frontiers | Research Topics

Conference research topic: 16th international symposium on schistosomiasis

Edited by
Roberta Lima Caldeira, Thiago Almeida Pereira,
Cristina Toscano Fonseca and Marina Moraes Mourão

Published in
Frontiers in Immunology
Frontiers in Microbiology
Frontiers in Public Health

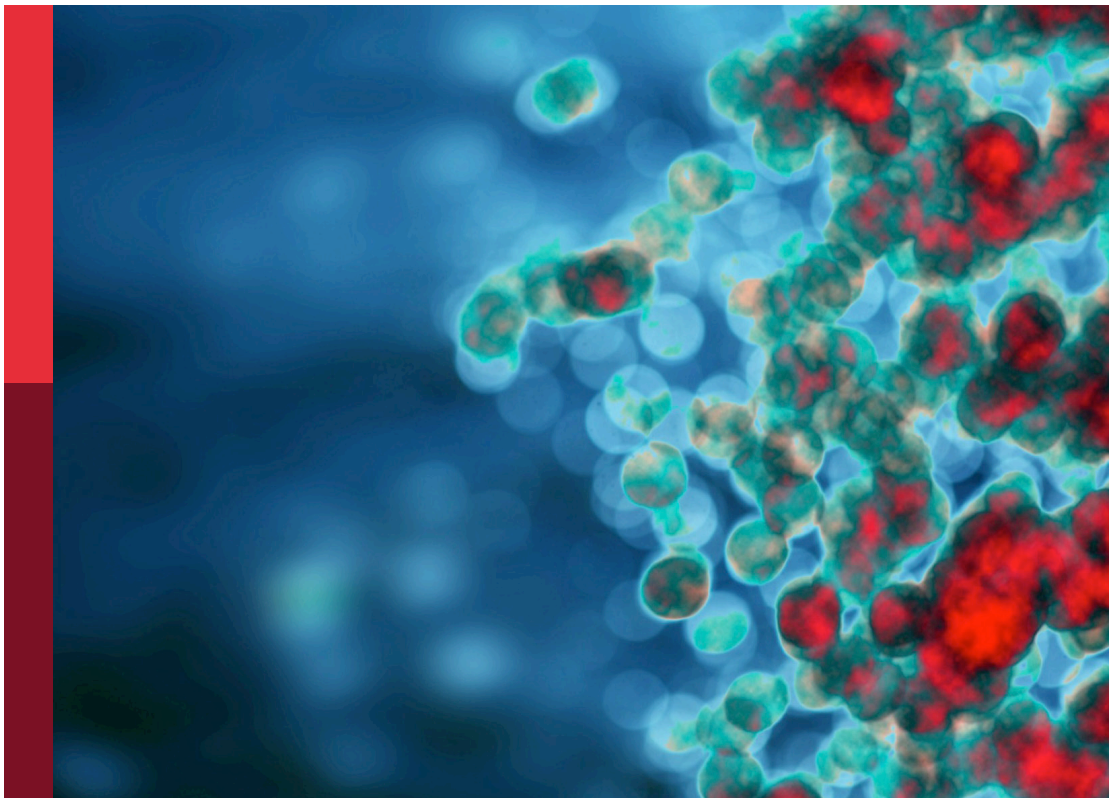

ISSN 1664-8714
ISBN 978-2-8325-5372-5
DOI 10.3389/978-2-8325-5372-5

About Frontiers

Frontiers is more than just an open access publisher of scholarly articles: it is a pioneering approach to the world of academia, radically improving the way scholarly research is managed. The grand vision of Frontiers is a world where all people have an equal opportunity to seek, share and generate knowledge. Frontiers provides immediate and permanent online open access to all its publications, but this alone is not enough to realize our grand goals.

Frontiers journal series

The Frontiers journal series is a multi-tier and interdisciplinary set of open-access, online journals, promising a paradigm shift from the current review, selection and dissemination processes in academic publishing. All Frontiers journals are driven by researchers for researchers; therefore, they constitute a service to the scholarly community. At the same time, the *Frontiers journal series* operates on a revolutionary invention, the tiered publishing system, initially addressing specific communities of scholars, and gradually climbing up to broader public understanding, thus serving the interests of the lay society, too.

Dedication to quality

Each Frontiers article is a landmark of the highest quality, thanks to genuinely collaborative interactions between authors and review editors, who include some of the world's best academicians. Research must be certified by peers before entering a stream of knowledge that may eventually reach the public - and shape society; therefore, Frontiers only applies the most rigorous and unbiased reviews. Frontiers revolutionizes research publishing by freely delivering the most outstanding research, evaluated with no bias from both the academic and social point of view. By applying the most advanced information technologies, Frontiers is catapulting scholarly publishing into a new generation.

What are Frontiers Research Topics?

Frontiers Research Topics are very popular trademarks of the *Frontiers journals series*: they are collections of at least ten articles, all centered on a particular subject. With their unique mix of varied contributions from Original Research to Review Articles, Frontiers Research Topics unify the most influential researchers, the latest key findings and historical advances in a hot research area.

Find out more on how to host your own Frontiers Research Topic or contribute to one as an author by contacting the Frontiers editorial office: frontiersin.org/about/contact

Conference research topic: 16th international symposium on schistosomiasis

Topic editors

Roberta Lima Caldeira — René Rachou Institute, Oswaldo Cruz Foundation (Fiocruz), Brazil

Thiago Almeida Pereira — Stanford University, United States

Cristina Toscano Fonseca — Grupo de Pesquisas em Biologia e Imunologia de Doenças Infecciosas e Parasitárias, Instituto René Rachou, Fundação Oswaldo Cruz, Brazil

Marina Moraes Mourão — Oswaldo Cruz Foundation (Fiocruz), Brazil

Citation

Caldeira, R. L., Pereira, T. A., Fonseca, C. T., Mourão, M. M., eds. (2024). *Conference research topic: 16th international symposium on schistosomiasis*. Lausanne: Frontiers Media SA. doi: 10.3389/978-2-8325-5372-5

Table of contents

frontiers | Frontiers in Immunology

TYPE Editorial
PUBLISHED 16 August 2024
DOI 10.3389/fimmu.2024.1462318

OPEN ACCESS

EDITED AND REVIEWED BY
Ian Marriott,
University of North Carolina at Charlotte, United States

*CORRESPONDENCE
Marina Moraes Mourão
mourao.marina@gmail.com
Roberta Lima Caldeira
roberta.caldeira@fiocruz.br
Thiago Almeida Pereira
thiagoap@stanford.edu
Cristina Toscano Fonseca
cristina.toscano@fiocruz.br

RECEIVED 09 July 2024
ACCEPTED 24 July 2024
PUBLISHED 16 August 2024

CITATION
Mourão MM, Caldeira RL, Pereira TA and Fonseca CT (2024) Editorial: Conference research topic: 16th international symposium on schistosomiasis NEW ('th') presented in superscript. *Front. Immunol.* 15:1462318. doi: 10.3389/fimmu.2024.1462318

Editorial: Conference research topic: 16th international symposium on schistosomiasis NEW ('th') presented in superscript

Marina Moraes Mourão[1]*, Roberta Lima Caldeira[1]*, Thiago Almeida Pereira[2]* and Cristina Toscano Fonseca[3]*

[1]Grupo de Helmintologia e Malacologia Médica, Instituto René Rachou, Fundação Oswaldo Cruz, Belo Horizonte, Brazil, [2]Institute for Stem Cell Biology and Regenerative Medicine, Stanford University School of Medicine, Stanford, CA, United States, [3]Grupo de Biologia e Imunologia de Doenças Infecciosas e Parasitárias, Instituto René Rachou, Fundação Oswaldo Cruz, Belo Horizonte, Brazil

KEYWORDS

International Symposium on Schistosomiasis, host-parasite interactions, vaccines, immunobiology, *Biomphalaria* sp., *Schistosoma* sp, diagnosis, public health

Editorial on the Research Topic
Conference research topic: 16th international symposium on schistosomiasis NEW ('th') presented in superscript

The International Symposium on Schistosomiasis is the foremost scientific gathering dedicated to this significant and neglected disease worldwide. Its 16th edition occurred in Minas Gerais, 2022, a Brazilian endemic state for the disease. The theme of this edition was "Schistosomiasis and Citizenship," with topics that addressed initiatives for disease control and elimination, the development of tools such as vaccines, medications, diagnostic tests, strategies for controlling the intermediate host, health education, and sanitation actions. In addition, epidemiological, clinical, and parasitological aspects, including the intermediate hosts, were broadly discussed.

The 16th symposium saw a turnout of 329 registered participants from 11 countries and 20 Brazilian states. Five keynote speeches, 98 studies presented as posters, ten panel discussions with 37 talks delivered by invited experts, and 24 selected from abstract submissions. The proceedings of the symposium encompassed 135 abstracts.

This Research Topic aims to widely disseminate some of the studies presented during the event and provide an opportunity for researchers who could not attend to share their study results on the event's theme. This Symposium edition includes 14 manuscripts, two reviews, and 12 original research articles from 108 authors worldwide.

Initiative for the control and elimination of schistosomiasis as a public health problem

The WHO's Guideline on the Control and Elimination of Human Schistosomiasis outlines six recommendations to assist national programs in endemic countries. These

recommendations focus on achieving morbidity control, eliminating schistosomiasis as a public health issue, and progressing towards interrupting transmission in line with the 2030 Agenda (1). Subsequently, members of the Oswaldo Cruz Foundation's Schistosomiasis Translational Program (Fio-schisto) and other experts from Brazil discussed the feasibility of this guideline for the Brazilian settings, published in the article of Menezes et al. The Fio-schisto proposes, for Brazil, interventions in basic sanitation as a priority measure envisioning eliminating schistosomiasis transmission, associated with the Information, Education, and Communication (IEC) strategy and other control measures, actively involving the school community. A two-stage immunological and molecular testing approach was recommended to verify transmission interruption during and after the intervention.

The paper by Wang et al. highlights the importance of education for transmission control. This study aimed to explore the Protection Motivation Theory (PMT) in predicting the likelihood of engaging in protective behavior against *Schistosoma* infection. They showed that in China, behavior intention is a complicated and indispensable part of changes in the population conduct, influenced by professional knowledge, socio-economic status, and personal characteristics. Effective dissemination of knowledge about schistosomiasis should be strengthened to ensure the effectiveness of protective measures against infection and severe disease.

To improve the species-specific recognition of the genus *Biomphalaria*, Araujo et al. used: 1) DNA barcoding methods, Barcode of Life Data System (BOLD) identification criteria and Best Close Match, 2) barcode gap, using the Kimura two-parameter model to calculate intraspecific and interspecific distance, and 3) sequences clustered/grouped into operational taxonomic units: Generalized Mixed Yule-Coalescent, Poisson Tree Processes, Automatic Barcode Gap Discovery, and Assemble Species by Automatic Partitioning. This work generated partial sequences of the *coi* gene and allowed the correct delimitation of most Brazilian *Biomphalaria* species using DNA barcoding and clustering/phylogenetic algorithms. This is a valuable work since there are 11 species of *Biomphalaria* sp. in Brazil, but only three species are of epidemiological importance for schistosomiasis.

Diagnosis development and evaluation

A new diagnostic test for schistosomiasis is essential for achieving schistosomiasis elimination as a public health problem by 2030 and certifying transmission interruption (1). Scientists worldwide are making significant efforts to develop and evaluate new diagnosis tools. During the symposium, several studies in the diagnosis area were presented. Two of these studies were reported in more detail in this Research Topic, and three other studies using point-of-care diagnosis were published in this Research Topic.

In their manuscript, Mesquita et al. evaluated the accuracy of eleven diagnostic tests for *S. mansoni* infection in a prospective blind study conducted in a low-endemic setting in Brazil. They evaluated point-of-care circulating cathodic antigen (POC-CCA) in the urine, PCR, qPCR, PCR-ELISA tests, and a loop-mediated isothermal amplification (LAMP) test in feces and urine samples. Additionally, they assessed three different ELISA tests without a good index test, thus using a latent class model to determine infection status. This study demonstrates the performance of all tests using different biological samples and proposes three different diagnostic strategies based on two tests: a sensitive ELISA-based test to initially screen for infection, and a confirmatory test based on molecular methods as a second step. This strategy proved more accurate and less expensive than any molecular test alone.

Given the broad distribution of *S. mansoni* infection in endemic countries, qPCR as a diagnostic test relies on infrastructure and logistics. Therefore, isothermal amplification techniques such as the Recombinase Polymerase Amplification (RPA) arise as an alternative. Mesquita et al. developed two RPA assays based on mitochondrial minisatellite DNA detection. The assays differed in their strategies. In the Real-Time RPA, amplification is detected based on the fluorescence emitted during amplification, while it is captured on the test line in the lateral flow format. Both formats performed well using full or half recommended volumes of reagents, were species-specific, and detected one copy of the target gene. No cross-amplification was observed.

To improve diagnosis, surveillance, and mapping of schistosomiasis cases in resource-limiting settings, Zacharia et al. provided a basis for the use of the dried urine spot method and POC-CCA. Collection, storage, and transportation of urine samples can be challenging in resource-limited settings. The authors demonstrated that the filter paper-based dried urine spot method could detect CCA antigens using the POC-CCA test without compromising the integrity of the results and is, therefore, an alternative to testing of fresh or stored samples.

Seeking a diagnostic assay to screen *S. japonicum* infection, Mu et al. developed a gold-immunochromatography assay (GICA) that detected antibodies against the *S. japonicum* saposin antigen (SjSAP-4). This antigen has a low predicted potential for cross-reactivity with antibodies against other parasite flukes and doesn't cross-react with antibodies against alveolar echinococcosis and trichinellosis. An interesting strategy was applied in the design and laboratory evaluation of the test suggesting its promise as a tool for screening cases in endemic settings and detecting the disease in non-endemic areas.

In the subsequent validation of the GICA test, Mu et al. assessed its performance in 412 individuals from *S. japonicum* endemic areas when compared with Kato-Katz (KK), POC-CCA, two in-house ELISA tests, and the droplet digital PCR assay (ddPCR) performed using feces, urine, serum, and saliva samples. Different sensibility and specificity values were observed depending on the index test used, highlighting the impact of the choice of index texts in diagnosis evaluation.

In diseased diagnosis, Zhong and Jin highlighted the importance of unisexual-schistosome exposure as a neglected phenomenon that should be considered when choosing a diagnostic strategy since unisexual-infected individuals lack the obvious clinical symptoms of the disease and might be less sensitive to praziquantel. In their mini-review, the authors summarized recent advances in our understanding of unisexual schistosomes and host-parasite interactions.

Host-parasite interaction and functional characterization

Defining host-parasite interactions is crucial to identifying novel strategies to help eliminate schistosomiasis. However, the lack of appropriate tools to study such interactions can be challenging, especially in the intermediate snail host. Duval et al. provided a new tool to study *Schistosoma-Biomphalaria* interactions using fluorescent non-transgenic cell trackers as a non-invasive tool for monitoring different stages of *S. mansoni* within the host without compromising viability and virulence. Combining this tool with vibratome histological techniques allows the visualization of the entire snail without damaging tissue structure. This novel protocol will help to elucidate the nuances of host-parasite interactions in the intermediate host.

The search for novel drugs against schistosomiasis is essential since the treatment relies on a single drug, praziquantel. Coelho et al. explored the functions and expression profile of Protein Arginine Methyltransferases (PRMTs), which catalyze posttranslational modifications, affecting both histone and non-histone proteins. The authors analyzed single-cell RNA-seq data and revealed that most *S. mansoni* (Sm) PRMTs are evenly distributed across various cell clusters in schistosomes. Functional interrogation using knockdown approaches decreased oviposition *in vitro* and *in vivo*. *Ex vivo* analysis revealed structural abnormalities in these worms. This study provides insights into SmCARM1 in *S. mansoni* biology, suggesting its potential as a drug target.

Schistosomes rely on the purine salvage pathway to secure their puric bases, resulting in an energy economy, which could be a choke point for parasite survival. Batista et al. interrogated the function of a gene family regulated by the Smp38 MAP kinase pathway, Hypoxanthine guanine phosphoribosyl transferases 1 and 3 (SmHGPRTases). It was shown that those proteins could be parasite-specific druggable targets, and that all members of the family participate in adenosine uptake. Ex vivo knocked-down in females exhibited immature eggs and impaired ovary development. Therefore, this study supports SmHGPRTases' importance as target candidates for schistosomiasis and parasite biology.

Continuing the theme of the search for new targets for drugs or vaccine development, Patrick Skelly and Da'dara presented a characterization of the gene encoding the schistosome tegumental acetylcholinesterase (AChE) in three major schistosome species. They demonstrated that schistosomes cleave exogenous acetylthiocholine and detangled the previous annotation of AChE enzymes. *S. mansoni* tegumental AChE (SmTAchE) is different from its human counterpart at a moderate level, and exposure to antibodies targeting SmTAChE impaired schistosomula viability. Thus, they propose it as a vaccine or therapeutic target. Therefore, this work aids in clarifying some of the questions regarding AChEs in this pathogen and highlights new therapeutic targets.

Vaccine development for schistosomiasis remains challenging despite intensive research. Understanding the natural mechanisms of self-cure in animal models such as the rhesus macaque or mice after multiple exposures to a radiation-attenuated cercarial vaccine may provide novel targets for vaccine development. Vance et al. compared the reactivity of sera pools from rhesus macaques after self-curing to four peptide arrays of secreted/exposed proteins from the alimentary tract and tegument of *S. mansoni*. The titer was the primary determinant for the rate of self-cure. Their screening provides the community with a list of candidate epitopes that could be combined to develop an effective vaccine.

Closing remarks

The 16th International Symposium on Schistosomiasis, held in Brazil, focused on disease control and elimination. It brought together participants from 11 countries to discuss various aspects, including the development of disease control tools and health education. The Research Topic dedicated to the symposium aimed at disseminating selected studies presented during the event to advance disease knowledge and control. Implementing WHO guidelines and improving species-specific recognition of the *Biomphalaria* genus was highlighted. Diagnostic tests for schistosomiasis were evaluated, including the accuracy of different tests and the development of new assays. Host-parasite interactions were studied, leading to the development of a new tool for tracking *S. mansoni* in the intermediate snail host. The functions of PRMTs and SmHGPRTases were explored as potential drug targets, and the gene encoding schistosome tegumental acetylcholinesterase was characterized as a potential vaccine or therapeutic target. Screening of self-cured macaques provided candidate epitopes for vaccine development. The 16th International Symposium on Schistosomiasis and the Pre-Symposium Research Topics (2) hold 48 manuscripts published in different sections of Frontiers, enriching this area of knowledge covering all aspects of schistosomiasis. These studies contribute to the search for new strategies to combat schistosomiasis.

Author contributions

MM: Writing – review & editing, Writing – original draft. RC: Writing – review & editing, Writing – original draft. TA: Writing – review & editing, Writing – original draft. CF: Writing – review & editing, Writing – original draft.

Acknowledgments

We would like to pay homage to all our colleagues we have lost since the last edition of the Symposium, in particular our dear friends Rodrigo Corrêa-Oliveira, Carlos Grault, and Donald McManus. The schistosomiasis community is grateful for their dedication and invaluable contribution to the field. We would also like to thank the scientists who contributed to the collaborative peer-review process and improved the exciting new research presented in this special edition.

Conflict of interest

The authors declare that the research was conducted in the absence of any commercial or financial relationships that could be construed as a potential conflict of interest.

The author(s) declared that they were an editorial board member of Frontiers, at the time of submission. This had no impact on the peer review process and the final decision.

Publisher's note

References

1. World Health Organization. *WHO guideline on control and elimination of human schistosomiasis*. Geneva: World Health Organization (2022). p. 144.

2. Fonseca CT, Pereira TA, Stothard JR, Caldeira RL, Mourão MM. Editorial: pre-conference research topic: 16th international symposium on schistosomiasis. *Front Immunol.* (2021) 12:774311. doi: 10.3389/fimmu.2021.774311

frontiers | Frontiers in Microbiology

TYPE Original Research
PUBLISHED 18 November 2022
DOI 10.3389/fmicb.2022.1043596

OPEN ACCESS

EDITED BY
Michal Letek,
Universidad de León,
Spain

REVIEWED BY
Wang Jiangyong,
South China Sea Fisheries Research Institute (CAFS), China
Sergei A. Subbotin,
California Department of Food and Agriculture, United States
Ulrich Femoe Membe,
University of Yaounde I, Cameroon

*CORRESPONDENCE
Bonnie Webster
b.webster@nhm.ac.uk
Roberta Lima Caldeira
roberta.caldeira@fiocruz.br

SPECIALTY SECTION
This article was submitted to Infectious Agents and Disease, a section of the journal Frontiers in Microbiology

RECEIVED 13 September 2022
ACCEPTED 17 October 2022
PUBLISHED 18 November 2022

CITATION
Mesquita SG, Lugli EB, Matera G, Fonseca CT, Caldeira RL and Webster B (2022) Development of real-time and lateral flow recombinase polymerase amplification assays for rapid detection of *Schistosoma mansoni*. *Front. Microbiol.* 13:1043596. doi: 10.3389/fmicb.2022.1043596

Development of real-time and lateral flow recombinase polymerase amplification assays for rapid detection of *Schistosoma mansoni*

Silvia Gonçalves Mesquita[1,2], Elena Birgitta Lugli[2], Giovanni Matera[3], Cristina Toscano Fonseca[4], Roberta Lima Caldeira[1]* and Bonnie Webster[2]*

[1]Grupo de Pesquisa em Helmintologia e Malacologia Médica, Instituto René Rachou, Fundação Oswaldo Cruz, Belo Horizonte, Brazil, [2]Wolfson Wellcome Laboratories, Department of Science, Natural History Museum, London, United Kingdom, [3]Department of Health Sciences, Unit of Microbiology, University "Magna Graecia" of Catanzaro, Catanzaro, Italy, [4]Grupo de Pesquisa em Biologia e Imunologia Parasitária, Instituto René Rachou, Fundação Oswaldo Cruz, Belo Horizonte, Brazil

Background: Accurate diagnosis followed by timely treatment is an effective strategy for the prevention of complications together with reducing schistosomiasis transmission. Recombinase Polymerase Amplification (RPA) is a simple, rapid, sensitive, and specific isothermal method with low resource needs. This research aimed at the development and optimisation of a real-time (RT) and a lateral flow (LF) RPA assay for the detection of *Schistosoma mansoni*.

Methodology: Recombinase Polymerase Amplification reactions were performed at full- (as recommended) and half-volumes (to reduce costs), with RT or LF detection systems targeting the *S. mansoni* mitochondrial minisatellite region. The specificity was assessed using gDNA from other *Schistosoma* species, helminths co-endemic with *S. mansoni*, human stool, and urine, and *Biomphalaria* snail hosts. The analytical sensitivity was evaluated using serial dilutions of gDNA, synthetic copies of the target, and single eggs. The ability of both assays to detect the *S. mansoni* DNA in human urine and stool samples was also tested. The long-term stability of the RT-RPA reagents was evaluated by storing the reaction components in different temperature conditions for up to 3 weeks.

Results: The RT- and the LF-RPA (SmMIT- and SmMIT-LF-RPA, respectively) presented similar results when used full- and half-volumes, thus the latter was followed in all experiments. The SmMIT-RPA was 100% specific to *S. mansoni*, able to detect a single egg, with a limit of detection (LOD) of down to 1 fg of gDNA and one synthetic copy of the target. The assay was able to detect *S. mansoni* DNA from stool containing 1 egg/g and in spiked urine at a concentration of 10 fg/μl. SmMIT-RPA reagents were stable for up to 3 weeks when kept at 19°C, and 2 weeks when stored at 27°C. The SmMIT-LF-RPA cross-reacted with Clinostomidae, presented the LOD of 10 fg and one synthetic copy of the target, being able to detect a single egg and 1 egg/g in a stool sample. The LOD in spiked urine samples was 10 pg/μl.

Conclusion: The half-volume SmMIT-RPA is a promising method to be used in the field. It is specific, sensitive, robust, and tolerant to inhibitors, with a long-term stability of the reaction components and the real-time visualisation of results.

KEYWORDS

Schistosomiasis, *Schistosoma mansoni*, Recombinase Polymerase Amplification, isothermal molecular diagnostics, mitochondrial minisatellite region, real-time RPA, lateral flow RPA

Introduction

Schistosomiasis is a neglected tropical disease associated with poverty and low sanitation conditions, causing more than 240 million cases worldwide and 1.4 million disability-adjusted life years (DALYs). It is estimated that 779 million people currently live at risk of infection in tropical and subtropical regions (Kyu et al., 2018; Panzner, 2022; World Health Organization, 2022). The clinical manifestations of the disease can be urogenital or intestinal depending on the species that is causing the infection. *Schistosoma mansoni* is the species that causes intestinal disease in Africa and the Americas. The infection occurs when people have contact with watercourses contaminated with cercariae shed by *Biomphalaria* snails. The cercariae actively penetrate human skin, losing their tail, and migrating as schistosomula *via* blood vessels until establishing infection within the mesenteric veins as mature adult worms. After copulation, the female worm laid up to 300 eggs per day that can be released into the environment through the host's faeces or become trapped in tissues, causing most of the chronic symptoms and complications of the disease (McManus et al., 2018; LoVerde, 2019; Nelwan, 2019). Nonspecific symptoms may occur in the early stage of the infection, such as fever, headache, fatigue, and myalgia and it is known as Katayama syndrome. Chronic schistosomiasis often produces gastrointestinal symptoms including diarrhea and abdominal pain, as well as hepatosplenic symptoms due to eggs lodged in the liver, e.g., fibrosis and portal hypertension (Colley et al., 2014). Less commonly, complications associated with ectopic migration of eggs can be observed in the brain and spinal cord (Vale et al., 2012).

The WHO Guidelines on Control and Elimination of Human Schistosomiasis were recently published. WASH (clean water, sanitation, and hygiene) and environmental interventions are highly recommended together with preventive chemotherapy (PC) by the mass drug administration (MDA) of Praziquantel targeting selected areas and groups (Lo et al., 2022; World Health Organization, 2022). MDA success is conditional to the precise assessment of schistosomiasis prevalence that will determine the appropriate strategy to be used (Utzinger et al., 2015). Therefore, estimating the true prevalence of schistosomiasis has a significant impact on the control and elimination measures (Turner et al., 2017).

The Kato-Katz (KK) technique is the method recommended by the WHO for the diagnosis of human intestinal schistosomiasis and it consists of the microscopic visualisation of eggs in the stool. This test is highly specific, cost-effective, and simple to perform, not needing much technological equipment other than the optic microscope (Katz et al., 1972). It has been extensively used for epidemiological surveys presenting a satisfactory performance in high prevalence settings. However, the KK's sensitivity varies depending on the period of infection, daily fluctuation of egg excretion, uneven distribution of eggs in the stool, endemicity, and/or co-endemicity of the area (Bärenbold et al., 2017; Cavalcanti et al., 2019; Diego et al., 2021; Ogongo et al., 2022). These limitations are mainly observed in moderate and low endemic areas, where 25–30% of positive cases can be missed (Berhe et al., 2004; Enk et al., 2008; McManus et al., 2018). Schistosomiasis prevalence and intensity of infection has decreased in many endemic regions over the past years, especially due to MDA and WASH improvements (Katz, 2018; Brasil, 2021; Lo et al., 2022). Since the occurrence of light infections is becoming more frequent, the development and implementation of new diagnostic tools are highly needed (Utzinger et al., 2015).

Antigen tests based on the detection of circulating anodic and cathodic antigens (CAA and CCA, respectively) can be used for the indirect detection of *S. mansoni* using urine and serum samples. The detection of antigens can be performed using two types of lateral flow assays named POC-CCA (commercially available) and UCP-LF-CAA. Both assays are more sensitive than KK, in particular, the UCP-LF-CAA, which is the most sensitive and specific antigen test currently available (Sousa et al., 2019; Assare et al., 2021). However, there are limitations related to these tests. CCA detection does not work for urogenital schistosomiasis. It has been shown to give false-positive results (Graeff-Teixeira et al., 2021) with performance issues recently reported related to different kit batches (Viana et al., 2019) and with complicated interpretation of trace results (Coelho et al., 2016). Although the UCP-LF-CAA assay is very promising and covers all *Schistosoma* species (Corstjens et al., 2014), it currently needs bespoke laboratory based equipment with 24 h needed to obtain results (Sousa et al., 2019).

Molecular PCR-based methods have been extensively used for schistosomiasis detection due to the high sensitivity, specificity, and

accuracy when compared to the KK technique (Pontes et al., 2003; Gomes et al., 2006, 2010; Cnops et al., 2012; Meurs et al., 2015; Frickmann et al., 2021; Siqueira et al., 2021). Despite having great advantages, the use of PCR-based methods is limited by the elevated cost and the need for advanced technological equipment and laboratory infrastructure, hampering large-scale implementation in endemic settings (Diego et al., 2021; Panzner, 2022).

Isothermal molecular methods stand out as promising alternatives to PCR for use at the point-of-care (POC)/point-of-need (PON). The loop-mediated isothermal amplification (LAMP) and the recombinase polymerase amplification (RPA) are the most common approaches used, providing fast and sensitive diagnosis and feasible in the field as they have low resource needs (Lobato and O'Sullivan, 2018; Li et al., 2021). Several LAMP assays have been developed for the detection of *S. mansoni* in both human and snail hosts over the past years, with favorable results (Abbasi et al., 2010; Hamburger et al., 2013; Fernández-Soto et al., 2014; Gandasegui et al., 2016, 2018; Caldeira et al., 2017; Mwangi et al., 2018; García-Bernalt Diego et al., 2019; Price et al., 2019; Mesquita et al., 2021). RPA was described in 2006 (Piepenburg et al., 2006) and since then it has been used mostly for the detection of *Schistosoma haematobium* (Rosser et al., 2015; Rostron et al., 2019; Archer et al., 2020, 2022; Frimpong et al., 2021) and *Schistosoma japonicum* (Sun et al., 2016; Xing et al., 2017; Guo et al., 2021; Deng et al., 2022), with only one study focused on *S. mansoni* targeting the ribosomal DNA (rDNA) regions 28S and the internal transcribed spacer (ITS; Poulton and Webster, 2018). Although this work represented a first and important step for the use of RPA for *S. mansoni* diagnosis, the lateral flow approaches lacked specificity with cross-reactivity with *S. haematobium* and *Schistosoma bovis* observed. One of the benefits of molecular based approaches is that they can be designed for different DNA biomarkers, allowing assays to be optimised to achieve high levels of sensitivity and specificity (Wang and Hu, 2014; Blasco-Costa et al., 2016). Once the isothermal molecular platform, such as LAMP and RPA, has been established and proved to work in the required settings then the molecular assays can be tailored to the need and sample type. This versatility of molecular platforms presents many cross-cutting opportunities and financial value.

Schistosoma mansoni molecular detection generally relies on stool samples, but urine, serum, and saliva can also be used for that purpose due to the presence of cell-free DNA (cfDNA; LoVerde, 2019). Each type of sample used as a source for DNA has its particularities. Stool samples are widely utilised as the source of both cfDNA and DNA from eggs, the latter often attached to a bead-beating and/or freezing step to facilitate egg disruption and DNA release (Pomari et al., 2019; Barda et al., 2020). Despite stool samples being non-invasive, they are inconvenient and require community sensitisation to ensure the collection of samples (Turner et al., 2017). Conversely, cfDNA presents great advantages as some bodily fluids such as urine are non-invasive, convenient, and usually easier to process, not requiring additional steps for sample preparation (Weerakoon and McManus, 2016). Sample type and sample preparation also have an effect on the downstream molecular assay to be used/tested. For example, PCR based approaches typically need samples that have been processed to remove inhibitors while isothermal assays are more tolerant to such inhibitors (Lobato and O'Sullivan, 2018). However, sample preparation and DNA extraction are currently among the factors that limit the use of molecular-based diagnostics in resource-poor settings and at the POC/PON due to the equipment requirements, costs, and time needs.

Moving from morbidity control to elimination as a public health problem requires more sensitive and specific diagnostic tests, especially to verify interruption of transmission, by detecting the infection in humans and snails (World Health Organization, 2022). Generally, as the demand for the novel test increase, its cost tends to decrease. Also, the cost-effectiveness of more accurate tests usually outweigh the actual cost of the test and the economic cost of the disease (Turner et al., 2017). For instance, it is estimated that in Brazil schistosomiasis generates annually a financial burden of nearly 41 million USD. More than 90% of that is related to indirect costs (e.g., loss of productivity and wages due to sick leave, hospitalisation, and premature deaths) that could be avoided by accurate diagnosis of infected people and timely treatment (Nascimento et al., 2019).

In this research, we developed and evaluated the performance of a real-time and a lateral flow RPA assay targeting the mitochondrial minisatellite region of *S. mansoni* to evaluate the diagnosis of the infection in humans and snails, especially in endemic areas where resources are limited.

Materials and methods

Samples used for assay development and optimisation

For analytical sensitivity and specificity testing, genomic DNA (gDNA) from *S. mansoni* and other *Schistosoma* species (*Schistosoma haematobium, Schistosoma curassoni,* and *Schistosoma bovis*) were obtained from the Schistosomiasis Collection at The Natural History Museum (SCAN; Emery et al., 2012). Further analytical specificity was evaluated using gDNA from other non-*Schistosoma* samples including the intermediate hosts *Biomphalaria glabrata, Biomphalaria tenagophila*, *Biomphalaria straminea,* and trematodes commonly found infecting *Biomphalaria* snails belonging to the families Clinostomidae, Echinostomatidae, Notocotylidae, Spirorchiidae, and Strigeidae, all obtained from the Medical Malacology Collection at René Rachou Institute, Fiocruz Minas (Fiocruz-CMM) via the Trematodes Biology Laboratory from the Federal University of Minas Gerais (UFMG). The Helminthology and Medical Malacology Laboratory (HMM) from Fiocruz Minas provided gDNA from helminths co-endemic with *S. mansoni* including *Ascaris*

lumbricoides, Ancylostomidae, *Enterobius vermicularis, Trichuris trichiura*, and *Fasciola hepatica*. Clinical stool samples were obtained under the Ethical Committee of Calabria Region approval (#108, 27 April 2017) and provided by the University "Magna Graecia" of Catanzaro. The data associated to all the specimens used in this study is provided on Supplementary material 1.

RPA primers and probe design

Recombinase Polymerase Amplification primers and the internal probe (TIB MolBio-Berlin, Germany) were designed targeting the *S. mansoni* mitochondrial minisatellite DNA region (GenBank accession number: L27240) following the guidelines from TwistDx™ (Cambridge, United Kingdom). To prevent the formation of primer-dimers, a phosphothioate backbone was added to the reverse primers for both the LF and RT assays (El Wahed et al., 2021) and the position of the 6-FAM and BHQ1 was reversed (compared to the design guidelines) within the RT probe. The primers were tested in-silico using BLAST (Altschul et al., 1990) to check the possibility of cross-reactivity. All primers and probes are described in Table 1 and shown in Figure 1.

RPA reaction setup

Real-time fluorescence-based RPA (SmMIT-RPA)

The RT SmMIT-RPA was performed using the TwistAmp® Exo Kit (TwistDX, Cambridge, United Kingdom). RPA reactions were set up as recommended by the manufacturer. Reactions were run in volumes of 50 µl (as recommended) or 25 µl (half-reactions; Supplementary material 2A). For the 50 µl reaction, a master mix was prepared containing the RPA rehydration buffer, water (if needed), forward and reverse primers, and the RT probe. This was then added to the lyophilised RPA pellet and homogenised by pipetting. The magnesium acetate (MgAc) was added to the lid of the RPA tube. Lastly, the DNA was added to the reaction tube. For the 25 µl reaction, a master mix was prepared and added to the lyophilised RPA pellet as above, and once homogenised it was split into two new tubes. The MgAc was added to the lid of each tube and finally, the DNA was added to the reaction. A positive (1 ng of *S. mansoni* gDNA) and negative (water) controls were included in all the runs. For both protocols, after the DNA addition, the tubes were quickly (~2 s) centrifuged, mixed (by inversion), then quickly (~2 s) centrifuged again. The centrifugation step mixes the MgAc with the other components which starts the RPA reaction. The tubes were incubated at 42°C for 20 min using the portable fluorometer AmpliFire (Douglas Scientific, Alexandria, MN, United States), with a manual mix after 4 min of incubation. Results could be seen in real-time *via* the device's touchscreen and exported as an excel file for analysis of the raw data. Samples were considered positive if the amplification curve, normalised by the background level during the initial 4 min of the reaction, crossed the threshold of 346 relative fluorescence units (RFU). To determine the threshold value, we calculated the mean RFU observed in the first 4 min of the reaction of all non-*S. mansoni* samples used during the standardisation phase. The threshold was then set by three standard deviations of the calculated means, which was 346 RFU. All the protocol steps and the amount of each reagent are detailed in Figure 2 and Supplementary material 2A.

TABLE 1 Mitochondrial primer and probe sequences designed for the LF-and RT-RPA.

Name	RPA method	Sequence (5′-3′)
SmMITnfo probe	LF	(6-FAM)ACTTGAGAAATTTTTTGATAAATTAG GTGTTC(THF)ACTGTGGTTGATTTTTTG(c3)
SmMITnfo reverse	LF	(Btn) TAACCCTATAAATCCTATTACCTTTCTACCAsC
SmMIT forward	LF/RT	ACAGAATTTTCAAAATTTTCCTTTTATTGTCT
SmMIT probe	RT	ACTTGAGAAATTTTTTGATAAATTAGGTGT (BHQ1)C(THF)AC(6-FAM) GTGGTTGATTTTTTG(c3)
SmMIT reverse	RT	TAACCCTATAAATCCTATTACCTTTCTACCAsC

6-FAM, 6-carboxyfluorescein; THF, tetrahydrofuran residue; BHQ1, black hole quencher; s, thiol group; c3, C3 Spacer; Btn, Biotin; LF, lateral flow; and RT, real time.

Lateral flow RPA (SmMIT-LF-RPA)

The SmMIT-LF-RPA was performed using the TwistAmp® Nfo Kit (TwistDX, Cambridge, United Kingdom). The reaction was set up as described above and detailed in Figure 2 and Supplementary material 2B. A positive (1 ng of *S. mansoni* gDNA) and negative (water) controls were included in all the runs. After incubation, 5 µl of the amplification product were added to a 0.5 ml tube together with 70 µl of the PCRD extraction buffer. The mixture was then added to PCRD lateral flow cassettes. Results were observed after 10 min and any changes in the results after that period were not acknowledged. Positive samples presented two lines (both test and control lines) while just the control line was present for negative samples.

RPA limit of detection

The LOD of the assays was evaluated using the samples as described below.

Genomic DNA and synthetic copies

Serial 10-fold dilutions from 1 ng to 1 fg of *S. mansoni* gDNA were prepared from an adult worm extracted using the DNeasy Blood & Tissue kit (Qiagen, Hilden, Germany) at an original concentration of 3.8 ng/µl, measured by Nanodrop Spectrophotometer (ThermoFisher, Massachusetts, United States). Synthetic copies of the target region were obtained (gBlocks, IDT, Newark, New Jersey, United States) and diluted from 1×10^5 copies/

```
  1 ttagtgttatagcccatactcctttagtcttttagtattatcgtctatagtacggtaggt
 61 gggtaaggtagaaaatgttgtttgtttgattctgtatttcgtgcagataagatgtttgta
121 gtctctacttggcagtggtagaagtgtttaacttgatgaaggggataggtgtatgttctg
181 tcctcttgtttttgaatagtggtttcggttttgttttttttttttttggtgggggttaaag
241 tataggattaagttaatttaatggtaagtaaaatgatttccgaaaaaagacctaaatttg
301 tgttatatatataatatatacaattataatatagaaggagaaaagatgtaaaaataggat
361 ttagggaggaggaaaatttataggttttgataataaatttttcttgtaaggggtaccct
421 tacagaattttcaaaatttttccttttattgtctaaaattaggtatcaattgaggtaattt
481 tacttgagaaatttttttgataaattaggtgttcaactgtggttgatttttttggatgatag
541 atttattaaaaatattaaaaggtatagtcaattgtggtagaaaggtaataggatttatag
601 ggttaccttcccttggtttc
```

FIGURE 1
Position of the Recombinase Polymerase Amplification (RPA) primers and probe within the Mitochondrion *Schistosoma mansoni* minisatellite DNA region. Bold sequences represent the primer sites and sequence in italics represents the probe site.

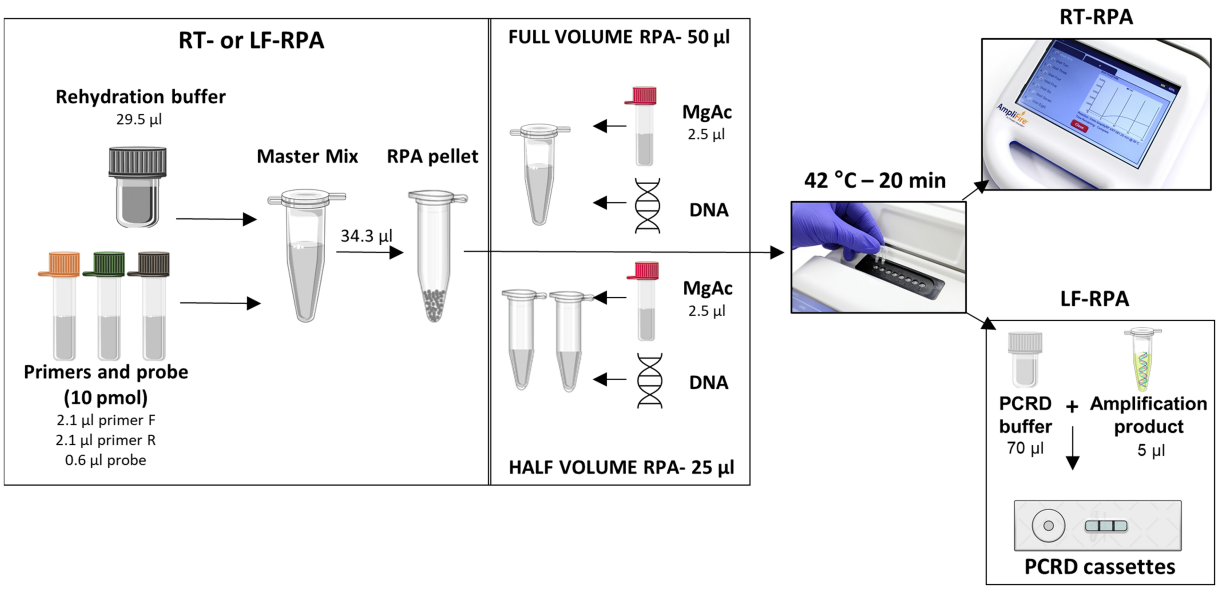

FIGURE 2
Set up of each RPA protocol used in this study. Images used in this figure were obtained at Agdia, Bioicons, and Mind the Graph websites.

µl down to 1 copy/µl. The analytical sensitivity of SmMIT-RPA was calculated by repeating 10 times the reaction using gDNA dilutions and three times using synthetic copies dilutions.

Schistosoma mansoni eggs

Single eggs of *S. mansoni* were provided by the Snail Schistosome Resource (SSR, Natural History Museum, United Kingdom-https://www.nhm.ac.uk/our-science/our-work/sustainability/schistosome-snail-resource.html) *via* the NIAID Schistosomiasis Resource Center (SRC, Biomedical Research Institute, United States-https://www.afbr-bri.org/schistosomiasis/). Individual eggs were isolated from a pool of eggs by capturing each one with a micropipette under a stereomicroscope. The DNA was then extracted using the SwiftX™ DNA kit (Xpedite Diagnostics, Germany) following protocol 1 from the manufacturer, with and without the heating step (Supplementary material 3). In brief, the protocol consists of the addition of buffer DL (50 µl) and magnetic beads (7.5 µl) to the tubes containing the single egg and incubate at room temperature (~19°C) or heated (95°C) for 5 min, followed by magnetic separation of the supernatant, which contains the extracted DNA. The direct addition of whole single eggs, with no DNA extraction procedure, in fresh (live eggs) and frozen conditions was also tested.

RPA specificity

For both the LF and RT assays, the specificity was assessed against gDNA from other organisms that may be present in clinical and field samples. This included host DNA (snail host DNA and DNA from human urine and stool). gDNA from the snail hosts *B. glabrata, B. straminea,* and *B. tenagophila* were tested together with other trematodes that are commonly found infecting *Biomphalaria* snails in the neotropical region (Clinostomidae, Echinostomatidae, Notocotylidae, Spirorchiidae, and Strigeidae). Helminths of medical importance that are often co-endemic with *S. mansoni* (*A. lumbricoides,* Ancylostomidae*, E. vermicularis, F. hepatica,* and *T. trichiura*) were tested together with other commonly occurring *Schistosoma* species (*S. bovis, S. curassoni, S. haematobium*).

RPA performance with urine and stool

Clinical stool samples

Stool samples that had been previously collected and characterised were used. One sample collected in Guinea Bissau, negative by both Kato-Katz and PCR methods, and one sample from Colombia, positive by Kato-Katz (1 egg/g) and by PCR. gDNA from these samples was extracted using the QIAamp DNA Stool Mini Kit (Qiagen, Hilden, Germany) following the manufacturer's protocol.

Spiked urine samples

Seven aliquots of 100 µl of urine from a non-infected donor were spiked with different concentrations of *S. mansoni* gDNA with final concentrations within the samples ranging between 1 ng/µl and 1 fg/µl. Two aliquots of 100 µl of urine from the same donor were spiked with a pool of gDNA from medically important helminths (*A. lumbricoides,* Ancylostomidae*, E. vermicularis, F. hepatica,* and *T. trichiura*), with and without *S. mansoni* DNA. One aliquot of 100 µl of urine without the addition of any DNA was also used. The urine samples were filtered using Whatman® qualitative filters paper grade 3:6 µm (Sigma-Aldrich, St. Louis, Missouri, United States). The filters were dried at room temperature and 6 mm holes were made using a hole puncher. The paper holes were used for the DNA extraction using the QIAamp DNA Blood Mini Kit (Qiagen, Hilden, Germany) and following the protocol described by Lodh et al. (2017).

SmMIT-RPA storage conditions

Aiming to simulate point-of-need settings, we evaluated alternative storage conditions of the RT primers, probe, and kit reagents for up to 3 weeks. The reaction components were stored protected from light, at 19 and 27°C, mixed or separate. Reactions were conducted on days 0, 1, 2, and 3, and on weeks 1, 2, and 3, so we could evaluate the efficiency of the reaction over time.

Results

Primers and probes

Primers and probes targeting 184 bp of the mitochondrial *S. mansoni* minisatellite DNA region were manually designed as detailed in Table 1. In-silico specificity, based on BLAST (Altschul et al., 1990), was 100% specific for *S mansoni*.

SmMIT-RPA and SmMIT-LF-RPA assay testing

Both real-time and lateral flow assays were successfully performed using full (50 µl) and half (25 µl) reaction volumes, keeping the final concentrations of each reaction component as in the original protocol (Table 2; Supplementary material 4). For that

TABLE 2 The performance of SmMIT-and SmMIT-LF-RPA assays.

Tests		SmMIT-RPA	SmMIT-LF-RPA
Volume	Full	Good performance	Good performance
	Half	Good performance	Good performance
Specificity	*Schistosoma* species	No cross-reactivity	No cross-reactivity
	Trematodes	No cross-reactivity	Cross-reactivity with Clinostomidae
	Helminths	No cross-reactivity	No cross-reactivity
	Biomphalaria snail hosts	No cross-reactivity	No cross-reactivity
	Human urine and stool	No cross-reactivity	No cross-reactivity
Analytical Limit of Detection	gDNA	1 fg	10 fg
	Synthetic copies	1 copy	1 copy
	Single Egg	Positive	Positive
Laboratory Validation	Stool	1egg/g	1 egg/g
	Urine	10 fg/µl	10 pg./µl
Storage	Primer mix+ Probe at 19°C	Stable until week 3	Not evaluated
	Primers separate + Probe at 19°C	Stable until week 3	
	Kit at 19°C	Stable until week 3	
	Primer mix+ Probe at 27°C	Stable until week 2	
	Primers separate + Probe at 27°C	Stable until week 2	
	Kit at 27°C	Stable until week 3	

reason, the adapted protocol was followed in all experiments performed and the results presented from here on in were obtained by using half reaction volumes (25 µl), as detailed in Figure 2.

Real-time fluorescence-based RPA (SmMIT-RPA)

SmMIT-RPA limit of detection

The SmMIT-RPA presented a high limit of detection being able to detect down to 1 fg of *S. mansoni* gDNA, one synthetic copy of the target, and a single *S. mansoni* egg in all conditions evaluated being: (i) DNA extracted with heated incubation; (ii) DNA extracted without heated incubation; (iii) fresh non-extracted egg; and (iv) frozen non-extracted egg (Figure 3; Table 2).

SmMIT-RPA specificity

The SmMIT-RPA assay was specific to *S. mansoni* with no cross-reactivity observed with snail or human DNA, DNA from other trematodes (including other *Schistosoma* species), and other helminths of medical importance (Figure 4; Table 2).

SmMIT-RPA performance using spiked urine and stool samples

The SmMIT-RPA presented a good performance when used on biological samples. *Schistosoma mansoni* DNA was detected in the positive stool sample known to contain 1 egg/g of stool (previously detected by the KK technique), and urine samples spiked with *S. mansoni* DNA at a final concentration of 10 fg/µl (Table 2; Supplementary material 5A) indicating high tolerance to molecular assay inhibitors present in urine (e.g., urea).

SmMIT-RPA storage condition

Our results showed that storing the primers and probe mixed together affected the assay performance giving false positive results. Keeping just the two primers mixed together or separately did not affect the RPA performance. However, the storage temperature influenced the results. Storing the primers and probe at 27°C reduced their longevity to 2 weeks, 1 week less than when stored at 19°C. The lyophilised RPA pellet, rehydration buffer, and MgAc produced consistent results after being stored for 3 weeks at both temperature conditions (19 and 27°C; Table 2). These results indicate that the SmMIT-RPA is a promising method able to produce robust results without the need for consistent cold chain for up to 3 weeks.

Lateral flow RPA (SmMIT-LF-RPA)

SmMIT-LF-RPA limit of detection

The SmMIT-LF-RPA detected down to one synthetic copy of the target region and one single egg either crude (frozen) or extracted with the SwiftX™ DNA kit (original protocol, i.e., with the heating step). The limit of detection of the assay using serial dilutions of the gDNA was 10 fg, 10-fold less sensitive than the SmMIT-RPA (Figure 5; Table 2).

SmMIT-LF-RPA specificity

The SmMIT-LF-RPA assay showed high specificity for *S. mansoni* with no cross-reactivity against *B. glabrata, B. straminea*, *B. tenagophila*, human urine, and stool; nor was there cross-reactivity to other co-endemic human helminths and other trematodes belonging to the families Echinostomatidae, Notocotylidae, Spirorchiidae, Strigeidae, and three other *Schistosoma* species. However, cross-reactivity was observed with a trematode from the Clinostomidae family (Figure 6; Table 2).

SmMIT-LF-RPA performance using urine and stool samples

A loss in LF sensitivity was observed when spiked urine samples were analysed. SmMIT-LF-RPA was able to detect 10 pg/µl of *S. mansoni* DNA, a 1,000-fold decrease when compared to the SmMIT-RPA. The assay was able to detect the presence of the *S. mansoni* DNA in the positive stool sample (1 egg/g by the KK technique; Table 2; Supplementary material 5B).

Discussion

Sensitive, specific, simple, and rapid diagnostic methods are essential to reach the World Health Organization (WHO) target of eliminating schistosomiasis as a public health problem (prevalence of heavy infections lower than 1%) by 2030 (WHO World Health Organization, 2022). To this end, Recombinase Polymerase Amplification (RPA) is an isothermal amplification method that presents great potential. It has been piloted for detection of urogenital schistosomiasis caused by *Schistosoma haematobium* (Rosser et al., 2015; Rostron et al., 2019; Archer et al., 2020; Frimpong et al., 2021) and intestinal schistosomiasis caused by *Schistosoma japonicum* (Sun et al., 2016; Xing et al., 2017; Guo et al., 2021; Deng et al., 2022), with promising results for its use in the field at the point-of-need (PON). Only one study has explored the development of a RPA assay to detect *Schistosoma mansoni* DNA, and this was done using the lateral flow RPA. The assay's molecular targets were the 28S and ITS rDNA regions and although analytical sensitivity was good, the assays were found to be non-specific to *S. mansoni* with cross-reactivity observed with other *Schistosoma* species, namely *S. haematobium* and *S. bovis* (Poulton and Webster, 2018). The development of a RT-RPA targeting these ribosomal regions may be advantageous for a genus-specific assay. The genus or species level diagnostic specificity need for schistosomiasis, will depend on the diagnostic use case, with species level specificity detailed as a priority within the WHO schistosomiasis diagnostic target product profile (World Health Organization, 2021). In the present study, real-time fluorescence-based (RT)

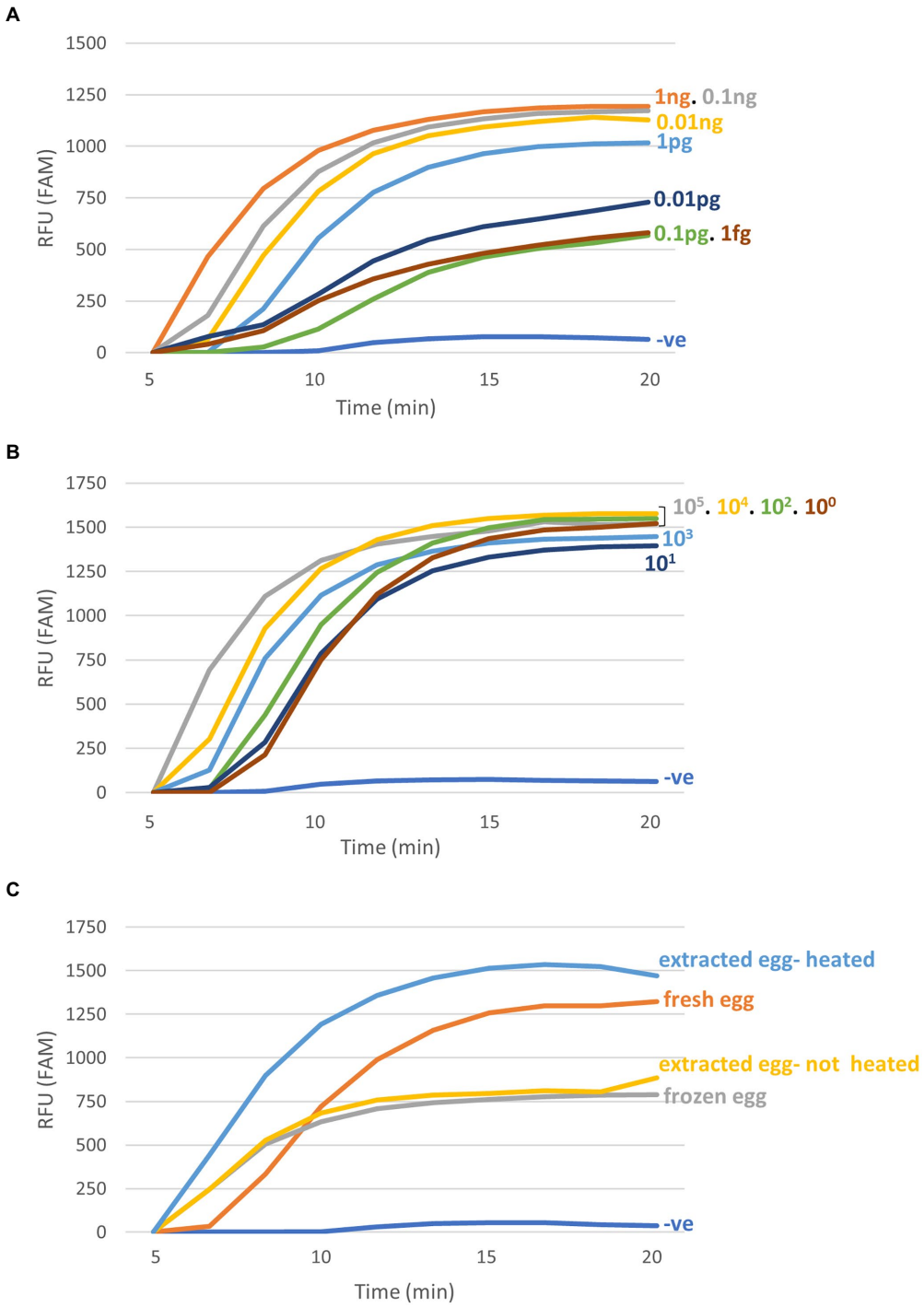

FIGURE 3
Limit of detection of the SmMIT-RPA. The assay was able to detect down to **(A)** 1 fg of the gDNA; **(B)** One synthetic copy of the target; **(C)** Single eggs extracted with the SwiftX™ DNA kit with or without the heating step, and single crude eggs, collected fresh and frozen (no DNA extraction procedure used). All graphs are displayed with the background baseline fluorescence subtracted. Legend: RFU-relative fluorescence units; ng-nanogram; pg-picogram, fg-femtogram; –ve-negative control (water).

and lateral flow (LF) RPA assays were developed targeting the mitochondrial minisatellite region (termed here as SmMIT-and SmMIT-LF-RPA, respectively RPA) with higher sensitivity and specificity to *S. mansoni*, compared to the assays developed by Poulton and Webster (2018), with further potential for its use in endemic settings.

The developed SmMIT-RPA assay was 100% specific for *S. mansoni* in this study, proving to be a good alternative for the

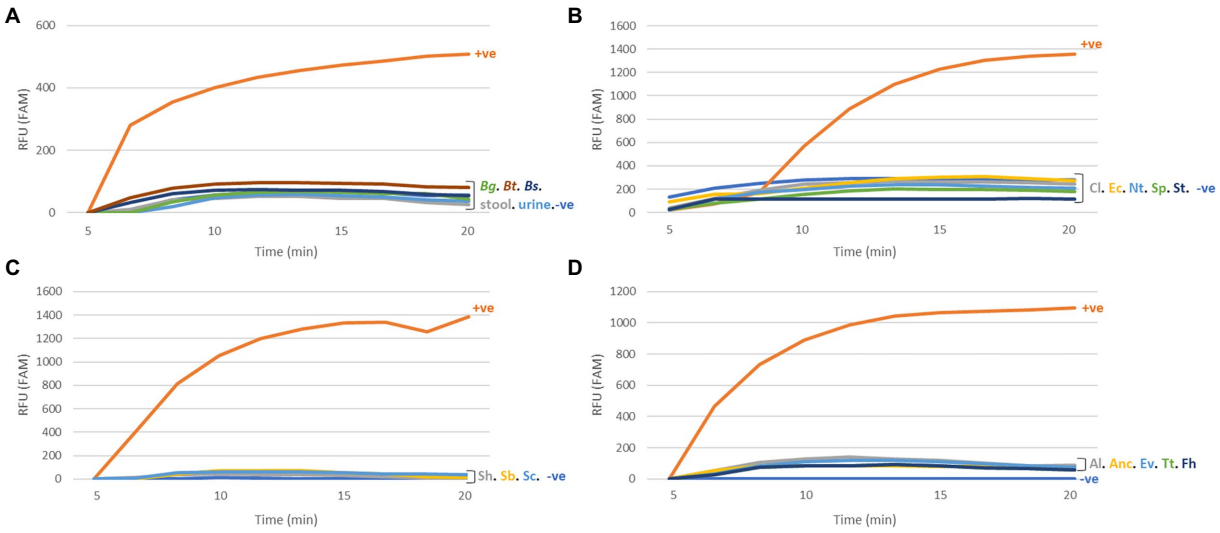

FIGURE 4
Specificity of the SmMIT-RPA. The assay was specific to *Schistosoma mansoni* with no cross-reactivity against **(A)** The host species; **(B)** Trematodes; **(C)** *Schistosoma* species; **(D)** Helminths of medical importance. All graphs are displayed with the background baseline fluorescence subtracted. Legend: RFU-relative fluorescence units; +ve-positive control (1 ng of *S. mansoni* gDNA); –ve-negative control (water); Bg, *B. glabrata*; Bt, *B. tenagophila*; Bs, *B. straminea*; Cl, Clinostomidae; Ec, Echinostomatidae; Nt, Notocotylidae; Sp, Spirorchiidae; St, Strigeidae; Sh, *S. haematobium*; Sb, *S. bovis*; Sc, *S. curassoni*; Al, *A. lumbricoides*; Anc, Ancylostomidae; Ev, *E. vermicularis*; Fh, *F. hepatica*; and Tt, *T. trichiura*.

detection of *S. mansoni* infections in both human and snail hosts, without any cross-reactivity with other *Schistosoma* species and trematodes tested. It will be important to further test this specificity in terms of the genetic diversity of *S. mansoni* geographical strains, to make sure that specificity does not limit its ability to detect *S. mansoni* from all endemic areas (Webster et al., 2013). This is particularly relevant as the mitochondrial minisatellite target, used here, may be prone to high mutation rates due to its mitochondrial origins. It would also be relevant to check for specificity and cross-reactivity within co-infections, where inter-species interactions can lead to the production of hybrid offspring, e.g., *S. mansoni/S. haematobium* parthenogenic hybrids that have been observed to occur in co-endemic areas (Huyse et al., 2013). As the target used here is a mitochondrial target, only the maternal line of the interactions will be detected, however such hybrids are never found without the presence of the original species and so a specific diagnostic, such as the SmMIT-RPA, will still provide a diagnosis. The SmMIT-RPA assay should be further tested on *Schistosoma rodhaini,* the sister species to *S. mansoni* to check its ability to distinguish between *S. mansoni, S. rodhaini* and *S. mansoni/S. rodhaini* hybrids. This is particularly important for snail xenomonitoring of *Biomphalaria* snails, as *S. rodhaini* and *S. mansoni/S. rodhaini* are not implicated in human infections (Rey et al., 2021).

It was expected that the SmMIT-LF-RPA would show the same specificity as the primers and probes designed for both assays were very similar, except for the specific modifications required for each approach. However, cross-reactivity with cercariae belonging to the Clinostomidae family was observed only in the SmMIT-LF-RPA. Trematodes in the family Clinostomidae belong to the superfamily Schistosomatoidea together with the family Schistosomatidae, to which *S. mansoni* belongs. The close phylogenetic relationship between both families may reflect genomic similarities. RPA is known to be highly specific, but it can also tolerate the presence of a few nucleotide mismatches within the primer and probe regions, which can lead to false-positive results (Lobato and O'Sullivan, 2018), hence the need for rigorous specificity testing. Currently, there is no data available in public databases for the mitochondrial minisatellite region of non-schistosome trematodes, limiting the in-silico evaluation of the primers' specificity. Species belonging to the Clinostomidae family have been reported parasitising *Biomphalaria* snails in Brazil, including the hosts species (*B. glabrata, B. straminea,* and *B. tenagophila*; Mesquita et al, 2020; Sousa et al., 2022). These trematodes are parasites of birds with fish being the second intermediate host. Human infections are rare and accidental due to the ingestion of raw fish. These infections have been reported in Asia and currently do not represent risks for human health in endemic areas for schistosomiasis (Lee et al., 2017; Kim et al., 2019). However, this cross-reactivity should be taken into account by the local malacological surveillance and schistosomiasis control program to measure the benefits and risks of using the SmMIT-LF-RPA for snail xenomonitoring. Further modifications of the primers and probe could be carried out to prevent the cross-reactivity with this non-*Schistosoma* trematode.

The SmMIT-RPA assay presented a high limit of detection (LOD) being able to detect down to 1 fg of *S. mansoni* DNA, with an analytical sensitivity of 20% at this level, but 100% for 1 ng. A reason for the low percentage of analytical sensitivity at low concentrations of *S. mansoni* DNA could be due to

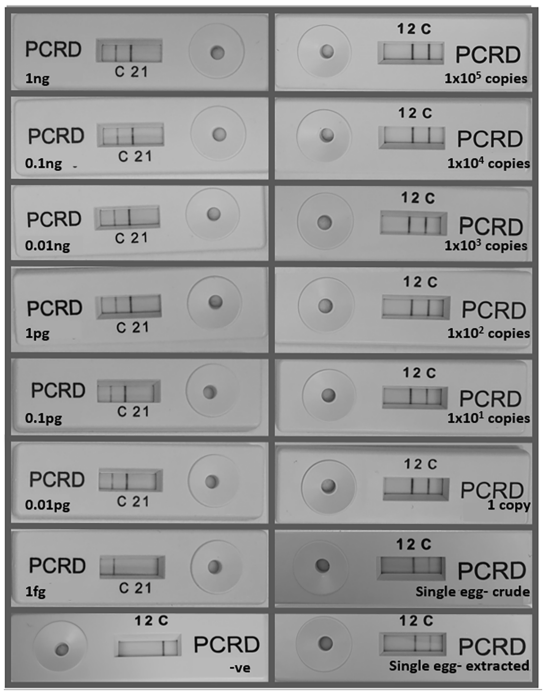

FIGURE 5
Limit of detection of the SmMIT-LF-RPA. The assay was able to detect down to 10 fg of the gDNA, one copy of the synthetic target DNA, and one single egg with or without DNA extraction. Legend: ng, nanogram; pg, picogram, fg, femtogram; +ve, positive control (1ng of *Schistosoma mansoni* gDNA); and –ve, negative control (water).

crowding agents in the RPA assay components. The crowding agents have an important role acting in the formation of the primer-recombinase complex (Piepenburg et al., 2006). However, they can also influence the reaction performance when there are low copies of the target due to its viscosity, which may be the reason for inconsistent results when low amounts of DNA were added to the reaction (Lobato and O'Sullivan, 2018). Moreover, analytical sensitivity does not always correspond to diagnostic sensitivity due to the nature of the starting material. When synthetic copies of the target were used, the LOD was 1 copy with an analytical sensitivity of 100%. This may be due to the higher purity of commercial samples compared to the gDNA dilutions obtained from adult worms' extracts. In comparison to the LOD of the SmMIT-RPA (down to 1 fg), the SmMIT-LF-RPA presented a 10-fold reduction (down to 10 fg) in the assay's analytical sensitivity. The difference in sensitivity between LF- and RT-RPA approaches has previously been reported for the assays developed for *S. haematobium,* with the LF assay able to detect 100 fg of the gDNA while the RT was able to detect down to 1 fg (Rosser et al., 2015; Rostron et al., 2019).

Both RPAs were able to detect the presence of DNA extracted using the SwiftX™ DNA kit from single *S. mansoni* eggs. This kit consists of the same components and steps as the discontinued Speed Xtract Nucleic Acid Kit (Qiagen, Hilden, Germany) and is a simple, fast, and efficient extraction method that requires few laboratory resources (e.g., pipettes and magnetic rack). A modification in the original protocol from the manufacturer was evaluated and the incubation of the sample was tested at both 95°C (as recommended) and at room temperature (~19°C), with the latter allowing to dispense with the requirement for a heating block that may rely on electricity. Both extraction conditions presented positive results. In addition, whole eggs (frozen and fresh) added directly to the reaction mix also produced positive results. This detection of *S. mansoni* DNA from single crude eggs reduces the requirements for sample preparation making both SmMIT-RPA and SmMIT-LF-RPA assays even more field-friendly while also reducing costs. However, clinical samples may present additional complications related to processing, egg disruption, and removal of inhibitors particularly related to stool samples. This has been demonstrated for other molecular assays where bead-beating and/or freezing prior to DNA extraction has been shown to increase DNA yields, improving the performance of molecular diagnostics (Pomari et al., 2019; Barda et al., 2020). The use of egg disruption strategies coupled with different DNA extraction methods needs to be further tested for RPA-based assays, particularly for clinical samples.

Recombinase Polymerase Amplification has been tested on multiple types of samples, e.g., urine, stool, blood, bodily fluids, and animal and plant products among others (Daher et al., 2016; Lobato and O'Sullivan, 2018). Moreover, the tolerance of the RPA reaction components to known PCR inhibitors found in clinical samples has been demonstrated in previous studies (Archer et al., 2022), including the direct addition of crude urine into the reaction mix (Rosser et al., 2015). The present study showed that both the LF-and RT-RPA approaches were able to detect *S. mansoni* DNA in clinical and spiked samples (stool and urine, respectively). Stool samples are the most used biological material for the molecular detection of *S. mansoni*, as it is the source of eggs and cfDNA. Promisingly, both LF-and RT-RPAs developed in this study were able to detect the infection in a stool sample having 1 egg/g that has previously been characterised as positive sample by KK and PCR. Several authors have also reported that urine samples can be used as the source of cfDNA of *S. mansoni* (Lodh et al., 2017; Fernández-Soto et al., 2019; Diab et al., 2021; Allam, 2022). In this study, urine samples were spiked with different amounts of gDNA to simulate the detection of cfDNA in clinical samples. As with testing of the gDNA standards, a difference was observed in the sensitivity of the SmMIT-RPA and SmMIT-LF-RPA, with the LF assay being less sensitive when using spiked urine samples. A 10-fold decrease in analytical sensitivity was observed for the LF-versus the RT-RPA assays using gDNA, whereas when the DNA was incorporated into the urine, there was a further loss of sensitivity for the LF assay (1,000-fold decrease). This may result from the RT-RPA having a higher tolerance to the presence of the inhibitors than the LF-RPA. However, additional studies should be conducted with larger numbers of clinical samples to investigate the effect of inhibitors on RPA outcome and whether they need to be removed.

The long-term stability of the lyophilised RT-RPA pellet and reagents has been previously evaluated by Chandu et al.

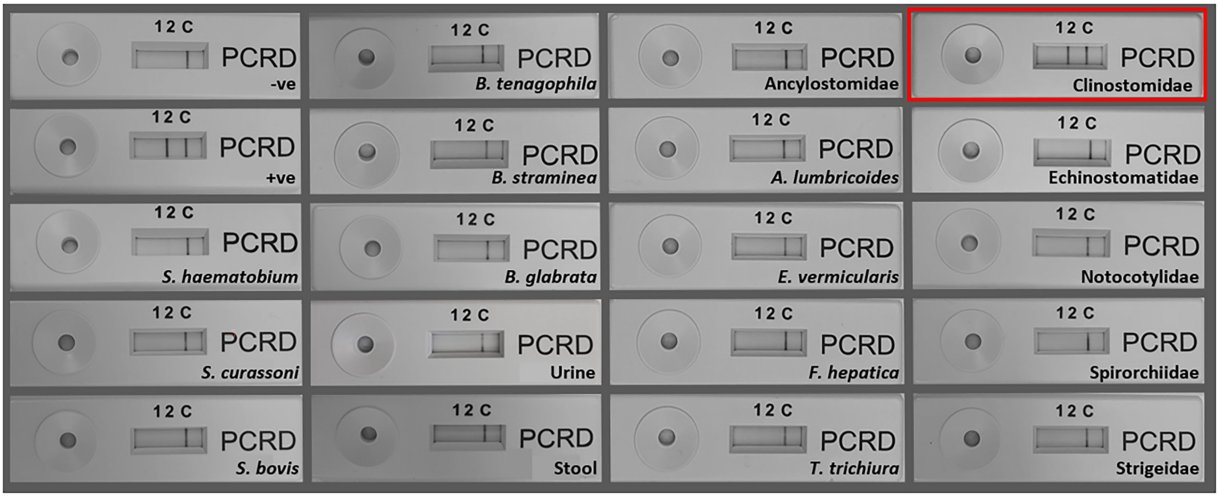

FIGURE 6
Specificity of the SmMIT-LF-RPA. The assay was specific to *Schistosoma mansoni* with no cross-reactivity with *S. haematobium, S. bovis, S. curassoni*, human stool, human urine *B. glabrata, B. straminea, B. tenagophila, A. lumbricoides,* Ancylostomidae, *E. vermicularis, T. trichiura, F. hepatica*, and trematodes belonging to the families, Echinostomatidae, Notocotylidae, Spirorchiidae, and Strigeidae. Cross-reactivity was observed for a Clinostomidae trematode (highlighted in red). Legend: +ve-positive control (1 ng of *S. mansoni* gDNA); –ve-negative control (water).

(2016), proving the robustness of the reagents kept at −15–8°C for 1 year, and at 22–28°C for up to 6 months. Our findings confirm the stability of the reagents plus the primers and probe for 3 weeks when stored at 19°C and up to 2 weeks when stored at 27°C, agreeing with results previously obtained by Lillis et al., (2016). Infra-structure limitations in endemic areas may hamper the use of molecular methods. For this reason, the ability to work without dependence of cold chain storage facilitates the use of the SmMIT-RPA in these contexts. The longevity of all reagents for a period longer than 3 weeks or at a temperature higher than 27°C, as well as the impact of humidity, should be evaluated in the future.

Even though RPA presents many advantages in terms of performance and accuracy, the costs of the assay might be a limiting factor considering its application in endemic settings, where usually there is limited availability of financial resources. In general, a qPCR reaction costs 1.5 USD per sample (not including the cost of DNA extraction and the thermocycler; Archer et al., 2022), whereas the KK technique, which is the recommended diagnostic test by WHO and local health authorities, costs approximately 0.1–0.3 USD per sample (not including the cost of microscope and personnel; Speich et al., 2010). The cost of a full-volume SmMIT-RPA per sample is 6.98 USD meanwhile the half-volume reaction cost is 3.49 USD. The SmMIT-LF-RPA has a higher cost per sample given the price of the cassettes, being 9.08 USD for each full-volume reaction, and 5.84 USD, for the half-volume reaction. The half-volume SmMIT-RPA is the most cost-effective protocol among the ones assessed in this study. Though it is 2.3 times more expensive than qPCR, the SmMIT-RPA is simpler and faster, the results are easier to interpret, and it is more field-friendly. The costs of each RPA assay are detailed in Supplementary material 6 and does not include the costs of DNA extractions as well as the cost of the fluorometer and other equipment needed (e.g., pipette, centrifuge, and vortex). The findings from this study represent important progress on price reduction by using half of the reaction volume without compromising good and consistent results for the detection of *S. mansoni*. The use of a smaller reaction volume, than that recommended by the manufacturer, has been tested before aiming at the elimination of the mixing step during incubation (Lillis et al., 2016), and this should be tested further with this SmMIT-RPA assay. Further optimisation of the assay and large-scale use may reduce the cost per reaction. Moreover, the cost-benefits of implementing a more sensitive and accurate diagnostic test should be considered. Accurate diagnosis enables timely treatment, the prevention of long-term complications and financial losses due to lack of productivity and sick leaves, as well as reducing the potential of emergence of new transmission foci (Turner et al., 2017). Thus, the impact of using a more expensive diagnostic test will be smaller in the long run given the benefits of its implementation.

The SmMIT-RPA presented a better performance overall when compared to the SmMIT-LF-RPA. Besides being more specific and sensitive, the SmMIT-RPA is advantageous as real-time visualisation of results does not require opening the reaction tubes after DNA amplification. RPA can amplify up to 10^4-fold the target in 10 min (Daher et al., 2016) and assays requiring end-point visualisation of the result can be prone to cross-contamination among the samples. Therefore, until a closed system is developed and available for the LF assay, there will be a risk of contamination when this approach is used.

Determining the precise prevalence of schistosomiasis in a specific area is conditional to a sensitive, specific, reproducible, and accessible diagnostic method. However, diagnostics improvements are very much needed for detection

of light infections in low prevalence settings, and for the verification of transmission interruption (Ogongo et al., 2022; World Health Organization, 2022). If good diagnostic tools are not available, the true prevalence of a specific area may be underestimated limiting the efficiency of schistosomiasis control programs (Panzner, 2022). The promising results obtained in this study suggest that the SmMIT-RPA may allow for a more accurate and rapid diagnosis of schistosomiasis and therefore may influence the decision-making processes involved in determining appropriate destination of public funding aimed at the elimination of schistosomiasis as a public health problem by 2030. Additional analysis will be conducted in order to validate the use of this assay for the detection of *S. mansoni* in clinical and field samples from endemic areas.

Data availability statement

The raw data supporting the conclusions of this article will be made available by the authors, without undue reservation.

Author contributions

BW, CF, RC, and SM: conceptualization. BW, RC, and SM: methodology and project administration. BW and SM: validation and data curation. SM: formal analysis, writing—original draft, and visualization. BW, EL, and SM: investigation. BW, GM, and RC: resources. BW, CF, EL, GM, and RC: writing—review and editing. BW, CF, and RC: supervision. BW, CF, and SM: funding acquisition. All authors contributed to the article and approved the submitted version.

Funding

This research has been financed by the Royal Society of Tropical Medicine and Hygiene (RSTMH) via the Small Grant Programme and was partially supported by the Coordenação de Aperfeiçoamento de Pessoal de Nível Superior – CAPES - Finance Code 001; SM is funded by CAPES via the PrINT programme, and Vice-Presidência de Educação, Informação e Comunicação (VPEIC-Fiocruz); CF is funded by CNPq Fellowship (grant number 303131/2018-7); and support was also provided *via* the Natural History Museum's Departmental Investment Fund and Conselho Nacional de Desenvolvimento Científico/Programa de Excelência em Pesquisa—Pesquisa e Ensaios Clínicos (PROEP/PEC; 420685/2017-0).

Acknowledgments

The authors would like to thank the Wellcome Trust funded Schistosome and Snail Resource (SSR; Wellcome Trust Biomedical Resource Grant 221368/Z/20/Z 2021-2026), NIAID Schistosomiasis Resource Center (SRC; NIH-NIAID Contract HHSN272201700014I), Schistosomiasis Collection at The Natural History Museum (SCAN), Medical Malacology Collection (Fiocruz-CMM), Helminthology, Medical Malacology Research Group from Fiocruz Minas (HMM), Trematodes Biology Laboratory from the Federal University of Minas Gerais (UFMG), and University "Magna Graecia" of Catanzaro for providing the samples used in this study; Agdia for the authorisation for using the images available on their website to create Figure 2; Bioicons (bioicons.com), Mind the Graph (mindthegraph.com), and SMART-Servier Medical Art (smart.servier.com) for the images used to create Figures 2 and Supplementary material 3; and Andy Wende and Ludovic Ebert from Xpedite Diagnostics for their assistance on the designing of DNA extraction assays.

Conflict of interest

The authors declare that the research was conducted in the absence of any commercial or financial relationships that could be construed as a potential conflict of interest.

Publisher's note

Supplementary material

The Supplementary material for this article can be found online at: https://www.frontiersin.org/articles/10.3389/fmicb.2022.1043596/full#supplementary-material

References

Abbasi, I., King, C. H., Muchiri, E. M., and Hamburger, J. (2010). Detection of Schistosoma mansoni and Schistosoma haematobium DNA by loop-mediated isothermal amplification: identification of infected snails from early prepatency. *Am. J. Trop. Med. Hyg.* 83, 427–432. doi: 10.4269/ajtmh.2010.09-0764

Allam, A. F. (2022). Performance of loop-mediated isothermal amplification (LAMP) for detection of Schistosoma mansoni infection compared with Kato–Katz and real-time PCR. *J. Helminthol.* 96:e28. doi: 10.1017/S0022149X22000153

Altschul, S. F., Gish, W., Miller, W., Myers, E. W., and Lipman, D. J. (1990). Basic local alignment search tool. *J. Mol. Biol.* 215, 403–410. doi: 10.1016/S0022-2836(05)80360-2

Archer, J., Barksby, R., Pennance, T., Rostron, P., Bakar, F., Knopp, S., et al. (2020). Analytical and clinical assessment of a portable, isothermal Recombinase polymerase amplification (RPA) assay for the molecular diagnosis of urogenital schistosomiasis. *Molecules* 25, 1–15. doi: 10.3390/molecules25184175

Archer, J., Patwary, F. K., Sturt, A. S., Webb, E. L., Phiri, C. R., Mweene, T., et al. (2022). Validation of the isothermal Schistosoma haematobium Recombinase polymerase amplification (RPA) assay, coupled with simplified sample preparation, for diagnosing female genital schistosomiasis using cervicovaginal lavage and vaginal self-swab samples. *PLoS Negl. Trop. Dis.* 16:e0010276. doi: 10.1371/journal.pntd.0010276

Assare, R. K., Tra-Bi, M. I., Coulibaly, J. T., Corstjens, P. L. A. M., Ouattara, M., Hurlimann, E., et al. (2021). Accuracy of two circulating antigen tests for the diagnosis and surveillance of Schistosoma mansoni infection in low-endemicity settings of Côte d'Ivoire. *Am. J. Trop. Med. Hyg.* 105, 677–683. doi: 10.4269/ajtmh.21-0031

Barda, B., Schindler, C., Wampfler, R., Ame, S., Ali, S. M., and Keiser, J. (2020). Comparison of real-time PCR and the Kato-Katz method for the diagnosis of soil-transmitted helminthiasis and assessment of cure in a randomized controlled trial. *BMC Microbiol.* 20, 1–8. doi: 10.1186/s12866-020-01963-9

Bärenbold, O., Raso, G., Coulibaly, J. T., N'Goran, E. K., Utzinger, J., and Vounatsou, P. (2017). Estimating sensitivity of the Kato-Katz technique for the diagnosis of Schistosoma mansoni and hookworm in relation to infection intensity. *PLoS Negl. Trop. Dis.* 11, 1–14. doi: 10.1371/journal.pntd.0005953

Berhe, N., Medhin, G., Erko, B., Smith, T., Gedamu, S., Bereded, D., et al. (2004). Variations in helminth fecal egg counts in Kato-Katz thick smears and their implications in assessing infection status with Schistosoma mansoni. *Acta Trop.* 92, 205–212. doi: 10.1016/j.actatropica.2004.06.011

Blasco-Costa, I., Cutmore, S. C., Miller, T. L., and Nolan, M. J. (2016). Molecular approaches to trematode systematics: 'best practice' and implications for future study. *Syst. Parasitol.* 93, 295–306. doi: 10.1007/s11230-016-9631-2

Brasil, M.D.S. (2021). Boletim Epidemiológio-Doenças Tropicais Negligenciadas. Available at: https://www.gov.br/saude/pt-br/media/pdf/2021/marco/3/boletim_especial_doencas_negligenciadas.pdf

Caldeira, R. L., Jannotti-Passos, L. K., and Dos Santos, C. O. (2017). Use of molecular methods for the rapid mass detection of Schistosoma mansoni (Platyhelminthes: Trematoda) in Biomphalaria spp. (Gastropoda: Planorbidae). *J. Trop. Med.* 2017, 1–6. doi: 10.1155/2017/8628971

Cavalcanti, M. G., Cunha, A. F. A., and Peralta, J. M. (2019). The advances in molecular and new point-of-care (POC) diagnosis of schistosomiasis pre-and post-praziquantel use-and the pursuit of more reliable approaches for low endemic and non-endemic areas. *Front. Immunol.* 10, 1–10. doi: 10.3389/fimmu.2019.00858

Chandu, D., Paul, S., Parker, M., Dudin, Y., King-Sitzes, J., Perez, T., et al. (2016). Development of a rapid point-of-use DNA test for the screening of Genuity® roundup ready 2 yield® soybean in seed samples. *Biomed. Res. Int.* 2016, 1–12. doi: 10.1155/2016/3145921

Cnops, L., Tannich, E., Polman, K., Clerinx, J., and Van Esbroeck, M. (2012). Schistosoma real-time PCR as diagnostic tool for international travellers and migrants. *Trop. Med. Int. Health* 17, 1208–1216. doi: 10.1111/j.1365-3156.2012.03060.x

Coelho, P. M. Z., Siqueira, L. M. V., Grenfell, R. F. Q., Almeida, N. B. F., Katz, N., Almeida, Á., et al. (2016). Improvement of POC-CCA interpretation by using Lyophilization of urine from patients with Schistosoma mansoni low worm burden: towards an elimination of doubts about the concept of trace. *PLoS Negl. Trop. Dis.* 10, 1–13. doi: 10.1371/journal.pntd.0004778

Colley, D. G., Bustinduy, A. L., Secor, W. E., and King, C. H. (2014). Human schistosomiasis. *Lancet* 383, 2253–2264. doi: 10.1016/S0140-6736(13)61949-2

Corstjens, P., De Dood, C. J., Kornelis, D., Tjon, K. F. E., Wilson, R. A., Kakiuki, T. M., et al. (2014). Tools for diagnosis, monitoring and screening of Schistosoma infections utilizing lateral-flow based assays and upconverting phosphor labels. *Parasitology* 141, 1841–1855. doi: 10.1017/S0031182014000626

Daher, R. K., Stewart, G., Boissinot, M., and Bergeron, M. G. (2016). Recombinase polymerase amplification for diagnostic applications. *Clin. Chem.* 62, 947–958. doi: 10.1373/clinchem.2015.245829

Deng, W., Wang, S., Wang, L., Lv, C., Li, Y., Feng, T., et al. (2022). Laboratory evaluation of a basic Recombinase polymerase amplification (RPA) assay for early detection of Schistosoma japonicum. *Pathogens* 11:319. doi: 10.3390/pathogens11030319

Diab, R. G., Tolba, M. M., Ghazala, R. A., Abu-Sheasha, G. A., Webster, B. L., and Mady, R. F. (2021). Intestinal schistosomiasis: can a urine sample decide the infection? *Parasitol. Int.* 80:102201. doi: 10.1016/j.parint.2020.102201

Diego, J. G. B., Fernández-Soto, P., Febrer-Sendra, B., Crego-Vicente, B., and Muro, A. (2021). Loop-mediated isothermal amplification in schistosomiasis. *J. Clin. Med.* 10, 1–13. doi: 10.3390/jcm10030511

El Wahed, A. A., Patel, P., Maier, M., Pietsch, C., Rüster, D., Böhlken-Fascher, S., et al. (2021). Suitcase lab for rapid detection of SARS-CoV-2 based on Recombinase polymerase amplification assay. *Anal. Chem.* 93, 2627–2634. doi: 10.1021/acs.analchem.0c04779

Emery, A., Allan, F., Rabone, M., and Rollinson, D. (2012). Schistosomiasis collection at the natural history museum (SCAN). *Parasit. Vectors* 5:185. doi: 10.1186/1756-3305-5-185

Enk, M. J., Lima, A. C. L., Drummond, S. C., Schall, V. T., and Coelho, P. M. Z. (2008). The effect of the number of stool samples on the observed prevalence and the infection intensity with Schistosoma mansoni among a population in an area of low transmission. *Acta Trop.* 108, 222–228. doi: 10.1016/j.actatropica.2008.09.016

Fernández-Soto, P., Gandasegui Arahuetes, J., Sánchez Hernández, A., López Abán, J., Vicente Santiago, B., and Muro, A. (2014). A loop-mediated isothermal amplification (LAMP) assay for early detection of Schistosoma mansoni in stool samples: A diagnostic approach in a murine model. *PLoS Negl. Trop. Dis.* 8:e3126. doi: 10.1371/journal.pntd.0003126

Fernández-Soto, P., Gandasegui, J., Rodríguez, C. C., Pérez-Arellano, J. L., Crego-Vicente, B., Diego, J. G. B., et al. (2019). Detection of Schistosoma mansoni-derived DNA in human urine samples by loop-mediated isothermal amplification (LAMP). *PLoS One* 14:e0214125. doi: 10.1371/journal.pone.0214125

Frickmann, H., Lunardon, L. M., Hahn, A., Loderstädt, U., Lindner, A. K., Becker, S. L., et al. (2021). Evaluation of a duplex real-time PCR in human serum for simultaneous detection and differentiation of Schistosoma mansoni and Schistosoma haematobium infections – cross-sectional study. *Travel Med. Infect. Dis.* 41:102035. doi: 10.1016/j.tmaid.2021.102035

Frimpong, M., Kyei-Tuffuor, L., Fondjo, L. A., Ahor, H. S., Adjei-Kusi, P., Maiga-Ascofare, O., et al. (2021). Evaluation of a real-time recombinase polymerase amplification assay for rapid detection of Schistosoma haematobium infection in resource-limited setting. *Acta Trop.* 216:105847. doi: 10.1016/j.actatropica.2021.105847

Gandasegui, J., Fernández-Soto, P., Hernández-Goenaga, J., López-Abán, J., Vicente, B., and Muro, A. (2016). Biompha-LAMP: A new rapid loop-mediated isothermal amplification assay for detecting Schistosoma mansoni in Biomphalaria glabrata snail host. *PLoS Negl. Trop. Dis.* 10:e05225. doi: 10.1371/journal.pntd.0005225

Gandasegui, J., Fernández-Soto, P., Muro, A., Simões Barbosa, C., Lopes de Melo, F., Loyo, R., et al. (2018). A field survey using LAMP assay for detection of Schistosoma mansoni in a low-transmission area of schistosomiasis in Umbuzeiro, Brazil: assessment in human and snail samples. *PLoS Negl. Trop. Dis.* 12, 1–16. doi: 10.1371/journal.pntd.0006314

García-Bernalt Diego, J., Fernández-Soto, P., Crego-Vicente, B., Alonso-Castrillejo, S., Febrer-Sendra, B., Gómez-Sánchez, A., et al. (2019). Progress in loop-mediated isothermal amplification assay for detection of Schistosoma mansoni DNA: towards a ready-to-use test. *Sci. Rep.* 9, 1–11. doi: 10.1038/s41598-019-51342-2

Gomes, L. I., Marques, L. H. D. S., Enk, M. J., de Oliveira, M. C., Coelho, P. M. Z., and Rabello, A. (2010). Development and evaluation of a sensitive PCR-ELISA system for detection of Schistosoma infection in feces. *PLoS Negl. Trop. Dis.* 4, 1–8. doi: 10.1371/journal.pntd.0000664

Gomes, A. L. D. V., Melo, F. L., Werkhauser, R. P., and Abath, F. G. C. (2006). Development of a real time polymerase chain reaction for quantitation of Schistosoma mansoni DNA. *Mem. Inst. Oswaldo Cruz* 101, 133–136. doi: 10.1590/S0074-02762006000900021

Graeff-Teixeira, C., Favero, V., Pascoal, V. F., de Souza, R. P., Rigo, F. D. V., LHD, A., et al. (2021). Low specificity of point-of-care circulating cathodic antigen (POC-CCA) diagnostic test in a non-endemic area for schistosomiasis mansoni in Brazil. *Acta Trop.*:217. doi: 10.1016/j.actatropica.2021.105863

Guo, Q., Zhou, K., Chen, C., Yue, Y., Shang, Z., Zhou, K., et al. (2021). Development of a Recombinase polymerase amplification assay for Schistosomiasis japonica diagnosis in the experimental mice and domestic goats. *Front. Cell. Infect. Microbiol.* 11, 1–12. doi: 10.3389/fcimb.2021.791997

Hamburger, J., Abbasi, I., Kariuki, C., Wanjala, A., Mzungu, E., Mungai, P., et al. (2013). Evaluation of loop-mediated isothermal amplification suitable for molecular monitoring of schistosome-infected snails in field laboratories. *Am. J. Trop. Med. Hyg.* 88, 344–351. doi: 10.4269/ajtmh.2012.12-0208

Huyse, T., Van den Broeck, F., Hellemans, B., Volckaert, F. A. M., and Polman, K. (2013). Hybridisation between the two major African schistosome species of humans. *Int. J. Parasitol.* 43, 687–689. doi: 10.1016/j.ijpara.2013.04.001

Katz, N. (2018). Inquérito Nacional de Prevalência da Esquistossomose mansoni e Geo-helmintoses. 76.

Katz, N., Chaves, A., and Pellegrino, J. (1972). A simple device for quantitative stool thick-smear technique in schistosomiasis mansoni. *Rev. do Inst. Med. Trop. São Paulo* 14, 397–400.

Kim, H., Cho, S. W., Oh, H., and Byeon, H. K. (2019). A case of unexpected Clinostomum complanatum infection initially presenting as foreign body in pharynx. *Kor. J. Parasitol.* 57, 175–177. doi: 10.3347/kjp.2019.57.2.175

Kyu, H. H., Abate, D., Abate, K. H., Abay, S. M., Abbafati, C., Abbasi, N., et al. (2018). Global, regional, and national disability-adjusted life-years (DALYs) for 359

diseases and injuries and healthy life expectancy (HALE) for 195 countries and territories, 1990-2017: A systematic analysis for the global burden of disease study 2017. *Lancet* 392, 1859–1922. doi: 10.1016/S0140-6736(18)32335-3

Lee, G. S., Park, S. W., Kim, J., Seo, K. S., You, K. W., Chung, J. H., et al. (2017). A case of endoscopically treated laryngopharyngitis resulting form Clinostomum complanatum infectio. *Kor. J. Gastroenterol.* 69, 177–180. doi: 10.4166/kjg.2017.69.3.177

Li, H. M., Qin, Z. Q., Bergquist, R., Qian, M. B., Xia, S., Lv, S., et al. (2021). Nucleic acid amplification techniques for the detection of Schistosoma mansoni infection in humans and the intermediate snail host: a structured review and meta-analysis of diagnostic accuracy. *Int. J. Infect. Dis.* 112, 152–164. doi: 10.1016/j.ijid.2021.08.061

Lillis, L., Siverson, J., Lee, A., Cantera, J., Parker, M., Piepenburg, O., et al. (2016). Factors influencing Recombinase polymerase amplification (RPA) assay outcomes at point of care. *Mol. Cell. Probes* 30, 74–78. doi: 10.1016/j.mcp.2016.01.009

Lo, N. C., Bezerra, F. S. M., Colley, D. G., Fleming, F. M., Homeida, M., Kabatereine, N., et al. (2022). Review of 2022 WHO guidelines on the control and elimination of schistosomiasis. *Lancet Infect. Dis.* 3099. doi: 10.1016/S1473-3099(22)00221-3

Lobato, I. M., and O'Sullivan, C. K. (2018). Recombinase polymerase amplification: basics, applications and recent advances. *Trends Anal. Chem.* 98, 19–35. doi: 10.1016/j.trac.2017.10.015

Lodh, N., Mikita, K., Bosompem, K. M., Anyan, W. K., Quartey, J. K., Otchere, J., et al. (2017). Point of care diagnosis of multiple schistosome parasites: species-specific DNA detection in urine by loop-mediated isothermal amplification (LAMP). *Acta Trop.* 173, 125–129. doi: 10.1016/j.actatropica.2017.06.015

LoVerde, P. T. (2019). Schistosomiasis. *Adv. Exp. Med. Biol.* 1154, 45–70. doi: 10.1007/978-3-030-18616-6_3

McManus, D. P., Dunne, D. W., Sacko, M., Utzinger, J., and Vennervald, B. J. (2018). Zhou X-N. Schistosomiasis. *Nat. Rev. Dis. Prim.* 4:13. doi: 10.1038/s41572-018-0013-8

Mesquita, S. G., FGDS, N., RGC, S., ODS, C., Fonseca, C. T., and Caldeira, R. L. (2021). A loop-mediated isothermal amplification assay for Schistosoma mansoni detection in Biomphalaria spp. from schistosomiasis-endemic areas in Minas Gerais, Brazil. *Parasit. Vectors* 14, 388–312. doi: 10.1186/s13071-021-04888-y

Mesquita, S. G., Rodrigues-Luiz, G. F., Reis-Cunha, J. L., Cardoso, M. S., De Mendonça, C. L. F., Bueno, L. L., et al. (2020). A multiplex PCR protocol for rapid differential identification of four families of trematodes with medical and veterinary importance transmitted by Biomphalaria Preston. *Acta Trop.* 2020:211.

Meurs, L., Brienen, E., Mbow, M., Ochola, E. A., Mboup, S., Karanj, D. M. S., et al. (2015). Is PCR the next reference standard for the diagnosis of Schistosoma in stool? A comparison with microscopy in Senegal and Kenya. *PLoS Negl. Trop. Dis.* 9:e03959. doi: 10.1371/journal.pntd.0003959

Mwangi, I. N., Agola, E. L., Mugambi, R. M., Shiraho, E. A., and Mkoji, G. M. (2018). Development and evaluation of a loop-mediated isothermal amplification assay for diagnosis of Schistosoma mansoni infection in Fecal samples. *J. Parasitol. Res.* 2018, 1–7. doi: 10.1155/2018/1267826

Nascimento, G. L., Pegado, H. M., Domingues, A. L. C., De Alencar Ximenes, R. A., Itria, A., Cruz, L. N., et al. (2019). The cost of a disease targeted for elimination in Brazil: the case of schistosomiasis mansoni. *Mem. Inst. Oswaldo Cruz* 114, 1–9. doi: 10.1590/0074-02760180347

Nelwan, M. L. (2019). Schistosomiasis: Life cycle, diagnosis, and control. *Curr. Ther. Res. Clin. Exp.* 91, 5–9. doi: 10.1016/j.curtheres.2019.06.001

Ogongo, P., Nyakundi, R. K., Chege, G. K., and Ochola, L. (2022). The road to elimination: Current state of Schistosomiasis research and Progress towards the end game. *Front. Immunol.* 13, 1–23. doi: 10.3389/fimmu.2022.846108

Panzner, U. (2022). *Clinical applications of isothermal diagnosis for human Schistosomiasis. Encyclopedia*, 2, 690–704. doi: 10.3390/ encyclopedia2020048

Piepenburg, O., Williams, C. H., Stemple, D. L., and Armes, N. A. (2006). DNA detection using recombination proteins. *PLoS Biol.* 4, 1115–1121. doi: 10.1371/journal.pbio.0040204

Pomari, E., Perandin, F., La Marca, G., and Bisoffi, Z. (2019). Improved detection of DNA Schistosoma haematobium from eggs extracted by bead beating in urine. *Parasitol. Res.* 118, 683–686. doi: 10.1007/s00436-018-6137-7

Pontes, L. A., Oliveira, M. C., Katz, N., Dias-Neto, E., and Rabello, A. (2003). Comparison of a polymerase chain reaction and the Kato-Katz technique for diagnosing infection with Schistosoma mansoni. *Am. J. Trop. Med. Hyg.* 68, 652–656. doi: 10.4269/ajtmh.2003.68.652

Poulton, K., and Webster, B. (2018). Development of a lateral flow recombinase polymerase assay for the diagnosis of Schistosoma mansoni infections. *Anal. Biochem.* 546, 65–71. doi: 10.1016/j.ab.2018.01.031

Price, M., Cyrs, A., Sikasunge, C. S., Mwansa, J., and Lodh, N. (2019). Testing the infection prevalence of Schistosoma mansoni after mass drug administration by comparing sensitivity and specificity of species-specific repeat fragment amplification by PCR and loop-mediated isothermal amplification. *Am. J. Trop. Med. Hyg.* 101, 78–83. doi: 10.4269/ajtmh.19-0121

Rey, O., Webster, B. L., Huyse, T., Rollinson, D., Van den Broeck, F., Kincaid-Smith, J., et al. (2021). Population genetics of African Schistosoma species. *Infect. Genet. Evol.* 89:104727. doi: 10.1016/j.meegid.2021.104727

Rosser, A., Rollinson, D., Forrest, M., and Webster, B. L. (2015). Isothermal Recombinase polymerase amplification (RPA) of Schistosoma haematobium DNA and oligochromatographic lateral flow detection. *Parasit. Vectors* 8, 446–445. doi: 10.1186/s13071-015-1055-3

Rostron, P., Pennance, T., Bakar, F., Rollinson, D., Knopp, S., Allan, F., et al. (2019). Development of a recombinase polymerase amplification (RPA) fluorescence assay for the detection of Schistosoma haematobium. *Parasit. Vectors* 12, 514–517. doi: 10.1186/s13071-019-3755-6

Siqueira, L. M. V., Senra, C., de Oliveira, A. A., NFDF, C., Gomes, L. I., Rabello, A., et al. (2021). A real-time PCR assay for the diagnosis of intestinal Schistosomiasis and cure assessment after the treatment of individuals with low parasite burden. *Front. Immunol.* 11, 1–13. doi: 10.3389/fimmu.2020.620417

Sousa, D. G. S., Carvalho-Costa, F. A., Monteiro, K. J. L., Silva, E. L., Castro, E. S., Sousa, R. L. T., et al. (2022). Larval trematodes hosted by Biomphalaria straminea in the Brazilian semiarid region: implications for schistosomiasis control. *Trop. Biomed.* 39, 1–10. doi: 10.47665/tb.39.1.003

Sousa, M. S., Van Dam, G. J., Pinheiro, M. C. C., De Dood, C. J., Peralta, J. M., Peralta, R. H. S., et al. (2019). Performance of an ultra-sensitive assay targeting the circulating anodic antigen (CAA) for detection of Schistosoma mansoni infection in a low endemic area in Brazil. *Front. Immunol.* 10:682. doi: 10.3389/fimmu.2019.00682

Speich, B., Knopp, S., Mohammed, K. A., Khamis, I. S., Rinaldi, L., Cringoli, G., et al. (2010). Comparative cost assessment of the Kato-Katz and FLOTAC techniques for soil-transmitted helminth diagnosis in epidemiological surveys. *Parasit. Vectors* 3, 1–11. doi: 10.1186/1756-3305-3-71

Sun, K., Xing, W., Yu, X., Fu, W., Wang, Y., Zou, M., et al. (2016). Recombinase polymerase amplification combined with a lateral flow dipstick for rapid and visual detection of Schistosoma japonicum. *Parasit. Vectors* 9, 476–479. doi: 10.1186/s13071-016-1745-5

Turner, H. C., Bettis, A. A., Dunn, J. C., Whitton, J. M., Hollingsworth, T. D., Fleming, F. M., et al. (2017). Economic considerations for moving beyond the Kato-Katz technique for diagnosing intestinal parasites as we move towards elimination. *Trends Parasitol.* 33, 435–443. doi: 10.1016/j.pt.2017.01.007

Utzinger, J., Becker, S. L., van Lieshout, L., van Dam, G. J., and Knopp, S. (2015). New diagnostic tools in schistosomiasis. *Clin. Microbiol. Infect.* 21, 529–542. doi: 10.1016/j.cmi.2015.03.014

Vale, T. C., de Sousa-Pereira, S. R., Ribas, J. G. R., and Lambertucci, J. R. (2012). Neuroschistosomiasis mansoni. *Neurologist* 18, 333–342. doi: 10.1097/NRL.0b013e3182704d1e

Viana, A. G., Gazzinelli-Guimarães, P. H., Castro, V. N. D., Santos, Y. L. D. O. D., Ruas, A. C. L., Bezerra, F. S. D. M., et al. (2019). Discrepancy between batches and impact on the sensitivity of point-of-care circulating cathodic antigen tests for Schistosoma mansoni infection. *Acta Trop.* 197:105049. doi: 10.1016/j.actatropica.2019.105049

Wang, S., and Hu, W. (2014). Development of "-omics" research in Schistosoma spp. and-omics-based new diagnostic tools for schistosomiasis. *Front. Microbiol.* 5:313. doi: 10.3389/fmicb.2014.00313

Webster, B. L., Webster, J. P., Gouvras, A. N., Garba, A., Lamine, M. S., Diaw, O. T., et al. (2013). DNA 'barcoding' of Schistosoma mansoni across sub-Saharan Africa supports substantial within locality diversity and geographical separation of genotypes. *Acta Trop.* 128, 250–260. doi: 10.1016/j.actatropica.2012.08.009

Weerakoon, K. G., and McManus, D. P. (2016). Cell-free DNA as a diagnostic tool for human parasitic infections. *Trends Parasitol.* 32, 378–391. doi: 10.1016/j.pt.2016.01.006

WHO World Health Organization (2020). Ending the neglected to attain the sustainable development goals-A road map for neglected tropical diseases 2021–2030. Geneva. 55

World Health Organization (2022). Diagnostic target product profiles for monitoring, evaluation and surveillance of schistosomiasis control programmes. 28. Available at: https://www.who.int/publications/i/item/9789240031104

World Health Organization (2022). WHO GUIDELINE on control and elimination of human schistosomiasis. 142 p.

Xing, W., Yu, X., Feng, J., Sun, K., Fu, W., Wang, Y., et al. (2017). Field evaluation of a recombinase polymerase amplification assay for the diagnosis of Schistosoma japonicum infection in Hunan province of China. *BMC Infect. Dis.* 17, 1–7. doi: 10.1186/s12879-017-2182-6

frontiers | Frontiers in Microbiology

TYPE Original Research
PUBLISHED 12 December 2022
DOI 10.3389/fmicb.2022.1064218

OPEN ACCESS

EDITED BY
Akram Da'dara,
Tufts University, United States

REVIEWED BY
Barbara Castro-Pimentel Figueiredo,
Federal University of Bahia, Brazil
Kentaro Kato,
Nagasaki University,
Japan

*CORRESPONDENCE
Marina Moraes Mourão
marina.mourao@fiocruz.br

SPECIALTY SECTION
This article was submitted to Microbial Immunology, a section of the journal Frontiers in Microbiology

RECEIVED 08 October 2022
ACCEPTED 14 November 2022
PUBLISHED 12 December 2022

CITATION
Batista ICA, Gava SG, Tavares NC, Calzavara-Silva CE and Mourão MM (2022) Hypoxanthine guanine phosphoribosyl transferases SmHGPRTases functional roles in *Schistosoma mansoni*. *Front. Microbiol.* 13:1064218. doi: 10.3389/fmicb.2022.1064218

Hypoxanthine guanine phosphoribosyl transferases SmHGPRTases functional roles in *Schistosoma mansoni*

Izabella Cristina Andrade Batista[1,2], Sandra Grossi Gava[1], Naiara Clemente Tavares[1], Carlos Eduardo Calzavara-Silva[2] and Marina Moraes Mourão[1]*

[1]Grupo de Helmintologia e Malacologia Médica, Instituto René Rachou, Fundação Oswaldo Cruz, Belo Horizonte, Brazil, [2]Grupo de Imunologia Celular e Molecular, Instituto René Rachou, Fundação Oswaldo Cruz, Belo Horizonte, Brazil

Introduction: Extracellular/environmental stimuli trigger cellular responses to allow *Schistosoma* sp. parasites adaptation and decide development and survival fate. In this context, signal transduction involving eukaryotic protein kinases (ePKs) has an essential role in regulatory mechanisms. Functional studies had shown the importance of MAPK pathway for *Schistosoma mansoni* development. In addition, early studies demonstrated that Smp38 MAPK regulates the expression of a large set of genes, among them the hypoxanthine-guanine phosphoribosyl transferase 1 (*SmHGPRTase* 1, Smp_103560), a key enzyme in the purine salvage pathway that is part of a family comprising five different proteins.

Methods: First, the regulation of this gene family by the MAPKs pathways was experimentally verified using Smp38-predicted specific inhibitors. In silico analysis showed significant differences in the predicted structure and the domain sequence among the schistosomal HGPRTase family and their orthologs in humans. In order to interrogate the *HGPRTases* (Smp_103560, Smp_148820, Smp_168500, Smp_312580 and Smp_332640, henceforth SmHGPRTase –1, –2, –3, –4, –5) functional roles, schistosomula, sporocysts, and adult worms were knocked-down using specific dsRNAs.

Results: Our results suggest that SmHGPRTases activity has an essential role in sporocysts and schistosomula development since significant differences in viability, size, and/ or shape were observed after the *in vitro* knockdown. Also, the knockdown of *SmHGPRTases* in schistosomula influenced the ovary development and egg maturation in female adult worms during mammalian infection. We also observed alterations in the movement of female adult worms knocked-down *in vitro*. Most of these results were shown when all gene family members were knocked-down simultaneously, suggesting a redundant function among them.

Discussion: Thus, this study helps to elucidate the functional roles of the *SmHGPRTase* gene family in the *S. mansoni* life cycle and provides knowledge for future studies required for schistosomiasis treatment and control.

KEYWORDS

***Schistosoma mansoni*, HGPRTase, RNA interference, functional genomics, host–parasite interaction**

Introduction

Schistosomiasis is a neglected tropical disease caused by trematode worms from the *Schistosoma* genus and is considered a major health and economic problem in developing countries. The transmission is related to precarious water treatment and sanitation conditions, combined with the presence of the snail vector (World Health Organization, 2018). *Schistosoma mansoni* is one of the main species causatives of schistosomiasis and can survive in the mammalian host for years or decades (Pearce and Sher, 1987). According to the World Health Organization, 78 countries reported transmission of this disease, and at least 241.3 million people required preventive chemotherapy with praziquantel (PZQ) in 2020 (World Health Organization, 2021).

To date, PZQ is the only treatment available for schistosomiasis. However, although this drug is effective against all species of *Schistosoma*, there are limitations to its use, including the development of resistance (Botros and Bennett, 2007; Doenhoff et al., 2008; Greenberg, 2013). Thereat, the search for new drug targets to support schistosomiasis treatment is extremely important.

The study of molecular interactions between hosts and parasite is essential to understanding this parasitic infection, its adaptation within the hosts, and pathogenesis (Cuesta-Astroz et al., 2019). Extracellular stimuli trigger cellular responses to allow the development and survival of parasites of the genus *Schistosoma*. Protein Kinases (PKs) play a major role in mediating these signals, which involve integrated networks that interact mostly by switching proteins activity status, performing essential functions in cell control (Hanks et al., 1988; Andrade et al., 2011). Despite the availability of many options that would allow the employment of piggyback strategies, specific targets regulated by those kinases could also be handy in order to avoid side effects (Boyle and Koleske, 2007; Eglen and Reisine, 2009).

Recent studies showed that the Smp38 MAPK signaling pathway is essential for the development, reproduction, and survival of *S. mansoni* (Avelar et al., 2019). Thus, despite being a promising target against the parasite, inhibition of hosts enzymes could be a concern and a barrier to be circumvented during drug development. Previous functional studies of the Smp38 gene have shown that this pathway regulates the expression of a large set of genes in *S. mansoni*, including the hypoxanthine-guanine phosphoribosyltransferase (*SmHGPRTase* 1; Avelar et al., 2019; Gava et al., 2019), an important protein in parasite biology, that has been extensively interrogated as a drug target (Senft and Crabtree, 1983; Dovey et al., 1984; Pereira et al., 2008; Romanello et al., 2019). This enzyme is included in a family of enzymes comprised by five different proteins whose role is to convert purine bases, hypoxanthine and guanine, to their respective nucleotides, inosine monophosphate (IMP) and guanosine monophosphate (GMP), in the presence of 5-phosphorylribose 1-pyrophosphate (PRPP; Senft and Crabtree, 1983). Studies demonstrated that *S. mansoni* adult worms were unable to incorporate ^{14}C-glycine into a purine ring, evidencing the dependence of an external supply of preformed bases for nucleotide synthesis and the absence of the *de novo* purine biosynthesis pathway (Miech et al., 1975). Since *S. mansoni* depends entirely on the salvage pathway to generate purines, enzymes like the SmHGPRTase family, involved in this pathway, could be critical to the parasite's life cycle and because of that many studies have shown that HGPRTases, regulated by PKs, are promising targets for the development of new drugs (Senft and Crabtree, 1983; Dovey et al., 1984). Example of that is the acyclic nucleoside phosphonates, which have previously been shown to be potent inhibitors of *Plasmodium falciparum* HGPRTase, while showing excellent selectivity for the parasite when compared with the human enzyme (Kaiser et al., 2017; Keough et al., 2018). Substructures of phosphoribosyl pyrophosphate (PRPP), an original substrate of HGPRT, are also being extensively studied for that and structure-based virtual screening and computational study had shown that these inhibitors can be potential drugs for *Trypanosoma cruzi* (Vidhya and Ponnuraj, 2021).

In the present report, we interrogate the functional roles of a gene family regulated by the MAP kinase pathway in *S. mansoni*, *SmHGPRTases*, in different stages of the parasite's life cycle and suggest that those proteins could be parasite-specific druggable targets.

Materials and methods

Target genes

In this study we have focused on the characterization of the hypoxanthine-guanine phosphoribosyl transferase (*SmHGPRTase*) gene family, regulated by Smp38 MAPK pathway. *S. mansoni* presents five different genes encoding SmHGPRTases, namely Smp_103560 (comprising two isoforms Smp_103560.1 and Smp_103560.2), Smp_148820, Smp_168500, Smp_312580 and Smp_332640; henceforth referred as *SmHGPRTase* 1, *SmHGPRTase* 2, *SmHGPRTase* 3, *SmHGPRTase* 4, and *SmHGPRTase* 5, respectively. According to the *S. mansoni* genome (v. 7) deposited in the WormBase Parasite database (Howe et al., 2017).

Parasites

All the experiments using animals were reviewed and approved by the Ethics Commission on Animal Use from Fundação Oswaldo Cruz under license numbers LW12/16 for hamsters and LM05/18 for mice.

The *S. mansoni* LE cercaria strain was acquired from the Mollusk rearing facility "Lobato Paraense" of René Rachou Institute – FIOCRUZ using *Biomphalaria glabrata* as the intermediate snail host.

To obtain *S. mansoni* adult worms and sporocysts, six-week-old female Golden hamsters (*Mesocricetus auratus*) were

infected subcutaneously with 400 cercariae each. Forty-two days after infection, animals were anesthetized with xylazine hydrochloride (10 mg/kg; Syntec) and ketamine hydrochloride (150 mg/kg; Syntec), followed by overdose euthanasia with 2.5% sodium thiopental (150 mg/kg; Cristália). Then, perfusion was performed (Pellegrino and Siqueira, 1956; Tavares and Mourão, 2021) to recover adult worms, eggs were recovered from hamsters' livers and sporocysts obtained as described by Mourão et al. (2009). Schistosomula were obtained by mechanical transformation of the cercariae (Milligan and Jolly, 2011).

Analysis of *SmHGPRTase* regulation by Smp38

According to Gava et al. (2019), the *SmHGPRTase 1* expression is down-regulated in Smp38 knocked-down schistosomula. To experimentally verify that regulation, an inhibitor previously identified by our group to bind in the ATP binding site of Smp38 was used (inhibitor NCC – 00001994 from the Managed Chemical Compound Collection – MCCC; Moreira et al., 2022) The inhibitor NCC – 00001994 was used at a final concentration of 10 µM in cultures containing 5,000 schistosomula in 1 ml of Glasgow Minimum Essential Medium (GMEM; Sigma-Aldrich) supplemented with 20 mM HEPES (Sigma-Aldrich), 0.1% lactalbumin hydrolysate (Vetec), 0.1% D-glucose (Sigma-Aldrich), 0.5 µM hypoxanthine (Sigma-Aldrich), 1 µM hydrocortisone (Sigma-Aldrich), 0.5% MEM vitamin solution (Gibco), 5% Schneider (Gibco), 1% penicillin and streptomycin (Gibco), and 2% heat-inactivated fetal bovine serum (FBS; Gibco). Parasites cultured with 0.2% of dimethyl sulfoxide (DMSO; negative control) were used as controls. To verify morphological alterations and viability, parasites were incubated for 30 h at 37°C, 5% CO_2, and 95% humidity, prior to the phenotypic assessment by inverted microscope (ABO 100 – ZEISS). Viability assessment was performed by the addition of 5 µg/ml of propidium iodide and visualization under a fluorescent inverted microscope (ABO 100 - ZEISS) using a 544 nm wavelength. After inhibitor exposure, the RNA was extracted, the cDNA was synthesized and the gene expression was analyzed by qPCR, as further detailed.

Protein modeling and analysis

The sequences of *S. mansoni* proteins used in this study were obtained from their predicted coding sequences in the *S. mansoni* genome (v. 7) deposited in the WormBase Parasite database[1] (Howe et al., 2017) and the sequence for human protein was obtained from the Uniprot database[2] (PDB ID P00492; Bateman et al., 2021). Protein domains (PF00156) coordinates were retrieved from the Pfam[3] (El-Gebali et al., 2019) and comparisons between *S. mansoni* and human sequences were performed using the MAFFT alignment program[4] (Katoh et al., 2019). The identity percentage between domains' sequences was calculated by pairwise comparisons using the Jalview software[5] (Waterhouse et al., 2009).

SmHGPRTase 1, SmHGPRTase 2, SmHGPRTase 3, SmHGPRTase 4, and SmHGPRTase 5 tridimensional modeling were carried out to compare the structures of *S. mansoni* proteins and the corresponding human orthologs. As SmHGPRTases 4 and 5 seems to be a duplication *in tandem* and present the same sequence, the *in silico* analysis for these two proteins was performed only once (SmHGPRTases 4/5). The proteins were first modeled using the Phyre2 web portal[6] (Kelley et al., 2015). After modeling, the predicted structures were aligned, and a subsequent comparison was carried out using the Chimera 1.13.1 program (Pettersen et al., 2004).

Single cell RNA-seq (scRNAseq) analysis

To verify the *SmHGPRTases* expression in the different cell types of adult *S. mansoni* worms, single-cell RNAseq (scRNAseq) data were obtained from the Gene Expression Omnibus database (GEO[7], BioProject PRJNA611783, SRASRP252217; Wendt et al., 2020). The RDS file containing the expression data in the different cell types was loaded in the R software (v4.1.2) (R Core Team, 2021) using the Seurat package (v4.1.1) (Satija et al., 2015) and used to build a heatmap with the package ComplexHeatmap (v2.10.0) (Gu et al., 2016).

Double-stranded RNA (dsRNA) synthesis

To functionally assess the SmHGPRTases proteins, specific primers containing the T7 promoter sequence were designed based on their nucleotide sequences in the *S. mansoni* genome (v. 7) available in the WormBase Parasite database and used in a PCR to amplify fragments ranging from 250 to 578 bp. The unspecific control, green fluorescent protein (GFP), was synthesized from a fragment cloned into a pCRII plasmid (AddGene). PCR products were analyzed in 1% agarose gel and purified using QIAquick Gel Extraction Kit (Qiagen), following the supplier's protocol. PCR products were previously cloned into pGEM-T Easy vector (Promega) and sequenced by Sanger sequencing using specific primers (Supplementary Table S1). After sequence confirmation, PCR products were used for double-stranded RNA (dsRNA)

1 https://parasite.wormbase.org/Schistosoma_mansoni_prjea36577
2 https://www.uniprot.org
3 https://pfam.xfam.org/
4 https://mafft.cbrc.jp/
5 http://www.jalview.org
6 http://www.sbg.bio.ic.ac.uk/phyre2
7 https://www.ncbi.nlm.nih.gov/geo/

synthesis. The dsRNAs were synthesized using the T7 RiboMAX Express RNAi System kit (Promega) according to the manufacturer's protocol. As the *SmHGPRTase 2* sequence is similar to *SmHGPRTases 4 and 5*, we used only one dsRNA targeting the three genes, thus, the results for these genes are represented as *SmHGPRtase 2/4/5* hereafter.

Ds-RNA exposure and phenotypic assessment in different life stages of *Schistosoma mansoni*

Sporocysts

The sporocysts (20,000/well) were maintained in 6-well polystyrene tissue culture plates with Chernin's balanced saline solution (CBSS) supplemented with 1 g/L glucose (Vetec), 1 g/L trehalose, and 1% penicillin/streptomycin (Gibco) at 28°C. In each well were added 50 nM of dsRNA (*SmHGPRT 1*, *SmHGPRT 2/4/5*, *SmHGPRT 3*, or *GFP*; Mourão et al., 2009). The parasites were also exposed to a combination of the dsRNAs targeting the five *SmHGPRTases* – termed as "combined group." This group consisted of 50 nM of each dsRNA of the *SmHGPRTases*, and 150 nM of GFP-dsRNA was used for the respective nonspecific control. Parasites not exposed to dsRNAs were included as an "untreated control." Parasite cultures were observed daily using an inverted microscope (ABO 100 – ZEISS) to verify phenotypic changes. The viability was assessed with the addition of 5 μg/ml of propidium iodide under a fluorescent inverted microscope (ABO 100 – ZEISS) using a 544 nm wavelength. Parasite images were recorded using the Axion Vision REL 4 software (ZEISS) for 10 days. The area (μm^2) of each sporocyst was measured using AxioVision 4.8 software. The experiments were performed in three independent biological replicates.

Schistosomula

Schistosomula cultures (30,000/well) were maintained in 6-well polystyrene tissue culture plates in 3 ml GMEM supplemented as previously mentioned in the inhibitor exposure section. After cercariae transformation, schistosomula were exposed to 100 nM of dsRNAs (*SmHGPRT 1*, *SmHGPRT 2/4/5*, *SmHGPRT 3*, or *GFP*; Andrade et al., 2011). DsRNAs at 200 nM (~70 nM of each dsRNA) were added to the "combined" and the unspecific controls. An untreated control was also included. Cultures were incubated at 37°C, 5% CO_2, and 95% humidity and were daily observed under a fluorescent inverted microscope (ABO 100 – ZEISS) to verify the viability as described previously for sporocysts. The experiments were performed in three independent biological replicates.

Adult worms

Adult worms recovered by perfusion were washed three times with Roswell Park Memorial Institute medium 1640 (RPMI) supplemented with 1% penicillin and streptomycin (Gibco). Worm pairs were manually separated, washed, and electroporated with 25 μg of each specific dsRNA (*SmHGPRT 1*, *SmHGPRT 2/4/5*, *SmHGPRT 3*, or *GFP*) using 4 mm cuvettes (Bio-Rad) at 125 V for 20 ms (Gava et al., 2019). For the combined group, were added 8.5 μg of each dsRNA (~25 μg total). An untreated control was also evaluated. Eight worm pairs were transferred to 6-well polystyrene tissue culture plates and maintained in RPMI 1640 medium supplemented with 2% penicillin and streptomycin (Gibco) and 10% FBS (Gibco) and incubated at 37°C, 5% CO_2, and 95% humidity in a CO_2 incubator.

Worm motility was assessed using 24-well polystyrene culture plates containing eight male or eight female worms per well, maintained as mentioned above. The worm's movement was recorded for 90 s using WormAssay software (Marcellino et al., 2012) for 10 days. The experiments were performed in three biological replicates.

RNA extraction, cDNA synthesis, and real-time quantitative PCR (qPCR) analysis

After dsRNA exposure, RNA extractions using the TRIzol Reagent (Invitrogen) were performed using 5,000 parasites on days 2, 4, and 7, for sporocysts, and days 2, 3, and 7 for schistosomula (Tavares et al., 2020). Differently, two pairs of worms on days 2, 4, and 7 were macerated with TRIzol Reagent (Invitrogen), and the RNA extractions were carried out associated with the SV Total RNA Isolation System (Promega), as described previously (Tavares et al., 2020). All RNA samples were treated with Turbo DNase (Ambion). The total RNA was quantified using Qubit RNA HS Assay Kit (Invitrogen) at a Qubit 2.0 Fluorometer (Invitrogen) and stored at −70°C.

To assess transcript knockdown on parasites exposed to dsRNAs, the cDNA was synthesized using ImProm-II™ Reverse Transcription System (Promega). Primers for qPCR were designed using the Primer 3 software[8] to amplify fragments ranging from 70 to 150 bp (Supplementary Table S1). qPCR was performed using GoTaq® qPCR Master Mix (Promega) on a ViiA 7 Real-Time PCR System (Thermo Scientific). The samples were normalized using the Cytochrome C oxidase I (Sm*cox*I, Smp_900000) and the actin-related protein 10 (Sm*arp*10, Smp_093230) expression levels geometric mean and all samples were assessed in three technical replicates. The relative expression was analyzed by comparing the expression levels of each gene to those from unspecific and untreated control groups (Livak and Schmittgen, 2001).

To investigate the mRNA expression profile of each target gene throughout different parasite's life stages, we also used the above protocol and relative qPCR analysis. In this evaluation, the transcription levels of each gene in miracidia, sporocysts,

8 http://primer3.sourceforge.net

cercariae, schistosomula, adult males, and adult females were normalized using the geometric mean transcription rate of three reference genes: Sm*cox*I, Sm*arp*10, and SmFAD-dependent oxidoreductase (Sm*fad*, Smp_089880).

High-performance liquid chromatography

To check whether adenosine levels were decreased after *SmHGPRTases*-knockdown, a High-Performance Liquid Chromatography (HPLC) method was performed to separate and quantify the adenosine content in the samples. First, a calibration curve of the adenosine at seven different concentrations (1,000, 500, 250; 125; 62.5; 31.25; 15.625 ng/ml) was generated. To perform the experiment, 150 µl of methanol containing 100 ng/ml of phenacetin (Sigma-Aldrich) were added to the reactions from the curve and samples. Following, parasites (four adult male worms, four adult female worms, ~3,000 sporocysts, and ~ 3,000 schistosomula) from unspecific control, and parasites treated with *SmHGPRTase 1*, *SmHGPRTase 2/4/5*, and *SmHGPRTase 3* -dsRNAs, separately or in combination, were macerated and centrifuged at 13,000 rpm for 10 min. The supernatant was transferred to a tube containing C18 resins (Sigma-Aldrich) and centrifuged. Then, the supernatant recovered from the resin was lyophilized in a Vacuum Concentrator (Eppendorf) for 30 min, then resuspended in 50 µl of Milli-Q water and transferred to LC–MS tubes (Sigma-Aldrich). The HPLC was performed on a Nexera UHPLC (Shimadzu) hyphenated system on a maXis ETD high-resolution ESI-QTOF mass spectrometer (Bruker) controlled by the Compass 1.5 software (Bruker). The 20 µl volume of the metabolite extracts were injected into a column Shim-Pack XR-ODS-III (C18, 2.2 µm, 2.0 × 150 mm – Shimadzu) at 30°C in a flow of 400 µl/min. The adenosine detection was based on the exact mass and retention time obtained from the standard calibration curve. Individual variations in extraction efficiency were normalized using the internal phenacetin standard. Adenosine detection and quantification were performed using the QuantAnalysis program from the Compass software. The experiments were performed in three biological replicates.

In vivo experiments

Knocked-down schistosomula exposed to the three *SmHGPRTases*-dsRNAs, which included all five enzymes in combination, were used for *in vivo* experiments. As mentioned before, schistosomula were also exposed to an unspecific dsRNAs. After 3 days of dsRNA exposure and transcript levels confirmation by RT-qPCR, 350 parasites from each experimental group, were subcutaneously inoculated in six-week-old female Swiss mice (*Mus musculus*). Forty-two days after infection, animals were euthanized by overdose as described before. Six mice were infected in each experimental group and three independent biological replicates were performed.

After adult worms' recovery by perfusion, they were counted, fixed in Alcohol-Formalin-Acetic Acid (AFA) and stained with chloride carmine (Machado-Silva et al., 1997). Then, confocal images were captured using an inverted microscope Eclipse Ti-E (Nikon) with Confocal C2 plus (Nikon) at 546 and 488 nm wavelengths. Confocal images of 12 to 15 female and 12 male worms from knocked-down parasites recovered from mice were analyzed. The ovary area and tubercles' height were measured and analyzed using the NIS-Elements software (Nikon).

Additionally, mice's livers and intestines were removed, weighed, and incubated with 10% KOH for egg recovery and quantification (Tavares and Mourão, 2021). The mice ileum was pressed with microscope slides to evaluate the egg maturation (stages 1, 2, 3, and 4; Mati and Melo, 2013).

Statistical analysis

First, a normality test using Shapiro–Wilk was performed for RT-qPCR data, adenosine levels assessment, egg maturation, and morphometric analyses. Then, the significant differences compared to control conditions were analyzed by t-test. For the parasite area, the normality test was performed using D'Agostino-Pearson, followed by *t*-test. For mortality rate and movement in adult worms, two-way analysis of variance (ANOVA) and Sidak as the *post hoc* test were used. Statistical significance was defined as $p \leq 0.05$. All graphics and statistical analyses were performed using GraphPad Prism 8 (La Jolla, CA, United States).[9]

Results

Smp38 MAPK pathway regulates *SmHGPRTases* expression

After the *in silico* analysis, we sought to confirm whether *SmHGPRTases* are regulated by the Smp38 MAPK pathway as previously described (Gava et al., 2019). Thus, schistosomula were exposed to Smp38 (NCC–00001994) predicted inhibitor (Moreira et al., 2022). After 30 h of culture, as described by Moreira et al. (2022) it was observed alterations in schistosomula phenotypes, like the presence of a dark middle-region and round bodies (Figures 1A,B). Additionally, the transcript levels of *SmHGPRTase 1*, *2/4/5,* and *3* were evaluated after the parasite exposure to the inhibitor. When the Smp38 predicted inhibitor was used, the *SmHGPRTase 1* and *3* transcript levels were decreased by 37 and 50% respectively, compared to parasites exposed to the vehicle control (DMSO 0.2%; Figure 1C). *SmHGPRTases 2/4/5* transcript

9 www.graphpad.com

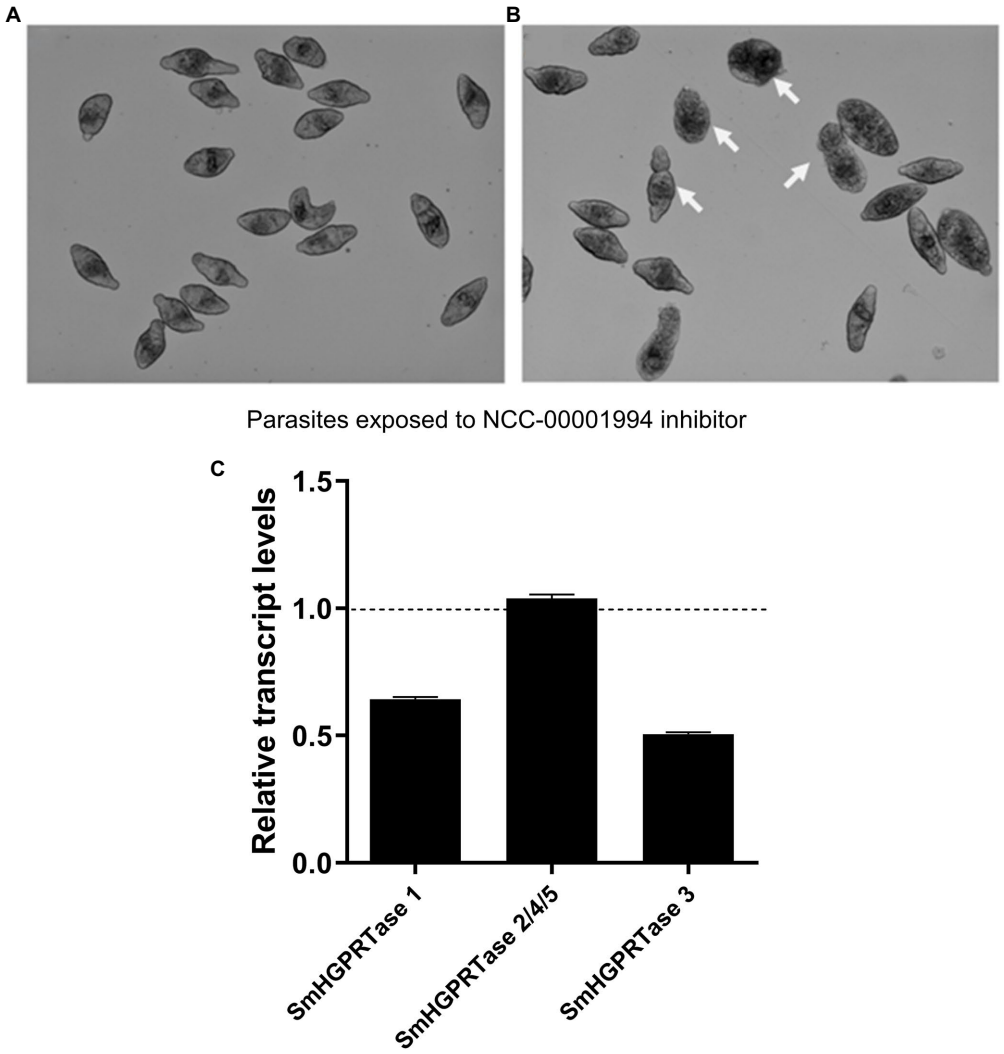

FIGURE 1
Experimental corroboration of Smp38 MAP kinase pathway in the regulation of the expression of *SmHGPRTase 1, 2/4/5,* and *3*. Representative images of schistosomula from the control **(A)** and schistosomula exposed to Smp38 predicted inhibitor NCC-00001994. **(B)** Arrows point to morphological changes in the parasites. **(C)** Bars representing the *SmHGPRTase 1, 2/4/5, 3* transcript levels in schistosomula exposed to Smp38 predicted inhibitor NCC-00001994. Data were normalized relative to the *SmHGPRTases* expression levels in parasites exposed to DMSO (dashed line).

levels were not altered after exposure to the predicted Smp38 inhibitor.

SmHGPRTases are different from their human orthologs

First of all, we aimed to comparing the *S. mansoni* SmHGPRTases target of this study to the human orthologs. Thus, an *in silico* analysis was performed comparing the five SmHGPRTases proteins identified in *S. mansoni* with their respective human counterparts.

The characteristic domain of an HGPRTase is the Phosphoribosyl transferase domain (Family Pribosyltran – PF00156), which catalyzes the substitution of the 5-phospho-a-D-ribose-1-diphosphate group 1-pyrophosphate (PRPP) with a purine base (adenine, guanine, hypoxanthine, or xanthine) to form the corresponding nucleoside in the nucleoside-5-monophosphate form (El-Gebali et al., 2019). The percentage of identity between the Phosphoribosyl transferase domain sequences from *S. mansoni* and their human ortholog counterpart is 50.61% for SmHGPRTase 1, 35.23% for SmHGPRTase 2, 40.49% for SmHGPRTase 3 and 36.87% for SmHGPRTases 4 and 5. The sequence position of each domain is represented in Supplementary Table S2.

By overlapping the predicted tridimensional structures of each HGPRTase protein, SmHGPRTase 1 presented the greatest identity with the human protein (39%; Figures 2A,B,F).

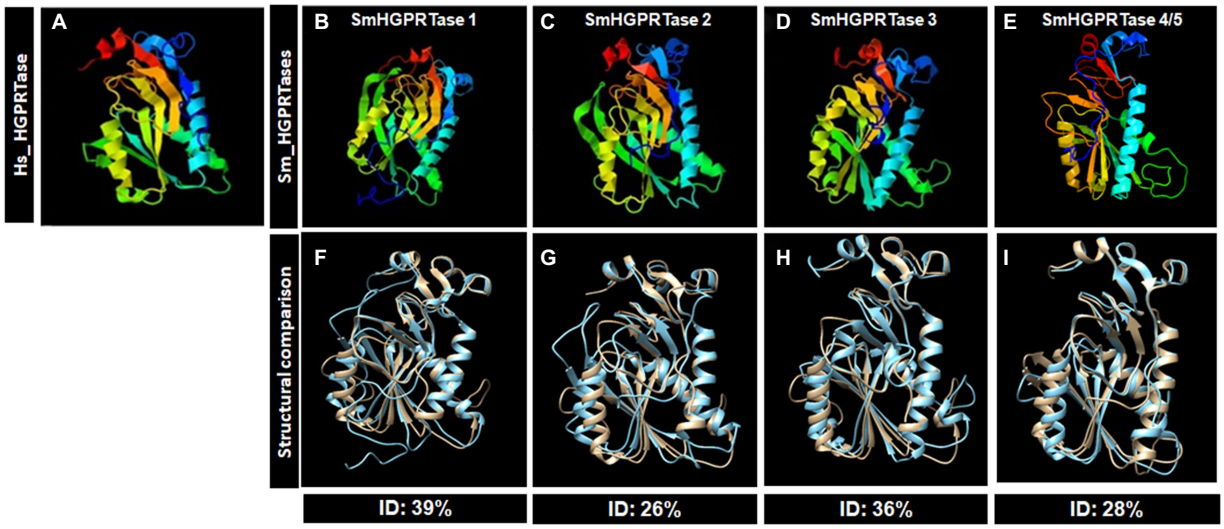

FIGURE 2
Predicted tridimensional structures for HGPRTases from *Schistosoma mansoni* and their human ortholog. Using the Phyre2 web portal the HGPRTase proteins from human **(A)** and *S. mansoni* (SmHGPRTase 1 – **B**, SmHGPRTase 2 – **C**, SmHGPRTase 3 – **D**, and SmHGPRTase 4/5 – **E**) were modeled and overlapped. Secondary structure elements are rainbow-colored from blue at the N-terminus to red at the C-terminus **(A–E)**. The percentage identities were calculated using the predicted models and the overlaps between the respective structures are represented below **(F–I)**. In gray, human protein; In blue, *Schistosoma* proteins.

Considering the domain sequences, the proteins with lower identity, SmHGPRTase 2 and SmHGPRTase 4/5, also showed low similarity when comparing the tridimensional structures (around 27%; Figures 2A,C,E,G,I), while SmHGPRTase 3 presented 36% identity with the human protein the tridimensional structures were compared (Figures 2A,D,H).

Expression profile of *SmHGPRTases* in different cell types of *Schistosoma mansoni*

First, an overall assessment of *SmHGPRTases* expression in the different cell lines was performed. The analysis of the scRNAseq data provided by Wendt et al. (2020) allowed the verification of the *S. mansoni SmHGPRTAses* expression in different cell types of *S. mansoni* adult worms (Figure 3). *SmHGPRtases 1* and *3* are highly expressed in almost all cell types, while *SmHGPRtase 2* is less expressed although in diverse cell types, and *SmHGPRtase 4* is more expressed in clusters of cells from the tegument (Supplementary Figure S1).

Expression profile of *SmHGPRTases* in different *Schistosoma mansoni* life stages

Once *SmHGPRTases 1* and *3* were experimentally proven to be regulated by Smp38 MAPK pathways and are distinct from their human counterpart, we hypothesized they could be promising candidates for further functional characterization. First, we sought, to investigate the expression profiles of each target gene throughout different *S. mansoni* life stages, the *SmHGPRTases* transcript levels were assessed in miracidia, sporocysts, cercariae, schistosomula, and male and female adult worms.

SmHGPRTase 1 exhibited the highest expression levels in sporocysts, followed by female adult worms, and the lowest levels in schistosomula. Miracidia, male adult worms, and cercariae presented approximately half of the amount exhibited by sporocysts (Figure 4A). *SmHGPRTases 2/4/5* also showed the highest expression levels in sporocysts and the second-highest expression levels in the female adult worm, followed by cercariae. Schistosomula and male adult worms presented low expression levels and miracidia presented the lowest levels (33 times less expressed than in sporocysts; Figure 4B). For *SmHGPRTase 3*, the highest expression levels were presented by female adult worms, which was twice the amount presented by miracidia which exhibited the second highest expression levels. Sporocysts presented the lowest expression levels (Figure 4C).

SmHGPRTase knockdown reduces adenosine levels in sporocysts and influences their viability

Once sporocysts presented the largest transcriptional levels of four *SmHGPRTases* (1 and *2/4/5*) we sought to evaluate the predicted functional roles of *SmHGPRTases*. The genes were knocked-down in sporocysts by exposure to specific dsRNAs for each gene or in combination by targeting the five *SmHGPRTases*.

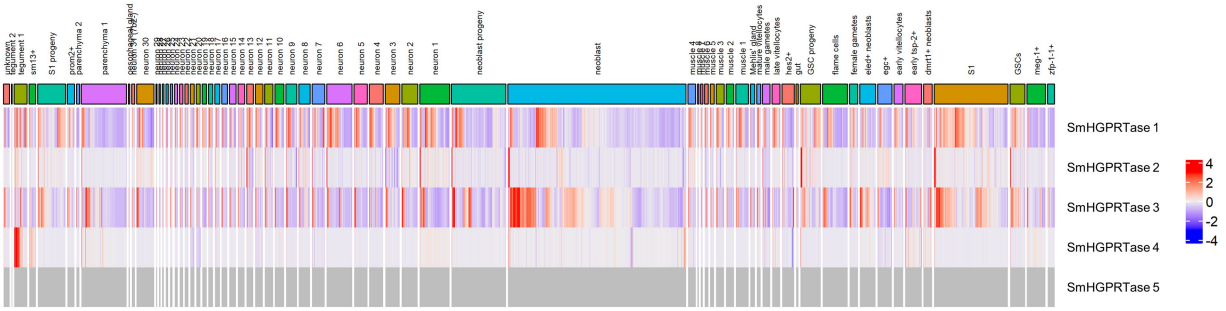

FIGURE 3
SmHGPRTAses expression patterns in different cell types observed in *Schistosoma mansoni* adult worms. The columns indicate the different cell types identified in adult worms and the lines represent the different *SmHGPRTAses* analyzed. The color scale indicates higher (red) or lower (blue) expression of transcripts. The undetectable expression is represented in gray.

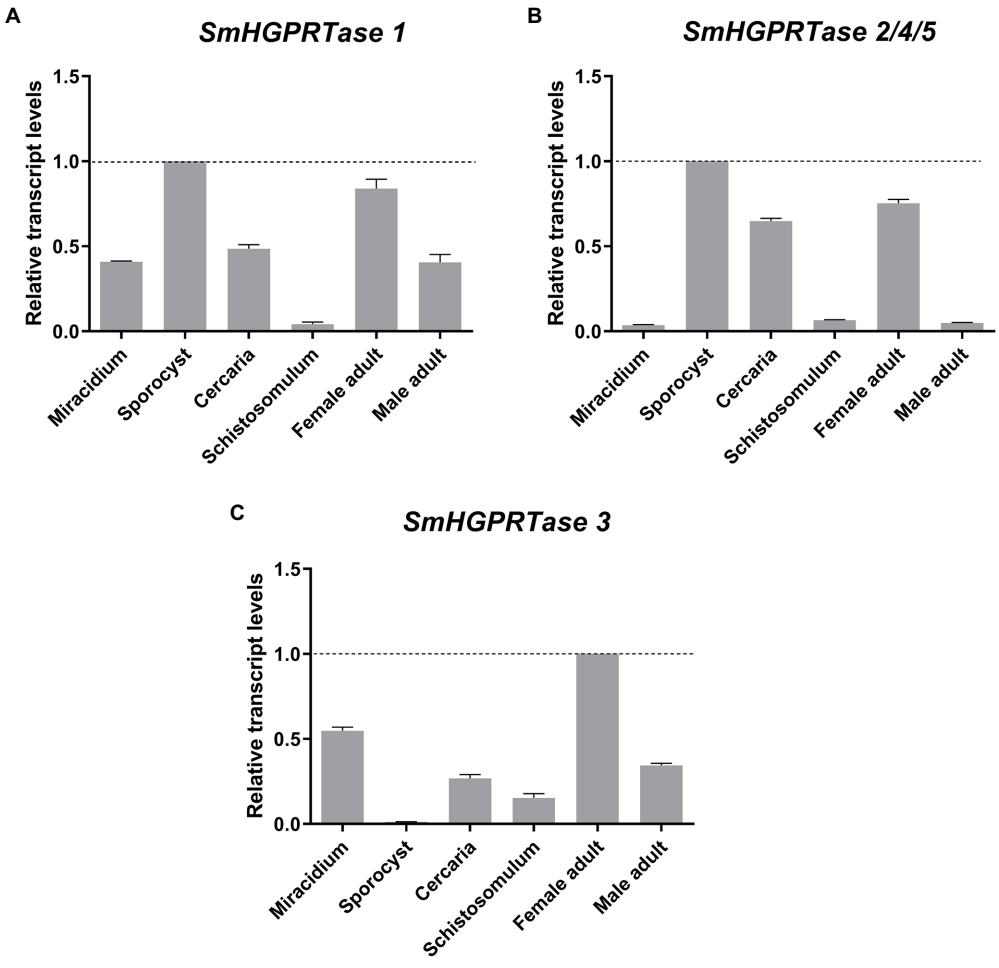

FIGURE 4
Expression profile of *SmHGPRTases* throughout different parasite's life stages. Bars showing the relative transcript levels of *SmHGPRTase 1* **(A)**, *SmHGPRTase 2/4/5* **(B)**, and *SmHGPRTase 3* **(C)** in the different *S. mansoni* life stages: miracidium, sporocyst, cercaria, schistosomulum, male, and female adult worm. **(A,B)** Data were normalized relative to the sporocyst stage (dashed line). **(C)** Data were normalized relative to the female adult worm stage (dashed line).

After knockdown, *SmHGPRTase 1* transcript levels were periodically evaluated in sporocysts (Figure 5A; Supplementary Figure S2) and we found that the lowest levels of transcript were achieved on the fourth day after dsRNA exposure, reducing by 71% regarding the untreated and unspecific controls. For *SmHGPRTase 2/4/5*, the highest transcript knockdown was

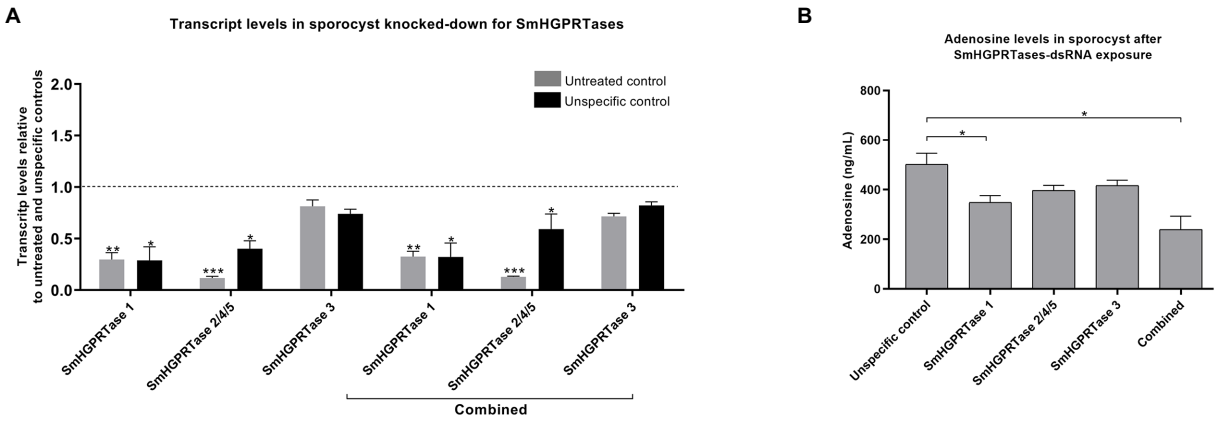

FIGURE 5
SmHGPRTases transcript levels after sporocysts exposure to dsRNAs and knockdown effects in adenosine levels. **(A)** Bars representing the transcript levels of *SmHGPRTase 1, SmHGPRTase 2/4/5,* and *SmHGPRTase 3* in sporocysts after exposure to the specific dsRNAs separately or in combination (combined) relative to the untreated (gray) or unspecific control (black) after 4days. Above the bars are represented the standard error of the mean of three replicates. The dashed line represents the normalized values in the controls. **(B)** Bars representing the adenosine levels in sporocysts in the respective groups: unspecific control, parasites treated with *SmHGPRTase 1*-dsRNA, *SmHGPRTase 2/4/5*-dsRNA, *SmHGPRTase 3*-dsRNA, and the combined group. Above the bars are represented the standard error of the mean of three replicates. After verifying the normality using the Shapiro–Wilk test, significant differences compared to control conditions were analyzed by unpaired *t*-test (*$p \leq 0.05$; **$p \leq 0.01$; ***$p \leq 0.001$).

achieved after 7 days of sporocysts exposure compared to the untreated and unspecific control groups, resulting in 77–89% reduction. In turn, *SmHGPRTase 3* transcript levels did not reduce after 2 days of dsRNA exposure and presented a reduction of 22–35% after 7 days of dsRNA exposure when compared to the controls. Similar knockdown effects were observed when we used a dsRNA combination targeting the five *SmHGPRTases,* likewise the best knockdown effect was detected on the fourth day of dsRNA exposure 68% for *SmHGPRTase 1,* 88–41% for *SmHGPRTase 2/4/5,* and 25% for *SmHGPRTase 3* in comparison to controls.

Once we determined the days when the transcript levels were lower after *SmHGPRTases* knockdown in sporocysts, biochemical tests were performed to check whether adenosine levels were also decreased, since these enzymes are supposed to be involved in the purine salvage pathway. We observed that the adenosine levels were 30% lower in the *SmHGPRTase 1* knocked-down sporocysts compared with the unspecific control. For the *SmHGPRTase* combined group, a 50% decrease in adenosine levels was observed when compared with the unspecific control after 4 days of dsRNA exposure (Figure 5B).

To assess the role of *SmHGPRTases* in sporocysts viability, knockdown parasites were daily observed. After 4 days of exposure to *SmHGPRTase 1*-dsRNA, a mortality of 8% rate in sporocysts was observed, 62% higher than the rate shown by the untreated control. This value was maintained until the seventh day, when the sporocysts reached a mortality rate of 19%, a value 57% higher than those found in the untreated and unspecific control groups. For sporocysts exposed to *SmHGPRTase 2/4/5*-dsRNA, a mortality rate of 13% after 7 days of exposure presented a significant increase when compared with the nonspecific control. The combined group had the highest sporocysts mortality rate, showing a mortality rate of 12% at third day of exposure to dsRNAs, representing a 75% increase in mortality compared to the two control groups. On the seventh day, this group reached the mortality rate of 22%, being approximately 65% higher than both control groups (Figure 6A).

Assessment of parasite phenotypes after the knockdown of *SmHGPRTase 1, 2/4/5*, and *3* was also performed. The sporocysts area was delimited considering the day in which each gene presented the lowest transcript levels. A significant reduction (8–13%) in the area of sporocysts exposed to *SmHGPRTase 1*- and *2/4/5*-dsRNA was noted when compared to control groups after 4 days of dsRNA exposure. *SmHGPRTase 3* knocked-down sporocysts did not show a significant alteration in their size (Figure 6B). Figures 6C–E show representative images evidencing the higher number of dead sporocysts in each group.

SmHGPRTases knockdown can be involved in schistosomula growth

In the schistosomula stage, transcript levels were optimally reduced during all assessments, resulting in up to ~85% for *SmHGPRTase 1* compared with both controls. Using *SmHGPRTase 2/4/5*-dsRNA the knockdown resulted in 40–71% after 3 days, and 62–78% after 7 days of exposure when compared with the untreated and unspecific controls. For *SmHGPRTase 3*, lower transcript levels were observed after 7 days of dsRNA exposure (50%). When in combination, the *SmHGPRTases* transcript levels only reduced after the third day of dsRNA exposure when reached its maximum knockdown for *SmHGPRTase 2/4/5* (68%). However, for *SmHGPRTase 1* and *SmHGPRTase 3,* the maximum knockdown was detected after

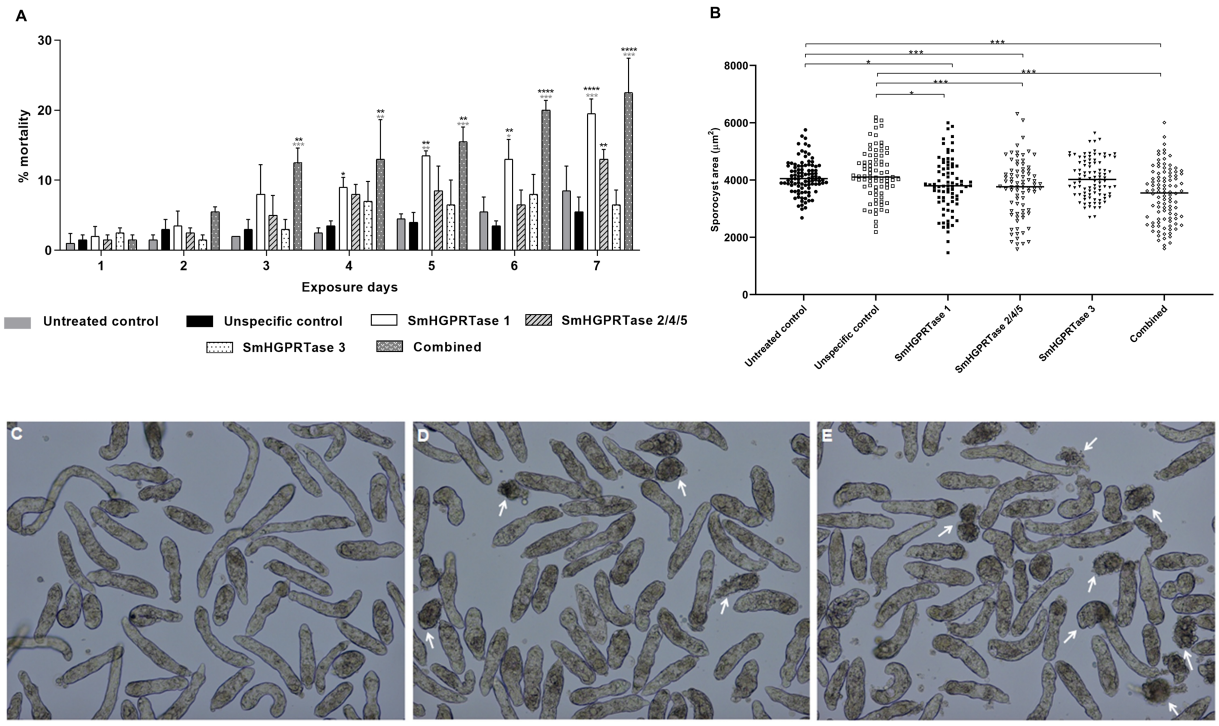

FIGURE 6
Viability of sporocysts exposed to *SmHGPRTases*-dsRNAs. **(A)** Bars representing the mortality percentage of sporocysts exposed to specific dsRNAs and control groups as described in the legend. Above the bars are represented the standard error of the mean of two biological replicates. As the statistical test, Two-way ANOVA with Sidak's multiple comparisons was used. Black asterisks represent significant differences from untreated control and gray asterisks from unspecific controls. **(B)** Area (μm^2) of sporocysts exposed to the SmHGPRTases-dsRNAs. Symbols represent a single parasite for each experimental group. Black circles, untreated control; White squares, unspecific control; Black square, parasites exposed to *SmHGPRTase 1*-dsRNA; White triangles, parasites exposed to *SmHGPRTase 2/4/5*-dsRNA; Black triangles, parasites exposed to *SmHGPRTase 3*-dsRNA; White rhombus, combined group. The horizontal black lines represent the median area of the sample population. After verifying the normality using the D'Agostino-Pearson test, significant differences compared to control conditions were analyzed by unpaired *t*-test. **(C–E)** Representative images of the untreated control group **(C)**, sporocysts exposed to *SmHGPRTase 1*-dsRNA **(D)**, and sporocyst from the combined group **(E)** 7days after dsRNA exposure. White arrows indicate changes in phenotype or dead sporocysts (*$p \leq 0.05$; **$p \leq 0.01$; ***$p \leq 0.001$; ****$p < 0.0001$).

seven days, reaching ~63%, and approximately 49%, respectively (Figure 7A; Supplementary Figure S3).

Concerning the measurement of adenosine levels for the schistosomula life stage, no statistically significant difference was observed when the adenosine levels obtained for knocked-down parasites were compared with the unspecific control (Supplementary Figure S4A). On the other hand, when the schistosomula area was delimited considering the day in which each gene presented the lowest transcript levels, it was observed 12% of area reduction for parasites treated with *SmHGPRTase 1*-dsRNA compared to the untreated control group and 8% compared to the unspecific control group. For *SmHGPRTase 2/4/5*-dsRNA, it was observed a reduction of 7% and for *SmHGPRTase 3*-dsRNA a reduction of 8% compared to the untreated control group. The combined group was also evaluated, and a significant reduction in the schistosomula area of 9% was observed when compared to the untreated control (Figures 7B,C). In addition to the size reduction, dark middle regions and round body in parasites from the combined group were noted (Supplementary Figure S5). The mortality rate in schistosomula did not present any significant differences among the groups (data not shown).

SmHGPRTase knockdown in female adult worms decreased adenosine levels and affect their motility *in vitro*

When adult worms were electroporated with the specific dsRNAs, *SmHGPRTase 1* presented the highest knockdown on the seventh days after exposure 70%. On the other hand, *SmHGPRTase 2/4/5* gene presented no transcript reduction on that day and reduced by 46% compared to untreated control group and 78% compared to nonspecific control group 2 days after electroporation. A decrease of 48–60% in the *SmHGPRTase 3* transcript levels was stable during all days the transcript levels were assessed. When the combined group was analyzed, similar results were seen for *SmHGPRTase 1* and *SmHGPRTase 3*, however, for *SmHGPRTase 2* lower transcript levels were detected. On the second, fourth, and seventh days after electroporation, a

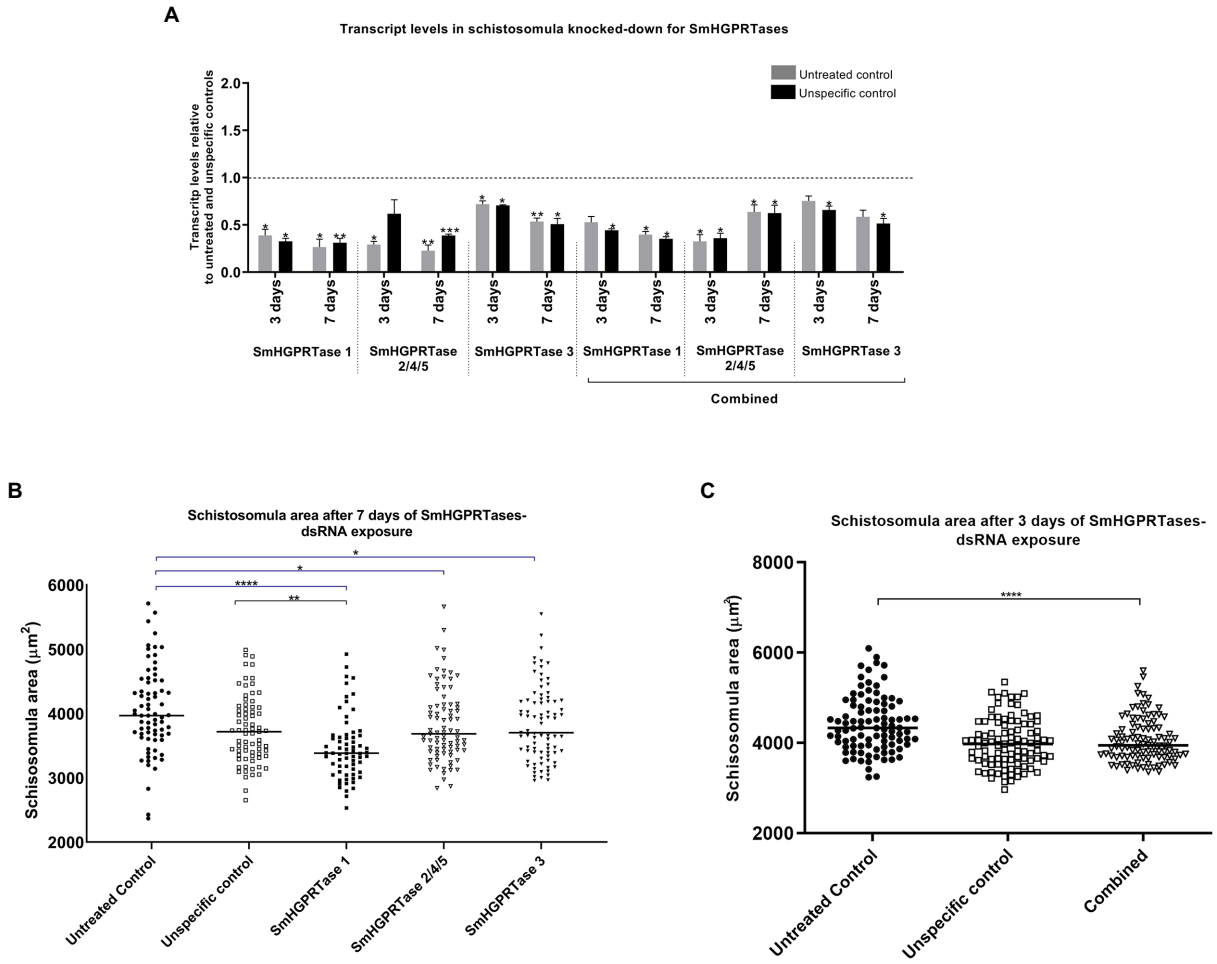

FIGURE 7
SmHGPRTases transcript levels and area of schistosomula after exposure to dsRNAs. **(A)** Bars representing the transcript levels of *SmHGPRTase 1, SmHGPRTase 2/4/5,* and *SmHGPRTase 3* in schistosomula after exposure to the specific dsRNAs separately or in combination (combined) relative to the untreated (gray) or unspecific control (black) after 3 and 7days. Above the bars are represented the standard error of the mean of three replicates. After verifying the normality using the Shapiro–Wilk test, significant differences compared to control conditions were analyzed by unpaired *t*-test. **(B)** Area (µm^2) of schistosomula exposed to the *SmHGPRTases-dsRNAs* after 7days. Symbols represent a single parasite for each experimental group. Black circles, untread control; White squares, unspecific control; Black square, parasites treated with *SmHGPRTase 1*-dsRNA; White triangles, parasites treated with *SmHGPRTase 2/4/5-dsRNA*; Black triangles, parasites treated with *SmHGPRTase 3*-dsRNA. **(C)** Area (µm^2) of schistosomula exposed to the combined group after 3days. Symbols represent a single parasite for each experimental group. Black circles, untread control; White squares, unspecific control; White triangles, combined group. The horizontal black lines represent the median area of the sample population. After verifying the normality using the D'Agostino-Pearson test, significant differences compared to control conditions were analyzed by unpaired *t*-test (*$p \leq 0.05$; **$p \leq 0.01$; ***$p \leq 0.001$; ****$p < 0.0001$).

decrease of 59–72%, 66–74%, and 49–64%, respectively (Figure 8A).

After that, the adenosine levels were checked to certify if they had decreased in adult worms. In female adult worms, the adenosine levels were reduced by approximately 45% for all the *SmHGPRTases* knocked-down parasites compared with the unspecific control (Figure 8B). On the other hand, for adult male worms no statistically significant difference in the adenosine levels was observed (Supplementary Figure S4B).

To analyze changes in the adult worms' viability after *SmHGPRTase* knockdown, the parasite's movement was quantified. Female adult worms electroporated with the combined *SmHGPRTases*-dsRNAs showed a significant reduction in their movement on the eighth (34%) and tenth day (43%) compared to the untreated and unspecific controls (Figure 8C). In male adult worms, no significant difference in their movement was observed (Supplementary Figure S6).

SmHGPRTases knockdown interferes in the ovary development and egg maturation in female adult worms *in vivo*

To evaluate the function of *SmHGPRTases* in the infection establishment, schistosomula exposed to the combined

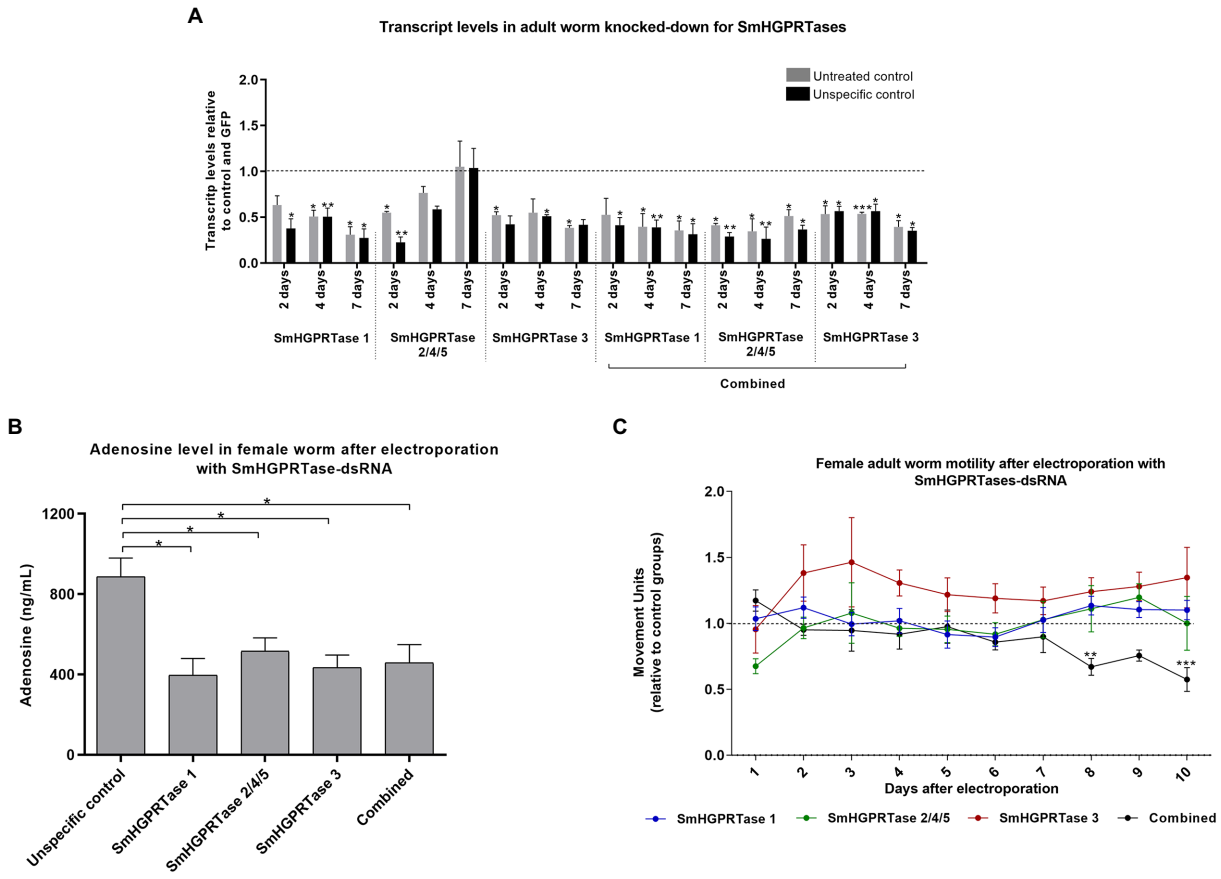

FIGURE 8
SmHGPRTases transcript levels after adult worm electroporation with dsRNAs and knockdown effects in adenosine levels and motility. **(A)** Bars representing the transcript levels of *SmHGPRTase 1, SmHGPRTase 2/4/5,* and *SmHGPRTase 3* in adult worms after electroporation with specific dsRNAs separately or in combination (combined) relative to the untreated (gray) or unspecific control (GFP; black) after 2, 4, and 7days. Above the bars are represented the standard error of the mean of three replicates. After verifying the normality using the Shapiro–Wilk test, significant differences compared to control conditions were analyzed by unpaired *t*-test. **(B)** Bars representing the adenosine levels in female adult worms in the respective groups: unspecific control, parasites exposed to *SmHGPRTase 1*-dsRNA, *SmHGPRTase 2/4/5*-dsRNA, *SmHGPRTase 3*-dsRNA, and the combined group. Above the bars are represented the standard error of the mean of three replicates. After verifying the normality using the Shapiro–Wilk test, significant differences compared to control conditions were analyzed by unpaired *t*-test. **(C)** Motility of female adult worms exposed to *SmHGPRTases*-dsRNAs. Dots represent the average of the movement units of female adult worms that were electroporated with *SmHGPRTases*-dsRNAs. Blue, parasites exposed to *SmHGPRTase 1*-dsRNA; Green, parasites exposed to *SmHGPRTase 2/4/5*-dsRNA; Red, parasites exposed to SmHGPRTase 3-dsRNA; Black, parasites exposed to the combination of the three *SmHGPRTases*-dsRNAs. The results were normalized according to the movement units of female adult worms from controls (dotted line). Standard errors of the mean of three biological replicates are represented above the dots. Statistical analysis was performed using Two-way ANOVA followed by the Sidak post-test (*$p \leq 0.05$; **$p \leq 0.01$; ***$p \leq 0.001$).

SmHGPRTases-dsRNAs were used for *in vivo* experiments using a murine model.

After perfusion, the number of recovered adult worms and eggs from the liver and intestine from the experimental groups did not show significant differences when compared to the controls (data not shown). However, the ileum of mice infected with schistosomula exposed to the combined *SmHGPRTases*-dsRNAs presented a significant increase in immature eggs. A significant increase of 8% of eggs in stage 3 was found in mice infected with knocked-down parasites when compared to the controls. Also, an increase (9%) in eggs on stage 2 when compared to the unspecific control was observed. Additionally, a significant reduction of 16% in mature eggs was observed in the combined group (Figures 9A–C). Representative images in Figures 9C–D highlight the differences among eggs found in the mice ileum.

Confocal microscopy was performed to verify if the parasite morphology was also altered in association with the high number of immature eggs noted after *SmHGPRTases* knockdown. A significant reduction of 36% in the ovary area was observed in female adult worms recovered from mice infected with schistosomula knocked-down for all *SmHGPRTases* when compared with controls (Figure 10A). Figures 10B–D demonstrates representative confocal images of the structural changes observed in female adult worms due to *SmHGPRTases* knockdown. No alterations were observed in male adult worms' reproductive systems (data not shown).

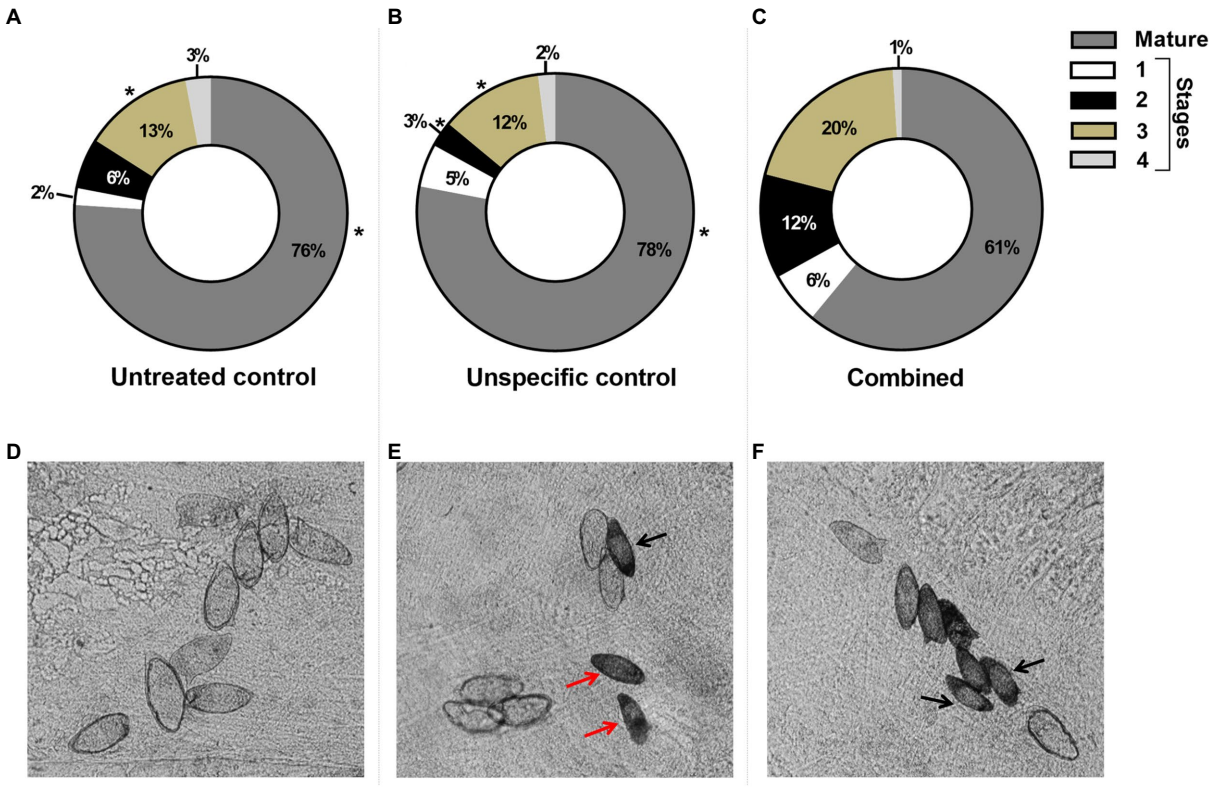

FIGURE 9
Egg maturation in the ileum of mice infected with schistosomula exposed to the dsRNAs of the five *SmHGPRTases* combined. The percentage of eggs in each maturation stage is represented in the circle section: mature (gray), stage 1 (white), stage 2 (black), stage 3 (beige), and stage 4 (light gray) for the untreated control group (**A**), GFP-dsRNA unspecific control (**B**), and the combined group (**C**). After verifying the normality using the Shapiro–Wilk test, significant differences compared to control conditions were analyzed by unpaired *t*-test (*$p \leq 0.05$). (**D–E**) Representative images of the maturation pattern in each experimental group. Black arrow, eggs in stage 2; Red arrow, eggs in stage 3.

Discussion

Functional studies have demonstrated that Smp38 is important for *S. mansoni* infection establishment in the mammalian host. This protein seems to be involved in the development of reproductive structures, the antioxidant defense, and egg maturation in this parasite (Avelar et al., 2019). In addition, studies have shown that Smp38 is essential in the regulation of miracidia ciliary movement and the early post-embryonic parasite development (Ressurreição et al., 2011a,b). The transcriptome of Smp38 knocked-down schistosomula showed that Smp38 regulates essential processes for the establishment of parasite homeostasis, including genes coding for proteins related to the structural composition of ribosomes, spliceosomes, and cytoskeleton, besides genes involved in the purine and pyrimidine metabolism pathways (Gava et al., 2019).

Analysis of Smp38 protein structure (Kelley et al., 2015) shows approximately 60% similarity with their respective human orthologs. The identity is even greater when only the domain sequences are compared. Accordingly, it would be interesting to explore parasite genes regulated by Smp38 MAPK pathway, that differ from the human orthologs or are parasite-specific, since several studies have proved the essential roles of Smp38 for *S. mansoni* development (Ressurreição et al., 2011a,b; Avelar et al., 2019; Gava et al., 2019). Thus, we sought to understand the biological functions of some genes that are regulated by this kinase in the parasite development, which may be responsible for the phenotypic alterations observed in Smp38 knocked-down parasites, among those genes are the hypoxanthine-guanine phosphoribosyl transferase 1 (*SmHGPRTase 1*) (Gava et al., 2019).

Different from their mammalian hosts, schistosomes lack the *de novo* purine biosynthesis pathway and depend on the salvage pathway for their purine requirements. One of the parasite's advantages in using the salvage pathway is the fact that the *de novo* biosynthesis requires a large amount of energy to synthesize puric bases. However, it also implies that schistosomes present a great dependence on an external supply of preformed puric bases in order to develop (Miech et al., 1975; Senft and Crabtree, 1983). For this reason, the salvage pathway has been raised as an interesting target for the development of new specific drugs to support schistosomiasis treatment (Ross and Jaffe, 1972; Craig et al., 1988; Yuan et al., 1992), among them, purine analogs inhibit enzymes of *S. mansoni* salvage pathway (Ross and Jaffe, 1972;

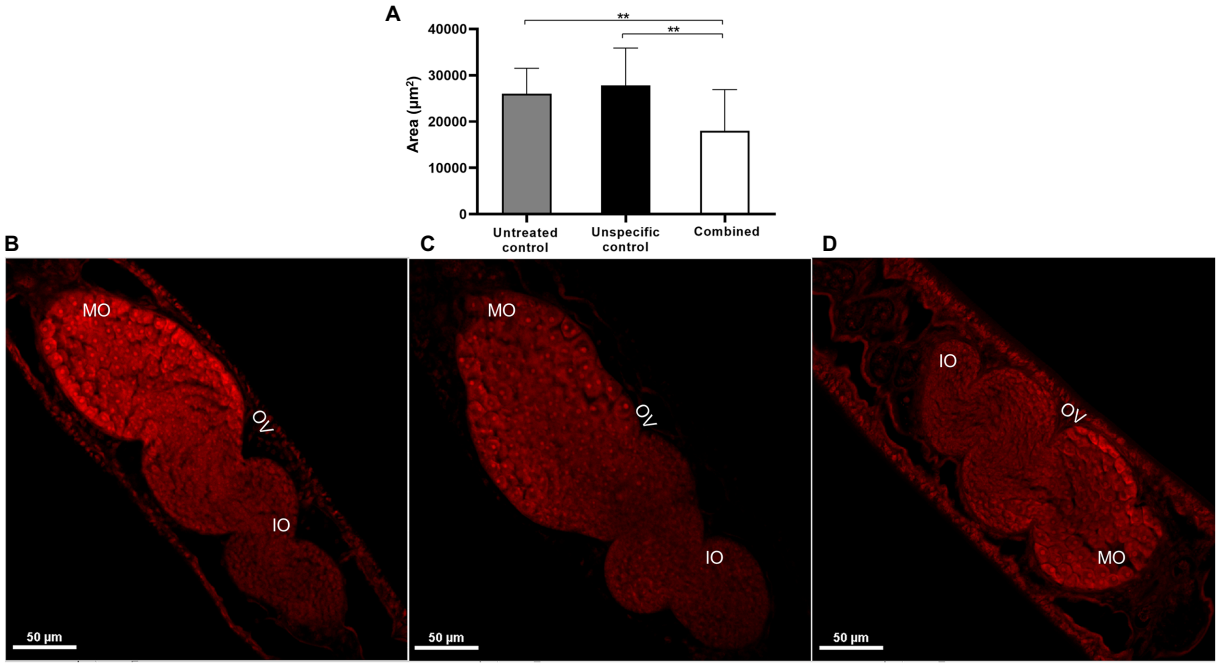

FIGURE 10
Phenotypic changes in female adult worms recovered from mice infected with *SmHGPRTases* knocked-down schistosomula. **(A)** Bars representing the ovary area of female adult worms from the untreated control (gray), unspecific control (black), and combined *SmHGPRTases* group (white). Above the bars are represented the standard error of the mean of three replicates. After verifying the normality using the Shapiro–Wilk test, significant differences compared to controls were analyzed by unpaired *t*-test (**$p \leq 0.01$). **(B–D)** Representative confocal images demonstrating female adult worms recovered from the untreated control **(B)**, unspecific control **(C)**, and the combined *SmHGPRTases* group **(D)**. MO, mature oocyte; IO, immature oocyte; OV, ovary. Scale bars: 50µm.

Miech et al., 1975). Tubercidin is one of those and causes the separation of *S. mansoni* worm pairs, loss of suction capacity of the ventral suction cup, alteration of the muscular activity pattern, and egg-laying inhibition (Ross and Jaffe, 1972). Hypoxanthine-guanine phosphoribosyl transferases (HGPRTases), targets of this study, are essential enzymes in the purine salvage pathway.

Since transcriptomic data are a snapshot of transcription rates, generating an insight of general biological data that requires posterior refinement, thus, we aimed at corroborating previously data generated by transcriptomics approach, using molecules predicted to bind to the Smp38 ATP-binding site to confirm the regulation of *SmHGPRTase* expression. We observed significant changes in the parasite phenotype indicating that they can be promising protein inhibitors, even more by the fact that these kinases are unique members of their families in *S. mansoni* (Rask-Andersen et al., 2014; Moreira et al., 2022). Besides that, we confirmed that Smp38 seems to regulate the expression of *SmHGPRTase 1*. In addition, we investigated whether Smp38 MAPK also regulates the expression of other *SmHGPRTase* family members. We observed that, although *SmHGPRTase 3* was not detected among the differentially expressed genes using the transcriptome data, the Smp38 inhibition seems to negatively regulate the expression of this gene. Analyzing the parasite's genome organization, we found that the five genes encoding SmHGPRTases are located on chromosome IV, in which *SmHGPRTases 1* and *3* appear to be regulated by Smp38 MAPK, and are proximally located. On the other hand, the genes encoding *SmHGPRTases 2, 4,* and *5,* which the expression does not appear to be regulated by this signaling pathway are also closely distributed evidencing *in tandem* duplications as already described by Wang et al. (2017). The gene duplication analysis revealed that genes derived from proximal duplications diverge less in gene structure and expression levels than the dispersed duplicated genes. The retention of duplicated genes is a mechanism described to contribute to the expansion of gene families associated with pathogenesis and consequent adaptations to parasitism for *S. mansoni* (Wang et al., 2017).

Previous studies showed that female adult worms recovered from mice infected with Smp38 knocked-down schistosomula showed a reduction in the ovary area and male adult worms presented a reduction in the tubercles' height (Avelar et al., 2019). Our results demonstrated that female adult worms recovered from mice, after 42 days of infection with *SmHGPRTases* knocked-down schistosomula, also presented similar phenotype reaffirming the fact that the Smp38 pathway may be related to the regulation of *SmHGPRTase* expression.

SmHGPRTases also show high expression in female adult worms. Previous studies suggest that these genes may be involved

in the parasite's sexual maturation (Romanello et al., 2019). Also, whole-mount *in situ* hybridization experiments show that SmHGPRTase 2 is present along the body of male and female worms, possibly indicating a sexual specialization role for this enzyme (Romanello et al., 2019). Genes that code for SmHGPRTases were also found up-regulated in parasites 28 days after infection in the mammalian host, suggesting a possible role for these enzymes in the synthesis of molecules necessary for egg production (Buddenborg et al., 2019). Our results corroborate these findings. Moreover, female adult worms knocked-down for all *SmHGPRTases* reduced their movement 8 days after dsRNA exposure *in vitro*.

Interestingly, when we checked the available single-cell RNAseq data, we observed that *SmHGPRTses 1* and *3* are more expressed in mature female worm's reproductive organs, including the cells from early, mature, and late vitellocytes, late female germ cells, and germline stem cell, in comparison with immature females (Wendt et al., 2020). This may explain the fact that egg maturation was altered, and adult worms recovered from mice infected with *SmHGPRTases* knocked-down schistosomula display phenotypic changes in the female reproductive organs.

In silico analysis showed that SmHGPRTases present important differences in protein structures and domain sequences when compared to their respective human ortholog. This data reaffirms other studies whereupon schistosomal HGPRTase structure has been compared with the human HGPRTase by circular dichroism. Significant differences were observed in thermostability and in the amino-acid side chains. The schistosomal protein contains 27% α-helix and 30% β-sheet, whereas the human enzyme contains 21% α-helix and 53% β-sheet (Yuan et al., 1993). In addition, the steady-state kinetics mechanism was determined and suggests that the design of a highly specific SmHGPRTase inhibitor, that binds exclusively to the enzyme-purine nucleotide binary complex, may be possible (Yuan et al., 1992). On the other hand, a study using isothermal titration calorimetry to determine kinetic parameters of SmHGPRTases 1, 2, and 3 observed that KM values for schistosomal HGPRTase are very similar to those determined for the human HGPRTase, indicating that SmHGPRTase alone is unlikely to be an efficient therapeutic target (Romanello et al., 2019).

Additionally, our data also show that *SmHGPRTase 1* and *SmHGPRTase 2/4/5* genes exhibited the highest expression levels in the sporocyst stage. In fact, in the snail host, extensive parasite asexual reproduction takes place, and several generations of multiplying sporocysts develop (Maldonado and Acosta Matienzo, 1947) which would demand energy and nucleotides for DNA synthesis, supporting the greater expression of *SmHGPRTases* in this stage. Corroborating these data, the analysis of the *in vivo* parasite transcriptome 3 days post-infection in *Biomphalaria pfeifferi* demonstrated an up-regulation of genes related to the purine salvage and nucleotide biosynthesis pathways (Buddenborg et al., 2019).

Small interfering RNAs (siRNAs) targeting *SmHGPRTase 1* have been used to interrogate this enzyme role in the parasite during the infection in mice. In the study, siRNAs were inoculated in the tail of *S. mansoni* infected mice, resulting in a 27% reduction in worm burden after a 60% reduction in the transcript levels (Pereira et al., 2008). This reduction could reflect the duplicity of functions among the HGPRTases present in the parasite and our results reinforce the importance of knocking down or inhibiting all genes of this family. This mechanism is evident by the higher mortality levels found in sporocysts when all the genes were knocked-down simultaneously. Our results also suggest that *SmHGPRTase 1* may be a major player for the sporocyst viability in regardregard to the other members of the family, since the mortality rate is also high when we knockdown this gene alone. However, it is important to point out that *SmHGPRTase 3* did not present a significant reduction in the transcript levels in sporocysts, consequently no significant phenotypic alterations can be attributed to the latter.

In summary, here we show that the Smp38 MAPK pathway regulates the expression of *SmHGPRTase 1* and *SmHGPRTase 3*. All members of the *SmHGPRTase* family seem to have a functional role in the adenosine uptake. Our results also suggest that SmHGPRTases activity is important for schistosomula development and that SmHGPRTase 1 and SmHGPRTase 2/4/5 are essential for sporocysts viability and development. Phenotypic alterations, for instance: parasites with dark central-region and reduction in female movement *in vitro*; were more evident when all gene family were knocked-down simultaneously, implying an overlap on the SmHGPRTase functions. SmHGPRTases also play a role in the parasite reproduction, demonstrated by the reduced ovary area in female adult worms and the significant increase in the number of immature eggs in the mice ileum. In conclusion, this study is a step forward in the elucidation of parasite biology and the functional roles of SmHGPRTases in *S. mansoni*, reinforcing the importance of these enzymes as therapeutic targets candidates in the parasite.

Data availability statement

Publicly available datasets were analyzed in this study. This data can be found here: ncbi.nlm.nih.gov/bioproject/, PRJNA611783, SRASRP252217.

Ethics statement

The animal study was reviewed and approved by Animals' procedures were approved by the Ethics Commission on Animal Use (CEUA) of the Oswaldo Cruz Foundation under the numbers LW-12/16 and LM-05/18. Experiments were performed under Brazil national guidelines following Law 11794/08.

Author contributions

MM, SG, and IB contributed to the conception and design of the study. MM contributed with reagents, materials, and analysis tools. IB and NT performed the *in vivo* experiments. IB performed the *in vitro* experiments and modeling analyses. IB and CC-S performed the statistical analyses. SG performed the single-cell analysis. MM, IB, SG, NT, and CC-S wrote the manuscript and contributed to manuscript revision and approved the submitted version. All authors contributed to the article and approved the submitted version.

Funding

This research was supported by grants from the European Commission's Seventh Framework Programme for research, under grant agreement no. 602080 (A-ParaDDisE), CAPES PCDD-Programa CAPES/Nottingham University (3661/2014), FAPEMIG (CBB-APQ-0520-13), Conselho Nacional de Desenvolvimento Cientifico e Tecnológico (CNPq) (Fellowship Grant number 302518/2018–5 and 317389/2021–1), Rede de Plataformas Tecnológicas Fiocruz (PDTIS). This study was also financed in part by the Coordenação de Aperfeiçoamento de Pessoal de Nível Superior – Brasil (CAPES) – Finance Code 001.

Acknowledgments

The authors would like to thank the snail and animal facility of the René Rachou Institute-Fiocruz for mollusk, mice, hamster, and parasite supply and the Program for Technological Development in Tools for Health-PDTIS/FIOCRUZ for the use of its facilities, including the mass spectrometry and Real-Time PCR platforms. They also thank the Programa de Pós-graduação em Ciências da Saúde of the René Rachou Institute-Fiocruz.

Conflict of interest

The authors declare that the research was conducted in the absence of any commercial or financial relationships that could be construed as a potential conflict of interest.

Publisher's note

All claims expressed in this article are solely those of the authors and do not necessarily represent those of their affiliated organizations, or those of the publisher, the editors and the reviewers. Any product that may be evaluated in this article, or claim that may be made by its manufacturer, is not guaranteed or endorsed by the publisher.

Supplementary material

The Supplementary material for this article can be found online at: https://www.frontiersin.org/articles/10.3389/fmicb.2022.1064218/full#supplementary-material

References

Andrade, L. F., Nahum, L. A., Avelar, L. G. A., Silva, L. L., Zerlotini, A., Ruiz, J. C., et al. (2011). Eukaryotic protein kinases (ePKs) of the helminth parasite *Schistosoma mansoni*. *BMC Genomics* 12:215. doi: 10.1186/1471-2164-12-215

Avelar, L. D. G. A., Gava, S. G., Neves, R. H., Silva, M. C. S., Araújo, N., Tavares, N. C., et al. (2019). Smp38 MAP kinase regulation in *Schistosoma mansoni*: roles in survival, oviposition, and protection against oxidative stress. *Front. Immunol.* 10:21. doi: 10.3389/fimmu.2019.00021

Bateman, A., Martin, M. J., Orchard, S., Magrane, M., Agivetova, R., Ahmad, S., et al. (2021). UniProt: the universal protein knowledgebase in 2021. *Nucleic Acids Res.* 49, D480–D489. doi: 10.1093/nar/gkaa1100

Botros, S. S., and Bennett, J. L. (2007). Praziquantel resistance. *Expert Opin. Drug Discovery* 2, S35–S40. doi: 10.1517/17460441.2.S1.S35

Boyle, S. N., and Koleske, A. J. (2007). Dissecting kinase signaling pathways. *Drug Discov. Today* 12, 717–724. doi: 10.1016/j.drudis.2007.07.019

Buddenborg, S. K., Kamel, B., Hanelt, B., Bu, L., Zhang, S. M., Mkoji, G. M., et al. (2019). The *in vivo* transcriptome of *Schistosoma mansoni* in the prominent vector species *Biomphalaria pfeifferi* with supporting observations from *Biomphalaria glabrata*. *PLoS Neglec. Trop. Dis.* 13:e0007013. doi: 10.1371/journal.pntd.0007013

Craig, S. P. 3rd, McKerrow, J. H., Newport, G. R., and Wang, C. C. (1988). Analysis of cDNA encoding the hypoxanthine-guanine phosphoribosyltransferase (HGPRTase) of *Schistosoma mansoni*; a putative target for chemotherapy. *Nucleic Acids Res.* 16, 7087–7101. doi: 10.1093/nar/16.14.7087

Cuesta-Astroz, Y., Santos, A., Oliveira, G., and Jensen, L. J. (2019). Analysis of predicted host–parasite interactomes reveals commonalities and specificities related to parasitic lifestyle and tissues tropism. *Front. Immunol.* 10:212. doi: 10.3389/fimmu.2019.00212

Mourão, M., Dinguirard, N., Franco, G. R., and Yoshino, T. P. (2009). Phenotypic screen of early-developing larvae of the blood fluke, *Schistosoma mansoni*, using RNA interference. *PLoS Negl. Trop. Dis.* 3:e502. doi: 10.1371/journal.pntd.0000502

Doenhoff, M. J., Cioli, D., and Utzinger, J. (2008). Praziquantel: mechanisms of action, resistance and new derivatives for schistosomiasis. *Curr. Opin. Infect. Dis.* 21, 659–667. doi: 10.1097/QCO.0b013e328318978f

Dovey, H. F., McKerrow, J. H., and Wang, C. C. (1984). Purine salvage in *Schistosoma mansoni* schistosomules. *Mol. Biochem. Parasitol.* 11, 157–167. doi: 10.1016/0166-6851(84)90062-8

Eglen, R. M., and Reisine, T. (2009). The current status of drug discovery against the human kinome. *Assay Drug Dev. Technol.* 7, 22–43. doi: 10.1089/adt.2008.164

El-Gebali, S., Mistry, J., Bateman, A., Eddy, S. R., Luciani, A., Potter, S. C., et al. (2019). The Pfam protein families database in 2019. *Nucleic Acids Res.* 47, D427–D432. doi: 10.1093/nar/gky995

Gava, S. G., Tavares, N. C., Falcone, F. H., Oliveira, G., and Mourão, M. M. (2019). Profiling transcriptional regulation and functional roles of *Schistosoma mansoni* c-Jun N-terminal kinase. *Front. Genet.* 10:1036. doi: 10.3389/fgene.2019.01036

Greenberg, R. M. (2013). New approaches for understanding mechanisms of drug resistance in schistosomes. *Parasitology* 140, 1534–1546. doi: 10.1017/S0031182013000231

Gu, Z., Eils, R., and Schlesner, M. (2016). Complex heatmaps reveal patterns and correlations in multidimensional genomic data. *Bioinformatics* 32, 2847–2849. doi: 10.1093/bioinformatics/btw313

Hanks, S. K., Quinn, A. M., and Hunter, T. (1988). The protein kinase family: conserved features and deduced phylogeny of the catalytic domains. *Science* 241, 42–52. doi: 10.1126/science.3291115

Howe, K. L., Bolt, B. J., Shafie, M., Kersey, P., and Berriman, M. (2017). WormBase ParaSite − a comprehensive resource for helminth genomics. *Mol. Biochem. Parasitol.* 215, 2–10. doi: 10.1016/j.molbiopara.2016.11.005

Kaiser, M. M., Baszczyński, O., Hocková, D., Poštová-Slavětínská, L., Dračínský, M., Keough, D. T., et al. (2017). Acyclic nucleoside phosphonates containing 9-deazahypoxanthine and a five-membered heterocycle as selective inhibitors of plasmodial 6-oxopurine phosphoribosyltransferases. *ChemMedChem* 12, 1133–1141. doi: 10.1002/cmdc.201700293

Katoh, K., Rozewicki, J., and Yamada, K. D. (2019). MAFFT online service: multiple sequence alignment, interactive sequence choice and visualization. *Brief. Bioinform.* 20, 1160–1166. doi: 10.1093/bib/bbx108

Kelley, L. A., Mezulis, S., Yates, C. M., Wass, M. N., and Sternberg, M. J. E. (2015). The Phyre2 web portal for protein modeling, prediction and analysis. *Nat. Protoc.* 10, 845–858. doi: 10.1038/nprot.2015.053

Keough, D. T., Rejman, D., Pohl, R., Zborníková, E., Hocková, D., Croll, T., et al. (2018). Design of *Plasmodium vivax* hypoxanthine-guanine phosphoribosyltransferase inhibitors as potential antimalarial therapeutics. *ACS Chem. Biol.* 13, 82–90. doi: 10.1021/acschembio.7b00916

Livak, K. J., and Schmittgen, T. D. (2001). Analysis of relative gene expression data using real-time quantitative PCR and the 2−ΔΔCT method. *Methods* 25, 402–408. doi: 10.1006/meth.2001.1262

Machado-Silva, J. R., Lanfredi, R. M., and Gomes, D. C. (1997). Morphological study of adult male worms of *Schistosoma mansoni* Sambon, 1907 by scanning electron microscopy. *Mem. Inst. Oswaldo Cruz* 92, 647–653. doi: 10.1590/S0074-02761997000500016

Maldonado, J. F., and Acosta Matienzo, J. (1947). The development of *Schistosoma mansoni* in the snail intermediate host, *Australorbis glabratus*. *P.R. J. Public Health Trop. Med.* 22, 331–373.

Marcellino, C., Gut, J., Lim, K. C., Singh, R., McKerrow, J., and Sakanari, J. (2012). WormAssay: A novel computer application for whole-plate motion-based screening of macroscopic parasites. *PLoS Neglect. Trop. Dis.* 6:e1494. doi: 10.1371/journal.pntd.0001494

Mati, V. L. T., and Melo, A. L. (2013). Current applications of oogram methodology in experimental schistosomiasis; fecundity of female *Schistosoma mansoni* and egg release in the intestine of AKR/J mice following immunomodulatory treatment with pentoxifylline. *J. Helminthol.* 87, 115–124. doi: 10.1017/S0022149X12000144

Miech, R. P., Senft, A. W., and Senft, D. G. (1975). Pathways of nucleotide metabolism in *Schistosoma mansoni*—VI adenosine phosphorylase. *Biochem. Pharmacol.* 24, 407–411. doi: 10.1016/0006-2952(75)90226-9

Milligan, J. N., and Jolly, E. R. (2011). Cercarial transformation and *in vitro* cultivation of *Schistosoma mansoni* schistosomules. *J. Vis. Exp.* 54:3191. doi: 10.3791/3191

Moreira, B. P., Batista, I. C. A., Tavares, N. C., Armstrong, T., Gava, S. G., Torres, G. P., et al. (2022). Docking-based virtual screening enables prioritizing protein kinase inhibitors with *in vitro* phenotypic activity against *Schistosoma mansoni*. *Front. Cell. Infect. Microbiol.* 12:913301. doi: 10.3389/fcimb.2022.913301

Pearce, E. J., and Sher, A. (1987). Mechanisms of immune evasion in schistosomiasis. *Contrib. Microbiol. Immunol.* 8, 219–232. PMID: 3304833

Pellegrino, J., and Siqueira, A. F. (1956). A perfusion technic for recovery of *Schistosoma mansoni* from experimentally infected guinea pigs. *Rev. Bras. Malariol. Doencas. Trop.* 8, 589–597.

Pereira, T. C., Pascoal, V. D. B., Marchesini, R. B., Maia, I. G., Magalhães, L. A., Zanotti-Magalhães, E. M., et al. (2008). *Schistosoma mansoni*: evaluation of an RNAi-based treatment targeting HGPRTase gene. *Exp. Parasitol.* 118, 619–623. doi: 10.1016/j.exppara.2007.11.017

Pettersen, E. F., Goddard, T. D., Huang, C. C., Couch, G. S., Greenblatt, D. M., Meng, E. C., et al. (2004). UCSF Chimera? A visualization system for exploratory research and analysis. *J. Comput. Chem.* 25, 1605–1612. doi: 10.1002/jcc.20084

R Core Team (2021). *A Language and Environment for Statistical Computing*. Vienna: R Foundation for Statistical Computing

Rask-Andersen, M., Zhang, J., Fabbro, D., and Schiöth, H. B. (2014). Advances in kinase targeting: current clinical use and clinical trials. *Trends Pharmacol. Sci.* 35, 604–620. doi: 10.1016/j.tips.2014.09.007

Ressurreição, M., Rollinson, D., Emery, A. M., and Walker, A. J. (2011a). A role for p38 MAPK in the regulation of ciliary motion in a eukaryote. *BMC Cell Biol.* 12:6. doi: 10.1186/1471-2121-12-6

Ressurreição, M., Rollinson, D., Emery, A. M., and Walker, A. J. (2011b). A role for p38 mitogen-activated protein kinase in early post-embryonic development of *Schistosoma mansoni*. *Mol. Biochem. Parasitol.* 180, 51–55. doi: 10.1016/j.molbiopara.2011.07.002

Romanello, L., Zeraik, A. E., de Freitas Fernandes, A., Torini, J. R., Bird, L. E., Nettleship, J. E., et al. (2019). *In vitro* and *in vivo* characterization of the multiple isoforms of *Schistosoma mansoni* hypoxanthine-guanine phosphoribosyltransferases. *Mol. Biochem. Parasitol.* 229, 24–34. doi: 10.1016/j.molbiopara.2019.02.005

Ross, A. F., and Jaffe, J. J. (1972). Effects of tubercidin and its ribonucleotides on various metabolic pathways in *Schistosoma mansoni*. *Biochem. Pharmacol.* 21, 3059–3069. doi: 10.1016/0006-2952(72)90198-0

Satija, R., Farrell, J. A., Gennert, D., Schier, A. F., and Regev, A. (2015). Spatial reconstruction of single-cell gene expression data. *Nat. Biotechnol.* 33, 495–502. doi: 10.1038/nbt.3192

Senft, A. W., and Crabtree, G. W. (1983). Purine metabolism in the schistosomes: potential targets for chemotherapy. *Pharmacol. Ther.* 20, 341–356. doi: 10.1016/0163-7258(83)90031-1

Tavares, N. C., Gava, S. G., Torres, G. P., de Paiva, C. Ê. S., Moreira, B. P., Lunkes, F. M. N., et al. (2020). *Schistosoma mansoni* FES tyrosine kinase involvement in the mammalian schistosomiasis outcome and miracidia infection capability in *Biomphalaria glabrata*. *Front. Microbiol.* 11:963. doi: 10.3389/fmicb.2020.00963

Tavares, N., and Mourão, M. (2021). Parasitemia evaluation in mice infected with *Schistosoma mansoni*. *Bio Protoc.* 11:e4017. doi: 10.21769/BioProtoc.4017

Vidhya, V. M., and Ponnuraj, K. (2021). Structure-based virtual screening and computational study towards identification of novel inhibitors of hypoxanthine-guanine phosphoribosyltransferase of *Trypanosoma cruzi*. *J. Cell. Biochem.* 122, 1701–1714. doi: 10.1002/jcb.30122

Wang, S., Zhu, X., and Cai, X. (2017). Gene duplication analysis reveals no ancient whole genome duplication but extensive small-scale duplications during genome evolution and adaptation of *Schistosoma mansoni*. *Front. Cell. Infect. Microbiol.* 7:412. doi: 10.3389/fcimb.2017.00412

Waterhouse, A. M., Procter, J. B., Martin, D. M., Clamp, M., and Barton, G. J. (2009). Jalview version 2--a multiple sequence alignment editor and analysis workbench. *Bioinformatics* 25, 1189–1191. doi: 10.1093/bioinformatics/btp033

Wendt, G., Zhao, L., Chen, R., Liu, C., O'Donoghue, A. J., Caffrey, C. R., et al. (2020). A single-cell RNA-seq atlas of *Schistosoma mansoni* identifies a key regulator of blood feeding. *Science* 369, 1644–1649. doi: 10.1126/science.abb7709

World Health Organization (2018). Schistosomiasis and soiltransmitted helminthiases: numbers of people treated in 2018. *Wkly. Epidemiol. Rec.*, 445–452.

World Health Organization (2021). Schistosomiasis - Situation and trends. Available at: https://www.who.int/data/gho/data/themes/topics/schistosomiasis (Accessed September 21, 2022).

Yuan, L., Craig, S. P. 3rd, McKerrow, J. H., and Wang, C. C. (1992). Steady-state kinetics of the schistosomal hypoxanthine-guanine phosphoribosyltransferase. *Biochemistry* 31, 806–810. doi: 10.1021/bi00118a024

Yuan, L., Wu, C. S. C., Craig, S. P. 3rd, Liu, A. F., and Wang, C. C. (1993). Comparing the human and schistosomal hypoxanthine-guanine phosphoribosyltransferases by circular dichroism. *Biochim. Biophys. Acta Protein Struct. Mol. Enzymol.* 1162, 10–16. doi: 10.1016/0167-4838(93)90121-7

frontiers | Frontiers in Microbiology

TYPE Original Research
PUBLISHED 15 December 2022
DOI 10.3389/fmicb.2022.1048457

OPEN ACCESS

EDITED BY
Leonard Peruski,
Centers for Disease Control and Prevention (CDC), United States

REVIEWED BY
Jean Tenena Coulibaly,
Félix Houphouët-Boigny University, Côte d'Ivoire
Georgette B. Salieb-Beugelaar,
Münster University of Applied Sciences, Germany

*CORRESPONDENCE
Cristina Toscano Fonseca
cristina.toscano@fiocruz.br

SPECIALTY SECTION
This article was submitted to Infectious Agents and Disease, a section of the journal Frontiers in Microbiology

RECEIVED 19 September 2022
ACCEPTED 04 November 2022
PUBLISHED 15 December 2022

CITATION
Mesquita SG, Caldeira RL, Favre TC, Massara CL, Beck LCNH, Simões TC, Carvalho GB, Neves FGS, de Oliveira G, Lacerda LSB, de Almeida MA, Carvalho OS, Mourão MM, Oliveira E, Silva-Pereira RA and Fonseca CT (2022) Assessment of the accuracy of 11 different diagnostic tests for the detection of *Schistosomiasis mansoni* in individuals from a Brazilian area of low endemicity using latent class analysis. *Front. Microbiol.* 13:1048457. doi: 10.3389/fmicb.2022.1048457

Assessment of the accuracy of 11 different diagnostic tests for the detection of *Schistosomiasis mansoni* in individuals from a Brazilian area of low endemicity using latent class analysis

Silvia Gonçalves Mesquita[1], Roberta Lima Caldeira[1], Tereza Cristina Favre[2], Cristiano Lara Massara[1], Lílian Christina Nóbrega Holsbach Beck[2], Taynãna César Simões[3], Gardênia Braz Figueiredo de Carvalho[4], Flória Gabriela dos Santos Neves[1], Gabriela de Oliveira[4], Larisse de Souza Barbosa Lacerda[4], Matheus Alves de Almeida[5], Omar dos Santos Carvalho[1], Marina Moraes Mourão[1], Edward Oliveira[5], Rosiane A. Silva-Pereira[4] and Cristina Toscano Fonseca[4]*

[1]Grupo de Pesquisa em Helmintologia e Malacologia Médica, Instituto René Rachou, Fundação Oswaldo Cruz, Belo Horizonte, Minas Gerais, Brazil, [2]Laboratório de Educação em Ambiente e Saúde, Instituto Oswaldo Cruz, Fundação Oswaldo Cruz, Rio de Janeiro, Brazil, [3]Núcleo de Estudos em Saúde Pública e Envelhecimento, Instituto René Rachou, Fundação Oswaldo Cruz, Belo Horizonte, Minas Gerais, Brazil, [4]Grupo de Pesquisa em Biologia e Imunologia de Doenças Infecciosas e Parasitárias, Instituto René Rachou, Fundação Oswaldo Cruz, Belo Horizonte, Minas Gerais, Brazil, [5]Grupo de Pesquisa em Genômica Funcional de Parasitos, Instituto René Rachou, Fundação Oswaldo Cruz, Belo Horizonte, Minas Gerais, Brazil

Background: Schistosomiasis is a parasitic disease associated with poverty. It is estimated that 7.1 million people are infected with *Schistosoma mansoni* in Latin America, with 95% of them living in Brazil. Accurate diagnosis and timely treatment are important measures to control and eliminate schistosomiasis, but diagnostic improvements are needed to detect infections, especially in areas of low endemicity.

Methodology: This research aimed to evaluate the performance of 11 diagnostic tests using latent class analysis (LCA). A cross-sectional survey was undertaken in a low endemicity area of the municipality of Malacacheta, Minas Gerais, Brazil. Feces, urine, and blood samples were collected from 400 residents older than 6 years of age, who had not been treated with praziquantel in the 12 months previous to the collection of their samples. The collected samples were examined using parasitological (Helm Test® kit Kato-Katz), nucleic acid amplification tests -NAATs (PCR, qPCR and LAMP on urine; PCR-ELISA, qPCR and LAMP on stool), and immunological (POC-CCA, the commercial anti-*Schistosoma mansoni* IgG ELISA kit from Euroimmun, and

two in-house ELISA assays using either the recombinant antigen PPE or the synthetic peptide Smp150390.1) tests.

Results: The positivity rate of the 11 tests evaluated ranged from 5% (qPCR on urine) to 40.8% (commercial ELISA kit). The estimated prevalence of schistosomiasis was 12% (95% CI: 9–15%) according to the LCA. Among all tests assessed, the commercial ELISA kit had the highest estimated sensitivity (100%), while the Kato-Katz had the highest estimated specificity (99%). Based on the accuracy measures observed, we proposed three 2-step diagnostic approaches for the active search of infected people in endemic settings. The approaches proposed consist of combinations of commercial ELISA kit and NAATs tests performed on stool. All the approaches had higher sensitivity and specificity than the mean values observed for the 11 tests (70.4 and 89.5%, respectively).

Conclusion: We showed that it is possible to achieve high specificity and sensitivity rates with lower costs by combining serological and NAATs tests, which would assist in the decision-making process for appropriate allocation of public funding aiming to achieve the WHO target of eliminating schistosomiasis as a public health problem by 2030.

KEYWORDS

schistosomiasis, *Schistosoma mansoni*, diagnostic tests, diagnosis, latent class analysis, clinical research, sensitivity, specificity

Introduction

Schistosomiasis is a debilitating neglected tropical disease (NTD) that currently affects about 240 million people in the tropical and subtropical regions. *Schistosoma mansoni* is the main species causing intestinal schistosomiasis in Africa and the Americas, where it is estimated that 25 million people are at risk of infection (PAHO, 2022). In Brazil, there are more than 1.5 million people infected (Ministério da Saúde, 2019), especially in the Northeast and Southeast regions (Carvalho et al., 2018; Katz, 2018). Data from the records of the Brazilian national schistosomiasis control programme-the Sistema de Informação do Programa de Controle da Esquistossomose (SISPCE), indicate that the prevalence of schistosomiasis in Brazil between the years 2009 and 2019 ranged from 3.22 to 5.20%, with an average of 4.29% (BRASIL M da S, 2021). Although these percentages may suggest that Brazil is due to meet the World Health Organization (WHO) target of eliminating schistosomiasis as a public health problem (defined as a prevalence of heavy infections lower than 1%) by 2030 (WHO, 2021), it is likely that these data are underestimated because of the microscopy-based diagnostic method used, namely the Kato-Katz (KK) test (Siqueira et al., 2011; Weerakoon et al., 2018; Ogongo et al., 2022). The KK test consists of the microscopic observation of eggs in fecal samples (Katz et al., 1972) and has a high analytical specificity, low cost, and relatively simple execution. For these reasons, this is the method recommended by both the WHO and the Brazilian Ministry of Health for the diagnosis of intestinal schistosomiasis and use in epidemiological surveys. However, the performance of the KK test is limited by the intensity of the host infection, the daily variation of parasite egg excretion and the uneven distribution of eggs within fecal samples (Ogongo et al., 2022). This is especially critical in low endemicity settings, where the KK test may overlook 25–30% of the infected people, underestimating the true prevalence of the disease (Berhe et al., 2004; Enk et al., 2008; McManus et al., 2018).

The development of new diagnostic tests and tools has been extensively explored in the past years, and it is listed in the new WHO 2021–2030 road map for neglected tropical diseases (WHO, 2021) as one of the actions required to control and eliminate NTDs, including schistosomiasis. Ideally, in order to properly evaluate the performance of a new diagnostic test, its sensitivity, specificity, and accuracy need to be compared to a reference standard test (RST), where the latter is able to indicate the true-positive and true-negative individuals (Alonzo and Pepe, 1999). Although recommended for use by health authorities in clinical settings, the KK test is not appropriate for use as a RST, because its lack of sensitivity would influence (i.e., bias) the assessment of the accuracy of any new test(s) under evaluation.

In this context, latent class analysis (LCA) is a useful analytical technique that can circumvent the problem of an absence of an appropriate RST. LCA is a statistical method described in Walter and Irwig (1988) that enables the evaluation of new diagnostic methods when an RST is not available by estimating the infection status of an individual based on the combined results of the tests conducted in a particular group. It is a promising tool for analyzing

new schistosomiasis diagnostic tests and many recent studies have relied on using this approach to assess the accuracy of new tests (Colley et al., 2013; Beltrame et al., 2017; Clements et al., 2017; Fuss et al., 2018; Koukounari et al., 2021). In order to address the need to improve schistosomiasis diagnosis, our study evaluated the sensitivity, specificity, and accuracy of 11 diagnostic tests using different samples (feces, urine, and blood) from 400 residents of a low endemicity area in Brazil (the municipality of Malacacheta) using the occurrence of infection estimated by LCA as a reference standard. Our findings allowed us to propose a 2-step diagnostic process, with an overall accuracy of 94%, involving the combination of serological and nucleic acid amplification tests (NAATs) for the active search for infected people in moderate and low prevalence settings.

Materials and methods

Ethics statement

This study followed the guidelines and regulations for clinical research—Resolution 196/1996 of the Brazilian National Health Council (CNS)—and is in line with the principles of the Declaration of Helsinki. The study was approved by both: (i) the Ethical Committee of the René Rachou Institute (IRR, Fiocruz Minas), CAAE 76273317.3.0000.5091, and approval numbers 2.400.880, 2.803.752, 3.802.104 and 3.918.849; and (ii) the Ethical Committee of the Oswaldo Cruz Institute (IOC, Fiocruz), CAAE 76273317.3.3001.5248, and approval number 2.426.395. For Ethical reasons, all participants of this study received the results of the parasitological diagnosis, and those with a positive KK result were treated using praziquantel tablets (Farmanguinhos/Fiocruz, Rio de Janeiro, RJ, Brazil), with a 60 mg/kg single dose, as recommended by the Brazilian Health Ministry (Brasil, 2014). As the KK test also allows the detection of soil-transmitted helminths (STH), the participants who had STH eggs in their feces received two albendazole tablets (400 mg) to be taken with a 15-day interval.

Study area

The study was conducted in the borough of Santa Rita (17°50′33″S; 42°4′22″W), in the city of Malacacheta, in the state of Minas Gerais, Brazil, between the 16th of October 2018 to the 16th of November 2018. The city of Malacacheta has a high percentage (17.3%) of extreme poverty and was considered by the Brazilian Ministry of Health as one of the 222 municipalities requiring priority action for schistosomiasis control (Portaria Ministerial no 1.556 de 28 de outubro de 2011). According to the data collected by the Brazilian national schistosomiasis control programme, the Programa de Controle da Esquistossomose (PCE), coordinated by the Brazilian Ministry of Health, 7,114 diagnostic tests were carried out in Malacacheta between 2010 and 2012, of which 1,646 (23.1%) were positive, among them 105 (6,4%) having high-intensity infection (http://tabnet.datasus.gov.br/cgi/tabcgi.exe?sinan/pce/cnv/pcebr.def, accessed on 04/25/2022). A school survey performed in 2013, based on two KK slides per stool sample, indicated an estimated prevalence of infection of 24.3% among schoolchildren (6–15 years; Favre et al., 2021). Data provided by a Basic Health Unit (BHU) in Malacacheta (personal communication) indicated a rise in the number of schistosomiasis cases among the inhabitants of the borough of Santa Rita during 2017. This, together with the socio-economic and environmental vulnerability of the residents, determined the choice of Santa Rita as the study area.

Study design

The current cross-sectional study was designed to assess by LCA the accuracy of parasitological, NAATs, and immunological methods for schistosomiasis diagnosis employing different biological samples (feces, blood, and urine). The study followed the recommendations of STARD 2015 (Bossuyt et al., 2015), and all the procedures were blindly performed by experienced members of the team supervised by a senior researcher according to Good Clinical Practices. The STARD 2015 checklist is available on Supplementary material 1.

Inclusion criteria

The target population was the residents of the borough of Santa Rita who both expressed an interest in joining the study and met the following eligibility criteria: (i) being resident in Santa Rita, (ii) being older than 6 years of age, (iii) willing to voluntarily provide blood, urine, and fecal samples, (iv) to have not received treatment for schistosomiasis in the previous 12 months prior to sample collection, and (v) signing the Informed Consent Form (ICF) and/or the Informed Term of Consent (ITC).

A total of 410 residents of the borough of Santa Rita were included in the study after the recruitment step, which was conducted at the local BHU Waldemar José Pereira. All the participants received unique ID numbers (from 001 to 410) to preserve their confidentiality. Ten individuals were excluded from the study either due to: one person had a previous treatment with praziquantel, one participant did not agree to provide one of the biological samples during the recruitment process, eight individuals did not deliver one of the three types of biological sample during the collection or delivery process.

Sample size calculation

The sample size used was calculated using epiDisplay package in the R software considering the sensitivity of the test with the lowest sensitivity (i.e., the KK test) among all the tests used in the current study the script below:

```
a <−n.for.survey(p = sens,delta = 0.10).
a
```

n < −ceiling(ceiling(a$n1)/p).
n

where, sens (sensitivity for the KK test) was 0.57; n.for survey (number of inhabitants of Santa Rita borough) was 1421; p (estimated prevalence of disease) was 0.281.

Thus, a sample size of 410 individuals was inferred as being required from a total population size of 1,421 residents, calculated assuming a 57% test sensitivity for Kato-Katz, a prevalence of infection of 28.1%, a 95% confidence level, a maximum marginal error of 10%, plus a 20% loss of enrolled participants during follow-up (Eldridge et al., 2006).

The sample size calculation described above, which was performed before the study was started, assumed a loss of 20% of the enrolled participants. However, the actual loss of enrolled participants was less than 2.4%. Therefore, our study was conducted with 400 participants, and its statistical power was not affected by loss of enrolled participants (Figure 1).

Sociodemographic questionnaire and history of schistosomiasis

At the BHU Waldemar José Pereira, after having a 10 ml sample of blood collected, the participants answered a questionnaire. The following information was obtained: age, gender and history of previous infection. The history of the schistosomiasis was assessed through questions concerning how many diagnostic tests had been previously performed prior to the current study (and, if any, what kind of biological material was used and what was the result of the test), and whether praziquantel was ever taken. The questionnaire was filled out by qualified research staff, based on the information provided by the participants. At the end of this phase of the study, the participants received containers for the collection of urine and feces together with the recommendations for the collection of the samples. Those samples were later handed to the Community Health Agents (CHAs) during home visits.

Sample collection

A temporary laboratory was set up at the Secretariat for Education building, which had four workstations, each exclusively used for one of the following: (i) stool sample preparation and slide reading for the KK test; (ii) blood sample preparation; (iii) urine sample preparation; (iv) POC-CCA execution. The blood samples were collected at the Basic Health Unit on the same day the questionnaire was conducted. Urine and stool samples were collected by the participant, preferably on the same day although a 7-day interval was allowed between the collection of each sample. Stool and urine samples were delivered by the participant to a team member that went house-to-house to get those samples. If the urine and stool samples were not provided within this 7-day period, the participant was subsequently removed from the study population.

Blood samples

Blood samples (10 ml) were collected from the participants using appropriately labelled BD vacutainer tubes. The tubes were transported to the temporary laboratory, where they were kept at room temperature for at least 1 h after obtaining the blood samples to allow complete clot formation and then centrifuged at 1000–1300×*g* at room temperature for 10 min to obtain the serum, which was aliquoted into cryogenic tubes and stored in the freezer at-70°C until use.

Fecal samples

Fecal samples were collected in appropriately pre-labelled containers and were processed on the same day of collection for parasitological and NAATs. The samples were separated into two portions: (i) ~84 mg for the preparation of two KK slides (~42 mg each), and (ii) ~500 mg cryopreserved to be used later for DNA extraction and molecular tests. The 500 mg portion was separated using 3D-printed models provided by the 3D Print Facility of the IRR.

Urine samples

The participants collected at least 35 ml of their first-morning urine. At the workstation, the samples underwent a chemical analysis using Combur10 Test® M test strips (Roche, Basel, Switzerland) to check and record any alterations in pH value, and detect the presence of leucocytes, protein, hemoglobin, and/or nitrite. This step was conducted by two experienced researchers simultaneously. For that, a test strip was immersed into every urine sample for about 1 s and then, after 1 min, the color presented on each pad of the strip was compared to the reference scale. The interpretation was conducted according to the manufacturer's instructions, and the Guidelines from the Brazilian Society for Clinical Pathology and Laboratory Medicine (SBPC/ML; Andriolo et al., 2017). After that, two drops of each urine sample were used for the POC-CCA test. The remaining volume was filtered in a cone folded Whatman® qualitative filter paper, Grade 3:6 µm (diameter 185 mm), previously labelled with the participant ID. After the filtration, the paper filters were left exposed on a sterilized bench to completely dry. They were then individually stored in hermetically sealed plastic bags, together with desiccant silica gel, and then transported at room temperature from the field to the laboratory, where the DNA extraction and NAATs tests were conducted.

Kato–Katz test

Two slides were prepared, each with ~42 mg of feces, as recommended by the Brazilian Ministry of Health. In order to estimate the parasite load of each participant, the instructions of the Helm Test® Kit (Bio-Manguinhos/Fiocruz, Rio de Janeiro, RJ, Brazil) were followed, such that the total number of eggs found on each of the two slides were added together and divided by 12 to calculate the number of eggs per gram of stool (eggs/g). The slides

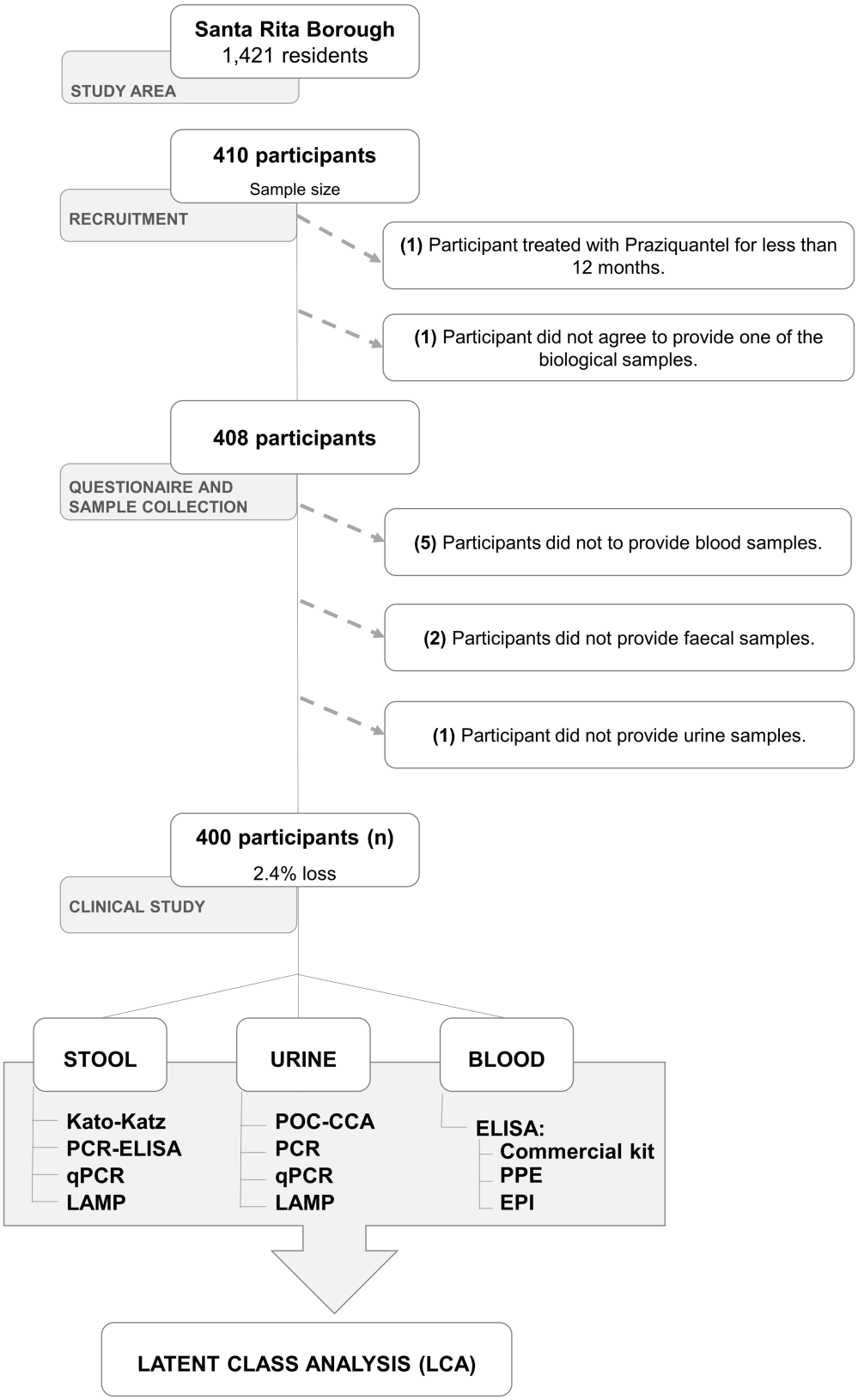

FIGURE 1
Flowchart detailing the study design. Legend: PCR-ELISA=polymerase chain reaction coupled with the enzyme-linked immunosorbent assay; qPCR=quantitative real-time PCR; LAMP=loop-mediated isothermal amplification; POC-CCA=point-of-care circulating cathodic antigens; Commercial kit=anti-*Schistosoma-mansoni* IgG commercial ELISA kit from Euroimmun; PPE=in-house anti-IgG ELISA test using the recombinant antigen PPE; EPI=in-house anti-IgG ELISA test using the Smp150390.1 peptide.

were read 3 h after preparation. For quality control, 10% of the slides were read by two technicians, and a third technician read 10% of the total slides of this study. In all instances, the technicians examined the slides "blind" and did not know the results when others had already read the same slides.

POC-CCA test

The POC-CCA (Urine CCA (Schisto) ECO test) was performed to detect the presence of the *S. mansoni* circulating cathodic antigen in fresh urine. When this was not possible, the samples were refrigerated until the next day. In this case, prior to testing, the urine was removed from the refrigerator and held at room temperature for up to 2 h before testing. The urine samples were tested by Urine CCA (Schisto) ECO test (Eco Diagnóstica, Nova Lima, MG, Brazil-product reference: TR.0301CA020, batch number: 201806011, expiration date: 01/31/2021), following Eco Diagnóstica's instructions for transport, storage, and use. After preparing a panel of properly labelled urine samples, with respective cassettes labelled with each participant's ID. Each sample was homogenized, and two drops of urine were transferred to the cassette. After the 21st minute, the result was interpreted by technicians who were unaware of the stool test results. At the time of reading, all tests were photographed, and these records were kept in the study files. According to the manufacturer, valid tests were categorized as negative, trace, or positive, with trace being considered as a positive result. Non-valid tests were repeated until a valid result was obtained.

Nucleic Acid Amplification tests

Source of samples used as positive controls for NAATs

Genomic DNA (gDNA) extracted from *S. mansoni* adult worms (LE strain) using the Wizard® Genomic DNA Purification Kit (Promega, Madison, WI, United States), following the manufacturer's protocol, was used as positive controls in all NAATs performed. The gDNA concentration was determined using Nanodrop Spectrophotometer (Thermo Fisher Scientific, Waltham, MA, USA) and diluted to working concentrations of either 1 ng/μl (for LAMP) or 5 ng/μl (for qPCR, PCR and PCR–ELISA). A schematic demonstration of molecular tests is illustrated in Supplementary material 2.

DNA extraction

DNA extraction from fecal samples

The gDNA from 400 fecal samples was extracted using three different commercial nucleic acid extraction kits: (i) QIAamp DNA Stool Mini Kit (Qiagen GmbH, Hilden, Germany), according to the manufacturer's protocol "DNA Isolation from Stool for Pathogen Detection and DNA Isolation from Large Amounts of Stool"; (ii) QIAamp Fast DNA Stool Mini Kit (Qiagen GmbH); and (iii) QIAamp PowerFecal Pro DNA Kit (Qiagen GmbH). Although the latter kit is designed to extract the DNA from 250 mg of stool, we used samples consisting of 500 mg of stool. However, the protocol was still effectively performed as recommended by the manufacturer by splitting each 500 mg fecal sample into two 250 mg halves and performing separately the "Experienced User Protocol" on each "half" until step 7. The two "halves" were then added (one at a time) to the MB Spin Column, and the remaining steps of the protocol followed treating the two pooled halves as a single sample (Qiagen, personal communication).

DNA extraction from urine samples

The gDNA from 400 urine samples was extracted using the commercial QIAamp DNA Blood Mini Kit (Qiagen GmbH, Hilden, Germany). Twelve circular pieces of 6 mm each were punched from every paper filter using a hole puncher. In order to avoid cross-contamination, the hole puncher was sterilized with ethanol 75% after each use. For each sample, all pieces of filter paper were transferred to a single 1.5 ml tubes with 600 μl nuclease free water and heated at 95°C for 10 min. The tubes were then incubated for 16–18 h at 22–25°C (Lodh et al., 2017). Up to 400 μl were transferred to a new labelled 2 ml tube, which was used for the DNA extraction following the manufacturer's protocol "Purification from Blood or Body Fluids (Spin Protocol)."

PCR-ELISA assay

A highly repetitive genome sequence of parasites from the genus *Schistosoma* (Gen Bank M61098) was amplified by PCR following the protocol described by Gomes et al. (2009, 2010) with a few modifications. Briefly, PCR was performed using a final volume of 20 μl, containing 2 μl of 10X PCR buffer, 2 μg of BSA (Sigma Aldrich, Saint Louis, MO, USA), 0.5 μM of each *S. mansoni*-specific primer (Table 1), 1.5 mM $MgCl_2$, 200 μM of each dNTPs (Promega, Madison, WI, USA), 2.0 U of Platinum™ Taq DNA Polymerase (Thermo Fisher Scientific), and 2 μl of gDNA purified from stool samples diluted 1:5 in linear acrylamide solution [30 μg/ml (*w*/*v*)]. The cycling programs were preceded by 12 min at 95°C, and then:15 cycles of 95°C for 1 min, 63°C for 1 min and 72°C for 30 s; 12 cycles of 80°C for 1 min, 63°C for 1 min and 72°C for 30 s; and 7 cycles of 80°C for 1 min, 65°C for 1 min and 72°C for 30 s; followed by a final elongation step at 72°C for 7 min. In each PCR assay, a negative control (PCR mix without DNA) and a positive control (gDNA from *S. mansoni* adult worms) were included. The presence of amplicons was detected in MaxiSorp® polystyrene microplates (Nunc™, Thermo Fisher Scientific) following the protocol described by Senra et al. (2018). The primers used are detailed in Table 1. The human *β-actin* (*ACTB*) gene was used as an internal control, and negative (PCR mix without DNA) and positive (using DNA extracted from adult *S. mansoni* worms as template) controls were both included. The cut-off of the PCR-ELISA used in this study was 0.136, as previously defined using a receiver

TABLE 1 Primers and probes used in the molecular tests.

Type	Amplicon	Target	Assay	Sequence	References
Forward Primer	121 bp	*S. mansoni* repetitive region	PCR and	5-Biosg/ GAT CTG AAT CCG ACC AAC CG-3′	Gomes et al. (2009)
Reverse Primer		*Sm1-7* (GenBank: M61098)	PCR-ELISA	5′- ATA TTA ACG CCC ACG CTC TC-3′	
Probe				5-6[FAM]/ TGG TTT CGG AGA TAC AAC GA-3′	
Forward Primer	120 bp	Human *β-actin* gene	PCR-ELISA	5-Biosg/ ACC TCA TGA AGA TCC TCA CC-3′	Musso et al. (1996)
Reverse Primer		(GenBank: AY582799.1)		5′- CCA TCT CTT GCT CGA AGT CC-3′	
Probe				5-6[FAM]/ TCT CCT TAA TGC ACG CAC G-3′	Gomes et al. (2010)
Forward primer	90 bp	*S. mansoni* repetitive region	qPCR	5′-CCG ACC AAC CGT TCT ATG A-3′	Siqueira et al. (2021)
Reverse Primer		*Sm1-7* (GenBank: M61098)		5′-CAC GCT CTC GCA AAT AAT CTA AA-3′	
Probe				5′-6[FAM]/TCG TTG TAT CTC CGA AACCAC TGG ACG/[3BHQ1]	
Forward Primer	92 bp	Human *β-actin* gene		5’-CCA TCT ACG AGG GGT ATG-3’	
Reverse Primer		(GenBank: AY582799.1)		3′-GGT GAG GAT CTT CAT GAG GTA-5’	
Probe				5′- 6[JOE]/CCT GCG TCT GGA CCT GGC TG/[3BHQ1]	
Internal forward Primer- FIP	NA	Mitochondrial *S. mansoni* minisatellite DNA region (GenBank: L27240)	LAMP	5′- GCC AAG TAG AGA CTA CAA ACA TCT TTG GGT AAG GTA GAA AAT GTT GT-3’	Fernández-Soto et al. (2014)
Internal Backward Primer- BIP				5′- AGA AGT GTT TAA CTT GAT GAA GGG GAA ACA AAA CCG AAA CCA CTA-3’	
External Forward Primer- F3	203 bp			5′- TTA TCG TCT ATA GTA CGG TAG G-3’	
External Backward Primer- B3				5′- ATA CTT TAA CCC CCA CCA A-3’	

bp = base pair; FAM = 6-Carboxyfluorescein; BHQ1 = Black Hole Quencher 1; JOE = 6-carboxy-4′,5′-dichloro-2′,7′-dimethoxyfluorescein; NA = not applicable.

operating characteristic curve (ROC Curve) analysis (Senra et al., 2018). This test was performed only on stool samples.

PCR

PCR assays were conducted as described above in Section 7.3 using 2 µl of gDNA from urine samples diluted 1:2 in linear acrylamide solution [30 µg/ml (*w/v*)] as template for each reaction. The results were visualized by electrophoresis using 6% polyacrylamide gels and analyzed by silver staining.

qPCR assay

The quantitative PCR (qPCR) reaction was performed according to Siqueira et al. (2021). Briefly, the reaction was done in a final volume of 20 µl containing 10 µl of TaqMan® Universal PCR Master Mix (Life Technologies, Thermo Fisher Scientific), 0.1 µM of each *S. mansoni*-specific primer, 0.25 µM of the *S. mansoni*-specific probe, 0.15 µM of each *β-actin* specific primer and 0.25 µM of the *β-actin* probe (Table 1), 2 µg of BSA, 2 µM $MgCl_2$, and 4 µl of gDNA extracted from stools and diluted 1:5 in linear acrylamide solution [30 µg/ml (w/v)]. Two controls were used for each reaction: a positive control (PCR mix plus gDNA from adult worms) and a negative control consisting of PCR mix only (i.e., no template control). All primers and probes used are listed in Table 1. The assays were performed in duplicate using microplates (MicroAmp® Fast Optical-Applied Biosystems, Foster City, CA, United States) sealed with adhesive film (Optical Adhesive Covers-Applied Biosystems, Foster City, CA, USA) on the StepOnePlus™ Real-Time PCR System (Thermo Fisher Scientific) under the universal cycling program with 45 cycles and annealing temperature of 60°C. Samples with observed Ct ≤ 42 were classified as positive, according to Siqueira et al. (2021). Samples that did not have amplification of the internal control (i.e., amplification of the *β-actin* gene) were retested, and a new DNA sample was extracted when necessary. For the urine samples, the reaction was done in a final reaction volume of 20 µl following the protocol described above, but with the follow modifications: 2.0 mM $MgCl_2$ and 4 µl of DNA diluted 1:3 in linear acrylamide solution [30 µg/ml (*w/v*)] were used. Additionally, for the urine sample, the Ct cut-off used was ≤ 44 defined through a standard curve analysis that showed amplification up to 0.38 fg of *S. mansoni* DNA. Samples that did not have amplification of the internal control gene were retested and a new DNA sample was re-extracted when necessary.

Lamp

The primers designed by Fernández-Soto et al. (2014) targeting the mitochondrial *S. mansoni* minisatellite DNA region (GenBank: L27240) were used in this study (Table 1).

The original protocol described by the authors was adapted to ensure the specificity of the reaction. The adapted protocol consisted of a final volume of 25 µl having: 1 × Isothermal Amplification Buffer (20 mM Tris–HCl, 10 mM $(NH4)_2SO_4$, 50 mM KCl, 2 mM $MgSO_4$, 0.1% Tween-20, pH 8.8 @ 25°C; New England Biolabs, Ipswich, MA, United States), 6 mM $MgSO_4$ (New England Biolabs), 1.4 mM of each dNTP (Invitrogen, Waltham, MA, United States), 40 pmol/µl of the internal primers FIP and BIP, 5 pmol/µl of the external primers F3 and B3, 1 M betaine (Sigma Aldrich), 8 U *Bst* 2.0 Warm-Start DNA polymerase (New England Biolabs), 2 µl of the DNA extracted from fecal samples or 5 µl of the DNA extracted from urine samples. The reaction tubes were incubated at 63°C for 50 min, followed by a 5-min incubation at 80°C to inactivate the polymerase. The result was visualized by naked eye after the addition of 2 µl of the DNA intercalating dye SYBR Green I (1000X, Life Technologies, Thermo Fisher Scientific). When positive, the reaction changed color from orange to yellow. When negative, the reaction remained orange. The reaction tubes were also exposed to UV light (320 nm) and the samples were considered positive when the reaction tube showed fluorescent signal, whilst the absence of amplification was inferred when no fluorescence was apparent. As a quality control, 3 µl of the reaction product was visualized on silver-stained 6% polyacrylamide gel. If the result observed by adding the SYBR Green I dye and by electrophoresis did not match, the reaction was repeated just once. After repeating, any discordant results were resolved by considering visual inspection of any color changes.

Serological tests

Schistosoma mansoni antigens

A synthetic peptide (SLPSNAHNNDNNSSD-biotin) containing amino acids 216–230 from the *S. mansoni* protein Smp150390.1 (Carvalho et al., 2017) was purchased from Biomatik (Ontario, Canada) and conjugated with biotin at the C-terminal end. The synthetic peptide had a purity of 96.22% and was resuspended in ultra-pure water to a final concentration of 2.5 mg/ml and stored at-70°C until use. A *S. mansoni* recombinant protein, called by the name PPE (rPPE), and encoded by a sequence similar to the *Smp_049300.3* gene, was expressed in *E. coli* ArcticExpress (DE3) cells (Agilent Technologies, Santa Clara, CA, United States) using the pET21a plasmid and purified by Ni^{2+} affinity chromatography using the Ni-NTA Fast Start Kit (Qiagen GmbH, Hilden, Germany). The resulting purified rPPE was stored at-70°C in PBS at 1 mg/ml until use.

ELISA tests

Three different ELISA tests were performed using sera from the participants of the study: the anti-*Schistosoma mansoni* IgG commercial ELISA Kit from Euroimmun (São Caetano do Sul, SP, Brazil), and two in-house ELISA tests using either the biotin-labelled synthetic Smp150390.1 (216–230) peptide or the recombinant PPE protein as antigens, respectively.

The anti-*Schistosoma mansoni* IgG ELISA test from Euroimmun (from here on in termed the commercial ELISA kit) was performed following the manufacturer's instructions using the buffers provided in the Kit. Briefly, microtiter plates adsorbed with *S. mansoni* purified soluble egg antigens were incubated with serum samples diluted 1:101 in sample buffer for 1 h at 37°C. The plates were washed four times with a wash buffer and the detection antibody (anti-human IgG-HRP) was then added and incubated for 30 min at 37°C. After an additional washing step, color reactions were developed by incubating the substrate for 30 min at room temperature. The reaction was stopped using the stop solution and the absorbance was measured at 450 nm using an ELISA microplate reader (Thermo Fisher Scientific). Sample reactivity was determined by the ratio between sample and calibrator absorbances. Values below 0.8 were taken to indicate non-reactive sera, while values higher than or equal to 1.1 indicated reactive sera. Values higher than or equal to 0.8, but lower than 1.1, were interpreted as indeterminate results.

Anti-IgG EPI (ELISA test to detect reactivity against the synthetic peptide) containing the epitope Smp150390.1 (216–230) and anti-IgG PPE ELISA tests (ELISA test to detect reactivity against the recombinant protein PPE), from here on in termed "ELISA EPI" and "ELISA PPE," respectively, were performed as follows. MaxiSorp 96-well microtiter plates (Nunc™, Thermo Fisher Scientific) were coated with either 25 µg/ml (synthetic peptide) or 8 µg/ml (rPPE) diluted in carbonate–bicarbonate buffer 0.05 M, pH 9.6, for 16 h at 4°C. The plates were blocked for 2 h at 37°C with 300 µl/well of PBS-T (phosphate-buffered saline, pH 7.2 with 0.05% Tween-20) with 10% FBS (fetal bovine serum; GIBCO, United States). One hundred microliters of each serum sample diluted either 1:40 (anti-IgG EPI test) or 1:100 (anti-IgG PPE test) in PBS-T was added per well and incubated for 2 h at 37°C. Serum samples were analyzed in duplicate. Plate-bound antibody was detected using 100 µl/well of a peroxidase-conjugated anti-human IgG (Sigma Aldrich) diluted 1:40,000 (anti-IgG EPI test) or 1:60,000 (anti-IgG PPE test) in PBS-T. Plates containing the detection antibody were incubated for 2 h at 37°C. Color reactions were developed by adding 100 µl of TMB (3,3′,5,5′-Tetramethylbenzidine) substrate (Sigma Aldrich) for 30 min at room temperature. The reaction was stopped with 50 µl of 2 M sulfuric acid solution, giving 4 N (4 Normal), per well, and the absorbance was measured at 450 nm using an ELISA microplate reader (Thermo Fisher Scientific). Sample reactivity was determined by the ratio between the mean sample absorbance and the mean calibrator (pool of sera samples from non-*Schistosoma mansoni* infected individuals) absorbance. Values below 0.95 were taken to indicate non-reactive sera and values higher than 1.05 indicated reactive sera. Values higher than or equal to 0.95, but lower than or equal to 1.05, were interpreted as indeterminate results. The ranges for classification of the serum reactivity were determined based on the inter- and intra-test coefficient of variation observed during the standardization

process. A schematic demonstration of ELISA tests is illustrated in Supplementary material 2.

Sera presenting indeterminate results in any of the ELISA tests were evaluated again, and the second result registered in the study database. For the construction of the latent class model, indeterminate results were considered as negative results.

Statistical analysis

Initially, samples were characterized based on the proportional distribution of individuals in relation to the history of infection with the parasite and any previous treatment. The latent class analysis (LCA) can be used in situations where the reference standard is partially unavailable or imperfect. The LCA method combines multiple test results in order to construct a standard reference outcome. The probability of each individual being classified as 'case' (classified as positive for *S. mansoni* infection) based on the 11 tests described above was estimated from the fit of the latent class model (LCM), which may include a random effect (Beath, 2017). The best model in terms of the number of classes into which individuals are classified was chosen based on the lowest value of the Bayesian Information Criterion (BIC). The posterior class probabilities for each observed pattern and class were determined. These were returned as a data frame together with the patterns for each observation. Thus, the outcome of interest could be defined. Individuals who presented a posterior class probability above 80% in the best fit LCM were considered as belonging to the 'case group'. Separate analyses of the individual accuracy of each of the 11 diagnosis tests were also performed. The 80% cut-off was defined based on the distribution of outcome probabilities (Supplementary material 3) in which there is a sharp decrease below the cut-off in the probability of being included in the 'case group' (from 81 to 68%).

Diagnostic test accuracy (DTA) is defined as the proportion of all the clinical diagnostic tests analyzed that give a correct result. The most common accuracy measures are: (i) sn = sensitivity, the probability of a positive test result in people with the infection; (ii) sp. = specificity, the probability of a negative test result in people without the infection; (iii) PPV = positive predictive value, the ratio of people with the infection to those who have a positive test result; (iv) NPV = negative predictive value, the ratio of people without the infection to those who have a negative test result; (v) LR+ = positive likelihood ratio, the ratio of the probability of a positive test result among those with the infection to that of a positive test result among those without the infection; (vi) LR- = negative likelihood ratio, the ratio of the probability of a negative test result among those with the infection to that of a negative test result among those without the infection; (vii) accuracy, the combined proportion of people who are true positives and true negatives among all the subjects tested. The LR is an overall measure of the discrimination of test result. The test is useless if LR = 1. The test is better the more LR differs from 1, that is, greater than 1 for LR+ and lower than 1 for LR-. The *Epi* package was used in the R software (epi.tests function) computes true and apparent prevalence, sensitivity, specificity, positive and negative predictive values, and positive and negative likelihood ratios from count data provided in a 2 by 2 table (Carstensen et al., 2022). The exact binomial confidence limits were calculated for test sensitivity, specificity, and positive and negative predictive values (Collett, 2002). Confidence intervals for positive and negative likelihood ratios were based on the formulae provided by Simel et al. (1991).

In order to calculate the summary statistics for the DTA, a pairwise meta-analysis model was selected. General pairwise meta-analysis calculates the effect size, such as relative risk and the odds ratio (OR) for binary data, and the mean difference for continuous data. DTA simultaneously combines two effect sizes, such as the sensitivity and specificity, or the positive predictive and negative predictive values. The bivariate model assumes a binomial distribution that directly models the sensitivity and specificity for within study variations, while assuming a bivariate normal distribution for between-study variation. "Different studies" were considered as different exclusive sets of tests grouped together according to the type of biological material they examined (i.e., urine, stool, or blood; Shim et al., 2019).

For calculating the confidence interval, the Clopper–Pearson method was used (Newcombe, 1998). In forest plots, the Higgins' I^2 of the heterogeneity was determined by subtracting the number of degrees of freedom from the Cochrane Q statistics, and then again dividing the resulting value by the Cochrane Q statistics. Thus, it quantifies the heterogeneity in a consistent manner. Heterogeneity may be suspected if the between-study variation is greater than the within-study variation in the forest plot (sensitivity and specificity). Methods for meta-analysis of fixed effects and random effects of single proportions were used to calculate an overall proportion (Borenstein et al., 2010; Barendregt et al., 2013). The packages in R software used were *random LCA*, *Epi*, *metaprop* and *metabin* for sensitivity, specificity, and diagnostic odds ratio; and *forest* for the forest plot (Beath, 2017; Balduzzi et al., 2019; Carstensen et al., 2022).

Rationale for calculating the cost of tests

The cost of each test assessed in this study was calculated according to the current price quoted in Brazilian reais (BRL) between June and July 2022. The exchange rate for American dollars (USD) was obtained from the Central Bank of Brazil (https://www.bcb.gov.br/) on 27/07/2022, when 1 USD = 5.3068 BRL. The costs of the 2-step protocols proposed in the present study were calculated using the following formulas:

$$n \times \text{cost of comercial ELISA kit} = X$$

$$\text{nPOS} \times \text{cost of molecular test on stool} = Y$$

$$\text{cost per individual of the proposed two} - \text{step protocol} = (X + Y) \div n$$

When n is the population size and *nPOS* is the number of individuals classified as positive by the commercial ELISA kit.

The cost for each sample does not include the price of equipment needed, personnel, and DNA extraction kits (for NAATs). The cost of DNA extraction kits is listed separately on Supplementary Material 4. The price of the discontinued QIAamp DNA Stool Mini Kit, the KK and POC-CCA kits were obtained previously (2017–18) and adjusted according to the General Market Price Index (IGP-M) from Getúlio Vargas Foundation (https://portal.fgv.br/). The calculation of the costs is described in detail in Supplementary Material 4.

Results

Demographic data

The participants answered a questionnaire enabling the determination of their demographic profile. The age of the study population ranged from 6 to 88 years, with 51.5% of participants with less than 30 years of age. The majority were female (65.5%). More than 56% of the participants had schistosomiasis at least once in their lives. All the demographic data collected by the questionnaire are detailed in Table 2. No adverse effects associated with either sample collection or treatment for worm infection were observed.

Kato-Katz technique

The KK technique enabled the detection of 22 individuals (5.5%) having *S. mansoni* eggs in their stools (Figure 2). Based on the egg count per gram of stool, the distribution of the intensity of *S. mansoni* infection was as follows: 81.8% of *S. mansoni*-infected participants had light infections (1–99 eggs/g), 9.1% of moderate infections (100–399 eggs/g), and 9.1% heavy infections (> 400 eggs/g; Gomes et al., 2017). Besides the detection of *S. mansoni* infection, KK also enables the detection in stools of the eggs of soil-transmitted helminths (STH). In this study, the presence of the nematode *Ascaris lumbricoides* was detected in six individuals (1.5% of all participants), and unspecified hookworms in one individual (0.2%). The occurrence of multiple infections (i.e., simultaneous coinfection of the same individual with both *S. mansoni* and STH) was not detected.

Immunological tests

POC-CCA identified 122 (30.5%) individuals as positive for the presence of circulating cathodic antigen (when also including the trace outcome; Figure 2). Serological tests were conducted to detect the presence of IgG antibodies in the sera of the study population. The commercial ELISA kit classified 163 individuals as positive (40.8% of the total study population), while 53% (212/400) had a non-reactive serum, and the remaining 6.3% (25/400) had indeterminate results, with both of the latter groups being considered negative for the purposes of the current study. A positivity rate of 33% (132/400) was observed when the ELISA EPI was performed, with 65.8% (263/400) of samples non-reactive and 1.3% (5/400) indeterminate results. Similarly, a positivity rate of 33.8% (135/400) was observed when the ELISA PPE was used. When this latter test was performed 65% (260/400) of samples were non-reactive and 1.3% (5/400) showed indeterminate results. The ELISA EPI and PPE had highly concordant results according to McNemar's test ($p = 0.901$; Figure 2).

Nucleic Acid Amplification Tests

NAATs applied to stool samples showed at least a three-fold increase in the schistosomiasis positivity rate compared to KK results. The LAMP assay had the highest positivity rate of the molecular methods of 30.8%, detecting the presence of the parasite DNA in 123 individuals. PCR-ELISA and qPCR also had notably higher positivity rates than KK of 18.5% (74/400) and 16.5% (66/400), respectively (Figure 2). There was evidence of agreement between the results of the PCR-ELISA and qPCR when applying McNemar's test ($p = 0.322$).

The positivity rate observed using LAMP assay on urine samples was relatively high, although lower than that observed when POC-CCA was used, with positive results for 22% of the study population (89/400). In contrast, the positivity rates observed when either PCR or qPCR were used on the urine samples were much lower, although similar to one another, being 6% (24/400) and 5.2% (21/400), respectively (Figure 2). Accordingly, McNemar's test only indicated an agreement between the results of the PCR and qPCR tests ($p = 0.728$).

Chemical analysis of the urine

All urine samples were submitted to chemical analysis using the Combur10 Test® M test strips, enabling detection of leucocytes in the urine from 39 (9.8%), proteins in 36 (9%), hemoglobin in 40 (10%), and nitrite in 19 (4.8%) individuals. For all of these parameters, their absence is the reference value (i.e., that expected in healthy individuals). Alterations in the pH of the urine was detected in 50.3% of the study population, with 36.8% (147/400) of them acidic (pH < 5.5) and 13.5% (54/400) alkaline (pH > 6.5).

TABLE 2 Summary of the demographic data of the study population (*N*=400).

Population characteristics	*n* (400)	%
Age		
6 - 8	35	8.8
9 - 11	40	10.0
12 - 14	38	9.5
15 – 29	93	23.2
30 – 47	95	23.8
48 - 88	99	24.8
Gender		
Female	262	65.5
Male	138	34.5
Previously tested for schistosomiasis		
Yes	258	64.5
No	130	32.5
Did not know	12	3.0
Among those previously tested	***n* (258)**	**%**
Biological material used for previous testing		
Faeces		
Blood	252	97.7
Blood and Faeces	4	1.6
Did not know/ Did not answer	2	0.01
	4	1.6
Previous test result		
Positive	145	56.2
Negative	97	37.6
Did not know	16	6.2
Previous treatment with praziquantel		
Yes	130	89.7
No	15	10.3
Time since previous treatment		
> 1 year	6	4.6
> 3 years	124	95.4

Multiple separate Fisher's Exact Tests were used to evaluate the existence of any individual (i.e., bivariate) associations between (i) each of the five urine parameters described above and (ii) the results of each of the four specific diagnostic tests for *S. mansoni* used on the urine samples (i.e., POC-CCA, LAMP, PCR, and qPCR). A significant association was observed only between the presence of protein in the urine and a negative result in POC-CCA ($p = 0.028$).

Diagnostic test accuracy

The LCA models with two-classes had a smaller BIC statistic compared to models with either one or three classes, therefore the two-classes LCA model was chosen. In this model, class 1 presented higher outcome probabilities for the majority of the tests and was assigned as the 'case group' in this study. The outcome probabilities table is available in Supplementary material 3. The estimated prevalence of schistosomiasis using LCA was 13.4%.

In this study, to evaluate the accuracy of the diagnostic tests, only individuals who presented the combination of test outcomes corresponding to probability higher than 80% of being included in Class 1 were classified within the "case group." As a result, 47 people were considered true positives according to this LCM, with a schistosomiasis prevalence of 12% (95% CI: 9–15%).

LCA was used in this study as the reference standard. Based on this, KK had an estimated sensitivity of 38% and a specificity of 99%. Among all the NAATs methods evaluated in this study, PCR-ELISA, and qPCR, both using stool samples, had the highest estimated values of sensitivity and specificity, being 96 and 92% for PCR-ELISA, and 96 and 94% for qPCR, respectively. Among NAATs performed, the lowest sensitivity rates were observed when using urine samples (6% PCR, 13% qPCR and 19% LAMP). Serological tests had the lowest specificities (67% commercial ELISA kit, 67% ELISA EPI and 69% ELISA PPE), although the commercial ELISA kit also had the highest sensitivity rate (100%). These and the remaining estimated parameters of each diagnostic test evaluated in the current study are listed in Table 3.

Based on the estimated sensitivity and specificity values of each test (Table 3), three different two-step diagnostic approaches are proposed for the active search of infected people in low and moderate endemicity settings (Figure 3). As the serological commercial ELISA kit had the highest sensitivity among all the tests evaluated, being 100% sensitive, this test is considered an excellent option when screening for true-negative individuals. However, considering the low specificity of this test (67%), it is advised to use a second test with high specificity in order to detect the true-positive among the positive results generated by the commercial ELISA kit. NAATs performed on stool had satisfactory specificity, especially PCR-ELISA and qPCR (92 and 94%, respectively), which are good candidates for the second step of the two-step protocol. Although LAMP had a lower specificity (75%) compared to these two latter tests, it is also considered a candidate for the second step due to its simplicity and feasibility of use in the field.

The estimated parameters for each proposition were calculated and are listed in Table 3. The mean value of sensitivity observed for the 11 tests was 70.4% whilst the specificity was 89.5%, as illustrated in Figure 4. The sensitivity of all three propositions was higher than the general estimated value. Proposition 2 (commercial ELISA kit + LAMP_stool) showed the lowest sensitivity value of 72%, while Propositions 1 and 3 had higher, sensitivity values of 96%. With regard to specificity, all three proposed two-step approaches had similar values ranging from the lowest of 91% (Proposition 2) to the highest of 98% (Proposition 1) and were higher than the general estimated value (89.5%). Propositions 1 (commercial ELISA kit + qPCR_stool)

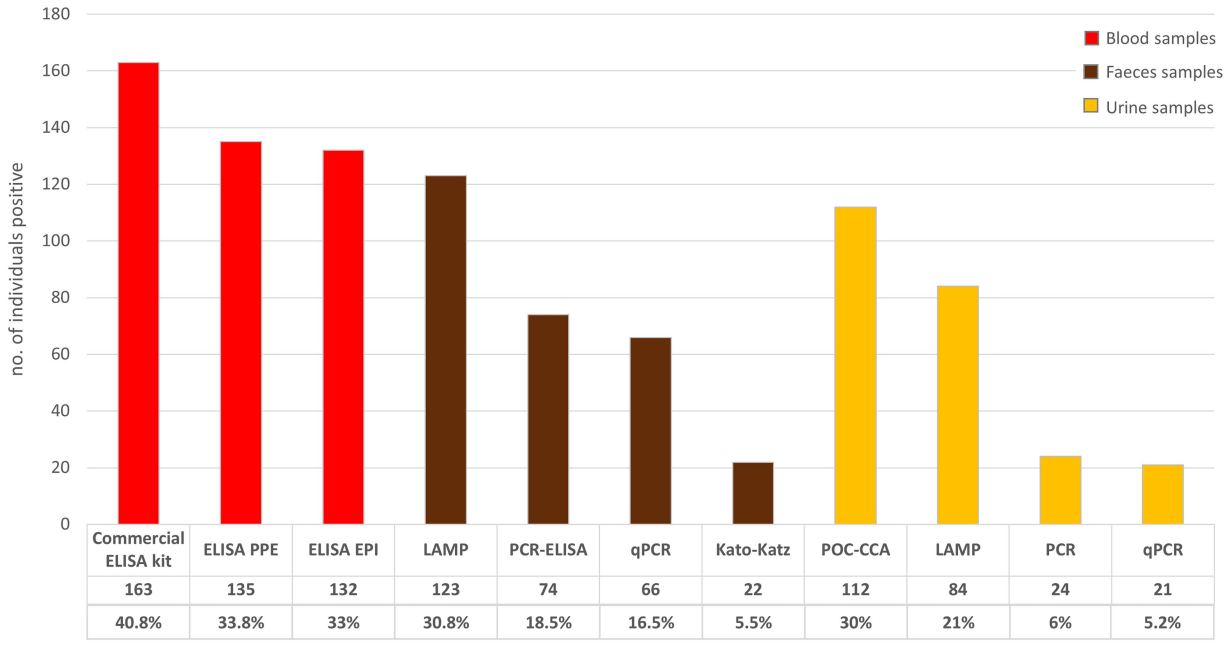

FIGURE 2
Detection of schistosomiasis infection according to different diagnostic tests and sample types. POC-CCA positive results include trace outcome and serologically negative results include indeterminate results.

and 3 (commercial ELISA kit + PCR-ELISA_stool) are the most promising candidate methods, with Proposition 1 marginally preferable it has a higher accuracy compared to Proposition 3 (98 and 96%, respectively).

Regarding the costs of each diagnostic test, Kato-Katz had the lower cost (US$ 0.97), followed by LAMP (US$ 2.39), PCR (US$ 2.73), ELISA tests (US$ 2.70–3.26), PCR-ELISA (US$ 4.61), qPCR (US$ 5.14) and POC-CCA (US$ 7.14; Table 3). The two-step diagnosis approach provided similar performance than molecular tests alone with lower costs (Table 3).

Discussion

There is an urgent need to eliminate schistosomiasis as a public health problem, and precisely diagnosing infected people is vital to achieve this goal. Given the current absence of a standard reference test, and the difficulties of diagnosing the infection in low endemicity areas, we sought to evaluate the performance of 11 diagnostic tests for the detection of *Schistosoma mansoni* infection using the occurrence of infection estimated by latent class analysis (LCA) as the reference standard. LCA is a statistical approach that has been successfully used to assess the accuracy of diagnostic methods for a range of diseases, including schistosomiasis (Ibironke et al., 2012; Colley et al., 2013; Beltrame et al., 2017; Clements et al., 2017; Ferreira et al., 2017; Koukounari et al., 2021). The latent class model (LCM) developed here enabled the estimation of a 12% (95% CI: 9–15%) schistosomiasis prevalence in the borough of Santa Rita, in Malacacheta, Minas Gerais, Brazil. Our findings also enabled the proposition of three different two-step approaches for the accurate diagnosis of *S. mansoni* infection in moderate and low endemicity settings.

We aimed to include a heterogeneous population in our study, with regard to age and gender, in order to enable extrapolation and translation of our findings to other settings. More than 64% of participants reported a past examination for schistosomiasis, with a positive test result for most of them.

Kato-Katz (KK) test is recommended by both the WHO and the Brazilian Ministry of Health (Gomes et al., 2017), for individual diagnosis and epidemiological surveys. In the present study, KK detected *S. mansoni* eggs in stool samples from 22 individuals, with a positivity rate of 5.5%. More than 80% of the KK-positive individuals presented light infections (less than 99 eggs/g). Due to the low sensitivity of KK in low endemicity settings, especially with regard to its ability to detect low intensity infections, it is expected that some infected people have been misdiagnosed as false-negative (McManus et al., 2018; Weerakoon et al., 2018).

In this study, the estimated parameters obtained confirmed that KK has a high specificity (99%) but insufficient sensitivity (38%). This lack of sensitivity is especially critical in regard to control and elimination strategies. According to the WHO, preventive chemotherapy (PC) through mass drug administration (MDA) of praziquantel remains the main strategy for schistosomiasis control and elimination, and to whom PC will be delivered depends on the prevalence of infection in the treated region (Lo et al., 2022). Therefore, timely treatment may be denied

TABLE 3 Estimated parameters of the 11 individual diagnostic tests evaluated, and the three 2-step diagnostic approaches proposed for the active search of infected people in moderate and low endemicity areas, in the current study.

Tests	Case (LCA)		Estimated Parameters									Cost/ Sample (USD) **
	YES	NO	p*	P	sn	sp	PPV	NPV	LR+	LR-	ac	
POC-CCA			0.30	0.12	0.57	0.73	0.22	0.93	2.13	0.58	0.71	7.14
+	27	95	LI=0.26	LI=0.09	LI=0.42	LI=0.68	LI=0.15	LI=0.89	LI=1.58	LI=0.42	LI=0.67	
-	20	258	LS=0.35	LS=0.15	LS=0.72	LS=0.78	LS=0.31	LS=0.96	LS=2.88	LS=0.82	LS=0.76	
LAMP_urine			0.22	0.12	0.19	0.77	0.10	0.88	0.84	1.05	0.70	2.39
+	9	80	LI=0.18	LI=0.09	LI=0.09	LI=0.73	LI=0.05	LI=0.84	LI=0.46	LI=0.90	LI=0.66	
-	38	277	LS=0.27	LS=0.15	LS=0.33	LS=0.82	LS=0.18	LS=0.91	LS=1.57	LS=1.21	LS=0.75	
PCR_urine			0.06	0.12	0.06	0.94	0.12	0.88	1,07	1.00	0.84	2.73
+	3	21	LI=0.04	LI=0.09	LI=0.01	LI=0.91	LI=0.03	LI=0.85	LI=0.33	LI=0.92	LI=0.80	
-	44	332	LS=0.09	LS=0.15	LS=0.18	LS=0.96	LS=0.32	LS=0.91	LS=3.46	LS=1.08	LS=0.87	
qPCR_urine			0.05	0.12	0.13	0.96	0.29	0.89	3.00	0.91	0.86	5.14
+	6	15	LI=0.03	LI=0.09	LI=0.05	LI=0.93	LI=0.11	LI=0.86	LI=1.23	LI=0.81	LI=0.82	
-	41	338	LS=0.08	LS=0.15	LS=0.26	LS=0.98	LS=0.52	LS=0.92	LS=7.36	LS=1.02	LS=0.89	
Kato-Katz			0.06	0.12	0.38	0.99	0.82	0.92	33.80	0.62	0.92	0.97
+	18	4	LI=0.03	LI=0.09	LI=0.25	LI=0.97	LI=0.60	LI=0.89	LI=11.95	LI=0.50	LI=0.89	
-	29	349	LS=0.08	LS=0.15	LS=0.54	LS=1.00	LS=0.95	LS=0.95	LS=95.60	LS=0.78	LS=0.94	
LAMP_stool			0.31	0.12	0.72	0.75	0.28	0.95	2.87	0.37	0.74	2.39
+	34	89	LI=0.26	LI=0.09	LI=0.57	LI=0.70	LI=0.20	LI=0.92	LI=2.23	LI=0.23	LI=0.70	
-	13	264	LS=0.36	LS=0.15	LS=0.84	LS=0.79	LS=0.36	LS=0.97	LS=3.69	LS=0.59	LS=0.79	
PCR-ELISA_stool			0.18	0.12	0.96	0.92	0.61	0.99	11.65	0.05	0.92	4.61
+	45	29	LI=0.15	LI=0.09	LI=0.85	LI=0.88	LI=0.49	LI=0.98	LI=8.18	LI=0.01	LI=0.89	
-	2	324	LS=0.23	LS=0.15	LS=0.99	LS=0.94	LS=0.72	LS=1.00	LS=16.60	LS=0.18	LS=0.95	
qPCR_stool			0.16	0.12	0.96	0.94	0.68	0.99	16.09	0.05	0.94	5.14
+	45	21	LI=0.13	LI=0.09	LI=0.85	LI=0.91	LI=0.56	LI=0.98	LI=10.58	LI=0.01	LI=0.91	
-	2	332	LS=0.21	LS=0.15	LS=0.99	LS=0.96	LS=0.79	LS=1.00	LS=24.47	LS=0.18	LS=0.96	
ELISA-EPI			0.33	0.12	0.32	0.67	0.11	0.88	0.96	1.02	0.63	3.26
+	15	117	LI=0.28	LI=0.09	LI=0.19	LI=0.62	LI=0.07	LI=0.84	LI=0.62	LI=0.83	LI=0.58	
-	32	236	LS=0.38	LS=0.15	LS=0.47	LS=0.72	LS=0.18	LS=0.92	LS=1.50	LS=1.26	LS=0.68	
ELISA-PPE			0.34	0.12	0.53	0.69	0.19	0.92	1.71	0.68	0.67	2.70
+	25	110	LI=0.29	LI=0.09	LI=0.38	LI=0.64	LI=0.12	LI=0.88	LI=1.25	LI=0.50	LI=0.62	
-	22	243	LS=0.39	LS=0.15	LS=0.68	LS=0.74	LS=0.26	LS=0.95	LS=2.33	LS=0.93	LS=0.72	
commercial-ELISA			0.41	0.12	1.00	0.67	0.29	1.00	3.04		0.71	2.81
+	47	116	LI=0.36	LI=0.09	LI=0.92	LI=0.62	LI=0.22	LI=0.98	LI=2.62	-	LI=0.66	
-	0	237	LS=0.46	LS=0.15	LS=1.00	LS=0.72	LS=0.36	LS=1.00	LS=3.53		LS=0.75	
Proposition 1			0.13	0.12	0.96	0.98	0.87	0.99	48.28	0.04	0.98	4.90
+	45	7	LI=0.10	LI=0.09	LI=0.85	LI=0.96	LI=0.74	LI=0.98	LI=23.13	LI=0.01	LI=0.96	
-	2	346	LS=0.17	LS=0.15	LS=0.99	LS=0.99	LS=0.94	LS=1.00	LS=100.78	LS=0.17	LS=0.99	
Proposition 2			0.16	0.12	0.72	0.91	0.52	0.96	7.98	0.30	0.89	3.78
+	34	32	LI=0.13	LI=0.09	LI=0.57	LI=0.87	LI=0.39	LI=0.93	LI=5.49	LI=0.19	LI=0.85	
-	13	321	LS=0.21	LS=0.15	LS=0.84	LS=0.94	LS=0.64	LS=0.98	LS=11.61	LS=0.48	LS=0.92	
Proposition 3			0.15	0.12	0.96	0.96	0.75	0.99	22.53	0.04	0.96	4.69
+	45	15	LI=0.12	LI=0.09	LI=0.85	LI=0.93	LI=0.62	LI=0.98	LI=13.68	LI=0.01	LI=0.93	
-	2	338	LS=0.19	LS=0.15	LS=0.99	LS=0.98	LS=0.85	LS=1.00	LS=37.11	LS=0.17	LS=0.98	

LI = limit inferior of the 95% confidence interval; LS = limit superior of the 95% confidence interval; prevalence; *p** = positivity rate; p = prevalence; sn = sensitivity; sp. = specificity; PPV = positive predictive value; NPV = negative predictive value, LR+ = positive likelihood ratio; LR– = negative likelihood ratio; ac = accuracy; ** cost/sample column does not include the price of equipment needed, personnel, and DNA extraction kits. The cost of each test was calculated according to the US Dollar exchange rate for 27/07/2022 from the Central Bank of Brazil (https://www.bcb.gov.br/) when 1 USD = 5.3068 BRL.

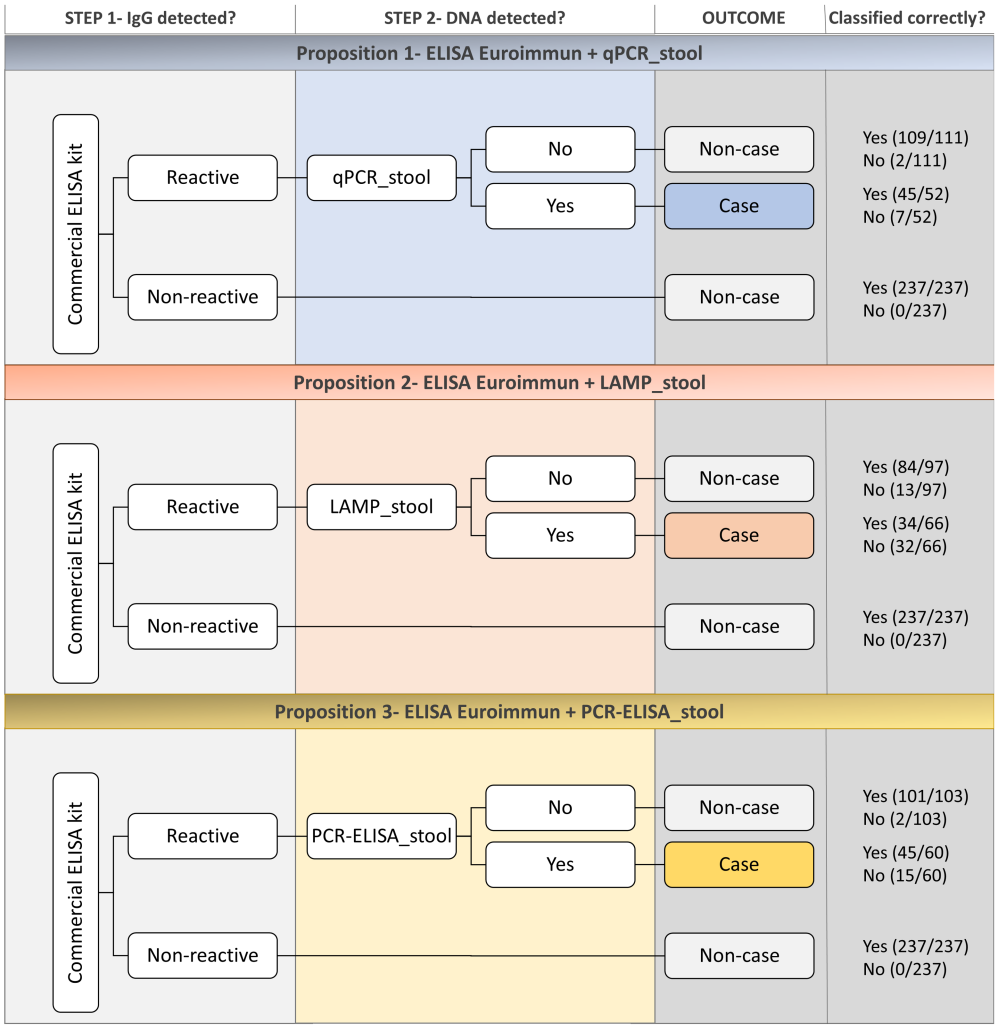

FIGURE 3
Flowchart illustrating the three different two-step diagnostic approaches proposed for the active search of infected people in endemic areas.

to those in need if the true prevalence is underestimated. It is important to reinforce that even low intensity infections are associated with morbidity (King, 2015), as well as parasite cycle maintenance.

Nucleic Acids Amplification Tests (NAATs) are highly sensitive alternatives to microscopic egg detection. Stool samples are usually used as the source of *S. mansoni* genetic material, and a pre-analytical phase is necessary to extract the DNA from eggs and remove inhibitors that can hamper the performance of NAATs. Nucleic acid extraction is an important process, which often requires additional steps to facilitate egg disruption (Pomari et al., 2019). PCR-based methods are more influenced by the presence of inhibitors than isothermal methods (Panzner, 2022). In the present study, qPCR, PCR-ELISA and LAMP were performed using stool samples. PCR-ELISA and qPCR, both targeting the highly repetitive nuclear region termed as *Sm1-7*, had similar positivity rates of 18 and 16%. An agreement was observed between the results of these two methods, probably due to their shared target. The LAMP assay detects the *S. mansoni* mitochondrial minisatellite region (named here *SmMIT*) and had a positivity rate of 31%. Promisingly, PCR-ELISA and qPCR had high sensitivities (96%) and specificity estimates (92 and 94%, respectively). The increased sensitivity of PCR-based methods compared to parasitological diagnosis was expected, in accordance with the findings from previous studies (Espírito-Santo et al., 2014; Siqueira et al., 2015; Senra et al., 2018; do Magalhães et al., 2020; Siqueira et al., 2021; Panzner, 2022). Although highly accurate, qPCR and PCR-ELISA are less field-friendly due to the need for technological equipment, experienced personnel to perform and interpret the results, and the time and costs involved (Li et al., 2021). Isothermal methods have recently become increasingly popular, as promising alternatives for the molecular detection of *S. mansoni* instead of PCR (Fernández-Soto et al., 2014; Gandasegui et al., 2018; García-Bernalt Diego et al., 2019). LAMP is a fast, simple, accurate and field-friendly isothermal method, which can be used at the point-of-care (POC; Notomi

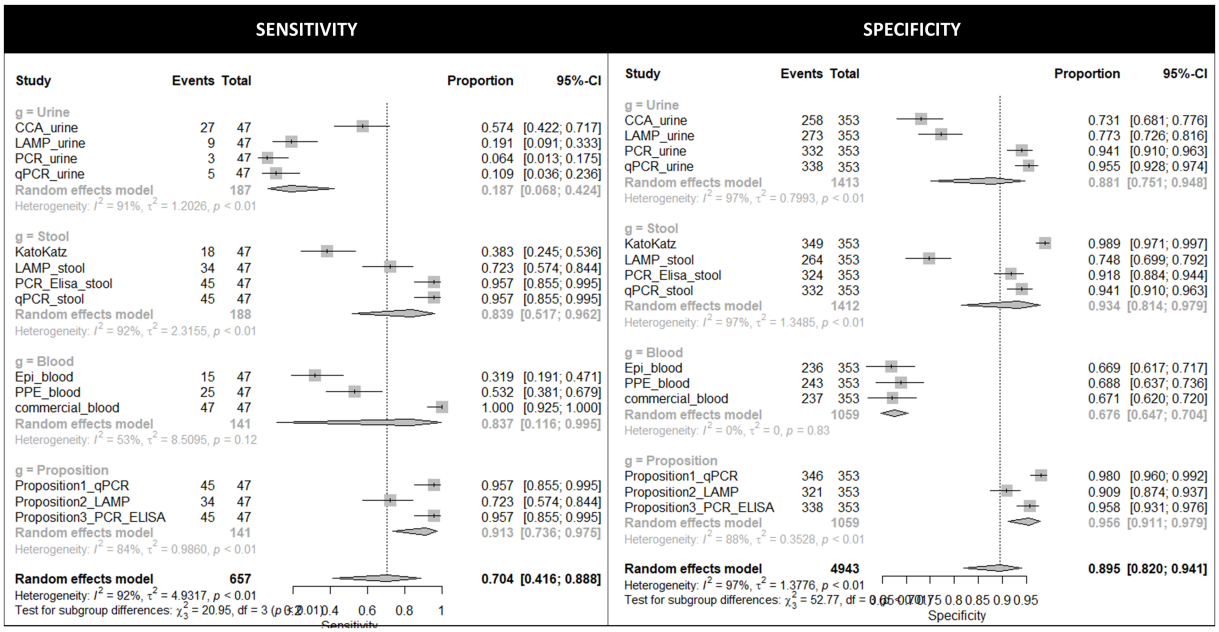

FIGURE 4
Forest plots illustrating the estimated sensitivity and specificity of the 11 individual diagnostic tests evaluated, and the three two-step diagnostic approaches proposed, in this study.

et al., 2000; Panzner, 2022). In contrast to previous reports, in this study, LAMP was less sensitive (72%) and specific (75%). Each NAAT assessed in this study has a different limit of detection, with LAMP being able to detect down to 100 fg (Fernández-Soto et al., 2014), PCR-ELISA 1.3 fg (Gomes et al., 2010) and qPCR 0.37 fg (Siqueira et al., 2021). The analytical sensitivity of the assays surely affected the accuracy observed. Given the POC potential of LAMP, future optimization of this assay is advised.

Alternatively, urine samples can also be used for *S. mansoni* detection. A chemical analysis of the urine was conducted to investigate whether the alterations in the standard parameters of the urine influence the outcome of the tests performed using urine samples. Among all the alterations observed, only the presence of protein was associated with a negative outcome of POC-CCA ($p = 0.028$). A previous study assessed variation in urine parameters and their association with the results of POC-CCA, in urine samples where leucocytes were detected it was less expected to observe a positive POC-CCA outcome (Graeff-Teixeira et al., 2021).

The commercially available POC-CCA test detects by lateral flow assay the circulating cathodic antigen released by *S. mansoni* in urine samples. Previous studies have shown that POC-CCA has a higher accuracy when compared to KK in high and moderate endemicity regions (Kittur et al., 2016; Bezerra et al., 2018; Viana et al., 2019). Nevertheless, POC-CCA may give ambiguous results, referred to as 'trace', which consists of a weak test line, with no consensus of whether it should be considered as a positive or negative result. Although the manufacturer of this test recommends trace results to be considered positive, there is little evidence of an association between this outcome and the actual presence of infection (Coelho et al., 2016). It has been stated that some illness, use of medicines, and excessive alcohol intake may influence the test result, especially with regard to trace outcomes (Ferreira et al., 2017). Here, 33 individuals were classified as positive by POC-CCA with a clear and strong signal, and 56 trace results. We followed the manufacturer's instructions and considered the trace results as positives, raising the positive rate from 8.2% (when traces considered negative) to 30% (when traces considered positive). When compared to KK, the POC-CCA test presented a 4-fold increase in positivity. POC-CCA presented a positivity rate of 30%, 3 times higher than the actual prevalence of 12% estimated by LCA. As previously mentioned, the performance of POC-CCA may vary according to the schistosomiasis prevalence and intensity of infection. Besides this, the test is less accurate among people with light infections and in low endemicity areas (Viana et al., 2019; da Ramírez et al., 2020) and may present false-positive results in non-endemic areas (Graeff-Teixeira et al., 2021). The outcome of POC-CCA from Eco Diagnóstica can also be influenced by the batch used (Viana et al., 2019). Furthermore, cross-reactivities have been reported previously due to pregnancy, neoplasia, autoimmune diseases, and other infections, including with soil transmitted helminths (STH; Coelho et al., 2016; Bezerra et al., 2018). However, in the present study, all the individuals positive for STH by KK were POC-CCA-negative.

Besides antigens, urine is also the source of *S. mansoni* cell-free DNA (cfDNA), extracellular DNA fragments which can also be found in serum, and saliva. The origin of cfDNA is still unclear, but it is believed to be released after cellular degradation,

apoptosis, or necrosis. The amount of cfDNA present in body fluids is associated with the intensity of parasite infection (Weerakoon and McManus, 2016). The performance of NAATs for cfDNA detection is dependent on accurate selection of the target (Ullah et al., 2021) which can be both the nuclear and/or mitochondrial DNA (Ullah et al., 2022). Several authors described the effective diagnosis of intestinal schistosomiasis by detecting cfDNA in urine and serum samples using different molecular methodologies (Ullah et al., 2022). The presence of *S. japonicum* cfDNA has been detected by PCR in mice as soon as the first week of infection, and by LAMP in rabbits 3 days-post-infection (Gomes et al., 2014; Xu et al., 2015). *Schistosoma haematobium* cfDNA becomes undetectable 2 weeks after treatment with praziquantel (Ibironke et al., 2012). Diagnostic tests based on the presence of eggs in stools are dependent on worm copulation and oviposition, which happens within 40 days-post-infection. Therefore, novel diagnostic methods based on cfDNA may enable the detection of the infection in the prepatent stage of schistosomiasis infection (Ullah et al., 2022). Three NAATs assays were conducted in this study to detect the presence of cfDNA in urine samples, two of them targeting the nuclear *Sm1-7* region and one targeting the *SmMIT* region. In the present study, qPCR and PCR assays targeted the *Sm1-7* region, and had positivity rates of 5 and 6%, respectively, whilst LAMP targeted the *SmMIT* region and had a positivity rate of 22.3%. As observed NAATs using stool samples, methods targeting the same region presented concordant results (i.e., PCR and qPCR; $p = 0.728$). The sensitivity estimates of the urine-based assays were very low, being 19% (LAMP), 13% (qPCR) and 6% (PCR). The unsatisfactory performances observed could be explained by the absence of the target regions in the urine. Nevertheless, previous studies have confirmed that *Sm1-7* (Lodh et al., 2013) and *SmMIT* (Fernández-Soto et al., 2019) markers can be detected in the urine from *S. mansoni*-infected people. Another possible explanation could be some aspect of the pre-analytical stage. However, the clinical urine samples collected here from the study population were processed according to the protocol described by Lodh et al. (2017). Additionally, prior to the application of this protocol on clinical samples, we had successfully validated it in the laboratory using spiked urine samples (data not shown). Given the convenience of urine collection, and the promising results reported by several authors, further investigation should be conducted to optimize the use of cfDNA from urine samples, as a target of NAATs for schistosomiasis diagnosis.

ELISA assays are high throughput tests widely used for the detection of specific antigens and antibodies in blood samples. Immunodiagnostics using antibody detection is more sensitive than KK and particularly useful for monitoring areas of controlled transmission and for the diagnosis of travelers (Cavalcanti et al., 2013). However, they often have low specificity, especially in endemic areas, as they may not be able to differentiate between past and current infection (Weerakoon et al., 2018; Ogongo et al., 2022). It is believed that in endemic areas, all residents will eventually be infected with *S. mansoni* at some point during their lives, thus, it might influence the performance of serological tests in those settings (LoVerde, 2019). The appropriate choice of parasite antigens to be used in ELISA assays is challenging, but vital for the development of accurate tests (Carvalho et al., 2017). The use of recombinant antigens is a promising alternative to increase specificity (Gomes et al., 2014). In the present study, three anti-IgG ELISA tests were conducted, one being a commercially available test (anti-*Schistosoma mansoni* IgG ELISA kit from Euroimmun) and the other two in-house tests: the ELISA EPI using the Smp150390.1 (216–230) peptide, and the ELISA PPE using the recombinant PPE antigens). Carvalho et al. (2017) reported the Smp150390.1 (216–230) peptide as capable of differentiating positive and negative individuals from endemic areas, and negative individuals from non-endemic areas, as well as being less reactive after treatment. Likewise, the recombinant PPE antigen was able to differentiate positive and negative sera (personal communication). The in-house tests employed in the present study provided similar positivity rates of 33% for the ELISA EPI assay and 33.8%, for ELISA PPE, with concordant results. The commercial ELISA kit presented the highest positivity rate of 40.8%. All the serological tests presented low and similar specificity estimates, with commercial ELISA and ELISA EPI kit presenting the lowest (67%), followed by ELISA PPE (69%). Regarding the estimated sensitivity, ELISA EPI was the least sensitive immunoassay (32%) followed by ELISA PPE (53%), while the commercial ELISA kit had a 100% sensitivity, the highest value among all 11 tests assessed. Our results demonstrate that as antigen complexity increases, sensitivity also increases. ELISA EPI test uses as an antigen one epitope from the parasite, ELISA PPE detects the immune response against several epitopes from one parasite protein, while the commercial ELISA kit detects antibody reactivity against epitopes from several proteins of the parasite egg. Therefore, the commercial ELISA kit may be a good candidate test for screening in the absence of the disease, but it will likely provide false-positive results due to either cross-reactivity or detection of past infections.

The recently launched WHO Guidelines on Control and Elimination of Human Schistosomiasis (World Health Organization, 2022) considered the use of a two-step diagnostic approach to detect *S. mansoni* infection, as a strategy for a more accurate diagnosis, especially in low endemicity areas. The combination of multiple tests has been previously evaluated by many authors to increase the accuracy of schistosomiasis detection (Alarcón de Noya et al., 2007; Carneiro et al., 2013; Gomes et al., 2014). We propose in this study three different two-step diagnostic approaches based on the sensitivity and specificity estimates of the 11 individual tests evaluated. The propositions combine the examination of serum samples using the commercial ELISA kit from Euroimmun for the accurate detection of all negative individuals, followed by the molecular detection of *S. mansoni* DNA in stool samples either by (i) qPCR, (ii) LAMP, or (iii) PCR-ELISA, for the accurate detection of true-positive individuals. Overall, the two-step approaches proposed provided similar sensitivity and specificity values observed when using the NAATs

alone but with lower costs. Therefore, the cost-effectiveness of the two-step approaches justify their use.

The implementation of novel diagnostic tests is often associated with increased cost. NAATs are usually more expensive than other tests due to the equipment requirement and sample preparation step. The costs associated with the DNA extraction increases substantially the price of each test. For instance, in the present study, the cost for DNA extraction ranged from 8.34 to 16.94 USD for each stool sample. By combining different tests, as suggested in the Proposition 1 (Figure 3), an economy of up to 4,100 USD could be made to examine the whole study population, keeping similar accuracy estimates. Schistosomiasis generates an estimated annual cost of nearly 41 million USD, which could be avoided by properly diagnosing infected people and providing timely treatment with praziquantel (Nascimento et al., 2019). Through these means, besides the economic savings, the health and social burden would also be overcome. Additionally, in the long-term, as the demand for the new products increases the prices tend to decrease (Turner et al., 2017).

Currently, the WHO recommends MDA with praziquantel to every person with 2 or more years of age in areas where the schistosomiasis prevalence is higher than 10% (Lo et al., 2022; World Health Organization, 2022). If KK was the only test result considered, MDA would not be conducted in the study area. The three 2-step protocols proposed in this study have observed prevalence of (i) 13%, (ii) 16%, and (iii) 15%. Therefore, the application of any of these approaches would result in the delivery of PCs to the whole study population regardless of which of the three 2-step protocols were used. Nevertheless, there is evidence that in some low endemicity areas, a relevant hurdle to the MDA strategy is community compliance, and the uptake of praziquantel in the absence of a positive test. In this scenario, the test-and-treat strategy is more targeted and may therefore be more acceptable to the treated population, as well as even more economically justified (Parker et al., 2008; Parker and Allen, 2011; Dabo et al., 2013; Mazigo et al., 2018).

It is believed that the persistence of schistosomiasis transmission is related not only to lack of sanitation and limited access to health care, but also to misdiagnosis of infected individuals with light infections that lead to delayed or absence of timely treatment (da Silva et al., 2022). Thus, to meet the WHO goal of eliminating schistosomiasis as a public health problem by 2030, it is undeniable that diagnostic improvements are necessary and should be prioritized, especially in low endemicity settings.

Study limitations

The absence of a standard reference test or absolute knowledge of the true positives is a significant limitation, but also the motivation for the research itself. We have overcome this inherent limitation by using LCA to evaluate the diagnostic tests, but the LCA estimated occurrence of infection is influenced by the particular outcome of each test conducted. In addition, this was a cross-sectional study. If a longitudinal study had been conducted, probably a higher prevalence of infection would have been observed given the known daily fluctuation of *S. mansoni* oviposition. Another limitation of our work is the use of three different kits for the DNA extraction from stool samples. The QIAamp DNA Stool Mini Kit has been previously used by members of our team and provided satisfactory results. As production of this kit has been discontinued, we had no choice but to utilize other methods, but this effect was minimized by using two different commercial kits from the same manufacturer. It is reported in the literature that co-infections could influence the outcome of some schistosomiasis diagnosis tests, for instance, HIV impact on the elimination of egg within the feces. However, in this study we did not collected information regarding co-infections other than the ones detected in the Kato-Katz method, therefore we could not address this issue.

Data availability statement

The original contributions presented in the study are included in the article/Supplementary material, further inquiries can be directed to the corresponding author.

Ethics statement

The studies involving human participants were reviewed and approved by Ethical Committee of the René Rachou Institute (IRR, Fiocruz Minas), CAAE 76273317.3.0000.5091, and approval numbers 2.400.880, 2.803.752, 3.802.104 and 3.918.849; and (ii) the Ethical Committee of the Oswaldo Cruz Institute (IOC, Fiocruz), CAAE 76273317.3.3001.5248, and approval number 2.426.395. Written informed consent to participate in this study was provided by participants or by the participants' legal guardian/next of kin.

Author contributions

RC, TF, CM, LB, MM, EO, RS-P, and CF: conceptualization. SM, RC, TF, CM, LB, GC, FN, GO, LL, MA, EO, RS-P, and CF: methodology and investigation. TS and CF: formal analysis. RC, TF, OC, MM, EO, RS-P, and CF: resources. RC, TF, CM, LB, TS, GC, MM, EO, RS-P, and CF: data curation. SM, TF, CM, LB, TS, EO, RS-P, and CF: writing—original draft. SM, RC, TF, CM, LB, TS, OC, MM, EO, RS-P, and CF: writing – editing. RC, TF, CM, LB, TS, GC, FN, GO, LL, MA, OC, MM, EO, RS-P, and CF: writing—review. SM and TS: visualization. RC and CF: supervision. RC and CF: project administration. RS-P and CF: funding acquisition. All authors contributed to the article and approved the submitted version.

Funding

This study was financed in part by: René Rachou Institute (IRR-Fiocruz), Oswaldo Cruz Institute (IOC-Fiocruz); Conselho Nacional de Desenvolvimento Científico/Programa de Excelência em Pesquisa—Pesquisa e Ensaios Clínicos (PROEP/PEC; 420685/2017-0); Fundação de Amparo à Pesquisa do Estado de Minas Gerais (FAPEMIG; APQ-01596-16 e APQ-00875-18). SGM is funded by Coordenação de Aperfeiçoamento de Pessoal de Nível Superior-Brasil (CAPES)—Finance Code 001; CAPES Print-Fiocruz Program, and Vice-Presidência de Educação, Informação e Comunicação (VPEIC-Fiocruz); CNPq (Fellowship Grant number: CTF-303131/2018-7; EO-313471/2019-3; MMM—317389/2021-1).

Acknowledgments

We would like to thank: the participants of the study who kindly engaged with high adherence to this research; the Secretariat of Education and the Secretariat of Health of the municipality of Malacacheta for their support of this research and for kindly providing the space for our field work; the community health agents for their noteworthy help during the recruitment, questionnaire survey and sample collection; the technicians who helped with the preparation of the stool samples and reading of the slides; Roberto Sena Rocha for his contribution on the conceptualization of the study; the 3D Print Facility of IRR for providing the 3D-printed models used for subsampling 500 mg of the stools; the Clinical Research Platform of Fiocruz for training and guiding the research team with regard to study protocols and good clinical practices, also for generating and managing the study database; and Luke Baton for language revision of the manuscript.

Conflict of interest

The authors declare that the research was conducted in the absence of any commercial or financial relationships that could be construed as a potential conflict of interest.

Publisher's note

All claims expressed in this article are solely those of the authors and do not necessarily represent those of their affiliated organizations, or those of the publisher, the editors and the reviewers. Any product that may be evaluated in this article, or claim that may be made by its manufacturer, is not guaranteed or endorsed by the publisher.

Supplementary material

The Supplementary material for this article can be found online at: https://www.frontiersin.org/articles/10.3389/fmicb.2022.1048457/full#supplementary-material

References

Alarcón de Noya, B., Ruiz, R., Losada, S., Colmenares, C., Contreras, R., Cesari, I. M., et al. (2007). Detection of schistosomiasis cases in low-transmission areas based on coprologic and serologic criteria. The Venezuelan experience. *Acta Trop.* 103, 41–49. doi: 10.1016/j.actatropica.2007.04.018

Alonzo, T., and Pepe, M. (1999). Using a combination of reference tests to assess the accuracy of a diagnostic test. *Stat. Med.* 18, 2987–3003. doi: 10.1002/sim.762

Andriolo, AÁP, de Machado, AMO, da Fonseca, AA, Antunes, BV, Bichara, CDA, dos Ferreira, CES, et al. (2017) Recomendações da Sociedade Brasileira de Patologia Clínica/Medicina Laboratorial (SBPC/ML): Realização de exames em urina. Barueri, SP: Manole, 306.

Balduzzi, S., Rücker, G., and Schwarzer, G. (2019). How to perform a meta-analysis with R: a practical tutorial. *Evid. Based Ment. Heal.* 22, 153–160. doi: 10.1136/ebmental-2019-300117

Barendregt, J. J., Doi, S. A., Lee, Y. Y., Norman, R. E., and Vos, T. (2013). Meta-analysis of prevalence. *J. Epidemiol. Community Health* 67, 974–978. doi: 10.1136/jech-2013-203104

Beath, K. J. (2017). Random LCA: an R package for latent class with random effects analysis. *J. Stat. Softw.* 81, 1–25. doi: 10.18637/jss.v081.i13

Beltrame, A., Guerriero, M., Angheben, A., Gobbi, F., Requena-Mendez, A., Zammarchi, L., et al. (2017). Accuracy of parasitological and immunological tests for the screening of human schistosomiasis in immigrants and refugees from African countries: an approach with latent class analysis. *PLoS Negl. Trop. Dis.* 11, e0005593–e0005515. doi: 10.1371/journal.pntd.0005593

Berhe, N., Medhin, G., Erko, B., Smith, T., Gedamu, S., Bereded, D., et al. (2004). Variations in helminth faecal egg counts in Kato-Katz thick smears and their implications in assessing infection status with *Schistosoma mansoni*. *Acta Trop.* 92, 205–212. doi: 10.1016/j.actatropica.2004.06.011

Bezerra, F. S. M., Leal, J. K. F., Sousa, M. S., Pinheiro, M. C. C., Ramos, A. N., Silva-Moraes, V., et al. (2018). Evaluating a point-of-care circulating cathodic antigen test (POC-CCA) to detect *Schistosoma mansoni* infections in a low endemic area in North-Eastern Brazil. *Acta Trop.* 182, 264–270. doi: 10.1016/j.actatropica.2018.03.002

Borenstein, M., Hedges, L. V., Higgins, J. P. T., and Rothstein, H. R. (2010). A basic introduction to fixed-effect and random-effects models for meta-analysis. *Res. Synth. Methods* 1, 97–111. doi: 10.1002/jrsm.12

Bossuyt, P. M., Reitsma, J. B., Bruns, D. E., Bruns, D. E., Glasziou, P. P., Irwig, L., et al. (2015). STARD 2015: an updated list of essential items for reporting diagnostic accuracy studies1. *Radiology* 277, 826–832. doi: 10.1148/radiol.2015151516

Brasil. Vigilância da Esquistossomose Mansoni-Diretrizes técnicas. (2014).

BRASIL M da S. Boletim Epidemiológico-Doenças Tropicais Negligenciadas. (2021). Available at: https://www.gov.br/saude/pt-br/media/pdf/2021/marco/3/boletim_especial_doencas_negligenciadas.pdf (Accessed November 11, 2022)

Carneiro, T. R., Peralta, R. H. S., Pinheiro, M. C. C., de Oliveira, S. M., Peralta, J. M., and Bezerra, F. S. M. (2013). A conventional polymerase chain reaction-based method for the diagnosis of human schistosomiasis in stool samples from individuals in a low-endemicity area. *Mem. Inst. Oswaldo Cruz* 108, 1037–1044. doi: 10.1590/0074-0276130202

Carstensen, B., Plummer, M., Laara, E., and Hills, M. (2022). Epi: Statistical analysis in epidemiology. Available at: https://cran.r-project.org/web/packages/Epi/index.html (Accessed November 11, 2022).

Carvalho, O., Mendonça, C. L. F., Marcelino, J. M. D. R., Jannotti-Passos, L. K., Fernandez, M. A., Leal, R. S., et al. (2018). Geographical distribution of intermediate hosts of *Schistosoma mansoni* in the states of Paraná, Minas Gerais, Bahia, Pernambuco and Rio Grande do Norte, Brazil. *Epidemiol e Serv saúde Rev do Sist Único Saúde do Bras* 27:e2017382. doi: 10.5123/S1679-49742018000300012

Carvalho, G. B. F., Resende, D. M., Siqueira, L. M. V., Lopes, M. D., Lopes, D. O., Coelho, P. M. Z., et al. (2017). Selecting targets for the diagnosis of Schistosoma mansoni infection: an integrative approach using multi-omic and

immunoinformatics data. *PLoS One* 12, e0182299–e0182216. doi: 10.1371/journal.pone.0182299

Cavalcanti, M. G., Silva, L. F., Peralta, R. H. S., Barreto, M. G. M., and Peralta, J. M. (2013). Schistosomiasis in areas of low endemicity: a new era in diagnosis. *Trends Parasitol.* 29, 75–82. doi: 10.1016/j.pt.2012.11.003

Clements, M. N., Donnelly, C. A., Fenwick, A., Kabatereine, N. B., Knowles, S. C. L., Meité, A., et al. (2017). Interpreting ambiguous 'trace' results in *Schistosoma mansoni* CCA tests: estimating sensitivity and specificity of ambiguous results with no gold standard. *PLoS Negl. Trop. Dis.* 11, e0006102–e0006118. doi: 10.1371/journal.pntd.0006102

Coelho, P. M. Z., Siqueira, L. M. V., Grenfell, R. F. Q., Almeida, N. B. F., Katz, N., Almeida, Á., et al. (2016). Improvement of POC-CCA interpretation by using Lyophilization of urine from patients with *Schistosoma mansoni* low worm burden: towards an elimination of doubts about the concept of trace. *PLoS Negl. Trop. Dis.* 10, 1, e0004778–13. doi: 10.1371/journal.pntd.0004778

Collett, D. (2002). *Modelling Binary Data*. London: Chapman and Hall/CRC.

Colley, D. G., Binder, S., Campbell, C., King, C. H., Tchuenté, L. A. T., N'Goran, E. K., et al. (2013). A five-country evaluation of a point-of-care circulating cathodic antigen urine assay for the prevalence of S*chistosoma mansoni*. *Am. J. Trop. Med. Hyg.* 88, 426–432. doi: 10.4269/ajtmh.12-0639

da Ramírez, A. P., Favero, V., Lindholz, C. G., de Veríssimo, C. M., Pascoal, V. F., RRF, C., et al. (2020). Schistosomiasis: an epidemiological update on Brazil's southernmost low endemic area in Esteio. *Rev. Soc. Bras. Med. Trop.* 53:e20200411. doi: 10.1590/0037-8682-0411-2020

da Silva, B. M., Ferreira, A. F., JAM, D. S., de Amorim, R. G., Domingues, A. L. C., Pinheiro, M. C. C., et al. (2022). High schistosomiasis-related mortality in Northeast Brazil: trends and spatial patterns. *Rev. Soc. Bras. Med. Trop.* 55:e0431, 1–8. doi: 10.1590/0037-8682-0431-2021

Dabo, A., Bary, B., Kouriba, B., Sankaré, O., and Doumbo, O. (2013). Factors associated with coverage of praziquantel for schistosomiasis control in the community-direct intervention (CDI) approach in Mali (West Africa). *Infect. Dis. Poverty* 2:11. doi: 10.1186/2049-9957-2-11

do Magalhães, F. C., Resende, S. D., Senra, C., Graeff-Teixeira, C., Enk, M. J., PMZ, C., et al. (2020). Accuracy of real-time polymerase chain reaction to detect *Schistosoma mansoni*–infected individuals from an endemic area with low parasite loads. *Parasitology* 147, 1140–1148. doi: 10.1017/S003118202000089X

Eldridge, S. M., Ashby, D., and Kerry, S. (2006). Sample size for cluster randomized trials: effect of coefficient of variation of cluster size and analysis method. *Int. J. Epidemiol.* 35, 1292–1300. doi: 10.1093/ije/dyl129

Enk, M. J., Lima, A. C. L., Drummond, S. C., Schall, V. T., and Coelho, P. M. Z. (2008). The effect of the number of stool samples on the observed prevalence and the infection intensity with *Schistosoma mansoni* among a population in an area of low transmission. *Acta Trop.* 108, 222–228. doi: 10.1016/j.actatropica.2008.09.016

Espírito-Santo, M. C. C., Alvarado-Mora, M. V., Dias-Neto, E., Botelho-Lima, L. S., Moreira, J. P., Amorim, M., et al. (2014). Evaluation of real-time PCR assay to detect *Schistosoma mansoni* infections in a low endemic setting. *BMC Infect. Dis.* 14:558. doi: 10.1186/s12879-014-0558-4

Favre, T. C., Massara, C. L., Beck, L. C. N. H., Cabello, R. K. S. A. A., and Pieri, O. S. (2021). Adherence to diagnosis followed by selective treatment of schistosomiasis mansoni and related knowledge among schoolchildren in an endemic area of Minas Gerais, Brazil, prior to and after the implementation of educational actions. *Parasite Epidemiol. Control* 13. doi: 10.1016/j.parepi.2021.e00208

Fernández-Soto, P., Gandasegui Arahuetes, J., Sánchez Hernández, A., López Abán, J., Vicente Santiago, B., and Muro, A. (2014). A loop-mediated isothermal amplification (LAMP) assay for early detection of *Schistosoma mansoni* in stool samples: a diagnostic approach in a murine model. *PLoS Negl. Trop. Dis.* 8:e3126. doi: 10.1371/journal.pntd.0003126

Fernández-Soto, P., Gandasegui, J., Rodríguez, C. C., Pérez-Arellano, J. L., Crego-Vicente, B., Diego, J. G. B., et al. (2019). Detection of *Schistosoma mansoni*-derived DNA in human urine samples by loop-mediated isothermal amplification (LAMP). *PLoS One* 14, e0214125–e0214116. doi: 10.1371/journal.pone.0214125

Ferreira, F. T., Fidelis, T. A., Pereira, T. A., Otoni, A., Queiroz, L. C., Amâncio, F. F., et al. (2017). Sensitivity and specificity of the circulating cathodic antigen rapid urine test in the diagnosis of *Schistosomiasis mansoni* infection and evaluation of morbidity in a low-endemic area in Brazil. *Rev. Soc. Bras. Med. Trop.* 50, 358–364. doi: 10.1590/0037-8682-0423-2016

Fuss, A., Mazigo, H. D., Tappe, D., Kasang, C., and Mueller, A. (2018). Comparison of sensitivity and specificity of three diagnostic tests to detect *Schistosoma mansoni* infections in school children in Mwanza region, Tanzania. *PLoS One* 13, 1–14. doi: 10.1371/journal.pone.0202499

Gandasegui, J., Fernández-Soto, P., Muro, A., Simões Barbosa, C., Lopes de Melo, F., Loyo, R., et al. (2018). A field survey using LAMP assay for detection of *Schistosoma mansoni* in a low-transmission area of schistosomiasis in Umbuzeiro, Brazil: assessment in human and snail samples. *PLoS Negl. Trop. Dis.* 12, e0006314–e0006316. doi: 10.1371/journal.pntd.0006314

García-Bernalt Diego, J., Fernández-Soto, P., Crego-Vicente, B., Alonso-Castrillejo, S., Febrer-Sendra, B., Gómez-Sánchez, A., et al. (2019). Progress in loop-mediated isothermal amplification assay for detection of *Schistosoma mansoni* DNA: towards a ready-to-use test. *Sci. Rep.* 9, 14744–14711. doi: 10.1038/s41598-019-51342-2

Gomes, E., Domingues, A., and Barbosa, C. (2017) in *Esquistossomose: manejo clínico e epidemiológico na atenção básica*. ed. F. P. Recife, 144.

Gomes, L. I., dos Marques, L. H. S., Enk, M. J., de Oliveira, M. C., Coelho, P. M. Z., and Rabello, A. (2010). Development and evaluation of a sensitive PCR-ELISA system for detection of Schistosoma infection in feces. *PLoS Negl. Trop. Dis.* 4:e664, 1–8. doi: 10.1371/journal.pntd.0000664

Gomes, L. I., Enk, M. J., and Rabello, A. (2014). Diagnosing schistosomiasis: where are we? *Rev. Soc. Bras. Med. Trop.* 47, 3–11. doi: 10.1590/0037-8682-0231-2013

Gomes, L. I., Marques, L. H. S., Enk, M. J., Coelho, P. M. Z., and Rabello, A. (2009). Further evaluation of an updated PCR assay for the detection of *Schistosoma mansoni* DNA in human stool samples. *Mem. Inst. Oswaldo Cruz* 104, 1194–1196. doi: 10.1590/S0074-02762009000800021

Graeff-Teixeira, C., Favero, V., Pascoal, V. F., de Souza, R. P., de Rigo, F. V., LHD, A., et al. (2021). Low specificity of point-of-care circulating cathodic antigen (POC-CCA) diagnostic test in a non-endemic area for schistosomiasis mansoni in Brazil. *Acta Trop.* 217:105863. doi: 10.1016/j.actatropica.2021.105863

Ibironke, O., Koukounari, A., Asaolu, S., Moustaki, I., and Shiff, C. (2012). Validation of a new test for *Schistosoma haematobium* based on detection of Dra1 DNA fragments in urine: evaluation through latent class analysis. *PLoS Negl. Trop. Dis.* 6, e1464–e1466. doi: 10.1371/journal.pntd.0001464

Katz, N. (2018) *Inquérito Nacional de Prevalência da Esquistossomose mansoni e Geo-helmintoses*. Belo Horizonte: CPqRR, 76.

Katz, N., Chaves, A., and Pellegrino, J. (1972). A simple device for quantitative stool thick-smear technique in schistosomiasis mansoni. *Rev do Inst Med Trop São Paulo1* 14, 397–400.

King, C. H. (2015). It's time to dispel the myth of "asymptomatic" schistosomiasis. *PLoS Negl. Trop. Dis.* 9:e0003504. doi: 10.1371/journal.pntd.0003504

Kittur, N., Castleman, J. D., Campbell, C. H., King, C. H., and Colley, D. G. (2016). Comparison of schistosoma mansoni prevalence and intensity of infection, as determined by the circulating cathodic antigen urine assay or by the Kato-Katz fecal assay: a systematic review. *Am. J. Trop. Med. Hyg.* 94, 605–610. doi: 10.4269/ajtmh.15-0725

Koukounari, A., Jamil, H., Erosheva, E., Shiff, C., and Moustaki, I. (2021). Latent class analysis: insights about design and analysis of schistosomiasis diagnostic studies. *PLoS Negl. Trop. Dis.* 15, e0009042–e0009023. doi: 10.1371/journal.pntd.0009042

Li, H. M., Qin, Z. Q., Bergquist, R., Qian, M. B., Xia, S., Lv, S., et al. (2021). Nucleic acid amplification techniques for the detection of *Schistosoma mansoni* infection in humans and the intermediate snail host: a structured review and meta-analysis of diagnostic accuracy. *Int. J. Infect. Dis.* 112, 152–164. doi: 10.1016/j.ijid.2021.08.061

Lo, N. C., Bezerra, F. S. M., Colley, D. G., Fleming, F. M., Homeida, M., Kabatereine, N., et al. (2022). Review of 2022 WHO guidelines on the control and elimination of schistosomiasis. *Lancet Infect. Dis.* 22, e327–e335. doi: 10.1016/s1473-3099(22)00221-3

Lodh, N., Mikita, K., Bosompem, K. M., Anyan, W. K., Quartey, J. K., Otchere, J., et al. (2017). Point of care diagnosis of multiple schistosome parasites: species-specific DNA detection in urine by loop-mediated isothermal amplification (LAMP). *Acta Trop.* 173, 125–129. doi: 10.1016/j.actatropica.2017.06.015

Lodh, N., Mwansa, J. C. L., Mutengo, M. M., and Shiff, C. J. (2013). Diagnosis of *Schistosoma mansoni* without the stool: comparison of three diagnostic tests to detect schiostosoma mansoni infection from filtered urine in Zambia. *Am. J. Trop. Med. Hyg.* 89, 46–50. doi: 10.4269/ajtmh.13-0104

LoVerde, P. T. (2019). Schistosomiasis. *Adv. Exp. Med. Biol.* 1154, 45–70. doi: 10.1007/978-3-030-18616-6_3

Mazigo, H. D., Amuasi, J. H., Osei, I., and Kinung'hi, S. M. (2018). Integrating use of point-of-care circulating cathodic antigen rapid diagnostic tests by community health workers during mass drug administration campaigns to improve uptake of praziquantel treatment among the adult population at Kome Island, North-Western. *BMC Public Health* 18:840. doi: 10.1186/s12889-018-5732-y

McManus, D. P., Dunne, D. W., Sacko, M., Utzinger, J., Vennervald, B. J., and Zhou, X.-N. (2018). Schistosomiasis. *Nat. Rev. Dis. Prim.* 4:13. doi: 10.1038/s41572-018-0013-8

Ministério da Saúde (2019). Secretaria de Vigilância em Saúde. Departamento de Vigilância Epidemiológica. Vigilância da Esquistossomose mansoni-Diretrizes

técnicas/ Ministério da Saúde, Secretaria de Vigilância em Saúde, Departamento de Vigilância das Doenças Transmissíveis. -4.ed.- Brasília: Ministério da Saúde. (2014).144p. Available at: https://portalarquivos2.saude.gov.br/images/pdf/2019/setembro/25/boletim-especial-21ago19-web.pdf

Musso, O., Sommer, P., Drouet, E., Cotte, L., Neyra, M., Grimaud, J. A., et al. (1996). In situ detection of human cytomegalovirus DNA in gastrointestinal biopsies from AIDS patients by means of various PCR-derived methods. *J. Virol. Methods* 56, 125–137. doi: 10.1016/0166-0934(95)01892-1

Nascimento, G. L., Pegado, H. M., Domingues, A. L. C., De Alencar Ximenes, R. A., Itria, A., Cruz, L. N., et al. (2019). The cost of a disease targeted for elimination in Brazil: the case of schistosomiasis mansoni. *Mem. Inst. Oswaldo Cruz* 114, e180347–e180349. doi: 10.1590/0074-02760180347

Newcombe, R. G. (1998). Two-sided confidence intervals for the single proportion: comparison of seven methods. *Stat. Med.* 17, 857–872. doi: 10.1002/(SICI)1097-0258(19980430)17:8<857::AID-SIM777>3.0.CO;2-E

Notomi, T., Okayama, H., Masubuchi, H., Yonekawa, T., Watanabe, K., Amino, N., et al. (2000). Notomi et al LAMP.pdf. *Nucleic Acids Res.* 28:e63, 63e–663e. doi: 10.1093/nar/28.12.e63

Ogongo, P., Nyakundi, R. K., Chege, G. K., and Ochola, L. (2022). The road to elimination: Current state of schistosomiasis research and Progress towards the end game. *Front. Immunol.* 13, 1–23. doi: 10.3389/fimmu.2022.846108

PAHO (2022). Pan American Health Organization. *Schistosomiasis*. Available at: https://www.paho.org/en/topics/schistosomiasis (Accessed November 11, 2022)

Panzner, U. (2022). Clinical applications of isothermal diagnosis for human schistosomiasis. *Encyclopedia* 2, 690–704. doi: 10.3390/ encyclopedia2020048

Parker, M., and Allen, T. (2011). Does mass drug administration for the integrated treatment of neglected tropical diseases really work? Assessing evidence for the control of schistosomiasis and soil-transmitted helminths in Uganda. *Heal. Res. Policy Syst.* 9:3. doi: 10.1186/1478-4505-9-3

Parker, M., Allen, T., and Hastings, J. (2008). Resisting control of neglected tropical diseases: dilemmas in the mass treatment of schistosomiasis and soil-transmitted helminths in north-West Uganda. *J. Biosoc. Sci.* 40, 161–181. doi: 10.1017/S0021932007002301

Pomari, E., Perandin, F., La Marca, G., and Bisoffi, Z. (2019). Improved detection of DNA *Schistosoma haematobium* from eggs extracted by bead beating in urine. *Parasitol. Res.* 118, 683–686. doi: 10.1007/s00436-018-6137-7

Senra, C., Gomes, L. I., Siqueira, L. M. V., Coelho, P. M. Z., Rabello, A., and Oliveira, E. (2018). Development of a laboratorial platform for diagnosis of schistosomiasis mansoni by PCR-ELISA. *BMC. Res. Notes* 11, 455–458. doi: 10.1186/s13104-018-3571-7

Shim, S. R., Kim, S.-J., and Lee, J. (2019). Diagnostic test accuracy: application and practice using R software. *Epidemiol. Health* 41:e2019007. doi: 10.4178/epih.e2019007

Simel, D. L., Samsa, G. P., and Matchar, D. B. (1991). Likelihood ratios with confidence: sample size estimation for diagnostic test studies. *J. Clin. Epidemiol.* 44, 763–770. doi: 10.1016/0895-4356(91)90128-V

Siqueira, L. M. V., Coelho, P. M. Z., de Oliveira, Á. A., Massara, C. L., de Carneiro, N. F., ACL, L., et al. (2011). Evaluation of two coproscopic techniques for the diagnosis of schistosomiasis in a low-transmission area in the state of Minas Gerais, Brazil. *Mem. Inst. Oswaldo Cruz* 106, 844–850. doi: 10.1590/S0074-02762011000700010

Siqueira, L. M. V., Gomes, L. I., Oliveira, E., de Oliveira, E. R., de Oliveira, Á. A., Enk, M. J., et al. (2015). Evaluation of parasitological and molecular techniques for the diagnosis and assessment of cure of *Schistosomiasis mansoni* in a low transmission area. *Mem. Inst. Oswaldo Cruz* 110, 209–214. doi: 10.1590/0074-02760140375

Siqueira, L. M. V., Senra, C., de Oliveira, A. A., de Carneiro, N. F., Gomes, L. I., Rabello, A., et al. (2021). A real-time PCR assay for the diagnosis of intestinal schistosomiasis and cure assessment after the treatment of individuals with low parasite burden. *Front. Immunol.* 11, 1–13. doi: 10.3389/fimmu.2020.620417

Turner, H. C., Bettis, A. A., Dunn, J. C., Whitton, J. M., Hollingsworth, T. D., Fleming, F. M., et al. (2017). Economic considerations for moving beyond the Kato-Katz technique for diagnosing intestinal parasites as we move towards elimination. *Trends Parasitol.* 33, 435–443. doi: 10.1016/j.pt.2017.01.007

Ullah, H., Arbab, S., Khan, M. I. U., Li, K., Muhammad, N., Suleman, Q. A., et al. (2021). Circulating cell-free mitochondrial DNA fragment: a possible marker for early detection of *Schistosoma japonicum*. *Infect. Genet. Evol.* 88:104683. doi: 10.1016/j.meegid.2020.104683

Ullah, H., Arbab, S., Li, K., Inayat, M., Khan, U., Qadeer, A., et al. (2022). Schistosomiasis related circulating cell-free DNA: a useful biomarker in diagnostics. *Mol. Biochem. Parasitol.* 251, 1–4. doi: 10.1016/j.molbiopara.2022.111495

Viana, A. G., Gazzinelli-Guimarães, P. H., de Castro, V. N., YLO, D. S., ACL, D. R., FSM, D. B., et al. (2019). Discrepancy between batches and impact on the sensitivity of point-of-care circulating cathodic antigen tests for *Schistosoma mansoni* infection. *Acta Trop.* 197:105049. doi: 10.1016/j.actatropica.2019.105049

Walter, S. D., and Irwig, L. M. (1988). Estimation of test error rates, disease prevalence and relative risk from misclassified data: a review. *J. Clin. Epidemiol.* 41, 923–937. doi: 10.1016/0895-4356(88)90110-2

Weerakoon, K. G., Gordon, C. A., and McManus, D. P. (2018). DNA diagnostics for schistosomiasis control. *Trop. Med. Infect. Dis.* 3, 1–20. doi: 10.3390/tropicalmed3030081

Weerakoon, K. G., and McManus, D. P. (2016). Cell-free DNA as a diagnostic tool for human parasitic infections. *Trends Parasitol.* 32, 378–391. doi: 10.1016/j.pt.2016.01.006

WHO (2021). *Ending-the-neglect-to-attain-the-SDGs-NTD-roadmap*. Geneva: WHO.

World Health Organization (2022). *WHO GUIDELINE on Control and Elimination of Human Schistosomiasis*. Geneva: World Health Organization.

Xu, J., Guan, Z. X., Zhao, B., Wang, Y. Y., Cao, Y., Zhang, H. Q., et al. (2015). DNA detection of *Schistosoma japonicum*: diagnostic validity of a LAMP assay for low-intensity infection and effects of chemotherapy in humans. *PLoS Negl. Trop. Dis.* 9, e0003668–e0003614. doi: 10.1371/journal.pntd.0003668

frontiers | Frontiers in Immunology

TYPE Original Research
PUBLISHED 31 January 2023
DOI 10.3389/fimmu.2023.1056469

OPEN ACCESS

EDITED BY
Marina Moraes Mourão,
Oswaldo Cruz Foundation (Fiocruz), Brazil

REVIEWED BY
Paul McCusker,
Queen's University Belfast, United Kingdom
Frédéric Chevalier,
Texas Biomedical Research Institute,
United States

*CORRESPONDENCE
Akram A. Da'dara
akram.Da_darah@tufts.edu

SPECIALTY SECTION
This article was submitted to Vaccines and Molecular Therapeutics, a section of the journal Frontiers in Immunology

RECEIVED 28 September 2022
ACCEPTED 16 January 2023
PUBLISHED 31 January 2023

CITATION
Skelly PJ and Da'dara AA (2023) A novel, non-neuronal acetylcholinesterase of schistosome parasites is essential for definitive host infection.
Front. Immunol. 14:1056469.
doi: 10.3389/fimmu.2023.1056469

A novel, non-neuronal acetylcholinesterase of schistosome parasites is essential for definitive host infection

Patrick J. Skelly and Akram A. Da'dara*

Molecular Helminthology Laboratory, Department of Infectious Disease and Global Health, Cummings School of Veterinary Medicine, Tufts University, North Grafton, MA, United States

Schistosomes are long-lived parasitic worms that infect >200 million people globally. The intravascular life stages are known to display acetylcholinesterase (AChE) activity internally as well as, somewhat surprisingly, on external tegumental membranes. Originally it was hypothesized that a single gene (SmAChE1 in *Schistosoma mansoni*) encoded both forms of the enzyme. Here, we demonstrate that a second gene, designated "*S. mansoni* tegumental acetylcholinesterase, SmTAChE", is responsible for surface, non-neuronal AChE activity. The SmTAChE protein is GPI-anchored and contains all essential amino acids necessary for function. AChE surface activity is significantly diminished following SmTAChE gene suppression using RNAi, but not following SmAChE1 gene suppression. Suppressing SmTAChE significantly impairs the ability of parasites to establish infection in mice, showing that SmTAChE performs an essential function for the worms *in vivo*. Living *S. haematobium* and *S. japonicum* parasites also display strong surface AChE activity, and we have cloned SmTAChE homologs from these two species. This work helps to clarify longstanding confusion regarding schistosome AChEs and paves the way for novel therapeutics for schistosomiasis.

KEYWORDS

acetylcholinesterase, host-parasite interaction, non-neuronal, tegument, schistosoma

Introduction

Schistosomiasis is a parasitic disease caused by helminth parasites of the genus *Schistosoma* (1, 2). Schistosomiasis ranks among the most important infectious diseases globally, affecting more than 200 million people world-wide, and over 700 million people live at risk of infection (2–6). In sub-Saharan Africa alone, mortality is put at ~280,000 deaths per year, with tens of millions having chronic morbidity (4, 7, 8). Furthermore, extensive pathological changes associated with schistosome infection can affect multiple organ systems, including the liver, spleen and the gastro-intestinal tract, especially in individuals with longstanding or heavy infections (9). Three major species cause schistosomiasis in humans: *S. mansoni*, *S. haematobium* and *S. japonicum*. Schistosomes have complex life cycles. Larvae

(cercariae) are released from infected intermediate, freshwater snail hosts. Upon encountering a human (the definitive host), cercariae penetrate the skin, transform into juvenile forms called schistosomula that migrate through the bloodstream to the liver where they mature into adult male or female parasites. The adults mate and females produce hundreds of eggs each day, some of which are released into the environment. In fresh water, the eggs hatch and give rise to free swimming larvae (miracidia) that seek and enter the snails to continue the life cycle.

In our laboratory, we study the molecular and cell biology of the schistosome tegument (skin) (10–16). The tegument of the intravascular life stages is a major site for host-parasite interaction, and proteins that make up the tegument represent potential therapeutic targets and vaccine candidates. Here we focus on schistosome tegumental acetylcholinesterase (AChE; EC. 3.1.1.7).

AChE, a widely distributed enzyme in animals, is best known for its ability to catalyze the breakdown of the neurotransmitter acetylcholine. This limits the interaction of acetylcholine with its receptors at cholinergic synapses. The immunolocalization of AChE in the neuromusculature of schistosomes, and the ability of anticholinesterase compounds to paralyze adult worms, are both consistent with a role for this enzyme in controlling neuromuscular activity in these parasites, as in other animals (17–20). Somewhat surprisingly, AChE has additionally been localized in the tegument of intravascular-stage schistosomes, and AChE activity has been associated with isolated tegumental membranes (17, 20–22). Indeed, more than 50% of total *S. mansoni* AChE activity can be detected at the surface of 24-h cultured schistosomula (23). The precise relationship between the tegumental and non-tegumental AChE in schistosomes has been unclear for many years. Earlier biochemical characterization suggested the existence of two different AChE enzymes differing in their solubility characteristics and quaternary structures (24, 25). One form, with a sedimentation coefficient of 6.5S, did not bind to heparin (26). Since this AChE is released from intact parasites by treating them with phosphatidylinositol-phospholipase C (Pi-PLC), it is considered to be the tegumental, host-interactive AChE (26, 27). A second AChE form had a sedimentation coefficient of 8S and bound heparin (26). In addition, in experiments with live parasites, the non-membrane permeable AChE inhibitor echothiophate (phospholine) selectively blocked the 6.5S enzyme but not the 8S form, suggesting that the 8S form is located internally (26). However, heterologous anti-AChE antibodies could not distinguish between two distinct schistosome AChE forms and a single identified AChE gene was proposed to encode both the internal (neuromuscular) and external (tegumental) enzymes (17). A gene encoding AChE was identified not just in *S. mansoni* (now designated SmAChE1) (28) but also in *S. haematobium* (17), S. *bovis* (28) and *S. japonicum* (29). However, not one of the proteins encoded by these genes is predicted to contain a GPI anchoring sequence, suggesting that none encode the surface form of AChE. A second AChE gene has been identified in *S. mansoni* (SmAChE2) but its reported sequence also lacks both a predicted GPI anchoring motif and a leader sequence (30). However, purified recombinant SmAChE1 and SmAChE2 do both cleave acetylthiocholine, and suppression of either gene diminishes the cholinesterase activity measured in extracts of gene-suppressed schistosomula compared with controls (30). Antibodies raised against recombinant fragments of SmAChE1 and SmAChE2 bind widely throughout the adult worms' internal structures as well as in the tegument. However, given that both AChEs share multiple conserved motifs, it is likely that antibodies against one will cross react with the other. Finally, while both SmAChE1 and SmAChE2 are reported to immunolocalize on the tegument "surface" (30) the resolution by immunofluorescence microscopy is not sufficient to support this claim.

Here, we set out to identify and characterize the gene encoding the surface AChE in the three major schistosome species that infect humans and to determine if the previously characterized AChE genes encode the enzymes responsible for surface activity.

Materials and methods

Mice and parasites

Female, 6–8 week-old Swiss-Webster CD1 mice were purchased from Charles River and maintained under specific pathogen-free conditions at the animal facility of Cummings School of Veterinary Medicine, Tufts University. All experimental procedures involving animals were carried out in accordance with approved guidelines of the Institutional Animal Care and Use Committee (IACUC) of Tufts University and all animal work was done in the vivarium at Cummings School of Veterinary Medicine, Tufts University.

Biomphalaria glabrata snails, infected with *Schistosoma mansoni* (Puerto Rican NMRI strain) were obtained from the NIAID Schistosomiasis Resource Center of the Biomedical Research Institute (BRI), Rockville, MD, USA, and maintained in our laboratory. Cercariae, infectious larvae, were prepared by exposing infected snails to light for 1-2 h to induce shedding. Cercarial numbers and viability were determined using a light microscope.

Schistosomula were prepared from cercariae by mechanical removal of the cercarial tails *via* vortexing and subsequent Percoll purification, as previously described (31). Schistosomula were cultured in complete DMEM/F12 medium (Invitrogen) supplemented with 10% heat-inactivated fetal bovine serum (FBS), 200 U/ml penicillin and 200 µg/ml streptomycin (Invitrogen), 1 µM serotonin (Sigma), 8 µg/ml human insulin (Sigma), 0.2 µM triiodothyronine at 37°C, in an atmosphere of 5% CO_2. Schistosomula numbers and viability were determined using a light microscope and the trypan blue exclusion test.

Adult male and female parasites were recovered by perfusion from Swiss Webster mice that were infected with 120 cercariae (*S. mansoni*) or 25 cercariae (*S. japonicum*) 7 weeks previously (32–34). Adult *S. haematobium* were recovered by perfusion of Golden Syrian hamsters that had been infected with 350 cercariae 12 weeks previously. In all cases, the mesenteric veins and the liver vasculature were examined for the presence of any parasites that were not washed out by perfusion. Both *S. japonicum* infected mice and *S. haematobium* infected hamsters were provided by BRI. Adult parasites were maintained in complete DMEM/F12 medium supplemented as described above. Schistosome eggs were isolated from livers of mice infected with *S. mansoni*, as previously described (34, 35).

Measuring acetylcholinesterase (AChE) activity

AChE activity was measured at room temperature by the modified Ellman method using acetylthiocholine iodide (ATCh) as substrate (36). The reaction mixture contained 1 mM acetylthiocholine and 1 mM 5,5'-dithiobis(2-nitrobenzoic acid) (DTNB) in 100 mM sodium phosphate, pH 7.2, in a total volume of 200 µl. DTNB is a membrane impermeant reagent (37, 38). Total parasite lysates were prepared by homogenizing a specific number of male or female parasites in ice-cold 100 mM phosphate buffer, Ph 7.2. Experiments were carried out on parasite lysates or on live, individual male or female parasites, or groups of cercariae, schistosomula or eggs, in PBS or in clear, serum-free DMEM/F12 medium containing reaction mixture. There was no significant difference in the activity between PBS and clear medium and in all subsequent experiments clear medium was used with living worms. Absorbance at 412 nm was monitored over time (mostly every 5 mins) using a Synergy HT spectrophotometer (Bio-Tek Instruments, Winooski, VT, USA). Note that parasites remained in the wells during this assay, and their presence did not impact readings. In some experiments the acetylcholinesterase inhibitor BW284c51 (1,5-bis(4-allyldimethylammoniumphenyl)pentan-3-onedibromide, Sigma-Aldrich) was added at a final concentration of 100 µM. Some experiments were conducted using butyrylthiocholine iodide (BuTCh, Sigma-Aldrich, 2.5 mM), and not acetylthiocholine, as substrate.

Cloning and characterization of the tegumental AChE (SmTAChE) of *S. mansoni*

Since initial studies showed that the surface AChE was not encoded by the known AChE gene (now called AChE1), this led us to search for another gene which could potentially encode the surface AChE. *S. mansoni* data bases (http://schistodb.net/, https://parasite.wormbase.org/index.html and http://www.genedb.org/Homepage/Smansoni) were queried for the presence of potential AChE sequences. Based on signature elements found in other acetylcholinesterases, several genes were identified including a strong candidate (ID: Smp_136690). All other early database hits displayed only modest sequence similarity over short distances and were filtered out on this basis. The Smp_136690 coding sequence was amplified using the following primers: SmAC2-F: 5'-TGACTATTTGGATACACTTATG-3', and SmAC2-R: 5'-TCTATGAAGTCATTTTACAAGG-3', designed from database information, and using AccuPrime Taq DNA Polymerase high fidelity (following 40 cycles at 95°C for 30 sec, 50°C for 30 sec and 68°C for 3 min), as per the manufacturer's recommendations (Thermo Fisher Scientific). cDNA synthesized from total RNA (obtained from a mixture of adult male and female worms) was used as a template for the PCR. The amplified product was purified and sequenced at Tufts University Core Facility and the final clone was designated SmTAChE. RNA isolation and cDNA synthesis is described below under "SmTAChE gene expression analysis". Sequence analysis using multiple tools (described below) was used to characterize potential AChEs.

Cloning of the tegumental AChEs of *S. haematobium* and *S. japonicum*

Analysis of the *S. haematobium* genome at schistoDB.net resulted in the identification of a gene (KL250835) encoding a protein with a high degree of sequence similarity to SmTAChE (now designated MS3_0012973 at *WormBase Parasite*, https://parasite.wormbase.org/index.html). The following oligonucleotides flanking the predicted open reading frame (ORF) were used to amplify the cDNA using RNA isolated from mixed adult stage parasites: ShAC2-F: 5'-AATATTCTTTCTTCCTATTGACAATG-3', ShAC2-R: 5'-ACATTTTCATCAATATAAAAAC-3'. The amplified coding DNA was sequenced and designated ShTAChE.

Analysis of the *S. japonicum* genome did not immediately reveal a gene encoding a protein similar to SmTAChE. However, extensive analysis revealed the presence of sequences encoding potential fragments of a SmTAChE homolog on two different contigs: Sjp_0045440 (now known to code for the first exon), and Sjp_0070510 (now known to encode the remaining 3 exons) (*WormBase ParaSite*: https://parasite.wormbase.org/index.html). To isolate the full predicted coding sequence, a rapid amplification of cDNA ends (RACE) experiment was performed using the 3', 5' SMARTer RACE kit, with mixed adult stage RNA and the following gene-specific primers, (following the manufacturer's instructions, Clontech): SjAC2GSP-S1: CAGGCAGTGCTAATCTACAAGTATACAATGGTGC-3' and SjAC2GSP-S2: GCTGAACATGTTGCTAGATTACCAAATGC, (for the 3'end), and SjAC2GSP-AS1: GCACCATTGTATACTTGTAGATTAGCACTGCCTG and SjAC2GSP-AS2: GCATTTGGTAATCTAGCAACATGTTCAGC-3' (for the 5'end). Several fragments with the predicted size were amplified and sequenced. In this manner the full ORF, encoding what we now call SjTAChE, was identified, and this confirmed that the two contigs abut.

In Silico analysis of the predicted tegumental AChEs

Several online tools were used to analyze the deduced amino acid sequence of the tegumental AChEs. For the prediction of GPI anchors and omega residues, the GPI-SOM (http://gpi.unibe.ch/) and the NetGPI (https://services.healthtech.dtu.dk/service.php?NetGPI) tools were used. Analysis of the signal peptide was performed using SignalP prediction software (https://services.healthtech.dtu.dk/service.php?SignalP-5.0). Analysis of potential N-glycosylation sites was performed using the NetNGlyc 1.0 Server (https://services.healthtech.dtu.dk/service.php?NetNGlyc-1.0). Multiple alignment analysis was conducted using CLUSTAL O (1.2.4) at http://www.ebi.ac.uk/Tools/msa/clustalo/. Phylogenetic analysis was performed at phylogeny.fr (http://www.phylogeny.fr/) (39–41) using default settings (Alignment: Muscle; Maximum number of iterations: 16; Curation: Gblocks; Phylogeny: PhyML; Statistical test for branch support: approximate likelihood ratio test (SH-like); Number of substitution rate categories: 4).

Anti-SmTAChE antibody production

An SmTAChE-specific peptide, comprising amino acid residues K^{328} – E^{346} (NH_2-KHRYDAVRKYLLPRYHKQE-COOH), was synthesized by Genemed Synthesis, Inc. (San Antonio, TX). Note that this peptide represents a sequence unique to SmTAChE and is not found in SmAChE1 (accession no. AAQ14321.1). A cysteine residue was added at the peptide's amino terminus, to facilitate conjugation to bovine serum albumin (BSA). Approximately 500 µg of peptide-BSA conjugate in Freund's Complete Adjuvant was used to immunize two New Zealand White rabbits subcutaneously. The rabbits were boosted with 100 µg of peptide alone in Incomplete Freund's Adjuvant 20, 40, and 60 days later. Ten days following the last immunization, serum was recovered from both rabbits, pooled and anti-SmTAChE antibodies were affinity-purified using the same peptide at Genemed Synthesis.

RNA interference

Schistosome parasites (adults and schistosomula) were treated with a synthetic siRNA (from IDT DNA Technologies) targeting either SmAChE1 (AF279461), or SmTAChE (OP018961) or no sequence in the schistosome genome (Control). Sequences of all siRNAs are provided in Table S1. siRNAs were delivered to parasites by electroporation, as described previously (31). Gene suppression was assessed post-treatment by comparing mRNA levels using reverse transcription quantitative PCR (RT-qPCR) and by comparative enzyme activity measurements in target versus control groups.

SmTAChE gene expression analysis

The level of expression of both the SmAChE1 and the SmTAChE gene in different life stages of the parasite, and in parasites treated with gene-specific siRNAs, was measured by RT-qPCR, using custom TaqMan gene expression systems (Applied Biosystems, CA). First, RNA from different life stages was isolated using TRIzol Reagent according to the manufacturer's instructions (Invitrogen). RNA was then treated with DNaseI to remove any genomic DNA, using a Turbo-DNase I kit (Ambion). cDNA was synthesized using 0.5 µg RNA, an oligo $(dT)_{12\text{-}18}$ primer and Superscript III RT (Invitrogen). For developmental expression, triose phosphate isomerase (TPI) was used as a reference gene, as previously (31). Primer sets and reporter probes labeled with 6-carboxyfluorescein (FAM) were obtained from Applied Biosystems, CA (Table S2). All samples were run in triplicate and underwent 40 amplification cycles on a StepOne Plus Real Time PCR System. For relative quantification, the ΔΔCt method was employed (31). For RNAi experiments, the schistosome alpha-tubulin gene was used as the "within-stage" endogenous control, as earlier (13, 31).

Pi-PLC treatment and western blot analysis

To monitor the expression of the SmTAChE protein, parasite samples were first homogenized in ice-cold lysis buffer (20 mM Tris-HCl, pH 8.0 containing 2% SDS). Protein concentration was determined using the Pierce Micro BCA Protein Assay Kit (ThermoFisher Scientific) according to the manufacturer's instructions. GPI-anchored proteins were recovered from live male worms by *in vitro* incubation with phosphatidylinositol-phospholipase C (Pi-PLC) (Sigma-Aldrich), as previously described (42). Briefly, 20 freshly perfused male parasites were washed three times in DMEM and were then incubated at 37°C for 1 h in the presence of Pi-PLC (from *Bacillus cereus*) at 1.25 Units/ml. The supernatant was removed and concentrated at 4°C using a 10-kDa cut-off Pierce Protein Concentrators (ThermoFisher Scientific). Proteins were resolved by SDS-PAGE under reducing conditions and blotted to PVDF membrane. Membranes were blocked using Tris-Buffered Saline (TBS) containing 0.05% Tween 20 (TBST) and 5% non-fat dry milk. The membrane was then probed overnight at 4° C with affinity purified rabbit anti-SmTAChE antibody at 1:1000 dilution. After three washes in TBST, bound primary antibody was detected using horseradish peroxidase-labeled anti-rabbit IgG (1:5000, GE Healthcare). Signals were detected using ECL Western Blotting Detection Reagents (GE Healthcare). Western blot images were captured using a ChemiDoc Touch Imaging System (Bio-Rad).

Immunolocalization of SmTAChE

Freshly perfused parasites were embedded in OCT compound and flash frozen in liquid nitrogen. Adult worm frozen sections (7 µm thick) were obtained using a cryostat and fixed in ice-cold acetone for 30 min at -20°C. Cultured schistosomula (7 day) were fixed in 4% paraformaldehyde for 20 min at room temp. Parasites/parasite sections were washed three times in PBS before being incubated with 1% BSA in PBS (blocking buffer) for 1h. The samples were incubated with primary, purified anti-SmTAChE, antibody at 1:100 dilution for 1h. After washing with PBST (PBS containing 0.05% Tween-20), parasites were then incubated with Alexa Fluor-488-anti-rabbit IgG (H+L, Invitrogen) diluted 1:100 in blocking buffer for 1h, as described (43). Samples were washed in PBS, mounted in Fluoromount and viewed using an inverted fluorescent microscope (TH4–100; Olympus, Tokyo, Japan) equipped with a Retiga 1300 camera (Q Imaging, BC, Canada).

Immunogold labeling and electron microscopy

Freshly perfused adult parasites were fixed overnight with 2% glutaraldehyde in 0.1M cacodylate buffer at 4°C. The samples were then dehydrated in a graded series of ethanol, then infiltrated and embedded in L.R. white acrylic resin. Ultramicrotomy was performed using a Leica Ultracut R ultramicrotome and the sections collected on gold grids. Grids were immunolabeled in a two-step method as follows: the grids were conditioned in PBS for 5 min x 3 at room temperature, followed by the blocking of non-specific labeling for 30 min at room temp using 5% non-fat dry milk in PBS. After rinsing, the grids were exposed to primary antibody diluted 1:30 for 1h at room temperature, followed by washing in PBS and then incubated with secondary antibody diluted 1:30 (10 nm gold-labeled goat anti-

rabbit IgG (H&L, GE Healthcare)) for 1h at room temperature, and finally rinsed thoroughly in water. Control parasite preparations were treated with secondary antibody alone. Grids were exposed to osmium vapor and/or lightly stained with lead citrate to improve contrast and were examined and photographed using a Philips CM 10 electron microscope at 80KV.

Infection of mice with SmTAChE gene suppressed schistosomula

One-day-old cultured schistosomula were electroporated with siRNA targeting SmTAChE, or with control siRNA, or with no siRNA (Table S1). Parasites were maintained in culture for 4 days, then counted and resuspended in phenol-red-free RPMI medium. Approximately 1000 schistosomula were used to infect each mouse by intramuscular injection (100 µl total volume) into the thigh muscles, using a 1 ml tuberculin syringe and a 25G-1 needle (12, 44). Mice were perfused 6 weeks later, and worm burdens were determined (32–34).

Statistical analysis

Data were assessed for normality using Shapiro-Wilk tests with GraphPad Prism 9.4. Bartlett's test for homogeneity of variances confirmed the assumption of equal variances. The student's *t*-test, one-way analysis of variance (ANOVA) with Tukey *post hoc* analysis and two-way ANOVA were used to compare the means between a target group and a control group using GraphPad Prism 9.4. P values less than 0.05 were considered significant.

Results

Schistosome parasites exhibit surface AChE activity

As shown in Figure 1A, intact, individual live male or female adult *S. mansoni* cleave exogenous acetylthiocholine. The larger male worms exhibit significantly higher (>2X) surface AChE activity compared to females ($p<0.001$). When the AChE activity of total lysates of individual male worms is set at 100%, the surface AChE activity (i.e., that displayed by live individual worms) is approximately 70% of this value (Figure 1B). As shown in Figure 1C, live schistosomula also display measurable AChE activity, and the greater the number of schistosomula the greater the activity recorded. In addition, essentially no AChE activity is detected in clear, conditioned, serum-free culture medium where 500 schistosomula had been cultured for 24 hours (Conditioned Media, Figure 1C), However, no AChE activity is detected using freshly shed live cercariae (Figure 1C). Furthermore, no activity is observed when butyrylthiocholine is incubated instead of acetylthiocholine with live schistosomula, as indicated in Figure 1D. Similarly, no butyrylcholinesterase activity was detected when live adult parasites were used in similar experiments (data not shown). Schistosome eggs, freshly isolated from the liver tissue of infected mice, exhibit substantial AChE activity (Figure 1E). Once again, the greater the

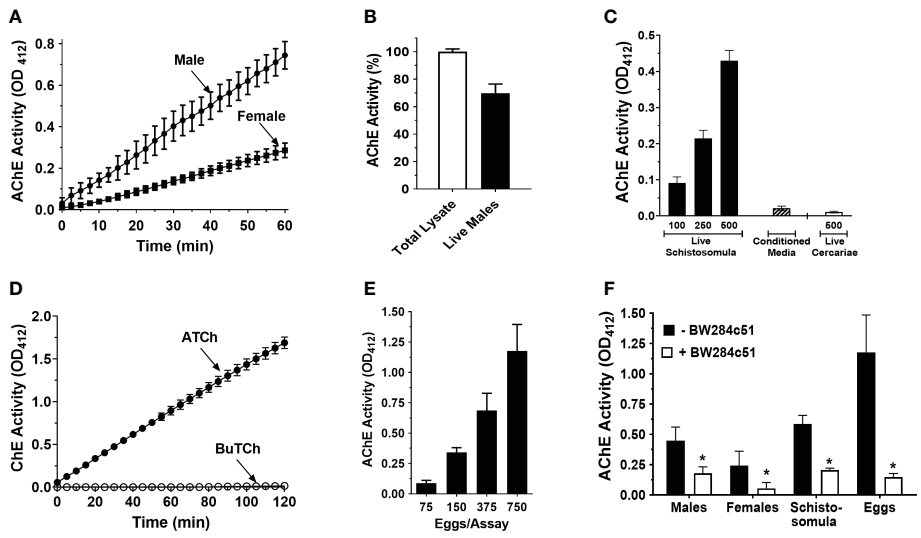

FIGURE 1
Acetylcholinesterase (AChE) activity (mean OD_{412} ± SD) in live *S. mansoni* parasites. **(A)** Acetylcholinesterase activity in individual live male (circles, n>10) or female parasites (squares, n>10). Male parasites display significantly higher surface AChE than females (two-way ANOVA, $p<0.0001$). **(B)** Surface AChE activity of individual live male parasites (at 60 min, black bar) compared to total AChE activity recorded in lysates of individual male parasites (white bar, set at 100%). **(C)** AChE activity in groups of live, 7-day-old cultured schistosomula (black bars) or in 24 h conditioned media (from 500 cultured schistosomula, hatched bar) or in groups of 500 cercariae (white bar), at 60 min (n≥3), **(D)** Cholinesterase (ChE) activity (mean OD_{412} ± SD) displayed by live schistosomula (groups of 1000, n=4) in the presence of acetylthiocholine (ATCh, 2.5 mM, closed circles) or butyrylthiocholine (BuTCh, 2.5 mM, open circles); no cholinesterase activity is detected when BuTCh is included as substrate. **(E)** AChE activity in groups of freshly recovered liver eggs at 60 min, (n>5). **(F)** Surface AChE activity of different schistosome life stages at 60 min, (1 male, 1 female, 500 schistosomula, or 750 eggs per assay, n≥4) in the presence (white bars) or absence (black bars) of the acetylcholinesterase inhibitor BW284c51 (100 µM final concentration; * t test, $p<0.05$).

number of parasites in the assay, the greater the activity seen. As shown in Figure 1F, the surface AChE activity of all life-stages is significantly inhibited in the presence of the selective AChE inhibitor, BW284c51 ($p<0.05$ in all cases).

Identifying the surface AChE enzyme

Figure 2A shows that treating adult male worms with siRNAs targeting SmAChE1 results in the successful suppression of this gene (by >75%, $p<0.01$ v either control). Three different siRNAs were evaluated, and preliminary analysis showed that all 3 siRNAs provided similar levels of gene suppression; therefore, SmAC1-siRNA1 was chosen in all subsequent RNAi experiments (Table S1). Figure 2B shows that this suppression had no significant impact on the ability of live worms to cleave exogenous acetylthiocholine (Figure 2B). There was no significant difference in the AChE activity displayed by the SmAChE1gene-suppressed worms versus controls. This result strongly suggests that a different gene, encoding a surface AChE, is responsible for the live worm activity detected. Therefore, as described in Methods, we performed an extensive *in silico* analysis of schistosome DNA databases in order to identify other potential acetylcholinesterase genes encoding proteins that might be responsible. In this manner Smp_136690 was identified to encode a strong candidate gene that we now designate SmTAChE (https://parasite.wormbase.org/Schistosoma_mansoni_prjea36577/Info/Index/; database version WBPS17). This gene is 23,068 bp (from the start to the stop codon) and, as depicted in Figure 3A (top), consists of 4 exons and 3 introns, unlike the SmAChE1 gene (Smp_154600) which contains 9 exons (Figure 3A, bottom). All introns have the consensus splicing site sequence (5'-GT/AG-3'). Both AChE genes are found on chromosome number 1, the largest autosomal chromosome; they are ~300 kb apart. Several oligonucleotides were designed based on the SmTAChE genomic sequence and used to amplify the complete 2,085 bp open reading frame, using adult *S. mansoni* cDNA as template. The GenBank accession number for the complete nucleotide sequence of the SmTAChE cDNA is OP018961. The ORF codes for the SmTAChE polypeptide of 694 amino acids. This is essentially a newly annotated version of a previously reported shorter (489 amino acid) sequence that was designated SmAChE2 (30). Due to substantial differences between the predicted sequences of these proteins (as shown in Figure S1), we elect to use the SmTAChE name for the new sequence reported here.

As shown in Figure 3B, phylogenetic analysis shows that SmTAChE (red text) is closely related to homologs from *S. haematobium* and *S. japonicum* (described below) and these are quite distinct from previously described schistosome AChE proteins (SmAChE1 and its homologs). All trematode AChEs (from schistosomes, liver flukes and cestodes) form a distinct clade, distant from the AChEs of animals from other phyla, such as nematodes and vertebrates. The multiple sequence alignment of all the sequences used to generate the phylogenetic tree is presented in Figure S2.

The SmTAChE sequence exhibits 36% amino acid sequence identity with SmAChE1, and 35% identity with the human AChE enzyme

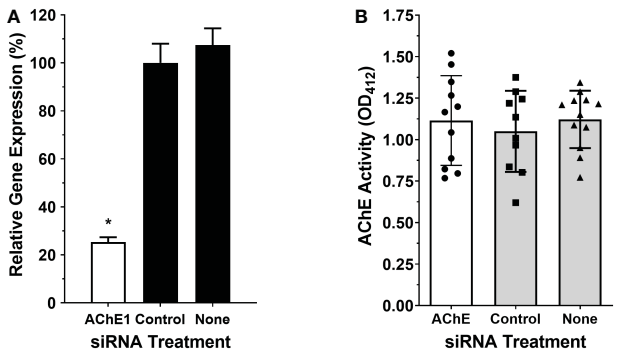

FIGURE 2
Suppression of SmAChE1 gene expression. Adult male parasites were treated either with an siRNA targeting SmAChE1, or with an irrelevant siRNA (Control) or with no siRNA (None), as indicated. **(A)** Relative expression of the SmAChE1 gene, measured by RT-qPCR seven days later. Treating parasites with siRNA targeting SmAChE1 significantly suppressed the expression of this gene (by ~ 70%; white bar, *$p < 0.05$ ANOVA) compared to controls. **(B)** AChE activity was measured in live individual male parasites treated with siRNA, as indicated. Mean AChE activity of the three groups of parasites did not differ significantly when tested 7 days post siRNA treatment. Each point represents data from an individual parasite, and the bars indicate the mean (± SD) for the group.

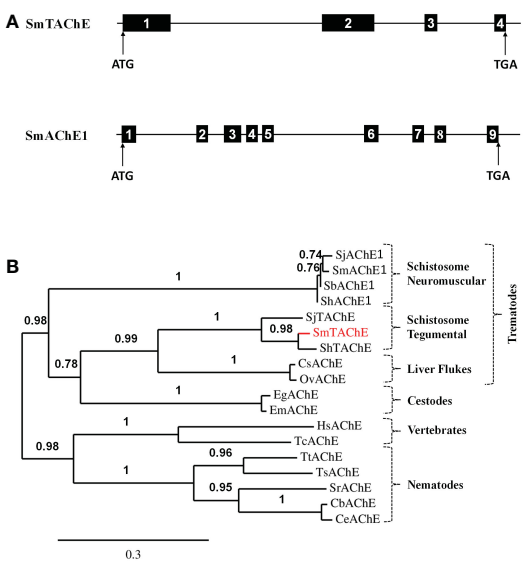

FIGURE 3
(A) Schematic representations of the SmTAChE (top) and SmAChE1 (bottom) genes. Black boxes represent the numbered exons and thin lines introns. The positions of the start (ATG) and stop (TGA) codons are noted. **(B)** Phylogenetic analysis of the following AChEs: *S. mansoni* SmTAChE, (Accession no: OP018961, red), *S. haematobium* ShTAChE, (OP018962), *S. japonicum* SjTAChE, (OP018963), *S. mansoni* SmAChE1, (AAQ14321.1), *S. haematobium* ShAChE1, (AAQ14322.1), *S. bovis* SbAChE1, (AAQ14323.1), *S. japonicum* SjAChE1, (ANH56887.1), *Echinococcus granulosus* EgAChE, (EUB57267.1) *Echinococcus multilocularis* EmAChE, (CDS43027.1), *Clonorchis sinensis* CsAChE, (GAA53463.1), *Opisthorchis viverrini* OvAChE, (XP_009168237.1), *Caenorhabditis briggsae* CbAChE, (XP_002643631.1), *Caenorhabditis elegans* CeAChE, (NP_510660.1), *Trichuris trichiura* TtAChE, (CDW55373.1), *Trichinella spiralis* TsAChE, (XP_003374589.1), *Strongyloides ratti* SrAChE, (CEF63281.1), *Homo sapiens* HsAChE, (NP_000656) and the electric eel *Torpedo californica* TcAChE, (P04058.2). Numbers on the branches reflect the branch support value, and the scale bar indicates 30% amino acid sequence divergence.

(HsAChE). As illustrated in Figure 4, SmTAChE contains all amino acids considered essential for AChE activity: the catalytic triad (S^{239}, E^{401}, H^{553}), the choline-binding site (W^{115}), six cysteines responsible for 3 intrachain disulfide bonding, the four charged residues involved in forming two salt-bridges, nine amino acids out of 14 aromatic residues that line the catalytic gorge in *Torpedo californica* AChE. In addition, SmTAChE contains the essential residues that form the oxyanion hole (G^{151}, G^{152}, and A^{240}) which plays an important role in catalysis (45). The SmTAChE sequence is predicted to contain three intrachain disulfide bonds formed between six conserved cysteine residues (C^{97}-C^{125}, C^{293}-C^{306}, C^{514}-C^{647}, indicated by blue dashed arrows in Figure 4) which are considered essential for correct secondary structure formation. Importantly, SmTAChE also contains a predicted signal peptide (M^{1} - S^{25}) and a strong predicted C-terminal GPI anchor sequence (^{669}GGIKPTGNYILILGSGLLLFIGIFYG^{694}, dashed underline in Figure 4) (30). The GPI-anchoring site (omega (ω)-residue, S^{668}) is indicated by ‡ in Figure 4.

SmTAChE developmental expression

The developmental expression of both the SmAChE1 and SmTAChE genes were examined in several schistosome life stages by RT-qPCR. As shown in Figure 5, both genes have lowest relative expression in the cercarial stage and, in both cases, expression increases greatly following infection – in schistosomula and in adult males and females. Both genes are very well expressed in eggs, strikingly so for SmTAChE. Based on available transcriptomic datasets (https://v7test.schisto.xyz/), the expression of both genes is high in adult male parasites.

Immunolocalization of SmTAChE

To localize SmTAChE, we first generated an anti-SmTAChE antibody targeting a unique synthetic peptide (K^{329}-E^{346}, underlined red text in Figure 4) found only in SmTAChE, and not in SmAChE1. As shown in Figure 6A, the antibody detects a major protein band of the expected size of SmTAChE (~75kDa, arrow) in extracts of adult male parasites (arrow), both among the Pi-PLC released proteins from live male parasites (Figure 6A, +Pi-PLC) and in a total male worm lysate (-Pi-PLC). Immunolocalization of SmTAChE was carried out using the anti-SmTAChE antibodies and whole, fixed 7-day cultured schistosomula (Figure 6B) or fixed, frozen sections of adult parasites (Figure 6C). Strong SmTAChE staining is observed, very predominantly in the tegument; a clear "green ring" of peripheral staining around the schistosomula is revealed (Figure 6B, white arrows). Likewise in adult worms, clear tegumental staining is

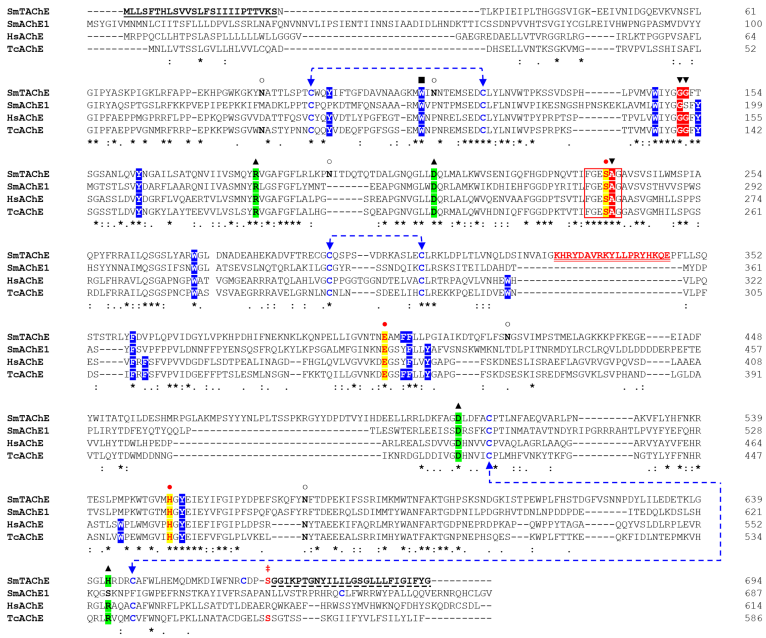

FIGURE 4
Alignment of the amino acid sequences of selected AChE proteins. The amino acid sequence of SmTAChE (Accession number OP018961), SmAChE1 (AAQ14321.1), human AChE (HsAChE, GPI-modified H form; NP_000656) and the Electric eel, *Torpedo californica* (TcAChE; GPI-modified form, P04058.2) were aligned using Clustal W. The catalytic triad residues (S^{239}, E^{401}, H^{553}, where amino acid positions correspond to the numbering of the SmTAChE sequence) are in red and indicated with ● and shaded in yellow. The 6 amino acid signature sequence (^{236}FGESAG^{241}) of cholinesterases around the active serine residue (S^{239}) is boxed. The choline-binding site (W^{115}) is indicated with ■. The three intrachain disulfide bonds formed using six conserved cysteines (C^{97}-C^{125}, C^{293}-C^{306}, C^{514}-C^{647}) are indicated with dashed blue lines. The four conserved charged residues involved in forming two salt-bridges are marked with ▲ and shaded in green. The positions of the 14 aromatic residues that line the catalytic gorge in *T. californica* AChE are shaded in blue (9 are identical in SmTAChE). The oxyanion hole residues are indicated with ▼ and shaded in red. Five potential N-glycosylation sites (with the consensus sequence NXS/T) are marked with ○. The amino acid sequence of the unique peptide (K^{329}-E^{346}) used to generate antibodies for SmTAChE is in red and double underlined. The signal peptide of SmTAChE (M^{1}-S^{25}) is underlined. The GPI anchor sequence of SmTAChE (G^{669} - G^{694}) is indicated with a dashed underline, and the omega (ω)-residue (S^{668}) is indicated with ‡. Identical residues in all sequences are marked with an asterisk (*); strongly similar residues (conserved substitution) are indicated with a colon (:); weakly similar residues (semi-conserved) indicated with a dot (.), and gaps, introduced to allow maximum alignment, are marked with dashes (–). The numbers (right) tally the amino acid count per line for each sequence.

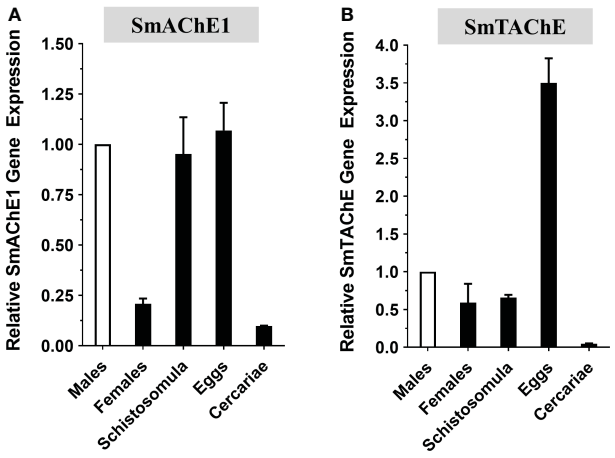

FIGURE 5
Developmental expression of acetylcholinesterase genes in different *S. mansoni* life stages as determined by RT-qPCR. **(A)** SmAChE1 gene expression. **(B)** SmTAChE Gene expression. All values are relative to the gene expression level of male parasites, set at 1 (Mean ± SD, n=3).

revealed in both the male longitudinal section (Figure 6C, top white arrows) and in the female cross section (Figure 6C, middle panel, white arrows). Control parasites, exposed to secondary antibody alone, do not display signal in the tegument or elsewhere, in either adult parasites or schistosomula (Figure 6B, C, bottom panels). Further analysis using e.g., confocal microscopy would help confirm expression of SmTAChE in the tegument of schistosomula. Localization of SmTAChE by immunogold electron microscopy (Figure 6D) does confirm that the protein is distributed in adult worm tegumental membranes. Immunogold particles are seen scattered widely throughout the section, sometimes in small clusters, including at the host interactive surface (red arrows). In addition, immunogold particles are also seen lining tegumental pits (green arrows). Very few immunogold particles are seen in control sections incubated with gold-labeled secondary anti-rabbit antibody alone (Figure S3).

The SmTAChE gene encodes the surface AChE

To evaluate whether the SmTAChE gene codes for the enzyme responsible for surface AChE activity, we first knocked-down expression of the gene using RNAi using 2 different siRNAs. Both siRNAs gave similar levels of suppression, and for all subsequent experiments SmAC2-siRNA1 was used. Figure 7A shows ~90% SmTAChE gene suppression in parasites treated with an siRNA targeting the gene compared to control parasites treated with a control (irrelevant) siRNA or no siRNA (none), as determined by RT-qPCR. To assess the impact of the knock-down on the surface AChE, the ability of live worms to cleave exogenous acetylthiocholine was compared between the groups, 7 days after RNAi treatment. As shown in Figure 7B, mean surface AChE activity is significantly reduced in live male parasites treated with siRNA specific for the SmTAChE gene, versus controls ($p < 0.0001$). No visible changes were observed to SmTAChE gene-suppressed parasites maintained in culture for 14 days, as assessed by light microscopy.

SmTAChE is essential for parasite survival *in vivo*

To investigate whether SmTAChE has an impact on parasite survival *in vivo*, we first suppressed its expression in schistosomula and, after 4 days in culture, these parasites were used to infect mice. Control mice were infected either with schistosomula treated with an irrelevant (control) siRNA or no siRNA, as previously described (12, 44). Mice were perfused six weeks later, and worm burdens were analyzed. As shown in Figure 8, in two independent experiments, almost no parasites were recovered from mice infected with schistosomula whose SmTAChE gene was suppressed compared to mice infected with schistosomula treated with no siRNA (Figure 8A) or mice infected with schistosomula treated with control siRNA (Figure 8B) ($p < 0.05$, for both experiments, Student's t test). This

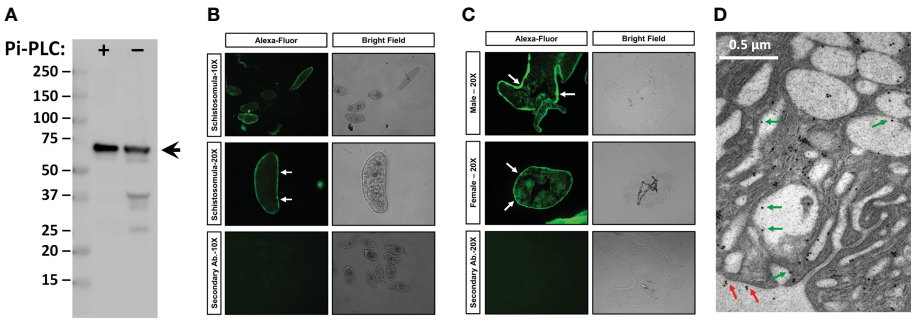

FIGURE 6
Immunolocalization of SmTAChE. **(A,** left) Anti-SmTAChE antibodies bind to a protein of the expected size of SmTAChE (~75 kDa, arrow) as seen by western blot analysis in a protein preparation obtained following Pi-PLC treatment of live adult males (**+**) and in a total male lysate (not treated with Pi-PLC, **-**). Numbers to the left indicate molecular mass markers (kDa). **(B)** Immunostaining of SmTAChE in 7-day old cultured schistosomula. **(C)** Immunostaining of SmTAChE in sections of adult male longitudinal section; (**C**, top panel) and adult female (cross section; **C**, middle panel) parasites. Magnification level (10X or 20X) is indicated to the left. An Alexa-Fluor 488 conjugated secondary antibody was used for detection and was used as a control. Both fluor (left panels) and bright (right panels) fields are shown for each section. Strong tegumental staining is seen in schistosomula and adults (white arrows). **(D)** Electron micrograph of the adult tegument showing immunogold labeling of SmTAChE. Red arrows indicate localization of gold particles on the external surface of the worm and green arrows indicate the presence of some gold particles lining tegumental pits.

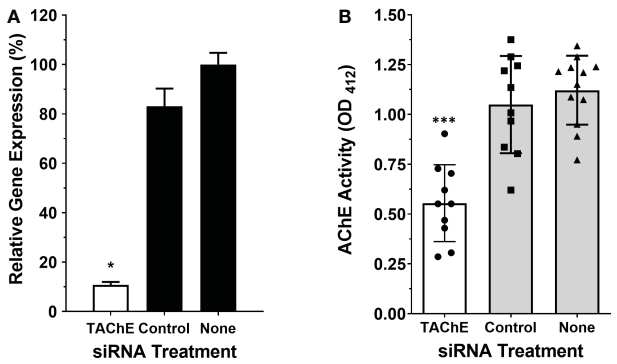

FIGURE 7
The SmTAChE gene encodes the surface AChE. Adult male parasites were treated either with an siRNA targeting SmTAChE, or with an irrelevant siRNA (Control) or with no siRNA (None), as indicated. **(A)** Treating parasites with siRNA targeting SmTAChE significantly suppressed the expression of this gene (by >90%; white bar, *p < 0.05 ANOVA) compared to controls, as revealed by RT-qPCR. **(B)** The AChE activity of all three groups of live parasites, one week after treatment, is shown, where each point represents the data from an individual parasite, and the bars indicates the mean for the group (± SD). Mean surface AChE activity is significantly lower in parasites treated with siRNA specific for SmTAChE (white bar) compared to parasites treated with control siRNA or with no siRNA (None) (grey bars, ***p < 0.0001, ANOVA, n ≥10).

important result shows that SmTAChE performs a vital function that is key for parasite survival.

Identification of SmTAChE homologs in *S. haematobium* and *S. japonicum*

Analysis of the *S. haematobium* genome resulted in the identification of a gene (MS3_0012973) encoding a potential protein with 85% sequence identity to SmTAChE, which we designate ShTAChE. The complete nucleotide sequence of ShTAChE cDNA is deposited at the NCBI GenBank under the accession number OP018962. In the case of *S. japonicum*, no single contig or scaffold was identified that contained a complete SmTAChE homolog. However, as detailed in Methods, two different contigs were identified in WormBase ParaSite, each encoding part of an SmTAChE homolog; based on these sequences and using the RACE technique, we isolated the complete *S. japonicum* TAChE coding region. The complete nucleotide sequence of SjTAChE cDNA is deposited at NCBI GenBank under the accession number OP018963. The predicted SjTAChE protein has 71% sequence identity with SmTAChE and 69% identity with ShTAChE. Analysis of the gene structures of the three schistosome TAChE genes shows them to be very similar; as shown in Figure S4, all genes contain 4 exons and 3 introns (Figure S4) and with all exon-splicing sites being identical in the three genes. Figure S5 shows the predicted amino acid sequences of the three schistosome TAChE proteins. Similar to SmTAChE, both ShTAChE and SjTAChE proteins are predicted to have a signal peptide and a GPI anchoring signal with conserved ω-site, as well as all motifs conserved in other members of the AChE family.

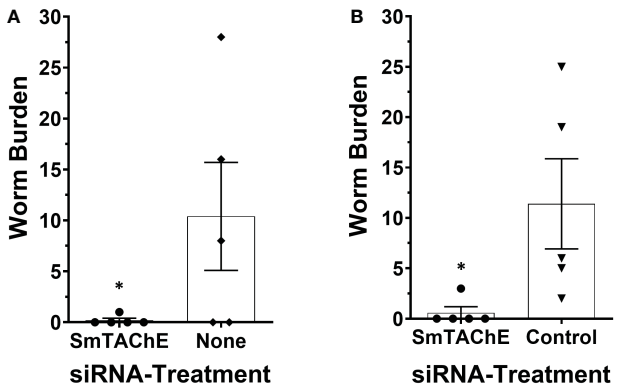

FIGURE 8
SmTAChE is essential for parasite survival *in vivo*. Schistosome recovery from mice 6 weeks after infection with SmTAChE-suppressed or control parasites. Results from two independent experiments are shown. **(A)** schistosomula were treated with siRNA specific for SmTAChE, or with no siRNA, prior to infection and in **(B)** schistosomula were treated with siRNA specific for SmTAChE or with control siRNA prior to infection. Each point represents the worm burden from one mouse, and the line represents the mean (± SD) for the group. In both instances, treatment with SmTAChE siRNA significantly reduced the number of recovered parasites (*P < 0.04, Students' t test).

Surface AChE activity of the three major human schistosome species

Here we compare the surface AChE activity displayed by male and female parasites of the three major human schistosome species. As shown in Figure 9, individual live adult male (Figure 9A) and live adult female (Figure 9B) schistosomes from all three species cleave exogenous acetylthiocholine. *S. haematobium* parasites have the highest AChE activity; individual male *S. haematobium* have approximately twice the surface activity found in individual *S. mansoni* or *S. japonicum* parasites, while individual female *S. haematobium* parasites have almost 7 times the surface activity of individual females of the other two schistosome species. (Quantitative data reported in Table S3) It is noteworthy that individual female *S. haematobium* display similar surface AChE activity to individual male parasites (Table S3). For *S. mansoni* and *S. japonicum*, live individual male AChE activity is about twice that of individual females.

The TAChE genes of all three schistosome species were targeted for suppression by treating male worms with a universal siRNA that targets the TAChEs of all three. In each case this treatment resulted in significant reductions in surface AChE activity seven days post treatment (white bars) compared to control parasites treated either with control siRNA or with no siRNA (grey bars) (Figures 9C-E).

Discussion

We demonstrated here for the first time that live, intact, intravascular-stage schistosomes can cleave exogenous acetylthiocholine. Adult male and female *S. mansoni*, as well as schistosomula, display this activity, as do freshly isolated parasite eggs. All such activity is blocked in the presence of the selective AChE inhibitor BW284c51. The majority of total adult male worm AChE activity (~70%) can be attributed to the action of the surface AChE.

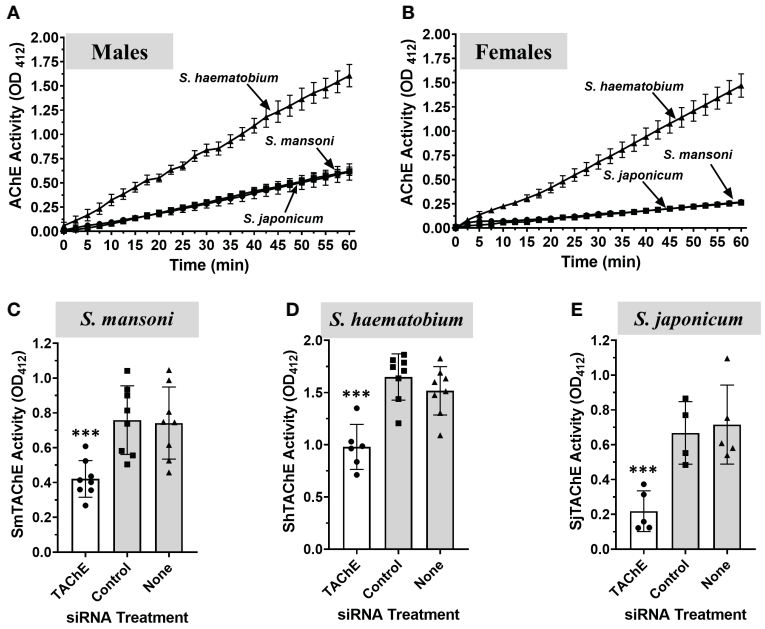

FIGURE 9
Surface AChE activity (mean OD_{412} ± SD) in live individual adults of the three medically most important schistosome species *S. mansoni*, *S. haematobium* and *S. japonicum*, as indicated (n≥5). **(A)** Live individual adult male parasites. **(B)** Live individual adult female parasites. *S. haematobium* parasites (both male and female) exhibit significantly higher surface AChE activity versus *S. mansoni* or *S. japonicum* parasites ($p < 0.001$, Two-Way ANOVA). No significant difference is observed between live *S. mansoni* and *S. japonicum* adult parasite AChE activity. **(C–E)** A universal siRNA targeting the tegumental AChE gene of the three species was designed and used to knock-down the expression of this gene in adult male parasites. Seven days later the surface AChE activity (mean OD_{412} ± SD) was measured in live, gene-suppressed versus control *S. mansoni* **(C)**, *S. haematobium* **(D)** or *S. japonicum* **(E)** adult males. Each point represents the data from one worm, and the line represents the mean (± SD) for the group. In all cases, gene suppression resulted is significant reductions in surface AChE activity (**C**, *S. mansoni;* ***$p < 0.001$), (**D**, *S. haematobium*; ***$p < 0.0001$) and (**E**, *S. japonicum*; ***$p < 0.008$, all by ANOVA). Values obtained at 60 min are presented.

While a tegumental butyrylcholinesterase (BuChE) has been identified in *S. mansoni* (SmBuChE (30),), we find that intact, live parasites display no evidence of host-interactive BuChE activity, suggesting that SmBuChE is not expressed on the external surface of the intravascular-stage worms. In addition, we were unable to detect secreted AChE activity, showing that AChE remains attached to the parasites surface and is not excreted or secreted by the worms to any great extent. In agreement with this, previous work detected AChE activity only in medium where live parasites had been treated with Pi-PLC, but not in the medium of control parasites (46).

A gene encoding an AChE was previously identified in *S. mansoni*, *S. haematobium*, *S. bovis* and *S. japonicum* (17, 21, 28, 29). The worms had been reported to display AChE activity both internally as well as on their external tegumental membranes and it was originally proposed that the identified gene encoded both internal and tegumental enzymes (17). However, we show here that suppression of this gene in *S. mansoni* (SmAChE1) using RNAi failed to significantly impact the surface AChE activity of live adult male parasites. In addition, neither SmAChE1 (and its homologs in other schistosome species), nor a second AChE identified in *S. mansoni* (SmAChE2 (30),), were predicted to contain a consensus C-terminal GPI anchoring sequence. Therefore, we hypothesized that another gene coded for the surface AChE. *In silico* analysis of the *S. mansoni* genome revealed the presence of a gene potentially encoding a 694 amino acid protein that has a high degree of identity with the previously published 488 amino acid SmAChE2 (30). Despite the fact that both sequences are encoded by the same gene (Smp_136690), substantial differences have emerged between the published SmAChE2 protein (30) and the sequence we present here. Our predicted AChE is essentially a newly annotated version of the previous sequence, and we elect to use the name SmTAChE for this enzyme. We cloned the complete coding sequence of this gene and, as detailed in Results, identified all domains and essential amino acids required for AChE activity in its predicted amino acid sequence. We have sequenced and analyzed multiple PCR products generated using adult parasite cDNA as template, but have never found a sequence that matches the published SmAChE2 sequence (30). Importantly, our SmTAChE sequence contains a leader sequence and a consensus GPI anchoring domain, supporting the biochemical evidence that the tegumental AChE is GPI linked (21, 27, 42). Indeed, we show here that experimental treatment of live schistosomes with Pi-PLC releases SmTAChE. Interestingly, it has been previously demonstrated that treating parasites with Pi-PLC significantly upregulates the synthesis of AChE (47).

Immunolocalization experiments reported here, using antibodies that are specific for SmTAChE, showed that the protein is prominently expressed in the tegument of the schistosomula and adult parasite stages, as expected if this protein is responsible for surface AChE activity. Most importantly, knocking down the expression of the SmTAChE gene resulted in a significant reduction in the surface AChE activity displayed by live parasites. These data prove that the tegumental surface AChE of *S. mansoni* is encoded by the SmTAChE gene and help to clarify longstanding confusion regarding schistosome AChE activity. To our surprise, SmTAChE

expression is not seen to be especially enriched in tegumental cells (neither cluster 1 nor cluster 2) in an *S. mansoni* single cell dataset (48, 49). Instead, expression is detected in many cell types with enrichment noted in several distinct neuronal cell groups and in flame cells (48, 49). More work is needed to better reconcile the transcriptomic versus tegument proteomic data sets.

Presumably SmTAChE is the protein earlier characterized as having a sedimentation coefficient of 6.5S that does not bind to heparin but that can be released from intact parasites by Pi-PLC treatment (26, 27). In support of this and as noted earlier, treatment of live schistosomes with Pi-PLC releases SmTAChE. We infer that SmAChE1 is the internal protein earlier characterized as having a sedimentation coefficient of 8S that binds heparin (26). Genes encoding both proteins are expressed in all intra-mammalian life stages of the parasites, and both exhibit minimal relative expression in the cercarial life stage.

In other animals, a key function of the AChE enzyme is to terminate synaptic transmission at cholinergic synapses by hydrolyzing the neurotransmitter acetylcholine, and we hypothesize that SmAChE1 largely fulfills this function in schistosomes. However, the function of the non-neuronal, tegumental enzyme SmTAChE is unknown (50). To examine the importance of this tegumental AChE enzyme for *S. mansoni in vivo*, SmTAChE gene-suppressed versus control schistosomula were used to infect mice and, after 6 weeks, worm burdens were compared between the groups. Almost no parasites are recovered from mice infected with schistosomula whose SmTAChE gene was suppressed compared to controls. This important result shows that the function(s) performed by SmTAChE are vital for parasite survival. The essential function fulfilled by SmTAChE is unclear. The enzyme may influence host vascular physiology, given that acetylcholine is a vasodilator (51–53). Additionally, SmTAChE may have an immunoregulatory role since several immune cells respond to acetylcholine (54, 55) and, due to SmTAChE action, it seems likely that immune signaling *via* acetylcholine would be impaired, at least in the vicinity of the worms. Glucose uptake is reported to be enhanced in the presence of acetylcholine in adult *S. haematobium* and *S. bovis* but not *S. mansoni* (56) and it is possible that the action of tegumental AChEs could impact this. Beyond schistosomes, AChEs are now reported to be distributed in a variety of non-neuronal tissues including in hematopoietic, osteogenic and various neoplastic cells, where the enzymes are predicted to express non-classical (and possibly non-enzymatic) activities (21, 57–59). Currently, there is substantial effort to understand the physiological significance and the molecular mechanisms of these non-neuronal cholinergic activities (60–65).

Since the suppression of SmTAChE gene expression severely impaired the ability of the worms to establish a robust infection, this validates SmTAChE as a therapeutic target for schistosomiasis. Indeed, it has been shown that human schistosomiasis can be treated using the drug metrifonate, an organophosphorus compound (13, 66). The active metabolite of metrifonate, dichlorvos (2,2-dichlorovinyl dimethyl phosphate), acts by inhibiting AChEs. It was suggested that tegumental AChE is the target for this therapy (20). While metrifonate is no longer commercially available as an anti-schistosome agent due to the need for multiple doses, reduced efficacy compared to the newer drug praziquantel (PZQ), and higher specificity to human AChE which can result in toxicity (66, 67), its earlier use in humans highlights the potential value of identifying schistosome-specific AChE inhibitors (against SmTAChE and/or SmAChE1) as novel therapies.

Since any new therapy for schistosomiasis should ideally target all three medically important species, we looked for evidence of surface AChE activity in *S. japonicum* and *S. haematobium*, in addition to *S. mansoni*. Adult male and female worms of all three species were observed to cleave exogenous acetylthiocholine with *S. haematobium* parasites exhibiting the highest surface AChE activity, when compared to the other two species. Both *S. mansoni* and *S. japonicum* adult worms express very similar levels of surface AChE activity. In contrast, individual adult male *S. haematobium* parasites display about two-fold greater activity compared to individual males of either *S. japonicum* or *S. mansoni*. Additionally, female *S. haematobium* exhibits strikingly high relative AChE surface activity - almost seven times that found in the other two species. These data are in general agreement with reports that tegument extracts of adult *S. haematobium* display substantially higher AChE activity compared to equivalent tegument extracts of *S. mansoni* (20). The requirement for such high surface AChE activity by *S. haematobium*, and whether it is related to living in its distinct, preferred intravascular niche (the vesicle plexus), is not known. Similarly, why *S. mansoni* eggs should display such a very high relative SmTAChE expression level (>3 times that of adult males) is unclear.

Finally, we investigated whether the surface AChEs of *S. haematobium* and *S. japonicum* are encoded by SmTAChE homologs. We first identified and cloned clear homologs from *S. haematobium* (ShTAChE) and *S. japonicum* (SjTAChE) and we identified that the genes encoding these proteins possess a very similar structure across all three species, and all three proteins are predicted to possess signal peptides and GPI anchoring sites. We next targeted the surface AChE gene from each species for suppression by RNAi. This yielded parasites with a significantly diminished ability to cleave exogenous acetylthiocholine compared to controls, confirming that the identified genes indeed encode the tegumental AChE in the three schistosome species.

The two *S. mansoni* AChE gene structures are quite divergent; SmAChE1 has 9 exons while SmTAChE has 4. In addition, the 687 amino acid SmAChE1 and the 694 amino acid SmTAChE display just moderate (~35%) amino acid sequence identity and this is about the same as that displayed by either of the schistosome AChEs versus (evolutionarily distant) human AChE (614 amino acids). Given the moderate level of amino acid sequence identity between the schistosome AChEs versus the human enzyme, it is likely that drugs preferentially inhibiting the schistosome enzymes could be developed. Unlike schistosomes, the human genome encodes a single AChE, and this makes any differential inhibitor screening (i.e., testing for inhibition of schistosome *vs*. human AChE) very feasible.

Heterologous anti-AChE antibodies (raised by immunizing rabbits with AChE from an electric eel, *Eletrophorus electricus*) bind to live *S. mansoni* schistosomula (68). Incubating these parasites with guinea pig serum (as a source of complement) results in ~ 50% killing of the parasites (68). Similarly, incubating schistosomula with antibodies raised against *S. mansoni* cercarial AChE (in the presence of guinea pig serum) leads to ~80% parasite killing (69). We infer that in these experiments the anti-AChE antibodies drive this effect by binding to the SmTAChE that is exposed on the external

surface of the worms; this provides a strong rationale for also considering surface located SmTAChE as a novel anti schistosome vaccine candidate. Blocking SmTAChE function using either new drugs, or immunologically, offers a new therapeutic approach to control schistosomiasis.

Data availability statement

The datasets presented in this study can be found in online repositories. The names of the repository/repositories and accession number(s) can be found in the article/Supplementary Material.

Ethics statement

The animal study was reviewed and approved by The Institutional Animal Care and Use Committee (IACUC) of Tufts University and all animal work was done in the vivarium at Cummings School of Veterinary Medicine, Tufts University.

Author contributions

PS: Conceptualization, data curation, writing and editing the manuscript. AD: Conceptualization, data curation and analysis. performed the experiments, writing the first draft and finalizing the manuscript. All authors contributed to the article and approved the submitted version.

Funding

This work was funded with support from the National Institutes of Health, National Institute of Allergy and Infectious Diseases [AI056273] and [AI137667].

Acknowledgments

We thank the NIAID Schistosomiasis Resource Center of the Biomedical Research Institute (Rockville, MD) for providing essential schistosome reagents through NIH-NIAID Contract HHSN272201700014I. NIH: *Biomphalaria glabrata* (NMRI) exposed to *Schistosoma mansoni* (NMRI).

Conflict of interest

The authors declare that the research was conducted in the absence of any commercial or financial relationships that could be construed as a potential conflict of interest.

Publisher's note

Supplementary material

The Supplementary Material for this article can be found online at: https://www.frontiersin.org/articles/10.3389/fimmu.2023.1056469/full#supplementary-material

SUPPLEMENTARY FIGURE 1
Sequence comparison of SmTAChE and SmAChE2. Both sequences derive from the gene Smp_136690; however, the SmTAChE protein (accession number OP018961) is substantially different from the published SmAChE2 sequence (30). The SmAChE2 sequence lacks a signal peptide(M^{1}-S^{25}) underlined in the SmTAChE sequence) and a GPI-anchoring signal (G^{669}-G^{694} double underlined in SmTAChE) and, likely due to differences in annotation, is missing many blocks of amino acids compared to SmTAChE. Differences between the sequences are depicted by red text highlighted in yellow.

SUPPLEMENTARY FIGURE 2
Alignment of multiple AChE sequences using Muscle (http://www.phylogeny.fr/). These data were used to generate the phylogenetic tree shown in . All accession numbers are indicated in the legend. Similar residues are highlighted in blue as most conserved according to BLOSUM62. Average BLOSUM62 score: Max: 3.0, Mid: 1.5, Low: 0.5.

SUPPLEMENTARY FIGURE 3
Control electron micrograph (EM) image. Very few immunogold particles are seen in sections, such as that shown, that were incubated with gold-labeled secondary anti-rabbit antibody alone.

SUPPLEMENTARY FIGURE 4
A schematic representation of the conserved tegumental AChE gene structure of three schistosome species. The gene encoding the tegumental AChE of *S. mansoni* (SmTAChE, topo) is compared to that of *S. haematobium* (ShTAChE, middle) and *S. japonicum* (SjTAChE, bottom). The sizes of exons and introns are indicated (numbers represent base pairs). The//indicates that the complete intron 1 of SjTAChE has not yet been characterized.

SUPPLEMENTARY FIGURE 5
Alignment of the amino acid sequences of the tegumental acetylcholinesterases (AChEs) of three schistosome species. The amino acid sequence of the tegumental *Schistosoma mansoni* AChE (*Sm*TAChE, accession number OP018961), tegumental *S. haematobium* AChE (*Sh*TAChE, accession number OP018962) and tegumental *S. japonicum* AChE (*Sj*TAChE, accession number OP018963) were aligned using Clustal W. The catalytic triad residues (S^{239}, E^{401}, H^{553}, where amino acid positions correspond to the numbering of the *Sm*TAChE sequence) are in red and indicated with ●. The signature sequence (^{236}FGESAG^{241}) of cholinesterases around the active serine residue (S^{239}) is boxed. The choline-binding site (W^{115}) is indicated with ■. The three intrachain disulfide bonds formed using six conserved cysteines are indicated with dashed blue lines. The boxed cysteine residue (C^{665}) is predicted to be involved in dimer formation. Predicted signal peptides are underlined and predicted GPI anchoring motifs are indicated with a dashed underline. All three sequences have a conserved omega (ω)-site (indicated with ‡). All other domains are described in the legend to . Red arrows (↓) depict amino acids encoded by DNA sequences at exon/exon junctions, further highlighting their conservation.

References

1. Steinmann P, Keiser J, Bos R, Tanner M, Utzinger J. Schistosomiasis and water resources development: systematic review, meta-analysis, and estimates of people at risk. *Lancet Infect Dis* (2006) 6(7):411–25. doi: 10.1016/S1473-3099(06)70521-7

2. Gryseels B. Schistosomiasis. *Infect Dis Clinics North America* (2012) 26(2):383–97. doi: 10.1016/j.idc.2012.03.004

3. King CH, Dangerfield-Cha M. The unacknowledged impact of chronic schistosomiasis. *Chronic Illn* (2008) 4(1):65–79. doi: 10.1177/1742395307084407

4. King CH. Parasites and poverty: the case of schistosomiasis. *Acta Tropica* (2010) 113 (2):95–104. doi: 10.1016/j.actatropica.2009.11.012

5. King CH, Dickman K, Tisch DJ. Reassessment of the cost of chronic helmintic infection: a meta-analysis of disability-related outcomes in endemic schistosomiasis. *Lancet* (2005) 365(9470):1561–9. doi: 10.1016/S0140-6736(05)66457-4

6. Hotez PJ, Alvarado M, Basanez MG, Bolliger I, Bourne R, Boussinesq M, et al. The global burden of disease study 2010: interpretation and implications for the neglected tropical diseases. *PloS Negl Trop Dis* (2014) 8(7):e2865. doi: 10.1371/journal.pntd.0002865

7. Gryseels B, Polman K, Clerinx J, Kestens L. Human schistosomiasis. *Lancet* (2006) 368(9541):1106–18. doi: 10.1016/S0140-6736(06)69440-3

8. Jia TW, Utzinger J, Deng Y, Yang K, Li YY, Zhu JH, et al. Quantifying quality of life and disability of patients with advanced schistosomiasis japonica. *PloS Negl Trop Dis* (2011) 5(2):e966. doi: 10.1371/journal.pntd.0000966

9. Warren KS. The secret of the immunopathogenesis of schistosomiasis: *in vivo* models. *Immunol Rev* (1982) 61:189–213. doi: 10.1111/j.1600-065X.1982.tb00377.x

10. Skelly P, Wilson R. Making sense of the schistosome surface. *Adv Parasitol* (2006) 63:185–284. doi: 10.1016/S0065-308X(06)63003-0

11. Nation CS, Da'Dara AA, Skelly PJ. NAD-catabolizing ectoenzymes of schistosoma mansoni. *Biochem J* (2022) 479(11):1165–80. doi: 10.1042/BCJ20210784

12. Krautz-Peterson G, Simoes M, Faghiri Z, Ndegwa D, Oliveira G, Shoemaker CB, et al. Suppressing glucose transporter gene expression in schistosomes impairs parasite feeding and decreases survival in the mammalian host. *PloS Pathog* (2010) 6(6):e1000932. doi: 10.1371/journal.ppat.1000932

13. Faghiri Z, Camargo SM, Huggel K, Forster IC, Ndegwa D, Verrey F, et al. The tegument of the human parasitic worm schistosoma mansoni as an excretory organ: the surface aquaporin SmAQP is a lactate transporter. *PloS One* (2010) 5(5):e10451. doi: 10.1371/journal.pone.0010451

14. Elzoheiry M, Da'dara AA, Bhardwaj R, Wang Q, Azab MS, El-Kholy EI, et al. Intravascular schistosoma mansoni cleave the host immune and hemostatic signaling molecule sphingosine-1-Phosphate *via* tegumental alkaline phosphatase. *Front Immunol* (2018) 9:1746. doi: 10.3389/fimmu.2018.01746

15. Da'dara AA, Elzoheiry M, El-Beshbishi SN, Skelly PJ. Vitamin B6 acquisition and metabolism in schistosoma mansoni. *Front Immunol* (2020) 11:622162. doi: 10.3389/fimmu.2020.622162

16. Da'dara AA, Angeli A, Ferraroni M, Supuran CT, Skelly PJ. Crystal structure and chemical inhibition of essential schistosome host-interactive virulence factor carbonic anhydrase SmCA. *Commun Biol* (2019) 2:333. doi: 10.1038/s42003-019-0578-0

17. Jones AK, Bentley GN, Oliveros Parra WG, Agnew A. Molecular characterization of an acetylcholinesterase implicated in the regulation of glucose scavenging by the parasite schistosoma. *FASEB J* (2002) 16(3):441–3. doi: 10.1096/fj.01-0683fje

18. Barker LR, Bueding E, Timms AR. The possible role of acetylcholine in schistosoma mansoni. *Br J Pharmacol Chemother* (1966) 26(3):656–65. doi: 10.1111/j.1476-5381.1966.tb01845.x

19. Pax RA, Siefker C, Bennett JL. Schistosoma mansoni: differences in acetylcholine, dopamine, and serotonin control of circular and longitudinal parasite muscles. *Exp Parasitol* (1984) 58(3):314–24. doi: 10.1016/0014-4894(84)90048-1

20. Camacho M, Tarrab-Hazdai R, Espinoza B, Arnon R, Agnew A. The amount of acetylcholinesterase on the parasite surface reflects the differential sensitivity of schistosome species to metrifonate. *Parasitology* (1994) 108(Pt 2):153–60. doi: 10.1017/S0031182000068244

21. Camacho M, Alsford S, Agnew A. Molecular forms of tegumental and muscle acetylcholinesterases of schistosoma. *Parasitology* (1996) 112(Pt 2):199–204. doi: 10.1017/S0031182000084766

22. Levi-Schaffer F, Tarrab-Hazdai R, Schryer MD, Arnon R, Smolarsky M. Isolation and partial characterization of the tegumental outer membrane of schistosomula of schistosoma mansoni. *Mol Biochem Parasitol* (1984) 13(3):283–300. doi: 10.1016/0166-6851(84)90120-8

23. Espinoza B, Parizade M, Ortega E, Tarrab-Hazdai R, Zilberg D, Arnon R. Monoclonal antibodies against acetylcholinesterase of schistosoma mansoni: production and characterization. *Hybridoma* (1995) 14(6):577–86. doi: 10.1089/hyb.1995.14.577

24. Goldlust A, Arnon R, Silman I, Tarrab-Hazdai R. Acetylcholinesterase of schistosoma mansoni: purification and characterization. *J Neurosci Res* (1986) 15 (4):569–81. doi: 10.1002/jnr.490150413

25. Tarrab-Hazdai R, Levi-Schaffer F, Gonzales G, Arnon R. Acetylcholinesterase of schistosoma mansoni. molecular forms of the solubilized enzyme. *Biochim Biophys Acta* (1984) 790(1):61–9. doi: 10.1016/0167-4838(84)90332-7

26. Tarrab-Hazdai R, Toker L, Silman I, Arnon R. Acetylcholinesterase from schistosoma mansoni: interaction of globular species with heparin. *Biochem J* (1999) 344 Pt 3:945–51. doi: 10.1042/bj3440945

27. Espinoza B, Tarrab-Hazdai R, Silman I, Arnon R. Acetylcholinesterase in schistosoma mansoni is anchored to the membrane via covalently attached phosphatidylinositol. *Mol Biochem Parasitol* (1988) 29(2-3):171–9. doi: 10.1016/0166-6851(88)90072-2

28. Bentley GN, Jones AK, Agnew A. Mapping and sequencing of acetylcholinesterase genes from the platyhelminth blood fluke schistosoma. *Gene* (2003) 314:103–12. doi: 10.1016/S0378-1119(03)00709-1

29. You H, Gobert GN, Du X, Pali G, Cai P, Jones MK, et al. Functional characterisation of schistosoma japonicum acetylcholinesterase. *Parasit Vectors* (2016) 9(1):328. doi: 10.1186/s13071-016-1615-1

30. Tedla BA, Sotillo J, Pickering D, Eichenberger RM, Ryan S, Becker L, et al. Novel cholinesterase paralogs of schistosoma mansoni have perceived roles in cholinergic signalling and drug detoxification and are essential for parasite survival. *PloS Pathog* (2019) 15(12):e1008213. doi: 10.1371/journal.ppat.1008213

31. Da'dara AA, Skelly PJ. Gene suppression in schistosomes using RNAi. *Methods Mol Biol* (2015) 1201:143–64. doi: 10.1007/978-1-4939-1438-8_8

32. Da'dara AA, Li YS, Xiong T, Zhou J, Williams GM, McManus DP, et al. DNA-Based vaccines protect against zoonotic schistosomiasis in water buffalo. *Vaccine* (2008) 26(29-30):3617–25. doi: 10.1016/j.vaccine.2008.04.080

33. Da'dara AA, Skelly PJ, Wang MM, Harn DA. Immunization with plasmid DNA encoding the integral membrane protein, Sm23, elicits a protective immune response against schistosome infection in mice. *Vaccine* (2001) 20(3-4):359–69. doi: 10.1016/S0264-410X(01)00374-7

34. Tucker MS, Karunaratne LB, Lewis FA, Freitas TC, Liang YS. Schistosomiasis. *Curr Protoc Immunol* (2013) 103:19 1 1– 1 58. doi: 10.1002/0471142735.im1901s103

35. Dalton JP, Day SR, Drew AC, Brindley PJ. A method for the isolation of schistosome eggs and miracidia free of contaminating host tissues. *Parasitology* (1997) 115(Pt 1):29–32. doi: 10.1017/S0031182097001091

36. Ellman GL, Courtney KD, Andres VJr., Feather-Stone RM. A new and rapid colorimetric determination of acetylcholinesterase activity. *Biochem Pharmacol* (1961) 7:88–95. doi: 10.1016/0006-2952(61)90145-9

37. Cline DJ, Redding SE, Brohawn SG, Psathas JN, Schneider JP, Thorpe C. New water-soluble phosphines as reductants of peptide and protein disulfide bonds: reactivity and membrane permeability. *Biochemistry* (2004) 43(48):15195–203. doi: 10.1021/bi048329a

38. Winther JR, Thorpe C. Quantification of thiols and disulfides. *Biochim Biophys Acta* (2014) 1840(2):838–46. doi: 10.1016/j.bbagen.2013.03.031

39. Dereeper A, Audic S, Claverie JM, Blanc G. BLAST-EXPLORER helps you building datasets for phylogenetic analysis. *BMC Evol Biol* (2010) 10:8. doi: 10.1186/1471-2148-10-8

40. Dereeper A, Guignon V, Blanc G, Audic S, Buffet S, Chevenet F, et al. Phylogeny.fr: robust phylogenetic analysis for the non-specialist. *Nucleic Acids Res* (2008) 36(Web Server issue):W465–9. doi: 10.1093/nar/gkn180

41. Edgar RC. MUSCLE: multiple sequence alignment with high accuracy and high throughput. *Nucleic Acids Res* (2004) 32(5):1792–7. doi: 10.1093/nar/gkh340

42. Castro-Borges W, Dowle A, Curwen RS, Thomas-Oates J, Wilson RA. Enzymatic shaving of the tegument surface of live schistosomes for proteomic analysis: a rational approach to select vaccine candidates. *PloS Negl Trop Dis* (2011) 5(3):e993. doi: 10.1371/journal.pntd.0000993

43. Skelly PJ, Dougan PM, Maule A, Day TA, Shoemaker CB. Cloning and characterization of a muscle isoform of a Na,K-ATPase alpha subunit (SNaK1) from schistosoma mansoni. *Parasitol Notes* (2001) 123(Pt 3):277–84. doi: 10.1017/S0031182001008484

44. Bhardwaj R, Krautz-Peterson G, Da'dara A, Tzipori S, Skelly PJ. Tegumental phosphodiesterase SmNPP-5 is a virulence factor for schistosomes. *Infect Immun* (2011) 79(10):4276–84. doi: 10.1128/IAI.05431-11

45. Zhang Y, Kua J, McCammon JA. Role of the catalytic triad and oxyanion hole in acetylcholinesterase catalysis: an ab initio QM/MM study. *J Am Chem Soc* (2002) 124 (35):10572–7. doi: 10.1021/ja020243m

46. Arnon R, Silman I, Tarrab-Hazdai R. Acetylcholinesterase of schistosoma mansoni–functional correlates. contributed in honor of professor Hans neurath's 90th birthday. *Protein Sci* (1999) 8(12):2553–61. doi: 10.1110/ps.8.12.2553

47. Espinoza B, Silman I, Arnon R, Tarrab-Hazdai R. Phosphatidylinositol-specific phospholipase c induces biosynthesis of acetylcholinesterase *via* diacylglycerol in schistosoma mansoni. *Eur J Biochem* (1991) 195(3):863–70. doi: 10.1111/j.1432-1033.1991.tb15776.x

48. Wendt G, Zhao L, Chen R, Liu C, O'Donoghue AJ, Caffrey CR, et al. A single-cell RNA-seq atlas of schistosoma mansoni identifies a key regulator of blood feeding. *Science* (2020) 369(6511):1644–9. doi: 10.1126/science.abb7709

49. Wendt GR, Reese ML, Collins JJ3rd. SchistoCyte atlas: A single-cell transcriptome resource for adult schistosomes. *Trends Parasitol* (2021) 37(7):585–7. doi: 10.1016/j.pt.2021.04.010

50. Soreq H, Seidman S. Acetylcholinesterase–new roles for an old actor. *Nat Rev Neurosci* (2001) 2(4):294–302. doi: 10.1038/35067589

51. Kellogg DLJr., Zhao JL, Coey U, Green JV. Acetylcholine-induced vasodilation is mediated by nitric oxide and prostaglandins in human skin. *J Appl Physiol (1985)* (2005) 98(2):629–32. doi: 10.1152/japplphysiol.00728.2004

52. Medow MS, Glover JL, Stewart JM. Nitric oxide and prostaglandin inhibition during acetylcholine-mediated cutaneous vasodilation in humans. *Microcirculation* (2008) 15(6):569–79. doi: 10.1080/10739680802091526

53. Holowatz LA, Thompson CS, Minson CT, Kenney WL. Mechanisms of acetylcholine-mediated vasodilatation in young and aged human skin. *J Physiol* (2005) 563(Pt 3):965–73. doi: 10.1113/jphysiol.2004.080952

54. Kawashima K, Fujii T, Moriwaki Y, Misawa H. Critical roles of acetylcholine and the muscarinic and nicotinic acetylcholine receptors in the regulation of immune function. *Life Sci* (2012) 91:1027–32. doi: 10.1016/j.lfs.2012.05.006

55. Kawashima K, Fujii T. The lymphocytic cholinergic system and its contribution to the regulation of immune activity. *Life Sci* (2003) 74(6):675–96. doi: 10.1016/j.lfs.2003.09.037

56. Camacho M, Agnew A. Schistosoma: rate of glucose import is altered by acetylcholine interaction with tegumental acetylcholine receptors and acetylcholinesterase. *Exp Parasitol* (1995) 81(4):584–91. doi: 10.1006/expr.1995.1152

57. Kawashima K, Fujii T. Basic and clinical aspects of non-neuronal acetylcholine: overview of non-neuronal cholinergic systems and their biological significance. *J Pharmacol Sci* (2008) 106(2):167–73. doi: 10.1254/jphs.FM0070073

58. Wessler IK, Kirkpatrick CJ. The non-neuronal cholinergic system: an emerging drug target in the airways. *Pulmonary Pharmacol Ther* (2001) 14(6):423–34. doi: 10.1006/pupt.2001.0313

59. Wessler I, Kilbinger H, Bittinger F, Kirkpatrick CJ. The biological role of non-neuronal acetylcholine in plants and humans. *Japanese J Pharmacol* (2001) 85(1):2–10. doi: 10.1254/jjp.85.2

60. Kirkpatrick CJ, Bittinger F, Nozadze K, Wessler I. Expression and function of the non-neuronal cholinergic system in endothelial cells. *Life Sci* (2003) 72(18-19):2111–6. doi: 10.1016/S0024-3205(03)00069-9

61. Maeda S, Jun JG, Kuwahara-Otani S, Tanaka K, Hayakawa T, Seki M. Non-neuronal expression of choline acetyltransferase in the rat kidney. *Life Sci* (2011) 89(11-12):408–14. doi: 10.1016/j.lfs.2011.07.011

62. de Almeida JP, Saldanha C. Nonneuronal cholinergic system in human erythrocytes: biological role and clinical relevance. *J Membr Biol* (2010) 234(3):227–34. doi: 10.1007/s00232-010-9250-9

63. Pickett MA, Dush MK, Nascone-Yoder NM. Acetylcholinesterase plays a non-neuronal, non-esterase role in organogenesis. *Development* (2017) 144(15):2764–70. doi: 10.1242/dev.149831

64. Fujii T, Mashimo M, Moriwaki Y, Misawa H, Ono S, Horiguchi K, et al. Expression and function of the cholinergic system in immune cells. *Front Immunol* (2017) 8:1085. doi: 10.3389/fimmu.2017.01085

65. Fujii T, Mashimo M, Moriwaki Y, Misawa H, Ono S, Horiguchi K, et al. Physiological functions of the cholinergic system in immune cells. *J Pharmacol Sci* (2017) 134(1):1–21. doi: 10.1016/j.jphs.2017.05.002

66. Kramer CV, Zhang F, Sinclair D, Olliaro PL. Drugs for treating urinary schistosomiasis. *Cochrane Database Systematic Rev* (2014) 2014(8):CD000053. doi: 10.1002/14651858.CD000053.pub3

67. Danso-Appiah A, Utzinger J, Liu J, Olliaro P. Drugs for treating urinary schistosomiasis. *Cochrane Database Systematic Rev* (2008) 2008(3):CD000053. doi: 10.1002/14651858.CD000053.pub2

68. Tarrab-Hazdai R, Levi-Schaffer F, Smolarsky M, Arnon R. Acetylcholinesterase of schistosoma mansoni: antigenic cross-reactivity with electrophorus electricus and its functional implications. *Eur J Immunol* (1984) 14(3):205–9. doi: 10.1002/eji.1830140302

69. Espinoza B, Tarrab-Hazdai R, Himmeloch S, Arnon R. Acetylcholinesterase from schistosoma mansoni: immunological characterization. *Immunol Lett* (1991) 28(2):167–74. doi: 10.1016/0165-2478(91)90116-R

frontiers | Frontiers in Microbiology

TYPE Original Research
PUBLISHED 24 February 2023
DOI 10.3389/fmicb.2023.1079855

OPEN ACCESS

EDITED BY
William Harold Witola,
University of Illinois at Urbana–Champaign,
United States

REVIEWED BY
Uriel Koziol,
University of the Republic,
Uruguay
Anna Victoria Protasio,
University of Cambridge,
United Kingdom

*CORRESPONDENCE
Marina Moraes Mourão
✉ marina.mourao@fiocruz.br

†These authors have contributed equally to this work and share first authorship

SPECIALTY SECTION
This article was submitted to Infectious Agents and Disease, a section of the journal Frontiers in Microbiology

RECEIVED 25 October 2022
ACCEPTED 01 February 2023
PUBLISHED 24 February 2023

CITATION
Coelho FS, Gava SG, Andrade LF, Geraldo JA, Tavares NC, Lunkes FMN, Neves RH, Machado-Silva JR, Pierce RJ, Oliveira G and Mourão MM (2023) *Schistosoma mansoni* coactivator associated arginine methyltransferase 1 (SmCARM1) effect on parasite reproduction. *Front. Microbiol.* 14:1079855. doi: 10.3389/fmicb.2023.1079855

Schistosoma mansoni coactivator associated arginine methyltransferase 1 (SmCARM1) effect on parasite reproduction

Fernanda Sales Coelho[1,2†], Sandra Grossi Gava[1†], Luiza Freire Andrade[1], Juliana Assis Geraldo[1], Naiara Clemente Tavares[1], Felipe Miguel Nery Lunkes[1], Renata Heisler Neves[3], José Roberto Machado-Silva[3], Raymond J. Pierce[4], Guilherme Oliveira[1,5] and Marina Moraes Mourão[1*]

[1]Grupo de Pesquisa em Helmintologia e Malacologia Médica, Instituto René Rachou, Fundação Oswaldo Cruz—FIOCRUZ, Belo Horizonte, Minas Gerais, Brazil, [2]Department of Clinical Research, London School of Hygiene and Tropical Medicine, London, United Kingdom, [3]Laboratório de Helmintologia Romero Lascasas Porto, Departamento de Microbiologia, Imunologia e Parasitologia, Faculdade de Ciências Médicas, Universidade do Estado do Rio de Janeiro, Rio de Janeiro, Brazil, [4]Université de Lille, CNRS, Inserm, CHU Lille, Institut Pasteur de Lille, U1019—UMR 9017—CIIL—Centre d'Infection et d'Immunité de Lille, Lille, France, [5]Instituto Tecnológico Vale, Belém, Pará, Brazil

Introduction: The human blood fluke parasite *Schistosoma mansoni* relies on diverse mechanisms to adapt to its diverse environments and hosts. Epigenetic mechanisms play a central role in gene expression regulation, culminating in such adaptations. Protein arginine methyltransferases (PRMTs) promote posttranslational modifications, modulating the function of histones and non-histone targets. The coactivator-associated arginine methyltransferase 1 (CARM1/PRMT4) is one of the *S. mansoni* proteins with the PRMT core domain.

Methods: We carried out *in silico* analyses to verify the expression of SmPRMTs in public datasets from different infection stages, single-sex versus mixed-worms, and cell types. The SmCARM1 function was evaluated by RNA interference. Gene expression levels were assessed, and phenotypic alterations were analyzed *in vitro*, *in vivo*, and *ex vivo*.

Results: The scRNAseq data showed that SmPRMTs expression is not enriched in any cell cluster in adult worms or schistosomula, except for Sm*carm*1 expression which is enriched in clusters of ambiguous cells and Sm*prmt*1 in NDF+ neurons and stem/germinal cells from schistosomula. Sm*prmt*1 is also enriched in S1 and late female germ cells from adult worms. After dsRNA exposure *in vitro*, we observed a Sm*carm*1 knockdown in schistosomula and adult worms, 83 and 69%, respectively. Sm*carm*1-knockdown resulted in reduced oviposition and no significant changes in the schistosomula or adult worm phenotypes. *In vivo* analysis after murine infection with Sm*carm*1 knocked-down schistosomula, showed no significant change in the number of worms recovered from mice, however, a significant reduction in the number of eggs recovered was detected. The *ex vivo* worms presented a significant decrease in the ovary area with a lower degree of cell differentiation, vitelline glands cell disorganization, and a decrease in the testicular lobe area. The worm tegument presented a lower number of tubercles, and the ventral sucker of the parasites presented a damaged tegument and points of detachment from the parasite body.

Discussion: This work brings the first functional characterization of SmCARM1 shedding light on its roles in *S. mansoni* biology and its potential as a drug target. Additional studies are necessary to investigate whether the reported effects of

Sm*carm*1 knockdown are a consequence of the SmCARM1-mediated methylation of histone tails involved in DNA packaging or other non-histone proteins.

KEYWORDS

***Schistosoma mansoni*, coactivator associated arginine methyltransferase 1, SmCARM1, epigenetics, reproduction**

Introduction

Schistosomiasis is a neglected parasitic disease with high rates of morbidity and mortality, producing significant economic losses, especially occurring in developing countries (Adepoju, 2020; WHO, 2022). The disease is caused by parasites of the genus *Schistosoma*, which have well-known and complex life cycles. Parasites require numerous and diverse mechanisms to change their anatomy and physiology and enable adaptation to different environments and hosts (Colley et al., 2014). Such adaptations are orchestrated by intense regulation of gene expression in which epigenetics mechanisms play a central role.

Schistosomiasis treatment relies on a single drug, praziquantel. The drug is effective with low side effects, but resistance has been described (Botros and Bennett, 2007; Doenhoff et al., 2008; Coeli et al., 2013). Since epigenetic proteins are promising targets for parasitic drug development, especially in helminths (Marek et al., 2013; Melesina et al., 2015) and a wide variety of epi-drugs are available; the piggy-back strategy might expedite the discovery of new specific leads and might allow the development of a new drug.

Eukaryotic chromatin remodeling promotes important parasite transcriptional changes and is mediated by nucleosome arrangements, DNA methylation, histone variants, non-coding RNAs, and posttranslational modifications (PTMs) of histones (Lee et al., 2010; Margueron and Reinberg, 2010). In this context, histone-modifying enzymes (HMEs) mediate the addition or removal of methyl, acetyl, or phosphate groups, among others, in the histone tails, remodeling the chromatin structure and altering the access to specific DNA segments (Jenuwein and Allis, 2001; Margueron and Reinberg, 2010). Histone methylation is an important PTM process that plays a crucial role in transcriptional control, splicing, DNA repair, and signaling (Dillon, 2004).

Protein arginine methyltransferases (PRMTs) promote the transference of methyl groups to the arginine residues of histones and other proteins (Lee et al., 1977). The eukaryotic PRMTs are classified into three different types. Type-I enzymes (PRMT1, PRMT3, PRMT4, PRMT6, and PRMT8) catalyze the formation of monomethyl arginine (MMA) and asymmetric dimethylarginine (aDMA), type-II enzymes (PRMT5 and PRMT9) form MMA and symmetric dimethylarginine (sDMA), while type-III enzymes (PRMT7) catalyze only MMA formation (Hartley and Lu, 2020). A type-IV enzyme catalyzes the monomethylation of the internal guanidino nitrogen atom and is reported only for yeast (RMT2; Bedford and Clarke, 2009). The posttranslational arginine methylation promoted by PRMTs modulates the function of histone proteins and non-histone targets, like transcription factors, coactivators, corepressors, and RNA-binding proteins. Accordingly, PRMTs regulate diverse cellular processes, including cell cycle, transcription, splicing, translation, signal transduction, and DNA damage and repair (Hwang et al., 2021).

Histone methylation processes play a role in *S. mansoni* development, as different life stages of the parasite present specific methylation profiles and the pharmacological inhibition of methyltransferases impacts the transition of miracidium to sporocyst (Roquis et al., 2018). *Schistosoma mansoni* possesses five proteins with the PRMT core domain (Smp_029240, Smp_025550, Smp_070340, Smp_171150, and Smp_337860; Padalino et al., 2018). The protein arginine methyltransferase 1 (SmPRMT1, Smp_029240) was the first and only characterized PRMT in *S. mansoni*. Mansure et al. demonstrated that SmPRMT1 methylates histone H4, besides SMYB1 and SmSmD3, proteins likely to be involved in RNA metabolism; suggesting the involvement of SmPRMT1 in chromatin remodeling and RNA editing and transport (Mansure et al., 2005). Additionally, Diao and collaborators demonstrated the immunogenic role of PRMT1 from *Schistosoma japonicum* pointing out this enzyme as a promising molecule for vaccine development (Diao et al., 2014).

The coactivator-associated arginine methyltransferase 1 (CARM1), also known as protein arginine methyltransferase 4 (PRMT4), regulates the expression of genes related to cell cycle progression and autophagy (El Messaoudi et al., 2006; Shin et al., 2016). CARM1 methylates the arginines 17 and 26 of histone H3 (H3R17, H3R26) and also functions as a coactivator in non-nuclear receptor systems like NF-κB, p53, INF-γ, MEF2C, and β-Catenin reviewed in Yue et al. (2007). In mice, CARM1-knockout embryos present small size and perinatal death (Yadav et al., 2003). Due to the important roles attributed to CARM1 orthologs and the lack of functional information in the *S. mansoni* parasite, here we aim at contributing to the functional characterization of this enzyme with a focus on schistosomula and adult stages, to shed light on the roles of SmCARM1 (Smp_070340) in *S. mansoni* biology and its potential as a drug target.

Materials and methods

Ethics statement

All procedures for the scientific use of animals were reviewed according to the Brazilian ethical guidelines (Law 11,794/08) and approved by the Ethics Committee for Animal Use (CEUA) of the Oswaldo Cruz Foundation under license numbers LW13/13 and LW12/16.

Reagents

The following reagents were used for parasite culture, Glasgow Minimum Essential Medium (GMEM), triiodothyronine, lactalbumin,

HEPES, MEM vitamin solution, Schneider's Insect Medium, hypoxanthine, and hydrocortisone were purchased from Sigma-Aldrich. Penicillin/streptomycin, RPMI 1640 medium, and Fetal Bovine Serum (FBS) were from Gibco; glucose from VETEC; TRIzol Reagent from Invitrogen.

All primers were purchased from IDT, Sm*carm*1-dsRNA_F: taatacgactcactatagggCATGGCATGGATCTAACTGC, Sm*carm*1-dsRNA_R: taatacgactcactatagggTGTTGTTGTTGCTGTTGTGC, Sm*carm*1-qPCR_F: TGCTGTTGAAGCATCTAATATGG, Sm*carm*1-qPCR_R: ATAATGACATCCACTGGTTCG; Sm*cox*I (Smp_900000) Sm*cox*I-qPCR_F: TACGGTTGGTGGTGTCACAG, Sm*cox*I-qPCR_R: ACGGCCATCACCATACTAGC; GFP-dsRNA_F: taatacgactcactata gggTCTTCAAGTCCGCCATG, GFP-dsRNA_R: taatacgactcactaggg TGCTCAGGTAGTGGTTGTC. The sequences in lowercase correspond to the T7 promoter sequence added to the 5′-end in primers designed for dsRNA synthesis.

Parasites

The "Lobato Paraense" snail facility at the René Rachou Institute—FIOCRUZ provided cercariae of *S. mansoni* (LE strain). The parasite cycle is maintained throughout passages between hamsters (*Mesocricetus auratus*) and snails (*Biomphalaria glabrata*).

As previously described, cercariae were mechanically transformed into schistosomula (Milligan and Jolly, 2011). Schistosomula were cultured in GMEM supplemented with 0.2 µM triiodothyronine; 0.1% glucose; 0.1% lactalbumin; 20 mM HEPES; 0.5% MEM vitamin solution; 5% Schneider's Insect Medium; and 0.5 µM hypoxanthine, 1 µM hydrocortisone, 1% penicillin/streptomycin, and 2% heat-inactivated FBS.

Hamsters (*M. auratus*) were infected with cercariae and subjected to perfusion (Pellegrino and Siqueira, 1956) after 45 days for obtaining adult worms. Males and females were washed, separated manually, and cultured in Roswell Park Memorial Institute 1640 (RPMI 1640) medium supplemented with 2% penicillin/streptomycin and 10% heat-inactivated FBS.

In silico analyses

To verify the expression data of SmPRMTs in the different cell types of adult *S. mansoni* worms, single-cell RNAseq (scRNAseq) data were obtained from the Gene Expression Omnibus database (GEO, https://www.ncbi.nlm.nih.gov/geo/, BioProject PRJNA611783, SRA SRP252217; https://www.collinslab.org/schistocyte/; Wendt et al., 2020). We also verified Sm*carm*1 expression in clusters of cells identified in schistosomula at the cellxgene platform[1] (Diaz Soria et al., 2020). The RDS file containing the expression data in the different cell types was loaded in the R software (v4.1.2; R Core Team, 2020) using the Seurat package (v4.1.1; Satija et al., 2015) and used to build a heatmap with the package ComplexHeatmap (v2.10.0; Gu et al., 2016). Additionally, we checked the SmPRMTs expression in a publicly available RNAseq dataset (Protasio et al., 2017) retrieved from WormBase ParaSite as counts of aligned reads per run per gene. Differential expression analysis was carried out using DESeq2 (v. 2_1.38.2; $padj < 0.05$; Love et al., 2014) and we used the pheatmap package (v1.0.12; Kolde, 2015) in R (v4.1.2; R Core Team, 2020) to construct a heatmap representing the log2 fold change for 18-, 28-, 35-, and 38-day post-infection (dpi) relative to 21 dpi.

Double-stranded RNA synthesis and parasite exposure

The Sm*carm*1 coding sequence was obtained from the GeneDB database.[2] The T7 promoter sequence was added to the 5′-end of primers designed to amplify a template of 569 bp for double-stranded RNAs (dsRNAs) synthesis. A fragment of 360 bp from the green fluorescent protein (GFP) cloned in the pCRII plasmid vector, was used as non-schistosome RNA interference (RNAi) control. The PCR amplified fragments were purified with the QIAquick Gel Extraction KIT (QIAGEN) and used for dsRNA synthesis using the T7 RiboMAX Express RNAi System kit (Promega) according to the supplier's protocol; except for the time of reactions which was changed to 16 h. DsRNAs annealing and integrity were verified in 1% agarose gel electrophoresis, and the quantification was estimated in a Nanodrop Spectrometer ND-1000 (Thermo Fischer Scientific).

Approximately 2,000 schistosomula were exposed to 100 nM of dsRNAs (Sm*carm*1 or GFP), immediately after mechanical transformation, in 24-well plate and incubated for 7 days at 37°C, 5% CO_2, and 95% humidity with 2 ml of GMEM supplemented as previously mentioned.

Eight adult worms (males and females, separately) were placed in 100 µl of RPMI 1640 medium with 25 µg of dsRNA. The worms were electroporated with specific Sm*carm*1-dsRNA or unspecific GFP-dsRNA into 4 mm cuvettes at 125 V for 20 ms and cultivated in 24-well plate with 1 ml RPMI 1640 medium supplemented with 10% heat-inactivated FBS and 2% penicillin/streptomycin. Similarly, to count the number of eggs laid, eight worm pairs were electroporated and cultured in six-well plate and the medium was changed daily.

RNA extraction, cDNA synthesis, and qPCR analysis

Seven days after dsRNA exposure, 1,000 schistosomula were separated for RNA extraction and relative expression analysis by quantitative real-time PCR (RT-qPCR). *Schistosoma mansoni* cytochrome C oxidase I gene (Sm*cox*I—Smp_900000) was used as the internal control gene. RNA extractions were performed using the TRIzol Reagent method followed by purification with the RNeasy Mini Kit (Qiagen), according to the manufacturer's guidelines. RNA samples were treated with the TURBO DNA-free kit (Ambion) to remove residual genomic DNA, quantified using the Nanodrop Spectrometer ND-1000, and stored at −70°C.

1 www.schistosomulacellatlas.org

2 http://www.genedb.org/Homepage/Smansoni

For adults, for 7 days, two worm pairs per day were removed and macerated with TRIzol Reagent for RNA extraction as described previously. Experiments were performed in four biological replicates.

The cDNAs were synthesized with equal amounts of the extracted RNAs using the SuperScript II Reverse Transcriptase (Invitrogen), with oligo(dT)18 following the manufacturer's protocol. Primers for qPCR analysis were designed using the Primer 3 program.[3] Primer efficiencies were estimated by titration analysis to be 100 ± 5% (data not shown), and the specificity was verified by the melting curve. qPCR reactions were performed on 7500 Real-Time PCR System (Applied Biosystems) with SYBR Green PCR Master Mix (Applied Biosystems) and 200 nM of each primer in a final volume of 25 µl. Internal controls to evaluate genomic DNA contaminations (RNA samples) and reagent purity (no cDNA) were included in all analyses. The $2^{-\Delta\Delta Ct}$ method (Livak and Schmittgen, 2001) was used for relative quantification and normalized with Sm*cox*I. Transcript levels were expressed as a percentage of difference relative to the unspecific (GFP) or negative control.

Phenotypic evaluation of schistosomula and adult worms

Schistosomula cultures were daily observed by inverted light microscopy (ABO 100, ZEISS) to verify viability and phenotypic changes, such as movement, color, and tegument integrity.

To evaluate the motility of the worms, we capture worm movement (eight males or females separately) for 1 min and 30 s for 7 days using the WormAssay software (Marcellino et al., 2012), in six replicates. Additionally, to verify the influence of SmCARM1 on oviposition, eggs laid in the media were counted daily in the cultures containing worm pairs, in five replicates.

In vivo experiments

After schistosomula exposure to dsRNAs for 2 days, 300 schistosomula were subcutaneously inoculated in Swiss mice (*Mus musculus*). Each experimental group consisted of at least six mice in three independent biological replicates. Before the infection, the Sm*carm*1 transcript levels in schistosomula were checked by qPCR, as described above. Schistosomula exposed to unspecific dsRNA-GFP and untreated parasites were used as controls. After 37 days adult worms were recovered by perfusion (Pellegrino and Siqueira, 1956). After perfusion, the worms recovered from the mice were separated into males and females and counted. Mouse livers were removed and individually weighed, crushed with a scalpel, and treated overnight with 10% KOH, for subsequent egg counting (Tavares and Mourão, 2021).

Morphometric and confocal analysis

The adult worms recovered after 37 days of mouse infection were fixed and stored in Alcohol-Formalin-Acetic Acid (AFA, 95% ethanol, 3% formaldehyde, and 2% glacial acetic acid), at room temperature, and stained with 2.5% chloride carmine, dehydrated in alcoholic series (70, 90%, and absolute), clarified in methyl salicylate with Canadian balsam (1:2), and prepared as whole-mounts (Neves et al., 1998). We analyzed at least six males and six females recovered from mice infected with schistosomula previously exposed to Sm*carm1*-, GFP-dsRNA, or untreated, from the three biological replicates.

Computer images (Image Pro Plus, Media Cybernetics), from male and female worms captured by a camera (640/480 pixels, RGB) coupled to a light microscope (BX50, Olympus), were used for morphometric analyses. We evaluated the number and area of testicular lobes, ovary area, presence of tubercles, presence of eggs and vitelline glands, and integrity of the tegument (Neves et al., 2004).

Whole mounts of male and female worms were also analyzed under confocal laser scanning microscopy (LSM-410, Zeiss) using a 543 nm laser and a BP560-615 IR filter, in reflected mode. We examined male (testicular lobes, seminal vesicle) and female (yolk glands, ovary, uterus, and ootype) reproductive systems, as well as the integrity of the tegument and the shape of the oral and ventral suckers.

Statistical analysis

All statistical analyses were performed using GraphPad Prism, v. 7 for Windows (GraphPad Software, www.graphpad.com). After verifying for outliers, using the ROUT method ($Q = 1\%$; Motulsky and Brown, 2006), and applying normality test analysis to check if the data follows a Gaussian distribution, statistical analyses used the Mann–Whitney test (Wilcoxon-Sum of Ranks, $p < 0.05$), Paired or Unpaired *t*-test ($p < 0.05$), as described in the respective figure legends.

Results

PRMTs expression in *Schistosoma mansoni*

At first, we aimed at analyzing existing RNAseq and single-cell RNAseq data available in the WormBase ParaSite, the Gene Expression Omnibus database, and cellxgene platform. All results for differential expression analysis retrieved for PRMTs (Smp_025550—SmPRMT7, Smp_029240—SmPRMT1,Smp_070340—SmCARM1,Smp_171150—SmPRMT6, and Smp_337860—SmPRMT3) are available in Supplementary Table S1. In this analysis, we found that PRMTs identified in the *S. mansoni* genome present a significative decrease in the expression profiles for male adult worms from single-sex infections, from 18- to 21-dpi (Supplementary Figure S1), except for Sm*prmt*6. Females from unisexual or mixed infections presented a similar expression profile of Sm*carm*1 from 21- to 35-dpi, with a significant reduction in expression. However, only females in the presence of male worms return to the transcript levels of those observed for 21 dpi, which is observed for all PRMTs, specially Sm*prmt*6. Whereas, in males, single or mixed infections do not differently impact the Sm*carm*1 expression profile.

The analysis of the scRNAseq data provided by Wendt et al. (2020) and Diaz Soria et al. (2020) allowed the assessment of the expression of *S. mansoni* SmPRMTs in different cell types of *S. mansoni* adult worms and schistosomula, respectively, (Figure 1). Sm*prmt*1 (Smp_029240) expression is enriched in Supplementary Figure S1 and

3 http://primer3.sourceforge.net

10.3389/fmicb.2023.1079855

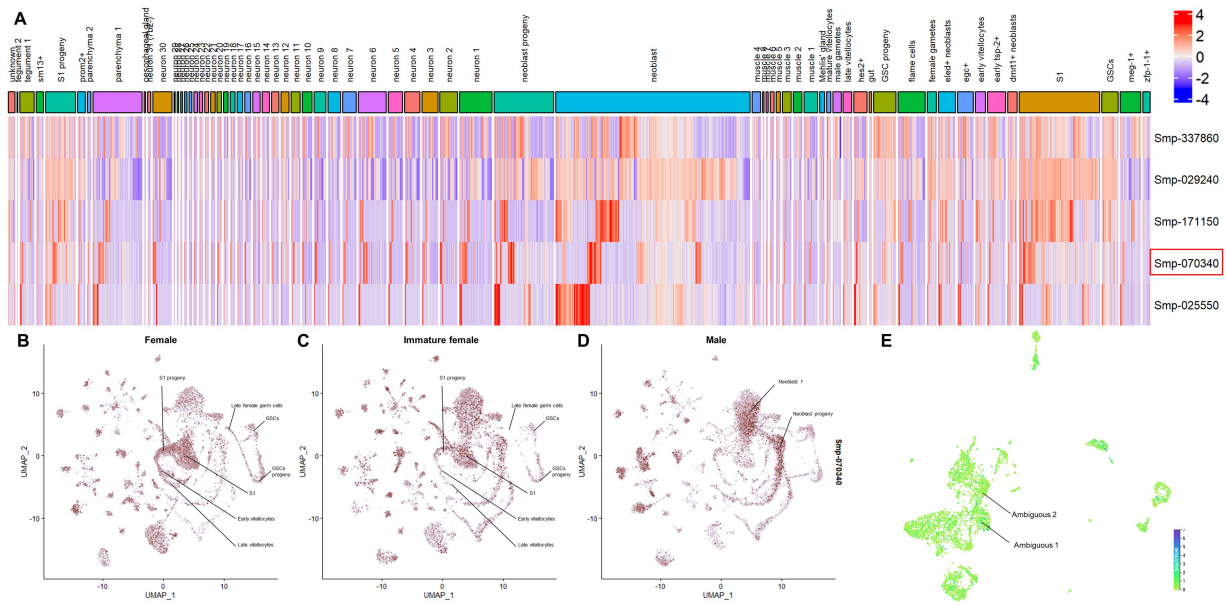

FIGURE 1
SmPRMTs expression in different cell types identified in *Schistosoma mansoni* adult worms. **(A)** SmPRMTs expression in different cell types identified in *S. mansoni* adult worms. The columns indicate the different cell types identified in adult worms and the lines represent the different SmPRMTs analyzed. The color scale indicates higher (red) or lower (blue) expression of transcripts. Sm*carm*1 (Smp_070340) is highlighted by a red box. **(B–D)** UMAP projections depicting the expression profiles of Sm*carm*1 in different cell clusters in **(B)** female, **(C)** immature female, and **(D)** male *S. mansoni* adult worms. Expression values are normalized and represented by colors (gray=not expressed, red=expressed). **(E)** UMAP projections depicting the expression profiles of Sm*carm*1 in 13 transcriptionally distinct cell types in schistosomula. Expression values are normalized and represented by colors ranging from light green (not expressed) to purple (highly expressed).

late female germ cells, whereas expression of the other SmPRMTs, including Sm*carm*1, is not enriched in any cell cluster. In schistosomula, Sm*prmt*1 expression is enriched in NDF+ neurons and stem/germinal cells, and Sm*carm*1 expression is enriched in clusters of ambiguous cells (Figure 1E), while expression of the other SmPRMTs is not enriched in any cell cluster.

In vitro Sm*carm*1 knockdown on schistosomula

There is a lack of functional characterization of PRMTs in the *S. mansoni* parasite. Since important roles have been attributed to CARM1 in other organisms, we further investigated whether SmCARM1 had effects on worm biology, so to that end we knocked-down the Sm*carm*1 transcripts by RNAi experiments. After 7 days of dsRNA exposure, schistosomula presented an average 83% reduction in Sm*carm*1 transcript levels (Figure 2) compared to the controls. No significant changes were observed in viability or evaluated phenotypes, such as movement, color, tegument integrity, or area in *in vitro* cultivated parasites (data not shown).

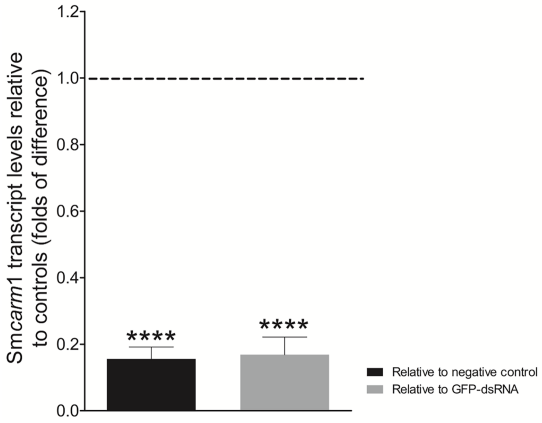

FIGURE 2
Sm*carm*1 transcript levels in schistosomula after dsRNA exposure. Bar graph depicting the Sm*carm*1 transcript levels in schistosomula after 7days of exposure to Sm*carm*1-dsRNA relative to negative (black) or unspecific GFP-dsRNA (gray). Data are represented as mean fold-difference (±SE) relative to controls (dashed line). Mann–Whitney test. ****$p<0.0001$.

In vitro Sm*carm*1 knockdown on adult worms

Adult worms electroporated with Sm*carm*1-dsRNA showed up to a 69% reduction in Sm*carm*1 transcript levels on the first day after electroporation (Figure 3A). Sm*carm*1-dsRNA knockdown resulted in a significant reduction of 54.9% in egg laying compared to the negative control (Figure 3B), although no relevant changes were observed in the movement of females or males for 7 days (Figures 3C,D).

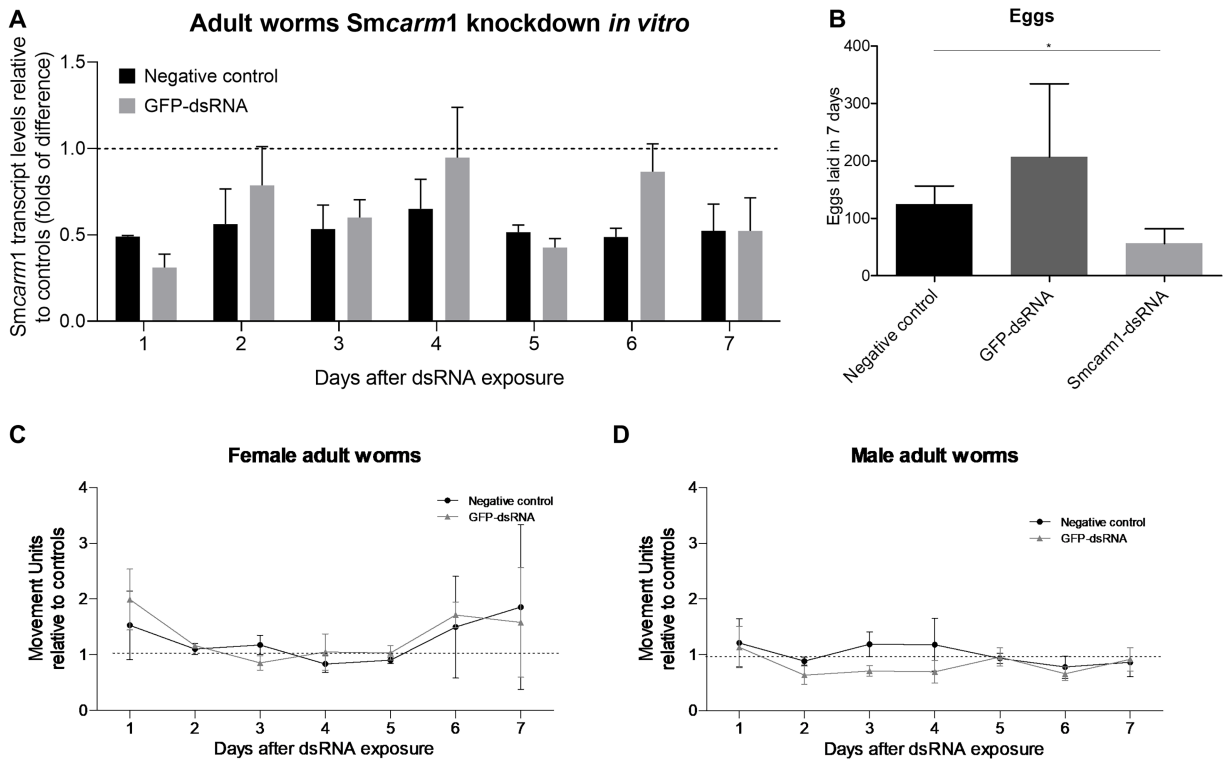

FIGURE 3
Smcarm1 knockdown in adult worms *in vitro*. **(A)** Smcarm1 transcript levels in adult worms after dsRNA exposure. Bar graph depicting the Smcarm1 transcript levels in adult worms during 7days of exposure to Smcarm1-dsRNA relative to negative (black) or unspecific GFP-dsRNA (gray). Data are represented as mean fold-difference (±SE) relative to controls (dashed line). Mann–Whitney test, $N=4$. **(B)** Bar graph depicting the number of eggs laid during 7days for adult worms from the negative control (black) and after electroporation with GFP-dsRNA (dark gray) or Smcarm1-dsRNA (light gray). Paired *t*-test (*$p<0.05$), $N=5$. Movement units from **(C)** female and **(D)** male adult worms knocked-down for Smcarm1 normalized with negative (black) or unspecific control (gray). The dotted line represents normalized movement units in the control. Two-way ANOVA, $N=6$.

Effect of Smcarm1 knockdown on worm development in a murine model

The conclusions drawn from *in vitro* experiments could be limited since parasites are not challenged by a real biological system. Therefore, we sought to investigate the role of SmCARM1 on *in vivo* infections. Before infection, the reduction of Smcarm1 transcript levels in schistosomula was confirmed by RT-qPCR (Supplementary Figure S2). After perfusion, there was no significant change in the number of worms, male or female, recovered from mice infected with Smcarm1 knocked-down schistosomula (Figure 4A). However, there was a significant reduction in the number of eggs recovered from the livers of these mice (Figure 4B).

Morphometric analyses showed that there was a significant decrease in the ovaries area in females recovered from mice infected with Smcarm1 knocked down schistosomula (Figure 5A). In addition to area reduction, it is possible to observe a lower degree of cell differentiation in the ovary (Figure 6) and disorganization of vitelline gland cells (immature cells without the characteristic cluster morphology when compared to the control, which, in turn, presents evident nucleus and characteristic organization of clusters; Figure 7).

Furthermore, there was a decrease in the area of the testicular lobes in male worms recovered from these mice (Figure 5B), however, without a variation in the number of lobes present in each group (data not shown). The testicular lobes were well-demarcated and without the presence of vacuoles (data not shown).

In the tegument of the adult worms recovered from mice infected with Smcarm1 knocked-down schistosomula, the presence of fewer tubercles is clearly observed (Figure 8). The ventral sucker of the parasites presented a damaged tegument and a few points of detachment to the parasite (Figure 9).

Discussion

The protein posttranslational modification (PTM) catalyzed by protein arginine methyltransferases (PRMTs) occurs in cytoplasmic and nuclear proteins. PRMTs can be recruited to gene promoters by transcription factors to methylate arginine residues in the histone tails (Rezai-Zadeh et al., 2003; An et al., 2004). Histone methylation can interfere with the binding of transcriptional effectors and plays diverse roles in regulating chromatin function. In addition, PRMTs can methylate coactivators (Xu et al., 2001; Chevillard-Briet et al., 2002), transcription elongation factors (Kwak et al., 2003; Boulanger et al., 2004), and heterogeneous nuclear ribonucleoproteins (hnRNPs; Xu and Henry, 2004; Yu et al., 2004) also regulating transcriptional initiation and elongation processes and the packaging and export of messenger ribonucleoprotein particles

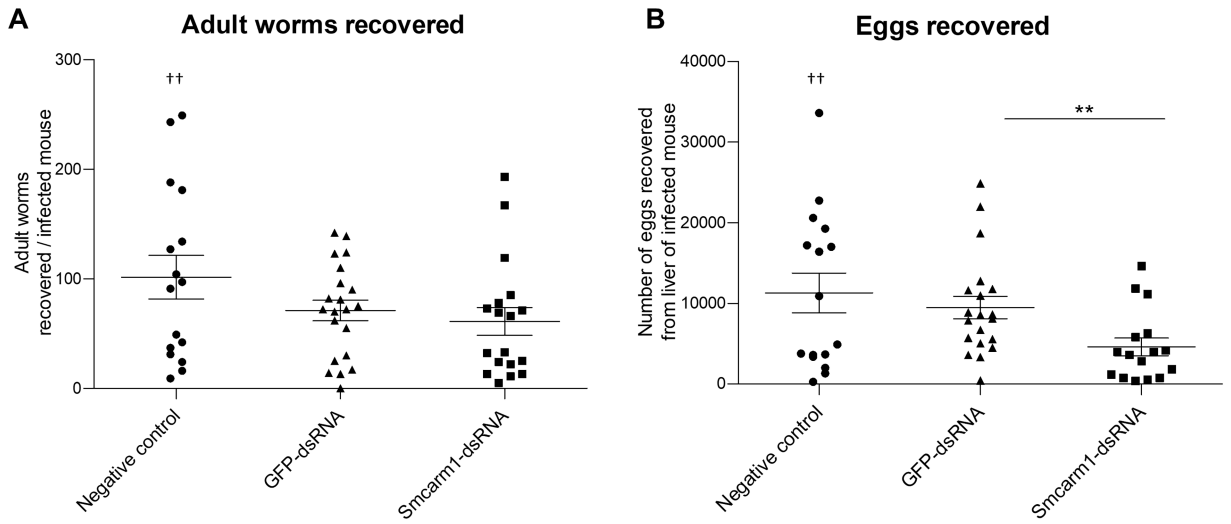

FIGURE 4
Analysis of *ex vivo* adult worms and evaluation of egg recovery from mice liver. Adult worms recovered from mice infected with schistosomula from negative control (●), unspecific GFP-dsRNA (▲), and Sm*carm*1-dsRNA (■). Each symbol in the chart represents **(A)** worm counts per mouse or **(B)** egg counts per mouse liver. Dead mouse is represented (†) above the plotted data. The horizontal lines represent the median values per group. Data were generated from three independent experiments and statistically analyzed using the Mann–Whitney test. $^{**}p<0.01$.

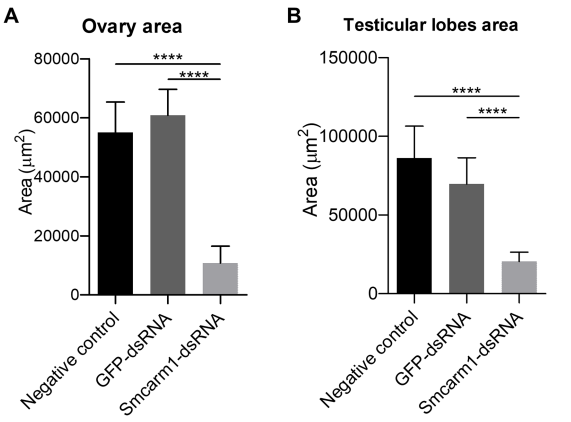

FIGURE 5
Morphometric analysis of *ex vivo* Sm*carm*1 knocked down adult worms. Morphometric analysis of **(A)** ovary from female and **(B)** testicular lobes from male adult worms recovered from mice infected with schistosomula from negative control (black), unspecific GFP-dsRNA (dark gray), and Sm*carm*1-dsRNA (light gray). Data were generated from three independent experiments and statistically analyzed using the Unpaired *t*-test. $^{****}p<0.0001$.

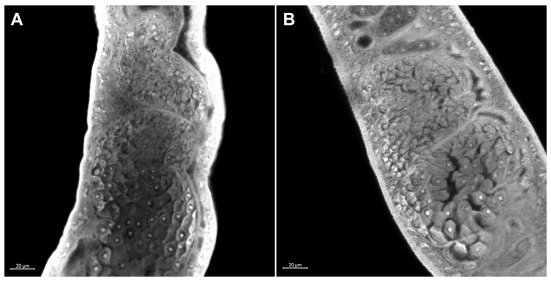

FIGURE 6
Morphology of the ovary of *ex vivo* Sm*carm*1 knocked-down adult worms. Morphological changes in the ovary of female adult worms recovered from mice infected with schistosomula from **(A)** negative control and **(B)** Sm*carm*1-dsRNA. The white bars indicate the scale 20µm.

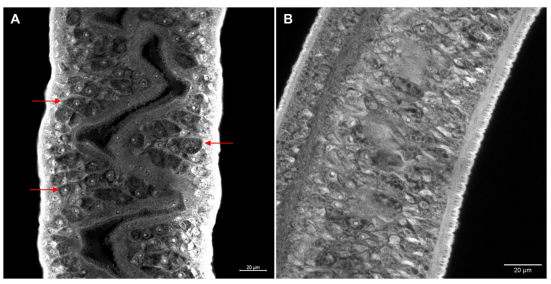

FIGURE 7
Morphology of *ex vivo* Sm*carm*1 knocked-down female adult worms. Morphological changes in the vitelline glands of female adult worms recovered from mice infected with schistosomula from **(A)** negative control and **(B)** Sm*carm*1-dsRNA. Red arrows highlight the cell organization of the vitelline glands and white bars indicate the scale 20µm.

(mRNP; reviewed in Bedford and Richard, 2005). Despite its importance, the methylation of arginine residues catalyzed by PRMTs, whether in histone tails or other proteins, has so far been poorly studied in the schistosome research field.

Publicly available RNAseq data show that the five PRMTs identified in the *S. mansoni* genome are more expressed at the initial stages (18 and 21 days) of infection in male adult worms, despite of the female presence. The expression of Sm*carm*1 in these initial stages could reflect the importance of this protein in the development of male adult worms. Focusing on Sm*carm*1, its expression recovers to similar levels of the early stage (21 dpi) for

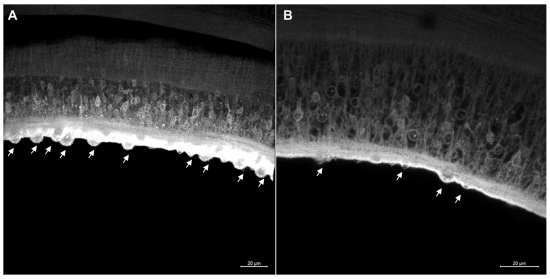

FIGURE 8
Tegument of *ex vivo* Sm*carm*1 knocked-down male adult worms. Morphological changes in the tegument of male adult worms recovered from mice infected with schistosomula from **(A)** negative control (De Andrade et al., 2014) and **(B)** Sm*carm*1-dsRNA. The arrows indicate the tubercles in the tegument and the white bars indicate the scale 20μm.

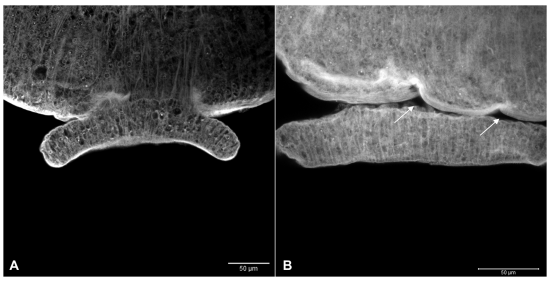

FIGURE 9
Ventral sucker with irregular tegument in *ex vivo* Sm*carm*1 knocked down adult worms. Morphological changes in the ventral sucker of male adult worms recovered from mice infected with schistosomula from **(A)** negative control and **(B)** Sm*carm*1-dsRNA. The arrows highlight points of the detachment of the ventral sucker to the parasite and white bars indicate the scale 50μm.

females from mixed, which is not true for females from single-sex infections. The same pattern of increase in expression is shared by all SmPRMTs, specially Sm*prmt6*, which might indicate a possible role of SmPRMTs in the complete female maturation that could be triggered by the presence of male worms.

Looking at the transcript expression at a single-cell resolution in adult worms (Wendt et al., 2020), we noticed that there is no enrichment in Sm*carm*1 expression at any specific cell clusters, with ubiquitous expressions in almost all cell types, including those related to the reproductive organs, like S1, vitellocytes, and germ cells. In the present work, the reduction of eggs recovered from mice after infection with Sm*carm*1-knockdown schistosomula strengthens the importance of this protein in the regulation of reproduction processes. Indeed, females recovered from mice infected with Sm*carm*1-knocked-down schistosomula presented a significant decrease in the area of the ovaries accompanied by a lower degree of cell differentiation and disorganization of vitelline gland cells. However, Sm*carm*1-knockdown *in vitro* in mature adult worms did not impact egg laying, indicating that Sm*carm*1 is probably more involved in the development of the reproductive organs during worm maturation than in egg formation. The same phenotype was observed with the *in vitro* knockdown of vasa/PL10-like (Sm*vlg1*), a gene related to germline development, in adult females. Mature knocked-down females showed a reduction in the volume of the ovaries, but this did not affect the number of eggs laid (Skinner et al., 2020).

The role of CARM1 in spermiogenesis has already been demonstrated in mice. The *carm*1 knockdown led to low sperm counts and deformed sperm heads showing that the gene is essential for the late stages of germ cell development (Bao et al., 2018). In male worms recovered from mice infected with Sm*carm*1-knockdown schistosomula, we observed a decrease in the area of testicular lobes, which might also influence the observed reduction in egg production.

The tegument of male worms recovered from mice infected with Sm*carm*1-knockdown schistosomula presented fewer tubercles and the ventral sucker presented a damaged tegument and points of detachment from the parasite body. Surprisingly, despite the possibility of a larger exposure of parasite antigens due to tegument damage and the loose ventral sucker adhesion to the worm body, which would impact the parasite adhesion to the host venules, no reduction in parasite numbers was detected. Sm*carm1* expression is enriched in clusters of ambiguous cells in the schistosomula, for which no specific markers or particular processes could be determined, so the role of SmCARM1 in this cell population remains to be elucidated.

Additional studies are necessary to investigate whether the reported effects of Sm*carm*1 knockdown are a consequence of the epigenetic role of SmCARM1 in the methylation of histone tails involved in DNA packaging or other nonhistone proteins associated with transcriptional regulation, splicing mechanism, or mRNA stability.

Data availability statement

The datasets presented in this study can be found in online repositories. The names of the repository/repositories and accession number(s) can be found in the article/Supplementary material.

Ethics statement

The animal study was reviewed and approved by Ethics Committee for Animal Use (CEUA) of the Oswaldo Cruz Foundation under license numbers LW13/13 and LW12/16.

Author contributions

MM, GO, and RP contributed to conception and design of the study. FC, LA, JG, NT, FL, and MM performed the experiments. FC, RN, and JM-S obtained and analyzed the confocal data. SG, FC, and MM performed the statistical analysis. SG performed *in silico* analyses. MM and GO contributed reagents, materials, and analysis tools. FC, SG, and MM wrote the manuscript. All authors contributed to the manuscript revision and approved the submitted version.

Funding

This work was supported by funding from the European Commission's Seventh Framework Program for research, under Grant agreement no. 602080 (A-ParaDDisE), Fundação de Amparo à Pesquisa do Estado de Minas Gerais (FAPEMIG; CBB-APQ-0520-13), and Conselho Nacional de Desenvolvimento Científico e Tecnológico (CNPq; 302518/2018–5 and 317389/2021–1) to MM. Coordenação de Aperfeiçoamento de Pessoal de Nível Superior (CAPES) Programa PCDD-Programa CAPES/Nottingham University (003/2014), CNPq (470673/2014–1, 309312/2012–4, and 304138/2014–2), CAPES (REDE 21/2015), and FAPEMIG (PPM-35 00189–13) to GO. FC and LA fellowships were financed by the CAPES (Finance code 001). SG fellowship was financed by Inova Fiocruz/Fundação Oswaldo Cruz. RP was supported by institutional funds from the CNRS, the Institut Pasteur de Lille, and Lille University.

Acknowledgments

The authors would like to thank the "Lobato Paraense" snail rearing facility of the René Rachou Institute for supplying the parasites and the Program for Technological Development in Tools for Health-PDTIS/FIOCRUZ for the use of its facilities. They also thank the Programa de Pós-graduação em Ciências da Saúde of the René Rachou Institute-Fiocruz. The authors thank the reviewers for their careful and insightful comments during the peer review process.

Conflict of interest

The authors declare that the research was conducted in the absence of any commercial or financial relationships that could be construed as a potential conflict of interest.

Publisher's note

All claims expressed in this article are solely those of the authors and do not necessarily represent those of their affiliated organizations, or those of the publisher, the editors and the reviewers. Any product that may be evaluated in this article, or claim that may be made by its manufacturer, is not guaranteed or endorsed by the publisher.

Supplementary material

The Supplementary material for this article can be found online at: https://www.frontiersin.org/articles/10.3389/fmicb.2023.1079855/full#supplementary-material

References

Adepoju, P. (2020). NTDs in the time of COVID-19. *Lancet Microb.* 1:e244. doi: 10.1016/s2666-5247(20)30153-1

An, W., Kim, J., and Roeder, R. G. (2004). Ordered cooperative functions of PRMT1, p300, and CARM1 in transcriptional activation by p53. *Cells* 117, 735–748. doi: 10.1016/j.cell.2004.05.009

Bao, J., Rousseaux, S., Shen, J., Lin, K., Lu, Y., and Bedford, M. T. (2018). The arginine methyltransferase CARM1 represses p300•ACT•CREMτ activity and is required for spermiogenesis. *Nucleic Acids Res.* 46, 4327–4343. doi: 10.1093/nar/gky240

Bedford, M. T., and Clarke, S. G. (2009). Protein arginine methylation in mammals: who, what, and why. *Mol. Cell* 33, 1–13. doi: 10.1016/j.molcel.2008.12.013

Bedford, M. T., and Richard, S. (2005). Arginine methylation: An emerging regulator of protein function. *Mol. Cell* 18, 263–272. doi: 10.1016/j.molcel.2005.04.003

Botros, S. S. S. S., and Bennett, J. L. J. (2007). Praziquantel resistance. *Expert Opin. Drug Discovery* 2, S35–S40. doi: 10.1517/17460441.2.S1.S35

Boulanger, M. C., Miranda, T. B., Clarke, S., Di Fruscio, M., Suter, B., Lasko, P., et al. (2004). Characterization of the drosophila protein arginine methyltransferases DART1 and DART4. *Biochem. J.* 379, 283–289. doi: 10.1042/BJ20031176

Chevillard-Briet, M., Trouche, D., and Vandel, L. (2002). Control of CBP co-activating activity by arginine methylation. *EMBO J.* 21, 5457–5466. doi: 10.1093/emboj/cdf548

Coeli, R., Baba, E. H., Araujo, N., Coelho, P. M. Z., and Oliveira, G. (2013). Praziquantel treatment decreases Schistosoma mansoni genetic diversity in experimental infections. *PLoS Negl. Trop. Dis.* 7:e2596. doi: 10.1371/journal.pntd.0002596

Colley, D. G., Bustinduy, A. L., Secor, W. E., and King, C. H. (2014). Human schistosomiasis. *Lancet* 383, 2253–2264. doi: 10.1016/S0140-6736(13)61949-2

De Andrade, L. F., Mourão, M. D. M., Geraldo, J. A., Coelho, F. S., Silva, L. L., Neves, R. H., et al. (2014). Regulation of Schistosoma mansoni development and reproduction by the mitogen-activated protein kinase signaling pathway. *PLoS Negl. Trop. Dis.* 8:e2949. doi: 10.1371/journal.pntd.0002949

Diao, W., Zhou, H., Pan, W., Liu, H., Shen, Y., Xu, Y., et al. (2014). Expression and immune characterization of a novel enzyme, protein arginine methyltransferase 1, from Schistosoma japonicum. *Parasitol. Res.* 113, 919–924. doi: 10.1007/s00436-013-3723-6

Diaz Soria, C. L., Lee, J., Chong, T., Coghlan, A., Tracey, A., Young, M. D., et al. (2020). Single-cell atlas of the first intra-mammalian developmental stage of the human parasite Schistosoma mansoni. *Nat. Commun.* 11, 6411–6416. doi: 10.1038/s41467-020-20092-5

Dillon, N. (2004). Heterochromatin structure and function. *Biol. Cell.* 96, 631–637. doi: 10.1016/j.biolcel.2004.06.003

Doenhoff, M. J., Cioli, D., and Utzinger, J. (2008). Praziquantel: mechanisms of action, resistance and new derivatives for schistosomiasis. *Curr. Opin. Infect. Dis.* 21, 659–667. doi: 10.1097/QCO.0b013e328318978f

El Messaoudi, S., Fabbrizio, E., Rodriguez, C., Chuchana, P., Fauquier, L., Cheng, D., et al. (2006). Coactivator-associated arginine methyltransferase 1 (CARM1) is a positive regulator of the Cyclin E1 gene. *Proc. Natl. Acad. Sci.* 103, 13351–13356. doi: 10.1073/pnas.0605692103

Gu, Z., Eils, R., and Schlesner, M. (2016). Complex heatmaps reveal patterns and correlations in multidimensional genomic data. *Bioinformatics* 32, 2847–2849. doi: 10.1093/bioinformatics/btw313

Hartley, A.-V., and Lu, T. (2020). Modulating the modulators: regulation of protein arginine methyltransferases by post-translational modifications. *Drug Discov. Today* 25, 1735–1743. doi: 10.1016/j.drudis.2020.06.031

Hwang, J. W., Cho, Y., Bae, G.-U. U., Kim, S.-N. N., and Kim, Y. K. (2021). Protein arginine methyltransferases: promising targets for cancer therapy. *Exp. Mol. Med.* 53, 788–808. doi: 10.1038/s12276-021-00613-y

Jenuwein, T., and Allis, C. D. (2001). Translating the histone code. *Science* 293, 1074–1080. doi: 10.1126/science.1063127

Kolde, R. (2015). Pheatmap: Pretty heatmaps.

Kwak, Y. T., Guo, J., Prajapati, S., Park, K. J., Surabhi, R. M., Miller, B., et al. (2003). Methylation of SPT5 regulates its interaction with RNA polymerase II and transcriptional elongation properties. *Mol. Cell* 11, 1055–1066. doi: 10.1016/S1097-2765(03)00101-1

Lee, H. W., Kim, S., and Paik, W. K. (1977). S-Adenosylmethionine:protein-arginine methyltransferase. Purification and mechanism of the enzyme. *Biochemistry* 16, 78–85. doi: 10.1021/bi00620a013

Lee, J. S., Smith, E., and Shilatifard, A. (2010). The language of histone crosstalk. *Cells* 142, 682–685. doi: 10.1016/j.cell.2010.08.011

Livak, K. J., and Schmittgen, T. D. (2001). Analysis of relative gene expression data using real-time quantitative PCR and the 2(-Delta Delta C(T)) method. *Methods* 25, 402–408. doi: 10.1006/meth.2001.1262

Love, M. I., Huber, W., and Anders, S. (2014). Moderated estimation of fold change and dispersion for RNA-seq data with DESeq2. *Genome Biol.* 15, 1–21. doi: 10.1186/s13059-014-0550-8

Mansure, J. J., Furtado, D. R., De Oliveira, F. M. B., Rumjanek, F. D., Franco, G. R., and Fantappié, M. R. (2005). Cloning of a protein arginine methyltransferase PRMT1 homologue from Schistosoma mansoni: evidence for roles in nuclear receptor signaling and RNA metabolism. *Biochem. Biophys. Res. Commun.* 335, 1163–1172. doi: 10.1016/j.bbrc.2005.07.192

Marcellino, C., Gut, J., Lim, K. C., Singh, R., McKerrow, J., and Sakanari, J. (2012). WormAssay: a novel computer application for whole-plate motion-based screening of macroscopic parasites. *PLoS Negl. Trop. Dis.* 6:e1494. doi: 10.1371/journal.pntd.0001494

Marek, M., Kannan, S., Hauser, A.-T., Moraes Mourão, M., Caby, S., Cura, V., et al. (2013). Structural basis for the inhibition of histone deacetylase 8 (HDAC8), a key epigenetic player in the blood fluke Schistosoma mansoni. *PLoS Pathog.* 9:e1003645. doi: 10.1371/journal.ppat.1003645

Margueron, R., and Reinberg, D. (2010). Chromatin structure and the inheritance of epigenetic information. *Nat. Rev. Genet.* 11, 285–296. doi: 10.1038/nrg2752

Melesina, J., Robaa, D., Pierce, R. J., Romier, C., and Sippl, W. (2015). Homology modeling of parasite histone deacetylases to guide the structure-based design of selective inhibitors. *J. Mol. Graph. Model.* 62, 342–361. doi: 10.1016/j.jmgm.2015.10.006

Milligan, J. N., and Jolly, E. R. (2011). Cercarial transformation and in vitro cultivation of Schistosoma mansoni schistosomules. *J. Vis. Exp.* 54, 4–7. doi: 10.3791/3191

Motulsky, H. J., and Brown, R. E. (2006). Detecting outliers when fitting data with nonlinear regression—a new method based on robust nonlinear regression and the false discovery rate. *BMC Bioinform.* 7:123. doi: 10.1186/1471-2105-7-123

Neves, R. H., Costa-Silva, M., Martinez, E. M., Branquinho, T. B., De Oliveira, R. M. F., Lenzi, H. L., et al. (2004). Phenotypic plasticity in adult worms of Schistosoma mansoni (Trematoda:Schistosomatidae) evidenced by Brightfield and confocal laser scanning microscopies. *Mem. Inst. Oswaldo Cruz* 99, 131–136. doi: 10.1590/S0074-02762004000200003

Neves, R. H., Dos Santos Pereira, M. J., De Oliveira, R. M. F., Gomes, D. C., and Machado-Silva, J. R. (1998). Schistosoma mansoni Sambon, 1907: morphometric differences between adult Worms from sympatric rodent and human isolates. *Mem. Inst. Oswaldo Cruz* 93, 309–312. doi: 10.1590/S0074-02761998000700061

Padalino, G., Ferla, S., Brancale, A., Chalmers, I. W., and Hoffmann, K. F. (2018). Combining bioinformatics, cheminformatics, functional genomics and whole organism approaches for identifying epigenetic drug targets in Schistosoma mansoni. *Int. J. Parasitol. Drugs Drug Resist.* 8, 559–570. doi: 10.1016/j.ijpddr.2018.10.005

Pellegrino, J., and Siqueira, A. F. A. F. (1956). A perfusion technic for recovery of Schistosoma mansoni from experimentally infected Guinea pigs. *Rev. Bras. Malariol. Doencas Trop.* 8, 589–597. Available at: http://www.ncbi.nlm.nih.gov/pubmed/13494879

Protasio, A. v., van Dongen, S., Collins, J., Quintais, L., Ribeiro, D. M., Sessler, F., et al. (2017). MiR-277/4989 regulate transcriptional landscape during juvenile to adult transition in the parasitic helminth Schistosoma mansoni. *PLoS Negl. Trop. Dis.* 11, 1–24. doi: 10.1371/journal.pntd.0005559

R Core Team (2020). R: A language and environment for statistical computing.

Rezai-Zadeh, N., Zhang, X., Namour, F., Fejer, G., Wen, Y.Der, Yao, Y. L., et al. (2003). Targeted recruitment of a histone H4-specific methyltransferase by the transcription factor YY1. *Genes Dev.* 17, 1019–1029. doi: 10.1101/gad.1068003

Roquis, D., Taudt, A., Geyer, K. K., Padalino, G., Hoffmann, K. F., Holroyd, N., et al. (2018). Histone methylation changes are required for life cycle progression in the human parasite Schistosoma mansoni. *PLoS Pathog.* 14, e1007066–e1007026. doi: 10.1371/journal.ppat.1007066

Satija, R., Farrell, J. A., Gennert, D., Schier, A. F., and Regev, A. (2015). Spatial reconstruction of single-cell gene expression data. *Nat. Biotechnol.* 33, 495–502. doi: 10.1038/nbt.3192

Shin, H.-J. R., Kim, H., Oh, S., Lee, J.-G., Kee, M., Ko, H.-J., et al. (2016). AMPK–SKP2–CARM1 signalling cascade in transcriptional regulation of autophagy. *Nature* 534, 553–557. doi: 10.1038/nature18014

Skinner, D. E., Popratiloff, A., Alrefaei, Y. N., Mann, V. H., Rinaldi, G., and Brindley, P. J. (2020). Functional analysis of vasa/PL10-like genes in the ovary of Schistosoma mansoni. *Mol. Biochem. Parasitol.* 236:111259. doi: 10.1016/j.molbiopara.2020.111259

Tavares, N., and Mourão, M. (2021). Parasitemia evaluation in mice infected with Schistosoma mansoni. *Bio Protoc.* 11, e4017–e4019. doi: 10.21769/bioprotoc.4017

Wendt, G., Zhao, L., Chen, R., Liu, C., O'Donoghue, A. J., Caffrey, C. R., et al. (2020). A single-cell RNA-seq atlas of Schistosoma mansoni identifies a key regulator of blood feeding. *Science* 369, 1644–1649. doi: 10.1126/science.abb7709

WHO (2022). Schistosomiasis and soil-transmitted helminthiases: progress report, 2021. *Wkly Epidemiol. Rec.* 97, 621–632.

Xu, W., Chen, H., Du, K., Asahara, H., Tini, M., Emerson, B. M., et al. (2001). A transcriptional switch mediated by cofactor methylation. *Science* 294, 2507–2511. doi: 10.1126/science.1065961

Xu, C., and Henry, M. F. (2004). Nuclear export of hnRNP Hrp1p and nuclear export of hnRNP Npl3p are linked and influenced by the methylation state of Npl3p. *Mol. Cell. Biol.* 24, 10742–10756. doi: 10.1128/mcb.24.24.10742-10756.2004

Yadav, N., Lee, J., Kim, J., Shen, J., Hu, M. C., Aldaz, C. M., et al. (2003). Specific protein methylation defects and gene expression perturbations in coactivator-associated arginine methyltransferase 1-deficient mice. *Proc. Natl. Acad. Sci. U. S. A.* 100, 6464–6468. doi: 10.1073/pnas.1232272100

Yu, M. C., Bachand, F., McBride, A. E., Komili, S., Casolari, J. M., and Silver, P. A. (2004). Arginine methyltransferase affects interactions and recruitment of mRNA processing and export factors. *Genes Dev.* 18, 2024–2035. doi: 10.1101/gad.1223204

Yue, W. W., Hassler, M., Roe, S. M., Thompson-Vale, V., and Pearl, L. H. (2007). Insights into histone code syntax from structural and biochemical studies of CARM1 methyltransferase. *EMBO J.* 26, 4402–4412. doi: 10.1038/sj.emboj.7601856

frontiers | Frontiers in Microbiology

TYPE Correction
PUBLISHED 29 March 2023
DOI 10.3389/fmicb.2023.1190341

OPEN ACCESS

APPROVED BY
Frontiers Editorial Office,
Frontiers Media SA, Switzerland

*CORRESPONDENCE
Marina Moraes Mourão
✉ marina.mourao@fiocruz.br

†These authors have contributed equally to this work and share first authorship

SPECIALTY SECTION
This article was submitted to Infectious Agents and Disease, a section of the journal Frontiers in Microbiology

RECEIVED 20 March 2023
ACCEPTED 21 March 2023
PUBLISHED 29 March 2023

CITATION
Coelho FS, Gava SG, Andrade LF, Geraldo JA, Tavares NC, Lunkes FMN, Neves RH, Machado-Silva JR, Pierce RJ, Oliveira G and Mourão MM (2023) Corrigendum: *Schistosoma mansoni* coactivator associated arginine methyltransferase 1 (SmCARM1) effect on parasite reproduction.
Front. Microbiol. 14:1190341.
doi: 10.3389/fmicb.2023.1190341

Corrigendum: *Schistosoma mansoni* coactivator associated arginine methyltransferase 1 (SmCARM1) effect on parasite reproduction

Fernanda Sales Coelho[1,2†], Sandra Grossi Gava[1†], Luiza Freire Andrade[1], Juliana Assis Geraldo[1], Naiara Clemente Tavares[1], Felipe Miguel Nery Lunkes[1], Renata Heisler Neves[3], José Roberto Machado-Silva[3], Raymond J. Pierce[4], Guilherme Oliveira[1,5] and Marina Moraes Mourão[1*]

[1]Grupo de Pesquisa em Helmintologia e Malacologia Médica, Instituto René Rachou, Fundação Oswaldo Cruz—FIOCRUZ, Belo Horizonte, Minas Gerais, Brazil, [2]Department of Clinical Research, London School of Hygiene and Tropical Medicine, London, United Kingdom, [3]Laboratório de Helmintologia Romero Lascasas Porto, Departamento de Microbiologia, Imunologia e Parasitologia, Faculdade de Ciências Médicas, Universidade do Estado do Rio de Janeiro, Rio de Janeiro, Brazil, [4]Université de Lille, CNRS, Inserm, CHU Lille, Institut Pasteur de Lille, U1019—UMR 9017—CIIL—Centre d'Infection et d'Immunité de Lille, Lille, France, [5]Instituto Tecnológico Vale, Belém, Pará, Brazil

KEYWORDS

***Schistosoma mansoni*, coactivator associated arginine methyltransferase 1, SmCARM1, epigenetics, reproduction**

A corrigendum on
Schistosoma mansoni coactivator associated arginine methyltransferase 1 (SmCARM1) effect on parasite reproduction

by Coelho, F. S., Gava, S. G., Andrade, L. F., Geraldo, J. A., Tavares, N. C., Lunkes, F. M. N., Neves, R. H., Machado-Silva, J. R., Pierce, R. J., Oliveira, G., and Mourão, M. M. (2023). *Front. Microbiol.* 14:1079855. doi: 10.3389/fmicb.2023.1079855

In the published article, there was an error. In the section Materials and methods, "*In silico* analyses," paragraph 1, it was previously stated that:

"Additionally, we checked the SmPRMTs expression in a publicly available RNAseq dataset (Protasio et al., 2017) retrieved from WormBase ParaSite as the median of transcripts per million units (TPMs) per gene."

The corrected sentence appears below:

"Additionally, we checked the SmPRMTs expression in a publicly available RNAseq dataset (Protasio et al., 2017) retrieved from WormBase ParaSite as counts of aligned reads per run per gene."

The authors apologize for this error and state that this does not change the scientific conclusions of the article in any way. The original article has been updated.

Publisher's note

References

Protasio, A. v., van Dongen, S., Collins, J., Quintais, L., Ribeiro, D. M., Sessler, F., et al. (2017). MiR-277/4989 regulate transcriptional landscape during juvenile to adult transition in the parasitic helminth Schistosoma mansoni. *PLoS Negl. Trop. Dis.* 11, 1–24. doi: 10.1371/journal.pntd.0005559

frontiers | Frontiers in Immunology

TYPE Original Research
PUBLISHED 03 April 2023
DOI 10.3389/fimmu.2023.1165480

OPEN ACCESS

EDITED BY
Thiago Almeida Pereira,
Stanford University, United States

REVIEWED BY
William Evan Secor,
Centers for Disease Control and Prevention (CDC), United States
Arnaud Chalin,
NG Biotech, France

*CORRESPONDENCE
Pengfei Cai
Pengfei.Cai@qimrberghofer.edu.au

†Deceased

SPECIALTY SECTION
This article was submitted to Parasite Immunology, a section of the journal Frontiers in Immunology

RECEIVED 14 February 2023
ACCEPTED 07 March 2023
PUBLISHED 03 April 2023

CITATION
Mu Y, McManus DP, Gordon CA, You H, Ross AG, Olveda RM and Cai P (2023) Development and assessment of a novel gold immunochromatographic assay for the diagnosis of schistosomiasis japonica. *Front. Immunol.* 14:1165480. doi: 10.3389/fimmu.2023.1165480

Development and assessment of a novel gold immunochromatographic assay for the diagnosis of schistosomiasis japonica

Yi Mu[1], Donald P. McManus[1†], Catherine A. Gordon[1], Hong You[1], Allen G. Ross[2], Remigio M. Olveda[3†] and Pengfei Cai[1*]

[1]Molecular Parasitology Laboratory, QIMR Berghofer Medical Research Institute, Brisbane, QLD, Australia, [2]Rural Health and Medical Research Institute, Charles Sturt University, Orange, NSW, Australia, [3]Department of Immunology, Research Institute for Tropical Medicine, Manila, Philippines

Background: The neglected zoonosis, schistosomiasis japonica, remains a major public health problem in the Philippines. The current study aims to develop a novel gold immunochromatographic assay (GICA) and evaluate its performance in the detection of *Schistosoma japonicum* infection.

Methods: A GICA strip incorporating a *S. japonicum* saposin protein, SjSAP4 was developed. For each GICA strip test, diluted serum sample (50 µl) was loaded and strips were scanned after 10 min to convert the results into images. ImageJ was used to calculate an R value, which was defined as the signal intensity of the test line divided by the signal intensity of the control line within the cassette. After determination of optimal serum dilution and diluent, the GICA assay was evaluated with sera collected from non-endemic controls (n = 20) and individuals living in schistosomiasis-endemic areas of the Philippines (n = 60), including 40 Kato Katz (KK)-positive participants and 20 subjects confirmed as KK-negative and faecal droplet digital PCR assay (F_ddPCR)-negative at a dilution of 1:20. An ELISA assay evaluating IgG levels against SjSAP4 was also performed on the same panel of sera.

Results: Phosphate-buffered saline (PBS) and 0.9% NaCl were determined as optimal dilution buffer for the GICA assay. The strips tested with serial dilutions of a pooled serum sample from KK-positive individuals (n = 3) suggested that a relatively wide range of dilutions (from 1:10 to 1:320) can be applied for the test. Using the non-endemic donors as controls, the GICA strip showed a sensitivity of 95.0% and absolute specificity; while using the KK-negative and F_ddPCR-negative subjects as controls, the immunochromatographic assay had a sensitivity of 85.0% and a specificity of 80.0%. The SjSAP4-incorperated GICA displayed a high concordance with the SjSAP4-ELISA assay.

Conclusions: The developed GICA assay exhibited a similar diagnostic performance with that of the SjSAP4-ELISA assay, yet the former can be

performed by local personnel with minimal training with no requirement for specialised equipment. The GICA assay established here represents a rapid, easy-to-use, accurate and field-friendly diagnostic tool for the on-site surveillance/screening of *S. japonicum* infection.

KEYWORDS

schistosomiasis, *Schistosoma japonicum*, GICA strip, lateral flow immunochromatographic test, ELISA, rapid diagnosis, point-of-care (POC), surveillance

1 Introduction

In the recently released new WHO roadmap for neglected tropical diseases (NTDs) 2021-2030, it has been emphasized that effective diagnostics are key components of NTD programmes, from confirmation of disease to mapping, screening, surveillance, monitoring and evaluation, representing a prerequisite for reaching the 2030 disease targets (1). Schistosomiasis, one of the major NTDs, affects more than 250 million people worldwide (2). Six species of schistosomes (trematode blood flukes) infect human beings, of which *Schistosoma mansoni*, *S. haematobium*, and *S. japonicum* are the major species. The control of the disease relies heavily on mass drug administration (MDA) employing praziquantel (PDZ) (3). Recently, both the prevalence and infection intensity of the disease have declined in many endemic areas due to the implementation of integrated control programs, including MDA, making conventional parasitological diagnostics (e.g., the microscopy-based Kato Katz (KK) and the miracidium hatching technique) less efficient in the detection of schistosomiasis. These situations thus necessitate the development and implementation of more cost-effective and accurate diagnostics for rapid mapping and monitoring schistosomiasis in the endemic areas.

In addition to conventional parasitological diagnostics, there are a number of other diagnostic methods available for the detection of schistosome infections (4–8). Improved coprological tests, such as the saline gradient method (9), formalin-ethyl acetate sedimentation-digestion (FEA-SD) (10) and Helmintex method (i.e., isolates eggs from fecal samples with the use of paramagnetic particles in a magnetic field) (11) showed an increased diagnostic sensitivity compared with the traditional techniques; yet are usually labour-intensive and have a lengthy processing time. In addition, polymerase chain reaction (PCR) technology-based molecular diagnostics, including real time quantitative (q)PCR- (12–15), droplet digital (dd) PCR-based assays (16–18), loop-mediated isothermal amplification (LAMP) (19–21), and recombinase polymerase amplification (RPA) (22–25) are alternative tools for schistosomiasis diagnosis due to their outstanding accuracy; however, these tests require experienced human resources and are expensive (e.g. the relatively high cost of DNA extraction, qPCR reagents and/or equipment), limiting their application in remote areas with limited resources.

Point-of-care (POC) diagnostics are at the forefront of government initiatives, non-government organisations, medical diagnostics companies as well as fundamental research (26). For NTDs, accurate POC testing facilitates rapid results *in situ*, enabling targeted intervention for drug treatment and providing insights into dynamic transmission of pathogens and the burden of diseases. The application of POC tests can increase acceptance of treatment and minimise the risk of potential development of drug resistance. Recently, the WHO called for expert consultation on diagnostics with a particular focus on POC testing for schistosomiasis and soil-transmitted helminths (27). As a powerful POC tool, immumochromatographic assay (ICA) has been widely developed with a particular application in epidemiological surveys in the field. Recently, a number of colloidal gold immunochromatographic assay (GICA) strips have been established and evaluated for the rapid diagnosis of parasitic diseases, such as schistosomiasis (28–31), toxoplasmosis (32), fascioliasis (33) and opisthorchiasis (34), as an alternative screening tool.

Current antigen detection (AgD)-based POC tests schistosomiasis are based on the probing proteoglycan components present in the gut vomit of juvenile and adult worms known as circulating anodic antigens (CAAs) or circulating cathodic antigens (CCAs) using lateral flow assays (2). The POC-CCA is a commercially available cassette assay that has been widely validated in the detection of active *S. mansoni* infection in high and moderate endemic areas. However, the assay showed lower potential in the diagnosis of other *Schistosoma* species (35–37). In addition, the assay suffers some pitfalls, such as cross-reactivity, underperformed specificity, and a 'Trace' reading problem (36, 38). To date, the antibody detection (AbD)-based GICA assays developed for schistosomiasis japonica diagnosis typically use crude worm or egg antigen, which can result in cross-reactions with other helminths during field clinical sample testing. Previously we, and others, identified a schistosome saposin protein, SjSAP4, which shows an unprecedented level of accuracy for diagnosing infected cohort subjects from *S. japonicum*-endemic areas in both China and the Philippines (39–41). In this study, we aimed to develop and assess a novel SjSAP4-incorporated GICA strip for the diagnosis of schistosomiasis japonica.

2 Methods

2.1 Ethics

The human research ethical approval for the study was obtained from the Human Research Ethics Committee, QIMR Berghofer

Medical Research Institute (QIMRB), Brisbane, Australia (Project Approval: P524) and the Institutional Review Board (IRB) of the Research Institute for Tropical Medicine (RITM), Manila, Philippines (IRB Number 2015-12). Written consent was obtained from all participants (for children aged 15 years or under written consent was obtained from their legal guardians).

2.2 Study cohort, sample collection, processing, and storage

The study recruited human subjects from 18 barangays moderately endemic (27% prevalence) for schistosomiasis japonica in the municipalities of Laoang and Palapag, Northern Samar, Philippines, in 2015 (3, 18, 39, 42). Fecal and serum samples were collected from the participating subjects. For each participant, two fecal samples (10–15 g each) were sought on different days within a week for the KK analysis. After fixing in 80% ethanol, the remainder of the first fecal sample (~10 g) was stored at 4°C. A blood sample (10 ml) was collected from each individual using a 10 ml serum silica vacutainer. The blood sample was set to clot at ambient temperature for 30 min. After centrifugation at 1500 × *g* for 10 min, the serum samples were aliquoted. All clinical samples were kept at 4°C and transported on wet ice to the RITM, where the samples were stored at -20°C. All samples were subsequently shipped to QIMRB, Brisbane, Australia on dry ice. In this study, a subset of serum samples (n = 60) collected from the endemic areas was tested with the GICA strips. Serum samples collected from healthy human subjects (n = 20) living in a non-endemic area (Qiqihar, Heilongjiang Province, China) for schistosomiasis served as controls.

2.3 Parasitological detection (Kato-Katz)

Kato-Katz analysis on fecal samples was performed by experienced technicians at RITM. For each fecal sample, three KK slides were examined. Infection burden was presented as the number of eggs per gram of feces (EPG). To increase the accuracy of the KK test, 10% of slides were randomly selected for re-examination by an experienced microscopist.

2.4 Cloning, expression and purification of recombinant SjSAP4

A gene fragment of SjSAP4 (GenBank No: ON241030, nt 1-534) with an additional pET28a vector-derived sequence -CCATGGGCAGCAGCCATCATCATCATCATCAC- at N-terminal was synthesized. The DNA fragment was amplified by PCR from the synthetic gene with forward primer: AACCATGGGCAGCAGCCATCAT and reverse primer: AACTCGAG-TAATGGACACA-ACTGTATTG. The PCR product was purified and further digested with restriction enzymes *Nco*I and *Xho*I, and the DNA fragment was then cloned into the pET-28a vector. Recombinant plasmid was confirmed by DNA sequencing and transformed into Rosetta (DE3) competent cells. Expression of the recombinant SjSAP4 (rSjSAP4) protein was induced by 0.2 mM IPTG. The rSjSAP4 protein was purified under native conditions using Ni-IDA Sepharose Cl-6B (Novagen, San Diego, CA, USA) according to the manufacturer's instructions. The purified rSjSAP4 protein was analyzed by 12% (w/v) SDS-PAGE and Western blot analysis (Supplementary Figure S1).

2.5 Preparation of the GICA strips

The GICA strips were developed by ZoonBio Biotechnology (Nanjing, China). The design of the GICA strip was illustrated in Figure 1. Briefly, rSjSAP4 protein was initially coated with colloidal gold particle (70 nm) and the gold-rSjSAP4 conjugate (10 μg/ml) was applied onto conjugate pad (glass fibre membrane) at a volume of 35 μl/cm and dried in a biochemical incubator for 12 hours at 37 °C. The buffer used for conjugate pad preparation contains 20 mM Tris, 5% (w/v) sucrose, and 2.5% (w/v) trehalose. By using an XYZ Biostrip Dispenser (HM3030, Shanghai Kinbio Tech. Co., Ltd, Shanghai, China), 1 mg/ml Protein G (Zoonbio Biotechnology, Nanjing, China) and 0.7 mg/ml mouse anti-His tag mAb (Zoonbio Biotechnology, Nanjing, China) were dispensed onto the nitrocellulose (NC) membrane (CN140, Sartorius, Goettingen, Germany) (porosity: 8 μm, wicking rate: 110-165s/4cm) at a volume of 1 μl/cm to form the test and control lines, respectively. The membrane was then dried at room temperature in a biochemical incubator for 6 hours. The absorbent pad (filter paper) coated membrane (NC membrane), conjugate pad (glass fibre membrane), and sample pad (glass fibre membrane), were laminated and pasted onto a plastic-backed support card with a 1–2 mm overlap as illustrated in Figure 1. The entire assembled scale board was cut lengthwise and divided into strips measuring 3 × 60 mm using a guillotine cutter (ZQ2002, Shanghai Kinbio Tech. Co., Ltd, Shanghai, China). The resulting strips were assembled in a plastic cassette, which was further placed into a silica gel desiccant-containing aluminium foil bag, and stored at room temperature.

2.6 GICA assay measurement and analysis

For each test, 50 μl diluted serum sample was added to each cassette. The strips were scanned at 10 min after sample loading. The tests were determined as invalid when the control band did not appear or when the tests were left to develop for more than 15 min. All images were uploaded to a computer and analysed by a Java-based image processing program, ImageJ to quantify the intensity of the bands. In order to convert the results to fully quantitative information, an R value, which was defined as the intensity of the test band divided by that of corresponding control band, was introduced.

2.7 ELISA

The ELISA assay was performed as described previously (39). MaxiSorp high protein-binding capacity 96-well ELISA plates

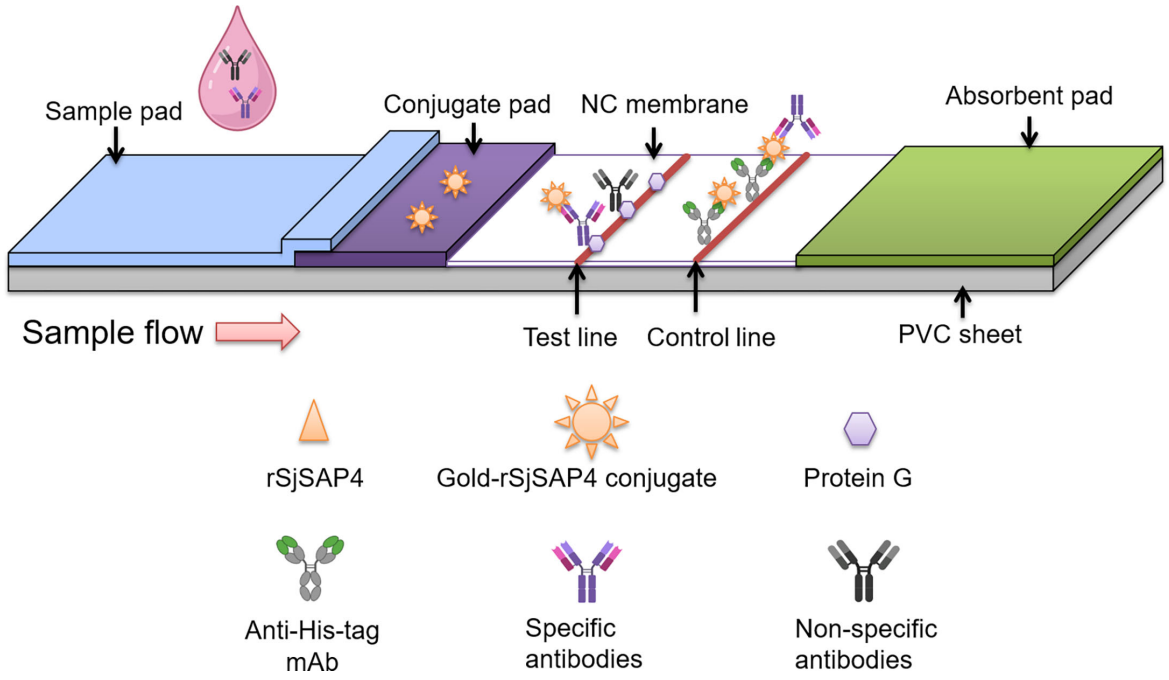

FIGURE 1
Schematic illustration of the rSjSAP4-incorporated GICA strip. The gold-rSjSAP4 conjugate is added to the conjugate pad. The recombinant protein G and a monoclonal mouse anti-His tag antibody is immobilized on the test (T) and control (C) line, respectively, on the NC membrane. Once serum samples containing specific anti-SjSAP4 antibodies or non-specific antibodies loaded onto the sample well, the conjugated anti-SjSAP4 antibody complexes and non-specific antibodies are captured by the protein G immobilized on the 'T' line. The gold-rSjSAP4 conjugate and conjugated anti-SjSAP4 antibody complexes are captured by the anti-His tag antibody on the 'C' line. A positive result is indicated by the appearance of pinkish red bands on both the 'T' and 'C' lines. A negative result is indicated by the appearance of only a single pinkish red band on the 'C' line. A test is determined as invalid if no bands appear on both 'T' and 'C' lines or if only one band appears on the 'T' line, and thus needs to be re-tested.

(Nunc, Roskilde, Denmark) were coated with 100 ng recombinant SjSAP4 in coating buffer (100 µl/well) overnight at 4°C. The plates were blocked with 1% (w/v) bovine serum albumin (BSA) in phosphate-buffered saline with 0.05% Tween-20 (PBST pH 7.4) for 1 h at 37°C. Serum samples diluted at 1:250 in blocking buffer were added to the wells and the plates were incubated for 1 h at 37°C. A mouse monoclonal anti-human IgG (Fc specific)-biotin antibody (Sigma-Aldrich Co, MO, USA) was then added as secondary antibody (1:20,000, 100 µL/well) for 1 h at 37°C. The plates were further incubated with Streptavidin-HRP (BD Pharmingen, CA, USA) (1:10,000, 100 µl/well) at 37°C for 0.5 h. Plates were washed 5 times with PBST after each step. Next, 100 µl 3,3′,5,5′-tetramethylbenzidine (TMB) substrate was added to each well to develop the colorimetric reaction, which was terminated after 5 min by adding 50 µl 2 M sulfuric acid per well. The ELISA plates were read at OD 450 nm with a microplate reader (BMG LABTECH, VIC, Australia).

2.8 Statistical analysis

To analyse the differences in R values of GICA tests with serum samples at different dilutions or with different dilution buffers, Student's *t*-test was used. Cut-off values for the GICA assay and SjSAP4-ELISA assay were set with the maximization of Youden's *J*-index. Pearson's correlation coefficient (r) was used for the assessment of the correlation between the R values of the GICA assay and OD values of the SjSAP4-ELISA assay. Agreement between the GICA strip and the SjSAP4-ELISA assay was determined using the Kappa statistic (https://www.graphpad.com/quickcalcs/kappa1/). Statistical analyses were performed using GraphPad Prism version 9.4.0 software (GraphPad Software, Inc., San Diego, CA, USA). Statistics were considered significant at a *p*-value less than 0.05.

3 Results

3.1 The detectable limit of the GICA assay

The developed GICA strips were tested with a pooled serum sample collected from KK-positive (KK (+)) individuals (n = 3) at a serial dilution (from 1:5 to 1:40960). The strips were scanned at 10 min after sample loading (Figure 2A). Based on R value analysis with a cut-off value of 0.076, the detectable limit of the GICA assay on testing the diluted serum samples was 1:20480. The established GICA strip showed the highest R value when the serum sample was tested at a dilution of 1:40. Six dilution ratios (from 1:10 to 1:320) had an R value higher than 1 (Figure 2B), indicating that a relatively wide range of dilution ratios may be applicable for the strip test. The hook effect was observed when serum samples diluted at 1:5 and 1:10 were tested (Figure 2B). A significant decrease in R value was observed when the sample was diluted to 1:640 and beyond (Figure 2B).

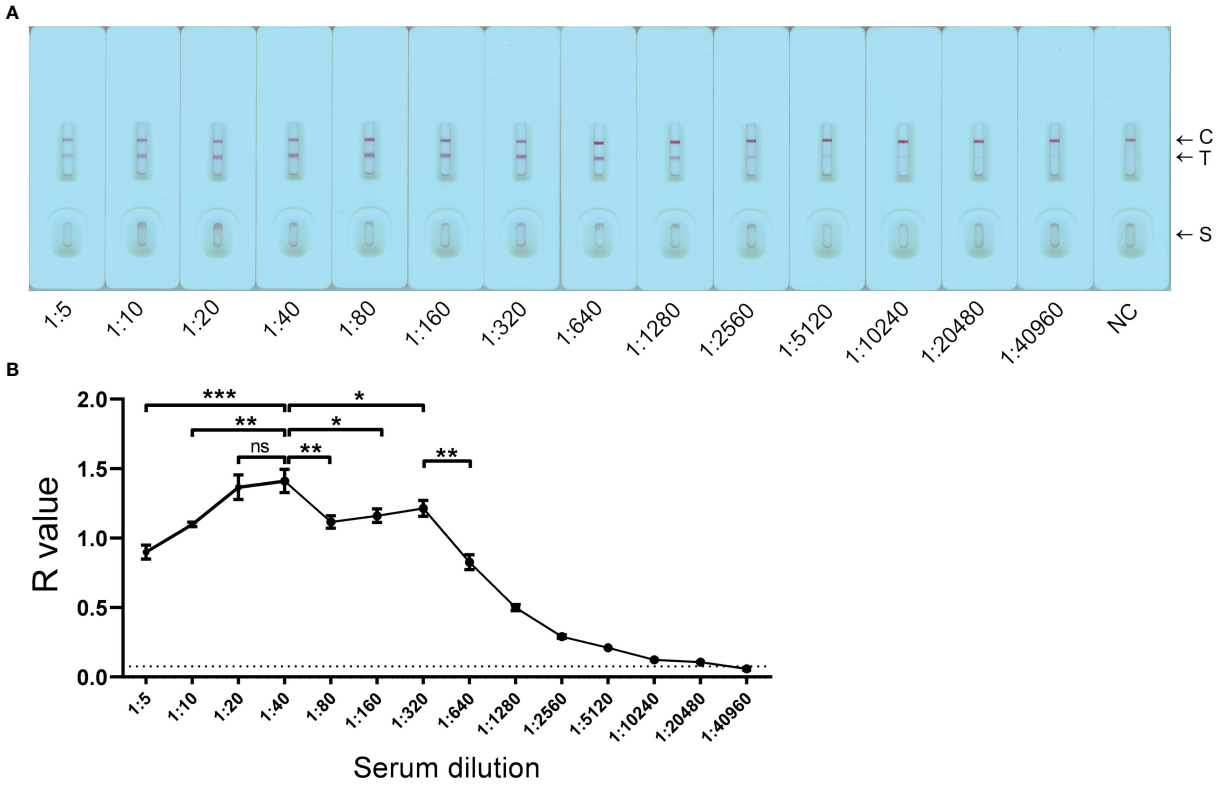

FIGURE 2
Detection limit of the GICA assay on pooled sera. **(A)** The GICA strips were tested with a pooled serum sample from KK-positive individuals (n = 3) with an EPG of 13, 14, and 20, respectively, at a series of dilutions (from 1:5 to 1:40960). C, Control line; T, Test line; S, Sample well; NC, a pooled serum sample from non-endemic controls (n = 3) tested at a dilution of 1:5. **(B)** R values of the GICA assay testing a pooled serum sample from KK (+) individuals (n = 3) at a series of dilutions. Dotted line: cut-off value determined as 2.1 times the mean R values of the pooled serum sample from non-endemic controls. The test was repeated in triplicate. *p* values were calculated using the Student's *t*-test (ns, no significant difference; *$p < 0.05$; **$p < 0.001$; ***$p < 0.001$).

3.2 Optimal dilution buffer for the developed GICA assay

The *S. japonicum*-positive human serum samples were diluted with PBS, 0.9% NaCl, PBST (1% Tween 20) and 2.5% sucrose containing 1% Tween 20 in 1:40 to determine the best serum dilution buffer solution (Figure 3A). As shown in Figure 3B, PBS diluted sera showed a significant higher R value compared to sera diluted with PBST (1% Tween 20) ($p < 0.01$) and 2.5% sucrose (1% Tween 20) ($p < 0.05$); while there was no difference in R values when using PBS and 0.9% NaCl as the dilution buffer. The assay was performed in triplicate. PBS was then selected as serum diluent for the subsequent GICA tests.

3.3 Assessment of diagnostic performance of the GICA assay

Serum samples collected from 80 subjects, including 40 KK (+) individuals, 20 endemic individuals confirmed as both KK-negative (KK (-)) and faecal droplet digital PCR assay-negative (F_ddPCR (-)) (18), and 20 healthy donors from a non-endemic area, were further tested with the GICA strips at a dilution of 1:20, given most of the KK (+) subjects harboring an EPG less than 10. Meanwhile, the SjSAP4-ELISA assay was performed on the same panel of serum samples. As shown in Figures 4A, B, individuals from the endemic areas had higher R values and OD values than non-endemic donors ($p < 0.0001$ and $p < 0.05$ for the KK (+) group, and KK (-) and F_ddPCR (-) group, respectively). Using the non-endemic group as control, the developed GICA strip showed a sensitivity of 95.0% and a specificity of 100% (Figure 4A), while the SjSAP4-ELISA assay had a sensitivity of 97.5% and absolute specificity (Figure 4B). Using the KK (-) and F_ddPCR (-) group as control, the GICA assay had a sensitivity of 85.0% and a specificity of 80.0% (Figure 4A), while the SjSAP4-ELISA assay displayed a sensitivity of 87.5% and a specificity of 90.0% (Figure 4B). A significant positive correlation between the developed GICA test and the SjSAP4-ELISA assay was observed (Pearson's correlation, r = 0.7231, $p < 0.0001$) (Figure 4C). The Kappa statistics analysis indicated that there is an almost perfect agreement between the GICA strip and SjSAP4-ELISA assay (κ value = 0.964 and 0.893 using the non-endemic donors, and KK (-) and F_ddPCR (-) subjects as control, respectively).

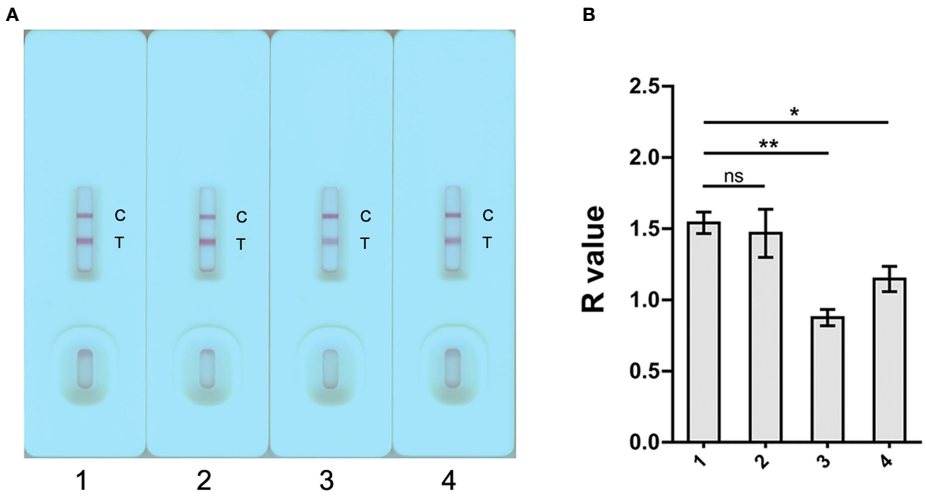

FIGURE 3
Determination of the optimal dilution buffer for the GICA assay. **(A)** Four dilution buffers, 1) PBS, 2) 0.9% NaCl, 3) 1% PBST, and 4) 2.5% sucrose containing 1% Tween 20, were selected to determine the optimal serum diluents. For each buffer, a pooled serum sample from three KK (+) individuals was tested in triplicate at a dilution of 1:40. **(B)** R value analysis revealed a significant impaired binding the gold-rSjSAP4 conjugate with antibodies in pooled serum samples when using PBST and 2.5% sucrose containing 1% Tween 20 as the dilution buffer compared with PBS. Data are represented as the mean ± SD from three different assays *p* values were calculated using the Student's *t*-test (ns, no significance; $*p < 0.05$; $**p < 0.01$).

3.4 Assessment of stability of the GICA strips

To establish the stability of the developed GICA strips, sealed cassettes were stored at room temperature and used at 12 months using serum samples collected from eight subjects, including one healthy control and seven KK (+) individuals (Figure 5A). R value analysis revealed that there was no difference in result interpretation between the freshly produced GICA strips and those sealed ones stored at room temperature for 12 months (Figure 5B). These results indicate that the GICA strips remain stable at least for 1 year when stored in the dark with desiccant at room temperature.

4 Discussion

In the Philippines, approximately 12 million Filipinos in 28 provinces across 12 geographical zones are potentially affected by schistosomiasis japonica, with two and half million directly exposed to the disease (43, 44). As of 2019, the national prevalence of the disease was reported to be 4.0% based on focal surveys (45). Nevertheless, the infection intensity of the disease is decreasing in endemic barangays of the Philippines where MDA has been implemented annually, and light infections with an EPG less than 99 are becoming more dominant (46). Development and deployment of rapid, easy-to-use, cost-effective, and field-deployable diagnostic tools represent an important component of an integrated and innovative control approach to achieve disease elimination. GICA is the most widely used POC diagnostic tool for the detection/screening of a variety of disorders/diseases, including infectious diseases (28, 47). In this study, we developed a novel recombinant protein-based GICA assay and assessed its performance in the diagnosis of human *S. japonicum* infection.

It has been noted that the application of SEA of *S. japonicum* or antigen purified from crude lysate of *S. mansoni* adult worms in GICA strip development caused significant cross-reaction with the antibodies to other parasitic flukes or soil-transmitted helminths, although showing a high sensitivity (28, 29, 48). Rodpai et al. recently developed an immunochromatographic test (Sj-ICT) for the diagnosis of schistosomiasis japonica using somatic extract from adult *S. japonicum* as target antigen (49). The diagnostic assay also showed cross-reactions with cases of *Opisthorchiasis viverrini*, *Clonorchiasis sinensis*, *Paragonimiasis heterotremus*, sparganosis, cysticercosis, trichinellosis and trichuriasis (49). These studies indicate that it is necessary to develop immunochromatographic tests by incorporating optimised recombinant antigens, such as tetraspanins, saposin family members and hepatic schistosomula antigens (30, 39, 50, 51), to minimise the potential risk of cross-reactions. In the current study, we used a *S. japonicum* saposin protein, SjSAP4 as the target antigen, which previously showed no cross-reaction with alveolar echinococcosis and trichinellosis in ELISA assays (41), for the development of GICA assay. In addition, a BLASTp search in the National Center Biotechnology Information (NCBI) database confirmed that there exist only homologous fragments sharing less than 30% sequence identity with SjSAP4 in other parasitic flukes, such as *C. sinensis* and *Fasciola hepatica*, making the potential cross-reactivity of SjSAP4 with these flukes less likely. Nevertheless, a further experimental validation of the developed SjSAP4-incorapted GICA strip with sera samples from patients infected with other helminths, particularly other parasitic flukes, is still needed to test the potential cross-reactivity.

Currently, there are mainly two types of design used for the development of GICA assays for the diagnosis of schistosomiasis. The first, as adopted by Xu et al. (10) and Shen et al. (29), the gold- or fluorescent protein-conjugated recombinant streptococcal

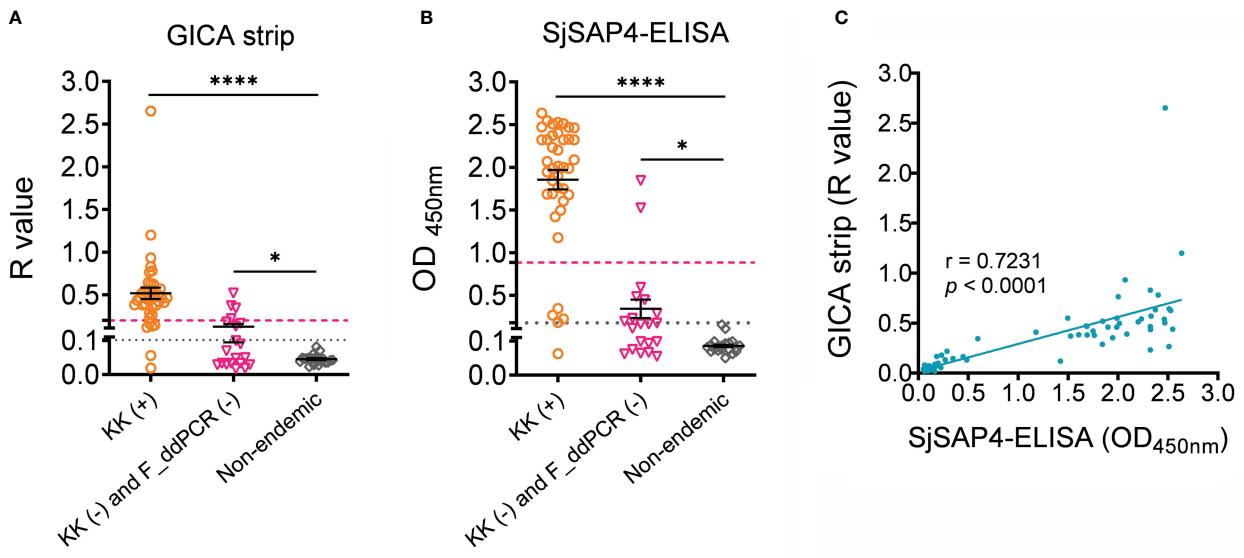

FIGURE 4
The performance of the SjSAP4-incorpated GICA and SjSAP4-ELISA assay in the diagnosis human schistosomiasis japonica. **(A, B)** Scatter plot showing the R values of the GICA assay (serum dilution 1:20) and OD values of the SjSPA4-ELISA assay (serum dilution 1:250) in testing serum samples from KK (+) individuals (n = 40), KK (-) and F_ddPCR (-) individuals (n = 20), and the non-endemic controls (n =20). Significance was analyzed by the Student's *t*-test (****, $p < 0.0001$; *, $p < 0.05$). Gray dotted line: cut-off value determined using non-endemic group as control; Magenta dashed line: cut-off value determined using the KK (-) and F_ddPCR (-) group as control. **(C)** Correlation between the R values of the GICA strip and OD values determined by the SjSAP4-ELISA assay (n = 80) using Pearson's correlation coefficient.

protein G (rSPG) is added onto the conjugate pad, while the schistosome antigen and rSPG are immobilized on the NC membrane, as the T and C line, respectively. For the second design as adopted by Rodpai et al. (49) and Pearson et al. (30), the gold-conjugated mouse anti-human IgG was sprayed onto the conjugate pad, while the schistosome antigen and goat anti-mouse IgG were dispensed as the T and C line, respectively, on the NC membrane. The two designs require high concentration of schistosome-derived antigens to be sprayed on the NC membrane. However, the recombinant SjSAP4 exhibits limited solubility in non-denatured solution, restricting the feasibility to adopt the above designs in developing GICA assay incorporating SjSAP4. In addition, our previous study showed that there are limited linear B-cell epitopes available on SjSAP4, suggesting its antigenicity is predominantly dependent on conformational B-cell epitopes (52), a finding that excludes the use of denatured rSjSAP4 in the development of the GICA assay. In this study, a novel GICA format, as shown in Figure 1, was then adopted. Based on the design, it is possible that the non-specific antibodies may compete with the conjugated anti-SjSAP4 antibody complexes for binding to the immobilized protein G on the 'T' line, which may partly explain why serum samples at relatively high concentrations (such as those diluted at 1:5 and 1:10) did not show a greater R value compared to those at relatively low concentrations (such as those diluted at 1:20 and 1:40) when tested with the developed GICA strips (Figure 2B), in addition to the hook effect.

As the results of immunochromatographic strips need to be read within a limited time after sample loading, the result read must be conducted by well-trained investigators to achieve an accurate assessment if naked eye determination method is employed. There can, however, be variability in visual interpretation of trace results due to individual differences in visual acuity and/or training (53). In regarding of interpretation optimization, a reference colour card (34) or lateral flow reader (54) was employed in previous studies to increase accuracy in result reads. In this study, the results of the established GICA assay were timely scanned and further analyzed *in silico* to eliminate the inter-reader variability, a procedure similar to that undertaken previously (35, 55). By introducing an R value, we convert the results of the developed GICA assay into a fully quantitative test, which can minimise the likelihood of potential system errors caused by variations in the absorbance rate of samples and/or color development time among different cassettes.

The current GICA assay is an AbD based assay. As antibodies can persist in the host after parasite clearance, an inherent limitation of AbD assays is their limited ability to differentiate between past and current infection. In this regard, determination of antibody decay rates post-infection could be a relevant subject to determine diagnostic value for some applications. Previously, by employing a murine schistosomiasis model, we found that the levels of SjSAP4-specific IgG antibodies start to decline at 7 months post-chemotherapy in one out of six mice (39). However, murine schistosomiasis usually represents a high dosage of infection, which cannot fully reflect the authentic situation of the disease in humans. Thus, a similar investigation, i.e., exploring the decay of specific antibodies against SjSAP4 in schistosomiasis patients after chemotherapy would be expected in the future. Using non-endemic donors as controls, some individuals in the KK (-) and F_ddPCR (-) group were positive for the GICA assay (positivity rate: 35%) and SjSAP4-ELISA assay (positivity rate: 40.0%). The antibody reaction observed in these subjects indicates that they may have previously been infected with *S. japonicum* in the

A

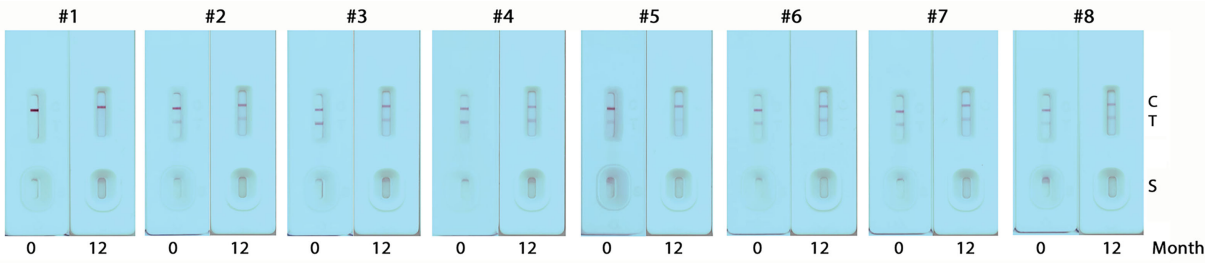

B

No	0 month		12 month	
	R value	Result interpretation	R value	Result interpretation
#1	0.021	-	0.049	-
#2	0.440	+	0.365	+
#3	1.136	+	0.509	+
#4	0.934	+	1.001	+
#5	0.217	+	0.201	+
#6	0.570	+	0.790	+
#7	0.626	+	0.638	+
#8	0.437	+	0.628	+

FIGURE 5
Stability assessment of the GICA strips. **(A)** Eight serum samples (one from healthy control (#1) and 7 from KK-positive subjects (#2 – #8)) diluted with PBS at 1:20 were used to assess the stability of the GICA strips stored at 25 for 12 months; **(B)** R values and read results for the eight serum samples tested with freshly produced GICA strips and those sealed and stored at 25°C for 12 months, respectively.

past (such as 3-12 months). It is worth noting that, the ability to discriminate between the current and previous infection can be improved for both assays by setting stringent cut-off values as we did in the case of individuals from endemic areas being used as controls, at the cost of sacrificing the diagnostic sensitivity to some extent. Nevertheless, the applications of such rapid and field-friendly POC tests for accurate diagnosis of schistosomiasis include: 1) Used as a screening tool for monitoring of transmission areas. For example, the developed GICA assay thus can be used for rapid mapping of schistosomiasis in the endemic zones in the Philippines, helping identify high-priority areas for targeted interventions. As the Department of Health (DOH) of the Philippines administers MDA for schistosomiasis every January through the Schistosomiasis Control and Elimination Program (56), the best time to carry out such rapid mapping should be at the end of the year. 2) Used as a screening tool for surveillance. In a limited prevalence or "post-elimination" situation, such as that in China, the GICA assay can also be used to determine if transmission blocking/elimination are actually achieved. 3) Testing individuals from non-endemic areas returning home after visiting schistosomiasis-endemic regions with suspicion of infection (travellers, migrants and international labourers), thereby helping prevent disease spread. 4) Determining the serological prevalence in endemic areas before and after the implementation of integrated interventions, thus monitoring the effect of these intervention measures. 5) Used to define the affected area of an *S. japonicum* infection focus, such as in Lindu, Napu, and Bada Highlands in Central Sulawesi, Indonesia (57), and two new endemic foci, Gonzaga and Calatrava, in the Philippines (58), by moving further away from the center until blood samples from surrounding areas are no longer positive.

As both are an indirect AbD based immunoassay, the SjSAP4-incorperated GICA and the SjSAP4-ELISA assay showed a high concordance. However, when the KK (-) and F_ddPCR (-) individuals were used as controls, the SjSAP4-incorperated GICA assay is inferior to the SjSAP4-ELISA assay in both sensitivity (85% vs 87.5%) and specificity (80% vs 90%), indicating that further optimisation steps are required to improve the performance of the immunochromatographic strip, such as validating the assay with serum samples at a higher dilution. Nevertheless, in contrast to GICA, the classic ELISA assay is labor-intensive and equipment-dependent, and requires a well-trained technician to perform. The stability assay of the GICA strips indicated that the validity period of the GICA strips was at least 12 months at room temperature, without loss of performance in the detection of *S. japonicum* infection. The GICA assay established here thus displays similar stability with the Sj-ICT and GICA assays previously developed by other groups (28, 49). In addition, due to high sensitivity of the established GICA strip, diluted finger-prick blood with a brief centrifugation to remove blood cells may also be suitable for the assay, which will further reduce the cost of the test.

5 Conclusions

In this study, a novel recombinant antigen-incorporated GICA assay was developed and assessed for the diagnosis of schistosomiasis japonica in subjects recruited from endemic areas in the Philippines. The application of the strip requires only a small serum volume and the results can be read within 10 min. The GICA strip showed a sensitivity of 95.0% and absolute specificity using the non-endemic individuals as controls. In addition, when the subjects confirmed as KK (-) and F_ddPCR (-) were employed as controls, the immunochromatographic test exhibited a sensitivity of 85.0% and a specificity of 80.0%. The GICA assay displayed a similar diagnostic ability with the conventional indirect ELISA method detecting serum IgG against rSjSAP4. The

developed immunochromatographic strips are stable for at least for 12 months stored at room temperature in sealed aluminium foil bag with desiccant, without loss of performance. The GICA assay established here represents a powerful tool for large-scale screening in rural schistosomiasis japonica-endemic areas where access to facilities and supplies is limited.

Data availability statement

The original contributions presented in the study are included in the article/Supplementary Material. Further inquiries can be directed to the corresponding author.

Author contributions

YM, DM and PC formulated the research aims and prepared the study protocol. PC supervised the research. DM, AR, RO and PC, provided study materials. YM, DM, CG, HY, AR, RO and PC developed the methodology, collected and analyzed the data. YM and PC drafted the original manuscript. CG, AR and PC critically reviewed and edited the manuscript. All authors contributed to the article and approved the submitted version.

Funding

This work was funded by the National Health and Medical Research Council (NHMRC) of Australia (ID: APP1160046, APP2008433, APP1102926, APP1037304 and APP1098244). DM was a NHMRC Leadership Fellow and Senior Scientist at QIMRB. The funders had no role in study design, data collection and analysis, decision to publish, or preparation of the manuscript.

Acknowledgments

We thank all study participants and the local field and clinical staff in Laoang and Palapag, Northern Samar, the Philippines, for their kind assistance in the collection of the clinical samples. We thank Dr. Xianyu Piao and Prof. Qijun Chen (Institute of Pathogen Biology, Chinese Academy of Medical Sciences) for providing serum samples collected from healthy donors. We also thank Dr. Thomas G. Egwang (Med Biotech Laboratories, Kampala, Uganda) and Mr. Moses Adriko (Vector Borne & NTD Control Division, Ministry of Health, Kampala, Uganda), for their critical review and edit of the manuscript.

Conflict of interest

The authors declare that the research was conducted in the absence of any commercial or financial relationships that could be construed as a potential conflict of interest.

Publisher's note

Supplementary material

The Supplementary Material for this article can be found online at: https://www.frontiersin.org/articles/10.3389/fimmu.2023.1165480/full#supplementary-material

SUPPLEMENTARY FIGURE 1
Recombinant SjSAP4 protein expression and identification. **(A)** SDS-PAGE gel electrophoresis analysis of rSjSAP4 expression in *E. coli*. M, protein marker; lane 1, empty vector; lane 2-3, bacterial extract before and after rSjSAP4 expression, respectively; lane 4-5, supernatant and precipitate of bacterial extract expressing rSjSAP4, respectively. **(B)** SDS-PAGE analysis of purified rSjSAP4. M, protein marker; lane 1, BSA; lane 2, purified rSjSAP4. **(C)** Western blot analysis of rSjSAP4 using the Odyssey system. M, protein marker; lane 1, purified rSjSAP4 probed with an anti-His-tag antibody.

References

1. WHO. *Ending the neglect to attain the sustainable development goals: a road map for neglected tropical diseases 2021–2030: overview*. Geneva: World Health Organization (2020).

2. McManus DP, Dunne DW, Sacko M, Utzinger J, Vennervald BJ, Zhou XN. Schistosomiasis. *Nat Rev Dis Primers* (2018) 4(1):13. doi: 10.1038/s41572-018-0013-8

3. Ross AG, Olveda RM, Chy D, Olveda DU, Li Y, Harn DA, et al. Can mass drug administration lead to the sustainable control of schistosomiasis? *J Infect Dis* (2015) 211 (2):283–9. doi: 10.1093/infdis/jiu416

4. Cavalcanti MG, Silva LF, Peralta RH, Barreto MG, Peralta JM. Schistosomiasis in areas of low endemicity: A new era in diagnosis. *Trends Parasitol* (2013) 29(2):75–82. doi: 10.1016/j.pt.2012.11.003

5. Weerakoon KG, Gobert GN, Cai P, McManus DP. Advances in the diagnosis of human schistosomiasis. *Clin Microbiol Rev* (2015) 28(4):939–67. doi: 10.1128/CMR.00137-14

6. Mesquita SG, Caldeira RL, Favre TC, Massara CL, Beck L, Simoes TC, et al. Assessment of the accuracy of 11 different diagnostic tests for the detection of schistosomiasis mansoni in individuals from a Brazilian area of low endemicity using latent class analysis. *Front Microbiol* (2022) 13:1048457. doi: 10.3389/fmicb.2022.1048457

7. Lv C, Deng W, Wang L, Qin Z, Zhou X, Xu J. Molecular techniques as alternatives of diagnostic tools in China as schistosomiasis moving towards elimination. *Pathogens* (2022) 11(3):287. doi: 10.3390/pathogens11030287

8. Tabios IKB, Sato MO, Tantengco OAG, Fornillos RJC, Kirinoki M, Sato M, et al. Diagnostic performance of parasitological, immunological, molecular, and ultrasonographic tests in diagnosing intestinal schistosomiasis in fieldworkers from endemic municipalities in the Philippines. *Front Immunol* (2022) 13:899311. doi: 10.3389/fimmu.2022.899311

9. Coelho PM, Jurberg AD, Oliveira AA, Katz N. Use of a saline gradient for the diagnosis of schistosomiasis. *Mem Inst Oswaldo Cruz* (2009) 104(5):720–3. doi: 10.1590/S0074-02762009000500010

10. Xu B, Gordon CA, Hu W, McManus DP, Chen HG, Gray DJ, et al. A novel procedure for precise quantification of *Schistosoma japonicum* eggs in bovine feces. *PloS Negl Trop Dis* (2012) 6(11):e1885. doi: 10.1371/journal.pntd.0001885

11. Lindholz CG, Favero V, Verissimo CM, Candido RRF, de Souza RP, Dos Santos RR, et al. Study of diagnostic accuracy of helmintex, kato-Katz, and POC-CCA methods for diagnosing intestinal schistosomiasis in Candeal, a low intensity transmission area in northeastern Brazil. *PloS Negl Trop Dis* (2018) 12(3):e0006274. doi: 10.1371/journal.pntd.0006274

12. Gordon CA, Acosta LP, Gobert GN, Olveda RM, Ross AG, Williams GM, et al. Real-time PCR demonstrates high prevalence of *Schistosoma japonicum* in the Philippines: Implications for surveillance and control. *PloS Negl Trop Dis* (2015) 9 (1):e0003483. doi: 10.1371/journal.pntd.0003483

13. Cnops L, Soentjens P, Clerinx J, Van Esbroeck MA. *Schistosoma haematobium*-specific real-time PCR for diagnosis of urogenital schistosomiasis in serum samples of international travelers and migrants. *PloS Negl Trop Dis* (2013) 7(8):e2413. doi: 10.1371/journal.pntd.0002413

14. Mu Y, Cai P, Olveda RM, Ross AG, Olveda DU, McManus DP. Parasite-derived circulating microRNAs as biomarkers for the detection of human *Schistosoma japonicum* infection. *Parasitology* (2020) 147(8):889–96. doi: 10.1017/S0031182019001690

15. Halili S, Grant JR, Pilotte N, Gordon CA, Williams SA. Development of a novel real-time polymerase chain reaction assay for the sensitive detection of *Schistosoma japonicum* in human stool. *PloS Negl Trop Dis* (2021) 15(10):e0009877. doi: 10.1371/journal.pntd.0009877

16. Weerakoon KG, Gordon CA, Gobert GN, Cai P, McManus DP. Optimisation of a droplet digital PCR assay for the diagnosis of *Schistosoma japonicum* infection: A duplex approach with DNA binding dye chemistry. *J Microbiol Methods* (2016) 125:19–27. doi: 10.1016/j.mimet.2016.03.012

17. Weerakoon KG, Gordon CA, Cai P, Gobert GN, Duke M, Williams GM, et al. A novel duplex ddPCR assay for the diagnosis of schistosomiasis japonica: Proof of concept in an experimental mouse model. *Parasitology* (2017) 144(8):1005–15. doi: 10.1017/S003118201700021X

18. Weerakoon KG, Gordon CA, Williams GM, Cai P, Gobert GN, Olveda RM, et al. Droplet digital PCR diagnosis of human schistosomiasis: Parasite cell-free DNA detection in diverse clinical samples. *J Infect Dis* (2017) 216(12):1611–22. doi: 10.1093/infdis/jix521

19. Gandasegui J, Fernandez-Soto P, Carranza-Rodriguez C, Perez-Arellano JL, Vicente B, Lopez-Aban J, et al. The rapid-heat LAMPellet method: A potential diagnostic method for human urogenital schistosomiasis. *PloS Negl Trop Dis* (2015) 9(7):e0003963. doi: 10.1371/journal.pntd.0003963

20. Gandasegui J, Fernandez-Soto P, Muro A, Simoes Barbosa C, Lopes de Melo F, Loyo R, et al. A field survey using LAMP assay for detection of *Schistosoma mansoni* in a low-transmission area of schistosomiasis in umbuzeiro, Brazil: Assessment in human and snail samples. *PloS Negl Trop Dis* (2018) 12(3):e0006314. doi: 10.1371/journal.pntd.0006314

21. Garcia-Bernalt Diego J, Fernandez-Soto P, Febrer-Sendra B, Crego-Vicente B, Muro A. Loop-mediated isothermal amplification in schistosomiasis. *J Clin Med* (2021) 10(3):511. doi: 10.3390/jcm10030511

22. Guo Q, Zhou K, Chen C, Yue Y, Shang Z , Zhou K, et al. Development of a recombinase polymerase amplification assay for schistosomiasis japonica diagnosis in the experimental mice and domestic goats. *Front Cell Infect Microbiol* (2021) 11:791997. doi: 10.3389/fcimb.2021.791997

23. Rostron P, Pennance T, Bakar F, Rollinson D, Knopp S, Allan F, et al. Development of a recombinase polymerase amplification (RPA) fluorescence assay for the detection of *Schistosoma haematobium*. *Parasit Vectors* (2019) 12(1):514. doi: 10.1186/s13071-019-3755-6

24. Mesquita SG, Lugli EB, Matera G, Fonseca CT, Caldeira RL, Webster B. Development of real-time and lateral flow recombinase polymerase amplification assays for rapid detection of *Schistosoma mansoni*. *Front Microbiol* (2022) 13:1043596. doi: 10.3389/fmicb.2022.1043596

25. MacGregor SR, McManus DP, Sivakumaran H, French JD, Gordon CA, Cai P, et al. Development of a novel CRISPR/Cas13-based assay for diagnosis of *Schistosoma japonicum* infection. *medRxiv* (2022). doi: 10.1101/2022.11.11.22282198

26. Heidt B, Siqueira WF, Eersels K, Dilien H, van Grinsven B, Fujiwara RT, et al. Point of care diagnostics in resource-limited settings: A review of the present and future of PoC in its most needed environment. *Biosensors (Basel)* (2020) 10(10):133. doi: 10.3390/bios10100133

27. WHO. *Public consultation: Target product profiles for diagnostic tests to meet schistosomiasis and soil-transmitted helminth programme needs*. Available at: https://www.who.int/news-room/articles-detail/public-consultation-target-product-profiles-for-diagnostic-tests-to-meet-schistosomiasis-and-soil-transmitted-helminth-programme-needs (Accessed Jan 31, 2023).

28. Xu R, Feng J, Hong Y, Lv C, Zhao D, Lin J, et al. A novel colloidal gold immunochromatography assay strip for the diagnosis of schistosomiasis japonica in domestic animals. *Infect Dis Poverty* (2017) 6(1):84. doi: 10.1186/s40249-017-0297-z

29. Shen Y, Ji R, Chai R, Yuan N, Zhang J, Jing Y, et al. A novel fluorescence immunochromatographic assay strip for the diagnosis of schistosomiasis japonica. *Parasit Vectors* (2021) 14(1):8. doi: 10.1186/s13071-020-04511-6

30. Pearson MS, Tedla BA, Mekonnen GG, Proietti C, Becker L, Nakajima R, et al. Immunomics-guided discovery of serum and urine antibodies for diagnosing urogenital schistosomiasis: A biomarker identification study. *Lancet Microbe* (2021) 2(11):e617–26. doi: 10.1016/S2666-5247(21)00150-6

31. Jiang SF, Zhang XP, Li BL, He YY, Liu J, Tang YH, et al. Evaluation of partially purified soluble egg antigens in colloidal gold immunochromatography assay card for rapid detection of anti-*Schistosoma japonicum* antibodies. *Southeast Asian J Trop Med Public Health* (2014) 45(3):568–75.

32. Shen Y, Wang Z, Li J, Xu R, Ji R, Lin J, et al. Preparation of colloidal gold immunochromatographic test strips for the diagnosis of. *Toxoplasma gondii. Food Agric Immunol* (2020) 31(1):630–41. doi: 10.1080/09540105.2020.1749569

33. Wang J, He K, Wu Z, Jin W, Wu W , Guo Y, et al. Development of a colloidal gold immunochromatographic strip for the rapid detection of antibodies against *Fasciola gigantica* in buffalo. *Front Vet Sci* (2022) 9:1004932. doi: 10.3389/fvets.2022.1004932

34. Sadaow L, Rodpai R, Janwan P, Boonroumkaew P, Sanpool O, Thanchomnang T, et al. An innovative test for the rapid detection of specific IgG antibodies in human whole-blood for the diagnosis of *Opisthorchis viverrini* infection. *Trop Med Infect Dis* (2022) 7(10):308. doi: 10.3390/tropicalmed7100308

35. Cai P, Mu Y, Weerakoon KG, Olveda RM, Ross AG, McManus DP. Performance of the point-of-care circulating cathodic antigen test in the diagnosis of schistosomiasis japonica in a human cohort from Northern Samar, the Philippines. *Infect Dis Poverty* (2021) 10(1):121. doi: 10.1186/s40249-021-00905-5

36. Peralta JM, Cavalcanti MG. Is POC-CCA a truly reliable test for schistosomiasis diagnosis in low endemic areas? the trace results controversy. *PloS Negl Trop Dis* (2018) 12(11):e0006813. doi: 10.1371/journal.pntd.0006813

37. Obeng BB, Aryeetey YA, de Dood CJ, Amoah AS, Larbi IA, Deelder AM, et al. Application of a circulating-cathodic-antigen (CCA) strip test and real-time PCR, in comparison with microscopy, for the detection of *Schistosoma haematobium* in urine samples from Ghana. *Ann Trop Med Parasitol* (2008) 102(7):625–33. doi: 10.1179/136485908X337490

38. Graeff-Teixeira C, Favero V, Pascoal VF, de Souza RP, Rigo FV, Agnese LHD, et al. Low specificity of point-of-care circulating cathodic antigen (POCCCA) diagnostic test in a non-endemic area for schistosomiasis mansoni in Brazil. *Acta Trop* (2021) 217:105863. doi: 10.1016/j.actatropica.2021.105863

39. Cai P, Weerakoon KG, Mu Y, Olveda DU, Piao X, Liu S, et al. A parallel comparison of antigen candidates for development of an optimized serological diagnosis of schistosomiasis japonica in the Philippines. *EBioMedicine* (2017) 24:237–46. doi: 10.1016/j.ebiom.2017.09.011

40. Cai P, Weerakoon KG, Mu Y, Olveda RM, Ross AG, Olveda DU, et al. Comparison of Kato Katz, antibody-based ELISA and droplet digital PCR diagnosis of schistosomiasis japonica: Lessons learnt from a setting of low infection intensity. *PloS Negl Trop Dis* (2019) 13(3):e0007228. doi: 10.1371/journal.pntd.0007228

41. Liu S, Zhou X, Piao X, Hou N, Shen Y, Zou Y, et al. Saposin-like proteins, a multigene family of *Schistosoma* species, are biomarkers for the immunodiagnosis of schistosomiasis japonica. *J Infect Dis* (2016) 214(8):1225–34. doi: 10.1093/infdis/jiw188

42. Mu Y, Weerakoon KG, Olveda RM, Ross AG, McManus DP , Cai P. Diagnostic performance of a urine-based ELISA assay for the screening of human schistosomiasis japonica: A comparative study. *Front Microbiol* (2022) 13:1051575. doi: 10.3389/fmicb.2022.1051575

43. Olveda RM, Gray DJ. Schistosomiasis in the Philippines: Innovative control approach is needed if elimination is the goal. *Trop Med Infect Dis* (2019) 4(2):66. doi: 10.3390/tropicalmed4020066

44. Department of Health. *Schistosomiasis control and elimination program* (2018). Available at: https://doh.gov.ph/node/211 (Accessed Jan 13, 2023).

45. Belizario VY Jr., de Cadiz AE, Navarro RC, Flores MJC, Molina VB, Dalisay SNM. The status of schistosomiasis japonica control in the Philippines: The need for an integrated approach to address a multidimensional problem. *Int J One Health* (2022) 8(1):8–19. doi: 10.14202/IJOH.2022.8-19

46. Leonardo L, Chigusa Y, Kikuchi M, Kato-Hayashi N, Kawazu S-i, Ma Angeles J, et al. Schistosomiasis in the Philippines: Challenges and some successes in control. *Southeast Asian J Trop Med* (2016) 47(4):651–66.

47. Li X, Yin Y, Pang L, Xu S, Lu F, Xu D, et al. Colloidal gold immunochromatographic assay (GICA) is an effective screening method for identifying detectable anti-SARS-CoV-2 neutralizing antibodies. *Int J Infect Dis* (2021) 108:483–6. doi: 10.1016/j.ijid.2021.05.080

48. Hoermann J, Kuenzli E, Schaefer C, Paris DH, Buhler S, Odermatt P, et al. Performance of a rapid immuno-chromatographic test (Schistosoma ICT IgG-IgM) for detecting *Schistosoma*-specific antibodies in sera of endemic and non-endemic populations. *PloS Negl Trop Dis* (2022) 16(5):e0010463. doi: 10.1371/journal.pntd.0010463

49. Rodpai R, Sadaow L, Boonroumkaew P, Phupiewkham W, Thanchomnang T, Limpanont Y, et al. Comparison of point-of-care test and enzyme-linked immunosorbent assay for detection of immunoglobulin G antibodies in the diagnosis of human schistosomiasis japonica. *Int J Infects Dis* (2021) 107:47–52. doi: 10.1016/j.ijid.2021.04.039

50. Xu X, Zhang Y, Lin D, Zhang J, Xu J, Liu YM, et al. Serodiagnosis of *Schistosoma japonicum* infection: Genome-wide identification of a protein marker, and assessment of its diagnostic validity in a field study in China. *Lancet Infect Dis* (2014) 14(6):489–97. doi: 10.1016/S1473-3099(14)70067-2

51. Hou N, Piao X, Jiang N, Liu S, Cai P, Liu B, et al. Novel hepatic schistosomula antigens as promising targets for immunodiagnosis and immunoprotection of schistosomiasis japonica. *J Infect Dis* (2022) 225(11):1991–2001. doi: 10.1093/infdis/jiac077

52. Mu Y, Gordon CA, Olveda RM, Ross AG, Olveda DU, Marsh JM, et al. Identification of a linear B-cell epitope on the *Schistosoma japonicum* saposin protein, SjSAP4: Potential as a component of a multi-epitope diagnostic assay. *PloS Negl Trop Dis* (2022) 16(7):e0010619. doi: 10.1371/journal.pntd.0010619

53. Colley DG, Andros TS, Campbell CH. Schistosomiasis is more prevalent than previously thought: what does it mean for public health goals, policies, strategies, guidelines and intervention programs? *Infect Dis Poverty* (2017) 6(1):63. doi: 10.1186/s40249-017-0275-5

54. Mewamba EM, Tiofack AAZ, Kamdem CN, Ngassam RIK, Mbagnia MCT, Nyangiri O, et al. Field assessment in Cameroon of a reader of POC-CCA lateral flow strips for the quantification of *Schistosoma mansoni* circulating cathodic antigen in urine. *PloS Negl Trop Dis* (2021) 15(7):e0009569. doi: 10.1371/journal.pntd.0009569

55. Casacuberta M, Kinunghi S, Vennervald BJ, Olsen A. Evaluation and optimization of the circulating cathodic antigen (POC-CCA) cassette test for detecting *Schistosoma mansoni* infection by using image analysis in school children in Mwanza Region, Tanzania. *Parasite Epidemiol Control* (2016) 1(2):105–15. doi: 10.1016/j.parepi.2016.04.002

56. DOH. *Guidelines on the implementation of the harmonized schedule and combined mass drug administration (HSCMDA) for the prevention and control of lymphatic filariasis. schistosomiasis, and soil-transmitted helminths (DOH Memorandum No 2016-0212).* (2016).

57. Anastasia H, Widjaja J. Engaging multi-sectoral collaboration to combat schistosomiasis in Napu Highlands, Poso District, Central Sulawesi. *J Phys Conf Ser* (2019) 1155(1):012111. doi: 10.1088/1742-6596/1155/1/012111

58. Leonardo L, Rivera P, Saniel O, Antonio Solon J, Chigusa Y, Villacorte E, et al. New endemic foci of schistosomiasis infections in the Philippines. *Acta Trop* (2015) 141 (Pt B):354–60. doi: 10.1016/j.actatropica.2013.03.015

frontiers | Frontiers in Immunology

TYPE Mini Review
PUBLISHED 19 April 2023
DOI 10.3389/fimmu.2023.1158805

OPEN ACCESS

EDITED BY
Roberta Lima Caldeira,
René Rachou Institute, Oswaldo Cruz Foundation (FIOCRUZ), Brazil

REVIEWED BY
Gabriel Rinaldi,
Aberystwyth University, United Kingdom
Wannaporn Ittiprasert,
George Washington University, United States

*CORRESPONDENCE
Yamei Jin
yameijin@shvri.ac.cn

SPECIALTY SECTION
This article was submitted to Parasite Immunology, a section of the journal Frontiers in Immunology

RECEIVED 04 February 2023
ACCEPTED 10 April 2023
PUBLISHED 19 April 2023

CITATION
Zhong H and Jin Y (2023) Single-sex schistosomiasis: a mini review. *Front. Immunol.* 14:1158805. doi: 10.3389/fimmu.2023.1158805

Single-sex schistosomiasis: a mini review

Haoran Zhong[1,2] and Yamei Jin[1,2]*

[1]National Reference Laboratory for Animal Schistosomiasis, Shanghai Veterinary Research Institute, Chinese Academy of Agricultural Sciences, Shanghai, China, [2]Key Laboratory of Animal Parasitology of Ministry of Agriculture and Rural Affairs, Shanghai Veterinary Research Institute, Chinese Academy of Agricultural Sciences, Shanghai, China

Schistosomiasis is a neglected tropical disease caused by dioecious blood flukes of the genus *Schistosoma* and second to malaria as a parasitic disease with significant socio-economic impacts. Mating is essential for maturation of male and female schistosomes and for females to lay of eggs, which are responsible for the pathogenesis and propagation of the life cycle beyond the mammalian host. Single-sex schistosomes, which do not produce viable eggs without mating, have been overlooked given the symptomatic paucity of the single-sex schistosomiasis and limited diagnostic toolkit. Besides, single-sex schistosomes are less sensitive to praziquantel. Therefore, these issues should be considered to achieve the elimination of this infection disease. The aim of this review is to summarize current progress in research of single-sex schistosomes and host-parasite interactions.

KEYWORDS

schistosome, single-sex infection, omics, host-parasite interaction, immune regulation

Introduction

Schistosomiasis is a neglected tropical disease caused by parasitic flatworms (blood flukes) of the genus *Schistosoma* that affects about 250 million people mainly in tropical and subtropical regions and accounts for 1.4–3.3 million disability-adjusted life years annually (1, 2). The World Health Organization (WHO) currently recommends mass administration of praziquantel (PZQ) for the control, worm/egg burden reduction and elimination of schistosomiasis (3). The increasing attention to schistosomiasis over the past few decades has led to significant improvements in agricultural and irrigation practices, as well as sanitation and hygiene (4, 5). Data from the national surveillance sites for schistosomiasis in China show that there have been no cases of *Schistosoma japonicum* infection of humans, bovines, or aquatic snails as the intermediate host in 2021 (6), demonstrating remarkable achievements in the control of schistosomiasis. The considerable expansion of preventive chemotherapy in tandem with scientific progress have improved the global control of schistosomiasis (2, 7). A publication by the WHO, titled “Ending the neglect to attain the Sustainable Development Goals: a road map for neglected tropical diseases 2021–2030”, proposes more ambitious targets, including the

elimination of schistosomiasis as a public health threat (8). Nevertheless, as a highly complex multi-host parasite, many questions remain unexplored.

Dioecious schistosomes mate and lay eggs within either the mesenteric or venules of the plexus venous of urogenital organs (depending on the species) (1). Most eggs are excreted in urine or feces, thereby contributing to propagate the life cycle. The presence of eggs in faecal or urine samples is considered the gold standard diagnostic tool (9). However, this approach is insufficient for detection of single-sex schistosomiasis (10). An opinion article published in 2018 proposed that exposure to single-sex schistosomes is an overlooked phenomenon, as no eggs are produced within the final host and infection is asymptomatic (11). Most importantly, a single-sex infection cannot be identified by traditional egg-based parasitological tests, which undoubtedly jeopardizes diagnostic accuracy of schistosomiasis (11). Other methods to theoretically detect egg-free single-sex schistosome infection include monitoring of schistosome gut-associated circulating anodic and cathodic antigens in serum or urine (12), and real-time polymerase chain reaction (PCR) analysis of schistosome DNA (13). When considering cost and convenience of rapid detection, circulating cathodic antigen is a direction worthy of further study in the future (14).

Both field and laboratory studies have reported cases of single-sex schistosome infections (15–18). Theoretically, single-sex schistosomes only mate in the host after encountering a worm of the opposite sex (17, 19). However, schistosomes produced by single-sex infections can also mate with the opposite sex of heterologous species and produce viable eggs (20–25). Another recent study indicated that both male and female *S. japonicum* can survive treatment with PZQ and retain normal reproductive potential (26). Therefore, it is necessary to address infections of single-sex schistosomes. Elucidation of the mechanisms underlying reproductive development of schistosomes and host-parasite interactions offers new perspectives for drug administration and therapies.

Single-sex schistosome infection occurs under natural conditions

Schistosomes mature only after mating and can subsequently survive in human hosts for 3–10 years (27, 28). Initial studies suggested that single-sex schistosome infections do not occur in nature but they can be generated in laboratory animals with cercariae produced from snails infected with single-sex miracidia (29, 30). However, subsequent field studies have found that single-sex schistosome infections do indeed occur in nature (15).

Single-sex miracidia can infect the tropical freshwater snail *Oncomelania hupensis* as the intermediate host (31). A field study conducted in the hilly areas of Anhui, China identified 67 (0.78%) of 8563 snails infected with schistosomes (32). Of the 46 snails selected for further studies, 21 (45.7%) were infected with female schistosomes, 23 (50.0%) with males, and only 2 (4.3%) with both sexes (32). Other field studies have reported similar results for *S. mansoni* and *S. haematobium* (31, 33). Besides, an ecological survey of definitive hosts conducted in 1993 found that 43 (20.8%) of 207 wild rats were infected with single-sex schistosomes, which included 38 (88.4%) infected with males and 5 (11.6%) with females (18). Another survey conducted along the Yangtze River (Hubei, China) identified 22 (5.5%) of 400 sentinel mice infected with schistosomes, of which 14 (63.6%) were infected with only males and 2 (9.1%) with only females (15). However, there is a lack of data from field investigations on how long single-sex schistosomes can survive in the host. Besides, schistosomes have numerous naturally permissive and non-adaptive hosts, thus surveillance is extremely difficult, which can potentially limit control measures (1). Moreover, single-sex schistosomes can remain "mating-ready" for up to 1 year in mice and still produce viable eggs (17, 34). These findings provide compelling proof that schistosomes can exist unpaired in natural environments.

Morphological differences between single-sex and bisexual worms

Morphological observations after dissection are commonly used to identify infections with single-sex schistosomes (35). Single-sex female (SF) worms and bisexual mated female (MF) worms have distinct morphological differences. In general, SF worms are about one-third of the length of MF worms, which renders detection relatively difficult (36). In *S. japonicum*, developed ovaries could be observed in MF worms at 18 day post infection (dpi) (2–3 days after mating) (37). From 21–25 dpi, MF worms continue to develop with proliferation of vitelline cells, while the ovaries and vitelline glands of SF worms were stunted which contains only stage I vitellocytes (38). An *in vitro* study found that when separated from the male, the female will lose the ability to produce viable eggs due to the loss of mature oocytes (39). Unlike females, there is no significant morphological difference between single-sex infected male worms (SM) and bisexual infected mated male worms (MM) (40, 41), although the testes of SM worms are slightly smaller (16).

Current omics studies of single-sex schistosomes

Laboratory models for stable single-sex infections can be established by infecting snails with single miracidia and identifying the sex of the cercariae released by individual snails by PCR (42). This model of single-sex infection has paved the way towards a better understanding of single-sex schistosomiasis in the mammalian host (42, 43).

Omics studies are useful to explore the reproductive development of schistosomes. Recent developments of sequence databases and improvements in proteomics and transcriptomics technologies have facilitated high-throughput studies of single-sex schistosomes and provided useful references for further studies of the reproductive mechanisms (44, 45).

Transcriptomics

Alexis et al. (29) identified differentially expressed genes (DEGs) between 42-day *S. mansoni* SF and MF worms. The results of *in situ* hybridization studies found that DEGs were mainly localized in the vitellocytes and ovary of MF worms vs. the vitellocytes and subtegumental cells of SF worms (29). The various predicted functions of DEGs in MF worms include oocyte maturation, apoptosis, protein degradation, and interactions between vitellocytes (29). The predicted functions of the DEGs 6767 (GenBank no. CCD61090) and 15402 (GenBank no. XP_002573676) of SF worms involve interactions that occur during mating (46).

An in-depth study conducted by Lu et al. (47) applied RNA-sequencing (RNA-seq) analyses for comparisons of isolated complete ovaries and testes from paired (46-day) and unpaired (67-day) *S. mansoni* and the adult worm. The results identified 96 genes comparatively enriched in testes of MM worms and 147 in the testes of SM worms. However, the mating procedure resulted in nearly 15-fold more differentially expressed genes (DEGs) in the ovaries between SF and MF worms (47). This enormous discrepancy in quantity is probably, as mentioned above, closely related to the intuitive morphological differences (16). Reference to the Kyoto Encyclopedia of Genes and Genomes classified the DEGs to metabolic and regulatory pathways (48). The results revealed that 849 DEGs from the ovaries of MF worms were involved in the Akt-, MAPK-, and Ras-signaling pathways, ribosome biogenesis, RNA transport, and endocytosis, whereas 435 DEGs from the ovaries of SF worms were involved in focal adhesion, lysosome function, and the MAPK signaling pathway (47). The schistosome egg-shell precursor gene p14 (Smp_131110), which was up-regulated in MF worms, encodes a female-specific tyrosinase that plays a pivotal role in egg shell synthesis (49). Notably, the transcript profiles of SF worms were more similar to either SM or MM worms than MF worms, which might be associated with the evolutionary background (50).

A meta-analysis of RNA-seq studies offered valuable expression data across all life stages of *S. mansoni* (51). In addition, an interactive web portal was established (51) of not only RNA-seq data, but also conserved structural domains and related pathways. Combined with the WormBase ParaSite database (52), this web portal allows researchers to visualize and analyze data for genomic studies of schistosomes.

Single-cell RNA-seq has also been used to comprehensively describe tissue types and physiology of schistosomes (53). A study by Wendt et al. (53) classified 43642 cells from the adult *S. mansoni* into 68 distinct cell populations. These data will help to further clarify the development of various cellular lineages during the schistosome life cycle to facilitate the development of novel therapeutics.

Proteomics

Proteomics has been used extensively in schistosomiasis research and has facilitated the discovery of critical molecules involved in reproductive development and as potential vaccine targets (16, 37, 45, 54–58). Schistosomes are highly complex organisms, thus dynamic analysis of the developmental stages is warranted (59). Based on the life cycle of *S. japonicum* (mating at 15 or 16 dpi, eggshell formation at 22 dpi, and egg laying at 24 dpi) (1), the proteomic profiles of SF and MF worms at 18, 21, 23, and 25 dpi were elucidated by our group (37, 45). In total, 2835 differentially expressed proteins (DEPs) were identified between SF and MF worms at different developmental stages (37). Relative to SF worms, 402, 322, 415, and 505 DEPs were up-regulated, while 230, 267, 290, and 404 DEPs were down-regulated in MF worms at 18, 21, 23, and 25 dpi, respectively (37). Gene ontology functional annotations demonstrated that 34 DEPs down-regulated in MF worms at all four time points were mainly involved in actin-related cell cycle-related functions, whereas 44 DEPs up-regulated in MF worms were involved in protein folding and hydrolysis, redox reactions, translation, and calcium ion binding (37, 60, 61). *Schistosoma japonicum* translationally controlled tumor protein (SjTCTP), which was highly expressed in MF worms at 18, 21, 23, and 25 dpi, is essential to the development of *S. japonicum* and recombinant SjTCTP was reported to stimulate partial protective immunity against schistosome infection in BALB/c mice (37).

Similarly, our group conducted comparative analysis of the proteomic profiles of SM and MM worms at 18, 21, 23, and 25 dpi (16), which confirmed 674 DEPs at different developmental stages. As compared to studies of female worms, there were significantly fewer DEPs both overall and at single time points, similar to the transcriptome changes described above (47). However, the proteomics and transcriptomics profiles were not always consistent, possibly because of differences in the timing and loci of gene transcription and translation or posttranscriptional regulation of proteins, suggesting that these differences were not coincidental (62, 63). Interestingly, bioinformatics analysis identified some DEPs closely associated with tumor proliferation in mammals, suggesting that the biological function of a protein might have similar functions in different tissues or organisms and could possibly be involved in the growth and differentiation of some cells in schistosomes (64, 65). *S. haematobium* is classified as a class I carcinogen by the International Agency for Research on Cancer that is associated with squamous cell carcinoma of the urinary bladder. Proteomic studies that reveal the functional role of DEPs during tumour development in the context of urogenital schistosomiasis are critical to identify not only targets for control, but biomarkers. Promising proteomic studies looking at *S. haematobium* worm tegument and soluble egg proteins validate this statement (66).

miRNomics: MicroRNA biology and computational analysis

MicroRNAs (miRNAs) are small non-coding RNAs that can negatively regulate the expression of target genes at the post-transcriptional level by binding to the 3'- and 5'-untranslated regions and coding sequences in order to repress translation or initiate degradation (67). Schistosome-derived miRNAs have been implicated in schistosome development and host-parasite interactions in schistosomiasis (68–70). The miRNA expression profiles of SF and MF *S. japonicum* have been reported (71, 72). Sun et al. (71) investigated differentially expressed miRNAs of 18- and 23-day SF and MF, and found similar miRNA profiles in 18-day SF and MF worms, whereas in 23-day MF worms, sja-bantam was significantly up-regulated, while sja-miR-1, sja-miR-7, sja-miR-7-5p, and sja-miR-71 were significantly up-regulated in 23-day SF worms (71). The predicted target genes of sja-bantam are reportedly related to development of the embryo and primary sexual characteristics, while the four up-regulated miRNAs in 23-day SF worms are associated with ribonucleoprotein complex assembly and microtubule-based processes (71, 73). A previous study by our group identified differentially expressed miRNAs between 25-day SF and MF worms (72), where sja-bantam and 19 other miRNAs were up-regulated in 25-day MF worms, while sja-miR-1, sja-miR-7-5p, and 14 other miRNAs were up-regulated in 25-day SF worms (72). Furthermore, comparisons of the expression profiles of sma-miR-277, sma-miR-4989, and related target genes in single-sex infected schistosomes suggested that sma-miR-277 and sma-miR-4989 have pivotal roles during juvenile-to-adult transition (74). Collectively, these findings indicate that differentially expressed miRNAs and related target genes might regulate the sexual status of female worms.

Although omics has provided tremendous insights into the mystery of single-sex schistosomes, relatively few studies have investigated epigenetics and small non-coding RNAs, other than miRNAs. A summary of recent studies of single-sex infected schistosomes is provided in Table 1.

Single-sex schistosomes regulate hepatic fibrosis in the host

Prolonged survival of schistosomes in the host can facilitate regulation of the host immune response through intricate

TABLE 1 Studies involving schistosome single-sex infections in the last 30 years.

Year	Natural/ Artificial	Species	Main content	Reference
1993	Natural	*S. mansoni*	Distribution of SF and SM within the host population	(18)
1994	Artificial	*S. japonicum*	Circulating antigen detection of SF and SM infection	(19)
1994	Artificial	*S. mansoni* & *S. intercalatum*	Single-sex schistosomes mated with the opposite sexes of heterologous species	(21)
1995	Artificial	*S. mansoni* & *S. haematobium*	Single-sex schistosomes mated with the opposite sexes of heterologous species	(20)
1995	Artificial	*S. mansoni* & *S. intercalatum*	Mating competition between males	(22)
1999	Artificial	*S. mansoni* & *S. haematobium*	Single-sex schistosomes mated with the opposite sexes of heterologous species	(25)
2001	Artificial	*S. mansoni*	PCR for sexing cercariae	(43)
2002	Natural	*S. mansoni*	Single-sex infected snails found in the field	(33)
2002	Artificial	*Schistosoma mansoni* & *S. margrebowiei*	Single-sex schistosomes mated with the opposite sexes of heterologous species	(23)
2003	Artificial	*S. mansoni* & *S. intercalatum*	Single-sex schistosomes mated with the opposite sexes of heterologous species	(24)
2004	Artificial	*S. mansoni*	Morphological observation of SF and MF	(38)
2006	Artificial	*S. mansoni*	Transcriptional analysis of 49-day SF and SM	(73)
2012	Artificial	*S. mansoni*	Transcriptional analysis of 49-day SF and MF	(29)
2012	Natural	*S. japonicum*	Single-sex infected schistosomes found in surveillance	(15)
2014	Natural	*S. japonicum*	Single-sex infected snails found in the field	(32)
2014	Artificial	*S. japonicum*	MicroRNA profiles of 18- and 23-day SF and MF	(71)
2016	Artificial	*S. mansoni*	Transcriptional analysis of 67-day SF and SM	(47)

(Continued)

TABLE 1 Continued

Year	Natural/ Artificial	Species	Main content	Reference
2017	Artificial	*S. mansoni*	Profiles of sma-mir-277/4989 and its target genes	(74)
2017	Artificial	*S. mansoni*	SF mitigates liver fibrosis after secondary infection	(75)
2018	Artificial	*S. mansoni*	Transcriptional analysis of all life stages of SF and SM	(51)
2018	/	/	Opinion article regarding the importance of single-sex infection	(11)
2018	Artificial	*S. mansoni*	Immunoregulation of SF and SM	(76)
2019	Artificial	*S. mansoni*	SF mitigates liver fibrosis after secondary infection	(77)
2020	Artificial	*S. japonicum*	Duplex RT-PCR for sexing cercariae	(42)
2020	Artificial	*S. japonicum*	Proteomic profiles of 25-day SF and MF	(45)
2020	Artificial	*S. japonicum*	MicroRNA profiles of 25-day SF and MF	(72)
2020	Artificial	*S. mansoni*	Single-cell RNA-seq analysis of 6–7 weeks SF and MF	(53)
2021	Artificial	*S. japonicum*	Survival and reproductive potential of SF and SM	(17)
2022	Artificial	*S. mansoni*	CCA and CAA of SF and SM	(12)
2022	Artificial	*S. japonicum*	Proteomic profiles of 18-, 21-, 23-, 25-day SF and MF	(37)
2022	Artificial	*S. japonicum*	Proteomic profiles of 18-, 21-, 23-, 25-day SM and MM	(16)
2022	Artificial	*S. japonicum*	PZQ treatment of SF and SM	(26)
2022	Artificial	*S. mansoni*	Transcriptional analysis of host infected with SF and SM	(78)
2022	Artificial	*S. mansoni*	BATT from male worms stimulate SF to develop	(79)
2023	Artificial	*S. japonicum*	Functional analysis of DEPs coming from SF and MF	(61)
2023	Artificial	*S. mansoni*	Single-sex infection boost immune response	(80)

SF, single-sex female worms; SM, single-sex male worms; MF, bisexual mated female worms; MM, bisexual mated male worms; PCR, polymerase chain reaction; RT-PCR, real-time polymerase chain reaction; CCA, circulating cathodic antigen; CAA, circulating anodic antigen; PZQ, praziquantel; BATT, β-alanyl-tryptamine; DEP, differentially expressed protein. /, not applicable.

mechanisms (81). Briefly, a T helper type 1 (Th1) response was generated during the initial phase of infection, which could target immature and mature migrating parasites (82). Schistosomes eggs trigger a dominate Th2 response regulated by regulatory T-cells (Tregs) (81). Granulomatous hypersensitivity to eggs trapped in the liver and intestinal tissues trigger the fundamental pathological causation of schistosomiasis, which could also be interpreted as a strong repair response (83) to suppress inflammation during the initial infection, but can also lead to tissue fibrosis (84). Mature female *S. japonicum* and *S. mansoni* produce hundreds of eggs per day, of which some become trapped in the liver, leading to hepatic inflammation, granuloma formation and fibrosis, and portal hypertension that leads to ascites (85). Without prompt treatment, schistosome-induced hepatic fibrosis is often irreversible (86). Therefore, targeting regulation of the host immune response could be useful for treatment or even reversal of schistosome-induced hepatic fibrosis.

Recent studies have investigated the immunomodulatory mechanisms of single-sex schistosomes in schistosome-induced hepatic fibrosis (75, 76, 78). Nicole et al. (75). demonstrated that primary infection of female *S. mansoni* (week 0–11) in secondary bisexually infected mice (week 12–19, then sacrificed) resulted in suppression of Th2-mediated granuloma and hepatic fibrosis, although no change in parasite load was observed. Mice with a primary infection of male *S. mansoni* also showed signs of reduced fibrosis, though not as evident as those initially infected with females (75), possibly due to high expression of cytotoxic T-lymphocyte-associated protein 4 (Ctla4) by Foxp3+ Tregs (87). Besides, the lack of relatively high production of Th1 cells implies that Th1 and Th2 responses might be regulated independently (75). Subsequent experiments indicated that Ctla4 had a preventive effect against schistosome-induced hepatic fibrosis (77).

When the timing of two infections were varied (primary infection at week 0–6 and secondary infection at week 7–14), protection against unisexual infection was not achieved when reinfection occurred more than 6 weeks later, thereby revealing the roles of male schistosomes in immune regulation (76). Male schistosomes triggered strong Th2 innate immune reactions during recurrent infection, which led to the strong recruitment of innate inflammatory cells, especially neutrophils and eosinophils, eventually resulting in reduced burdens of worms and eggs (76). However, the reduction to the parasite load in mice with primary infection of male schistosomes had a limited effect on granuloma size and hepatic fibrosis, which might be related to the high level of Th2 cytokines, such as interleukin-13, which promotes fibrosis (88).

A recent comparative transcriptomic analysis has helped to clarify the differences in immune regulation between male and female schistosomes (78). In this study, the number of DEGs in the

spleens of mice infected with male schistosomes was more than two-fold greater than mice infected with females, suggesting greater involvement of males (78). Further analysis found that male schistosomes drove dendritic cell maturation and induced T cell differentiation *via* up-regulation of the costimulatory molecule CD86, whereas infection with unisexual female worms had little effect on the host immune system (78).

Overall, infection by single-sex schistosomes (either sex) can induce immune responses in the host, which subsequently causes a Th1/Th2 imbalance, although further studies are needed to better clarify the effects of female schistosomes. These findings provide promising targets for new immune modulatory strategies against schistosome-induced hepatic fibrosis and possibly other diseases. The different outcomes of single-sex schistosome-induced hepatic fibrosis are presented in Figure 1.

Challenges and future perspectives

Several unresolved challenges and problems remain due to insufficient knowledge of single-sex schistosomes, including (i) the application of traditional egg-based parasitological tests for detection of single-sex infections; (ii) detection of antigens or nucleic acids as diagnostic criteria, as positive results might be due to past schistosome exposure or cross-reactions, rather than a single-sex schistosome infection (89, 90), and the reliance on morphological observations after dissection, which can create logistical difficulties; (iii) greater resistance of long-lived single-sex schistosomes to PZQ than paired worms (26); and (iv) the application of Omics studies to identify potential diagnostic and therapeutic targets. Extracellular vesicles (EVs) released from schistosome eggs and worms at different developmental stages were identified and considered to be important vectors in the regulation of host-parasite interactions (70). Studies have reported that the cargo of schistosome-derived EVs include sja-miR-1 (91), sma-miR-10 (92), sja-miR-71a (69), sja-miR-125b (93), sja-miR-2162 (94), sja-bantam (93) and novel sja-miRNA-33 (95), which mediate cross-species host-parasite interactions. However, the expression profiles of the EVs of single-sex schistosomes remain unknown. Thus, further analysis is warranted to provide new insights into immune regulation by single-sex schistosomes.

The development of *in vitro* culture methods for schistosomes has helped to validate the reliability of targets screened from Omics studies (96). In fact, a recent transcriptomic study indicated that male schistosomes can stimulate synthesis of the pheromone β-alanyl-tryptamine *via* nonribosomal peptide synthetase to facilitate normal development and laying of eggs by female schistosomes cultured *in vitro* (79). The results of this study suggest avenues for therapeutic intervention and demonstrated the unlimited potential of single-sex schistosome research.

The recently proposed "hygiene hypothesis" has made it possible to apply the immunomodulatory effects of schistosomes for the prevention and treatment of autoimmune disorders, other than liver fibrosis (69, 94, 95, 97). Schistosome infection and schistosome-derived proteins, peptides, miRNAs and EVs have been reported for the treatment of human immune-related disorders, including allergic asthma (98), arthritis (99), colitis (100), diabetes (101), sepsis (102), cystitis (103), and cancers (104, 105). In addition, human models of male schistosome cercariae infection, which produced no eggs or associated pathology, may provide foundations for subsequent studies (12, 106, 107). Nonetheless, further studies are needed to elucidate the distinct immunomodulatory mechanisms of male and female schistosomes and potential impacts on human diseases.

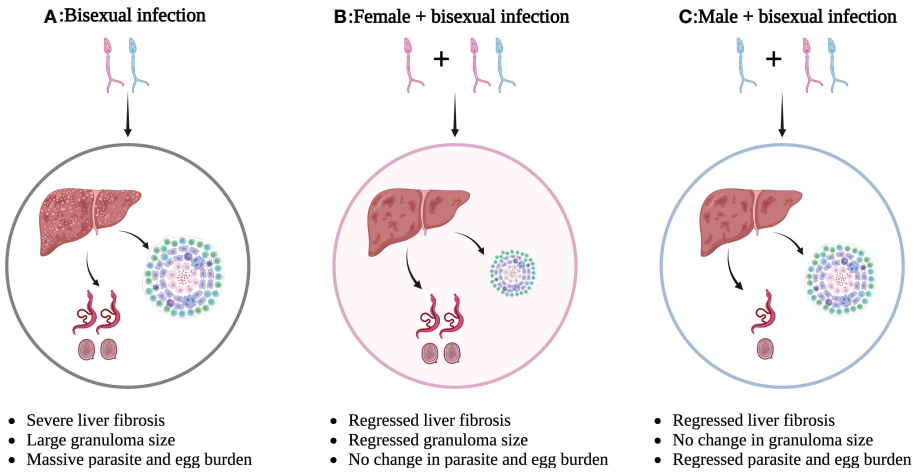

FIGURE 1
Different outcomes of single-sex schistosome-induced hepatic fibrosis. **(A)** Bisexual schistosome infection leads to severe liver fibrosis with large granuloma size and massive parasite/egg burden; **(B)** Bisexual schistosome infection after female infection leads to regressed liver fibrosis with smaller granuloma size, but no change in parasite/egg burden; **(C)** Bisexual schistosome infection after male infection leads to regressed liver fibrosis with regressed parasite/egg burden, but no change in granuloma size. This figure was created with Biorender.com. Arrows indicate the result of the next step.

Conclusions

Current control measures to reduce the infection rate of snails and definitive hosts could greatly increase the incidence of infection with single-sex schistosomes. These measures target the egg load in definitive hosts to reduce infection of snails, but also increase the risk for snails becoming hosts to mono-miracidia and production of only one sex of cercariae that can infect the definitive host (80).

Exposure to single-sex schistosomes is a neglected phenomenon that may become a threat of the control and elimination of schistosomiasis as a public health issue. The continued development of diagnostic and treatment protocols is imperative and further investigations of the reproductive development of schistosomes, as well as single-sex schistosomes, may provide essential references. In addition, future studies of the interactions between single-sex schistosomes and the host are warranted as a theoretical basis for autoimmune disorders, other than schistosomiasis.

Author contributions

YJ and HZ: conceptualization, validation, investigation, resources, and writing – review and editing. HZ: writing – original draft preparation and visualization. YJ: supervision, project administration, and funding acquisition. Both authors contributed to the article and approved the submitted version.

Funding

This work was supported by the Natural Science Foundation of Shanghai (no. 20ZR1469300) and the Chinese National Natural Science Foundation (no. 31672245).

Acknowledgments

We thank International Science Editing for revising the manuscript and their valuable comments.

Conflict of interest

The authors declare that the research was conducted in the absence of any commercial or financial relationships that could be construed as a potential conflict of interest.

Publisher's note

References

1. Colley DG, Bustinduy AL, Secor WE, King CH. Human schistosomiasis. *Lancet* (2014) 383(9936):2253–64. doi: 10.1016/s0140-6736(13)61949-2

2. Lo NC, Bezerra FSM, Colley DG, Fleming FM, Homeida M, Kabatereine N, et al. Review of 2022 who guidelines on the control and elimination of schistosomiasis. *Lancet Infect Dis* (2022) 22(11):e327–335. doi: 10.1016/s1473-3099(22)00221-3

3. Webster JP, Molyneux DH, Hotez PJ, Fenwick A. The contribution of mass drug administration to global health: past, present and future. *Philos Trans R Soc Lond B Biol Sci* (2014) 369(1645):20130434. doi: 10.1098/rstb.2013.0434

4. Zhou YB, Liang S, Jiang QW. Factors impacting on progress towards elimination of transmission of schistosomiasis japonica in China. *Parasit Vectors* (2012) 5:275. doi: 10.1186/1756-3305-5-275

5. Grover E, Paull S, Kechris K, Buchwald A, James K, Liu Y, et al. Predictors of bovine Schistosoma japonicum infection in rural sichuan, China. *Int J Parasitol* (2022) 52(8):485–96. doi: 10.1016/j.ijpara.2022.04.002

6. Zhang LJ, Xu ZM, Yang F, He JY, Dang H, Li YL, et al. Progress of schistosomiasis control in people's republic of China in 2021. *Zhongguo Xue Xi Chong Bing Fang Zhi Za Zhi* (2022) 34(4):329–36. doi: 10.16250/j.32.1374.2022132

7. Kokaliaris C, Garba A, Matuska M, Bronzan RN, Colley DG, Dorkenoo AM, et al. Effect of preventive chemotherapy with praziquantel on schistosomiasis among school-aged children in sub-Saharan Africa: a spatiotemporal modelling study. *Lancet Infect Dis* (2022) 22(1):136–49. doi: 10.1016/s1473-3099(21)00090-6

8. WHO. *Ending the neglect to attain the sustainable development goals. a global strategy on water, sanitation, and hygiene to combat neglected tropical diseases 2021–2030*. Geneva: World Health Organization (2021).

9. Chen C, Guo Q, Fu Z, Liu J, Lin J, Xiao K, et al. Reviews and advances in diagnostic research on Schistosoma japonicum. *Acta Trop* (2021) 213:105743. doi: 10.1016/j.actatropica.2020.105743

10. Nation CS, Da'dara AA, Marchant JK, Skelly PJ. Schistosome migration in the definitive host. *PloS Negl Trop Dis* (2020) 14(4):e0007951. doi: 10.1371/journal.pntd.0007951

11. Lu DB, Deng Y, Ding H, Liang YS, Webster JP. Single-sex schistosome infections of definitive hosts: implications for epidemiology and disease control in a changing world. *PloS Pathog* (2018) 14(3):e1006817. doi: 10.1371/journal.ppat.1006817

12. Casacuberta-Partal M, van Lieshout L, van Diepen A, Sijtsma JC, Ozir-Fazalalikhan A, Koopman JPR, et al. Excretion patterns of *Schistosoma mansoni* antigens CCA and CAA by adult male and female worms, using a mouse model and *ex vivo* parasite cultures. *Parasitology* (2022) 149(3):306–13. doi: 10.1017/S0031182021001839

13. Sun MT, Gu MM, Zhang JY, Yu QF, Lamberton PHL, Lu DB. Meta-analysis of variable-temperature PCR technique performance for diagnosising Schistosoma japonicum infections in humans in endemic areas. *PloS Negl Trop Dis* (2022) 16(1): e0010136. doi: 10.1371/journal.pntd.0010136

14. Sousa-Figueiredo JC, Betson M, Kabatereine NB, Stothard JR. The urine circulating cathodic antigen (Cca) dipstick: a valid substitute for microscopy for mapping and point-of-Care diagnosis of intestinal schistosomiasis. *PloS Negl Trop Dis* (2013) 7(1):e2008. doi: 10.1371/journal.pntd.0002008

15. Tu ZW, Cai SX, Huang XB, Su ZM, Gao H, Chen YY, et al. Surveillance and forecast for schistosome infectivity of Yangtze river and hanbeihe river during flooding in hubei province. *Zhongguo Xue Xi Chong Bing Fang Zhi Za Zhi* (2012) 24(2):193–5,9.

16. Zhong H, Wu L, Ren Y, Qin F, Jin Y. Comparative proteomic profiles of *Schistosoma japonicum* male worms derived from single-sex and bisexual infections. *Int J Parasitol* (2022) 52(13-14):815–28. doi: 10.1016/j.ijpara.2022.09.005

17. Lu DB, Yu QF, Zhang JY, Sun MT, Gu MM, Webster JP, et al. Extended survival and reproductive potential of single-sex male and female Schistosoma japonicum within definitive hosts. *Int J Parasitol* (2021) 51(11):887–91. doi: 10.1016/j.ijpara.2021.03.005

18. Morand S, Pointier J, Borel G, Theron A. Pairing probability of schistosomes related to their distribution among the host population. *Ecology* (1993) 74(8):2444–9.

19. Qiu L, Zhang Y, Chen W, Li H, Xue H. Relationship between the sex of Schistosoma japonicum and circulating antigen detection. *Zhongguo ji sheng chong xue yu ji sheng chong bing za zhi* (1994) 12(3):221–2.

20. Khalil SB, Mansour NS. Worm development in hamsters infected with unisex and cross-mated *Schistosoma mansoni* and *Schistosoma haematobium*. *J Parasitol* (1995) 81(1):8–11.

21. Tchuente LA, Imbert-Establet D, Southgate VR, Jourdane J. Interspecific stimulation of parthenogenesis in *Schistosoma intercalatum* and *S. mansoni*. *J Helminthol* (1994) 68(2):167–73. doi: 10.1017/s0022149x00013717

22. Tchuem Tchuente LA, Southgate VR, Imbert-Establet D, Jourdane J. Change of mate and mating competition between males of *Schistosoma intercalatum* and *S. mansoni*. *Parasitology* (1995) 110(Pt 1):45–52. doi: 10.1017/s0031182000081038

23. Cosgrove CL, Southgate VR. Mating interactions between *Schistosoma mansoni* and *S. margrebowiei*. *Parasitology* (2002) 125(Pt 3):233–43. doi: 10.1017/s0031182002002111

24. Cosgrove CL, Southgate VR. Interactions between *Schistosoma intercalatum* (zaire strain) and *S. mansoni*. *J Helminthol* (2003) 77(3):209–18. doi: 10.1079/JOH2002165

25. Webster BL, Southgate VR, Tchuem Tchuenté LA. Mating interactions between *Schistosoma haematobium* and *S. mansoni*. *J Helminthol* (1999) 73(4):351–6. doi: 10.1017/s0022149x99000591

26. Wang N, Peng HQ, Gao CZ, Cheng YH, Sun MT, Qu GL, et al. *In vivo* efficiency of praziquantel treatment of single-sex Schistosoma japonicum aged three months old in mice. *Int J Parasitol Drugs Drug Resist* (2022) 20:129–34. doi: 10.1016/j.ijpddr.2022.11.002

27. Warren KS, Mahmoud AA, Cummings P, Murphy DJ, Houser HB. Schistosomiasis mansoni in Yemeni in California: duration of infection, presence of disease, therapeutic management. *Am J Trop Med Hyg* (1974) 23(5):902–9. doi: 10.4269/ajtmh.1974.23.902

28. Chabasse D, Bertrand G, Leroux JP, Gauthey N, Hocquet P. Developmental bilharziasis caused by *Schistosoma mansoni* discovered 37 years after infestation. *Bull la Societe pathologie exotique ses filiales* (1985) 78(5):643–7.

29. Cogswell AA, Kommer VP, Williams DL. Transcriptional analysis of a unique set of genes involved in *Schistosoma mansoni* female reproductive biology. *PloS Negl Trop Dis* (2012) 6(11):e1907. doi: 10.1371/journal.pntd.0001907

30. Shaw JR. *Schistosoma mansoni*: Pairing *in vitro* and development of females from single sex infections. *Exp Parasitol* (1977) 41(1):54–65. doi: 10.1016/0014-4894(77)90129-1

31. Woolhouse ME, Chandiwana SK, Bradley M. On the distribution of schistosome infections among host snails. *Int J Parasitol* (1990) 20(3):325–7. doi: 10.1016/0020-7519(90)90147-f

32. Shi HP, Lu DB, Shen L, Shi T, Gu J. Single- or mixed-sex Schistosoma japonicum infections of intermediate host snails in hilly areas of anhui, China. *Parasitol Res* (2014) 113(2):717–21. doi: 10.1007/s00436-013-3700-0

33. Eppert A, Lewis FA, Grzywacz C, Coura-Filho P, Caldas I, Minchella DJ. Distribution of schistosome infections in molluscan hosts at different levels of parasite prevalence. *J Parasitol* (2002) 88(2):232–6. doi: 10.1645/0022-3395(2002)088[0232:Dosiim]2.0.Co;2

34. Shaw JR, Erasmus DA. *Schistosoma Mansoni*: An examination of the reproductive status of females from single sex infections. *Parasitology* (1981) 82(1):121–4. doi: 10.1017/s0031182000041913

35. Smithers SR, Terry RJ. The infection of laboratory hosts with cercariae of *Schistosoma mansoni* and the recovery of the adult worms. *Parasitology* (1965) 55(4):695–700. doi: 10.1017/s0031182000086248

36. Li P. The development of Schistosoma japonicum in unisexual and bisexual infections. *Acta Zoologica Sin* (1959) 11(4):499–506.

37. Zhong H, Ren Y, Qin F, Li X, Hou L, Gu S, et al. Schistosoma japonicum translationally controlled tumour protein, which is associated with the development of female worms, as a target for control of schistosomiasis. *Int J Parasitol* (2022) 52(8):569–79. doi: 10.1016/j.ijpara.2022.01.005

38. Neves RH, Costa-Silva M, Martinez EM, Branquinho TB, de Oliveira RM, Lenzi HL, et al. Phenotypic plasticity in adult worms of *Schistosoma mansoni* (trematoda: schistosomatidae) evidenced by brightfield and confocal laser scanning microscopies. *Mem Inst Oswaldo Cruz* (2004) 99(2):131–6. doi: 10.1590/s0074-02762004000200003

39. Popiel I, Cioli D, Erasmus DA. The morphology and reproductive status of female *Schistosoma mansoni* following separation from male worms. *Int J Parasitol* (1984) 14(2):183–90. doi: 10.1016/0020-7519(84)90047-x

40. Armstrong JC. Mating behavior and development of schistosomes in the mouse. *J Parasitol* (1965) 51:605–16.

41. Beckmann S, Quack T, Burmeister C, Buro C, Long T, Dissous C, et al. *Schistosoma mansoni*: Signal transduction processes during the development of the reproductive organs. *Parasitology* (2010) 137(3):497–520. doi: 10.1017/S0031182010000053

42. Liu S, Piao X, Hou N, Cai P, Ma Y, Chen Q. Duplex real-time PCR for sexing Schistosoma japonicum cercariae based on w chromosome-specific genes and its applications. *PloS Negl Trop Dis* (2020) 14(8):e0008609. doi: 10.1371/journal.pntd.0008609

43. Boissier J, Durand P, Moné H. PCR effectiveness for sexing *Schistosoma mansoni* cercariae: application for sexing clonal cercarial populations. *Mol Biochem Parasitol* (2001) 112(1):139–41. doi: 10.1016/s0166-6851(00)00344-3

44. Zhang M, Hong Y, Han Y, Han H, Peng J, Qiu C, et al. Proteomic analysis of tegument-exposed proteins of female and male Schistosoma japonicum worms. *J Proteome Res* (2013) 12(11):5260–70. doi: 10.1021/pr400476a

45. Li X, Qiao H, Qin F, Cheng G, Liu J, Li H, et al. Comparative analysis of ITRAQ-based proteome profiles of Schistosoma japonicum female worms coming from single-sex infections and bisexual infections. *J Proteomics* (2020) 213:103597. doi: 10.1016/j.jprot.2019.103597

46. Protasio AV, Tsai IJ, Babbage A, Nichol S, Hunt M, Aslett MA, et al. A systematically improved high quality genome and transcriptome of the human blood fluke *Schistosoma mansoni*. *PloS Negl Trop Dis* (2012) 6(1):e1455. doi: 10.1371/journal.pntd.0001455

47. Lu Z, Sessler F, Holroyd N, Hahnel S, Quack T, Berriman M, et al. Schistosome sex matters: a deep view into gonad-specific and pairing-dependent transcriptomes reveals a complex gender interplay. *Sci Rep* (2016) 6:31150. doi: 10.1038/srep31150

48. Kanehisa M, Goto S. Kegg: kyoto encyclopedia of genes and genomes. *Nucleic Acids Res* (2000) 28(1):27–30. doi: 10.1093/nar/28.1.27

49. Fitzpatrick JM, Hirai Y, Hirai H, Hoffmann KF. Schistosome egg production is dependent upon the activities of two developmentally regulated tyrosinases. *FASEB J* (2007) 21(3):823–35. doi: 10.1096/fj.06-7314com

50. Platt TR, Brooks DR. Evolution of the schistosomes (Digenea: schistosomatoidea): the origin of dioecy and colonization of the venous system. *J Parasitol* (1997) 83(6):1035–44.

51. Lu Z, Zhang Y, Berriman M. A web portal for gene expression across all life stages of. *Schistosoma mansoni. bioRxiv* (2018) 308213(11). doi: 10.1101/308213

52. Howe KL, Bolt BJ, Cain S, Chan J, Chen WJ, Davis P, et al. Wormbase 2016: expanding to enable helminth genomic research. *Nucleic Acids Res* (2016) 44(D1):D774–80. doi: 10.1093/nar/gkv1217

53. Wendt G, Zhao L, Chen R, Liu C, O'Donoghue AJ, Caffrey CR, et al. A single-cell RNA-seq atlas of *Schistosoma mansoni* identifies a key regulator of blood feeding. *Science* (2020) 369(6511):1644–9. doi: 10.1126/science.abb7709

54. Shang Z, Guo Q, Zhou X, Yue Y, Zhou K, Tang L, et al. Characterization of aspartyl aminopeptidase from Schistosoma japonicum. *Acta Trop* (2022) 232:106519. doi: 10.1016/j.actatropica.2022.106519

55. Li X, Cheng G, Qin F, Liu J, Li H, Jin Y. Function of the *lesswright* (*Lwr*) gene in the growth, development, and reproduction of Schistosoma japonicum. *Vet Parasitol* (2019) 272:31–9. doi: 10.1016/j.vetpar.2019.06.010

56. Cheng G, Li X, Qin F, Xu R, Zhang Y, Liu J, et al. Functional analysis of the *frzb2* gene in Schistosoma japonicum. *Vet Res* (2019) 50(1):108. doi: 10.1186/s13567-019-0716-1

57. Hong Y, Sun A, Zhang M, Gao F, Han Y, Fu Z, et al. Proteomics analysis of differentially expressed proteins in schistosomula and adult worms of Schistosoma japonicum. *Acta Trop* (2013) 126(1):1–10. doi: 10.1016/j.actatropica.2012.12.009

58. Liu M, Ju C, Du XF, Shen HM, Wang JP, Li J, et al. Proteomic analysis on cercariae and schistosomula in reference to potential proteases involved in host invasion of Schistosoma japonicum larvae. *J Proteome Res* (2015) 14(11):4623–34. doi: 10.1021/acs.jproteome.5b00465

59. Wang J, Yu Y, Shen H, Qing T, Zheng Y, Li Q, et al. Dynamic transcriptomes identify biogenic amines and insect-like hormonal regulation for mediating reproduction in Schistosoma japonicum. *Nat Commun* (2017) 8:14693. doi: 10.1038/ncomms14693

60. Conesa A, Götz S, García-Gómez JM, Terol J, Talón M, Robles M. Blast2go: a universal tool for annotation, visualization and analysis in functional genomics research. *Bioinformatics* (2005) 21(18):3674–6. doi: 10.1093/bioinformatics/bti610

61. Zhong H, Qin F, Ren Y, Li X, Hou L, Gu S, et al. Functional characterization of differentially expressed proteins coming from unisexual and bisexual infected *Schistosoma japonicum* female worms. *Exp Parasitol* (2023) 248:108504. doi: 10.1016/j.exppara.2023.108504

62. Zhai Q, Fu Z, Hong Y, Yu X, Han Q, Lu K, et al. ITRAQ-based comparative proteomic analysis of adult Schistosoma japonicum from water buffalo and yellow cattle. *Front Microbiol* (2018) 9:99. doi: 10.3389/fmicb.2018.00099

63. Lv L, Wang Y, Feng W, Hernandez JA, Huang W, Zheng Y, et al. ITRAQ-based differential proteomic analysis in mongolian gerbil brains chronically infected with *Toxoplasma gondii*. *J Proteomics* (2017) 160:74–83. doi: 10.1016/j.jprot.2017.03.012

64. Bommer UA, Telerman A. Dysregulation of TCTP in biological processes and diseases. *Cells* (2020) 9(7):1632. doi: 10.3390/cells9071632

65. Lee SR, Hong ST, Choi KW. Regulation of epithelial integrity and organ growth by tctp and coracle in *Drosophila*. *PloS Genet* (2020) 16(6):e1008885. doi: 10.1371/journal.pgen.1008885

66. Sotillo J, Pearson MS, Becker L, Mekonnen GG, Amoah AS, van Dam G, et al. In-depth proteomic characterization of *Schistosoma haematobium*: towards the development of new tools for elimination. *PloS Negl Trop Dis* (2019) 13(5):e0007362. doi: 10.1371/journal.pntd.0007362

67. Bartel DP. MicroRNAs: genomics, biogenesis, mechanism, and function. *Cell* (2004) 116(2):281–97. doi: 10.1016/s0092-8674(04)00045-5

68. Yu J, Yu Y, Li Q, Chen M, Shen H, Zhang R, et al. Comprehensive analysis of miRNA profiles reveals the role of Schistosoma japonicum miRNAs at different developmental stages. *Vet Res* (2019) 50(1):23. doi: 10.1186/s13567-019-0642-2

69. Wang L, Liao Y, Yang R, Yu Z, Zhang L, Zhu Z, et al. Sja-mir-71a in schistosome egg-derived extracellular vesicles suppresses liver fibrosis caused by schistosomiasis *via* targeting semaphorin 4d. *J Extracell Vesicles* (2020) 9(1):1785738. doi: 10.1080/20013078.2020.1785738

70. Zhong H, Jin Y. Multifunctional roles of microRNAs in schistosomiasis. *Front Microbiol* (2022) 13:925386. doi: 10.3389/fmicb.2022.925386

71. Sun J, Wang S, Li C, Ren Y, Wang J. Novel expression profiles of microRNAs suggest that specific miRNAs regulate gene expression for the sexual maturation of female Schistosoma japonicum after pairing. *Parasit Vectors* (2014) 7:177. doi: 10.1186/1756-3305-7-177

72. Han Y, Feng J, Ren Y, Wu L, Li H, Liu J, et al. Differential expression of microRNA between normally developed and underdeveloped female worms of Schistosoma japonicum. *Vet Res* (2020) 51(1):126. doi: 10.1186/s13567-020-00851-4

73. Fitzpatrick JM, Hoffmann KF. Dioecious *Schistosoma mansoni* express divergent gene repertoires regulated by pairing. *Int J Parasitol* (2006) 36(10-11):1081–9. doi: 10.1016/j.ijpara.2006.06.007

74. Protasio AV, van Dongen S, Collins J, Quintais L, Ribeiro DM, Sessler F, et al. Mir-277/4989 regulate transcriptional landscape during juvenile to adult transition in the parasitic helminth *Schistosoma mansoni*. *PloS Negl Trop Dis* (2017) 11(5):e0005559. doi: 10.1371/journal.pntd.0005559

75. Koslowski N, Sombetzki M, Loebermann M, Engelmann R, Grabow N, Osterreicher CH, et al. Single-sex infection with female *Schistosoma mansoni* cercariae mitigates hepatic fibrosis after secondary infection. *PloS Negl Trop Dis* (2017) 11(5):e0005595. doi: 10.1371/journal.pntd.0005595

76. Sombetzki M, Koslowski N, Rabes A, Seneberg S, Winkelmann F, Fritzsche C, et al. Host defense versus immunosuppression: unisexual infection with male or female *Schistosoma mansoni* differentially impacts the immune response against invading cercariae. *Front Immunol* (2018) 9:861. doi: 10.3389/fimmu.2018.00861

77. Sombetzki M, Rabes A, Bischofsberger M, Winkelmann F, Koslowski N, Schulz C, et al. Preventive ctla-4-Ig treatment reduces hepatic egg load and hepatic fibrosis in *Schistosoma mansoni*-infected mice. *BioMed Res Int* (2019) 2019:1704238. doi: 10.1155/2019/1704238

78. Winkelmann F, Rabes A, Reinholdt C, Koslowski N, Koczan D, Reisinger EC, et al. Sex-specific modulation of the host transcriptome in the spleen of *Schistosoma mansoni*-infected mice. *Front Cell Infect Microbiol* (2022) 12:893632. doi: 10.3389/fcimb.2022.893632

79. Chen R, Wang J, Gradinaru I, Vu HS, Geboers S, Naidoo J, et al. A male-derived nonribosomal peptide pheromone controls female schistosome development. *Cell* (2022) 185(9):1506–20.e17. doi: 10.1016/j.cell.2022.03.017

80. Reinholdt C, Winkelmann F, Koslowski N, Reisinger EC, Sombetzki M. Unisexual infection with *Schistosoma mansoni* in mice has the potential to boost the immune response against eggs after challenge infection. *Front Immunol* (2023) 14:1125912. doi: 10.3389/fimmu.2023.1125912

81. Pearce EJ, MacDonald AS. The immunobiology of schistosomiasis. *Nat Rev Immunol* (2002) 2(7):499–511. doi: 10.1038/nri843

82. Wynn TA, Thompson RW, Cheever AW, Mentink-Kane MM. Immunopathogenesis of schistosomiasis. *Immunol Rev* (2004) 201:156–67. doi: 10.1111/j.0105-2896.2004.00176.x

83. Zhong H, Gui X, Hou L, Lv R, Jin Y. From inflammation to fibrosis: novel insights into the roles of high mobility group protein box 1 in schistosome-induced liver damage. *Pathogens* (2022) 11(3):289. doi: 10.3390/pathogens11030289

84. Wilson MS, Mentink-Kane MM, Pesce JT, Ramalingam TR, Thompson R, Wynn TA. Immunopathology of schistosomiasis. *Immunol Cell Biol* (2007) 85(2):148–54. doi: 10.1038/sj.icb.7100014

85. Chuah C, Jones MK, Burke ML, McManus DP, Gobert GN. Cellular and chemokine-mediated regulation in schistosome-induced hepatic pathology. *Trends Parasitol* (2014) 30(3):141–50. doi: 10.1016/j.pt.2013.12.009

86. Schwartz C, Fallon PG. Schistosoma "eggs-iting" the host: granuloma formation and egg excretion. *Front Immunol* (2018) 9:2492. doi: 10.3389/fimmu.2018.02492

87. Taylor MD, Harris A, Babayan SA, Bain O, Culshaw A, Allen JE, et al. Ctla-4 and Cd4+ Cd25+ regulatory T cells inhibit protective immunity to filarial parasites. *vivo. J Immunol* (2007) 179(7):4626–34. doi: 10.4049/jimmunol.179.7.4626

88. Fichtner-Feigl S, Strober W, Kawakami K, Puri RK, Kitani A. Il-13 signaling through the il-13alpha2 receptor is involved in induction of TGF-beta1 production and fibrosis. *Nat Med* (2006) 12(1):99–106. doi: 10.1038/nm1332

89. Cai YC, Xu JF, Steinmann P, Chen SH, Chu YH, Tian LG, et al. Field comparison of circulating antibody assays versus circulating antigen assays for the detection of schistosomiasis japonica in endemic areas of China. *Parasit Vectors* (2014) 7:138. doi: 10.1186/1756-3305-7-138

90. Lamberton PH, Kabatereine NB, Oguttu DW, Fenwick A, Webster JP. Sensitivity and specificity of multiple kato-Katz thick smears and a circulating cathodic antigen test for *Schistosoma mansoni* diagnosis pre- and post-repeated-praziquantel treatment. *PloS Negl Trop Dis* (2014) 8(9):e3139. doi: 10.1371/journal.pntd.0003139

91. Wang Y, Fan X, Lei N, He X, Wang X, Luo X, et al. A microRNA derived from Schistosoma japonicum promotes schistosomiasis hepatic fibrosis by targeting host secreted frizzled-related protein 1. *Front Cell Infect Microbiol* (2020) 10:101. doi: 10.3389/fcimb.2020.00101

92. Meningher T, Barsheshet Y, Ofir-Birin Y, Gold D, Brant B, Dekel E, et al. Schistosomal extracellular vesicle-enclosed miRNAs modulate host T helper cell differentiation. *EMBO Rep* (2020) 21(1):e47882. doi: 10.15252/embr.201947882

93. Liu J, Zhu L, Wang J, Qiu L, Chen Y, Davis RE, et al. *Schistosoma japonicum* extracellular vesicle miRNA cargo regulates host macrophage functions facilitating parasitism. *PloS Pathog* (2019) 15(6):e1007817. doi: 10.1371/journal.ppat.1007817

94. He X, Wang Y, Fan X, Lei N, Tian Y, Zhang D, et al. A schistosome miRNA promotes host hepatic fibrosis by targeting transforming growth factor beta receptor III. *J Hepatol* (2020) 72(3):519–27. doi: 10.1016/j.jhep.2019.10.029

95. Wang Y, Gong W, Zhou H, Hu Y, Wang L, Shen Y, et al. A novel miRNA from egg-derived exosomes of Schistosoma japonicum promotes liver fibrosis in murine schistosomiasis. *Frontier Immunol* (2022) 13:860807. doi: 10.3389/fimmu.2022.860807

96. Wang J, Chen R, Collins JJ3rd. Systematically improved *in vitro* culture conditions reveal new insights into the reproductive biology of the human parasite *Schistosoma mansoni*. *PloS Biol* (2019) 17(5):e3000254. doi: 10.1371/journal.pbio.3000254

97. Alexandre-Silva GM, Brito-Souza PA, Oliveira ACS, Cerni FA, Zottich U, Pucca MB. The hygiene hypothesis at a glance: early exposures, immune mechanism and novel therapies. *Acta Trop* (2018) 188:16–26. doi: 10.1016/j.actatropica.2018.08.032

98. Liu P, Li J, Yang X, Shen Y, Zhu Y, Wang S, et al. Helminth infection inhibits airway allergic reaction and dendritic cells are involved in the modulation process. *Parasite Immunol* (2010) 32(1):57–66. doi: 10.1111/j.1365-3024.2009.01161.x

99. Osada Y, Horie Y, Nakae S, Sudo K, Kanazawa T. Stat6 and il-10 are required for the anti-arthritic effects of *Schistosoma mansoni via* different mechanisms. *Clin Exp Immunol* (2019) 195(1):109–20. doi: 10.1111/cei.13214

100. Liu Y, Ye Q, Liu YL, Kang J, Chen Y, Dong WG. Schistosoma japonicum Attenuates dextran sodium sulfate-induced colitis in mice *via* reduction of endoplasmic reticulum stress. *World J Gastroenterol* (2017) 23(31):5700–12. doi: 10.3748/wjg.v23.i31.5700

101. Yan K, Wang B, Zhou H, Luo Q, Shen J, Xu Y, et al. Amelioration of type 1 diabetes by recombinant fructose-1,6-bisphosphate aldolase and cystatin derived from Schistosoma japonicum in a murine model. *Parasitol Res* (2020) 119(1):203–14. doi: 10.1007/s00436-019-06511-7

102. Tang H, Liang YB, Chen ZB, Du LL, Zeng LJ, Wu JG, et al. Soluble egg antigen activates M2 macrophages *via* the stat6 and pi3k pathways, and Schistosoma japonicum alternatively activates macrophage polarization to improve the survival rate of septic mice. *J Cell Biochem* (2017) 118(12):4230–9. doi: 10.1002/jcb.26073

103. Mbanefo EC, Le L, Zee R, Banskota N, Ishida K, Pennington LF, et al. Ipse, a urogenital parasite-derived immunomodulatory protein, ameliorates ifosfamide-induced hemorrhagic cystitis through downregulation of pro-inflammatory pathways. *Sci Rep* (2019) 9(1):1586. doi: 10.1038/s41598-018-38274-z

104. Jiang P, Wang J, Zhu S, Hu C, Lin Y, Pan W. Identification of a Schistosoma japonicum microRNA that suppresses hepatoma cell growth and migration by targeting host *fzd4* gene. *Front Cell Infect Microbiol* (2022) 12:786543. doi: 10.3389/fcimb.2022.786543

105. Mu Y, McManus DP, Hou N, Cai P. Schistosome infection and schistosome-derived products as modulators for the prevention and alleviation of immunological disorders. *Front Immunol* (2021) 12:619776. doi: 10.3389/fimmu.2021.619776

106. Janse JJ, Langenberg MCC, Kos-Van Oosterhoud J, Ozir-Fazalalikhan A, Brienen EAT, Winkel BMF, et al. Establishing the production of male *Schistosoma mansoni* cercariae for a controlled human infection model. *J Infect Dis* (2018) 218 (7):1142–6. doi: 10.1093/infdis/jiy275

107. Langenberg MCC, Hoogerwerf MA, Koopman JPR, Janse JJ, Kos-van Oosterhoud J, Feijt C, et al. A controlled human *Schistosoma mansoni* infection model to advance novel drugs, vaccines and diagnostics. *Nat Med* (2020) 26(3):326–32. doi: 10.1038/s41591-020-0759-x

frontiers | Frontiers in Cellular and Infection Microbiology

TYPE Original Research
PUBLISHED 24 April 2023
DOI 10.3389/fcimb.2023.1167787

OPEN ACCESS

EDITED BY
Omar Hamarsheh,
Al-Quds University, Palestine

REVIEWED BY
Kifaya Azmi,
Al-Quds University, Palestine
Ahmad Amro,
Al-Quds University, Palestine

*CORRESPONDENCE
Sandra Grossi Gava
sandra.grossi@fiocruz.br
Roberta Lima Caldeira
roberta.caldeira@fiocruz.br

SPECIALTY SECTION
This article was submitted to Parasite and Host, a section of the journal Frontiers in Cellular and Infection Microbiology

RECEIVED 17 February 2023
ACCEPTED 22 March 2023
PUBLISHED 24 April 2023

CITATION
de Araújo AD, Carvalho OS, Gava SG and Caldeira RL (2023) DNA barcoding as a valuable tool for delimiting mollusk species of the genus *Biomphalaria* Preston, 1910 (Gastropoda: Planorbidae). *Front. Cell. Infect. Microbiol.* 13:1167787. doi: 10.3389/fcimb.2023.1167787

DNA barcoding as a valuable tool for delimiting mollusk species of the genus *Biomphalaria* Preston, 1910 (Gastropoda: Planorbidae)

Amanda Domingues de Araújo, Omar dos Santos Carvalho, Sandra Grossi Gava* and Roberta Lima Caldeira*

Helminthology and Medical Malacology Research Group, René Rachou Institute, Fiocruz Minas, Belo Horizonte, Minas Gerais, Brazil

Introduction: The genus *Biomphalaria* in Brazil includes 11 species and one subspecies, three of which are intermediate hosts of *Schistosoma mansoni*. Due to the recent evolution of this group, some species are difficult to identify based on morphological characters, making the use of genetic markers necessary for species identification. This study aimed to evaluate the use of partial sequences of the cytochrome c oxidase I (*coi*) gene for the identification of *Biomphalaria* species using phylogenetic reconstruction and species delimitation algorithms. The study tested the use of DNA barcoding technique for species delimitation within the genus.

Methods: DNA barcoding was performed by sequencing a partial region of the *coi* gene from specimens, and the sequences were analyzed using phylogenetic reconstruction and algorithms to delimit Operational Taxonomic Units (OTUs).

Results: The study found that the use of the *coi* gene in the reconstruction of the phylogeny of the genus might be an alternative for understanding the evolution and dispersion of species. However, this marker alone is not enough to solve complex taxonomic problems within the genus. A total of 223 sequences were analyzed, 102 of which could be separated using the barcode gap, enabling the correct identification of seven taxa.

Discussion: The study demonstrated that accurate mollusk identification is necessary for effective schistosomiasis control. The DNA barcoding methodology was found to be promising for accurate mollusk identification, which is crucial for concentrating schistosomiasis control efforts in places where it is needed.

KEYWORDS

DNA barcode, mollusks, *Biomphalaria*, medical malacology collection, molecular idenlification, cytochrome c oxidase *coi*

1 Introduction

Schistosoma mansoni Sambon, 1907 is the etiologic agent of schistosomiasis mansoni, a disease that affects about 130 million people in South America, the Caribbean, Africa, Madagascar, and the Middle East (James et al., 2018; McManus et al., 2018).

Mollusks of the genus *Biomphalaria* (Preston, 1910) belong to the family Planorbidae, which has approximately 300 species, of which about 10% are within the *Biomphalaria* genus (Jarne et al., 2010). There are 26 morphospecies and one subspecies of the latter genus described in Latin America. In Brazil, in particular, there are 11 species and one subspecies, of which three are intermediate hosts of *S. mansoni* under natural conditions – *Biomphalaria glabrata* (Say, 1818), *Biomphalaria tenagophila* (d'Orbigny, 1835) and *Biomphalaria straminea* (Dunker, 1835). 1848) – while another three are considered potential hosts, as they can be infected under laboratory conditions – *Biomphalaria peregrina* (d'Orbigny, 1835), *Biomphalaria amazonica* Paraense, 1966 and *Biomphalaria cousini* Paraense, 1966 (Corrêa, 1971; Paraense and Corrêa, 1973; Teodoro et al., 2010).

In the genus *Biomphalaria*, there are two different species complexes, whose members are practically indistinguishable by the morphology of their shells and by most characters of the genital system: (i) the *Biomphalaria straminea* complex, containing the species *B. straminea*, *Biomphalaria kuhniana* (Clessin, 1883) and *Biomphalaria intermedia* Paraense & Deslandes, 1962; and (ii) the *Biomphalaria tenagophila* complex, containing the species/subspecies *B. tenagophila tenagophila*, *Biomphalaria tenagophila guaibensis* Paraense, 1984 and *Biomphalaria occidentalis* Paraense, 1981 (Paraense, 1988; Caldeira et al., 1998; Spatz et al., 1999). Distinguishing between these taxa is one of the main challenges of research that aims to elucidate the phylogeny of the genus *Biomphalaria* using molecular techniques, such as the present work (Caldeira et al., 2000; Vidigal et al., 2004).

The study of the *Biomphalaria* genus has always been motivated by the epidemiological and ecological aspects of the relationship between these planorbids and *S. mansoni*. Despite this, the amount of research effort devoted to studies of the phylogeny and systematics of these groups has always been relatively small, even though elucidating the phylogenetic relationships of this group could change our understanding of its host-parasite relationships, which is fundamental for the development and planning of schistosomiasis control programs (Jarne et al., 2011).

Little is known about the evolution of the genus *Biomphalaria* due to the difficulty of placing fossils in the history of this species group, mainly because the morphometry of the shell is not used as an essential taxonomic characteristic, due to its simplicity and lack of relevant attributes regarding phylogeny (Cabrera et al., 2016). What can be said is that the evolution of mollusks of this genus is very recent, with the ancestral taxa within this genus beginning to split between the Pliocene and Pleistocene, around 1.8 million years ago, a fact that is consistent with the fossil record (Kaesler and Parodiz, 1970; Wanninger and Wollesen, 2019). Precisely for this reason, the characteristics used to distinguish between the species is quite limited; especially among closely-related species such as those of the *B. straminea* complex (Jarne et al., 2011). The morphological differences between *B. straminea* and *B. kuhniana* are very subtle and practically indistinguishable, with differences being limited to the number of muscular layers in the penis wall (three in *B. straminea* and two in *B. kuhniana*) (Paraense, 1988) and distal segment of the spermiduct very winding in *B. straminea* and straight or slighetly wavy in *B. kuhniana* (Paraense, 1988). Additionally, the molecular technique used for species differentiation within the genus (PCR/RFLP) generates a similar banding pattern between the two species (Caldeira et al., 1998), which creates several controversies in their differentiation.

The similarities between *B. tenagophila* and *B. occidentalis* are also numerous, again confusing human differentiation between, and identification of, the two species. For a long time, it was believed that the rates of infection by *S. mansoni* in the state of São Paulo were very low since infected mollusks were not found in the field. However, in 1981, the researcher Lobato Paraense described a new species, *B. occidentalis*, refractory to infection by the parasite, and that was previously confused with *B. tenagophila*, as they were almost indistinguishable by the shell morphology (Paraense, 1981). As a result of this description, in a large area in western Brazil, the distribution map of this last species has been undergoing constant change and readjustment (Scholte et al., 2012; Fernandez et al., 2014; Carvalho et al., 2020).

Traditionally, the DNA barcode technique consists of the amplification and sequencing of a fragment of the *cytochrome* c *oxidase I* (*coi*) gene, using pairs of universal primers – most often those proposed by Folmer et al. in 1994 – and subsequent comparison for specific identification with a universal database (BOLD) (Ratnasingham and Hebert, 2007). Therefore, the main objective of this work was to generate new DNA barcodes for the species of *Biomphalaria* found in Brazil, and to evaluate the use of the *coi* gene as a potential molecular marker for the identification of species of the genus *Biomphalaria*.

One of the main advantages of DNA barcoding is its ability to rapidly and accurately identify species, in the most variable life stages and genders, as well as identifying organisms by parts or pieces and discriminating individuals in a matrix with various mixed species (Casiraghi et al., 2010; Leray and Knowlton, 2015). It is also possible to identify species that are difficult to distinguish based on traditional morphological characteristics (Hebert et al., 2003; Casiraghi et al., 2010).

DNA barcoding is a useful tool for taxonomists, with good cost-effectiveness and the ability to allow non-experts to have access to quick and accurate identifications. This tool can be used in four ways (McManus et al., 2018): screening in collections, based on existing sequences in databases (James et al., 2018); identification of specimens where morphological identification is not possible (immature, partial, damaged or very small individuals), or even to resolve inconsistencies (in dimorphic species where identification is only possible in one sex) (Paéibo, 1990; Hebert et al., 2003; Casiraghi et al., 2010) (Jarne et al., 2010); as a powerful supplementary tool to other forms of identification and thus help in delimiting closely related species phylogenetically (Schindel and

Miller, 2005; Sun et al., 2016); and (Corrêa, 1971) the possibility of discovering previously undescribed species (Hebert et al., 2004). In addition, DNA barcoding is a relatively low-cost and scalable technique, with the potential for high-throughput analysis of large numbers of samples. This makes it particularly useful for large-scale biodiversity surveys and monitoring programs (Hebert et al., 2003; Leray and Knowlton, 2015).

2 Methods

2.1 Construction of the database and illustrative maps

Nucleotide sequences of the partial region of the *coi* gene were obtained from a search of the public GenBank database (https://www.ncbi.nlm.nih.gov/genbank). Additional new sequences were obtained by us through DNA Sanger sequencing of mollusks deposited in the Medical Malacology Collection (Fiocruz-CMM) located at the Instituto René Rachou (IRR – Fiocruz/Minas). These specimens were selected according to the known geographic distribution of each species that occurs within Brazilian territory, prioritizing the type localities.

Data referring to the exact geographic coordinates of each collection point were added to each specimen used from Fiocruz-CMM and for sequences obtained from GenBank for which this information was available. For sequences in the database without any indication of the exact location of collection, the coordinates of the city in which they were collected were assigned.

From the coordinates and cartographic data of the IBGE (2021), a thematic map was constructed to illustrate the geographic distribution of the specimens in this study using the free software QGIS version 3.20 (QGIS, 2021).

2.2 Molecular studies

2.2.1 - DNA extraction, amplification, and purification of the *coi* gene fragment

For specimens obtained from the Fiocruz-CMM collection, a cryopreserved fragment of the cephalopodal region was treated with proteinase K (0,1µg/µL) for at least 12 hours, precisely to degrade the proteins present in the mucus of the mollusk. Next, extraction is carried out with the commercial kit Wizard Genomic DNA Purification according to the manufacturer's instructions

For the amplification of an ~600 bp region of the *coi* gene, the primers LCO1490 (5'-GGTCAACAAATCATAAAGATATTGG-3') and HCO2198 (5'-TAAACTTCAGGGTGACCAAAAAATCA-3') were used (Folmer et al., 1994). All PCR reactions were performed using the Platinum® Taq DNA Polymerase kit (Invitrogen) following the manufacturer's instructions and according to amplification conditions described by Folmer (Folmer et al., 1994).

DNA purification was performed using the *Wizard® SV Gel and PCR Clean-Up System Kit* (Promega), according to the manufacturer's instructions, using the PCR product directly in the purification columns. The purity and concentration of the purified PCR products were verified on a NanoDrop™ 2000 spectrophotometer (ThermoFisher Scientific).

2.2.2 - Sequencing

The samples were sequenced by the Sanger method on an ABI 3730xL automatic sequencer (Applied Biosystems), using the same primers described above for amplification, at the Capillary Electrophoresis DNA Sequencing Platform of the IRR.

2.3 Data analysis

2.3.1 Alignments

The reliability of the nucleotides obtained from sequencing was visually checked and verified using MEGA X software (Kumar et al., 2018) to obtain consensus sequences applying the MUSCLE algorithm (Edgar, 2004). Additionally, CodonCode Aligner© v. 9.0.2 (CodonCode Corporation, 2019) was used to assign *Phred* quality values to each base. The *Phrap* program was then used to construct consensus sequences using the assigned quality values, with a minimum quality value of 20. The resulting consensus sequences were compared with those obtained by visual inspection to eliminate ambiguous bases. The consensus sequences were submitted to Nucleotide BLAST (BLASTn) (Altschul et al., 1990), and the BOLD species identification system (Ratnasingham and Hebert, 2007) (https://www.boldsystems.org/index.php/IDS_OpenIdEngine) to confirm the species identification and detect contamination with other organisms.

Sequences generated for *Biomphalaria* species in this study were combined with previously published sequences obtained from the GenBank database. MAFFT online version 7 (https://mafft.cbrc.jp/alignment/server/ (Katoh et al., 2019),) was employed to align all sequences. The resulting alignment was subsequently exported in FASTA format and visually inspected and edited in MEGA X. After trimming, the resulting sequences had sizes ranging from 517 to 655 bp.

2.3.2 Phylogenetic reconstruction of the partial *coi* gene sequences

For the phylogenetic reconstruction, ModelFinder (Kalyaanamoorthy et al., 2017) implemented in *PhyloSuite* (Zhang et al., 2020) was used to find the evolutionary model that best fit the sequence alignment, according to the Corrected Akaike Information criterion (AICc).

Phylogenetic reconstruction was conducted using either Maximum Likelihood (ML) estimation (Felsenstein, 1981) or Bayesian Inference (BI) (Drummond et al., 2002). A *coi* sequence of the genus *Helisoma* sp. (Swainson, 1840), which also belongs to the Planorbidae family, was selected as an outgroup for tree rooting (GenBank accession number: KM612179.1).

ML trees were inferred using the IQ-TREE software v. 1.6.8 (Nguyen et al., 2015), with the evolutionary model K81u+R3+F for

5000 ultrafast *bootstraps* (Minh et al., 2013) and the Shimodaira-Hasegawa approximate likelihood ratio test (SH-aLRT) (Guindon et al., 2010) to determine the support values of the branches.

For BI the *MrBayes* software v. 3.2.6 (Ronquist et al., 2012) was used, with the evolutionary model HKY+I+G+F previously calculated by *ModelFinder* (Kalyaanamoorthy et al., 2017). Two independent parallel searches (Markov chains) were performed with 10^7 generations (sampled every 1000 generations) and 25% of the initial data were discarded as burn-in.

The ML and BI trees were visualized and edited using the software *FigTree* v. 1.4.4 (Rambaut, 2018), with final editing performed using Inkscape v.1.1 (Inkscape Project, 2021).

2.3.3 Verification of polymorphic sites and genetic divergence between populations

Genetic polymorphism indices were calculated for the partial region of the *coi* gene using the software *DnaSP* v. 6 (Rozas et al., 2017). The following indices of genetic diversity and their standard deviation were calculated: the number and diversity of mitochondrial haplotypes (h, Hd), nucleotide diversity (π) (Nei, 1987), both with and without the Jukes-Cantor correction (Jukes and Cantor, 1969; Nei, 1987; Lynch and Crease, 1990), the average number of differences between nucleotides between pairs of sequences (k) (Tajima, 1983; Nei, 1987). The number of singleton-type and parsimonious informative polymorphic sites were also estimated, in addition to the fixed divergence between populations (Hey, 1991) and nucleotide divergence between populations.

2.3.4 Specimen identification and species delimitation

In order to verify the accuracy of the partial *coi* sequences for the identification of *Biomphalaria* specimens using DNA barcoding methodology, *BOLD Identification Criteria* (thresh-ID) and *Best Close Match* (BCM) analyses were carried out (Meier et al., 2006) using the *ape* v. 5.5 (Paradis and Schliep, 2019) and *spider* v. 1.5.0 (Brown et al., 2012) packages of the R software v. 4.0.5 (R Foundation for Statistical Computing, 2021).

In order to define the barcode gap, the Kimura two-parameter (K2P) model (Tamura et al., 2004) was used to calculate the intraspecific and interspecific distances (Meyer and Paulay, 2005) between the species using the *spider* v. 1.5.0 (Brown et al., 2012) package in the R software v. 4.0.5 (R Foundation for Statistical Computing, 2021).

Additionally, the sequences were clustered/grouped into Operational Taxonomic Units (OTUs), grouping organisms by their similarity, in this case in relation to a genetic marker (Blaxter et al., 2005), using the criteria of four algorithms; *Generalized Mixed Yule-Coalescent* (GMYC) (Reid and Carstens, 2012; Fujisawa and Barraclough, 2013), *Poisson Tree Processes* (bPTP) (Zhang et al., 2013), *Automatic Barcode Gap Discovery* (ABGD) (Puillandre et al., 2012) and *Assemble Species by Automatic Partitioning* (ASAP) (Puillandre et al., 2021).

3 Results

3.1 *coi* sequence database and specimen distribution map

Overall, the molecular data set analyzed consisted of 223 *Biomphalaria* nucleotide sequences, comprised of 83 previously published sequences obtained from GenBank (Supplementary Table 1) and 140 sequences newly-generated in this study (Supplementary Table 2). In addition, a single sequence was selected as an outgroup for phylogenetic analysis (*Helisoma* sp. - KM612179.1). The 11 species and one subspecies from Brazil are represented among the samples obtained, and all type localities are represented among the samples (except for the species *B. kuhniana*). The new sequences obtained in this study were deposited in GenBank (under Accession Numbers MZ778865 - MZ778963) and their IDs are listed in Supplementary Table 2.

Based on the geographic location associated with each sequence, a map was constructed to illustrate the distribution in Central and South America of the specimens used in this study, not including those retrieved from GenBank databases located in Egypt and China (Figure 1).

3.2 Phylogenetic reconstruction of mollusks of the genus *Biomphalaria* using the partial region of the *coi* gene

Phylogenetic inference produced well-supported clades that corresponded to the species studied, except for: (i) *B. cousini*, which formed two distantly-related lineages, one of which clustered with *B. amazonica*; (ii) *B. kuhniana* and *B. straminea*, whose sequences were polyphyletic, but together formed a single well-delimited monophyletic clade, within which the sequences of each of these two taxa were interspersed; (iii) The clades produced with sequences from *B. oligoza* and *B. peregrina* and *B. tenagophila guaibensis* were paraphyletic (Figure 2; Supplementary Figure 1). Since the topology of the trees are very similar, as well as the support values of the branches, we have provided only the representation of the tree from Bayesian Inference (Drummond et al., 2002) (Supplementary Figure 1).

3.3 Polymorphic sites and genetic divergence between *Biomphalaria* populations

Analysis of invariant and variable sites showed that most of the sites are invariant and most of the variable sites are parsimony-informative sites for most species (Table 1). The genetic polymorphism indices were also obtained for partial sequences of the *coi* gene from populations of *Biomphalaria* (Table 2).

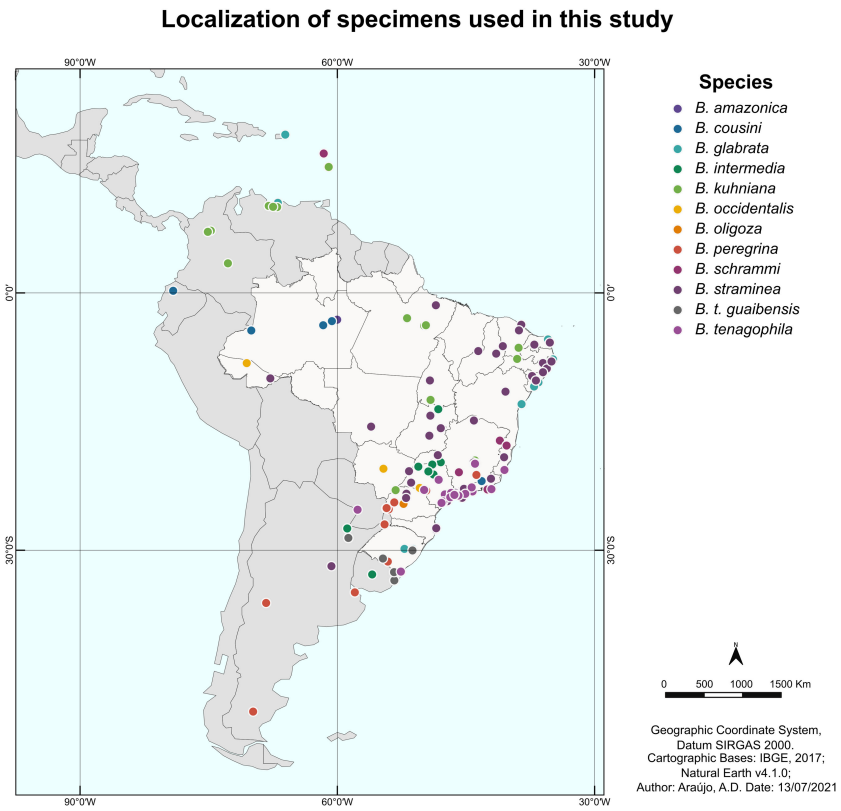

FIGURE 1
Map of Latin America showing the location of the specimens of the genus *Biomphalaria* used in this study. Each point represents the geographic location of a specimen, and the colors represent the different species used in the current study.

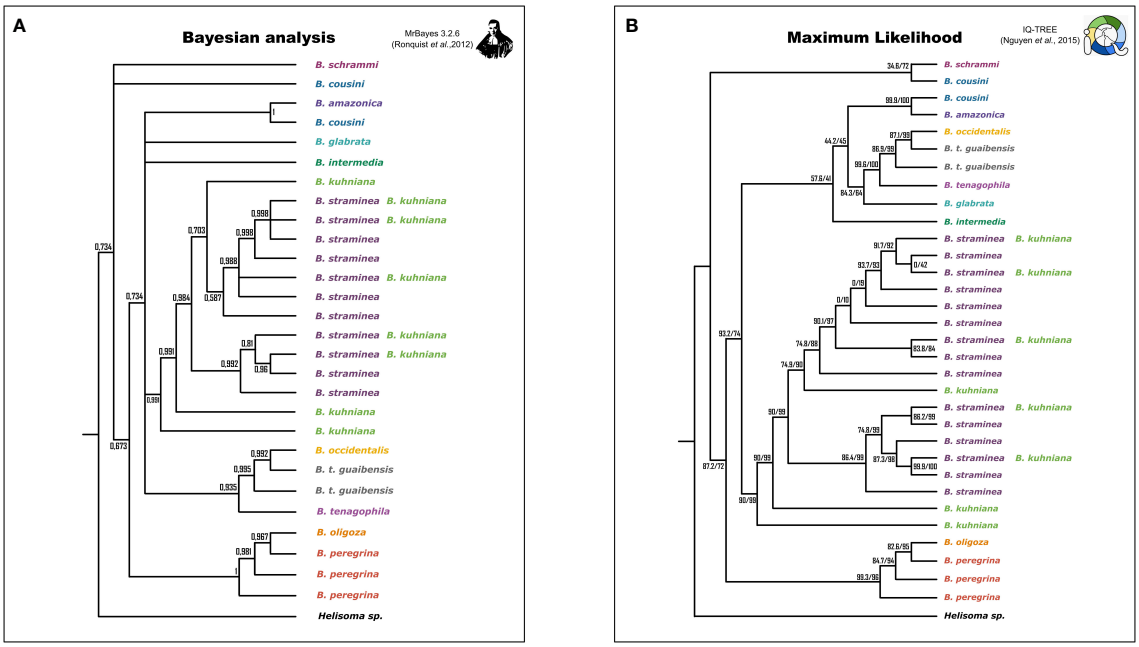

FIGURE 2
Simplified representation of the phylogenetic trees generated by Bayesian Inference (BI) and Maximum Likelihood (ML) criteria. Species are represented by different colors. Trees generated by MrBayes have posterior probability values represented on the branches **(A)**. Trees generated by IQ-TREE have two support values for comparison, ultrafast bootstraps (MINH et al., 2013) and the Shimodaira-Hasegawa test (SH-aLRT) (Guindon et al., 2010) **(B)**.

10.3389/fcimb.2023.1167787

TABLE 1 Polymorphic sites in the partial sequences of the *coi* gene from populations of *Biomphalaria*.

Species	Number of sequences analyzed	Invariant Sites (monomorphic)	Variable Sites (polymorphic)	Singleton type sites	Parsimonious information sites
All	223	312	193	25	168
B. amazonica	2	655	0	0	0
B. cousini	8	498	119	18	101
B. glabrata	22	502	44	12	32
B. intermedia	25	554	60	13	47
B. kuhniana	25	549	65	28	37
B. occidentalis	7	543	7	7	0
B. oligoza	3	586	2	2	0
B. peregrina	14	494	52	30	22
B. schrammi	8	541	60	36	24
B. straminea	70	481	56	15	41
B. t. guaibensis	8	504	13	0	13
B. tenagophila	31	527	22	6	16
B. straminea species complex	120	426	111	28	83
B. tenagophila species complex	46	469	48	7	41

Analysis of invariable and variable sites obtained using the DnaSP v. 6. The table describes the analyzed species, number of analyzed sequences, number of invariant (monomorphic) sites, number of variable (polymorphic) sites, and the numbers of singleton-type and parsimonious informative sites.

The calculated divergence of DNA sequences between populations showed that: (i) there are no fixed differences between the species *B. amazonica* and *B. cousini*, (ii) fixed differences between the species within each of the different species complexes are smaller than those between these species and the other species which are not members of the species complex; and (iii) *B. schrammi* has the greatest number of differences when compared to most of the other species of the genus (Supplementary Figure 2). Also, in order to measure the distance between species, the average number of nucleotide divergences between populations (k) was calculated (Supplementary Figure 3). The greatest nucleotide divergences were observed for *B. cousini* and *B. schrammi*, with the divergence between the two species being the largest observed of the pairwise comparisons. The smallest nucleotide divergences from the pairwise comparisons were between the closest species already reported in the literature; that is, *B. kuhniana* and *B. straminea*, *B. t. guaibensis* and *B. occidentalis*, and *B. peregrina* and *B. oligoza*.

3.4 *Biomphalaria* species delimitation

BOLD Identification Criteria (thresh-ID) and *Best Close Match* (BCM) analyses showed similar results, with *B. tenagophila*, *B. glabrata*, *B. t. guaibensis*, *B. occidentalis*, and *B. oligoza* all showing 100% of the sequences correctly identified. In both analyses, *B. intermedia* had 24 (96%) correctly identified sequences, and one sequence without identification. *Biomphalaria peregrina*, had ten sequences correctly identified (71.4%), and four without identification. For *B. schrammi*, the two analyzes were able to correctly identify only two sequences (25%), and the other six sequences could not be identified. The biggest differences found between the two analyses were in the sequences of the two species *B. straminea* and *B. kuhniana* (Figures 3A, B). For *B. straminea*, using BCM analysis, 46 sequences were considered correct (65.7%), four were considered incorrect (5.7%), 19 were ambiguous (27.1%) and one sequence could not be identified. Using the BOLD analysis, 16 sequences were considered correct (22.9%), 53 were ambiguous (75.7%) and one could not be identified. For *B. kuhniana*, using the BCM analysis, 15 sequences were considered correct (60%), five incorrect (20%), two ambiguous (8%) and three without identification, while using the BOLD analysis, 15 sequences were considered correct (60%), three incorrect (12%), four ambiguous (16%) and three without identification.We calculated intra- and interspecific distances in order to define the barcode gap using the K2P model (Figure 4). The intraspecific distances calculated for all sequences presented a bimodal distribution, while the interspecific distances showed a trimodal distribution (Figure 4). The histograms of pairwise distances of each species (Figure 5) indicated the absence of a barcode gap for specific differentiation of *B. straminea B. kuhniana B. intermedia B. t. guaibensis B. occidentalis B. peregrina* and *B. oligoza*. Of the 223 analyzed sequences, it was possible to calculate the barcode gap for only 102, which corresponds to 45.7% of the analyzed sequences. Thus,

10.3389/fcimb.2023.1167787

TABLE 2 Genetic polymorphism indices in partial sequences of the *COI* gene from populations of *Biomphalaria*.

Groups	Total number of mutations (η)	Total number of haplotypes (h)	Haplotype diversity (Hd)	Standard Deviation of Haplotype Diversity	Nucleotide diversity (π)	Nucleotide diversity (Jukes-Cantor), (π(JC))	Average number in nucleotide diversity (k)
All	273	119	0.987	0.0029	0.07235	0.07707	36.536
B. amazonica	0	1	0	0	0	0	0
B. cousini	126	6	0.929	0.084	0.09609	0.10693	59.286
B. glabrata	45	14	0.948	0.029	0.02331	0.02377	12.727
B. intermedia	66	18	0.977	0.016	0.02635	0.02698	16.180
B. kuhniana	69	20	0.98	0.017	0.02391	0.02438	14.683
B. occidentalis	7	4	0.714	0.181	0.00364	0.00366	2.000
B. oligoza	2	2	0.667	0.314	0.00227	0.00227	1.333
B. peregrina	53	11	0.956	0.045	0.0254	0.02604	13.868
B. schrammi	62	7	0.964	0.077	0.03417	0.03523	20.536
B. straminea	58	31	0.937	0.019	0.01718	0.01748	9.227
B. t. guaibensis	13	3	0.679	0.122	0.0143	0.01454	7.393
B. tenagophila	22	16	0.912	0.033	0.01119	0.01131	6.142
B. straminea species complex	124	58	0.969	0.008	0.03753	0.03896	20.156
B. tenagophila species complex	50	23	0.946	0.016	0.02606	0.02674	13.472

The table describes analyses of the total number of mutations (η), total number of haplotypes (h), haplotype diversity (Hd) and its standard deviation, nucleotide diversity (π), nucleotide diversity (Jukes-Cantor) (π(JC)), and the average number in nucleotide diversity (k) obtained using the software DnaSP v. 6.

58.3% of the analyzed species have a barcode gap, which can be used to delimit them from one another using this methodology.

In the formation of Operational Taxonomic Units (OTU), different clusters/clades were generated for each algorithm used (Table 3). The clusters/clades generated by ABGD, ASAP, and sGMYC were the closest to the current delineation of the species of the *Biomphalaria* genus. Despite the large number of groups created by bPTP, and mGMYC, they were congruent with the geographic locality of the specimens. The ABGD algorithm divided *B. cousini* into three different groups, with one of them being shared with the *B. amazonica* sequences, as inferred by phylogenetic reconstruction. *Biomphalaria schrammi* and *B. peregrina* were also divided into two groups, the latter sharing a cluster with the *B. oligoza* sequences. The sequences of *B. kuhniana* and *B. straminea* were pooled, as well as *B. occidentalis*, *B. tenagophila*, and *B. t. guaibensis*. ASAP was the algorithm that generated the least number of clusters. However, *B. cousini* was partitioned into three different clusters by the ASAP method, with the same division observed for the ABGD algorithm. These latter two methods, therefore, generated groups, each comprised of multiple species, as follows. ABGD: (i) *B. amazonica* and *B. cousini*, (ii) *B. kuhniana* and *B. straminea*, (iii) *B. oligoza* and *B. peregrina*, and (iv) all three species of the *Biomphalaria tenagophila* complex (*B. occidentalis*, *B. tenagophila*, and *B. t. guaibensis*). ASAP: (i) *B. amazonica*, *B. cousini*, *B. intermedia*, *B. kuhniana*, and *B. straminea*, (ii) *B. oligoza* and *B. peregrina*, and (iii) all three species of the *Biomphalaria tenagophila* complex. Using the sGMYC algorithm, 14 groups were formed, as follows. *Biomphalaria cousini* was divided into two groups, with one of them shared with *B. schrammi* sequences, while the other group was shared with a single large group comprised of *B. amazonica*, *B. glabrata*, *B. intermedia*, *B. occidentalis*, *B. tenagophila* and *B. t. guaibensis*. *Biomphalaria kuhniana* was divided into six different groups, sharing four of them with *B. straminea*, which was itself divided into eight groups (Supplementary Figure 1).

4 Discussion

The correct identification of mollusks that are the intermediate hosts of *Schistosoma* is a fundamental prerequisite for understanding the epidemiology of schistosomiasis and mobilizing efforts for disease surveillance and control (Rollinson et al., 2009). The Fiocruz-CMM combines both classical taxonomy through (i) comparison of morphological characters of the shell, as well as male and female reproductive organs (Lobato Paraense and Deslandes, 1958a; Lobato Paraense and Deslandes, 1958b; Paraense, 1975; Paraense, 1981; Paraense, 1984; Paraense, 1988; Paraense, 1990; Paraense et al., 1992; Estrada et al., 2006), and (ii) use of molecular tools, such as PCR-RFLP of the internal transcribed spacer (*ITS*) of the *ribosomal RNA* gene, to distinguish *Biomphalaria* species (Vidigal et al., 2000; Teodoro et al., 2010). Despite this, some inconsistencies between the

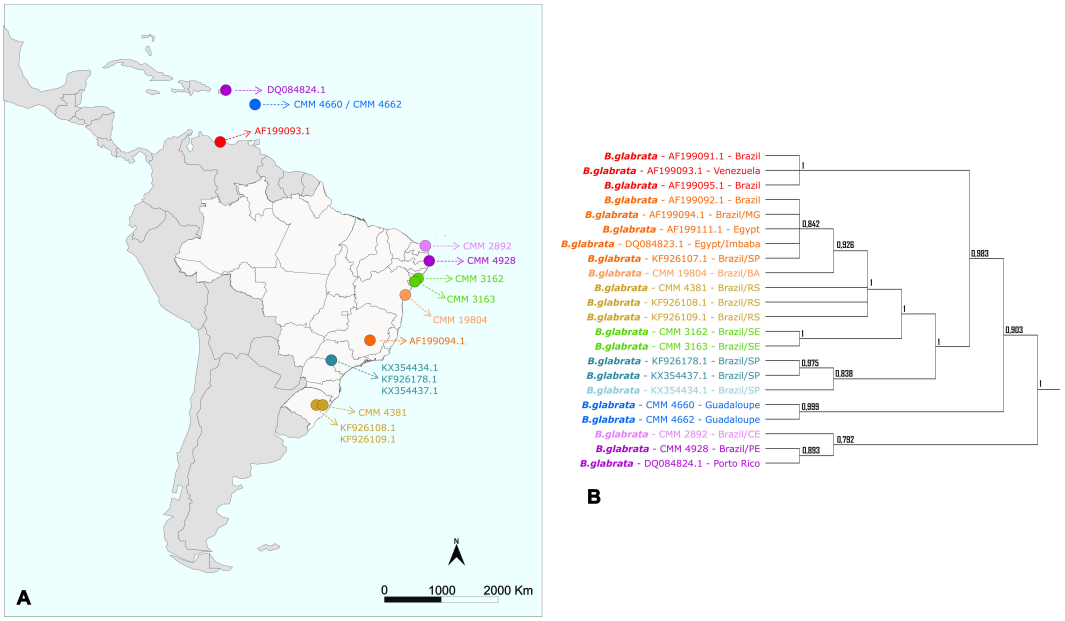

FIGURE 3
Number of sequences classified by the *Best Close Match* (BCM) and *BOLD Identification Criteria*. The bar graphs illustrate the absolute number of sequences identified using two different criteria: **(A)** *Best Close Match* (Meier et al., 2006) and **(B)** *BOLD Identification Criteria*, using the R software (version 4.0.5) and the package *spider* (version 1.5.0). The colors represent the four possible outcomes: correct (green), incorrect (red), ambiguous (yellow), and no identification (blue).

results of the identifications have already been reported (Aguiar-Silva et al., 2014). This highlights the importance of combining methodologies in the taxonomy of mollusks of the genus *Biomphalaria* for species identification following the Iterative taxonomy process, in order to refine and define the boundaries between species using multiple different lines of evidence (Yeates et al., 2011).

This study confirmed that the species identification within the genus *Biomphalaria* is not a simple task, a fact that had already been mentioned by Doctor Lobato Paraense, in the 1960s (Paraense and Deslandes, 1959). The anatomy of the reproductive tract has been an effective tool in mollusk identification within the genus (Paraense and Deslandes, 1959). However, a resolution limit is reached for groups of closely related species (Paraense, 1981;

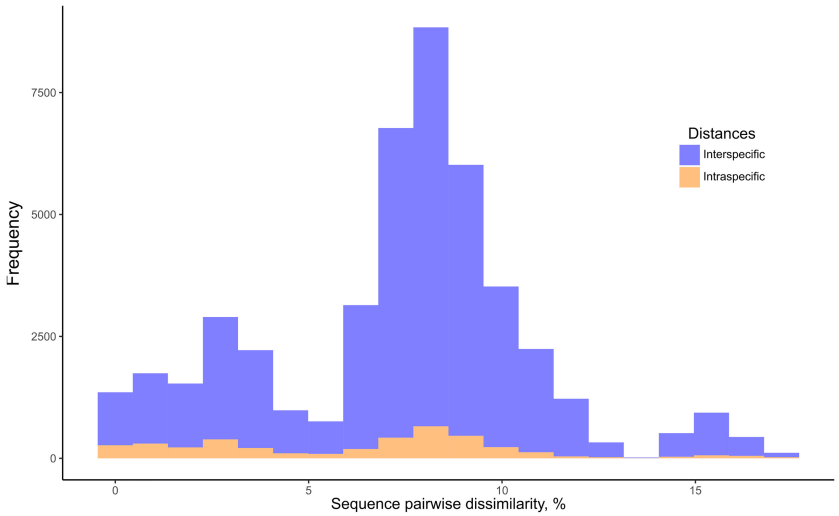

FIGURE 4
Frequency distribution of intraspecific and interspecific distances of *Biomphalaria* partial *coi* sequences. Histogram of intraspecific (orange) and interspecific (blue) distances based on the *Biomphalaria* partial *coi* sequences. Pairwise K2P distances were expressed as percentage dissimilarity (K2P * 100).

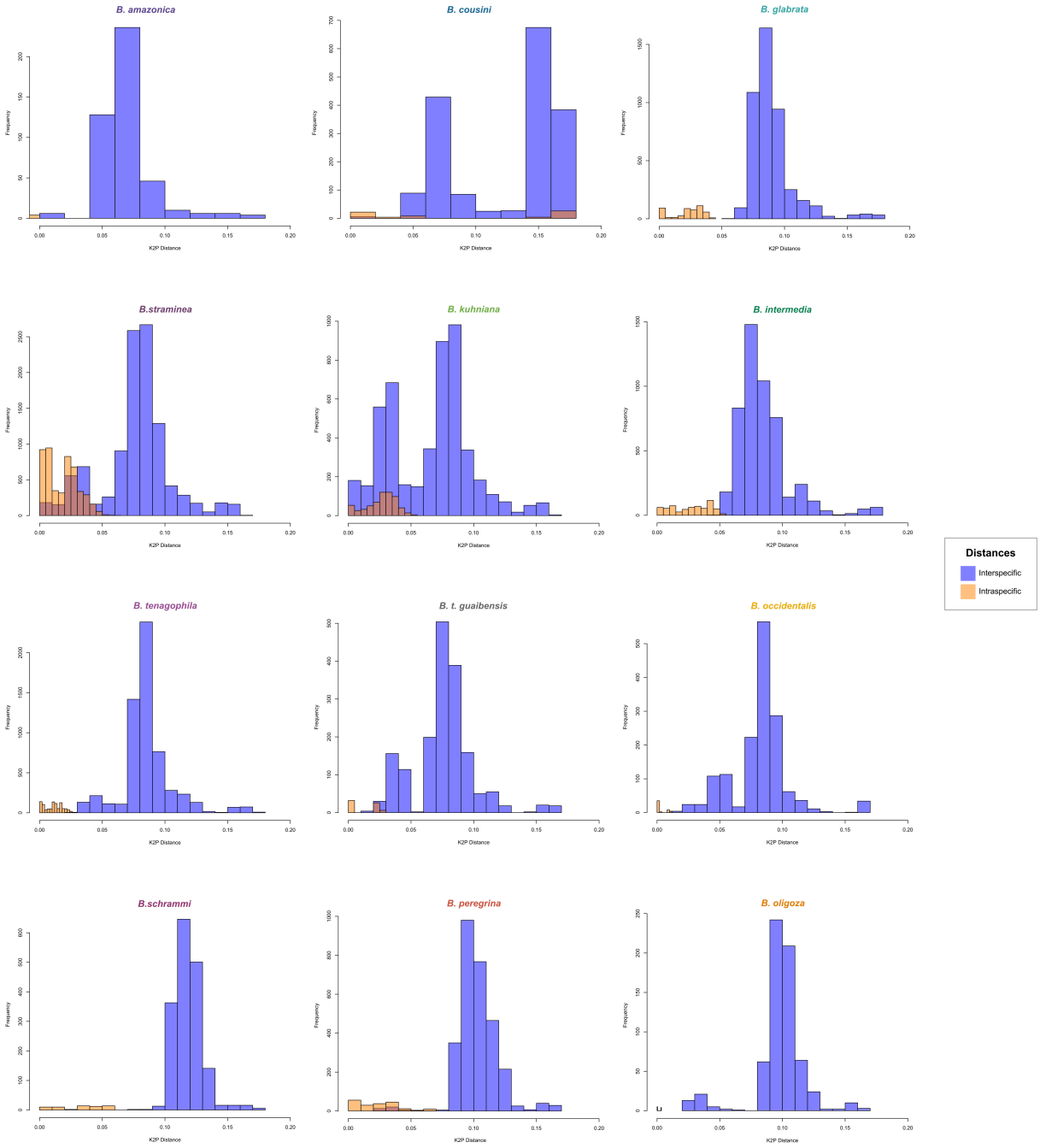

FIGURE 5
Frequency distribution of intraspecific and interspecific distances of *Biomphalaria* partial *coi* sequences according to species. Histogram of intraspecific (orange) and interspecific (blue) distances based on the *Biomphalaria coi* partial sequences. Pairwise distances were expressed as percentage dissimilarity for each species: *B. amazonica*, *B. cousini*, *B. glabrata*, *B. straminea*, *B. kuhniana*, *B. intermedia*, *B. tenagophila*, *B. t. guaibensis*, *B. occidentalis*, *B. schrammi*, *B. peregrina*, and *B. oligoza*.

Paraense, 1988), such as the *B. straminea* complex, *B. peregrina*/*B. oligoza*, and the *B. tenagophila* complex, as a consequence of intraspecific variation or incomplete variation, incomplete speciation, or the "gray zone of speciation" that exists between species due to recent evolution (De Queiroz, 2007; Jarne et al., 2011).

Biomphalaria straminea is a species that originated from the northern region of South America and has been expanding its habitat throughout Brazil and surrounding countries, mainly due to human activity and its high capacity to survive long periods of drought combined with its high fertility (Wang et al., 2013; Attwood et al., 2015). It is known that this species was recently introduced into both China (Meier Brook, 1975; Dudgeon and Yipp, 1983; Tang, 1983; Yipp, 1990; Yang et al., 2018), and the Caribbean (Paraense et al., 1981; Pointier et al., 1993) from strains originating from South America. The reconstructed phylogenies in this work

TABLE 3 Number of Operational Taxonomic Units (OTUs) according to *Biomphalaria* species.

Species	ABGD	ASAP	sGMYC	mGMYC	bPTP
B. amazonica	1	1	1	1	2
B. cousini	3	3	2	5	6
B. glabrata	1	1	1	15	10
B. intermedia	1	1	1	15	16
B. kuhniana	1	1	6	20	20
B. occidentalis	1	1	1	5	1
B. oligoza	1	1	1	2	2
B. peregrina	2	1	1	10	10
B. schrammi	2	1	1	4	7
B. straminea	1	1	8	50	26
B. tenagophila	1	1	1	24	17
B. t. guaibensis	1	1	1	6	3
TOTAL	**11**	**7**	**14**	**153**	**118**

Table with the number of clusters generated by the species delimitation algorithms used in this study. The table shows the absolute number of clusters by species and overall for the entire data set of 223 sequences.

reflect this introduction, with northeastern Brazilian specimens grouped with specimens from China, and specimens from the Caribbean grouped with specimens from northern Brazil, Venezuela, and Colombia.

In the reconstructed phylogeny, the *B. straminea* complex indicated a low resolution between *B. kuhniana* and *B. straminea*, which formed a polyphyletic clade. The same was observed between *B. cousini* and *B. amazonica*. This polyphyly may be the result of clades with recent evolution or imperfect taxonomy, in which not all the genus species diversity has been documented (Meyer and Paulay, 2005). Furthermore, due to the proximity between the species, there is a possibility that there is some level of hybridization between them (DeJong et al., 2001; Teodoro et al., 2011). Mitochondrial gene flow *via* hybridization has already been reported for several groups of animals, including planorbid mollusks (Mello-Silva et al., 1998), although it is not well understood. Hybridization is one of the sources of non-monophyly between clades of different groups of living beings, causing introgression (Anderson and Hubricht, 1938).

The clade representing the *B. glabrata* species is monophyletic and well supported (100%) in both the BI and ML analyses, with subdivision into at least five different groups. This fact can be explained by the Refuge Theory (Haffer, 1969), which suggests that climatic oscillations in the Pleistocene period may have been responsible for the habitat fragmentation and consequent geographic separation of *B. glabrata* populations, forming genetically-distinct clades (Dejong et al., 2003).

The phylogenetic trees inferred in this study corroborate what was indicated by previous studies that: (i) the Greater Antilles – Cuba, Hispaniola (Haiti and the Dominican Republic), Jamaica, and Puerto Rico – were colonized very early in *B. glabrata* evolution; (ii) specimens from southeastern Brazil were probably introduced into northeastern Brazil; and (iii) the Lesser Antilles and Venezuela appear to have been colonized by *B. glabrata* more recently, probably due to deforestation and human occupation (Mavárez et al., 2002; Dejong et al., 2003). Furthermore, as reported in 1998, our work also presents evidence of colonization of the South Region of Brazil with lineages from the North Region, probably related to recent human dispersal (Figure 6) (Carvalho O dos et al., 1998).

Of the 223 sequences used in this study, the barcode gap was successfully calculated for 102 (45.7%). However, of the 12 taxa studied, only seven (58.3%) can be differentiated from each other using DNA barcoding methodology. Among the invertebrate host species of *S. mansoni* in Brazil, only *B. straminea* could not be differentiated using this methodology, due to its genetic proximity to *B. kuhniana*. This result is promising regarding the use of DNA barcoding for taxonomy by the schistosomiasis epidemiology service in Brazil. In addition, due to the resolution observed using the *Best Close Match* (BCM) and *BOLD Identification Criteria* analyses, DNA barcoding methodology has a great potential to provide greater objectivity for mollusk identification, and can be used for the verification of identification performed by other methods (Ohlweiler et al., 2020). For species of the *B. tenagophila* complex, despite the proximity between the taxa, the DNA sequences were correctly identified by DNA barcoding methodology, with the analyses performed by *BOLD Identification Criteria* and *BCM*. Other authors also successfully separated the species of this complex, using DNA barcoding and phylogenetics, with high support values associated with each of the clades, and concluded that, for this species complex, molecular data may be more informative for species discrimination than morphology (Ohlweiler et al., 2020).

For some taxa, including *B. kuhniana* and *B. straminea*, the intraspecific divergence of the *coi* gene often surpassed the interspecific divergence, making coalescence methods for the formation of Operational Taxonomic Units (OTUs) inadequate

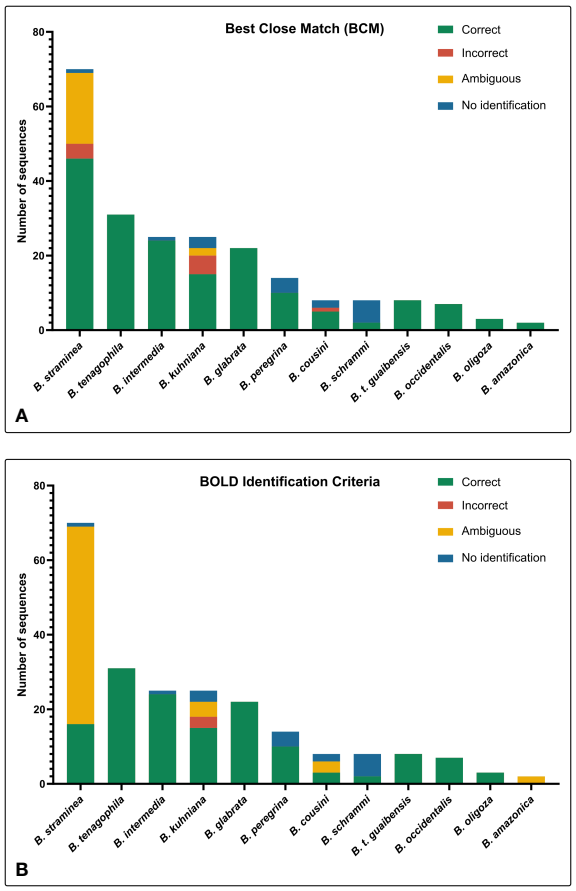

FIGURE 6
Distribution map and tree generated by Bayesian Inference of the *Biomphalaria glabrata* specimens used in this study. **(A)** Map with the geographical distribution of *Biomphalaria* specimens in Latin America. **(B)** Simplified phylogenetic tree obtained by Bayesian Inference (BI). The colors represent the large groups separated by the phylogeny of the species.

for species delimitation. We observed the formation of many clusters within each species, some of them with only one sequence, others with sequences from different species within the same cluster, an artifact of the high variability observed for the *coi* gene. The use of nuclear markers with lower rates of evolution can be an alternative for the delimitation of species using these approaches.

The cluster analyses using species delimitation algorithms showed that the genetic divergence within populations was significant enough to generate substructuring within clades and differentiated clusters, which was also observed by other authors (Palasio et al., 2017). However, the genetic diversity observed among the species was not reflected in the morphological characters used in the classical taxonomy for distinguishing between species. Thus, it is evident that these morphological traits do not present enough characteristics to reflect the biodiversity of *Biomphalaria* in nature. The origin of such biodiversity inside the genus in South America may be a reflection of tropical forest fragmentation, which can cause speciation by allopatry result of the formation of distinct and isolated environments in recurrent episodes of vicariance (Colinvaux, 1987). This fragmentation of habitats has been substantially exacerbated by human intervention, particularly through the destruction of natural habitats through deforestation. (Barnosky et al., 2011).

The analysis of the variable sites revealed that *B. cousini* is the taxon with the highest number of polymorphic sites among the evaluated sequences. The number of polymorphic sites within the population indicates the intrapopulation genetic variability (Caldeira et al., 2001), showing that among all the analyzed species, *B. cousini* is the one that exhibits the greatest genetic diversity. Comparison of K2P genetic distances (Tamura et al., 2004) between the *B. cousini* sequences also showed values larger than 18%, values greater than the distance between this group and any other taxon in this study. One of the possible reasons for the diversity within this species may be the isolation of populations caused by the geographic barrier imposed by the Amazon rainforest, which also ends up preventing the dissemination of species from Venezuela, for example, *Biomphalaria prona* (Dejong et al., 2003; Jarne et al., 2011). Another relevant point for this discussion is that hybridization between *B. cousini* and *B. amazonica* has already been observed (Teodoro et al., 2011), which may have caused this high diversity among specimens of *B. cousini* and the proximity to *B. amazonica*, a fact already reported by Dr. Paraense in the description of the species, in 1966 (Paraense, 1966). These data may encourage discussion about the possibility of the existence of cryptic species within the currently recognized taxon *B. cousini*.

The systematics of mollusks is very nebulous and undergoes recurrent modifications (Wanninger and Wollesen, 2019). As observed for mussels of the genus *Pecten* (Canapa et al., 2000), this study showed that *B. straminea* and *B. kuhniana* are very similar, with small genetic distances, a fact that may raise the question of whether both may belong to the same species or are undergoing a recent speciation event.

5 Conclusions

Although the use of molecular data does not guarantee correct phylogenetic trees, and the study involving only one mitochondrial molecular marker is far from ideal and may not reliably reflect the evolution of the genus, this study demonstrated that the use of a region of the *coi* gene in the reconstruction of the phylogeny of the *Biomphalaria* genus can be an alternative to understanding the evolution and dispersion of the species. Despite the relationships established here, it must be considered that associating a single mitochondrial gene to the taxonomic history of a species is impossible, highlighting the need to expand studies with other molecular markers. The usefulness of the DNA barcoding methodology for mollusks of the genus *Biomphalaria* is well-suited to providing a better representation of this genus in public databases and the use of integrative methodologies for the correct identification of mollusks. This work contributed significantly to the number of partial sequences of the *coi* gene deposited in public databases, thus allowing a greater number of possible comparisons in future studies. Additionally, it was possible to obtain the correct delimitation of most

of the *Biomphalaria* species whose occurrence is reported in Brazil using DNA barcoding and clustering/phylogenetic algorithms. Despite the high intraspecific diversity observed, two of the three species that act as intermediate hosts for *S. mansoni* in Brazil were successfully distinguished using the DNA barcoding technique based on the *coi* gene fragment. Further studies using both mitochondrial and nuclear markers are essential to elucidate the relationships between two of the most closely-related groups: *B. kuhniana* and *B. straminea*, and *B. cousini* and *B. amazonica*.

Data availability statement

The datasets presented in this study can be found in online repositories. The names of the repository/repositories and accession number(s) can be found in the article/Supplementary Material.

Author contributions

Conceptualization: RC, OC. Methodology & Investigation: AA, SG, RC. Formal analysis: AA, SG, RC. Resources: RC. Writing - original draft: AA. Writing – editing: AA, RC, SG, OC Writing – review: AA, RC, SG, OC. Visualisation: AA. Supervision: RC, SG. Project Administration: RC, SG. Funding acquisition: RC. All authors contributed to the article and approved the submitted version.

Funding

This work was funded by Fapemig (APQ-01533-22), Fiocruz (Oswaldo Cruz Foundation) and by the Coordenação de Aperfeiçoamento de Pessoal de Nível Superior–Brasil (CAPES) – Finance Code 001.

Acknowledgments

The authors would like to thank: the Medical Malacology Collection (Fiocruz-CMM, Instituto René Rachou, Oswaldo Cruz Foundation, Brazil) for providing samples; the Program for Technological Development in Tools for Health-PDTIS/FIOCRUZ for the use of its facilities; the Programa de Pós-graduação em Ciências da Saúde of the René Rachou Institute-Fiocruz; and Dr. Luke Baton for revising and commenting upon the manuscript.

Conflict of interest

The authors declare that the research was conducted in the absence of any commercial or financial relationships that could be construed as a potential conflict of interest.

Publisher's note

All claims expressed in this article are solely those of the authors and do not necessarily represent those of their affiliated organizations, or those of the publisher, the editors and the reviewers. Any product that may be evaluated in this article, or claim that may be made by its manufacturer, is not guaranteed or endorsed by the publisher.

Supplementary material

The Supplementary Material for this article can be found online at: https://www.frontiersin.org/articles/10.3389/fcimb.2023.1167787/full#supplementary-material

References

Aguiar-Silva, C., Mendonça, C. L., da Cunha Kellis Pinheiro, P., Mesquita, S., dos Carvalho, O., and Caldeira, R. (2014). Evaluation and updating of the Medical Malacology Collection (Fiocruz-CMM) using molecular taxonomy. *Springerplus* 3, 446. doi: 10.1186/2193-1801-3-446

Altschul, S. F., Gish, W., Miller, W., Myers, E. W., and Lipman, D. J. (1990). Basic Local Alignment Search Tool. *J. Mol. Biol.* 215, 403–410. doi: 10.1016/S0022-2836(05)80360-2

Anderson, E., and Hubricht, L. (1938). Hybridization in tradescantia. III. the evidence for introgressive hybridization. *Am. J. Bot.* 25, 396–402. doi: 10.1002/j.1537-2197.1938.tb09237.x

Attwood, S. W., Huo, G.-N., and Qiu, J.-W. (2015). Update on the distribution and phylogenetics of *Biomphalaria* (Gastropoda: Planorbidae) populations in Guangdong province, China. *Acta Trop.* 141, 258–270. doi: 10.1016/j.actatropica.2014.04.032

Inkscape Project (2021) *Inkscape project*. Available at: https://inkscape.org.

Barnosky, A. D., Matzke, N., Tomiya, S., Wogan, G., Swartz, B., Quental, T. B., et al. (2011). Has the earth's sixth mass extinction already arrived? *Nature* 471, 51–57. doi: 10.1038/nature09678

Blaxter, M., Mann, J., Chapman, T., Thomas, F., Whitton, C., Floyd, R., et al. (2005). Defining operational taxonomic units using DNA barcode data. *Philos. Trans. R Soc. B Biol. Sci.* 360, 1935–1943. doi: 10.1098/rstb.2005.1725

Brown, S. D. J., Collins, R. A., Boyer, S., Lefort, M., Malumbres-Olarte, J., Vink, C. J., et al. (2012). Spider: An R package for the analysis of species identity and evolution, with particular reference to DNA barcoding. *Mol. Ecol. Resour* 12, 562–565. doi: 10.1111/j.1755-0998.2011.03108.x

Cabrera, F., Martinez, S., and Norbis, W. (2016). Recognition of *Biomphalaria* species (Gastropoda: Planorbidae) using the spiral growth variability, with description of a new fossil species. *Nautilus (Philadelphia)* 130, 5–12.

Caldeira, R. L., Vidigal, T. H., Matinella, L., Simpson, A. J., and Carvalho, O. S. (2000). Identification of planorbids from Venezuela by polymerase chain reaction amplification and restriction fragment length polymorphism of internal transcriber spacer of the RNA ribosomal gene. *Mem Inst Oswaldo Cruz* 95, 171–177. doi: 10.1590/S0074-02762000000200007

Caldeira, R. L., Vidigal, T. H. D. A., Paulinelli, S. T., Simpson, A. J. G., and Carvalho, O. S. (1998). Molecular identification of similar species of the genus *Biomphalaria* (Mollusca: Planorbidae) determined by a polymerase chain reaction-restriction fragment length polymorphism. *Mem Inst Oswaldo Cruz* 93 (SUPPL), 219–225. doi: 10.1590/S0074-02761998000700039

Caldeira, R. L., Vidigal, T. H. D. A., Simpson, A. J. G., and Carvalho, O. S. (2001). Genetic variability in Brazilian populations of *Biomphalaria straminea* complex detected by simple sequence repeat anchored polymerase chain reaction amplification. *Mem Inst Oswaldo Cruz* 96, 535–544. doi: 10.1590/S0074-02762001000400016

Canapa, A., Barucca, M., Marinelli, A., and Olmo, E. (2000). Molecular data from the 16S rRNA gene for the phylogeny of Pectinidae (Mollusca: Bivalvia). *J. Mol. Evol.* 50, 93–97. doi: 10.1007/s002399910010

Carvalho, O. S., Mendonça, C. L. F., Teles, H. M. S., Finau, J., Caldeira, R. L., Scholte, R. G. C., et al. (2020). Moluscos hospedeiros intermediários de *Schistosoma mansoni* do Brasil. *Belo Horizonte/Instituto Renè Rachou/Fiocruz*.

Carvalho O dos, S., Nunes, I. M., and Caldeira, R. L. (1998). First report of *Biomphalaria glabrata* in the state of Rio Grande do Sul, Brazil. *Mem Inst Oswaldo Cruz* 93, 39–40. doi: 10.1590/S0074-02761998000100008

Casiraghi, M., Labra, M., Ferri, E., Galimberti, A., and Mattia, F. (2010). DNA Barcoding: theoretical aspects and practical applications. *Tools Identifying Biodivers Prog. Probl*, 269–273.

CodonCode Corporation (2019) *Sequence assembly and alignment software - CodonCode*. Available at: https://www.codoncode.com/index.htm (Accessed July 17, 2021).

Colinvaux, P. (1987). Amazon Diversity in light of the paleoecological record. *Quat Sci. Rev.* 6, 93–114. doi: 10.1016/0277-3791(87)90028-X

Corrêa, L. R. (1971). Susceptibility of *Biomphalaria amazonica* to infection with two strains of *Schistosoma mansoni*. *Rev. Inst Med. Trop. Sao Paulo* 13, 387–390.

DeJong, R. J., Morgan, J. A. T., Paraense, W. L., Pointier, J.-P., Amarista, M., Ayeh-Kumi, P. F. K., et al. (2001). Evolutionary relationships and biogeography of *Biomphalaria* (Gastropoda: Planorbidae) with implications regarding its role as host of the human bloodfluke, *Schistosoma mansoni*. *Mol. Biol. Evol.* 18, 2225–2239. doi: 10.1093/oxfordjournals.molbev.a003769

Dejong, R. J., Morgan, J. A. T., Wilson, W. D., Al-Jaser, M. H., Appleton, C. C., Coulibaly, G., et al. (2003). Phylogeography of *Biomphalaria glabrata* and *B. pfeifferi*, important intermediate hosts of *Schistosoma mansoni* in the new and old world tropics. *Mol. Ecol.* 12, 3041–3056. doi: 10.1046/j.1365-294X.2003.01977.x

De Queiroz, K. (2007). Species concepts and species delimitation. *Syst. Biol.* 56, 879–886. doi: 10.1080/10635150701701083

Drummond, A. J., Nicholls, G. K., Rodrigo, A. G., and Solomon, W. (2002). Estimating mutation parameters, population history and genealogy simultaneously from temporally spaced sequence data. *Genetics* 161 (1307 LP), 1320. doi: 10.1093/genetics/161.3.1307

Dudgeon, D., and Yipp, M. W. (1983). A report on the gastropod fauna of aquarium fish farms in Hong Kong, with special reference to an introduced human schistosome host species, *Biomphalaria straminea* (Pulmonata: Planorbidae). *Malacol Rev.* 16, 93–94.

Edgar, R. C. (2004). MUSCLE: multiple sequence alignment with high accuracy and high throughput. *Nucleic Acids Res.* 32, 1792–1797. doi: 10.1093/nar/gkh340

Estrada, V. E., Velásquez, L. E., Caldeira, R. L., Bejarano, E. E., Rojas, W., and Carvalho, O. S. (2006). Phylogenetics of south American *Biomphalaria* and description of a new species (Gastropoda: Planorbidae). *J. Molluscan Stud.* 72, 221–228. doi: 10.1093/mollus/eyl003

Felsenstein, J. (1981). Evolutionary trees from DNA sequences: A maximum likelihood approach. *J. Mol. Evol.* 17, 368–376. doi: 10.1007/BF01734359

Fernandez, M. A., de Mattos, A. C., da Silva, E. F., dos Santos, S. B., and Thiengo, S. C. (2014). A malacological survey in the Manso Power Plant, state of Mato Grosso, Brazil: new records of freshwater snails, including transmitters of schistosomiasis and exotic species. *Rev. Soc. Bras. Med. Trop.* 47, 498–506. doi: 10.1590/0037-8682-0138-2014

Folmer, O., Black, M., Hoeh, W., Lutz, R., and Vrijenhoek, R. (1994). DNA Primers for amplification of mitochondrial cytochrome c oxidase subunit I from diverse metazoan invertebrates. *Mol. Mar. Biol. Biotechnol.* 3, 294–299. doi: 10.1071/ZO9660275

Fujisawa, T., and Barraclough, T. G. (2013). Delimiting species using single-locus data and the generalized mixed Yule coalescent approach: A revised method and evaluation on simulated data sets. *Syst. Biol.* 62, 707–724. doi: 10.1093/sysbio/syt033

Guindon, S., Dufayard, J.-F., Lefort, V., Anisimova, M., Hordijk, W., and Gascuel, O. (2010). New algorithms and methods to estimate maximum-likelihood phylogenies: Assessing the performance of PhyML 3.0. *Syst. Biol.* 59, 307–321. doi: 10.1093/sysbio/syq010

Haffer, J. (1969). Speciation in Amazonian forest birds. *Science* 165, 131–137. doi: 10.1126/science.165.3889.131

Hebert, P. D. N., Cywinska, A., Ball, S. L., and DeWaard, J. R. (2003). Biological identifications through DNA barcodes. *Proc. R Soc. B Biol. Sci.* 270, 313–321. doi: 10.1098/rspb.2002.2218

Hebert, P. D. N., Penton, E. H., Burns, J. M., Janzen, D. H., and Hallwachs, W. (2004). Ten species in one: DNA barcoding reveals cryptic species in the neotropical skipper butterfly astraptes fulgerator. *Proc. Natl. Acad. Sci.* 101, 14812–14817. doi: 10.1073/pnas.0406166101

Hey, J. (1991). The structure of genealogies and the distribution of fixed differences between DNA sequence samples from natural populations. *Genetics* 128, 831–840. doi: 10.1093/genetics/128.4.831

IBGE (2021). Available at: https://www.ibge.gov.br/geociencias/downloads-geociencias.html (Accessed July 16, 2021).

James, S. L., Abate, D., Abate, K. H., Abay, S. M., Abbafati, C., Abbasi, N., et al. (2018). Global, regional, and national incidence, prevalence, and years lived with disability for 354 diseases and injuries for 195 countries and territories, 1990-2017: A systematic analysis for the global burden of disease study 2017. *Lancet* 392, 1789–1858. doi: 10.1016/S0140-6736(18)32279-7

Jarne, P., David, P., Pointier, J.-P., and Koene, J. M. (2010). "Basommatophoran gastropods," in *The evolution of primary sexual characters in animals*. Ed. AC-AJL Leonard (Oxforf: Oxford University press), 173–196.

Jarne, P., Pointier, J.-P., and David, P. (2011). "Biosystematics of *Biomphalaria* spp. with an emphasis on *Biomphalaria glabrata*," in *Biomphalaria snails and larval trematodes* (New York, NY: Springer New York), 1–32. doi: 10.1007/978-1-4419-7028-2_1

Jukes, T. H., and Cantor, C. R. (1969). Evolution of protein molecules. *Mamm. Protein Metab.*, 21–132. doi: 10.1016/B978-1-4832-3211-9.50009-7

Kaesler, R. L., and Parodiz, J. J. (1970). The tertiary non-marine Mollusca of South America. *Syst. Zool* 19, 306. doi: 10.2307/2412214

Kalyaanamoorthy, S., Minh, B. Q., Wong, T. K. F., von Haeseler, A., and Jermiin, L. S. (2017). ModelFinder: fast model selection for accurate phylogenetic estimates. *Nat. Methods* 14, 587–589. doi: 10.1038/nmeth.4285

Katoh, K., Rozewicki, J., and Yamada, K. D. (2019). MAFFT online service: multiple sequence alignment, interactive sequence choice and visualization. *Brief Bioinform.* 20, 1160–1166. doi: 10.1093/bib/bbx108

Kumar, S., Stecher, G., Li, M., Knyaz, C., and Tamura, K. (2018). MEGA X: Molecular evolutionary genetics analysis across computing platforms. *Mol. Biol. Evol.* 35, 1547–1549. doi: 10.1093/molbev/msy096

Leray, M., and Knowlton, N. (2015). DNA Barcoding and metabarcoding of standardized samples reveal patterns of marine benthic diversity. *Proc. Natl. Acad. Sci.* 112, 2076–2081. doi: 10.1073/pnas.1424997112

Lobato Paraense, W., and Deslandes, N. (1958a). Observations on *Taphius havanensis* (Pulmonata, planorbidae). *Rev. Bras. Biol.* 18, 87–91.

Lobato Paraense, W., and Deslandes, N. (1958b). *Taphius pronus* (Martens, 1873) (Pulmonata, planorbidae). *Rev. Bras. Biol.* 18, 367–373.

Lynch, M., and Crease, T. J. (1990). The analysis of population survey data on DNA sequence variation. *Mol. Biol. Evol.* 7, 377–394.

Mavárez, J., Amarista, M., Pointier, J.-P., and Jarne, P. (2002). Fine-scale population structure and dispersal in *Biomphalaria glabrata*, the intermediate snail host of *Schistosoma mansoni*, in Venezuela. *Mol. Ecol.* 11, 879–889. doi: 10.1046/j.1365-294X.2002.01486.x

McManus, D. P., Dunne, D. W., Sacko, M., Utzinger, J., Vennervald, B. J., and Zhou, X.-N. (2018). Schistosomiasis. *Nat. Rev. Dis. Prim* 4, 13. doi: 10.1038/s41572-018-0013-8

Meier, R., Shiyang, K., Vaidya, G., and Ng, P. K. L. (2006). DNA Barcoding and taxonomy in diptera: A tale of high intraspecific variability and low identification success. *Syst. Biol.* 55, 715–728. doi: 10.1080/10635150600969864

Meier Brook, C. (1975). A snail intermediate host of *Schistosoma mansoni* introduced into Hong Kong. *Bull. World Health Organ* 51, 661.

Mello-Silva, C. C., Grault, C. E., da, C. V. A., and Barbosa, F. S. (1998). Possible hybridization of Brazilian planorbid snails and its importance in population dynamics. *Mem Inst Oswaldo Cruz* 93, 227–232. doi: 10.1590/S0074-02761998000700040

Meyer, C. P., and Paulay, G. (2005). DNA Barcoding: Error rates based on comprehensive sampling. *PloS Biol.* 3, e422. doi: 10.1371/journal.pbio.0030422

Minh, B. Q., Nguyen, M. A. T., and von Haeseler, A. (2013). Ultrafast approximation for phylogenetic bootstrap. *Mol. Biol. Evol.* 30, 1188–1195. doi: 10.1093/molbev/mst024

Nei, M. (1987). *Molecular evolutionary genetics*. (New York: Columbia University Press). doi: 10.7312/nei-92038

Nguyen, L.-T., Schmidt, H. A., von Haeseler, A., and Minh, B. Q. (2015). IQ-TREE: A fast and effective stochastic algorithm for estimating maximum-likelihood phylogenies. *Mol. Biol. Evol.* 32, 268–274. doi: 10.1093/molbev/msu300

Ohlweiler, F. P., Rossignoli T de, J., Palasio, R. G. S., and Tuan, R. (2020). Taxonomic diversity of *Biomphalaria* (Planorbidae) in São Paulo state, Brazil. *Biota Neotrop* 20(2): e20200975. doi: 10.1590/1676-0611-bn-2020-0975

Pääbo, S. (1990). Amplifying ancient DNA. In MA Innis, DH Gelfand, JJ Sninsky, TJ White (eds). *PCR Protocols: a Guide to Methods and Applications* (San Diego: Academic Press), 159–166.

Palasio, R. G. S., Guimarães MC de, A., Ohlweiler, F. P., and Tuan, R. (2017). Molecular and morphological identification of *Biomphalaria* species from the state of São Paulo, Brazil. *Zookeys* 2017, 11–32. doi: 10.3897/zookeys.668.10562

Paradis, E., and Schliep, K. (2019). Ape 5.0: an environment for modern phylogenetics and evolutionary analyses in R. *Bioinformatics* 35, 526–528. doi: 10.1093/bioinformatics/bty633

Paraense, W. L. (1966). *Biomphalaria amazonica* and *B. cousini*, two new species of neotropical planorbid molluscs. *Rev. Bras. Biol.* 26, 115–126.

Paraense, W. L. (1975). Estado atual da sistemática dos planorbídeos brasileiros.(Mollusca, Gastropoda). *Arq do Mus Nac Do Rio Janeiro* 55, 105–128.

Paraense, W. L. (1981). *Biomphalaria occidentalis* sp. n. from South America (Mollusca basommatophora pulmonata). *Mem Inst Oswaldo Cruz* 76, 199–211. doi: 10.1590/S0074-02761981000200011

Paraense, W. L. (1984). *Biomphalaria tenagophila guaibensis* ssp. n. from southern Brazil and Uruguay (Pulmonata: Planorbidae). I. Morphology. *Mem Inst Oswaldo Cruz* 79, 465–469. doi: 10.1590/S0074-02761984000400012

Paraense, W. L. (1988). *Biomphalaria kuhniana* (Clessin, 1883), planorbid mollusc from South America. *Mem Inst Oswaldo Cruz* 83, 1–12. doi: 10.1590/s0074-02761988000100001

Paraense, W. L. (1990). *Biomphalaria obstructa* (Morelet, 1849): a study of topotypic specimens (Mollusca: Pulmonata: Planorbidae). *Mem Inst Oswaldo Cruz* 85, 391–399. doi: 10.1590/S0074-02761990000400002

Paraense, W. L., and Corrêa, L. R. (1973). Susceptibility of *Biomphalaria peregrina* from Brazil and Ecuador to two strains of *Schisotosoma mansoni*. *Rev. Inst Med. Trop. Sao Paulo* 15, 127–130.

Paraense, W. L., and Deslandes, N. (1959). The renal ridge as a reliable character for separating *Taphius glabratus* from *Taphius tenagophilus*. *Am. J. Trop. Med. Hyg* 8, 456–472. doi: 10.4269/ajtmh.1959.8.456

Paraense, W. L., Pointier, J. P., Delay, B., Pernot, A. F., Incani, R. N., Balzan, C., et al. (1992). *Biomphalaria prona* (Gastropoda: Planorbidae): a morphological and biochemical study. *Mem Inst Oswaldo Cruz* 87, 171–179. doi: 10.1590/S0074-02761992000200001

Paraense, W. L., Zeledón, R., Rojas, G., and Zeledon, R. (1981). *Biomphalaria straminea* and other planorbid molluscs in Costa Rica. *J. Parasitol.* 67, 282. doi: 10.2307/3280654

Pointier, J. P., Paraense, W. L., and Mazille, V. (1993). Introduction and spreading of *Biomphalaria straminea* (Dunker, 1848) (Mollusca: Pulmonata: Planorbidae) in Guadeloupe, French West Indies. *Mem Inst Oswaldo Cruz* 88, 449–455. doi: 10.1590/S0074-02761993000300016

Puillandre, N., Brouillet, S., and Achaz, G. (2021). ASAP: assemble species by automatic partitioning. *Mol. Ecol. Resour* 21, 609–620. doi: 10.1111/1755-0998.13281

Puillandre, N., Lambert, A., Brouillet, S., and Achaz, G. (2012). ABGD, automatic barcode gap discovery for primary species delimitation. *Mol. Ecol.* 21, 1864–1877. doi: 10.1111/j.1365-294X.2011.05239.x

QGIS (2021). Available at: https://www.qgis.org/en/site/ (Accessed July 16, 2021).

Rambaut, A. (2018) *FigTree*. Available at: http://tree.bio.ed.ac.uk/software/figtree/ (Accessed julho 15, 2021).

Ratnasingham, S., and Hebert, P. D. N. (2007). BOLD: The barcode of life data system (http://www.barcodinglife.org). *Mol. Ecol. Notes* 7, 355–364. doi: 10.1111/j.1471-8286.2007.01678.x

Reid, N. M., and Carstens, B. C. (2012). Phylogenetic estimation error can decrease the accuracy of species delimitation: a Bayesian implementation of the general mixed Yule-coalescent model. *BMC Evol. Biol.* 12, 196. doi: 10.1186/1471-2148-12-196

R Foundation for Statistical Computing (2021) *R: A language and environment for statistical computing*. Available at: https://www.r-project.org/.

Rollinson, D., Webster, J. P., Webster, B., Nyakaana, S., Jørgensen, A., and Stothard, J. R. (2009). Genetic diversity of schistosomes and snails: implications for control. *Parasitology* 136, 1801–1811. doi: 10.1017/S0031182009990412

Ronquist, F., Teslenko, M., van der Mark, P., Ayres, D. L., Darling, A., Höhna, S., et al. (2012). MrBayes 3.2: Efficient Bayesian phylogenetic inference and model choice across a Large model space. *Syst. Biol.* 61, 539–542. doi: 10.1093/sysbio/sys029

Rozas, J., Ferrer-Mata, A., Sánchez-DelBarrio, J. C., Guirao-Rico, S., Librado, P., Ramos-Onsins, S. E., et al. (2017). DnaSP 6: DNA sequence polymorphism analysis of Large data sets. *Mol. Biol. Evol.* 34, 3299–3302. doi: 10.1093/molbev/msx248

Schindel, D. E., and Miller, S. E. (2005). DNA Barcoding a useful tool for taxonomists. *Nature* 435, 17–17. doi: 10.1038/435017b

Scholte, R. G. C., Carvalho, O. S., Malone, J. B., Utzinger, J., and Vounatsou, P. (2012). Spatial distribution of *Biomphalaria* spp., the intermediate host snails of *Schistosoma mansoni*, in Brazil. *Geospat Health* 6, 95. doi: 10.4081/gh.2012.127

Spatz, L., Vidigal, T. H. D. A., Caldeira, R. L., Neto, E. D., Cappa, S. M. G., and Carvalho, O. S. (1999). Study of *Biomphalaria tenagophila tenagophila*, *B. t. guaibensis* and *B. occidentalis* by polymerase chain reaction amplification and restriction enzyme digestion of the ribosomal RNA intergenic spacer regions. *J. Molluscan Stud.* 65, 143–149. doi: 10.1093/mollus/65.2.143

Sun, S., Li, Q., Kong, L., Yu, H., Zheng, X., Yu, R., et al. (2016). DNA Barcoding reveal patterns of species diversity among northwestern pacific molluscs. *Sci. Rep.* 6, 1–17. doi: 10.1038/srep33367

Tajima, F. (1983). Evolutionary relationship of DNA sequences in finite populations. *Genetics* 105, 437–460. doi: 10.1093/genetics/105.2.437

Tamura, K., Nei, M., and Kumar, S. (2004). Prospects for inferring very large phylogenies by using the neighbor-joining method. *Proc. Natl. Acad. Sci.* 101, 11030–11035. doi: 10.1073/pnas.0404206101

Tang, C. T. (1983). "A survey of *Biomphalaria straminea* (Dunker, 1848) (Planorbidae) for trematode infection, with a report on larval flukes from other Gastropoda in Hong Kong," in *Proceedings of the Second International Workshop in Malacology Hong Kong*. 393–408.

Teodoro, T. M., Jannotti-Passos, L. K., Carvalho O dos, S., Grijalva, M. J., Baús, E. G., and Caldeira, R. L. (2011). Hybridism between *Biomphalaria cousini* and *Biomphalaria amazonica* and its susceptibility to *Schistosoma mansoni*. *Mem Inst Oswaldo Cruz* 106, 851–855. doi: 10.1590/S0074-02762011000700011

Teodoro, T. M., Janotti-Passos, L. K., Carvalho O dos, S., and Caldeira, R. L. (2010). Occurrence of *Biomphalaria cousini* (Mollusca: Gastropoda) in Brazil and its susceptibility to *Schistosoma mansoni* (Platyhelminths: Trematoda). *Mol. Phylogenet Evol.* 57, 144–151. doi: 10.1016/j.ympev.2010.05.019

Vidigal, T. H. D. A., Caldeira, R. L., Simpson, A. J. G., and Carvalho, O. S. (2000). Further studies on the molecular systematics of *Biomphalaria* snails from Brazil. *Mem Inst Oswaldo Cruz* 95, 57–66. doi: 10.1590/S0074-02762000000100009

Vidigal, T. H. D. A., Spatz, L., Kissinger, J. C., Redondo, R. A. F., Pires, E. C. R., Simpson, A. J. G., et al. (2004). Analysis of the first and second internal transcribed spacer sequences of the ribosomal DNA in *Biomphalaria tenagophila* complex (Mollusca: Planorbidae). *Mem Inst Oswaldo Cruz* 99, 153–158. doi: 10.1590/S0074-02762004000200007

Wang, W., Liang, Y.-S., Hong, Q.-B., and Dai, J.-R. (2013). African Schistosomiasis in mainland China: risk of transmission and countermeasures to tackle the risk. *Parasit Vectors* 6, 249. doi: 10.1186/1756-3305-6-249

Wanninger, A., and Wollesen, T. (2019). The evolution of molluscs. *Biol. Rev.* 94, 102–115. doi: 10.1111/brv.12439

Yang, Y., Huang, S.-Y., Pei, F.-Q., Chen, Y., Jiang, Q.-W., Deng, Z.-H., et al. (2018). Spatial distribution and habitat suitability of *Biomphalaria straminea*, intermediate host of *Schistosoma mansoni*, in Guangdong, China. *Infect. Dis. Poverty* 7, 109. doi: 10.1186/s40249-018-0492-6

Yeates, D. K., Seago, A., Nelson, L., Cameron, S. L., Joseph, L., and Trueman, J. W. H. (2011). Integrative taxonomy, or iterative taxonomy? *Syst. Entomol* 36, 209–217. doi: 10.1111/j.1365-3113.2010.00558.x

Yipp, M. W. (1990). Distribution of the schistosome vector snail, *Biomphalaria straminea* (Pulmonata: Planorbidae) in Hong Kong. *J. Molluscan Stud.* 56, 47–55. doi: 10.1093/mollus/56.1.47

Zhang, D., Gao, F., Jakovlić, I., Zou, H., Zhang, J., Li, W. X., et al. (2020). PhyloSuite: An integrated and scalable desktop platform for streamlined molecular sequence data management and evolutionary phylogenetics studies. *Mol. Ecol. Resour* 20, 348–355. doi: 10.1111/1755-0998.13096

Zhang, J., Kapli, P., Pavlidis, P., and Stamatakis, A. (2013). A general species delimitation method with applications to phylogenetic placements. *Bioinformatics* 29, 2869–2876. doi: 10.1093/bioinformatics/btt499

frontiers | Frontiers in Public Health

TYPE Original Research
PUBLISHED 01 September 2023
DOI 10.3389/fpubh.2023.1249637

OPEN ACCESS

EDITED BY
Cristina Toscano Fonseca,
Fundação Oswaldo Cruz, Brazil

REVIEWED BY
Marta Guimarães Cavalanti,
Federal University of Rio de Janeiro, Brazil
Edward Oliveira,
Oswaldo Cruz Foundation (Fiocruz), Brazil
Silvia Mesquita,
Natural History Museum (United Kingdom), United Kingdom

*CORRESPONDENCE
Pengfei Cai
✉ Pengfei.Cai@qimrberghofer.edu.au

†PRESENT ADDRESS
Kosala G. Weerakoon,
Department of Parasitology, Faculty of Medicine and Allied Sciences, Rajarata University of Sri Lanka, Saliyapura, Sri Lanka

‡Deceased

RECEIVED 29 June 2023
ACCEPTED 17 August 2023
PUBLISHED 01 September 2023

CITATION
Mu Y, Rivera J, McManus DP, Weerakoon KG, Ross AG, Olveda RM, Gordon CA, You H, Jones MK and Cai P (2023) Comparative assessment of the SjSAP4-incorporated gold immunochromatographic assay for the diagnosis of human schistosomiasis japonica. *Front. Public Health* 11:1249637. doi: 10.3389/fpubh.2023.1249637

Comparative assessment of the SjSAP4-incorporated gold immunochromatographic assay for the diagnosis of human schistosomiasis japonica

Yi Mu[1], Jonas Rivera[1,2], Donald P. McManus[1‡], Kosala G. Weerakoon[1†], Allen G. Ross[3], Remigio M. Olveda[4‡], Catherine A. Gordon[1,5], Hong You[1,6], Malcolm K. Jones[1,6] and Pengfei Cai[1,2]*

[1]Molecular Parasitology Laboratory, QIMR Berghofer Medical Research Institute, Brisbane, QLD, Australia, [2]School of Biomedical Sciences, The University of Queensland, Brisbane, QLD, Australia, [3]Rural Health and Medical Research Institute, Charles Sturt University, Orange, NSW, Australia, [4]Department of Immunology, Research Institute for Tropical Medicine, Manila, Philippines, [5]School of Public Health, Faculty of Medicine, The University of Queensland, Brisbane, QLD, Australia, [6]School of Veterinary Science, The University of Queensland, Brisbane, QLD, Australia

Background: Schistosomiasis, a disease caused by parasites of the genus *Schistosoma*, remains a global public health threat. This study aimed to validate the diagnostic performance of a recently developed gold immunochromatographic assay (GICA) for the detection of *S. japonicum* infection in a rural endemic area of the Philippines.

Methods: Human clinical samples were collected from 412 subjects living in Laoang and Palapag municipalities, Northern Samar, the Philippines. The presence of *Schistosoma*-specific antibodies in serum samples was tested with the SjSAP4-incorporated GICA strips and the results were converted to fully quantitative data by introducing an *R* value. The performance of the established GICA was further compared with other diagnostic tools, including the Kato-Katz (KK) technique, point-of-care circulating cathodic antigen (POC-CCA), droplet digital (dd) PCR, and enzyme-linked immunosorbent assays (ELISAs).

Results: The developed GICA strip was able to detect KK positive individuals with a sensitivity of 83.3% and absolute specificity. When calibrated with the highly sensitive faecal ddPCR assay, the immunochromatographic assay displayed an accuracy of 60.7%. Globally, the GICA assay showed a high concordance with the SjSAP4-ELISA assay. The schistosomiasis positivity rate determined by the GICA test was similar to those obtained with the SjSAP4-ELISA assay and the ddPCR assay performed on serum samples (SR_ddPCR), and was 2.3 times higher than obtained with the KK method.

Conclusion: The study further confirms that the developed GICA is a valuable diagnostic tool for detecting light *S. japonicum* infections and implies that this point-of-care assay is a viable solution for surveying endemic areas of low-intensity schistosomiasis and identifying high-priority endemic areas for targeted interventions.

KEYWORDS

schistosomiasis, *Schistosoma japonicum*, gold immunochromatographic assay (GICA), POC-CCA, droplet digital PCR, diagnosis, SjSAP4, ASSURED criteria

1. Introduction

Schistosomiasis, a debilitating disease caused by parasites of the genus *Schistosoma*, severely affects the health and socio-economic well-being of more than 250 million people in 78 of the world's poorest countries (1). In the past three decades, human mass drug administration (MDA), in which the effective oral drug praziquantel was delivered, has been the main strategy for the control of schistosomiasis globally (2). In Asia, hepatosplenic schistosomiasis caused by the zoonotic *Schistosoma japonicum* infection remains prevalent in China, the Philippines, and small foci in Central Indonesia (3). In the Philippines, the transmission of schistosomiasis is year-round due to high year-round precipitation. Added to this, the frequent flooding and strong typhoons, insufficient drug coverage and low compliance with MDA, and the presence of water buffaloes as a major reservoir animal host, meaning that the disease is still highly prevalent in the country. These issues necessitate multi-faceted interventions, such as bovine vaccination, development and implementation of cost-effective diagnostics for rapid mapping and monitoring of the disease in both humans and bovines, along with MDA to provide sustainable control, and beyond, elimination of the disease (4).

Currently, there are a diverse set of diagnostic tools available for the detection of schistosome infections (5–9). Parasitological detection techniques (e.g., the Kato-Katz (KK), urine filtration, and miracidia hatching technique (MHT)), while demonstrating a considerable specificity, had a compromised sensitivity when applied in endemic areas with low prevalence and/or reduced infection intensity of schistosomiasis (5). Improved coprological tests, such as the saline gradient method (10), and Helmintex method (11) showed a higher sensitivity compared with the traditional parasitological procedures; yet usually take longer time in sample processing and are labour-intensive. A variety of immunologic tests such as the circumoval precipitin test (COPT), indirect hemagglutination assay (IHA), the enzyme linked immunosorbent assay (ELISA), and rapid diagnostic tests (RDTs), were cost-effective and widely used during infection control and transmission control stages (8), although may suffer from a relatively low specificity if the crude extracted antigens were incorporated and it is difficult to distinguish between past and current infections. In addition, molecular detection methods mainly based on using polymerase chain reaction (PCR) and its derivative techniques, including nested PCR, real-time quantitative (q)PCR (12–15), droplet digital (dd) PCR assays (16–18), loop-mediated isothermal amplification (LAMP) (19–21), recombinase polymerase amplification (RPA) (22–24), and recently clustered regularly interspaced short palindromic repeats (CRISPR)-assisted diagnostic tests (25, 26) are promising tools for the detection of schistosomes; however at present, the prospect of large scale application of these methods in field areas remains obscure due to their relatively high cost.

The new roadmap for NTDs 2021–2030 recently released by the WHO (27) and revised guidelines for schistosomiasis (28) emphasised the need to develop and evaluate diagnostic tools to facilitate surveillance, control and elimination strategies (29). The WHO is seeking expert consultation on diagnostics with a particular focus on Point-of-care (POC) tests (30). Current antigen detection (AgD)-based POC tests for schistosomiasis are based on the probing of proteoglycan components present in the gut vomit of juvenile and adult worms known as circulating anodic antigens (CAAs) or circulating cathodic antigens (CCAs) using lateral flow assays (31–33). The POC-CCA assay is a commercially available cassette test that has been widely used for the detection of active *S. mansoni* infection in both Africa and South America (11, 34–36). However, the assay showed less potential for the diagnosis of other *Schistosoma* species (37–39). In addition, the assay suffers some pitfalls, such as cross-reactivity, underperformed specificity, and a "trace" reading issue (34, 38). The up-converting phosphor-lateral flow CAA (UCP-LF CAA) assay can detect all *Schistosoma* species quantitatively, exhibiting more accurate diagnostic performance than the POC-CCA assay. While the UCP-LF CAA assay has been suggested to be a promising tool for the diagnosis of low-intensity schistosome infections (40), it requires a large volume of samples, an additional filter device and concentration step and a special UCP-LF strip reader (41), and is, as of writing, not available as a commercial test currently.

To date, a number of antibody detection (AbD)-based lateral flow immunochromatographic assay (LFIA) strips have been developed for the rapid diagnosis of schistosomiasis japonica (42–45). However, these crude antigen-incorporated assays were found to be cross-reactive with other helminths. Recently, we developed a novel gold immunochromatographic assay (GICA) strip incorporating a recombinant saposin protein of *S. japonicum*, rSjSAP4, an unprecedented antigen for serological diagnosis of schistosomiasis (46–48). A preliminary assessment of the GICA cassette showed its potential in the rapid screening of schistosomiasis japonica (49). In this study, we further assess and validate the performance of the developed GICA cassettes with a large sample size, and calibrate its performance with the KK technique, ddPCR, POC-CCA and in-house ELISA assays that have been employed for the detection of *S. japonicum* infection against the same human cohort as reference (18, 46).

2. Materials and methods

2.1. Ethics approval and consent to participate

The human research ethics approval for conducting this study was obtained from the Institutional Review Board of the Research Institute for Tropical Medicine (RITM), Manila, the Philippines (number 2015–12) and the Human Research Ethics Committee, QIMR Berghofer Medical Research Institute (QIMRB), Brisbane, Australia (Ethics Approval: P524). Written informed consent was received from

each study participant (written informed consent was obtained from their legal guardians for those aged 15 years and under).

2.2. Sample collection, processing, and storage

Human clinical samples (faeces, serum, urine, and saliva) were collected from 412 subjects from 18 barangays in Palapag and Laoang, Northern Samar, the Philippines (18, 46, 47). Individual stool samples (10–15 g) were collected from each participant. Two faecal samples were sought from each individual on different days within a week for the KK analysis. The remainder of the first faecal sample (~10 g) was fixed in 80% ethanol. Blood sample (~10 mL) was collected from each individual with serum separation tubes. The blood samples were allowed to clot for 30 min at ambient temperature, and serum samples were then collected after centrifugation at 1500 × *g* for 10 min. Spot urine samples (~30 mL) were collected into 50 mL Falcon tubes and stored at 4°C. Saliva (~2 mL) was collected into a 5 mL centrifuge tube using the passive drool method under the supervision of a well-trained medical technologist. All processed samples were stored at 4°C and transported on wet ice to the RITM, Manila, where the samples were stored at −20°C. Subsequently, all samples were shipped to QIMRB, Brisbane, Australia, on dry ice. Faecal samples were then stored at 4°C, while serum, urine and saliva samples were stored at −80°C, for further analysis. Serum samples collected from healthy donors ($n = 23$) residing in a non-endemic area for schistosomiasis japonica (Qiqihar, Heilongjiang Province, China), were used as controls.

2.3. Parasitological detection

The KK slides were examined by experienced technicians at the RITM. For each stool sample, three KK thick smear slides were prepared and examined under a light microscope. Infection intensity for *S. japonicum* was defined as the number of eggs per gram of faeces (EPG). In order to improve the accuracy of the KK analysis, 10% of slides were randomly selected and subjected to re-examination by an experienced microscopist.

2.4. Preparation and measurement of the GICA strips

The GICA strips were developed by Zoonbio Biotechnology (Nanjing, China) (49). Briefly, colloidal gold particles with a mean particle diameter of 70 nm were used to coat recombinant protein rSjSAP4. The gold-rSjSAP4 conjugate was suspended in the buffer containing 20 mM Tris, 5% (w/v) sucrose, and 2.5% (w/v) trehalose at a final concentration of 10 μg/mL, and dispensed onto conjugate pad (glass fibre membrane) at a volume of 35 μL/cm. The pad was dried in a biochemical incubator for 12 h at 37°C. By using an XYZ Biostrip Dispenser (HM3030, Shanghai Kinbio Tech. Co., Ltd., Shanghai, China), protein G (1 mg/mL) (Zoonbio Biotechnology, Nanjing, China) and mouse anti-His tag mAb (0.7 mg/mL) (Zoonbio Biotechnology, Nanjing, China) were dispensed onto the nitrocellulose (NC) membrane (CN140, Sartorius, Goettingen, Germany) at a volume of 1 μL/cm to form the test and control lines, respectively. The NC membrane was then dried at room temperature in a biochemical incubator for 6 h. The absorbent pad (filter paper), coated NC membrane, conjugate pad, and sample pad, were laminated and pasted onto a plastic-backed support card with a 1–2 mm overlap. The assembled scale board was cut lengthwise into strips measuring 3 × 60 mm using a guillotine cutter (ZQ2002, Shanghai Kinbio Tech. Co., Ltd., Shanghai, China). The resulted strips were placed in a plastic cassette, which was further packaged into a silica gel desiccant-containing aluminium foil bag, and stored at room temperature.

The GICA strips were initially tested on 40 KK-positive [KK (+)] subjects, 20 KK-negative [KK (−)] and 20 control individuals in a previous pilot study (49). For the current study, the GICA cassettes were further tested for comparison with the other diagnostics following our previous pilot study protocol (49). Briefly, for each test, 50 μL diluted serum sample (1:20) was added to each cassette which was scanned at 10 min after sample loading. All images were further analysed by a Java-based image processing program, ImageJ to determine an *R* value, which was defined as the intensity of the test (*T*) line divided by that of the corresponding control (*C*) line, converting the results into fully quantitative data. The tests were determined as invalid when the control band did not appear or when the tests were left to develop for more than 15 min. GICA cassettes from the same batch were used for testing all the serum samples.

2.5. Comparative analysis using the KK, ddPCR, POC-CCA, and ELISA assays as references

The performance of the GICA was further calibrated using other diagnostic tests, including the KK, POC-CCA (37), two ELISA assays (Sj23-LHD-ELISA and SjSAP4-ELISA) (46), and four ddPCR assays performed on feces, serum, urine, and saliva, which were designated as F_ddPCR, SR_ddPCR, U_ddPCR, and SL_ddPCR, respectively (18), as references.

2.6. Statistical analysis

All statistical analyses were performed using GraphPad Prism version 9 software (GraphPad Software, Inc., California, United States). For analysis of differences in the *R* values between the control group and groups with variable *S. japonicum* egg burdens, one-way ANOVA followed by Holm-Sidak multiple comparison or the Mann–Whitney *U* test was used. A cut-off *R* value was set for the GICA assay with the maximization of Youden index (*J*) on testing of 108 KK (+) individuals and 23 healthy controls. McNemar's test[1] was used to determine the differences between the sensitivities determined by the GICA and the other diagnostic methods on testing 108 KK (+) individuals, and the differences between the positivity rates obtained with the GICA and other diagnostics across the different groups stratified by egg burdens. Calibrated by the different reference tests, sensitivity, specificity, positive predictive value (PPV), negative predictive value (NPV) and accuracy were analyzed for the developed GICA. Agreement between the GICA and the other diagnostics assays was determined using the

1 https://www.graphpad.com/quickcalcs/McNemar1.cfm

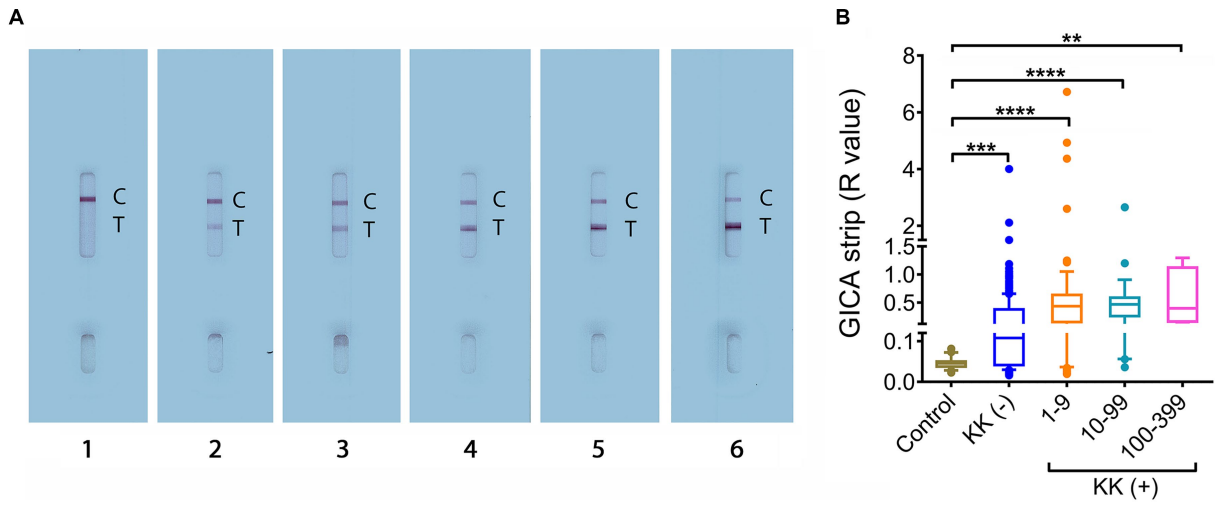

FIGURE 1
R value analysis for the developed GICA cassettes. **(A)** GICA strips showing different ranks of *R* values. Lanes 1–6, strips displaying an *R* value between 0–0.1, 0.1–0.5, 0.5–1, 1–2, 2–3, and > 3, respectively; **(B)** The distribution of *R* values in the controls, KK (–) individuals and different KK (+) groups. (Controls, $n = 23$; KK (–), $n = 304$; KK (+), $n = 108$; EPG 1–9, $n = 78$; EPG 10–99, $n = 26$; EPG 100–399, $n = 4$). Boxes represent the interquartile range of the data with lines across the boxes indicating the median values. The hash marks below and above the boxes indicate the 10th and 90th percentiles, respectively. *p* values were calculated using Kruskal-Wallis test (ns = no significant difference, **, $p < 0.01$;***, $p < 0.001$, ****, $p < 0.0001$).

Kappa statistic,[2] The strength of agreement was measured according to the κ value scores divided into: <0, no agreement; 0.00–0.20 slight agreement; 0.21–0.40 fair agreement; 0.41–0.60 moderate agreement; 0.61–0.80 substantial agreement; and 0.81–1.00 perfect agreement (50). Pearson's correlation coefficient (*r*) was used to assess the correlation between the immunochromatographic assay and the SjSAP4-ELISA assay for the KK (+) individuals and the entire cohort.

3. Results

3.1. Study population

The target population comprised 412 subjects [male: $n = 218$ (52.9%), 39.2 ± 16.1 years; female, $n = 194$ (47.1%), 41.5 ± 15.1 years] from a rural schistosomiasis-endemic area, Northern Samar, the Philippines. The human cohort had a moderate schistosomiasis japonica prevalence (26.2%) but a low intensity of infection based on the KK analysis on faecal samples (6 slides on two stool samples), according to the categorization by WHO. Detailed information of the study cohort can be found in previous studies (18, 51, 52).

3.2. Transforming the GICA into a fully quantitative assay by introducing an *R* value

The GICA cassettes were tested using optimized conditions (i.e., PBS was used as the dilution buffer and serum samples were diluted at a dilution of 1:20) (49). For each GICA cassette, the result was converted into an *R* value, which was calculated by dividing the band intensity of the "T" line with that of the corresponding "C" line. Figure 1A shows GICA cassettes displaying different levels of *R* values. The difference in *R* values between the controls and the target cohort stratified by different infection intensities were further assessed. The *R* values were significantly higher in groups with 1–9 EPG ($n = 78$, $p < 0.0001$), 10–99 EPG ($n = 26$, $p < 0.0001$) and 100–399 EPG ($n = 4$, $p < 0.01$), as well as the KK (–) individuals ($n = 304$, $p < 0.001$) compared with the non-endemic controls ($n = 23$) (Figure 1B).

3.3. Diagnostic performance of the GICA cassettes in KK (+) individuals

We further analysed diagnostic performance of the GICA strips in the detection of KK (+) subjects ($n = 108$). The *R* values in KK (+) group were significantly higher than those of the healthy controls ($p < 0.0001$) (Figure 2A). When an *R* cut-off value was set at 0.0864, which maximised the Youden's *J*-index, the GICA strip showed a sensitivity of 83.3% and absolute specificity. The ROC analysis revealed that the established GICA had an AUC level of 0.8945 ($p = 0.0001$) (Figure 2B). The sensitivity of the GICA was significantly lower than these of the F_ddPCR and SR_ddPCR tests (98.1%, $p = 0.0008$ and 94.4%, $p = 0.019$, respectively), but higher than these of the U_ddPCR, SL_ddPCR, POC-CAA and Sj23-LHD-ELISA assays (59.3%, 38.9%, 29.6%, and 42.6%, respectively, $p < 0.0001$ in all comparisons) (Figure 2C).

3.4. Positivity rate analysis

We then compared the positivity rate determined by the GICA with those obtained with other diagnostic tests in the detection of *S. japonicum* infection (Table 1). In the subgroup with moderate

2 https://www.graphpad.com/quickcalcs/kappa1/

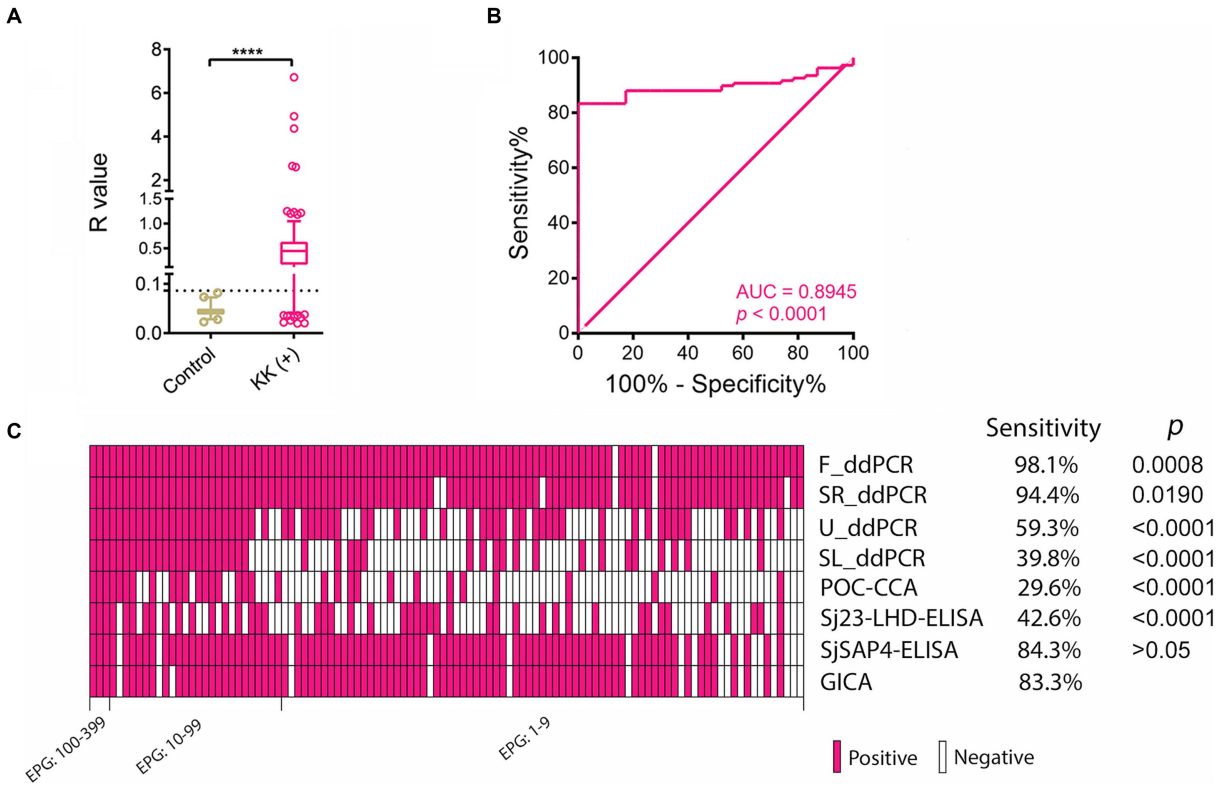

FIGURE 2
The performance of the SjSAP4-incorporated GICA cassettes in diagnosing the KK (+) individuals. **(A)** Scatter plots showing the *R* values of the non-endemic controls ($n = 23$) and KK (+) subjects ($n = 108$). Boxes represent the interquartile range of the data with lines across the boxes indicating the median values. The hash marks below and above the boxes indicate the 10th and 90th percentiles, respectively. Dashed line: *R* cut-off value. *p* value was determined using the Mann–Whitney *U* test (****, $p < 0.0001$); **(B)** Receiver operating characteristic curve (ROC) analysis was performed to assess the capability of the GICA assay in discriminating the non-endemic controls ($n = 23$) and KK (+) subjects ($n = 108$); **(C)** Clustered results for the eight diagnostics on testing the KK (+) individuals ($n = 108$). Samples are sorted from left to right in a decreased order of egg burden. The differences in sensitivity were compared between the GICA and other diagnostic methods. *p* values were determined by McNemar's test.

TABLE 1 Positivity rates of schistosomiasis japonica determined by different diagnostics in the different subgroups and entire cohort, respectively.

Diagnostic test	KK (+) moderate	KK (+) light[§]				KK (−)		Entire cohort	
	(EPG: 100–399)	(EPG: 10–99)		(EPG: 1–9)		(EPG: 0)		(EPG: 0–399)	
	Positive, % (*n*/*n*)	Positive, % (*n*/*n*)	*p**	Positive, % (*n*/*n*)	*p**	Positive, % (*n*/*n*)	*p**	Positive, % (*n*/*n*)	*p**
GICA[†]	100 (4/4)	88.5 (23/26)		80.8 (63/78)		53.0 (161/304)		60.9 (251/412)	
F_ddPCR	100 (4/4)	100 (26/26)	>0.05	97.4 (76/78)	0.0036	66.1 (201/304)	0.0011	74.5 (307/412)	<0.0001
SR_ddPCR	100 (4/4)	100 (26/26)	>0.05	92.3 (72/78)	>0.05	57.6 (175/304)	>0.05	67.2 (277/412)	>0.05
U_ddPCR	100 (4/4)	88.5 (23/26)	>0.05	47.4 (37/78)	<0.0001	43.4 (132/304)	0.0273	47.6 (196/412)	0.0001
SL_ddPCR	100 (4/4)	76.9 (20/26)	>0.05	24.4 (19/78)	<0.0001	20.4 (62/304)	<0.0001	25.5 (105/412)	<0.0001
POC-CCA[†]	100 (4/4)	57.7 (15/26)	0.0433	16.7 (13/78)	<0.0001	6.3 (19/304)	<0.0001	12.4 (51/412)	<0.0001
Sj23-LHD-ELISA[#]	100 (4/4)	53.8 (14/26)	0.0077	35.9 (28/78)	<0.0001	18.1 (55/304)	<0.0001	24.5 (101/412)	<0.0001
SjSAP4-ELISA[#]	100 (4/4)	92.3 (24/26)	>0.05	80.8 (63/78)	>0.05	56.3 (171/304)	>0.05	63.6 (262/412)	>0.05

[§]Individuals with a light infection were arbitrarily divided into two subgroups with EPG of 10–99 and 1–9, respectively. [†] *R* cut-off value for the developed GICA: 0.0864; *R* cut-off value for the POC-CAA assay: 0.1344 (37). [#]OD_{450nm} cut-off values for ELISA assays: Sj23-LHD-ELISA, 0.2185; SjSAP4-ELISA, 0.1832 (46). **p* values were determined by McNemar's test.

infection (EPG: 100–399), all the diagnostics had absolute positivity rate. In the subgroup with EPGs between 10–99, the positivity rate assessed by the GICA (88.5%) was significantly higher than those provided by the Sj23-LHD-ELISA (53.8%, $p = 0.0077$) and the POC-CCA cassette (57.7%, $p = 0.0433$), yet no difference was observed when it was compared with those determined by the other diagnostics. In subjects with an extremely low infection intensity (EPG: 1–9), the positivity rate determined by the GICA strips (80.8%) was significantly lower than that obtained with the F_ddPCR test (97.4%, $p < 0.0001$), but significantly higher than those

provided by the U_ddPCR, Sj23-LHD-ELISA, SL_ddPCR and POC-CCA assays (47.4%, 35.9%, 24.4%, and 16.7%, respectively, $p < 0.0001$ in all comparisons). In the KK (−) subjects, the positivity rate determined by the GICA (53.8%) was only significantly lower than that judged by the F_ddPCR test (66.1%, $p < 0.0001$) (Table 1). The clustered results for the eight molecular and immunological diagnostics on testing the KK (−) individuals ($n = 304$) are shown in Supplementary Figure S1. The global positivity rate of the target cohort provided by the GICA (60.9%) was significantly lower than that obtained with the F_ddPCR test (74.5%, $p < 0.0001$), but higher than those deduced from the U_ddPCR (47.6%, $p = 0.0001$), SL_ddPCR (25.5%, $p < 0.0001$), Sj23-LHD-ELISA (24.5%, $p < 0.0001$), and POC-CCA (12.4%, $p < 0.0001$) assays. There were no differences in positivity rates obtained with the GICA test and the SjSAP4-ELISA assay in the different subgroups and the entire cohort, respectively. Similarly, no differences were found between the positivity rates determined by the immunochromatographic cassettes and the SR_ddPCR test in all different groups.

We further analysed the schistosomiasis positivity rates in the different age groups determined by the nine diagnostics (Figure 3). Positivity rates deduced from five diagnostics, the F_ddPCR, SR_ddPCR, U_ddPCR, SjSAP4-ELISA, and GICA strips were higher than that determined by the KK in all age groups (Figure 3A). The positivity rate determined by the developed GICA for each age group was between 1.85 and 2.77 times higher than that assessed by the KK procedure (Figure 3B). The overall schistosomiasis positivity rate of the cohort determined by the established GICA was comparable with those assessed by the SjSAP4-ELISA and SR_ddPCR, and was about 2.3 times higher than that obtained with the KK technique (Figure 3).

3.5. Performance of the developed GICA strip with the other diagnostics as references

By employing various diagnostic tools as reference, we further evaluated the diagnostic performance, including sensitivity, specificity,

A

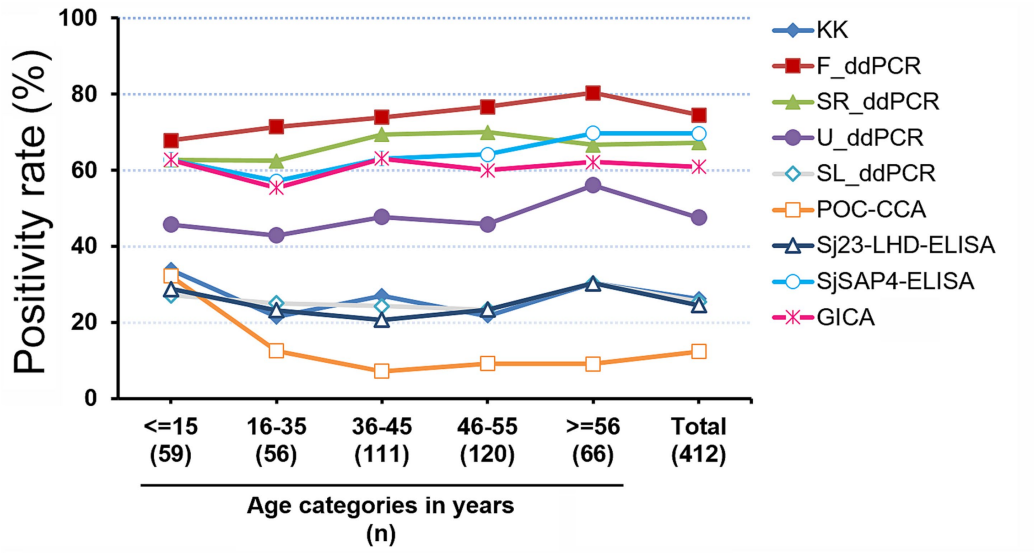

B

Diagnostics	Age categories in years (n)					Total (n = 412)
	<=15 (59)	16-35 (56)	36-45 (111)	46-55 (120)	>=56 (66)	
F_ddPCR	2.00	3.33	2.73	3.54	2.65	2.84
SR_ddPCR	1.85	2.92	2.57	3.23	2.20	2.56
U_ddPCR	1.35	2.00	1.77	2.12	1.85	1.82
SL_ddPCR	0.80	1.17	0.90	1.08	1.00	0.97
POC-CCA	0.95	0.58	0.27	0.42	0.30	0.47
Sj23-LHD-ELISA	0.85	1.08	0.77	1.08	1.00	0.94
SjSAP4-ELISA	1.85	2.67	2.33	2.96	2.30	2.66
GICA	1.85	2.58	2.33	2.77	2.05	2.33

FIGURE 3
Schistosomiasis japonica positivity rates in the different age groups. **(A)** The schistosomiasis positivity rates determined by all nine diagnostic tests for the human cohort stratified by different age groups. *R* cut-off value for the developed GICA: 0.0864; *R* cut-off value for the POC-CAA assay: 0.1344 (37); OD cut-off values for the ELISA assays: 0.2185 (Sj23-LHD-ELISA) and 0.1832 (SjSAP4-ELISA) (46). **(B)** Fold changes in schistosomiasis positivity rates obtained with the eight molecular and immunological diagnostics vs. that determined by the KK for the investigated cohort stratified by different age groups.

10.3389/fpubh.2023.1249637

TABLE 2 Performance of the GICA using different diagnostic tests as reference.

GICA[†]	Reference test		% Sensitivity (95% CI)	% Specificity (95% CI)	% PPV (95% CI)	% NPV (95% CI)	% Accuracy (95% CI)	Kappa index (95% CI)
	+	–						
	KK							
+	90	161	83.3 (74.9–89.8)	47.0 (41.3–52.8)	35.9 (29.9–42.1)	88.8 (82.9–93.2)	56.6 (51.6–61.4)	0.213 (0.143–0.283)
–	18	143						
	F_ddPCR							
+	198	53	64.5 (58.9–69.9)	49.5 (39.6–59.5)	78.9 (73.3–83.8)	32.3 (25.2–40.1)	60.7 (55.8–65.4)	0.119 (0.026–0.213)
–	109	52						
	SR_ddPCR							
+	177	74	64.0 (57.8–69.6)	45.2 (36.6–54.0)	70.5 (64.5–76.1)	37.9 (30.4–45.9)	57.8 (52.8–62.6)	0.087 (−0.010–0.183)
–	100	61						
	U_ddPCR							
+	123	128	62.8 (55.6–69.5)	40.7 (34.1–47.6)	49.0 (42.7–55.4)	54.7 (46.6–62.5)	51.2 (46.3–56.1)	0.035 (−0.058–0.128)
–	73	88						
	SL_ddPCR							
+	70	181	66.7 (56.8–75.6)	41.0 (35.5–46.8)	27.9 (22.4–33.9)	78.3 (71.1–84.4)	47.6 (42.7–52.5)	0.053 (−0.02–0.126)
–	35	126						
	POC-CCA[†]							
+	39	212	76.5 (62.5–97.2)	41.3 (36.2–46.6)	15.5 (11.3–20.6)	92.6 (87.3–96.1)	43.2 (38.4–48.1)	0.066 (0.016–0.116)
–	12	149						
	Sj23-LHD-ELISA[#]							
+	86	165	85.2 (76.7–91.4)	47.0 (41.3–52.7)	34.3 (28.4–40.5)	90.7 (85.1–94.7)	56.3 (51.4–61.2)	0.214 (0.147–0.281)
–	15	146						
	SjSAP4-ELISA[#]							
+	241	10	92.0 (88.0–95.0)	93.3 (88.1–96.8)	96.0 (92.8–98.1)	87.0 (80.8–91.7)	92.5 (89.5–94.8)	0.840 (0.786–0.894)
–	21	140						

[†]*R* cut-off value for the GICA strip: 0.0864; *R* cut-off value for the POC-CCA assay: 0.1344 (37). [#]OD_{450nm} cut-off values for the serum ELISA assays: Sj23-LHD-ELISA, 0.2185; SjSAP4-ELISA, 0.1832 (46).

PPV, NPV, and accuracy for the developed GICA strips (Table 2). The GICA test showed the highest sensitivity (92.0%) when the SjSAP4-ELISA assay detecting the serum IgG against the same antigen, SjSAP4, was used as the reference. When the different ddPCR tests were employed as reference tests, the established GICA showed a similar sensitivity between 62.8–66.7%. The developed immunochromatographic assay showed the highest accuracy (92.5%) when the SjSAP4-ELISA assay was adopted as the reference. When calibrated with the F_ddPCR test, the SjSAP4-GICA showed an accuracy of 60.7%. The immunochromatographic GICA displayed a perfect agreement with the SjSAP4-ELISA assay ($\kappa = 0.840$), a fair agreement with the KK technique ($\kappa = 0.213$) and Sj23-LHD-ELISA assay ($\kappa = 0.214$), and a slight agreement with the other diagnostics ($\kappa < 0.2$) (Table 2).

3.6. Correlation analysis

The associations between the developed GICA test and SjSAP4-ELISA assay were investigated in the KK (+) subjects ($n = 108$) and the entire study cohort ($n = 412$). Within the KK (+) subgroup, there was a significant positive correlation ($r = 0.3249$, $p = 0.0006$) between the GICA test and the SjSAP4-ELISA assay (Figure 4A). When analysing the entire cohort, a higher significant correlation ($r = 0.5078$, $p < 0.0001$) was observed between the two assays (Figure 4B).

4. Discussion

Schistosomiasis continues to be a major public health problem in the developing world. It is encouraging that it has been successfully controlled in a few of countries, such as China, which is steadily moving towards the goal of schistosomiasis japonica elimination (53). However, in the Philippines, a focal survey performed in 2017 showed that there were still 435 barangays having a high prevalence of human schistosomiasis of >5% (54). Currently, the Philippines government administers MDA in schistosomiasis endemic areas annually through the Schistosomiasis Control and Elimination Program (55). The currently used parasitological approaches, primarily the KK, are not sensitive enough for the diagnosis of schistosomiasis in endemic areas with reduced intensities due to MDA implementation (5). Thus, it is appropriate that the WHO's 2021–2030 roadmap to eliminate NTDs

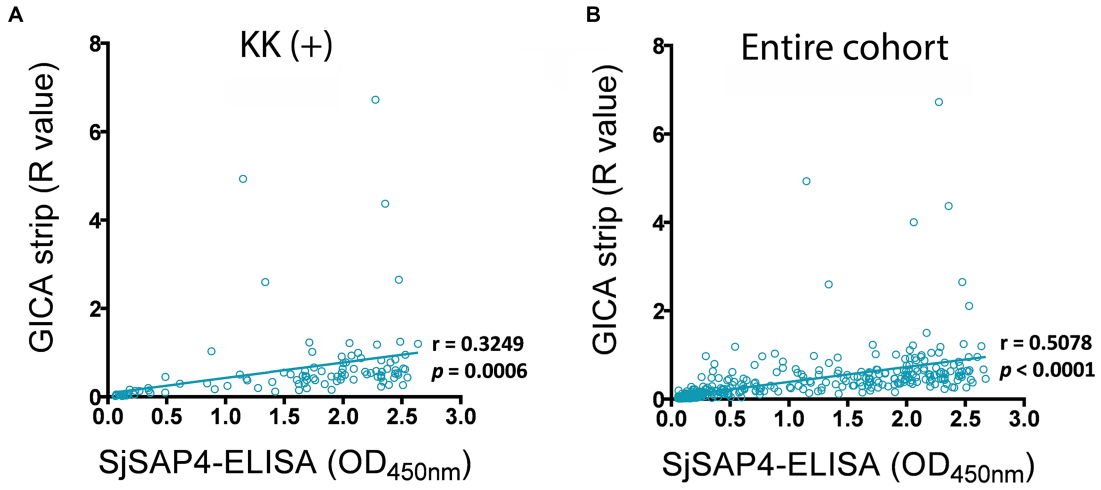

FIGURE 4
Correlation analysis for the GICA and ELISA assays. Correlations between the GICA test and the SjSAP4-ELISA assay on testing the **(A)** KK (+) individuals ($n = 108$) and **(B)** whole cohort ($n = 412$) using Pearson's correlation coefficient.

includes a focus on the development of improved diagnostics for schistosomiasis (27). In this study, we assessed the performance of the recently developed SjSAP4-incorporated GICA test by probing samples collected from a well-defined Philippines cohort, using eight other diagnostics as references.

As stated previously, the sensitivity of the KK technique is compromised in areas with lower infection intensities (51). In the KK (−) individuals, high positivity rates were obtained with both molecular methods, the F_ddPCR (66.1%) and SR_ddPCR (57.6%), and immunodiagnostic tests, the GICA (53%) and SjSAP4-ELISA (56.3%), indicating the KK failed to detect many light infections. This corresponded with a total prevalence, determined by the above mentioned molecular and immunodiagnostic assays, that was 2.33 to 2.84 times higher than that obtained with the KK (26.2%) (Figure 4B). Nevertheless, the KK is still useful for determining infection intensities and prevalence in moderate to high endemic areas, when combined with multiple slides across different days, can be used as a useful standard for comparing other diagnostics. In this study, when tested on the serum samples from KK (+) subjects ($n = 108$), the SjSAP4-incorporated GICA elicited 83.3% sensitivity and absolute specificity, with an AUC value of 0.8945 (Figure 2), indicating a "very good" diagnostic accuracy (56). Although the sensitivity has been decreased from 95% in testing a small subset of these KK (+) subjects ($n = 40$) in a previous study (49), to 83.3% in the current study as the sample size increases, these results indicate that the newly developed GICA strip has strong diagnostic potential in identifying light *S. japonicum* infections, with its performance competitive with the recently developed point of care immunochromatographic test (POC-ICT) incorporated with MS3_01370 antigen for the diagnosis of urogenital schistosomiasis (44).

Molecular methods, such as PCR assays, have been widely used in the detection of schistosome infections and showed high diagnostic performance (5). Although the substantial costs of required reagents and equipment and the requirement of well-trained personnel limit their application in screening of schistosomiasis in resource-poor endemic areas (5), PCR assays can be used as reference tests, which could be more accurate than the traditional parasitological detection procedures, for the evaluation of other laboratory developed diagnostics. For instance, the F_ddPCR and SR_ddPCR assays showed a higher sensitivity compared with those of the POC-CCA, GICA and ELISA assays in identifying the KK (+) individuals (Figure 2C). The developed GICA had a sensitivity of 62.8–66.7% when calibrated with ddPCR tests (Table 2). This relatively low sensitivity could arise as no accurate cut-off values have been set for the ddPCR assays, which may incur some false positives. Furthermore, the relatively lower sensitivity of serological tests compared with PCR, can be also due to some individuals having an abnormally reduced humoral immune response, as seen in previous studies (57). The concordances between the GICA and ddPCR tests are also very poor ($\kappa = 0.053$–0.119) (Table 2). This is probably due to the differences in test targets, i.e., ddPCR analysis detects the parasite-derived DNA in samples while the GICA probes host antibodies against SjSAP4. Nevertheless, it is impressive that the SjSAP4-incorporated GICA strip showed 60.7% accuracy when the F_ddPCR assay was employed as a reference test (Table 2). PCR tests, unlike AbD based assays, can be used to determine infection intensities. In our previous study, we found that the ddPCR results, presented as the target gene copy number index (CNI) showed a high degree of correlation with KK-determined EPGs (18), indicating ddPCR assays can measure the CNI as a direct quantitative measure of parasite burden. In contrast, either in field observation by an operator or converting to an *R* value, the AbD based GICA tests cannot reliably differentiate infection intensities. Falsely attributing past infections as active infections occurs for a much longer period of time for serological based techniques compared with molecular methods performed on faecal samples (58). This may contribute to the fact that the SjSAP4-GICA has a relatively low specificity when calibrated with the F_ddPCR test as standard.

Unsurprisingly, the SjSAP4-GICA recorded similar outcomes to the SjSAP4-ELISA. Overall, the developed GICA assay exhibited a diagnostic performance commensurate with that of the SjSAP4-ELISA. There was no significant difference in the positivity rate for the GICA assay and the SjSAP4-ELISA in the group of individuals with

an EPG of 10–99 (88.5% vs. 92.3%, $p > 0.05$), an EPG of 1–9 (80.8% vs. 80.8%, $p > 0.05$) and in the KK (−) individuals (53.0% vs. 56.3%, $p > 0.05$) (Table 1); similarly, the prevalence of schistosomiasis japonica determined by the GICA assay and SjSAP4-ELISA assay was comparable (60.9% vs. 65.5%, $p > 0.05$), which was about 2.5-fold higher than that determined by the KK method (26.2%) (Figure 4B). Also, the SjSAP4-incorporated GICA strip recorded the highest sensitivity (92.0%) and accuracy (92.5%) and near-perfect agreement ($\kappa = 0.840$) when the SjSAP4-ELISA was used as the reference test (Table 2). When using the F_ddPCR as reference, the GICA assay and the SjSAP4-ELISA assay test displayed similar performance in sensitivity (64.5% vs. 67.4%), specificity (55.2% vs. 47.6%), accuracy (60.7% vs. 62.4%) and agreement (0.119 vs. 0.132) (Table 2; Supplementary Table S1). In this study, we converted the GICA test into a fully quantitative test, which enabled us to assess the correlation between the GICA and SjSAP4-ELISA. The two assays showed significant positive correlations in the KK (+) individuals and the entire human cohort. All these observations indicate that the two assays had a high concordance, which is logical as both are AbD based assay targeting the same antigen. Nevertheless, compared with the rapid GICA, the classic ELISA assay is tedious and labor-intensive, has stringent equipment requirements, and needs well-trained personal to perform.

The POC-CCA assay has been extensively evaluated for the diagnosis of schistosomiasis mansoni in different endemic areas (59–62). In *S. mansoni* infections with a prevalence level of less than 50% (based on the KK procedure), the POC-CCA assay exhibits a 1.5–6 fold higher prevalence than that determined by the KK (63). Of the diagnostics available, it has been suggested that the POC-CCA test best fulfils the ASSURED (A = affordable by the affected individuals; S = sensitive; S = specific; U = user-friendly; *R* = rapid turn-around time and robust performance (e.g., reagents tolerate tropical climate); E = equipment-free; and D = delivered to those in need) criteria for in resource-limited settings (41). However, the diagnostic performance of the assay is *Schistosoma* species-dependent. For instance, in the detection of *S. mekongi* in endemic areas of Lao PDR, the POC-CCA showed a low sensitivity (24.1%) (64). Also, the POC-CCA test had a moderate sensitivity of 63.3%, in the diagnosis of *S. japonicum* patients with infection intensities of EPGs ≥10 (37), while showed a poor sensitivity (29.6%) in identifying *S. japonicum* infection in individuals with extremely low egg burdens (EPG: 1–9) (37). Furthermore, the prevalence determined by the POC-CCA was the lowest among all diagnostics investigated here (Table 1), and only half of that determined by the KK and one in fifth of that deduced by the GICA (Figure 4B). The poor diagnostic sensitivity of the POC-CCA for low intensity *S. japonicum* infections stems from a number of reasons, which has been discussed in a previous study, such as species septicity of capturing antibody incorporated in the POC-CCA cassette (37). Additionally, a relatively high *R* value has been set to retain a considerable specificity due to the concerned issues of low specificity (34) and cross-reactivity with other helminths (65), resulting in a reduced sensitivity for the assay. In all, it can be concluded that the POC-CCA is unsuitable for the diagnosis of schistosomiasis japonica in its current format. In contrast, the relatively high performance of the established GICA would, therefore, be an upgrade for schistosomiasis japonica diagnosis.

In this study, all the tested GICA cassettes were scanned and analysed *in silico*, i.e., a Java-based image processing program, ImageJ, was used to convert results into quantitative *R* values. This would reduce variability from an operator's training or visual acuity and, also, limit system errors from colour development times and sample absorbance rates (49). Essentially, the ImageJ *R* values would allow fair comparisons between multiple studies with different cassette batches/types. In a rapid field screening, the images of tested GICA strips can be captured by smartphones on-site, and uploaded to a computer for real-time analysis using ImageJ software. However, in some applications where a conversion of an *R* value is inaccessible, the diagnostic performance exhibited here may not be well reflected in those scenarios. Accordingly, other readout methods, such as a semi-quantitative visual scoring method using a color interpretive card as a reference, need to be developed for the interpretation of the GICA. Alternatively, a chromogenic rapid test reader can also be employed to quantify the intensities of bands appearing on the "T" line of the GICA cassettes, providing a quantitative readout. In this regard, parallel studies that assess the agreement and/or correlation between the results determined by ImageJ and those obtained with other readout methods, would, therefore, be of substantial value. Interestingly, Schary et al. recently develop an open-source, all-in-one smartphone-based system for quantitative analysis of lateral flow assays (LFAs) (66). The system includes an *R* Shiny software package with similar function to the Image J for image editing, analysis, data extraction, calibration and quantification of the assays (66). Further combining the smartphone-based *R* Shiny software will increase the potential of the GICA test in the field application.

The current study has the following limitations: (1) The Standards for Reporting Diagnostic accuracy studies (STARD) rules recommend using a "reference test" to evaluate the accuracy of a newly developed diagnostic test (67). However, none of the reference assays employed in this study can be a gold standard test. The KK technique has previously been referred to as a gold standard for intestinal schistosomiasis testing; but the KK lacks sensitivity in low-intensity infections. Further, the Sj23-LHD-ELISA and POC-CCA displayed insufficient sensitivity in the diagnosis of schistosomiasis japonica. And the Sj23-LHD-ELISA and SjSAP4-ELISA have an inherent limitation in the discrimination of current versus previous infections. As regards ddPCR assay, studies have demonstrated the higher sensitivity of this technique compared to conventional qPCR assay (68, 69). The ddPCR assay developed for schistosomiasis diagnosis was able to detect as little as 0.05 fg of template genomic DNA, much less than that in conventional PCR using the same primers, i.e., 0.1 pg (16). The SR_ddPCR, U_ddPCR, and SL_ddPCR assays detect the parasite-derived cfDNA in body fluids, while the F_ddPCR targets schistosome DNA derived from viable and/or decayed eggs and possibly the cell-free DNA released from worms and eggs in faecal samples. The ultra-sensitive nature of ddPCR assay may cause the problem of false positives due to cross-contamination of the samples, assay specificity and/or the detection of a past infection (70). In addition, no stringent CNI cut-off values have been set for these ddPCR assays, a fact that may magnify the problem (18). (2) As a new diagnostic approach, the developed GICA was only tested with serum samples collected from one endemic region. Further evaluations of the assay in different *S. japonicum*-endemic areas with variable intensities of infection and with a much larger sample size will be important in verifying the generalization. (3) The SjSAP4-incorporatd GICA cassettes were tested with only one serum dilution, which means that an optimal serum dilution remains to be determined for the assay.

5. Conclusion

The newly developed GICA was able to identify KK (+) subjects in a Philippine cohort with 83.3% sensitivity and 100% specificity. Targeting the whole cohort, a comparison of the GICA with other diagnostic methods further revealed the performance of this immunochromatographic test. In terms of diagnostic performance, the SjSAP4-GICA is comparable to the SjSAP4-ELISA assay but superior to U_ddPCR, SL_ddPCR, POC-CCA and Sj23-LHD-ELISA assays. While F_ddPCR and SR_ddPCR tests may perform better than the GICA strips, these PCR tests are time-consuming and labor-intensive, and requires expensive reagents and equipment. Currently, the SjSAP4-GICA is between $1.5–4.0 per test, depending on the order volume. Overall, the developed GICA stands to meet the ASSURED criteria the best, but further optimization steps are still required. A potential application scenario of the SjSAP4-GICA is its use as the first approach of the two-step diagnostic process suggested by the WHO for schistosomiasis, i.e., started with a high sensitivity test for screening and followed with a second, high specificity test for confirmation (71). Integration of the developed GICA cassettes into the current surveillance strategies in *S. japonicum* endemic areas may help identify high-priority areas for targeted interventions.

Data availability statement

The original contributions presented in the study are included in the article/Supplementary material, further inquiries can be directed to the corresponding author.

Ethics statement

The studies involving humans were approved by the Institutional Review Board of the Research Institute for Tropical Medicine (RITM), Manila, the Philippines and the Human Research Ethics Committee, QIMR Berghofer Medical Research Institute (QIMRB), Brisbane, Australia. The studies were conducted in accordance with the local legislation and institutional requirements. Written informed consent for participation in this study was provided by the participants' legal guardians/next of kin.

Author contributions

YM, DM, and PC conceptualized the study design and directed the project. YM, JR, KW, RO, and PC developed the methodology. KW, DM, RO, AR, and PC contributed to the acquisition of clinical sample resources. YM, JR, KW, CG, HY, MJ, and PC analyzed, reviewed and interpreted the data. YM, JR, and PC drafted the original manuscript. KW, AR, CG, HY, MJ, and PC revised the manuscript. DM and PC contributed to the funding acquisition. PC supervised the project. All authors contributed to the article and approved the submitted version.

Funding

This study was supported by the National Health and Medical Research Council (NHMRC) of Australia (IDs: APP1160046, APP2008433, APP1102926, APP1037304, and APP1098244). DM was a NHMRC Leadership Fellow and Senior Scientist at QIMRB. The funders had no role in study design, data collection and analysis, decision to publish, or preparation of the manuscript.

Acknowledgments

We appreciate all study participants and the local field and clinical staff in Laoang and Palapag, Northern Samar, the Philippines, for their assistance in the collection, storage and shipment of the human clinical samples. Thanks also given to Dr. Xianyu Piao and Prof. Qijun Chen (Institute of Pathogen Biology, Chinese Academy of Medical Sciences) for providing sera collected from healthy individuals.

Conflict of interest

The authors declare that the research was conducted in the absence of any commercial or financial relationships that could be construed as a potential conflict of interest.

Publisher's note

Supplementary material

The Supplementary material for this article can be found online at: https://www.frontiersin.org/articles/10.3389/fpubh.2023.1249637/full#supplementary-material

References

1. McManus DP, Dunne DW, Sacko M, Utzinger J, Vennervald BJ, Zhou XN. Schistosomiasis. *Nat Rev Dis Primers*. (2018) 4:13. doi: 10.1038/s41572-018-0013-8

2. Olveda RM, Tallo V, Olveda DU, Inobaya MT, Chau TN, Ross AG. National survey data for zoonotic schistosomiasis in the Philippines grossly underestimates the true burden of disease within endemic zones: implications for future control. *Int J Infect Dis*. (2016) 45:13–7. doi: 10.1016/j.ijid.2016.01.011

3. Gordon CA, Kurscheid J, Williams GM, Clements A, Li Y, Zhou XN, et al. Asian schistosomiasis: current status and prospects for control leading to elimination. *Trop Med Infect Dis*. (2019) 4:40. doi: 10.3390/tropicalmed4010040

4. Olveda RM, Gray DJ. Schistosomiasis in the Philippines: innovative control approach is needed if elimination is the goal. *Trop Med Infect Dis*. (2019) 4:66. doi: 10.3390/tropicalmed4020066

5. Cavalcanti MG, Silva LF, Peralta RH, Barreto MG, Peralta JM. Schistosomiasis in areas of low endemicity: a new era in diagnosis. *Trends Parasitol*. (2013) 29:75–82. doi: 10.1016/j.pt.2012.11.003

6. Weerakoon KG, Gobert GN, Cai P, McManus DP. Advances in the diagnosis of human schistosomiasis. *Clin Microbiol Rev*. (2015) 28:939–67. doi: 10.1128/CMR.00137-14

7. Mesquita SG, Caldeira RL, Favre TC, Massara CL, Beck LCNH, Simões TC, et al. Assessment of the accuracy of 11 different diagnostic tests for the detection of schistosomiasis mansoni in individuals from a Brazilian area of low endemicity using latent class analysis. *Front Microbiol*. (2022) 13:1048457. doi: 10.3389/fmicb.2022.1048457

8. Lv C, Deng W, Wang L, Qin Z, Zhou X, Xu J. Molecular techniques as alternatives of diagnostic tools in China as schistosomiasis moving towards elimination. *Pathogens*. (2022) 11:287. doi: 10.3390/pathogens11030287

9. Tabios IKB, Sato MO, Tantengco OAG, Fornillos RJC, Kirinoki M, Sato M, et al. Diagnostic performance of parasitological, immunological, molecular, and Ultrasonographic tests in diagnosing intestinal schistosomiasis in fieldworkers from endemic municipalities in the Philippines. *Front Immunol*. (2022) 13:899311. doi: 10.3389/fimmu.2022.899311

10. Coelho PM, Jurberg AD, Oliveira AA, Katz N. Use of a saline gradient for the diagnosis of schistosomiasis. *Mem Inst Oswaldo Cruz*. (2009) 104:720–3. doi: 10.1590/S0074-02762009000500010

11. Lindholz CG, Favero V, Verissimo CM, RRF C, de Souza RP, Dos Santos RR, et al. Study of diagnostic accuracy of Helmintex, Kato-Katz, and POC-CCA methods for diagnosing intestinal schistosomiasis in Candeal, a low intensity transmission area in northeastern Brazil. *PLoS Negl Trop Dis*. (2018) 12:e0006274. doi: 10.1371/journal.pntd.0006274

12. Gordon CA, Acosta LP, Gobert GN, Olveda RM, Ross AG, Williams GM, et al. Real-time PCR demonstrates high prevalence of *Schistosoma japonicum* in the Philippines: implications for surveillance and control. *PLoS Negl Trop Dis*. (2015) 9:e0003483. doi: 10.1371/journal.pntd.0003483

13. Cnops L, Soentjens P, Clerinx J, Van Esbroeck M. A *Schistosoma haematobium*-specific real-time PCR for diagnosis of urogenital schistosomiasis in serum samples of international travelers and migrants. *PLoS Negl Trop Dis*. (2013) 7:e2413. doi: 10.1371/journal.pntd.0002413

14. Mu Y, Cai P, Olveda RM, Ross AG, Olveda DU, McManus DP. Parasite-derived circulating microRNAs as biomarkers for the detection of human *Schistosoma japonicum* infection. *Parasitology*. (2020) 147:889–96. doi: 10.1017/S0031182019001690

15. Halili S, Grant JR, Pilotte N, Gordon CA, Williams SA. Development of a novel real-time polymerase chain reaction assay for the sensitive detection of *Schistosoma japonicum* in human stool. *PLoS Negl Trop Dis*. (2021) 15:e0009877. doi: 10.1371/journal.pntd.0009877

16. Weerakoon KG, Gordon CA, Gobert GN, Cai P, McManus DP. Optimisation of a droplet digital PCR assay for the diagnosis of *Schistosoma japonicum* infection: a duplex approach with DNA binding dye chemistry. *J Microbiol Methods*. (2016) 125:19–27. doi: 10.1016/j.mimet.2016.03.012

17. Weerakoon KG, Gordon CA, Cai P, Gobert GN, Duke M, Williams GM, et al. A novel duplex ddPCR assay for the diagnosis of schistosomiasis japonica: proof of concept in an experimental mouse model. *Parasitology*. (2017) 144:1005–15. doi: 10.1017/S003118201700021X

18. Weerakoon KG, Gordon CA, Williams GM, Cai P, Gobert GN, Olveda RM, et al. Droplet digital PCR diagnosis of human schistosomiasis: parasite cell-free DNA detection in diverse clinical samples. *J Infect Dis*. (2017) 216:1611–22. doi: 10.1093/infdis/jix521

19. Gandasegui J, Fernández-Soto P, Carranza-Rodríguez C, Pérez-Arellano JL, Vicente B, López-Abán J, et al. The rapid-heat LAMPellet method: a potential diagnostic method for human urogenital schistosomiasis. *PLoS Negl Trop Dis*. (2015) 9:e0003963. doi: 10.1371/journal.pntd.0003963

20. Gandasegui J, Fernández-Soto P, Muro A, Simões Barbosa C, Lopes de Melo F, Loyo R, et al. A field survey using LAMP assay for detection of *Schistosoma mansoni* in a low-transmission area of schistosomiasis in Umbuzeiro, Brazil: assessment in human and snail samples. *PLoS Negl Trop Dis*. (2018) 12:e0006314. doi: 10.1371/journal.pntd.0006314

21. Garcia-Bernalt Diego J, Fernandez-Soto P, Febrer-Sendra B, Crego-Vicente B, Muro A. Loop-mediated isothermal amplification in schistosomiasis. *J Clin Med*. (2021) 10:511. doi: 10.3390/jcm10030511

22. Guo Q, Zhou K, Chen C, Yue Y, Shang Z, Zhou K, et al. Development of a recombinase polymerase amplification assay for schistosomiasis japonica diagnosis in the experimental mice and domestic goats. *Front Cell Infect Microbiol*. (2021) 11:791997. doi: 10.3389/fcimb.2021.791997

23. Rostron P, Pennance T, Bakar F, Rollinson D, Knopp S, Allan F, et al. Development of a recombinase polymerase amplification (RPA) fluorescence assay for the detection of *Schistosoma haematobium*. *Parasit Vectors*. (2019) 12:514. doi: 10.1186/s13071-019-3755-6

24. Mesquita SG, Lugli EB, Matera G, Fonseca CT, Caldeira RL, Webster B. Development of real-time and lateral flow recombinase polymerase amplification assays for rapid detection of *Schistosoma mansoni*. *Front Microbiol*. (2022) 13:1043596. doi: 10.3389/fmicb.2022.1043596

25. MacGregor SR, McManus DP, Sivakumaran H, Egwang TG, Adriko M, Cai P, et al. Development of CRISPR/Cas13a-based assays for the diagnosis of schistosomiasis. *EBioMedicine*. (2023) 94:104730. doi: 10.1016/j.ebiom.2023.104730

26. Cherkaoui D, Mesquita SG, Huang D, Lugli EB, Webster BL, McKendry RA. CRISPR-assisted test for *Schistosoma haematobium*. *Sci Rep*. (2023) 13:4990. doi: 10.1038/s41598-023-31238-y

27. WHO. *Ending the neglect to attain the sustainable development goals: a road map for neglected tropical diseases 2021–2030: overview*. Geneva: World Health Organization (2020).

28. Lo NC, Bezerra FSM, Colley DG, Fleming FM, Homeida M, Kabatereine N, et al. Review of 2022 WHO guidelines on the control and elimination of schistosomiasis. *Lancet Infect Dis*. (2022) 22:e327–35. doi: 10.1016/S1473-3099(22)00221-3

29. Utzinger J, Becker S, Van Lieshout L, Van Dam G, Knopp S. New diagnostic tools in schistosomiasis. *Clin Microbiol Infect*. (2015) 21:529–42. doi: 10.1016/j.cmi.2015.03.014

30. WHO. TPP scope schistosomiasis monitoring & evaluation narrative. (2021). Available at: https://www.who.int/news-room/articles-detail/public-consultation-target-product-profiles-for-diagnostic-tests-to-meet-schistosomiasis-and-soil-transmitted-helminth-programme-needs (Accessed February 11, 2023).

31. Corstjens PL, Nyakundi RK, de Dood CJ, Kariuki TM, Ochola EA, Karanja DMS, et al. Improved sensitivity of the urine CAA lateral-flow assay for diagnosing active *Schistosoma* infections by using larger sample volumes. *Parasit Vectors*. (2015) 8:241. doi: 10.1186/s13071-015-0857-7

32. Hoekstra PT, Madinga J, Lutumba P, van Grootveld R, Brienen EAT, Corstjens PLAM, et al. Diagnosis of schistosomiasis without a microscope: evaluating circulating antigen (CCA, CAA) and DNA detection methods on banked samples of a community-based survey from DR Congo. *Trop Med Infect Dis*. (2022) 7:315. doi: 10.3390/tropicalmed7100315

33. Mewamba EM, Tiofack AAZ, Kamdem CN, Ngassam RIK, Mbagnia MCT, Nyangiri O, et al. Field assessment in Cameroon of a reader of POC-CCA lateral flow strips for the quantification of *Schistosoma mansoni* circulating cathodic antigen in urine. *PLoS Negl Trop Dis*. (2021) 15:e0009569. doi: 10.1371/journal.pntd.0009569

34. Graeff-Teixeira C, Favero V, Pascoal VF, de Souza RP, Rigo FV, Agnese LHD, et al. Low specificity of point-of-care circulating cathodic antigen (POCCCA) diagnostic test in a non-endemic area for schistosomiasis mansoni in Brazil. *Acta Trop*. (2021) 217:105863. doi: 10.1016/j.actatropica.2021.105863

35. Adriko M, Standley CJ, Tinkitina B, Tukahebwa EM, Fenwick A, Fleming FM, et al. Evaluation of circulating cathodic antigen (CCA) urine-cassette assay as a survey tool for *Schistosoma mansoni* in different transmission settings within Bugiri District, Uganda. *Acta Trop*. (2014) 136:50–7. doi: 10.1016/j.actatropica.2014.04.001

36. Mulindwa J, Namulondo J, Kitibwa A, Nassuuna J, Nyangiri OA, Kimuda MP, et al. High prevalence of *Schistosoma mansoni* infection and stunting among school age children in communities along the Albert-Nile, northern Uganda: a cross sectional study. *PLoS Negl Trop Dis*. (2022) 16:e0010570. doi: 10.1371/journal.pntd.0010570

37. Cai P, Mu Y, Weerakoon KG, Olveda RM, Ross AG, McManus DP. Performance of the point-of-care circulating cathodic antigen test in the diagnosis of schistosomiasis japonica in a human cohort from Northern Samar, the Philippines. *Infect Dis Poverty*. (2021) 10:121. doi: 10.1186/s40249-021-00905-5

38. Peralta JM, Cavalcanti MG. Is POC-CCA a truly reliable test for schistosomiasis diagnosis in low endemic areas? The trace results controversy. *PLoS Negl Trop Dis*. (2018) 12:e0006813. doi: 10.1371/journal.pntd.0006813

39. Obeng BB, Aryeetey YA, de Dood CJ, Amoah AS, Larbi IA, Deelder AM, et al. Application of a circulating-cathodic-antigen (CCA) strip test and real-time PCR, in comparison with microscopy, for the detection of *Schistosoma haematobium* in urine samples from Ghana. *Ann Trop Med Parasitol*. (2008) 102:625–33. doi: 10.1179/136485908X337490

40. Knopp S, Corstjens PL, Koukounari A, Cercamondi CI, Ame SM, Ali SM, et al. Sensitivity and specificity of a urine circulating anodic antigen test for the diagnosis of *Schistosoma haematobium* in low endemic settings. *PLoS Negl Trop Dis*. (2015) 9:e0003752. doi: 10.1371/journal.pntd.0003752

41. Ajibola O, Gulumbe BH, Eze AA, Obishakin E. Tools for detection of schistosomiasis in resource limited settings. *Med Sci (Basel)*. (2018) 6:39. doi: 10.3390/medsci6020039

42. Xu R, Feng J, Hong Y, Lv C, Zhao D, Lin J, et al. A novel colloidal gold immunochromatography assay strip for the diagnosis of schistosomiasis japonica in domestic animals. *Infect Dis Poverty*. (2017) 6:84. doi: 10.1186/s40249-017-0297-z

43. Shen Y, Ji R, Chai R, Yuan N, Zhang J, Jing Y, et al. A novel fluorescence immunochromatographic assay strip for the diagnosis of schistosomiasis japonica. *Parasit Vectors*. (2021) 14:8. doi: 10.1186/s13071-020-04511-6

44. Pearson MS, Tedla BA, Mekonnen GG, Proietti C, Becker L, Nakajima R, et al. Immunomics-guided discovery of serum and urine antibodies for diagnosing urogenital schistosomiasis: a biomarker identification study. *Lancet Microbe*. (2021) 2:e617–26. doi: 10.1016/S2666-5247(21)00150-6

45. Jiang SF, Zhang XP, Li BL, He YY, Liu J, Tang YH, et al. Evaluation of partially purified soluble egg antigens in colloidal gold immunochromatography assay card for rapid detection of anti-*Schistosoma japonicum* antibodies. *Southeast Asian J Trop Med Public Health*. (2014) 45:568–75.

46. Cai P, Weerakoon KG, Mu Y, Olveda DU, Piao X, Liu S, et al. A parallel comparison of antigen candidates for development of an optimized serological diagnosis of schistosomiasis japonica in the Philippines. *EBioMedicine*. (2017) 24:237–46. doi: 10.1016/j.ebiom.2017.09.011

47. Cai P, Weerakoon KG, Mu Y, Olveda RM, Ross AG, Olveda DU, et al. Comparison of Kato Katz, antibody-based ELISA and droplet digital PCR diagnosis of schistosomiasis japonica: lessons learnt from a setting of low infection intensity. *PLoS Negl Trop Dis*. (2019) 13:e0007228. doi: 10.1371/journal.pntd.0007228

48. Liu S, Zhou X, Piao X, Hou N, Shen Y, Zou Y, et al. Saposin-like proteins, a multigene family of *Schistosoma* species, are biomarkers for the Immunodiagnosis of schistosomiasis japonica. *J Infect Dis*. (2016) 214:1225–34. doi: 10.1093/infdis/jiw188

49. Mu Y, McManus DP, Gordon CA, You H, Ross AG, Olveda RM, et al. Development and assessment of a novel gold immunochromatographic assay for the diagnosis of schistosomiasis japonica. *Front Immunol*. (2023) 14:1165480. doi: 10.3389/fimmu.2023.1165480

50. Landis JR, Koch GG. The measurement of observer agreement for categorical data. *Biometrics*. (1977) 33:159–74. doi: 10.2307/2529310

51. Ross AG, Olveda RM, Chy D, Olveda DU, Li Y, Harn DA, et al. Can mass drug administration lead to the sustainable control of schistosomiasis? *J Infect Dis*. (2015) 211:283–9. doi: 10.1093/infdis/jiu416

52. Mu Y, Weerakoon KG, Olveda RM, Ross AG, McManus DP, Cai P. Diagnostic performance of a urine-based ELISA assay for the screening of human schistosomiasis japonica: a comparative study. *Front Microbiol*. (2022) 13:1051575. doi: 10.3389/fmicb.2022.1051575

53. Wang W, Bergquist R, King CH, Yang K. Elimination of schistosomiasis in China: current status and future prospects. *PLoS Negl Trop Dis*. (2021) 15:e0009578. doi: 10.1371/journal.pntd.0009578

54. DOH. (2018) Schistosomiasis control and elimination program. Available at: https://doh.gov.ph/node/211 (Accessed May 23, 2023).

55. DOH. Guidelines on the implementation of the harmonized schedule and combined mass drug administration (HSCMDA) for the prevention and control of lymphatic filariasis. schistosomiasis, and soil-transmitted helminths (DOH Memorandum No 2016-0212). (2016).

56. Simundic AM. Measures of diagnostic accuracy: basic definitions. *EJIFCC*. (2009) 19:203–11.

57. Xie SY, Yuan M, Ji MJ, Hu F, Li ZJ, Liu YM, et al. Immune responses result in misdiagnosis of *Schistosoma japonicum* by immunodiagnosis kits in egg-positive patients living in a low schistosomiasis transmission area of China. *Parasit Vectors*. (2014) 7:95. doi: 10.1186/1756-3305-7-95

58. Guegan H, Fillaux J, Charpentier E, Robert-Gangneux F, Chauvin P, Guemas E, et al. Real-time PCR for diagnosis of imported schistosomiasis. *PLoS Negl Trop Dis*. (2019) 13:e0007711. doi: 10.1371/journal.pntd.0007711

59. Sanneh B, Joof E, Sanyang AM, Renneker K, Camara Y, Sey AP, et al. Field evaluation of a schistosome circulating cathodic antigen rapid test kit at point-of-care for mapping of schistosomiasis endemic districts in the Gambia. *PLoS One*. (2017) 12:e0182003. doi: 10.1371/journal.pone.0182003

60. Fuss A, Mazigo HD, Tappe D, Kasang C, Mueller A. Comparison of sensitivity and specificity of three diagnostic tests to detect *Schistosoma mansoni* infections in school children in Mwanza region, Tanzania. *PLoS One*. (2018) 13:e0202499. doi: 10.1371/journal.pone.0202499

61. Fusco D, Rakotozandrindrainy R, Rakotoarivelo RA, Andrianarivelo MR, Rakotozandrindrainy N, Rasamoelina T, et al. A cluster randomized controlled trial for assessing POC-CCA test based praziquantel treatment for schistosomiasis control in pregnant women and their young children: study protocol of the freeBILy clinical trial in Madagascar. *Trials*. (2021) 22:822. doi: 10.1186/s13063-021-05769-6

62. Neumayr A, Chernet A, Sydow V, Kling K, Kuenzli E, Marti H, et al. Performance of the point-of-care circulating cathodic antigen (POC-CCA) urine cassette test for follow-up after treatment of *S. mansoni* infection in Eritrean refugees. *Travel Med Infect Dis*. (2019) 28:59–63. doi: 10.1016/j.tmaid.2018.09.004

63. Kittur N, Castleman JD, Campbell CH, King CH, Colley DG. Comparison of *Schistosoma mansoni* prevalence and intensity of infection, as determined by the circulating cathodic antigen urine assay or by the Kato-Katz fecal assay: a systematic review. *Am J Trop Med Hyg*. (2016) 94:605–10. doi: 10.4269/ajtmh.15-0725

64. Vonghachack Y, Sayasone S, Khieu V, Bergquist R, van Dam GJ, Hoekstra PT, et al. Comparison of novel and standard diagnostic tools for the detection of *Schistosoma mekongi* infection in Lao People's Democratic Republic and Cambodia. *Infect Dis Poverty*. (2017) 6:127. doi: 10.1186/s40249-017-0335-x

65. Homsana A, Odermatt P, Southisavath P, Yajima A, Sayasone S. Cross-reaction of POC-CCA urine test for detection of *Schistosoma mekongi* in Lao PDR: a cross-sectional study. *Infect Dis Poverty*. (2020) 9:114. doi: 10.1186/s40249-020-00733-z

66. Schary W, Paskali F, Rentschler S, Ruppert C, Wagner GE, Steinmetz I, et al. Open-source, adaptable, all-in-one smartphone-based system for quantitative analysis of point-of-care diagnostics. *Diagnostics (Basel)*. (2022) 12:589. doi: 10.3390/diagnostics12030589

67. Bossuyt PM, Reitsma JB, Bruns DE, Gatsonis CA, Glasziou PP, Irwig L, et al. STARD 2015: an updated list of essential items for reporting diagnostic accuracy studies. *BMJ*. (2015) 351:h5527. doi: 10.1136/bmj.h5527

68. Kojabad AA, Farzanehpour M, Galeh HEG, Dorostkar R, Jafarpour A, Bolandian M, et al. Droplet digital PCR of viral DNA/RNA, current progress, challenges, and future perspectives. *J Med Virol*. (2021) 93:4182–97. doi: 10.1002/jmv.26846

69. Choi C-H, Kim E, Yang S-M, Kim DS, Suh SM, Lee GY, et al. Comparison of real-time PCR and droplet digital PCR for the quantitative detection of *Lactiplantibacillus plantarum* subsp. *plantarum*. *Foods*. (2022) 11:1331. doi: 10.3390/foods11091331

70. Mahendran P, Liew JWK, Amir A, Ching XT, Lau YL. Droplet digital polymerase chain reaction (ddPCR) for the detection of *plasmodium knowlesi* and *plasmodium vivax*. *Malar J*. (2020) 19:241. doi: 10.1186/s12936-020-03314-5

71. WHO. *Guideline on control and elimination of human schistosomiasis*. Geneva: World Health Organization (2022).

frontiers | Frontiers in Immunology

TYPE Original Research
PUBLISHED 11 September 2023
DOI 10.3389/fimmu.2023.1216710

OPEN ACCESS

EDITED BY
Thiago Almeida Pereira,
Stanford University, United States

REVIEWED BY
Catherine A. Gordon,
The University of Queensland, Australia
Marta Guimarães Cavalanti,
Federal University of Rio de Janeiro, Brazil

*CORRESPONDENCE
Abdallah Zacharia
naayz@ymail.com

RECEIVED 04 May 2023
ACCEPTED 28 August 2023
PUBLISHED 11 September 2023

CITATION
Zacharia A, Makene T, Kinabo C, Ogweno G, Lyamuya F and Ngasala B (2023) Dried urine spot method for detection of *Schistosoma mansoni* circulating cathodic antigen in resource-limited settings: a proof of concept study. *Front. Immunol.* 14:1216710. doi: 10.3389/fimmu.2023.1216710

Dried urine spot method for detection of *Schistosoma mansoni* circulating cathodic antigen in resource-limited settings: a proof of concept study

Abdallah Zacharia[1]*, Twilumba Makene[1], Clemence Kinabo[1], George Ogweno[2], Faraja Lyamuya[3] and Billy Ngasala[1]

[1]Department of Parasitology and Medical Entomology, Muhimbili University of Health and Allied Sciences, Dar es Salaam, Tanzania, [2]National Institute for Medical Research, Mwanza, Tanzania, [3]Neglected Tropical Diseases Control Program, Ministry of Health, Dodoma, Tanzania

Background: Among the challenges in schistosomiasis surveillance and mapping surveys is the lack of a sensitive diagnostic method especially in low transmission setting. Currently, the WHO recommends the use point-of-care circulating cathodic antigen (Schisto POC-CCA) tests for surveillance and mapping of intestinal schistosomiasis. However, Schisto POC-CCA test has its drawbacks, one of which is the timely availability of test kits. One approach to overcoming this challenge is to develop a low-cost sampling method that allows for the collection and transport of urine specimens even in resource-limited settings.

Objective: To develop a simple and efficient method for the collection and detection of *Schistosoma mansoni* (*S. mansoni*) CCA using urine spotted onto filter paper.

Methodology: To develop a dried urine spot (DUS) method, various dried matrix extraction parameters were tested and optimized using predesigned steps. The parameters include the size of filter paper (determined by the number of punches), volume of solvents, and type of solvent. Moreover, we optimized the incubation conditions (time and temperature). Urine and stool specimens to conduct the experiments were collected from volunteer fishermen in Mwanza and this project staff. Data were entered into the Microsoft Excel spreadsheet and IBM Statistical Package for the Social Sciences, version 20 for analysis.

Results: The optimal results were obtained when the procedure was run under the following conditions: Five punches of filter paper containing DUS were dissolved in 150 µl of distilled water and incubated at room temperature for 24 hours in an Eppendorf tube. More than 93% of the assays performed under these conditions produced results that were either comparable to or significantly better than the standard method.

Conclusion: This study demonstrates the feasibility of collecting urine specimen (DUS) using filter paper and detecting *Schistosoma* CCA from DUS specimen using the Schisto POC-CCA cassette test.

KEYWORDS

dried matrix spot, dried urine spot, extraction, elution, Schistosoma mansoni, circulating cathodic antigens, filter paper

1 Introduction

Schistosomiasis is a parasitic disease caused by a trematode that belongs to the genus *Schistosoma*. Globally, approximately 240 million people are infected (about 90% live in sub-Saharan Africa), causing about 70 million disability-adjusted life years lost (1, 2). Widely used schistosomiasis diagnostic techniques include the Kato-Katz thick-smear and urine filtration for intestinal schistosomiasis and urogenital schistosomiasis respectively (3). But these methods have several pitfalls. First, they are time-consuming and require skilled laboratory technologists. In addition, they need good-quality microscopes and light sources (electricity), which makes them difficult to use in resource-limited areas (4). Moreover, the procedures are less sensitive when used in low-endemic settings (3). Hence, a highly sensitive and rapid diagnostic test is of paramount importance for successful schistosomiasis surveillance and mapping during the elimination stage (5).

Recently, there has been the development of more sensitive diagnostic tests based on the detection of *Schistosoma* antigens. The most commonly developed tests utilize the circulating antigens produced by adult worms. These antigens include circulating cathodic antigens (CCA) and circulating anodic antigens (CAA) (6). The CCA and CAA detection tests are useful for control programs because they are more sensitive than microscopy and hence provide more accurate information regarding the prevalence of *Schistosoma* infections (7, 8). Currently, the WHO has recommended the use of point-of-care CCA cassettes (Schisto POC-CCA) for mapping the prevalence and surveillance of *Schistosoma mansoni* by control programs (9). Despite its high sensitivity and specificity, the CAA test could not be used in the field as it involves steps that require laboratory equipment (8, 10). But also, the Schisto POC-CCA cassettes are commercially available from a single manufacture (Rapid Medical Diagnostics; Cape Town, South Africa) (11). The presence of a single manufacture impedes the timely availability of the tests (10). Additionally, schistosomiasis control programs in most endemic countries rely on the support of their implementing partners (donors), and the implementation of their activities are heavily reliant on the availability of the support from those partners (12). Furthermore, there are times when, as was the case during the COVID-19 pandemic, industrial production is reduced and transportation of materials within and across continents is difficult. Therefore, if there is a delay in receiving Schisto POC-CCA cassettes from the supplier or the support from the partners to purchase the cassettes, the program may require the use of cost-effective sample collection and storage methods that could be used even in a resource-limited setting where there is a high burden of schistosomiasis, especially when time for data (specimen) collection is a critical aspect of the particular work. This demand for the development of a simple and cost-effective sampling technique that will be used during sample collection, transportation, and storage in resource-limited settings.

Schistosoma circulating antigens are stable and detectable in urine, blood, and serum specimens. Urine specimens have several advantages over blood and serum. First, a sample of urine can stay for several days without a cold chain. Also, urine collection is noninvasive and doesn't require trained medical personnel. Moreover, a large volume can easily be collected (11). However, liquid urine has an increased risk of infection (leakage). Furthermore, in resource-limited settings, the liquid urine is difficult to transport (heavy load of urine containers) and store (large space requirement). A dried urine spot (DUS) using filter papers is considered simple and cost-effective compared to liquid urine. DUS can be easily prepared in a field setting with less skills, easily transported, and stored with a minimum risk of infection (13). Studies have reported the use of filter papers for the detection of *Schistosoma* eggs and nucleic acid amplification (13, 14). However, no study was conducted to determine the use of DUS for the detection of *Schistosoma* antigens.

We aimed to develop a simple, less expensive and efficient method for collecting and detecting *Schistosoma mansoni* (*S. mansoni*) CCA using filter paper-based DUS in resource-limited settings. The method was developed by assessing and optimizing the performance of various dried matrix spot (DMS) parameters in order to find those that best fit for the filter paper-based DUS for maximum detection of *Schistosoma* CCA using the Schisto POC-CCA cassette test.

2 Methods

2.1 Type of the study

This laboratory-based experimental study was conducted to devise a method for collecting DUS on filter paper and extracting *S. mansoni* CCA from the collected DUS. The experimental study was

carried out to test the feasibility of the predesigned steps for filter paper-based DUS method, as well as optimization of the materials and reagents to be used in the procedure and some parameters such as incubation temperature, solvent type and volume, and incubation time. The experiments were performed at parasitology laboratory of the National Institute for Medical Research (Mwanza Centre).

2.2 Development of dried urine spot method

2.2.1 Sample collection

Fourteen volunteer fishermen aged 18 and older, as well as one volunteer study staff member with no history of exposure to *S. mansoni* risk environments, provided urine and stool specimens. Fishermen and volunteer staff member were given pre-labeled wide-mouthed urine and stool containers after providing informed consent for the collection of fresh urine and stool specimens. They were asked to collect approximately 30 mL of fresh urine and about 20 g of fresh stool specimens. Both urine and stool specimens were immediately transported to the National Institute for Medical Research (NIMR) Mwanza laboratory and processed using the Schisto POC-CCA cassettes (Rapid Medical Diagnostics, Cape Town, South Africa; batch number 220701075), and filtration technique (Shenzhen combined biotech co., Ltd (15), Guangdong, China) for direct urine tests, while stool samples were processed using the formal-ether sedimentation method and Kato-Katz techniques (Vestergaard Frandesen Group, Lausanne Switzerland) (16). The results of all procedures were reported as positive in case of the presence of *Schistosoma* eggs or CCA and negative in case of the absence of *Schistosoma* eggs or CCA. Furthermore, positive Schisto POC-CCA test results were further classified as trace, 1+, 2+, and 3+ according to the visibility of colour reaction of the particular test (17), whereas Kato-Katz results were further classified as light (1-99 EPG), moderate (100-399 EPG), and heavy (> 400 EPG) intensities (18). As with the direct urine test, the Schisto POC-CCA cassette procedure was used to conduct direct tests of the three solvents (normal saline, phosphate buffered saline, and distilled water) as part of quality control.

2.2.2 Preparation of dried urine spots

Using a Pasteur pipette, urine was spotted on prelabeled 3x4-inch Whatman No. 3 (GE Healthcare UK Limited, Buckinghamshire, UK; Lot number 16988762) filter papers. To aid in the identification of the spots both immediately after application and after drying, urine was spotted on four printed circles. Five to 6 drops of urine were sufficient to saturate one printed circle. Four types of DUS were prepared using three positive urine specimens from fishermen with Kato-Katz (standard Schisto POC CCA) results: one light (2+), one moderate (3+), and one heavy (3+), as well as one urine sample from volunteer staff with negative Kato-Katz and Schisto POC-CCA results. The spotted filter papers were air dried for 24 hours in a fly-free box before being stored at room temperature in a small ziplock bag with a desiccant. The same procedure was used to prepare dried solvent spots using the three extraction solvents tested during the experiments (normal saline, phosphate buffered saline, and distilled water) as no template controls.

2.2.3 Optimization of the number of punches and solvent volume

A series of trial-and-error experiments were conducted to determine the number of DUS punches that can be dissolved in a solvent and yield a sufficient volume (2 drops of Schisto POC-CCA pipette ≈ 100 µl) of eluate for Schisto POC-CCA cassette testing, as well as having strong visual (colour) resemblance with original urine sample. Briefly, using a single hole handheld punching machine (6 mm diameter), filter paper with DUS was punched into an Eppendorf tube (1.5 ml capacity) and a specific volume of solvent (phosphate buffered saline, distilled water or normal saline) was added. The Eppendorf tube was then incubated at room temperature for approximately 2 hours. Following incubation, a micropipette with a 100 µl marked tip was used to measure the volume of the eluate before visual (colour) observation. The visual observation was given a grade of weak if the elute just slightly resembled the original urine, moderate if it did so somewhat, and strong if it did so closely. The trial started with 3 punches into 120 µl of solvent and ended with 5 punches into 150 µl of solvent.

2.2.4 Extraction of *Schistosoma mansoni* circulating cathodic antigen

The maximum recovery of three different eluting solvents (phosphate buffered saline pH 9, distilled water, and normal saline) at different temperatures (4^0 C, room temperature, and 37^0 C) and time conditions (2 hours and 24 hours) were determined 24 hours and 7 days after storing DUS in ziplock bags at room temperature. Figure 1 depicts the step-by-step procedure. In brief, the filter paper containing DUS as prepared in Section 2.2.2 was transferred from the storage area to the punching bench. Then, the precise location of the specimen spot on the filter paper was pinpointed. This was followed by punching 5 DUS disks (punches with 6 mm diameter each) in a prelabeled Eppendorf tube. The Eppendorf tube containing the 5 punches was then filled with one of the three solvents in the amount of 150 µl. The five DUS punches were pressed to the bottom of the tube with the pointed end of an unused micropipette tip to ensure that they were completely dissolved in the solvent. The tube was then incubated at one of three temperatures and one of the two incubation time. Therefore, 36 Eppendorf tubes were prepared on each of the four types of DUS specimens (18 Eppendorf tubes after 24 hours and the other 18 Eppendorf tubes 7 days after storage). Each one of the 18 Eppendorf tubes differed from the others in one of the following ways: the type of solvent it contained, the temperature at which it was incubated, or the time of incubation (Figure 2). As part of quality control, the same procedure was performed for dried solvent spots.

2.2.5 Detection of *Schistosoma mansoni* circulating cathodic antigens

The *S. mansoni* CCA detection was carried out in accordance with the Schisto POC-CCA procedure manual, with minor

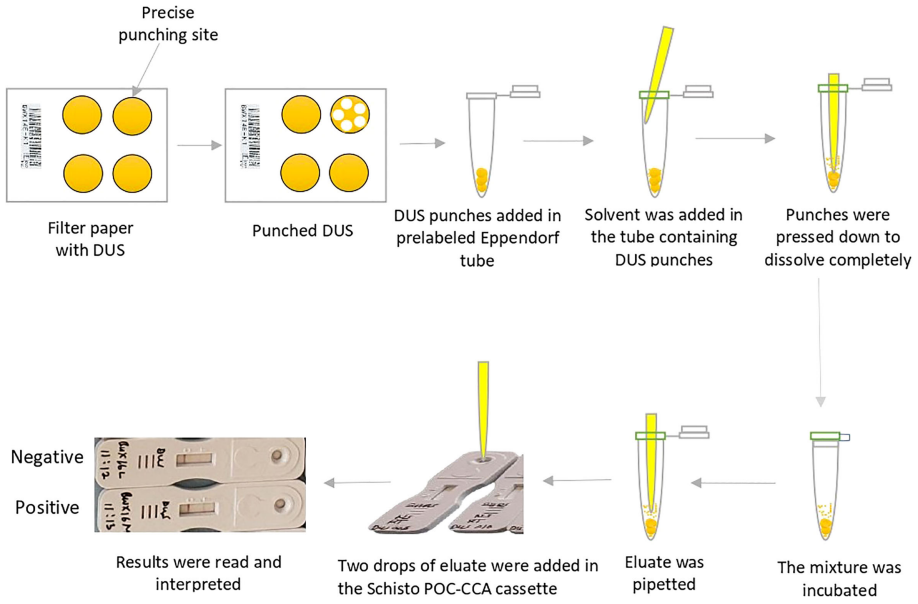

FIGURE 1
Step-by-step procedure for *Schistosoma mansoni* circulating cathodic antigens extraction from dried urine spot.

modifications. To summarize, all assay materials including Eppendorf tubes containing the mixture of filter paper-based DUS punches and the extracting solvents were first brought to room temperature. To separate the eluate from the punches and allow the pipette to reach the bottom of the tube, the dissolved punches were pressed on one side of the Eppendorf tube with the pipette provided in the Schisto POC-CCA kit. The pipette was then removed from the tube, squeezed, and reinserted with the tip touching the bottom of the tube. By gently releasing the pipette, the eluate was allowed to fill up. Two drops of eluate (equivalent to 90-100 µl) were transferred into the circular well of the prelabeled Schisto POC-CCA test cassette by gently squeezing the pipette. The eluate was allowed to completely absorb into the specimen pad contained within the circular well. The time for reading the results was then marked on the test cassette. Twenty minutes after the sample was added to the circular well, the result was read and recorded in the results form as negative or positive (trace, 1+, 2+, or 3+) (15).

2.3 Data analysis

The collected data was entered into Microsoft Excel spreadsheet before being transferred to the Statistical Package for the Social Sciences Version 20 for analysis. The prevalence of *Schistosoma* infection among fishermen was calculated for each diagnostic technique. For each DUS extraction condition, the visual Schisto POC-CCA cassette score of the Schisto POC-CCA test was compared to the score of its respective standard Schisto POC-CCA test. The score was classified as below if it was below the standard, same if it was similar to the standard, and high if it was higher than the standard. Each DUS extraction condition's performance was evaluated by looking at the proportion of their tests that scored below, similar, and higher than the standard.

2.4 Ethics statement

The study protocol was reviewed and approved by the Muhimbili University of Health and Allied Sciences Ethical Review Board (reference no. DA.282/298/01.C/1297). Permission to conduct the study in the Mwanza region was requested from the President's Office - Regional Administration and Local Government, and the Regional Administrative Secretary of the Mwanza region. Specimens for the experiments were obtained from 14 anonymised volunteer fishermen at a fishing camp along Lake Victoria in the Mwanza region, as well as one volunteer project staff member who had no history of *S. mansoni* exposure. The participants were informed about the purpose of this study and gave their written consent. All participants were informed of their schistosomiasis testing results, and all *Schistosoma*-infected participants were offered free treatment (single 40mg/kg dose of Praziquantel).

3 Results

3.1 Schistosomiasis infection among fishermen

According to the formal-ether, Kato-Katz, and Schisto POC-CCA techniques, the number of *S. mansoni* positive fishermen were 7, 6, and 9, respectively. The average intensity of infection was 172 EPG, with a range of 24 to 528 EPG. Of the 6 positive fishermen by

the Kato-Katz technique, 3 had light-intensity of infections, 2 had moderate-intensity of infections and 1 had heavy-intensity of infection. Out of 9 fishermen with Schisto POC-CCA positive results, 5 had 2+ and 4 had 3+ visual score results. There was no *Schistosoma haematobium* egg in any of the fishermen urine and volunteer project staff. Furthermore, all direct solvent tests yielded negative results.

3.2 Optimization of the number of punches and solvent volume

Table 1 shows the results of each trial conducted to optimize the number of DUS punches and solvent volume. The results show that the trial using 5 punches in 150 µl of any of the three solvents produced a sufficient volume of eluate for Schisto POC-CCA cassette testing. Furthermore, the eluate colour from this trial (5 punches in 150 µl) strongly matched the original urine sample.

3.3 Performance of optimized dried urine spot extraction conditions

A total of 144 assays were run to evaluate different conditions for *S. mansoni* CCA extraction from DUS samples. These conditions included the type of extraction solvent, incubation time, and temperature (Figure 2). When 24-hour-old DUS specimens were incubated for 24 hours at room temperature or 37^0 C, the same results as the standard were obtained for all solvents. Similar results were obtained when DUS samples dissolved in normal saline and distilled water were incubated for 2 hours at 4^0 C, 2 hours at room temperature, 2 hours at 37^0 C, and 24 hours at 4^0 C. It was found that, when a DUS sample with Kato-Katz light intensity results was dissolved in phosphate buffered saline and incubated for 2 hours at 4^0 C, 2 hours at room temperature, 2 hours at 37^0 C, and 24 hours at 4^0 C, it had poor CCA recovery when compared to the same urine sample tested using the standard direct urine test (Figure 3). When 7 days-old DUS specimens were incubated for 24 hours at any of the 3 temperatures, the same or better results than the standard were obtained for all solvents. The DUS (with Kato-Katz light intensity results) dissolved in normal saline incubated for 2 hours at 4^0 C, room temperature, and 37^0 C, and in distilled water and phosphate buffered saline incubated for 2 hours at 37 ^{0}C, have lower CCA recovery when compared to the standard direct urine test. The DUS (with Kato-Katz heavy intensity results) dissolved in normal saline incubated for 2 hours at 4 ^{0}C and 37^0 C, dissolved in distilled water incubated for 2 hours at 4^0 C, and dissolved in phosphate buffered saline incubated for 2 hours at 37 ^{0}C all showed low recovery (Figure 4). Furthermore, all dried solvent spots yielded negative results for both 24 hours-old and 7 days-old samples.

In general, distilled water outperformed other solvents across all DUS assays when compared to the standard assays. A total of 47 (98.0%) out of 48 DUS assays that used distilled water produced the same or high performance than their respective standard assays, while 43 (89.6%) DUS assays that used normal saline and 40 (83.3%) DUS assays that used phosphate buffered saline produced the same or high performance than their respective standard assays. Furthermore, 2 (4.2%) DUS assays that used distilled water outperformed their respective standard assays, while only 1 (2.1%) DUS assay for each of normal saline and phosphate buffered saline outperformed their respective standard assays (Table 2).

In terms of incubation temperature, the DUS assays performed better at room temperature than at other temperatures (4^0 C and 37^0 C). A total of 45 (93.7%) out of 48 DUS assays incubated at room temperature yielded the same or higher performance than their respective standard assays, while 43 (89.6%) DUS assays incubated at 4^0 C and 42 (87.5%) DUS assays incubated at 37 ^{0}C yielded the same or higher performance than their respective standard assays. Furthermore, 3 (6.2%) DUS assays incubated at room temperature outperformed their respective standard assays, while 1 (2.1%) DUS assay incubated at 37^0 C outperformed its respective standard assay. No DUS assay had performed better than its respective standard assay when incubated at 4^0 C (Table 3).

Regarding incubation time, DUS assays incubated for 24 hours performed better than those incubated for 2 hours when both are compared to the standard assays. A total of 71 (98.7%) out of 72 DUS assays incubated for 24 hours yielded the same or higher performance than their respective standard tests, while 59 (81.9%) out of 72 DUS assays incubated for 2 hours yielded the same or higher performance as their respective standard assays. Furthermore, 4 (5.6%) DUS assays incubated for 24 hours outperformed their respective standard assays. No DUS assay had performed better than its respective standard assay when incubated for 2 hours (Table 4).

TABLE 1 Summarizes the results of optimization of DUS punches and solvent volume.

Trial no.	Number of punches	Volume of solvent (µl)	Resulted eluate volume (µl)	Visual (colour) resemblance with original urine sample
1st	3	120	< 100	Strong
2nd	3	135	≥ 100	Week
3rd	4	135	< 100	Strong
4th	4	150	≥ 100	Moderate
5th	5	150	≥ 100	Strong

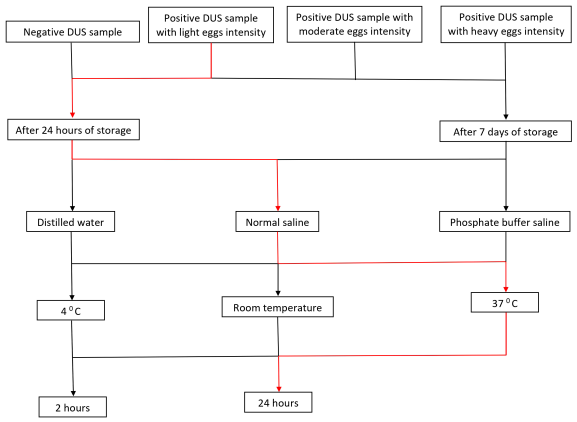

FIGURE 2
Flow chart illustrating the conditions that have been included in each experiment. Note: a red line depicts an assay experiment performed on the DUS sample with light intensity of infection that has been stored for 24 hours. The assay has been done using normal saline as extraction solvent, incubated at 37 ^{0}C for 24 hours.

4 Discussion

DMS is a sample collection strategy that involves soaking and drying a small volume of a fluid, such as blood, urine, saliva or sweat, onto filter paper (19). DMS is increasingly being used to collect specimens for various purposes ranging from quantitative approaches like therapeutic drug monitoring to qualitative approaches like disease diagnosis or doping testing (19). The method has had a significant impact on several fields of study, including newborn screening, epidemiology (field testing), infectious diseases, environmental research, forensics, therapeutic drug monitoring, illicit drug analysis, toxicology, and toxico- and pharmacokinetic studies of drugs and candidate drugs (20). DUS is a DMS method that has recently gained a lot of attention. DUS sampling is a filter paper method that has been used to collect urine to test for by-products of adrenal and sex steroid hormones and their respective metabolic pathways, providing a gauge for understanding the body's hormone metabolism (21, 22). Furthermore, DUS sampling has been used to test drugs (19), neurotransmitters, and elements such as iodine and metals such as arsenic (21, 22). Barry and colleagues were the first to develop procedures for DUS sampling method during procedures for the detection of phenylketonuria and the *Lactobacillus arabinosus* microbiological assay (23, 24).

The WHO recommends the use of Schisto POC-CCA for mapping of schistosomiasis of *Schistosoma mansoni* in endemic countries (25). This study developed methods for preparation of DUS on filter papers and detecting *Schistosoma* CCA in the DUS eluate using the Schisto POC-CCA cassette test. Many parameters influence assay performance and must be assessed and optimized, as in most assay development studies, to produce a standardized protocol that gives maximum recovery (maximum results) of the analyte of interest. The efficiency of the assay parameters must be assessed and optimized in order to produce a standardized protocol before an assay can be provisionally accepted and moved on to the validation stage (26). In this study, parameters assessment and optimization included trial and error experiments with extensive reagents (solvents) and filter paper measurements and evaluation of critical components (volume of urine to saturate on filter paper, volume of solvent, solvent type, and number of filter paper punches to dissolve) as well as assay conditions (incubation times and incubation temperatures), and result interpretation (definition of negative and positive results, further classification of positive results, and their meaning).

Several methods for preparing DUS have been tested and used. The methods include directly soaking filter paper in client urine. In this method, the client is instructed to saturate the provided filter paper with his or her urine by urinating directly on it. The other method is for a client to collect his or her urine in a container and then dip the provided filter paper in the urine. After saturating the filter paper, the client is instructed to hang it on a towel rack or other object to dry for 2 to 24 hours at room temperature without allowing the filter paper to touch anything. After drying, the client should place the filter paper in a ziploc bag with desiccant and bring it to the laboratory in person or by mail. These methods are commonly used for clients who require 24-hour urine collection and are typically performed at the client's home (27, 28). The third method involves providing a client with a urine container in which the urine is collected and delivered to the laboratory or expert personnel in the field. The personnel then complete all of the remaining procedures for preparing DUS. Personnel may prepare the DUS in this procedure by either dipping the filter paper in the urine container or transferring (spotting) urine onto the filter paper using pipette (29, 30). In our study, we opted for the third method of DUS preparation; transferring (spotting) urine onto the filter paper by using pipette. This is because most of the clients in schistosomiasis studies are children or people with very low knowledge of handling urine as potentially hazardous specimen. In addition, the use of expert personnel is ideal because it ensure that appropriate volume of urine (5-6 drops for the case of our study) is saturated and evenly distributed on the required area of the filter paper as it is usually assumed that the analytes (including *Schistosoma* CCA) are distributed uniformly in the urine.

Analyte extraction is the most important stage of DMS (including DUS) sample preparation before analyte detection. Elution is the commonly used method for extracting analytes from DUS. Through this method, analytes are extracted from DUS by washing the spots with a suitable solvent (19, 31, 32). In this study, we also employed elution to extract *Schistosoma* CCA from DUS on filter paper. Because the amount of urine specimen spotted onto filter paper is limited, the elusion process is critical for obtaining sufficient analytes concentrations for accurate test results. Therefore, the analyte concentration in the eluate from a DUS must quantitatively reflect the original liquid urine sample concentration. Researchers have tried to identify things that must be considered during the elution process in order to achieve maximum dissociation of analyte from filter paper. The first things to consider are DUS size and solvent volume. Before using DUS specimens in a specific test, appropriate-sized pieces of filter paper specimens must be sampled by punching from the large DUS paper and dissolving them in an appropriate volume of solvent. To ensure that we achieve maximum extraction of *Schistosoma* CCA, we considered DUS size by optimizing the various number of DUS punches and dissolving them in different solvent volumes (Table 1). We assumed that by

10.3389/fimmu.2023.1216710

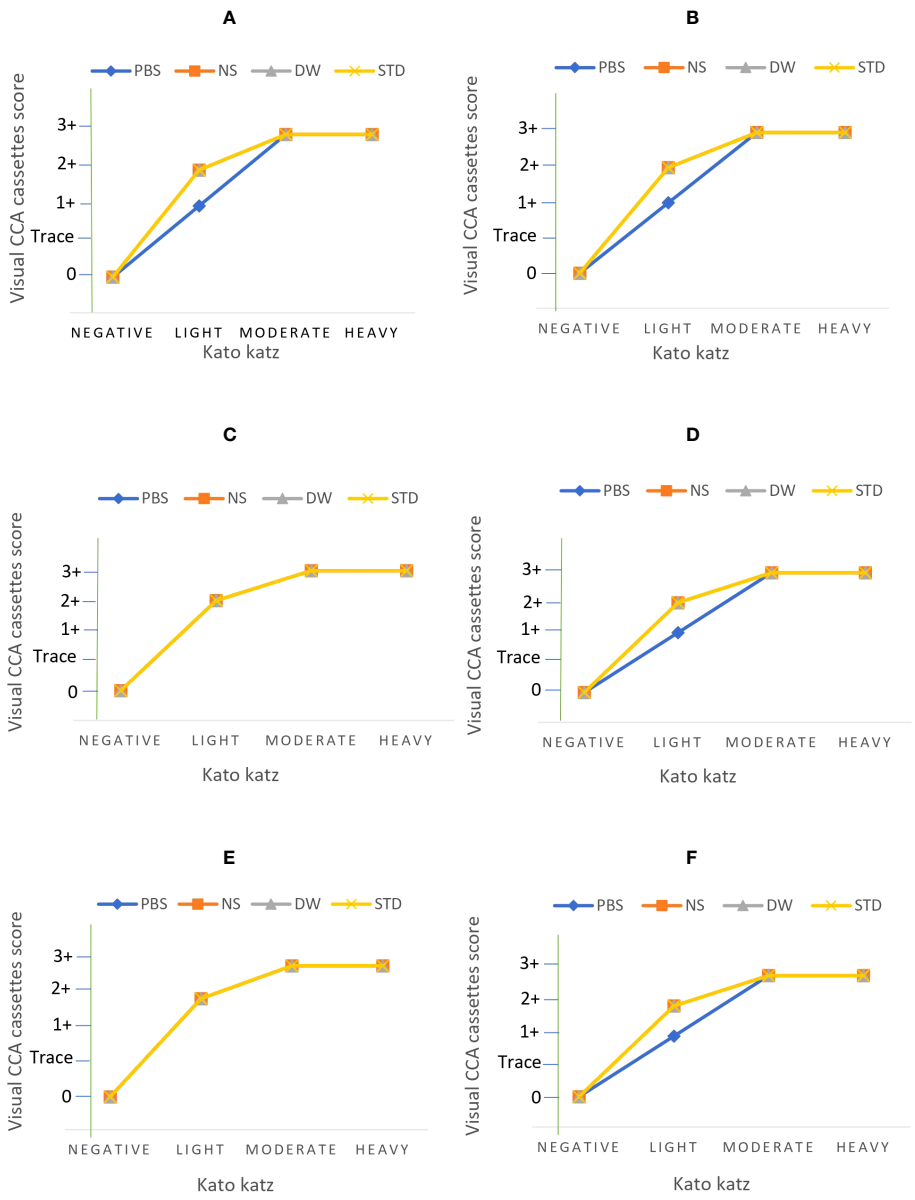

FIGURE 3
Results of assays performed on DUS samples 24 hours after preparation at the following extraction conditions; **(A)** 4 ^{0}C incubation for 24 hours, **(B)** 4 ^{0}C incubation for 2 hours, **(C)** room temperature incubation for 24 hours, **(D)** room temperature incubation for 2 hours, **(E)** 37 ^{0}C incubation for 24 hours, and **(F)** 37 ^{0}C incubation for 2 hours. Note: PBS stands for phosphate buffered saline, NS stands for normal saline, DW stands for distilled water, and STD stands for standard diagnostic test.

eluting DUS in such a way that the eluate resembled the original urine sample, most of the analytes (including *Schistosoma* CCA) would be dissociated from the filter paper in greater quantities. In this study, this assumption was met by dissolving five punches (6 mm diameter each) of DUS made on Whatman 3 filter paper in 150 µl of each of the three solvents (distilled water, phosphate buffered saline, and normal saline).

The other parameter that should be taken into consideration during DUS elution is the type of solvent used. The effects of different elution solvents on the DMS analytes concentrations in eluate have been extensively evaluated and need to be taken into consideration when developing a DMS method (33). For example, a urine sample may contain multiple excreted analytes; failing to adequately select the appropriate elution solvent may result in increased extraction of non-target analytes, increasing the possibility of cross-reactivity and, ultimately, a decreased ability to detect the analyte of interest by a specific diagnostic test method. Furthermore, some elution solvents may react and denature the analyte of interest, reducing its detection. We did not look into the chemical reactions that take place between the solvents we assessed and *Schistosoma* CCA. However, because the *Schistosoma* CCA is a glycoprotein, we attempted to use the most common solvents used for protein extraction (distilled water, phosphate buffered saline and normal saline). Our findings showed that, among these solvents, distilled water performed better than the other two solvents. When compared to phosphate buffered saline and normal saline, aqueous

10.3389/fimmu.2023.1216710

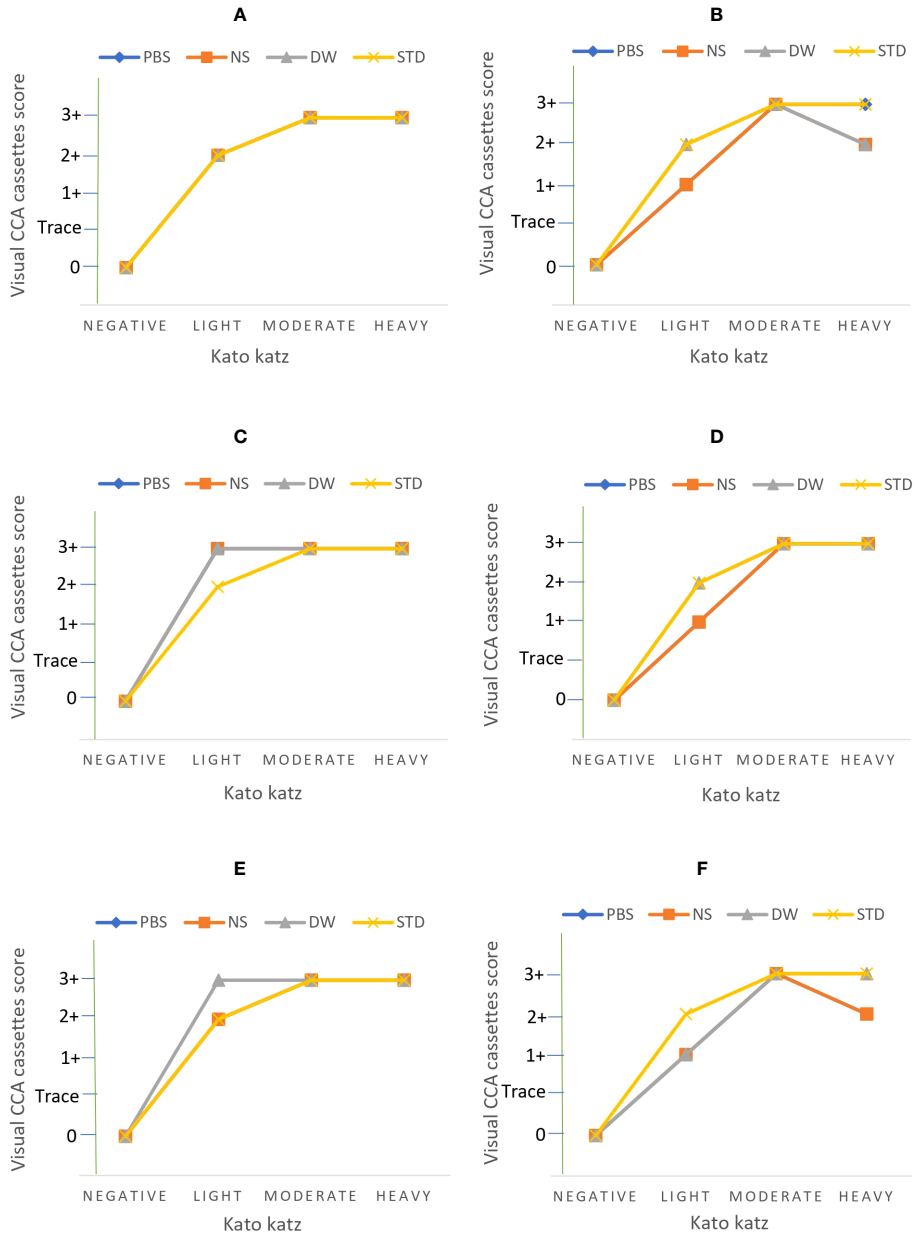

FIGURE 4
Results of assays performed on DUS samples 7 days after preparation at the following extraction conditions; **(A)** 4 ^{0}C incubation for 24 hours, **(B)** 4 ^{0}C incubation for 2 hours, **(C)** room temperature incubation for 24 hours, **(D)** room temperature incubation for 2 hours, **(E)** 37 ^{0}C incubation for 24 hours, and **(F)** 37 ^{0}C incubation for 2 hours. PBS stands for phosphate buffered saline, NS stands for normal saline, DW stands for distilled water, and STD stands for standard diagnostic test.

TABLE 2 Shows the overall performance of DUS Schisto POC-CCA assays for each solvent when compared to their respective standard Schisto POC-CCA assays.

Solvent	Performance n (%)			Total number of tests
	Below	Same	Higher	
Phosphate buffered saline	8 (16.7)	39 (81.2)	1 (2.1)	48
Normal saline	5 (10.4)	42 (87.5)	1 (2.1)	48
Distilled water	1 (2.1)	45 (93.8)	2 (4.2)	48
Total	14 (9.7)	126 (87.5)	4 (2.8)	144

n, number of tests.

TABLE 3 Shows the overall performance of DUS Schisto POC-CCA assays for each incubation temperature condition when compared to their respective standard Schisto POC-CCA assays.

Temperature	Performance n (%)			Total number of tests
	Below	Same	Higher	
4 ^{0}C	5 (10.4)	43 (89.6)	0 (0.0)	48
Room temperature	3 (6.2)	42 (87.5)	3 (6.2)	48
37 ^{0}C	6 (12.5)	41 (85.4)	1 (2.1)	48
Total	14 (9.7)	126 (87.5(	4 (2.8)	144

n, number of tests.

TABLE 4 Shows the overall performance of DUS Schisto POC-CCA assays for each incubation time condition when compared to their respective standard Schisto POC-CCA assays.

Incubation time	Performance n (%)			Total number of tests
	Below	Same	Higher	
2 hours	13 (18.1)	59 (81.9)	0 (0.0)	72
24 hours	1 (1.4)	67 (93.1)	4 (5.6)	72
Total	14 (9.7)	126 (87.5)	4 (2.8)	144

n, number of tests.

solutions are commonly used as protein analyte elution solvents. In general, an aqueous solvent is used for protein analytes extraction as it promotes analyte stability hence increasing its detection (34).

The temperature and time of elution are also important things to consider. Elution methods frequently require DUS to be dissolved in tubes containing the elution solution at specific temperature and time. Most procedures have method-specific incubation temperatures that range from 4 ^{0}C to room temperature (25 ^{0}C) for an hour to 24-hours (33). *Schistosoma* CCA is a very temperature-stable glycoprotein that is not easily distracted by minor temperature changes (35); however, temperature may have indirect effects by causing other analytes in DUS or elution solvents to affect the dissociation or nature of CCA and thus its concentration in the eluate. In our study, we included the core internal human body temperature (37 ^{0}C) in addition to the two common temperatures (4 ^{0}C and room temperature). However, after these temperatures were optimized, many assays incubated at room temperature performed better. In contrast, other studies found that 37 ^{0}C was the optimal temperature for extracting urine analytes from DUS on filter papers (31, 32). In terms of incubation time, we discovered that incubating the elution solution for 24 hours yielded the best results when compared to 2 hours. The same results were reported in methods that used elution to extract urine analytes from DUS on filter papers (32).

5 Conclusion

This study provides proof of the feasibility of collecting urine samples (DUS) using filter paper and detecting *Schistosoma* CCA from DUS samples using the Schisto POC-CCA cassette test. Because DMS methods are cost-effective, the use of filter paper-based DUS for urine collection and detection of *Schistosoma* CCA will ease the schistosomiasis work for control programs and researchers in resource-limited settings by allowing them to test both recent samples for clinical care and older samples, regardless of transportation and storage issues.

6 Study limitations

One of the important limitations of this study was the lack of technique to actually quantify the concentration of *Schistosoma* CCA in the DUS eluates and their original urine samples. However, to mitigate this we carefully compared the visual appearance of the eluate with its original urine sample. Another constraint was the use of filter paper from a single manufacturer. The qualities of filter papers produced by various companies vary. The difference could be attributed to the materials used or the manufacturing process. The materials used to manufacture the filter paper were also suggested to have effects on the analytes in the DUS. For example, it has been proposed that hydroxyl and carboxylic groups on the hydrophilic surface of cellulose interact with the *Schistosoma* circulating anodic antigen, resulting in low antigen recovery. Moreover, filter paper from different manufacturers may have different pore sizes and fiber densities. These variations may influence the quality of the filter paper to maintain the *Schistosoma* CCA. Another limitation of the study is that it was a proof-of-concept study with limited sample sizes. To validate the results of this study, we recommend a larger study with a larger sample size to be conducted.

Data availability statement

The original contributions presented in the study are included in the article/supplementary material. Further inquiries can be directed to the corresponding author.

Ethics statement

The studies involving humans were approved by Muhimbili University of Health and Allied Sciences Ethical Review Board. The studies were conducted in accordance with the local legislation and institutional requirements. The participants provided their written informed consent to participate in this study.

Author contributions

AZ conceptualized the study. AZ, TM, CK and FL designed the study. AZ, CK and GO participated in data acquisition. AZ analysed and interpreted the data. AZ, TM drafted the manuscript. BN revised the work critically for important intellectual content. All authors contributed to the article and approved the submitted version.

Funding

This publication was supported by the Coalition for Operation Research on Neglected Tropical Diseases, which is funded at The Task Force for Global Health primarily by Bill & Melinda Gates Foundation, the United States Agency for International Development through its Neglected Tropical Diseases Program, and with UK aid from the British people. The grant was administered by the African Research Network for Neglected Tropical Diseases (ARNTD). The contents are the responsibility of AZ and do not necessarily reflect the views of COR-NTD, USAID, UK aid or the ARNTD. The grant number for this project is OPP1190754.

Acknowledgments

The authors would like to express their gratitude to everyone at the National Institute for Medical Research Mwanza Center who assisted them during the laboratory work. Thank you especially to the center director and the laboratory manager. The authors would also like to thank the owner of the fishing camp for allowing us to communicate with the fishermen at his establishment. Finally, we would like to thank all of the fishermen who agreed to participate in this study and provided urine and stool samples.

Conflict of interest

The authors declare that the research was conducted in the absence of any commercial or financial relationships that could be construed as a potential conflict of interest.

Publisher's note

References

1. Aula OP, Mcmanus DP, Jones MK, Gordon CA. Schistosomiasis with a focus on Africa. *Trop Med Infect Dis* (2021) 6(109):1–40. doi: 10.3390/tropicalmed6030109

2. Mazigo HD, Uisso C, Kazyoba P, Nshala A, Mwingira UJ. Prevalence, infection intensity and geographical distribution of schistosomiasis among pre-school and school aged children in villages surrounding Lake Nyasa, Tanzania. *Sci Rep* (2021) 11(1):1–11. doi: 10.1038/s41598-020-80317-x

3. Weerakoon KGAD, Gobert GN, Cai P, McManus DP. Advances in the diagnosis of human schistosomiasis. *Clin Microbiol Rev* (2015) 28(4):939–67. doi: 10.1128/CMR.00137-14

4. Danso-Appiah A, Minton J, Boamah D, Otchere J, Asmah RH, Rodgers M, et al. Accuracy of point-of-care testing for circulatory cathodic antigen in the detection of schistosome infection: systematic review and meta-analysis. *Bull World Health Organ.* (2016) 94(7):522–533A. doi: 10.2471/BLT.15.158741

5. COR-NTD. *Developing a M & E framework for schistosomiasis and prioritizing operational research to achieve schistosomiasis elimination: Meeting Report 22 December 2020.* (2021) Decatur: Coalition for Operational Research on Neglected Tropical Diseases.

6. Hoekstra PT, Schwarz NG, Adegnika AA, Andrianarivelo MR, Corstjens PLAM, Rakotoarivelo RA, et al. Fast and reliable easy-to-use diagnostics for eliminating bilharzia in young children and mothers: An introduction to the freeBILy project. *Acta Trop* (2020) 21:105631. doi: 10.1016/j.actatropica.2020.105631

7. Utzinger J, Becker SL, van Lieshout L, van Dam GJ, Knopp S. New diagnostic tools in schistosomiasis. *Clin Microbiol Infect* (2015) 21(6):529–42. doi: 10.1016/j.cmi.2015.03.014

8. Hoekstra PT, van Dam GJ, van Lieshout L. Context-Specific Procedures for the diagnosis of human schistosomiasis – A Mini Review. *Front Trop Dis* (2021) 2:1–10. doi: 10.3389/fitd.2021.722438

9. Corstjens PLAM, de Dood CJ, Knopp S, Clements MN, Ortu G, Umulisa I, et al. Circulating anodic antigen (CAA): A highly sensitive diagnostic biomarker to detect active schistosoma infections—improvement and use during SCORE. *Am J Trop Med Hyg* (2020) 103:50–7. doi: 10.4269/ajtmh.19-0819

10. Ibironke O, Koukounari A, Asaolu S, Moustaki I, Shiff C. Validation of a new test for *Schistosoma haematobium* based on detection of Dra1 DNA fragments in urine: Evaluation through latent class analysis. *PloS Negl Trop Dis* (2012) 6(1):1–6. doi: 10.1371/journal.pntd.0001464

11. Shane HL, Verani JR, Abudho B, Montgomery SP, Blackstock AJ, Mwinzi PNM, et al. Evaluation of urine CCA assays for detection of *Schistosoma mansoni* infection in Western Kenya. *PloS Negl Trop Dis* (2011) 5(1):1–7. doi: 10.1371/journal.pntd.0000951

12. Chitsulo L, Engels D, Montresor A, Savioli L. The global status of schistosomiasis and its control Europe. *Acta Trop* (2000) 77(1):41–51. doi: 10.1016/S0001-706X(00)00122-4

13. Ibironke OA, Phillips AE, Garba A, Lamine SM, Shiff C. Diagnosis of *Schistosoma haematobium* by detection of specific DNA fragments from filtered urine samples. *Am J Trop Med Hyg* (2011) 84(6):998–1001. doi: 10.4269/ajtmh.2011.10-0691

14. Ibironke O, Koukounari A, Asaolu S, Moustaki I, Shiff C. Validation of a new test for *Schistosoma haematobium* based on detection of Dra1 DNA fragments in urine: Evaluation through latent class analysis. *PLoS Negl Trop Dis* (2012) 6(1):1–6.

15. Rapid Medical Diagnostics. *Schisto POC-CCA rapid test for qualitative detection of Bilharzia (Schistosomiasis)*. Noordhoek: Rapid Medical Diagnostics (2018).

16. WHO. *Bench aids for diagnosis of intestinal parasites. 2nd ed.* Geneva: World Health Organization (2019). p. 32.

17. Coulibaly JT, N'Gbesso YK, Knopp S, N'Guessan NA, Silué KD, van Dam GJ, et al. Accuracy of urine circulating cathodic antigen test for the diagnosis of Schistosoma mansoni in preschool-aged children before and after reatment. *PloS Negl Trop Dis* (2013) 7(3):1e2109. doi: 10.1371/journal.pntd.0002109

18. WHO Expert Committee. *Prevention and control of Schistosomiasis and Soil transmitted helminthiasis*. Geneva: Switzerland (2002).

19. Michely JA, Meyer MR, Maurer HH. Dried urine spots - a novel sampling technique for comprehensive LC-MSn drug screening. *Anal Chim Acta* (2017) 982:112–21. doi: 10.1016/j.aca.2017.05.033

20. Hannon H, Therrell B. (2014)., in: *Overview of the history and applications of dried blood samples*, . New Jersey: John Wiley & Sons, Inc.

21. Neoteryx. *Dried urine sampling is a good choice for delivering data* (2021). Available at: https://www.neoteryx.com/microsampling-blog/dried-urine-sampling-is-a-good-choice-for-delivering-data.

22. ZRT. *Provider data sheet about dried urine testing*. Beaverton: ZRT Laboratory (2015).

23. Berry HK, ScheelL C, Marks J. Microbiological test for leucine, valine, and isoleucine using urine sample dried on filter paper. *Clin Chem* (1962) 8:242–5. doi: 10.1093/clinchem/8.3.242

24. Berry HK. Procedures for testing urine specimens dried on filter paper. *Clin Chem* (1959) 5(8):603–8. doi: 10.1093/clinchem/5.6.603

25. WHO. *WHO guideline on control and elimination of human schistosomiasis*. Geneva: World Health Organization (2022).

26. Waugh C, Clark G. Factors affecting test reproducibility among laboratories. *Rev Sci Tech.* (2021) 40(1):131–43. doi: 10.20506/rst.40.1.3213

27. Mei JV, Zobel SD, Hall EM, De Jesús VR, Adam BW, Hannon WH. Performance properties of filter paper devices for whole blood collection. *Bioanalysis* (2010) 2 (8):1397–403. doi: 10.4155/bio.10.73

28. Newman M, Curran DA. Reliability of a dried urine test for comprehensive assessment of urine hormones and metabolites. *BMC Chem* (2021) 15(1):1–13. doi: 10.1186/s13065-021-00744-3

29. Breier AC, Cé J, Coelho JC. Correlation of the levels of glycosaminoglycans between urine and dried urine in filter paper samples and their stability over time under different storage temperatures. *Clin Chim Acta* (2014) 433:49–53. doi: 10.1016/j.cca.2014.02.022

30. Protti M, Sberna PM, Sberna AE, Ferrante R, Mandrioli R, Mercolini L. Enhanced urinary stability of peptide hormones and growth factors by dried urine microsampling. *J Pharm BioMed Anal* (2021) 204:114234. doi: 10.1016/j.jpba.2021.114234

31. Jain R, Quraish R, Ambekar A, Verna A, Gupta P. Dried urine spots for detection of benzodiazepines. *Indian J Pharmacol* (2017) 49(6):465–9. doi: 10.4103/ijp.IJP_578_16

32. Jain R, Quraish R, Verna A, Ambekar A. Development and clinical evaluation of a dried urine spot method for detection of morphine among opioid users. *Indian J Pharmacol* (2019) 51(1):40–4. doi: 10.4103/ijp.IJP_305_18

33. Kalou M. Application of enzyme immunoassay methods using dried blood spot specimens. In: Li W, Lee M, editors. *Dried blood spots: applications and techniques*. New Jersey: John Willey and Sons Inc (2014).

34. Luckwell J, Danielsson Å, Johnson B, Clegg S, Green M, Pierce A. Applications and chemistry of cellulose papers for dried blood spots. In: Li W, Lee M, editors. *Dried blood spots: applications and techniques*. New Jersey: John Willey and Sons Inc (2014).

35. Kildemoes AO, Vennervald BJ, Tukahebwa EM, Kabatereine NB, Magnussen P, de Dood CJ, et al. Rapid clearance of *Schistosoma mansoni* circulating cathodic antigen after treatment shown by urine strip tests in a Ugandan fishing community – Relevance for monitoring treatment efficacy and re-infection. *PloS Negl Trop Dis* (2017) 11(11):1–16. doi: 10.1371/journal.pntd.0006054

frontiers | Frontiers in Immunology

TYPE Methods
PUBLISHED 27 November 2023
DOI 10.3389/fimmu.2023.1293009

OPEN ACCESS

EDITED BY
Thiago Almeida Pereira,
Stanford University, United States

REVIEWED BY
Wannaporn Ittiprasert,
George Washington University,
United States
Soraya Gaze,
Oswaldo Cruz Foundation (Fiocruz), Brazil

*CORRESPONDENCE
David Duval
david.duval@univ-perp.fr
Ronaldo De Carvalho Augusto
ronaldo.augusto@univ-perp.fr

†These authors have contributed equally to this work

RECEIVED 12 September 2023
ACCEPTED 07 November 2023
PUBLISHED 27 November 2023

CITATION
Duval D, Poteaux P, Gourbal B, Rognon A and Augusto RDC (2023) Fluorescent non transgenic schistosoma to decipher host-parasite phenotype compatibility.
Front. Immunol. 14:1293009.
doi: 10.3389/fimmu.2023.1293009

Fluorescent non transgenic schistosoma to decipher host-parasite phenotype compatibility

David Duval*†, Pierre Poteaux†, Benjamin Gourbal, Anne Rognon and Ronaldo De Carvalho Augusto*

IHPE, Université de Perpignan Via Domitia, CNRS, Ifremer, Université de Montpellier, Perpignan, France

Schistosomiasis is considered as a significant public health problem, imposing a deeper understanding of the intricate interplay between parasites and their hosts. Unfortunately, current invasive methodologies employed to study the compatibility and the parasite development impose limitations on exploring diverse strains under various environmental conditions, thereby impeding progress in the field. In this study, we demonstrate the usefulness for the trematode parasite *Schistosma mansoni*, leveranging a fluorescence-imaging-based approach that employs fluorescein 5-chloromethylfluorescein diacetate (CMFDA) and 5-chloromethylfluorescein diacetate (CMAC) as organism tracker for intramolluscan studies involving the host snail *Biomphalaria glabrata*. These probes represent key tools for qualitatively assessing snail infections with unmatched accuracy and precision. By monitoring the fluorescence of parasites within the snail vector, our method exposes an unprecedented glimpse into the host-parasite compatibility landscape. The simplicity and sensitivity of our approach render it an ideal choice for evolutionary studies, as it sheds light on the intricate mechanisms governing host-parasite interactions. Fluorescent probe-based methods play a pivotal role in characterizing factors influencing parasite development and phenotype of compatibility, paving the way for innovative, effective, and sustainable solutions to enhance our understanding host-parasite immunobiological interaction and compatibility.

KEYWORDS

biomphalaria, host/parasite interaction, fluorescent vital probe, Schistosoma, vibratome section, 3D histochemistry

Introduction

Schistosomiasis is considered as a neglected human parasitic disease that however affects more than 240 million people worldwide, predominantly in developing countries (1). The disease is caused by a flatworm parasite of the *schistosoma* genus, which has a complex life cycle that involves freshwater snails as intermediate hosts and mammals as definitive hosts. Currently, the sole chemotherapy employed in the treatment of schistosomiasis, the Praziquantel, is limited in its effectiveness as it targets exclusively

adult worms and does not prevent reinfection (2). To address these challenges, a growing number of studies are seeking to expand the current approach through novel strategies, specifically by advancing our understanding of the interplay between the intermediate snail host and the parasite (3, 4). In contact with freshwater, *Schistosoma* sp. eggs release ciliated larvae called miracidia, which seek to invade a compatible snail host and developed in the first intramolluscan parasite stage called the mother sporocysts (or primary sporocysts). Each mother sporocyst can give rise to hundreds of daughters sporocysts (or secondary sporocysts), which can eventually transform into thousands of cercariae, the third intra-molluscan stage of the parasite that are dedicated to infect the definitive mammalian host by being released in the fresh water environment. Sporocysts are sac-like bodies enriched in stem cells with a phase of rapid asexual proliferation before undergoing embryogenesis to generate hundreds of new generations of either daughter sporocysts or cercariae. Indeed, from a single miracidium an virtually unlimited number of clonal sporocysts can be generated and even transplanted between snails for many generations (5–7). In the *Biomphalaria glabrata-Schistosoma mansoni* model, the concept of compatibility has been described as a complex molecular dialog between both protagonists involving multiple molecules with distinct roles (8–19). The parasite antigens *S. mansoni* polymorphic mucins (*Sm*PoMucs) and the *B. glabrata* immune receptors fibrinogen-related proteins (FREPs), two repertoires of polymorphic interacting molecules were proposed as the major components for defining the compatible/incompatible status of a specific snail/schistosome combination (18, 20, 21).

Hence sporocyst developmental trajectory is not exclusively dependent on the parasite genomic background, subsequently, it is also impacted by intrinsic factors from snail host, coinfections, or environmental stressors (22, 23–25). Individual parasites that enter the same snail can exhibit different fates; some may develop, and others may become encapsulated and killed by humoral factors. This suggests that infectivity is not a general characteristic of the parasite, but rather, it depends on the genotype of the specific host it enters. Similarly, susceptibility to infection is not a general characteristic of the host; instead, it is influenced by the genotype of the parasite it harbors. Moreover, environmental cues, such as coinfections to different parasite species, can modify the host phenotype by activating or inhibiting cellular and immune functions. Overall, the multifactorial nature of compatibility and the specificity of host-parasite interactions are crucial aspects when investigating *B.glabrata-S.mansoni* model. Understanding the mechanisms that govern the interaction between schistosomes and their intermediate snail hosts is a fundamental requirement for developing efficacious control strategies, as the exponential escalation of parasite numbers heightens the risk of disease propagation.

We theorize the use of fluorescent cell trackers as a non-invasive method in *B. glabrata-S. mansoni* compatibility studies. Fluorescent probes are valuable tools to understand cell-to-cell interaction which enable visualization and tracking *in vivo* and *in vitro* systems. These assays are instrumental in elucidating the behavior of specific pathogens within a heterogeneous milieu, providing insights into cell proliferation, viability, cytotoxicity, and motility. Fluorescent probes have been successfully used for unicellular parasites such as Trypanosoma, Leishmania, and Entamoeba sp. (26–28) and on multicellular parasites such as cestodes and nematodes to follow migration through hosts tissues, on studies of competition between different parasite species or to measure physiological stress (29–33). In these aspects, different vital stains offer the potential for labeling and monitoring cells *in vivo* and also being able to distinguish live parasites from dead ones (31). It is desirable to have tracking agents which have long-term stability, are non-toxic, and do not affect cell function. Here, we selected two different labels: CellTracker™ Green CMFDA (5-chloromethylfluorescein diacetate) and CMAC (5-chloromethylfluorescein diacetate) and performed an extensive analysis of their influence on the free-swimming parasite stage of *S. mansoni*, miracidium, as well as trackers sporocyst development into *B. glabrata* snail host.

Our results demonstrated that the fluorescent non-transgenic schistosome technique may have broad applications in the field of parasitology, as it provides a non-invasive, sensitive, and specific tool for tracking free-swimming parasites, parasite stages within snail-host. Moreover, even with the recent progress in the Crispr method, a single study managed to exhibit the feasibility of knocking along with GFP insertion in developing schistosome eggs (34). While this approach offers the advantage of visualizing fluorescence within the parasite, it demands cutting-edge molecular biology skills and comes with a substantial cost, rendering its implementation impractical in regions pivotal to the schistosomiasis eradication efforts. Our findings have the potential to provide valuable insights into the mechanisms underlying the compatibility of *Biomphalaria glabrata-Schistosoma mansoni* model.

Materials and methods

Ethics statement

Our laboratory holds permit #39910-2022121915564694 (APAFIS number) for experiments on animals from both the French Ministry of Agriculture and Fisheries, and the French Ministry of National Education, Research, and Technology. The housing, breeding, and animal care of the utilized animals followed the ethical requirements of our country. The researchers also possess an official certificate for animal experimentation from both French ministries (Decree # 87–848, October 19, 1987). Animal experimentation followed the guidelines of the French CNRS. The different protocols used in this study had been approved by the French veterinary agency from the DDPP Languedoc-Roussillon (Direction Départementale de Protection des Populations), Montpellier, France (authorization # 007083) and the Ethic committee CEEA-LR (# C66-136-01).

Parasite recovery procedure

Golden hamsters (*Mesocricetus auratus*) were infested with 700 cercariae of *Schistosoma mansoni* NMRI strain. Seven weeks post-infection, hamsters' livers were recovered in saline solution (150 mM NaCl), and ground and eggs were filtered using sieves. Eggs were hatched in sterile fresh water and miracidia were manually collected by pipetting and transferred to a 1.5mL Eppendorf tube for down stream analysis. *Biomphalaria glabrata* (BgBre2 strain) snails were exposed to artificial light (60 W) to enable the snails to shed cercariae which were manually collected by pipetting and transferred to a 1.5mL Eppendorf tube for labeling.

Optimizing labeling assays

Florescent probes 5-chloromethylfluorescein diacetate (CellTracker™ Green CMFDA, 492/516 nm, C7025, ThermoFisher), 7-amino-4-chloromethylcoumarin (CMAC, DAPI, C2110, 353/466 nm, ThermoFisher) and CellTracker™ red CMTPX (C34552, 577/602nm ThermoFisher) were prepared by dissolving it on DMSO (10 mM stock). On the day of use, a labeling medium was prepared by diluting stock solution to final concentrations: 1µM, 5µM, 10µM, and 100µM. Control labeling was set by exposure to DMSO following the same dye protocol, fixed in 1 to 4% paraformaldehyde for 5 to 10 minutes, and washed twice with phosphate buffered saline (PBS) at room temperature before being placed over the slide and covered with a fluorescence mounting medium (Dako Omnis, GM304). In this study, results and pictures obtained with the green labeling were mainly presented.

Toxicity assays

Miracidia were exposed for one hour to several concentrations (1µM, 5µM, 10µM, 100µM) of both DMSO-solubilized fluorescent CellTracker™. Control miracidia was either unexposed or exposed to DMSO following the same procedure as that carried out with the different dyes. Non-swimming larvae were counted, viability percentages were calculated and were compared to a control condition (unexposed or DMSO-exposed concentration). Three replicates were performed and at least 20 larvae were counted for each exposure condition.

Parasites, snails, and compatibility

Compatibility trials between miracidia and *B. glabrata* strains were conducted as previously described (35). For all experimental trials, 20 to 30 snails were infected per condition with 10 miracidia prelabeled with 5µM of fluorescence dye. Two control groups were considered – a negative control, for which snails were infected with unlabeled miracidia in aquarium water and a DMSO control group, for which snails were infected with miracidia exposed to DMSO. Two weeks later, we assessed the prevalence (percentage of infected snails) and intensity (number of developed mother sporocysts per infected snail) of infection for each experimental group. Three independent experiments were performed. Prevalence and intensity were first measured by direct observation of snails after 4 to 5 days of exposure to parasites under fluorescence stereo-microscope (Nikon, SMZ18) or inverted microscope (Nikon, TS100). Then, at 15 days post-exposure, the snail bodies were removed and fixed in modified Raillet-Henry solution to determine the occurrence and the exact number of mother sporocysts established in snail tissue.

Vibratome section preparation and histolabeling

B. glabrata snails are fixed overnight in 4% paraformaldehyde (PAF) after shell removal. Then, fixed snails are washed twice in PBS. Thick sections of snail tissues from foot to digestive glands are cut on the Leica VT1000S vibratome with 0.7 mm/s sectioning speed and 300 to 400-µm thickness in PBS. Thick sections generated by vibratome were observed under fluorescence stereo-microscope and/or confocal microscopy using a Zeiss LSM 700 microscope (Bioenvironment platform from UPVD). For histolabeling analysis, sections are incubated with DAPI (reference 5748, Biotechne) to stain nuclei during 1 min. After 2 washes in PBS, some sections are incubated during 5 to 10 min with Texas Red™-X Phalloidin (591/608 nm, T7471, ThermoFischer) to detect F-actin. After rinsing, tissue sections are mounted on slides with Dako mounting medium to be stored at 4°C. Images obtained with stereo and confocal microscopes are performed with NIS-Elements BR (Nikon) and Zen (Zeiss) softwares, respectively. For confocal microscopy observation, pictures were imported into ImageJ software.

Statistical analysis

A non-parametric Kruskal-Wallis test (36) was performed followed by a *post-hoc* Dunn test (37) to unveil the potential significant differences occurring between the survival rate of CMAC or CMFDA-exposed and control conditions (unexposed or DMSO-exposed miracidia). A significant difference was considered following a p-value<0.05 for the Kruskal-Wallis test and following p-value<0.025 for the Dunn posthoc test.

Results

Free-swimming miracidia toxicity assays

The toxicological effects of CMAC and CMFDA labeling on miracidia of *S. mansoni* were studied by assessing their swimming behavior. For those experiments, the CMAC and CMFDA labeling was performed for 1hr with 1µM, 5µM, 10µM, and 100µM concentrations. For CMAC- and CMFDA-labeled free swimming parasite stages, no significant changes in the survival rate were

10.3389/fimmu.2023.1293009

noticed following both Kruskal-Wallis and Dunn test statistical analysis for miracidia ($p>0.05$ for all analyzed groups; Figure 1A, B).

Nontoxic fluorescent cell tracker tools are efficient for schistosoma larvae staining

To first determine whether different concentrations of CMAC and CMFDA can be used individually to detect live parasites by fluorescence microscopy, we repeated the same concentrations as in the initial toxicity assay while varied the exposure time from 5 to 60 minutes (data not shown). Furthermore, all live parasites fluoresced when visualized after CMAC or CMFDA uptake with corresponding microscopy imaging of the same miracidia samples providing visual confirmation of a physiological normal phenotype (Figure 2, Video S01, S02, S03, S04). An optimal concentration of 10µM for 10 minutes was set to obtain maximal efficient dye retention for combining: i) minimum manipulation, ii) sort exposition, and iii) survival rate. These labeling parameters enabled us to archive live labeling without compromising miracidia survival rates for downstream approaches. For example, fluorescent-labeled parasites have the ability to penetrate into snails demonstrating that the labeling time do not seem to reduce their virulence (Video S05).

Briefly, both fluorescent dyes can cross the plasma membrane and remains internalized in some specific cells. For CMFDA probe, it can be metabolized by intracellular esterase into a fluorescent compound that is unable to pass through cell membranes again. Fluorescent labeling is thus sequestered exclusively in cells exhibiting esterase activity. In confocal microscopy, cellular-scale labeling can be explored. Herewith labeled cells related to neural mass can be noticed and with close to greater fluorescence intensity, perikaryon of neurons linked to multiciliated papilla in the median area of the organism (38–40); (Figure 3). Also, another perikaryon can be noticeably observed by the 3D reconstitution of a confocal series of pictures with a very strong fluorescence level: neurons related to lateral papillae, and, more precisely, to multiciliated receptors associated with lateral papillae and terebratorial multiciliated receptors (Video S06, S07) (38, 41).

There is a relatively close correlation of labeled tissues with cells exhibiting acetylcholine esterase activity in miracidia (42) especially neural mass, multiciliated receptors and lateral sides of the terebratorium (strong assumption for multiciliated receptors, that are side orientated) (39, 41). Indeed, this enzyme appeared particularly associated with neural tissues, multiciliated receptors extensions of neuronal cells. The activation of CMFDA could also occur potentially thanks to the presence of acetylcholine esterase in neurons of *S. mansoni* miracidium. This information could also give tools for the study of neural system of this organism and especially its esterase-related activity.

Fluorescent probes do not affect the miracidia infection and sporocyst development

To further assess the suitability of fluorescent probes for compatibility studies, the prevalence and intensity of live labeled miracidia to *B. glabrata* snails was investigated. *S. mansoni* miracidia were exposed to 10 µM of CMAC and CMFDA or to the respective controls (DMSO or freshwater). Two weeks after infection, the mean prevalence observed in each treated group was higher than 95% (Figure 4A). Both labeling probe approaches, along with their respective controls, exhibited no discernible trend in the intensity of infection. Specifically, the intensity of infection, measured as the mean number of sporocysts per infected snail, demonstrated consistency for both the CMAC-labeled group (mean of sporocysts per snail = 5) and the CMFDA-labeled group (mean of sporocysts per snail = 4.6) at a concentration of 10 µM for 10 minutes (Figure 4B). Notably, no statistically significant differences

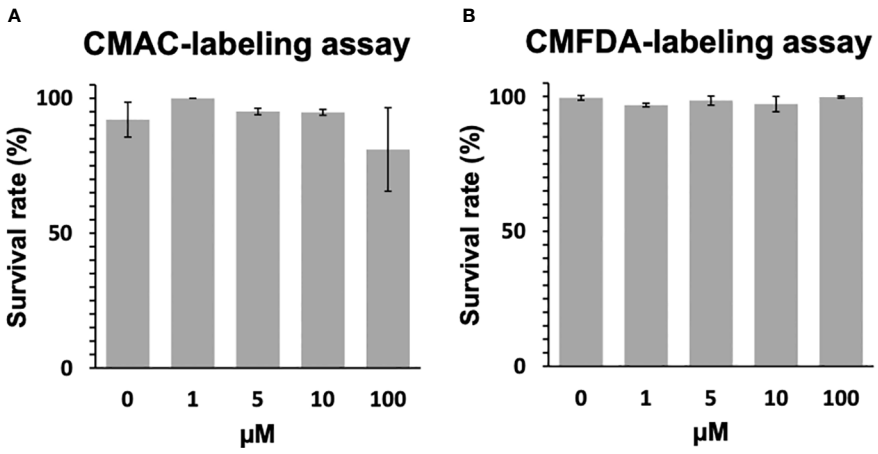

FIGURE 1
Toxicity assay of CMAC and CMFDA cell trackers. The viability of labeled and unlabeled miracidia populations was assessed in this study. **(A)** The survival rate of CMAC-labeled miracidia slightly decreased when they were exposed to 100 µM for 1 hour. **(B)** The survival rate of CMFDA-labeled miracidia faintly varies between all conditions after 1 hour of exposure. No significant differences were observed between the control and exposed conditions following statistical analysis ($p>0.05$).

10.3389/fimmu.2023.1293009

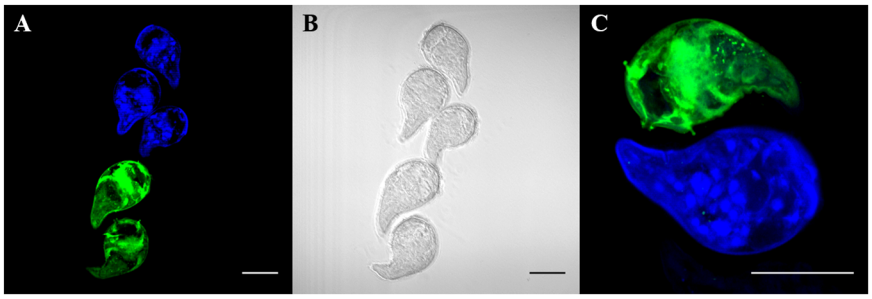

FIGURE 2
Live labeling of free-swimming miracidia with fluorescent probes CMAC and CMFDA. Fluorescent labeled miracidia were fixed and mounted on slides. Fluorescent labeling was done separately and put together for observation. **(A)** Blue and green fluorescent miracidia after labeling and rinsing. **(B)** Phase contrast microscopy of **(A, C)** High magnification of labeled miracidia. Live miracidia labeled by CMAC (blue) and CMFDA (green). All scale bars indicate 50 µm.

emerged in either the prevalence or the intensity of infection across all analyzed groups when compared to their respective controls ($p>0.05$; Figures 4A, B). We performed ANOVA by using the labeling approach as factor, prevalence, and infection intensity as the dependent variables. These findings revealed that the labeling process did not have any statistically significant impact on these variables ($p > 0.05$). Sporoscyst derived from CMFDA-labeled miracidia showed detectable fluorescence throughout *B. glabrata* snail host infection within the snail body (Video S08).

By demonstrating that CMFDA-labeled probes could effectively be used to stain live miracidia and newly developed sporocyst, a further experiment was conducted to determine how long CMFDA-labeled miracidia and sporocysts could be detected *in vivo* within *B. glabrata* snail tissue. Here, we demonstrated that fluorescent CMFDA-labeled sporocyst could be easily detected in live snails at least 15 days after infection (Figure 5). However, differential staining of individual was supported by observations of fluorescence dilution effect over sporocyst development starting 5 days post-infection (Figure S1). At this stage, mother sporocysts, which appeared to developed normally, have a vermiform shape. After 15 days of sporocyst development inside the snails, the fluorescence level of mother sporocyst decreases revealing blisters that seem empty. Consistently, this reduction is associated with the development of daughter sporocysts inside the mother sporocysts. Interestingly, the shape and the fluorescence level in each mother sporocyst differ from one parasite to another showing an asynchronized development and different abilities to differentiate and grow inside the host.

Other life cycle stages of the parasite are not affected by CMFDA labeling

30 days after infection, direct observations through the translucent shell of living snail demonstrate the presence of

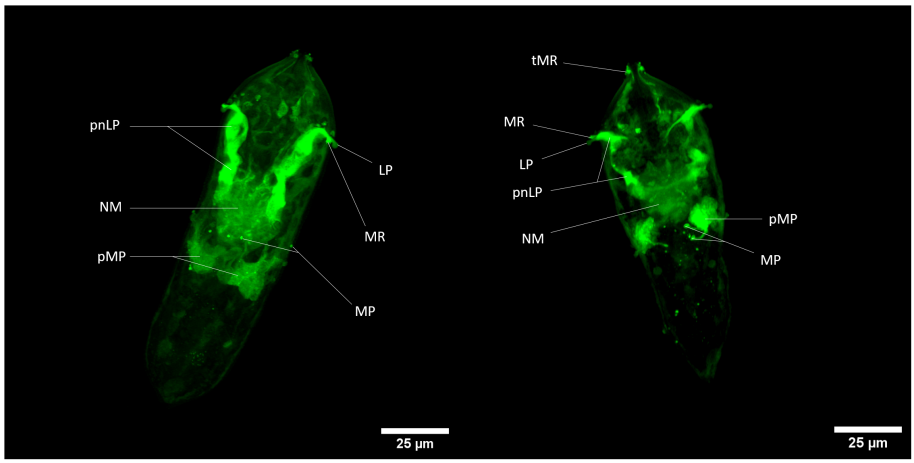

FIGURE 3
Z-stack of CMFDA-labeled miracidium of *Schistosoma mansoni*. LP, Lateral Papilla; MP, Multiciliated Papilla; MR, Multiciliated Receptor; NM, Neural Mass; pMP, perikaryon of Multiciliated Papilla; pnLP, perikaryon of the neuron to Lateral Papilla; sC, stem Cells; tMR, terebratorial Multiciliated Receptors. Scale bars are 25 µm long.

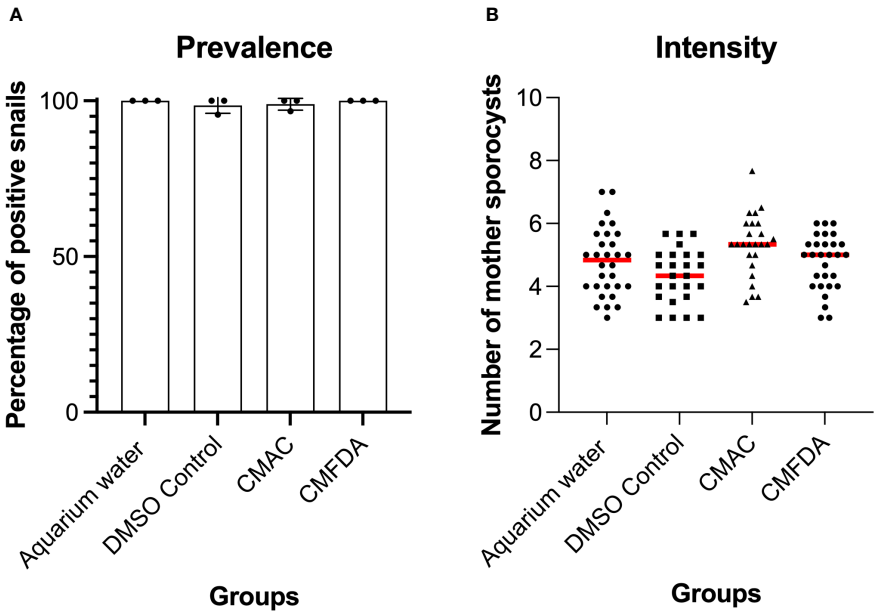

FIGURE 4
Prevalence **(A)** and intensity **(B)** of Biomphalaria glabrata infected by 10 labeled CMAC, CMFDA, and their respective controls with unlabeled miracidia in aquarium water and a DMSO control group. No significant differences were observed between the control and exposed conditions following statistical analysis ($p>0.05$).

daughter sporocysts but unlabeled. Likewise, we no longer observe any fluorescence on the 3-week-old daughter sporocysts collected during their migration to the hepatopancreas and ovotestis area. However, parasites are able to achieve their development cycle. All the parasite-Cell tracker combinations were able to produce cercariae (data not shown, n=16 snails per dye). In addition, these cercariae are also infective and the adult stage are fertile since parasite eggs have been obtained (data not shown, n=3 mice).

Combination of vital fluorescent dyes and vibratome histological procedure to evaluate *in vivo* host/parasite interactions

Snail/parasite compatibility is characterized by the presence of parasites that are able to develop into mother sporocysts and others that are recognized and killed by the immune system of the host mainly following cellular encapsulation by the hemocytes (snail innate immune cells). Both phenotypes are observed within the

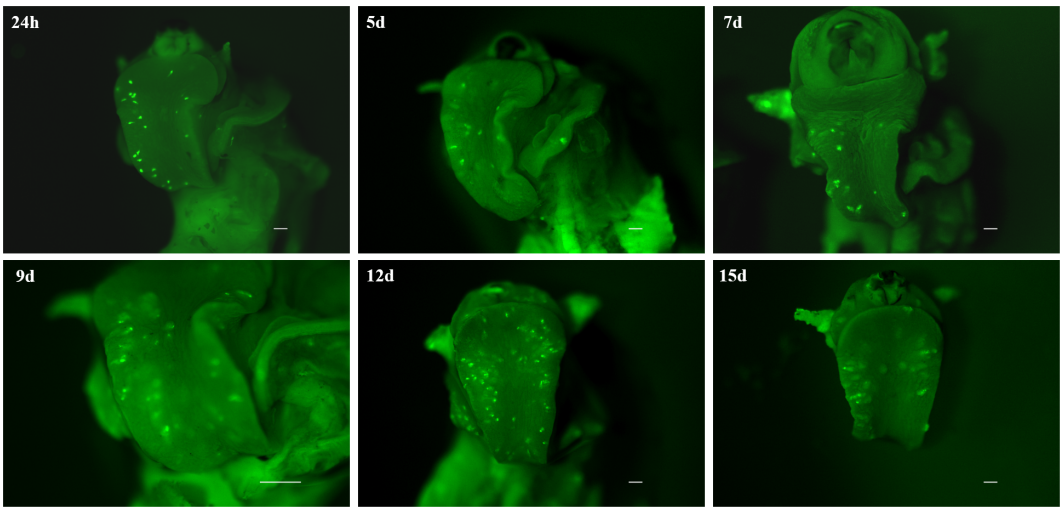

FIGURE 5
Fluorescence time series monitoring of CMFDA-labeled sporocysts inside Biomphalaria glabrata 24 h, 5 days, 7d ays, 9 days, 12 days, and 15 days post-infection. Parasite location is mainly observed in the head-foot region. All scare bars indicate 500 µm.

same snail exposed to several parasites, some of those miracidia can develop in sporoscyts while others can be immediately recognized and killed by hemocytes or plasmatic factors. No tool exists to separate infected from uninfected BgBAR snails in a exposed population with 20 miradicia of *S. mansoni* venezualian strain for which the prevalence of infection is around 60% (35). The use of dye-labeled parasite make feasible the selection of infected snails within the same population to carry out comparative omic experiments on the first hours of the host/parasite interaction. Infection intensity can vary from 5 to 50% depending on snail-parasite strain combinations used. As vibrating microtome is an effective procedure for generating thick sections that can be used for immunohistochemistry, we employed a robust methodology involving vibratome sectioning and combination with laser scanning confocal microscopy, to observe in 3D the relationships between parasite and snail and thus provide finely comprehensive insights into the studied system. Indeed, after 12h post-infection, encapsulated and damaged parasite forms can be discriminate from developing sporocysts by observing clusters of well-single fluorescent cells (Figures 6A, B). The presence of many snail cells probably hemocytes around the parasite reinforces this conclusion (Figures 6C, D, Video S09, S10). Some other immune-cytological labels can also be coupled easily (Figure 7, Video S11, S12). Simple and combined implementation of these different approaches can save time compared to conventional immunohistology techniques requiring paraffin-embedded samples and thin sections (21). Finally, multiple infections with parasites labeled with different fluorescent dyes can be performed in order to study interstrain competition within the same individual snail (Figure 8, Video S13, S14).

Discussion

The intricate interplay between parasites and their hosts, especially in diseases like schistosomiasis, requires a comprehensive understanding of intermediate host-parasite compatibility that govern their interaction. Understanding the mechanisms that govern the interaction between schistosomes and their intermediate snail hosts is a fundamental requirement for developing efficacious control strategies, as the exponential escalation of parasite numbers heightens the risk of disease propagation. This depth of understanding is essential to develop effective control strategies that can target specific vulnerabilities in the parasite's life cycle and the host's immune response. Current methodologies for studying host-parasite compatibility t face strong limitations, hindering a holistic exploration of various strains under diverse environmental conditions. This study introduces a groundbreaking approach that harnesses the potential of fluorescent probes, providing a non-invasive tool for tracking

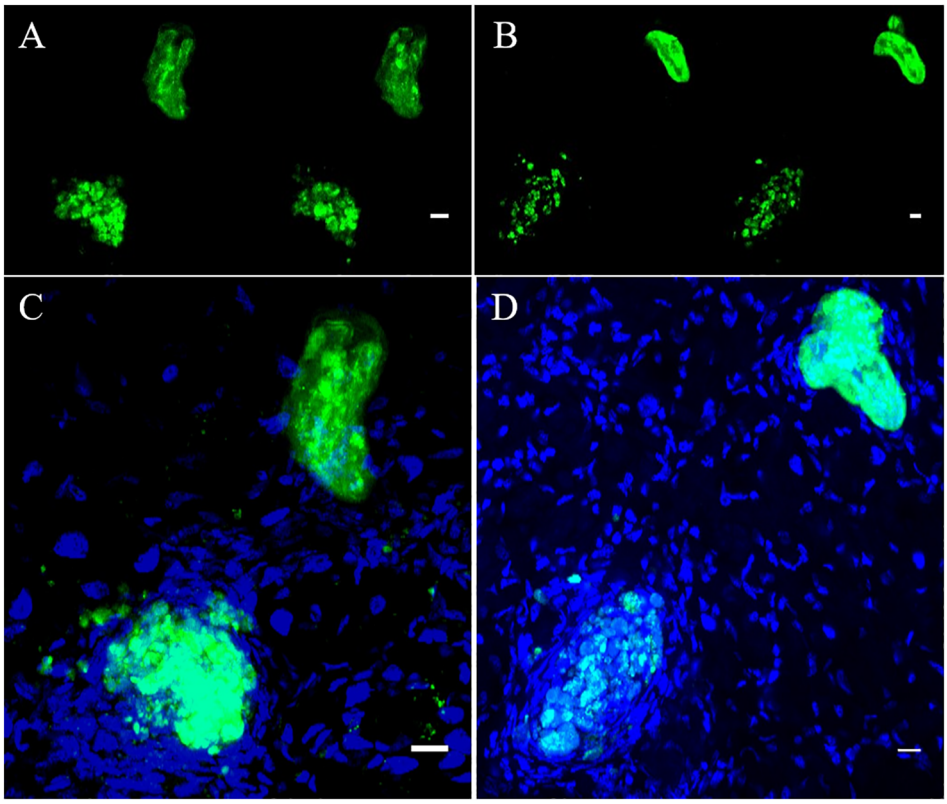

FIGURE 6
Green fluorescent parasites encapsulated or living inside snail. **(A, B)** are two adjacent focal planes selected from image stack **(C, D)**. which are 2 independent pictures from 2 infected snails obtained by z-stack scanning. Blue stain (DAPI) represents nuclei of snail and parasite cells. All scare bares indicates 10 µm.

10.3389/fimmu.2023.1293009

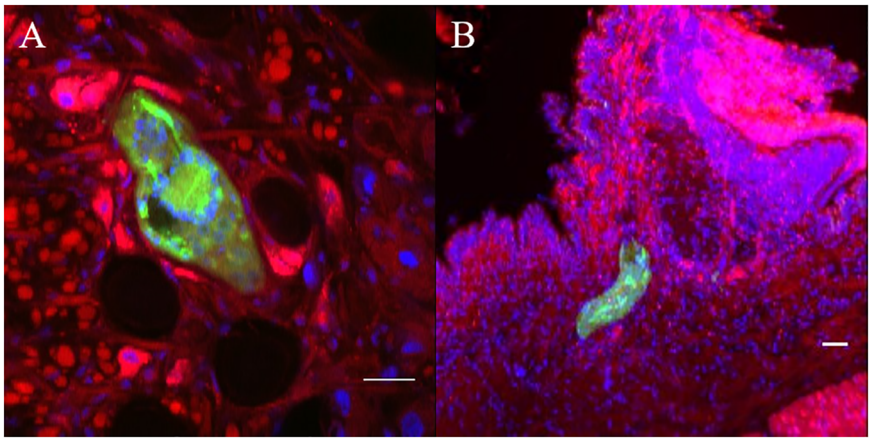

FIGURE 7
Confocal imaging of Biomphalaria glabrata and Schistosoma mansoni through vibratome sections. **(A, B)** CMFDA-labeled sporocysts were highlighted in green, snail actin filaments were stained with phalloidin in red, and snail cell nuclei were counterstained with DAPI in blue. Scare bares indicates 20 µm.

infections and shedding new insights about host-parasite interactions. Besides the notorious rewards of cell trackers for *in-vitro* cell applications, live-labelling have been successfully used as valuable tools for monitoring intracellular parasites for which no genetic tools exist (43). The sensitivity of CMAC and CMFDA are being used in a wide range of context thanks to the property that this fluorescent dye can, i) easily pass through cell membranes, ii) it is well retained in cells, and iii) it passed to daughter cells through several generations but it is not transferred to adjacent cells in a tissue or cell populations.

In this study, we employed fluorescent cell tracker probes to investigate the early stages of sporocyst development within their snail host, by tracking freshwater schistosome larvae stage, the miracidia. Our toxicity assays on free-swimming miracidia, essential for evaluating the viability of our method, underscored the non-toxic nature of fluorescent labeling using CMAC and CMFDA. These probes, whatever the concentrations used, exhibited no significant adverse effects on miracidia survival rates and behavior. This critical finding not only demonstrates the safety of our approach but also lays the foundation for its broad applicability on snail host-parasite studies.

In the past fluorescent probes have yet been used in studies with *S. mansoni* adult worms, but it is the first time that live-labelling was used to evaluate the developmental dynamic from one parasite stage

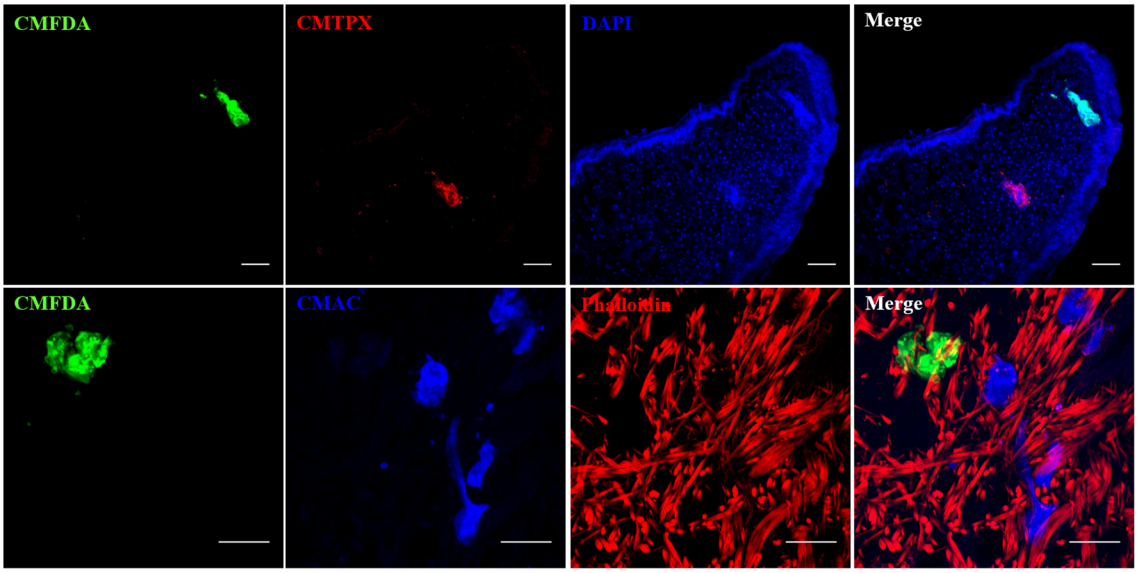

FIGURE 8
Multiple combinations of parasite labeling. Miracidia were labeled separately with CMFDA, CMTPX or CMAC dye. Then, multi-infestation were performed with differently labeled parasite. Depending on the type of the fluorescent dye, supplementary staining on snail tissue section was carried with DAPI or phalloidin. Scale bar is 50 µm.

to another as this is the case herein in the transition from freshwater stages, the miracidia to sporocysts in the intermediate snail hosts of *S. mansoni* parasites. Previous studies have used the fluorescent probe resorufin, a substrate for P-glycoprotein (PgP), to evaluate the activity of the excretory system of *S. mansoni* in drug-screening studies (44, 45). Moreover, the fluorescent Hoechst 33258 (bisbenzimide) probe was proposed as a marker of membrane integrity of adult *S. mansoni* worms, due to its affinity for DNA in a context of tegumental lesions (45). Indeed, the evaluation of the presence of tegumental damages and excretory activity in adult worms, were currently under deep investigations in the context of *S. mansoni* resistance to praziquantel, the only available drug to cure schistosomiasis (7, 46–48).

A notable achievement of our method is the extended detectability of fluorescent labeled sporocysts within the snail host. Our results revealed that CMFDA-labeled sporocysts remained detectable for up to 15 days post-infection, significantly advancing the temporal scope of parasite tracking. This temporal resolution is invaluable for unraveling the intricate and evolving nature of schistosoma-snail relationships.

We further deepened our exploration of snail-parasite interactions through vibratome sectioning and histochemistry. This methodology facilitated the visualization of the entire snail body with minimal tissue disruption.

Our research findings have the potential to significantly advance compatibility studies between the snail vector *B. glabrata* and the parasite *S. mansoni*, thereby contributing to the development of novel disease control strategies aimed at reducing the presence of infective parasite forms in freshwater. Furthermore, non-toxic *in vivo* labeling approach introduces an accessible and cost-effective tool that can democratize research in laboratories located in endemic countries. In practical terms, the present work empowers researchers to undertake detailed examinations of first steps of *S. mansoni* development within snail host by employing specific *in vivo* labelling. Besides *B. glabrata-S.mansoni* model compatibility studies, the proposed approach aims to shed light on scenarios that mirror the realities of epidemiologically active sites, where vector snails may encounter, and potentially host, multiple parasite strains and/or species. While studies of coinfection in vector snails are scarce in the literature (49, 50), *in vivo* labelling by fluorescente probes addresses this gap by offering a means to tackle the first steps of parasite infection and development reducing the complexities of studying multiple cycles in laboratory conditions and analyzing the resultant outcomes effectively. In conclusion, this innovative approach holds the potential to unveil valuable insights of compatibility of *B. glabrata-S.mansoni* model and into the intricate dynamics of coinfection, contributing to a deeper understanding of disease transmission and potentially informing more targeted control interventions.

Data availability statement

The original contributions presented in the study are included in the article/Supplementary Material. Further inquiries can be directed to the corresponding authors.

Author contributions

DD: Conceptualization, Data curation, Formal Analysis, Funding acquisition, Investigation, Methodology, Project administration, Resources, Software, Supervision, Validation, Visualization, Writing – original draft, Writing – review & editing. PP: Conceptualization, Data curation, Formal Analysis, Investigation, Methodology, Validation, Visualization, Writing – review & editing, Software, Writing – original draft. BG: Conceptualization, Data curation, Formal Analysis, Investigation, Methodology, Software, Supervision, Visualization, Writing – review & editing, Writing – original draft. AR: Conceptualization, Investigation, Resources, Writing – review & editing, Data curation, Methodology. RA: Data curation, Investigation, Methodology, Visualization, Writing – original draft, Writing – review & editing, Formal Analysis, Resources, Software, Supervision, Validation.

Funding

The author(s) declare financial support was received for the research, authorship, and/or publication of this article. This study is set within the framework of the "Laboratoires d'Excellences (LABEX)" TULIP (ANR-10-LABX-41) and CeMEB (ANR-10-LABX-04-01). The funders had no role in study design, data collection and analysis, decision to publish, or preparation of the manuscript. DD, PP and BG were supported by the ANR AEROSNAIL (ANR-19-CE11-0016-01) from the French National Research Agency (ANR). RA was supported by ANR (ANR-22-CPJ1-0056-01) -Tropical diseases of today, European diseases of tomorrow: a systems biology approach to understand, predict and control their emergence.

Acknowledgments

Thanks to the technical staff of the IHPE laboratory, Damien Pouzol and Olivier Portela for the maintenance of mollusc strains and their expertise on animal experimentation. We are greatful to Paradev Compagny for have facilitated the parasite egg collection. We acknowledge the "Réseau d'Histologie Expérimentale de Montpellier" - RHEM facility supported by SIRIC Montpellier Cancer (Grant INCa_Inserm_DGOS_12553), the European regional development foundation and the occitanian region (FEDER-FSE 2014-2020 Languedoc Roussillon) for expertise, especially Dr Hélène Hirbec and Anne Guillou-Duvoid for advices on using vibratome. The authors also want to thank Julien Portela for his help with the video editing.

Conflict of interest

The authors declare that the research was conducted in the absence of any commercial or financial relationships that could be construed as a potential conflict of interest.

Publisher's note

Supplementary material

The Supplementary Material for this article can be found online at: https://www.frontiersin.org/articles/10.3389/fimmu.2023.1293009/full#supplementary-material

SUPPLEMENTARY FIGURE 1
High magnification of a green sporocyst 5 days after parasite exposure. The observed sporocyst appears as a misshapen sac characterized by an extremity where fluorescence seems to accumulate. In detail boxes, scare bars are 100 µm.

SUPPLEMENTARY VIDEO 1
Swimming behavior of miracidia after CMFDA labeling and rinsing in Volvic water. Observation was done under stereo-microscope using NIS Element BR software taking an image every 100 msec. Living miracidia can be examined in their natural state without previously being killed by chemical fixation.

SUPPLEMENTARY VIDEO 2
Swimming behavior of miracidia after CMAC labeling and rinsing in Volvic water. Observation was done under stereo-microscope using NIS Element BR software taking an image every 100 msec.

SUPPLEMENTARY VIDEO 3
Miracidia exposure to CMFDA CellTracker in a 1.5ml tube. Observation was done under stereo-microscope using NIS Element BR software.

SUPPLEMENTARY VIDEO 4
Miracidia exposure to CMAC CellTracker in a 1.5ml tube. Observation was done under stereo-microscope using NIS Element BR software.

SUPPLEMENTARY VIDEO 5
Behavior of the CMFDA-labeled live miracidia of *Schistosoma mansoni* penetration *Biomphalaria glabratra* tissue. Note that at the end of the penetration when the parasite is entirely in snail, a lighter region around the parasite is visible suggesting an immediate cellular reaction induced by a changing local environment due to the entry parasite process.

SUPPLEMENTARY VIDEO 6
3-D reconstitution of multiple series confocal pictures from one CMFDA-labeled miracidium. Scale bar: 25µm.

SUPPLEMENTARY VIDEO 7
Unfolding of the different focal plans of a CMFDA-labeled miracidium. Scale bar: 25µm.

SUPPLEMENTARY VIDEO 8
Live green sporocyst of Schistosoma mansoni derived from with CMFDA-labeled miracidia into a living snail Biomphalaria glabrata 3 days after exposition. An image was taken every 0.7 sec.

SUPPLEMENTARY VIDEO 9
Unfolding of the different focal plans of a vibratome cut containing two CMFDA-labeled parasites in host tissues. One is encapsulated (bottom left), the other one is intact (top right). Scale bar: 10 µm.

SUPPLEMENTARY VIDEO 10
Unfolding of the different focal plans of a vibratome cut containing two CMFDA-labeled parasites in host tissues. One is encapsulated (bottom left), the other one is intact (top right). Scale bar: 10 µm.

SUPPLEMENTARY VIDEO 11
3D reconstitution of multiple series confocal pictures from CMFDA-labeled parasite in host tissues. Actin is labeled in red (phalloidin) and nuclei in blue (DAPI). Scale bar: 20µm.

SUPPLEMENTARY VIDEO 12
Unfolding of the different focal plans of a vibratome cut containing one CMFDA-labeled parasite in host tissues. Actin is labelled in red (phalloidin) and nuclei in blue (DAPI). Scale bar: 20 µm.

SUPPLEMENTARY VIDEO 13
Unfolding of the different focal plans of a vibratome cut containing one CMFDA-labeled parasite and one CMTPX-labeled parasite in host tissues. Scale bar: 50µm.

SUPPLEMENTARY VIDEO 14
Unfolding of the different focal plans of a vibratome cut containing one CMFDA-labeled parasite and several CMAC-labeled parasites in host tissues. Actin is labelled in red (phalloidin). Scale bar: 50µm.

References

1. Kokaliaris C, Garba A, Matuska M, Bronzan RN, Colley DG, Dorkenoo AM, et al. Effect of preventive chemotherapy with praziquantel on schistosomiasis among school-aged children in sub-Saharan Africa: a spatiotemporal modelling study. *Lancet Infect Dis* (2022) 22:136–49. doi: 10.1016/S1473-3099(21)00090-6

2. Vale N, Gouveia MJ, Rinaldi G, Brindley PJ, Gärtner F, Correia Da Costa JM. Praziquantel for schistosomiasis: single-drug metabolism revisited, mode of action, and resistance. *Antimicrob Agents Chemother* (2017) 61:e02582–16. doi: 10.1128/AAC.02582-16

3. Shiff C. Why reinvent the wheel? Lessons in schistosomiasis control from the past. *PloS Negl Trop Dis* (2017) 11:e0005812. doi: 10.1371/journal.pntd.0005812

4. WHO. *WHO | Field use of molluscicides in schistosomiasis control programmes: an operational manual for programme managers* (2017). WHO. Available at: http://www.who.int/schistosomiasis/resources/9789241511995/en/ (Accessed 3 Jul 2018).

5. Jourdane J, Theron A. Schistosoma mansoni: Cloning by microsurgical transplantation of sporocysts. *Exp Parasitol* (1980) 50:349–57. doi: 10.1016/0014-4894(80)90038-7

6. Wang B, Collins JJ, Newmark PA. Functional genomic characterization of neoblast-like stem cells in larval Schistosoma mansoni. *eLife* (2013) 2:e00768. doi: 10.7554/eLife.00768

7. Mouahid G, Rognon A, de Carvalho Augusto R, Driguez P, Geyer K, Karinshak S, et al. Transplantation of schistosome sporocysts between host snails: A video guide. *Wellcome Open Res* (2018) 3:3. doi: 10.12688/wellcomeopenres.13488.1

8. Bender RC, Goodall CP, Blouin MS, Bayne CJ. Variation in expression of Biomphalaria glabrata SOD1: A potential controlling factor in susceptibility/resistance to Schistosoma mansoni. *Dev Comp Immunol* (2007) 31:874–8. doi: 10.1016/j.dci.2006.12.005

9. Yoshino TP, Dinguirard N, Kunert J, Hokke CH. Molecular and functional characterization of a tandem-repeat galectin from the freshwater snail Biomphalaria glabrata, intermediate host of the human blood fluke Schistosoma mansoni. *Gene* (2008) 411:46–58. doi: 10.1016/j.gene.2008.01.003

10. Mourão M, Dinguirard N, Franco GR, Yoshino TP. Role of the Endogenous Antioxidant System in the Protection of Schistosoma mansoni Primary Sporocysts against Exogenous Oxidative Stress. *PloS Negl Trop Dis* (2009) 3:e550. doi: 10.1371/journal.pntd.0000550

11. Ittiprasert W, Miller A, Myers J, Nene V, El-Sayed NM, Knight M. Identification of immediate response genes dominantly expressed in juvenile resistant and susceptible Biomphalaria glabrata snails upon exposure to Schistosoma mansoni. *Mol Biochem Parasitol* (2010) 169:27–39. doi: 10.1016/j.molbiopara.2009.09.009

12. Moné Y, Mitta G, Duval D, Gourbal BEF. Effect of amphotericin B on the infection success of Schistosoma mansoni in Biomphalaria glabrata. *Exp Parasitol* (2010) 125:70–5. doi: 10.1016/j.exppara.2009.12.024

13. Hanington PC, Forys MA, Loker ES. A somatically diversified defense factor, FREP3, is a determinant of snail resistance to schistosome infection. *PloS Negl Trop Dis* (2012) 6:e1591. doi: 10.1371/journal.pntd.0001591

14. Portela J, Duval D, Rognon A, Galinier R, Boissier J, Coustau C, et al. Evidence for specific genotype-dependent immune priming in the lophotrochozoan *biomphalaria glabrata* snail. *J Innate Immun* (2013) 5:261–76. doi: 10.1159/000345909

15. Pila EA, Tarrabain M, Kabore AL, Hanington PC. A Novel Toll-Like Receptor (TLR) Influences Compatibility between the Gastropod Biomphalaria glabrata, and the Digenean Trematode Schistosoma mansoni. *PloS Pathog* (2016) 12:e1005513. doi: 10.1371/journal.ppat.1005513

16. Mitta G, Gourbal B, Grunau C, Knight M, Bridger JM, Théron A. The Compatibility Between Biomphalaria glabrata Snails and Schistosoma mansoni. *Adv Parasitol Elsevier* (2017) 97:111–45. doi: 10.1016/bs.apar.2016.08.006

17. Pila EA, Li H, Hambrook JR, Wu X, Hanington PC. Schistosomiasis from a snail's perspective: advances in snail immunity. *Trends Parasitol* (2017) 33:845–57. doi: 10.1016/j.pt.2017.07.006

18. Li H, Hambrook JR, Pila EA, Gharamah AA, Fang J, Wu X, et al. Coordination of humoral immune factors dictates compatibility between Schistosoma mansoni and Biomphalaria glabrata. *eLife* (2020) 9:e51708. doi: 10.7554/eLife.51708

19. Bu L, Zhong D, Lu L, Loker ES, Yan G, Zhang S-M. Compatibility between snails and schistosomes: insights from new genetic resources, comparative genomics, and genetic mapping. *Commun Biol* (2022) 5:940. doi: 10.1038/s42003-022-03844-5

20. Galinier R, Roger E, Moné Y, Duval D, Portet A, Pinaud S, et al. A multistrain approach to studying the mechanisms underlying compatibility in the interaction between Biomphalaria glabrata and Schistosoma mansoni. *PloS Negl Trop Dis* (2017) 11:e0005398. doi: 10.1371/journal.pntd.0005398

21. Portet A, Pinaud S, Tetreau G, Galinier R, Cosseau C, Duval D, et al. Integrated multi-omic analyses in Biomphalaria-Schistosoma dialogue reveal the immunobiological significance of FREP-SmPoMuc interaction. *Dev Comp Immunol* (2017) 75:16–27. doi: 10.1016/j.dci.2017.02.025

22. Elhelu O. Susceptibility of snails to infection with schistosomes is influenced by temperature and expression of heat shock proteins. *Epidemiol Open Access* (2015) 05. doi: 10.4172/2161-1165.1000189

23. Knight M, Elhelu O, Smith M, Haugen B, Miller A, Raghavan N, et al. Susceptibility of snails to infection with schistosomes is influenced by temperature and expression of heat shock proteins. *Epidemiology (Sunnyvale)* (2015) 5(2):189. doi: 10.4172/2161-1165.1000189

24. Haggerty CJE, Halstead NT, Civitello DJ, Rohr JR. Reducing disease and producing food: Effects of 13 agrochemicals on snail biomass and human schistosomes. *J Appl Ecol* (2022) 59:729–41. doi: 10.1111/1365-2664.14087

25. Lynch AE, Noble LR, Jones CS, Routledge EJ. Common aquatic pollutants modify hemocyte immune responses in Biomphalaria glabrata. *Front Immunol* (2022) 13. doi: 10.3389/fimmu.2022.839746

26. Paul J, Srivastava S, Bhattacharya S. Molecular methods for diagnosis of Entamoeba histolytica in a clinical setting: An overview. *Exp Parasitol* (2007) 116:35–43. doi: 10.1016/j.exppara.2006.11.005

27. Dagley MJ, Saunders EC, Simpson KJ, McConville MJ. High-content assay for measuring intracellular growth of *leishmania* in human macrophages. *ASSAY Drug Dev Technol* (2015) 13:389–401. doi: 10.1089/adt.2015.652

28. Schuster S, Krüger T, Subota I, Thusek S, Rotureau B, Beilhack A, et al. Developmental adaptations of trypanosome motility to the tsetse fly host environments unravel a multifaceted *in vivo* microswimmer system. *eLife* (2017) 6: e27656. doi: 10.7554/eLife.27656

29. Kurtz J, van der Veen IT, Christen M. Fluorescent vital labeling to track cestodes in a copepod intermediate host. *Exp Parasitol* (2002) 100:36–43. doi: 10.1006/expr.2001.4681

30. Trejo-Chávez H, García-Vilchis D, Reynoso-Ducoing O, Ambrosio JR. *In vitro* evaluation of the effects of cysticidal drugs in the Taenia crassiceps cysticerci ORF strain using the fluorescent CellTracker CMFDA. *Exp Parasitol* (2011) 127:294–9. doi: 10.1016/j.exppara.2010.06.025

31. Grego M, Stachowitsch M, De Troch M, Riedel B. CellTracker Green labelling vs. rose bengal staining: CTG wins by points in distinguishing living from dead anoxia-impacted copepods and nematodes. *Biogeosciences* (2013) 10:4565–75. doi: 10.5194/bg-10-4565-2013

32. Kilarski WW, Martin C, Pisano M, Bain O, Babayan SA, Swartz MA. Inherent biomechanical traits enable infective filariae to disseminate through collecting lymphatic vessels. *Nat Commun* (2019) 10:2895. doi: 10.1038/s41467-019-10675-2

33. Renahan T, Sommer RJ. Nematode interactions on beetle hosts indicate a role of mouth-form plasticity in resource competition. *Front Ecol Evol* (2021) 9:752695. doi: 10.3389/fevo.2021.752695

34. Ittiprasert W, Moescheid MF, Chaparro C, Mann VH, Quack T, Rodpai R, et al. Targeted insertion and reporter transgene activity at a gene safe harbor of the human blood fluke, Schistosoma mansoni. *Cell Rep Methods* (2023) 3:100535. doi: 10.1016/j.crmeth.2023.100535

35. Theron A, Rognon A, Gourbal B, Mitta G. Multi-parasite host susceptibility and multi-host parasite infectivity: a new approach of the Biomphalaria glabrata/Schistosoma mansoni compatibility polymorphism. *Infect Genet Evol J Mol Epidemiol Evol Genet Infect Dis* (2014) 26:80–8. doi: 10.1016/j.meegid.2014.04.025

36. Kruskal WH, Wallis WA. Use of ranks in one-criterion variance analysis. *J Am Stat Assoc* (1952) 47:583–621. doi: 10.1080/01621459.1952.10483441

37. Dunn OJ. Multiple comparisons using rank sums. *Technometrics* (1964) 6:241–52. doi: 10.1080/00401706.1964.10490181

38. Pan SC. The fine structure of the miracidium of Schistosoma mansoni. *J Invertebr Pathol* (1980) 36:307–72. doi: 10.1016/0022-2011(80)90040-3

39. Eklu-Natey DT, Wüest J, Swiderski Z, Striebel HP, Huggel H. Comparative scanning electron microscope (SEM) study of miracidia of four human schistosome species. *Int J Parasitol* (1985) 15:33–42. doi: 10.1016/0020-7519(85)90098-0

40. Samuelson JC, Caulfield JP. Role of pleated septate junctions in the epithelium of miracidia of Schistosoma mansoni during transformation to sporocysts *in vitro*. *Tissue Cell* (1985) 17:667–82. doi: 10.1016/0040-8166(85)90003-5

41. Poteaux P, Gourbal B, Duval D. Time series analysis of tegument ultrastructure of *in vitro* transformed miracidium to mother sporocyst of the human parasite Schistosoma mansoni. *Acta Trop* (2023) 240:106840. doi: 10.1016/j.actatropica.2023.106840

42. Bruckner DA, Voge M. The nervous system of larval schistosoma mansoni as revealed by acetylcholinesterase staining. *J Parasitol* (1974) 60:437–46. doi: 10.2307/3278359

43. Boleti H, Ojcius DM, Dautry-Varsat A. Fluorescent labelling of intracellular bacteria in living host cells. *J Microbiol Methods* (2000) 40:265–74. doi: 10.1016/S0167-7012(00)00132-9

44. Sato H, Kusel JR, Thornhill J. Functional visualization of the excretory system of adult Schistosoma mansoni by the fluorescent marker resorufin. *Parasitology* (2002) 125:527–35. doi: 10.1017/s0031182002002536

45. Couto FFB, Coelho PMZ, Araújo N, Kusel JR, Katz N, Mattos ACA. Use of fluorescent probes as a useful tool to identify resistant *Schistosoma mansoni* isolates to praziquantel. *Parasitology* (2010) 137:1791–7. doi: 10.1017/S003118201000065X

46. Liang Y-S, Wang W, Dai J-R, Li H-J, Tao Y-H, Zhang J-F, et al. Susceptibility to praziquantel of male and female cercariae of praziquantel-resistant and susceptible isolates of Schistosoma mansoni. *J Helminthol* (2010) 84:202–7. doi: 10.1017/S0022149X0999054X

47. Buchter V, Hess J, Gasser G, Keiser J. Assessment of tegumental damage to Schistosoma mansoni and S. haematobium after *in vitro* exposure to ferrocenyl, ruthenocenyl and benzyl derivatives of oxamniquine using scanning electron microscopy. *Parasit Vectors* (2018) 11:580. doi: 10.1186/s13071-018-3132-x

48. Wendt GR, Collins JN, Pei J, Pearson MS, Bennett HM, Loukas A, et al. Flatworm-specific transcriptional regulators promote the specification of tegumental progenitors in Schistosoma mansoni. *eLife* (2018) 7:e33221. doi: 10.7554/eLife.33221

49. Bonfim TCDS, Tunholi-Alves VM, Martins FG, Mota EM, Maldonado A, Pinheiro J, et al. Biological and histological changes in reproductive patterns of Biomphalaria glabrata experimentally co-infected by Echinostoma paraensei and Angiostrongylus cantonensis. *Exp Parasitol* (2018) 195:66–70. doi: 10.1016/j.exppara.2018.10.005

50. Bonfim TCDS, Martins FG, Tunholi-Alves VM, Lima MG, Mota EM, Maldonado A, et al. Evaluation of changes in the carbohydrate metabolism of Biomphalaria glabrata Say 1818 exposed to experimental coinfection by Angiostrongylus cantonensis (Nematoda) and Echinostoma paraensei (Trematoda). *J Invertebr Pathol* (2020) 170:107314. doi: 10.1016/j.jip.2019.107314

frontiers | Frontiers in Immunology

TYPE Review
PUBLISHED 05 December 2023
DOI 10.3389/fimmu.2023.1268998

OPEN ACCESS

EDITED BY
Rafael Toledo,
University of Valencia, Spain

REVIEWED BY
Moses Adriko,
Vector Borne and NTD Control Division, Uganda
Selorme Adukpo,
University of Ghana, Ghana

*CORRESPONDENCE
Ricardo Riccio Oliveira
ricardo.riccio@fiocruz.br

†These authors have contributed equally to this work and share first authorship

‡These authors have contributed equally to this work and share last authorship

RECEIVED 31 July 2023
ACCEPTED 17 November 2023
PUBLISHED 05 December 2023

CITATION
Menezes CA, Montresor LC, Jangola STG, de Mattos AC, Domingues ALC, Júnior AM, Silva CCM, Barbosa CS, de Mendonça CLF, Massara CL, Fonseca CT, de Oliveira EJ, Gomes ECdS, da Silva EF, Bezerra FSdM, Silva FP Jr, de Siqueira IC, Silva JRMe, Heller L, Farias LP, Beck LCNH, Santos MCS, Lima MG, Mourão MdM, Enk MJ, Fernandez MA, Katz N, Carvalho OdS, Parreiras PM, Neves RH, Gava SG, de Oliveira SA, Thiengo SC, Favre TC, Graeff-Teixeira C, Pieri OS, Caldeira RL, da Silva-Pereira RA, Rocha RS and Oliveira RR (2023) FioSchisto's expert perspective on implementing WHO guidelines for schistosomiasis control and transmission elimination in Brazil. *Front. Immunol.* 14:1268998. doi: 10.3389/fimmu.2023.1268998

FioSchisto's expert perspective on implementing WHO guidelines for schistosomiasis control and transmission elimination in Brazil

Camilla Almeida Menezes[1†], Langia Colli Montresor[2†], Soraya Torres Gaze Jangola[2†], Aline Carvalho de Mattos[3], Ana Lúcia Coutinho Domingues[4], Arnaldo Maldonado Júnior[3], Clélia Christina Mello Silva[3], Constança Simões Barbosa[5], Cristiane Lafetá Furtado de Mendonça[2], Cristiano Lara Massara[2], Cristina Toscano Fonseca[2], Edward José de Oliveira[2], Elainne Christine de Souza Gomes[5], Elizângela Feitosa da Silva[3], Fernando Schemelzer de Moraes Bezerra[6], Floriano Paes Silva-Jr[3], Isadora Cristina de Siqueira[1], José Roberto Machado e Silva[7], Leo Heller[2], Leonardo Paiva Farias[1], Lilian C. Nobrega Holsbach Beck[3], Mariana Cristina Silva Santos[2], Mariana Gomes Lima[3], Marina de Moraes Mourão[2], Martin Johannes Enk[8], Monica Ammon Fernandez[3], Naftale Katz[2], Omar dos Santos Carvalho[2], Patrícia Martins Parreiras[2], Renata Heisler Neves[7], Sandra Grossi Gava[2], Sheilla Andrade de Oliveira[5], Silvana Carvalho Thiengo[3], Tereza Cristina Favre[3], Carlos Graeff-Teixeira[9‡], Otávio Sarmento Pieri[3‡], Roberta Lima Caldeira[2‡], Rosiane A. da Silva-Pereira[2‡], Roberto Sena Rocha[2‡] and Ricardo Riccio Oliveira[1*‡]

[1]Instituto Gonçalo Moniz, Fundação Oswaldo Cruz - FIOCRUZ, Salvador, Brazil, [2]Instituto René Rachou, Fundação Oswaldo Cruz - FIOCRUZ, Belo Horizonte, Brazil, [3]Instituto Oswaldo Cruz, Fundação Oswaldo Cruz - FIOCRUZ, Rio de Janeiro, Brazil, [4]Centro de Ciências da Saúde, Departamento de Medicina Clínica, Universidade Federal de Pernambuco, Recife, Brazil, [5]Instituto Aggeu Magalhães, Fundação Oswaldo Cruz - FIOCRUZ, Recife, Brazil, [6]Centro de Ciências da Saúde, Departamento de Análises Clínicas e Toxicológicas, Universidade Federal do Ceará, Fortaleza, Brazil, [7]Faculdade de Ciências Médicas, Universidade Estatual do Rio de Janeiro, Rio de Janeiro, Brazil, [8]Seção de Parasitologia, Instituto Evandro Chagas, Ananindeua, Brazil, [9]Centro de Ciências da Saúde, Núcleo de Doenças Infecciosas, Universidade Federal do Espírito Santo, Vitória, Brazil

The World Health Organization (WHO) recognizes schistosomiasis as one of the Neglected Tropical Diseases targeted for global elimination in the 2030 Agenda of the Sustainable Development Goals. In Brazil, schistosomiasis mansoni is considered a public health problem, particularly prevalent among vulnerable

10.3389/fimmu.2023.1268998

populations living in areas with poor environmental and sanitary conditions. In 2022, the WHO published a Guideline encompassing recommendations to assist national programs in endemic countries in achieving morbidity control, eliminating schistosomiasis as a public health problem, and advancing towards interrupting transmission. The perspectives presented here, collectively prepared by members of the Oswaldo Cruz Foundation's (Fiocruz) Schistosomiasis Translational Program (FioSchisto), along with invited experts, examine the feasibility of the WHO recommendations for the Brazilian settings, providing appropriate recommendations for public health policies applicable to the epidemiological reality of Brazil, and suggests future research to address relevant issues. In Brazil, the provision of safe water and sanitation should be the key action to achieve schistosomiasis elimination goals. The agencies involved in measures implementation should act together with the Primary Care teams for planning, executing, monitoring, and evaluating actions in priority municipalities based on their epidemiological indicators. Host snails control should prioritize judicious ecological interventions at breeding sites. The Information, Education, and Communication (IEC) strategy should be associated with water and sanitation and other control actions, actively involving school community. To identify infected carriers, FioSchisto recommends a two-stage approach of immunological and molecular tests to verify transmission interruption during the intervention and beyond. Praziquantel administration should be done under medical supervision at the Primary Care level. MDA should be considered in exceptional settings, as a measure of initial attack strategy in locations presenting high endemicity, always integrated with water and sanitation, IEC, and snail control. To assist decision-making, as well as the monitoring and evaluation of strategic actions, there is a need for an Information System. FioSchisto considers this systematization essential to make investments in strategic research to support the improvement of schistosomiasis control actions. Efforts toward schistosomiasis elimination in Brazil will succeed with a paradigm shift from the vertical prescriptive framework to a community-centered approach involving intersectoral and interdisciplinary collaboration.

KEYWORDS

Schistosoma mansoni, schistosomiasis, neglected tropical diseases, control and elimination, Brazil

1 Introduction

Schistosomiasis, one of the oldest parasitic infections in humans, has co-evolved with humanity over centuries. Currently, an estimated 250 million people worldwide are infected with the disease, while approximately 700 million people are at risk of infection. Schistosomiasis has been recognized as one of the Neglected Tropical Diseases (NTDs), caused by blood flukes such as *Schistosoma mansoni*, *S. haematobium*, and *S. japonicum*. The disease primarily affects impoverished regions and individuals, remaining endemic in 78 countries (1). It is acquired through the skin and mucous membrane contact with water containing the infective forms of the parasite and is more prevalent in areas lacking adequate water and sanitation (2).

The transmission of schistosomiasis relies on infected individuals excreting helminth eggs within their feces and urine and aquatic snails acting as intermediate hosts that release infective cercariae into water sources used by humans in their daily activities. Schistosomiasis transmission is a complex process influenced by numerous complexes contributing factors. As a result, controlling the disease requires implementing multiple preventive measures. These measures include early diagnosis and timely treatment, the monitoring and control of intermediate hosts, health educational initiatives, and sanitation efforts to modify the environmental conditions that facilitate *Schistosoma* spp. transmission. These actions must be implemented in a coordinated and integrated manner as part of a comprehensive control program (2).

Align with the United Nations' 2030 agenda established in 2015, the World Health Organization (WHO) has set a goal of eliminating schistosomiasis as a public health issue worldwide. The aim is to reduce the prevalence of severe infections (≥ 400

10.3389/fimmu.2023.1268998

eggs per gram of feces) to less than 1% by 2030 and halt transmission in at least 25 out of the 78 endemic countries during the same period. To achieve these goals, the WHO published in 2022 guidelines for the control and elimination of human schistosomiasis. These guidelines provide a set of recommendations to guide national schistosomiasis programs in endemic countries to achieve morbidity control, elimination of the disease as a public health issue, and to make progress toward interrupting transmission. WHO guidelines prioritize mass drug administration (MDA) while also advocating for sustainable preventive measures such as water and sanitation (1).

Research conducted in Brazil, where schistosomiasis mansoni is a significant public health concern, has shown that periodic mass treatment of people living in endemic communities if implemented without concurrent improvements in water supply and sanitation infrastructure resulted in temporary impact in the reduction of disease prevalence (3). In light of this, the present discussion, collaboratively conducted by members of the Oswaldo Cruz Foundation's Schistosomiasis Translational Program (FioSchisto) and invited experts, explores the feasibility of implementing WHO recommendations for Brazilian settings. The outcome is a set of recommendations for public health policies that apply to the country's epidemiological context and suggests pertinent research topics to be addressed.

2 Analysis of WHO recommendations for schistosomiasis control and transmission elimination

This section will discuss the six WHO recommendations for the control and elimination of schistosomiasis by 2030 (1), as shown in Table 1, from the perspective of the Brazilian context, where low endemicity areas are widespread and *S. mansoni* is the only species occurring.

2.1 Analysis of recommendations 1, 2, and 3

2.1.1 Background

The first three WHO's recommendations for the control and elimination of schistosomiasis emphasize the strategy of MDA using praziquantel in different epidemiological scenarios. Some challenges and criticisms need to be considered regarding these recommendations. The first challenge relates to the possibility of an insufficient stock of medication available to meet global demand. As for the criticisms, there is scientific evidence suggesting that praziquantel mass administration may only provide temporary benefits.

Studies conducted in Brazil have demonstrated that periodic treatment of endemic communities without adequate water supply and sanitation has a transient effect. Examples of this scenario occurred in some locations in the municipalities of Ipojuca in Pernambuco and Conde in Bahia, which maintains the

TABLE 1 WHO recommendations for schistosomiasis control and elimination.

Recommendation 1	
In endemic communities with a prevalence of *Schistosoma* spp. infection ≥ 10%, WHO recommends annual preventive chemotherapy with a single dose of praziquantel at ≥ 75% treatment coverage in all age groups from 2 years old, including adults, pregnant women after the first trimester, and lactating women, to control schistosomiasis morbidity and advance towards eliminating the disease as a public health problem.	
Strong recommendation	Certainty of evidence: moderate
Recommendation 2	
In endemic communities with a prevalence of *Schistosoma* spp. infection < 10%, WHO suggests one of two approaches based on programmatic objectives and resources: (i) where there has been a program of regular preventive chemotherapy, to continue the intervention at the same or reduced frequency towards interruption of transmission; or (ii) where there has not been a program of regular preventive chemotherapy, to use a clinical approach of test-and-treat, instead of preventive chemotherapy targeting a population.	
Conditional recommendation	Certainty of evidence: very low
Recommendation 3	
In endemic communities with a prevalence of *Schistosoma* spp. infection ≥ 10% that demonstrate a lack of an appropriate response to annual preventive chemotherapy, despite adequate treatment coverage (≥ 75%), WHO suggests consideration of biannual (twice yearly) instead of annual preventive chemotherapy.	
Conditional recommendation	Certainty of evidence: very low
Recommendation 4	
WHO recommends that health facilities provide access to treatment with praziquantel to control morbidity due to schistosomiasis in all infected individuals regardless of age, including infected pregnant excluding the first trimester, lactating women, and pre-SAC aged < 2 years. The decision to administer treatment in children under 2 years of age should be based on testing and clinical judgment.	
Strong recommendation	Certainty of evidence: moderate
Recommendation 5	
WHO recommends WASH interventions, environmental interventions (water engineering and focal snail control with molluscicides), and behavioral change interventions as essential measures to help reduce transmission of *Schistosoma* spp. in endemic areas.	
Strong recommendation	Certainty of evidence: low
Recommendation 6	
In communities approaching the interruption of transmission (defined as having no autochthonous human cases reported for 5 consecutive years), WHO suggests a verification framework that consists of: 1. Testing for *Schistosoma* infection in humans with a diagnostic that has high sensitivity and specificity. This may require the use of a two-step diagnostic process starting with a high-sensitivity test confirmed with a second, high-specificity test. 2. Testing for *Schistosoma* infection in snails with a diagnostic that has high sensitivity and specificity. This may require the use of a two-step diagnostic process starting with a high-sensitivity test confirmed with a second, high-specificity test. 3. Testing for *Schistosoma* infection in non-human mammalian hosts, as applicable, with a diagnostic that has high sensitivity and specificity. This may require the use of a two-step diagnostic process starting with a high-sensitivity test confirmed with a second, high-specificity test.	
Conditional recommendation	Certainty of evidence: low

endemicity of the disease after successive mass treatments over two decades (4–8).

In 2009, the Executive Council of the Pan American Health Organization (PAHO) reiterated the WHO recommendation to implement an annual MDA scheme targeting school-age children in endemic areas of the Americas. At that time, the Brazilian Ministry of Health argued that schistosomiasis control measures should focus on strengthening the diagnosis and treatment capabilities at the primary healthcare level, as well as improving sanitation conditions (9). According to the Ministry of Health's latest Health Surveillance Guide (10), several crucial measures need to be taken to attain the required health standards for safeguarding and enhancing the living conditions of at-risk populations vulnerable to schistosomiasis and other infectious diseases that aggravate poverty. These measures include ensuring access to safe drinking water and sanitation, managing solid waste disposal, adopting appropriate practices for the use of land, improving drainage, controlling vectors, and managing non-human reservoirs.

Since 2014, the Ministry of Health has limited its recommendation of MDA to communities where the Kato-Katz positivity rates are ≥ 25%, which are a small minority, and always in conjunction with the aforementioned genuinely preventive measures (2). In Brazil, MDA has been implemented only once in communities where Kato-Katz positivity rates were 10% or higher. This initiative took place in different locations considered a priority by the Pernambuco State Health Department, in the four-year periods of 2011-2014 (11), 2015-2018 (12) e 2019-2022 (13). Despite the implementation of MDA, the failure to improve environmental sanitation and provide clean water to the communities left the population at a persistent risk of reinfection (14, 15).

A recent publication considers that the Americas and Asia may have had already achieved the elimination of schistosomiasis as a public health problem and are heading toward the interruption of transmission (16). This consideration should be viewed with caution regarding Brazil, as it has not yet been validated that the proportion of exams with severe infections (≥ 400 epg by Kato-Katz) in the country is lower than 1%, which is a prerequisite stipulated by the WHO (1). According to data from the Surveillance and Control Program for Schistosomiasis (SISPCE) (2), in 2016, 9% of the 53 localities that underwent MDA in the state of Pernambuco sustained percentages of severe infections equal to or higher than 1%.

In 2018, the Brazilian Ministry of Health formulated an Action Plan to tackle schistosomiasis for the period 2019-2021. For this, 472 municipalities across 11 states were chosen based on epidemiological data from official information systems over the previous five years, as well as results from the National Survey of Schistosomiasis and Soil-transmitted Helminthiasis (INPEG) conducted between 2011 and 2015. Factors such as population data, Municipal Human Development Index, and water and sanitation conditions of the municipalities in the period 2017-2018 were also considered. However, the original plan was not implemented due to the COVID-19 pandemic. The Ministry of Health is developing a new version, taking into account the goal of eliminating schistosomiasis as a public health problem by 2030 (1) and incorporating the latest recommendations provided by the WHO (17).

It is expected that the goal of eliminating schistosomiasis as a public health problem in Brazil will be achieved in the coming years, leading to an official recommendation by the WHO to proceed towards control and elimination of transmission. This new stage will require the implementation of a test-and-treat scheme dependent on highly sensitive and specific diagnostic tests. Consequently, both MDA and the identification of infected individuals based on Kato-Katz (18) will no longer be applicable. To achieve the goal of interrupting transmission, it will be crucial to prioritize the preventive measures emphasized in the Ministry of Health's Health Surveillance Guide (10).

2.1.2 Recommendations from FioSchisto

FioSchisto understands that the WHO recommendations regarding the mass administration of praziquantel do not apply to the current eco-epidemiological context of Brazil. Instead, interventions should genuinely prioritize preventive measures in both localities that have not yet achieved the goal of eliminating schistosomiasis as a public health problem and those moving towards interrupting transmission. Furthermore, municipalities interested in validating the goal of eliminating schistosomiasis as a public health problem should first identify the target communities, as these are the operational units of actions for schistosomiasis control (1, 2, 17), not the municipalities.

The FioSchisto highlights the need for improved information systems to assist in the decision-making process regarding the recommended strategic actions for the elimination of schistosomiasis as a public health problem and the interruption of transmission, as well as the monitoring and evaluation of these actions. The existing system (SISPCE) is deemed inadequate in terms of its ability to register, consolidate, and provide the required information. A robust information system should encompass data at both the individual and target population levels throughout the baseline, intervention, and follow-up stages.

Although FioSchisto acknowledges that MDA may not universally apply to the current Brazilian epidemiological settings, we recognize that there are still areas with a high frequency of positive parasitological tests. For such areas, the local health system and respective health authorities must mobilize attention to establish an effective strategy for local action, prioritizing actions based at water supply, sanitation, and health education, and may consider MDA as an initial attack strategy.

2.1.3 Investment in research

The FioSchisto recognizes that the 10% positivity threshold established by WHO for Kato-Katz testing applies specifically to different MDA schemes and not to other interventions. These interventions are indicated regardless of the level of positivity observed in the communities. It is worth noting that the threshold defined by WHO for MDA is based on studies conducted in Sub-Saharan Africa, where the epidemiological conditions differ from those in Brazil. Thus, the determination of appropriate cut-off points for different intervention schemes

depends on adequate studies of the country's reality. The FioSchisto emphasizes the need for investment in research to better understand the epidemiological context and to guide the development of appropriate interventions for the Brazilian context.

2.2 Analysis of recommendation 4

2.2.1 Background

The fourth WHO recommendation emphasizes that the use of praziquantel is indicated for all infected individuals, with exceptions for pregnant women in the first trimester, breastfeeding women, and children under two years of age. It also states that access to treatment should be provided by healthcare services in adequate facilities.

The praziquantel leaflet, approved by the Brazilian National Health Surveillance Agency (ANVISA), states that the treatment is not recommended for children under four years of age. Similarly, praziquantel treatment is contraindicated in the first trimester of pregnancy. However, due to the lack of scientific evidence on the safety of praziquantel use during pregnancy, treatment for pregnant women from the second trimester onwards should only be carried out after rigorous medical evaluation. In this case, praziquantel administration is classified as a category B risk.

According to ANVISA, during lactation, the prescribing physician should also carefully evaluate the administration of praziquantel since the medication can reach breast milk in concentrations equivalent to up to 20% of plasma concentration. In case of indication and use of praziquantel during lactation, breastfeeding should be interrupted on the day of treatment and during the three following days after administration.

2.2.2 Recommendations from FioSchisto

FioSchisto considers that praziquantel can be administered to patients under the mentioned conditions, but it should be done under careful medical evaluation and supervision. However, the indication and administration of praziquantel for children under four years of age, pregnant women, or lactating women should be implemented on an individual basis and in appropriate medical facilities, which does not apply at the population or large-scale level.

Additionally, FioSchisto recommends that primary healthcare teams in each municipality should be in charge of the schistosomiasis treatment using praziquantel. Thus, it is recommended that this team is properly trained and capacitated in the treatment of schistosomiasis. It is the responsibility of each municipality to provide the necessary support and resources to enable the implementation of this training.

2.2.3 Investment in research

Considering that praziquantel is currently the only available medication for treating schistosomiasis, investment in research for the development of new drugs is necessary. In addition to that, the well-known low efficacy against immature forms of *Schistosoma* sp., the continuous use of the medication for over four decades, and the parasite's ability to develop resistance to praziquantel make it necessary to develop new therapeutic approaches. Furthermore, it should be noted that the current formulation of praziquantel is not recommended for children under four years of age, according to the medication's package insert.

The pediatric praziquantel, which is being produced by Farmanguinhos-Fiocruz through a Pediatric Praziquantel consortium initiative led by Merck, will be available in the short term. This will be an important advancement in the treatment of schistosomiasis for children under four years of age, who have been historically excluded from therapeutic interventions. However, since the clinical trial for this new drug has not been conducted in Brazil and considering the large variation among human and parasite populations, it is recommended that its safety and efficacy should be also demonstrated in the Brazilian settings.

2.3 Analysis of recommendation 5

2.3.1 Background

The fifth WHO recommendation focuses on WASH interventions and chemical control of snails. The term WASH stands for Water, Sanitation, and Hygiene. However, the document introduces these interventions as of low certainty of evidence and states that "WASH interventions are expected to provide modest benefits in limiting Schistosoma transmission". For WHO, WASH interventions should be a "complementary measure" to reduce the prevalence of schistosomiasis.

As there is no exact translation of this term in the technical language used in Brazil, the expression "basic sanitation" is considered for this purpose. According to Brazilian legislation (19), basic sanitation comprises actions related to water supply, sanitation, solid waste management, and drainage of rainwater. Therefore, the concept of "basic sanitation" is more comprehensive than the actions covered by the WASH expression. In this study, the term "basic sanitation" is used from this point on, considering the above-mentioned conceptual difference.

While the inequality in access to sanitation infrastructure poses a hindrance to achieving universalization, there have been notable advances in this field in Brazil. Since the first national prevalence surveys in the 1950s, the country has gone from 15.5% to 86% coverage of households with water supply in 2019. For sanitation services, Brazil went from 9% of households served to 68% during the period (20). This increase represents significant additions in access to sanitary infrastructure over the decades, which may be compatible with efforts toward fulfilling Human Rights in Water and Sanitation (21).

Brazil has been consistently developing models to control schistosomiasis that can substantially reduce the prevalence and incidence indicators of the disease. The strategies include drug treatment, provision of water, sanitation and hygiene facilities, and actions that involve community participation and primary healthcare within the Unified Health System (SUS).

Studies conducted in Brazil have shown the effectiveness of basic sanitation interventions in reducing infection rates. For example, in the 1960s, in a locality in the municipality of Cabo, in Pernambuco, infection rates were progressively reduced in areas

with basic sanitation interventions compared to areas without intervention (22). Also in Pernambuco, in the municipality of São Lourenço da Mata, sanitary facilities such as septic tanks (OR 0.60; 95% CI 0.44-0.84) and general sewage systems (OR 0.20; 95% CI 0.14-0.29) were significantly associated with a decrease in the probability of infection (23). Another study, conducted in 482 municipalities in the state of Minas Gerais, showed that the variable "percentage of households with general sewage systems" contributed as an explanatory factor for infection rates, along with other social, demographic, and health conditions evaluated in the population. Additionally, the variable "percentage of households with sewage discharged into rivers, lakes, or seas" provided indicative evidence for the occurrence of the disease (24).

Similarly, an experience in municipalities of the states of Espírito Santo and Minas Gerais demonstrated that providing dry toilets and water, as well as facilities that encourage hygiene practices by the population, such as community laundries, domestic washing tanks, drinking fountains, faucets, and showers, constituted relevant alternatives to individualized drug treatment (25, 26). A district in the municipality of Sabará, Minas Gerais, showed a positive response to the implementation of a treated water system between 1980 and 2007, with a reduction in the prevalence of schistosomiasis from 36.7% to 2.5% (27, 28). In this state, studies in an endemic area over 25 years showed that severe forms of the disease were strongly associated with the absence of piped water (OR 7.7; 95% CI 2.6-23.1) and the habit of bathing in water collections (OR 5.7; 95% CI 1.3-25.5), the latter being a consequence of the former. In the observed periods (1981, 1992, and 2005), water supply coverage increased from 33.7% to 96%, safe sanitation increased from 71.7% to 97.6%, and the prevalence of the disease decreased from 70.4% to 1.7% (29–31).

The effectiveness of interventions in the school environment, compared to actions in the community, has been reported and should be considered. An ecological study using prevalence data from the INPEG (32) and national household and public and private school sanitation data showed that access to safe drinking water in schools was a protective factor for the disease (PRR 0.982; 95% CI 0.970 - 0.995) (33). This reinforces that water contact patterns are influenced by the availability of safe water supply, sanitation, and health education (34–36).

From a historical perspective, an ecological study analyzed data from three national surveys of schistosomiasis (1947-1953, 1975-1979, and 2010-2015), with a sample of 1,721 municipalities and 1,182,339 schoolchildren aged 7-14. The study found a protective effect of access to sanitary sewerage (RR 0.996; 95% CI 0.994 - 0.998), that increased from a mean coverage of 2.6% to 30.6% in the studied municipalities over 70 years. This result suggests that interventions in sanitation at the collective level have the potential to insert an effective barrier in the transmission cycle of schistosomiasis (37).

The local and nationwide findings reaffirm international studies that emphasize the increase in access to clean water, sanitation, and hygiene practices as important measures to reduce the chances of infection by the parasite (38). A meta-analysis published in 2014 supports that safe water supply (OR 0.53; 95% CI 0.47 - 0.61) and sanitation (OR 0.59; 95% CI 0.47 - 0.73) are associated with significantly lower chances of occurrence of schistosomiasis (39). It is important to highlight that this publication included 44 relevant studies, with Brazil contributing with 15 studies for water data and 11 studies for sanitation, reinforcing the country's leadership in research on the topic.

Regarding the chemical control of snails, during the 20th century, the use of molluscicides was among the strategies most advocated by governments and health agents (40–42). Since the 1960s, the most commonly used molluscicide has been niclosamide (40). In theory, the lethal concentration for snails, considered low, is non-toxic for vertebrates, including fish and humans. However, due to the technical complexity of the process of applying molluscicides in the environment, their irregular dispersion can lead to a higher accumulation in some areas, which can cause fish mortality and health problems in humans (43). Moreover, *Biomphalaria* sp. is known to undergo natural dormancy in certain periods, resulting in the inefficacy of niclosamide application.

Some countries, such as Brazil, have imposed restrictions on the use of niclosamide in the environment due to concerns regarding its harmful effects on non-target organisms (44). Niclosamide was approved many decades ago for anticestodal treatment in humans and has recently been evaluated in anticancer therapy and the treatment of the Zika virus (45, 46). This demonstrates its action on various signaling pathways in humans and other organisms, underscoring the need for a comprehensive risk evaluation of its environmental use. Furthermore, the decrease in the cost of praziquantel, after the end of its patent in the early 1990s, has made the use of niclosamide less cost-effective and potentially obsolete for schistosomiasis control.

Considering the evidence on the importance of long-lasting measures for snail control in the management of schistosomiasis, the promotion of environmental modifications that contribute to the reduction of snail populations, such as the modification of natural habitats, has been encouraged. Countries such as Japan, Morocco, Saudi Arabia, and Venezuela have achieved success with strategies such as the removal of aquatic vegetation, drainage of flooded areas, the lining of irrigation canals, and modification of watercourses, with careful attention to minimizing undesirable environmental impacts (47–50). In contrast, in areas with schistosomiasis transmission, environmental modifications that potentially contribute to the increase and expansion of snail populations, such as dam construction and expansion of irrigation, should be avoided (51, 52).

2.3.2 Recommendations from FioSchisto

In contrast to the WHO, FioSchisto proposes that genuinely preventive and long-lasting interventions against schistosomiasis should be prioritized in Brazil. It includes basic sanitation, health education, and interventions in snail breeding sites. The group recommends that a more appropriate approach should consider the following key aspects: the current public policy in Brazil based on decentralized control of endemic diseases; the autonomy of primary health care in addressing local health issues; the One Health concept; and environmental control measures of the disease, including interventions in basic sanitation.

The main basic sanitation measures that should be considered for schistosomiasis control in the country, after a thorough evaluation of the socio-environmental conditions of the affected locality, are described in Table 2.

In selecting the localities to prioritize basic sanitation interventions, it is important to adopt a watershed perspective. So it may be necessary to implement actions not only in endemic areas but also in contiguous areas that share the same watershed and are epidemiologically significant. In situations where there are increased migratory flows, due to development projects such as irrigation, dams, and mining works, basic sanitation actions must be properly planned and simultaneously implemented. In these cases, the risk of the introduction of schistosomiasis should be evaluated, and the necessary preventive environmental measures should be implemented.

It is recommended to establish effective and permanent communication between federal agencies and municipal health and environment departments to discuss, evaluate, plan, and implement sanitary interventions. Structural implementations should consider the sanitary reality of each region, given that the country has highly heterogeneous environmental, epidemiological, and socioeconomic conditions. The primary criterion for prioritizing interventions must be the prevalence of schistosomiasis and other sanitation-reducible diseases.

Health promotion, disease prevention, and control actions should be developed at the municipal level, taking into account local peculiarities. It is important to recognize that behavioral changes cannot be imposed through top-down interventions alone. Instead, it should be adapted through the understanding of risk factors and cultural patterns and in association with structural changes in the living environment.

Health professionals, including trained Community Health Agents, are essential and should be always included in the development of activities to inform and promote discussions about the disease, and the factors involved in transmission, prevention, and control. These actions should occur in the community and the school environment, as children and young people, are particularly important in the parasite transmission cycle. These discussions provide an opportunity to address that access to water and sanitation is a fundamental human right and a responsibility of public services, transcending beyond the scope of the disease itself.

TABLE 2 Main sanitation measures to be considered for schistosomiasis control in Brazil.

Basic sanitation measures
Supply of water for human consumption, with sufficient quantity and quality that meets potability standards.
Sanitary sewage disposal, with static or dynamic solutions, providing adequate sewage treatment to control pathogens and whose operation and maintenance are within reach of the community and service providers
Improvement of intra-household sanitary conditions.
Collection and proper disposal of solid waste, when relevant.
Drainage of rainwater, when applicable.

Regarding intervention in snail breeding sites, FioSchisto does not recommend the use of molluscicides, such as niclosamide, for snail control in Brazil due to its toxicity. Whenever possible, it is recommended to use snail control alternatives that are more appropriate and aligned with the One Health concept, particularly in low-endemicity areas, which are predominant in Brazil.

The FioSchisto suggests maintaining the recommendations outlined in the Technical Guidelines of the Ministry of Health (53) for snail control, with some updates and adjustments. As physical control methods in snail breeding sites, environmental management is considered, based on measures such as the rectification, coating, or channeling of watercourses, aimed at increasing the speed of water and making it difficult for intermediate hosts to attach. These measures should be planned and implemented in a way to minimize environmental impacts. Periodic cleaning and removal of aquatic vegetation on the banks of watercourses should be considered as a form of maintenance. Another recommended measure is the filling or drainage of places where water accumulates and creates an environment favorable to snail proliferation. In situations where contact with watercourses is necessary for crossing, the construction of bridges should be considered.

2.3.3 Investment in research

Investments in research are essential, especially in the areas of environmental, biological, and chemical control of intermediate hosts.

Regarding environmental control, there is still a need for a better understanding of the effects of implementing basic sanitation on the control of schistosomiasis and other parasitic diseases. From one side, basic sanitation encompasses a set of possible technologies and interventions (among other variations, collective vs individual systems for water; onsite vs offsite solutions for sanitation). On the other, the epidemiological, environmental, and socioeconomic context influences the possible effects of these interventions. This poses the need for fine-tuning in the research of the effects of different solutions for basic sanitation in different contexts, about the control of schistosomiasis.

Regarding biological control, there is a need to investigate the use of other native species within the same hydrographic basin proving it is sustainable and free of undesirable environmental effects. This approach can reduce or eliminate populations of schistosomiasis-transmitting snails. Another alternative is the release of snail populations resistant to *S. mansoni* infection in transmission foci. So, through crossbreeding with susceptible local populations, the trait of resistance or reduced susceptibility can be disseminated. It is strongly encouraged that these studies be carried out on populations of *Biomphalaria glabrata*, the main intermediate host of *S. mansoni* in Brazil. Also, the use of post-genomic methodologies for genetic modification of intermediate hosts to promote castration or resistance to *S. mansoni* infection shows promise.

Regarding chemical control, the focus should be on the development of solutions with high specificity and low environmental impact. It is suggested to search for new chemical products with molluscicidal or schistosomicidal action that are

specific and target essential molecular targets for the survival and development of the snail and/or the parasite.

2.4 Analysis of recommendation 6

2.4.1 Background

The sixth and final WHO's recommendation addresses a strategy for confirming the interruption of schistosomiasis transmission in communities, defined as the absence of autochthonous cases reported in humans in a specific community for five consecutive years. This recommendation suggests testing for schistosomiasis infection in humans, snails, and other mammalian hosts.

Regarding the verification of the interruption of transmission, in the absence of sensitive monitoring tools, there is a risk of premature interruption of the controlling measurement, which can lead to a significant increase in the number of cases in a short period of time. Therefore, the use of an accurate test for the diagnosis of schistosomiasis is important not only for the certification of disease elimination, but throughout the intervention period, especially when the control actions are guided by diagnosis performed at individual level and guides control actions. It is worth mentioning that the quantification of the parasitic load is necessary to indicate the elimination of the disease as a public health problem. But, considering the reality of the Brazilian health systems, except Kato-Katz, no other diagnostic methods are currently available for quantification of the parasitic load.

For the diagnosis of *S. mansoni* infection in the intermediate hosts, the main limitation is related to the transportation of the mollusks. Brazilian legislation is restrictive for the transport of biological material, turning the sample transport difficult and the mollusk-monitoring unfeasible. In addition to the high shipping fees, the time elapsed between collection and shipment of biological material is too long, resulting in the death of snails and in the waste of human and financial resources used in the process, making monitoring efforts unviable.

2.4.2 Recommendations from FioSchisto

FioSchisto considers that population surveys seeking the identification of infected individuals should use diagnostic methods with sensitivity greater than that achieved by the analysis of two slides of Kato-Katz. Thus, for areas that have not achieved the status of interrupting transmission, the group recommends the use of commercial serological tests. It is known that the currently available serological tests registered at ANVISA have limitations in terms of specificity. This limitation can be compensated by the epidemiological profile of the endemic areas, resulting in a high positive predictive value of the test in areas with high infection prevalence. Additionally, it should be noted that ELISA tests for other infections are routinely performed, and the operational capacity for conducting these tests already exists.

For localities in the process of eliminating transmission, where the predictive values of serological tests are compromised given the low incidence of the disease, and since no single diagnostic test is capable of accurately detect schistosomiasis in this epidemiological scenario, FioSchisto endorses the two-step diagnostic strategy recommended by WHO. It is suggested that the first screening stage should be performed using commercial serological tests with high sensitivity and the second stage should use a molecular test, such as quantitative Polymerase Chain Reaction (qPCR) (54), which, despite being more complex, have higher sensitivity compared to Kato-Katz method and a higher level of specificity. It is worth noting that the COVID-19 pandemic has shown that Brazil has the infrastructure needed to perform molecular tests, improving diagnosis and reducing costs if implemented on a larger scale.

Thus, by implementing the test-and-treat strategy, all individuals with schistosomiasis positivity are identified and treated. To make it possible, it is necessary to determine a new testing workflow so that samples are concluded as negative with the highest possible accuracy after multiple stages of analysis. The flowchart described in Figure 1 demonstrates the action plan proposed by FioSchisto for verifying the interruption of transmission in eligible locations.

Regarding testing in snails, in each monitoring cycle specific identification of the snails should be performed, in addition to detecting *S. mansoni*. The sampling strategy must consider local weather conditions and snail biology. Monitoring should be carried out annually during the dry season when breeding sites typically harbor a larger number of snails. The collection should be performed by trained teams so that a significant number of snails are collected (at least 20 per point), to increase the chances of detecting the parasite. In areas of low endemicity, where the probability of collecting snails positive for the parasite is low, it is necessary to increase the number of snails collected (100 specimens per point, of varying sizes). It is important to mention that these numbers may vary depending on the snail species. In intermittent watercourses, the collection should be performed when there is still enough water to harbor a dense population of snails. The transmission sites in areas considered epidemiologically important should be periodically monitored. The collection sites should be georeferenced, and the maximum amount of information should be recorded.

For the collection, transport, and processing of mollusks, FioSchisto recommends following the instructions in the "Guidelines for Surveillance and Control of Mollusks of Epidemiological Importance: Technical Guidelines" from the Schistosomiasis Surveillance and Control Program (SISPCE) (53). The identification of mollusks should be done using morphological taxonomy (55) and, when necessary, in association with molecular taxonomy (56, 57). Considering the difficulties described above, FioSchisto recommends that specific legislation be developed for the transportation of biological material that is of public health importance, thus facilitating access to reference laboratories. For the detection of *S. mansoni* in snails in areas of high and medium endemicity, where *B. glabrata* is the transmitting species, the classical parasitological methods of light exposure and crushing the snails between glass plates (58) should be prioritized due to their low cost. Considering trematodes diversity in Brazil, morphological identification of cercaria can provide robust results, particularly in endemic areas (59). In areas where *B. straminea* and *B. tenagophila*

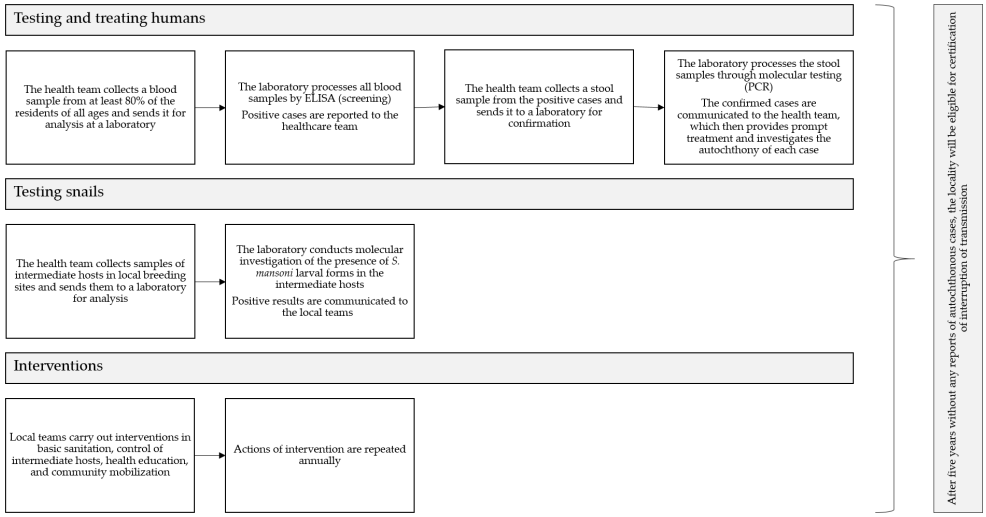

FIGURE 1
Action plan suggested by FioSchisto to verify interruption of schistosomiasis transmission in eligible locations.

are the transmitting species, as well as in low-endemicity areas, regardless of the transmitting species, molecular methods are indicated due to the inefficiency of parasitological methods under such epidemiological conditions. In this case, a pool of at least 10 to 20 snails from the same collection point should be used. DNA extraction should follow the literature recommendations (60) and extraction methods should be performed according to the standardized protocols of each laboratory. It is suggested to use the extracted DNA to identify the snail species and to detect the presence of *S. mansoni* (56). Associated with the monitoring of infected snails, it is recommended to investigate the occurrence of naturally infected wild rodents and other mammalians, and their function as maintainer of transmission of *S. mansoni*.

The WHO criterion for interruption of transmission should be used, i.e., no autochthonous cases reported for five consecutive years. The main operational indicators for mollusk control are the percentage of breeding sites surveyed, which indicates whether monitoring actions are being carried out according to the agreed plan; the percentage of positive snails; and the percentage of active transmission foci. These indicators demonstrate whether sanitation, environmental control, and mollusk control actions are effective in eliminating schistosomiasis transmission foci.

2.4.3 Investment in research

In the case of human testing, it is necessary to perform a laboratory and clinical validation of the serological diagnostic tests for schistosomiasis registered by ANVISA. There is also a need for studies that evaluate the effectiveness of the two-step diagnosis strategy and also of the test-and-treat strategy in reducing the number of infection cases in endemic areas. To drive future research efforts, an action plan was outlined:

- It is suggested to create a multicenter sample biobank of serum, urine, feces, and genetic material to be used in the validation of currently available tests and development of point-of-care tests.
- It is also suggested that in the case of fecal samples, unfixed frozen samples and samples processed *via* Helmintex should be stored.
- The case-finding strategy should also be validated because the higher the surveillance, the lower the prevalence tends to be.
- Equally important is the development of a point-of-care test to be used as the first test in diagnosis. For the production of this test, FioSchisto suggests the prioritization of antigens already used in ELISA assays. In the Brazilian states not yet equipped and capable to perform serological tests for schistosomiasis, it is recommended training and implementation of the required measures.

In the case of testing mollusks, it is necessary to provide financial support for biological material collection and transportation. New alternatives for sending preserved mollusks without the use of liquid fixatives, fixed in alcohol, or previously processed by regional teams, can aid increase the efficiency of monitoring methods.

Among promising monitoring techniques, environmental DNA (eDNA) appears to be of great relevance, as it allows the detection of cercariae without the need for mollusks collection. However, this technique still needs better standardization, and its reliability and reproducibility must be evaluated. Another promising method is near-infrared vibrational spectroscopy (NIR), already used for the detection of Zika virus and other arboviruses. NIR is a rapid method that does not require reagents and has good cost-benefit. An estimate regarding the diagnosis of Zika virus showed that NIR was 18 times faster and 110 times cheaper than RT-qPCR (61). However, the equipment is still not widely available, and the standardization of its use for *S. mansoni* detection and *Biomphalaria* spp. identification should be investigated (62).

3 Discussion

The successive WHO guidelines from 1953, 1961, 1965, 1967, 1973, and 1980 for the evaluation and control of schistosomiasis focused on the chemical control of snails until the early 1980s. This focus was gradually replaced by collective treatment until the end of the 1990s. Recently, targeted chemotherapeutic control for the most vulnerable groups has gained prominence. Other control measures, although recommended, did not have as much priority over the decades.

Brazil conducted national prevalence surveys of schistosomiasis since the 1940s and, faced with the expansion of the disease, control programs were created, such as the Special Schistosomiasis Control Program (PECE) in 1975, and the SISPCE (current program), which allowed disease mapping and implementation of control measures nationwide. These measures included coproscopic surveys, epidemiological surveillance of cases, environmental surveillance of intermediate hosts, and measures that precede and accompany all control activities, such as education, health, and community mobilization (2). However, since the beginning of Brazilian control programs, preventive chemotherapy as an isolated measure had already proven to be ineffective in reducing the prevalence of the disease (63), especially in areas that remained refractory to treatment (64).

The great diversity of ecological, socioeconomic, and cultural situations has an impact on the epidemiology of schistosomiasis and the dynamics of *S. mansoni* transmission in Brazil. The disease is not evenly distributed and low endemic areas are predominant, where it is very likely that the proportion of severe infections (≥ 400 epg by Kato-Katz) is less than 1% (32). The reduction in schistosomiasis prevalence and parasite load in infected individuals is the result of control programs that historically have used a combination of approaches, such as mass treatment, molluscicide application, and increased coverage of safe water supply and sanitation (65–67).

Studies conducted in Brazil have shown that periodic mass treatment of people living in endemic communities without improvements in water supply and sanitation infrastructure has a transient effect (3). Regarding molluscicides, although studies have shown that the use of niclosamide is capable of reducing snail populations and producing a substantial short-term impact on the prevalence and incidence of human infection, it has the disadvantage of low cost-effectiveness (27), toxic action on non-target organisms (68) and the need for frequent applications (65, 67). The literature has shown that niclosamide interferes with the development of zebrafish (*Danio rerio*) through various mechanisms (69). Considering that these studies were conducted at environmentally realistic concentrations, the adverse and toxic effects observed in zebrafish, an animal model universally used for toxicological and genetic testing due to its 70% genetic homology with humans, may also affect wildlife and humans (70).

The FioSchisto, as Fiocruz, and the WHO converge on a common premise: diseases are now recognized as resulting from dysfunction within ecosystems, characterized by their complex interactions. Human health is intimately linked to animal and environmental health. With that being said, the position established by FioSchisto in this document presents itself as a collaborative partner in a directed effort towards a comprehensive understanding of the mechanisms that can lead to the control and elimination of these infectious agents. Within this framework, which encompasses diverse and complementary approaches, research on schistosomiasis in Brazil aims to contribute to the development of strategies and affirmative actions, opening dialogue and a different perspective for collective consideration on the elimination of schistosomiasis.

According to this statement, FioSchisto firmly believes in the inappropriateness of WHO recommendations to the Brazilian reality and the need for their adaptation to the Brazilian context. The emphasis on mass administration of praziquantel and chemical control of snails does not apply to Brazil, given the eco-epidemiological context, socioeconomic particularities, public health policies, and history of disease control. In this scenario, it is necessary to identify infection carriers, provide selective treatment, and improve basic sanitation and surveillance, which is considered the main measure to meet the goal of eliminating schistosomiasis.

To identify infection carriers, FioSchisto recommends two-stage immunological and molecular testing (screening and confirmation) to assess the interruption of transmission throughout the intervention period. It is crucial for the Brazilian government to invest in research for the diagnosis of schistosomiasis and, once appropriate methods are developed, to ensure their prompt availability to all healthcare facilities. Furthermore, it is crucial that the healthcare system is adequately prepared to diagnose possible cases imported by travelers from other countries, involving other species of *Schistosoma*, and to identify associated clinical forms that are not observed in Brazil, such as urinary tract disorder and female genital schistosomiasis.

Praziquantel administration should be conducted under medical supervision within primary health care. The WHO recommendation for mass treatment should only be considered as an initial attack strategy in areas with high endemicity, and it should always be integrated with health education, snail control, and sanitation actions. Additionally, would be highly important to test the new pediatric formulation in the Brazilian population to expedite its use.

Comprehensive health and environmental education should be associated with basic sanitation interventions and other control actions, involving the school community, the general population, and health teams. Snail control should prioritize interventions in breeding sites, with modification of habitats through vegetation removal, drainage of flooded areas, lining of irrigation channels, and careful alteration of water flow.

All agencies involved in basic sanitation should work together with primary health care teams for effective planning, execution, monitoring, and evaluation of actions in municipalities considered a priority from an epidemiological perspective. It is also necessary to promote continuing education programs to keep primary healthcare teams up to date on disease surveillance and control strategies, following the current guidelines of the Ministry of Health. To assist decision-making, as well as monitoring and

evaluation of strategic actions, there is a need for an information system that allows for the recording, consolidation, and sharing of relevant data.

The main actions of basic sanitation include the supply of safe drinking water, safe sanitation by sewerage or onsite solutions, and hygiene measures, which may also include solid waste management and drainage of rainwater. Adequate interventions in sewage disposal can contribute to introducing a barrier in the disease transmission cycle by eliminating contact between the eggs present in feces and the intermediate host. It is important to highlight that the design of these interventions must consider the local context and measures for sewage treatment and disposal that effectively remove eggs and miracidia, and ensure sustainability in the system operation.

Access to safe sanitation systems helps prevent wastewater from flowing into ditches or stormwater drainage systems. Localities with poor sanitation conditions may have higher transmission rates because they provide ideal conditions for the breeding of snails (71, 72). Countries that have successfully eliminated the infection, such as Japan (50) and Puerto Rico (73), have done so through intense economic development, government-funded projects, effective community participation, and primarily, increased access to basic sanitation interventions, resulting in a reduction in transmission sites (74, 75).

The FioSchisto considers that the recommendations regarding interventions in basic sanitation, which are part of the guidelines of the Ministry of Health (2) remain valid as a priority measure envisioning the elimination of schistosomiasis transmission. Therefore, it is reiterated that interventions in basic sanitation, when reaching levels of salubrity to protect and improve the living conditions of populations, can have a lasting and effective effect on the control of schistosomiasis, even in areas with low prevalence. There is undeniable evidence of its effect also in the control of other water and sewage-related diseases, such as diarrheal diseases, hepatitis A and E, arboviruses (dengue, Zika, and chikungunya), giardiasis, and different helminthiases. Furthermore, efforts to eliminate schistosomiasis in Brazil will only succeed with a shift in paradigm from the vertical, prescriptive framework to a community-centered approach involving strong intersectoral and interdisciplinary collaboration.

Author contributions

CM: Conceptualization, Methodology, Writing – original draft, Writing – review & editing, Formal Analysis. LM: Conceptualization, Formal Analysis, Methodology, Writing – original draft, Writing – review & editing, Visualization. SJ: Conceptualization, Formal Analysis, Methodology, Writing – original draft, Writing – review & editing. AM: Conceptualization, Methodology, Writing – review & editing, Validation. AD: Conceptualization, Methodology, Writing – review & editing. AJ: Conceptualization, Methodology, Writing – review & editing, Validation. CM: Conceptualization, Methodology, Writing – review & editing. CB: Conceptualization, Methodology, Writing – review & editing. CM: Conceptualization, Methodology, Writing – review & editing. CL: Conceptualization, Methodology, Writing – review & editing. CF: Conceptualization, Methodology, Writing – review & editing. EO: Conceptualization, Methodology, Writing – review & editing. EG: Conceptualization, Methodology, Writing – review & editing. ES: Conceptualization, Methodology, Writing – review & editing. FB: Conceptualization, Methodology, Writing – review & editing. FS: Conceptualization, Methodology, Writing – review & editing. Id: Conceptualization, Methodology, Writing – review & editing. JM: Conceptualization, Methodology, Writing – review & editing. LH: Conceptualization, Methodology, Writing – review & editing. LF: Conceptualization, Methodology, Writing – review & editing. LB: Conceptualization, Methodology, Writing – review & editing. MS: Conceptualization, Methodology, Writing – review & editing. ML: Conceptualization, Methodology, Writing – review & editing. MM: Conceptualization, Methodology, Writing – review & editing. ME: Conceptualization, Methodology, Writing – review & editing. MF: Conceptualization, Methodology, Writing – review & editing. NK: Conceptualization, Methodology, Writing – review & editing. OC: Conceptualization, Methodology, Writing – review & editing. PP: Conceptualization, Methodology, Writing – review & editing. RN: Conceptualization, Methodology, Writing – review & editing. SG: Conceptualization, Methodology, Writing – review & editing. Sd: Conceptualization, Methodology, Writing – review & editing. ST: Conceptualization, Methodology, Writing – review & editing. TF: Conceptualization, Methodology, Writing – review & editing. CG-T: Conceptualization, Investigation, Methodology, Supervision, Validation, Writing – original draft, Writing – review & editing. OP: Conceptualization, Investigation, Methodology, Supervision, Validation, Writing – original draft, Writing – review & editing. RC: Conceptualization, Investigation, Methodology, Supervision, Validation, Writing – original draft, Writing – review & editing. RS: Conceptualization, Investigation, Methodology, Supervision, Validation, Writing – original draft, Writing – review & editing. RR: Conceptualization, Investigation, Methodology, Supervision, Validation, Writing – original draft, Writing – review & editing. RO: Conceptualization, Investigation, Methodology, Supervision, Validation, Writing – original draft, Writing – review & editing.

Funding

The author(s) declare that no financial support was received for the research, authorship, and/or publication of this article.

Acknowledgments

We acknowledge the Vice-Presidency of Research and Biological Collections (VPPCB) of FIOCRUZ for their unwavering support to the translational FioSchisto program. We also extend our heartfelt thanks to FIOCRUZ for their comprehensive support, and to the FIOCRUZ unit in Bahia for their generous contribution towards the publication costs of this work.

Conflict of interest

The authors declare that the research was conducted in the absence of any commercial or financial relationships that could be construed as a potential conflict of interest.

The author(s) declared that they were an editorial board member of Frontiers, at the time of submission. This had no impact on the peer review process and the final decision.

Publisher's note

References

1. WHO. *Ending the Neglect to Attain the Sustainable Development Goals: A Road Map for Neglected Tropical Diseases 2021–2030* (Geneva: World Health Organization), Vol. 63. (2020).

2. BRASIL. *Vigilância Da Esquistossomose Mansoni: Diretrizes Técnicas* (Brasília: Ministério da Saúde). (2014). p. 144.

3. Lima e Costa MF, Guerra HL, Pimenta FGJr., Firmo JO, Uchoa E. [Evaluation of a program for the control of schistosomiasis in municipalities located on the basin of the Sao Francisco River, Minas Gerais, Brazil]. *Rev da Sociedade Bras Medicina Trop* (1996) 29(2):117–26.

4. Araujo MI, Hoppe B, Medeiros MJr., Alcantara L, Almeida MC, Schriefer A, et al. Impaired T helper 2 response to aeroallergen in helminth-infected patients with asthma. *J Infect Dis* (2004) 190(10):1797–803. doi: 10.1086/425017

5. Duarte Hde O, Droguett EL, Moura M, Gomes EC, Barbosa C, Barbosa V, et al. An ecological model for quantitative risk assessment for schistosomiasis: the case of a patchy environment in the coastal tropical area of northeastern Brazil. *Risk Anal an Off Publ Soc Risk Anal* (2014) 34(5):831–46. doi: 10.1111/risa.12139

6. Figueiredo JP, Oliveira RR, Cardoso LS, Barnes KC, Grant AV, Carvalho EM, et al. Adult worm-specific Ige/Igg4 balance is associated with low infection levels of schistosoma mansoni in an endemic area. *Parasite Immunol* (2012) 34(12):604–10. doi: 10.1111/pim.12001

7. Gomes ECS, Silva I, Nascimento W, Loyo RM, Domingues ALC, Barbosa CS. Urban schistosomiasis: an ecological study describing a new challenge to the control of this neglected tropical disease. *Lancet regional Health Americas* (2022) 8:100144. doi: 10.1016/j.lana.2021.100144

8. Oliveira RR, Figueiredo JP, Cardoso LS, Jabar RL, Souza RP, Wells MT, et al. Factors associated with resistance to schistosoma mansoni infection in an endemic area of Bahia, Brazil. *Am J Trop Med hygiene* (2012) 86(2):296–305. doi: 10.4269/ajtmh.2012.11-0204

9. PAHO. *49th Directing Council: Final Report* (Washington: Pan American Health Organization). (2009). p. 191.

10. BRASIL. *Guia De Vigilância Em Saúde* (Brasília: Ministério da Saúde). (2021). p. 1126.

11. Pernambuco. *Programa De Enfretamento Das Doenças Negligenciadas No Estado De Pernambuco Sanar – 2011 / 2014* (Recife: Secretaria Estadual de Saúde), Vol. 39. (2013).

12. Pernambuco. *Plano Integrado De Ações Para O Enfretamento Às Doenças Negligenciadas No Estado De Pernambuco Sanar / 2015 - 2018* (Recife: Secretaria Estadual de Saúde), Vol. 46. (2015).

13. Pernambuco. *Programa Para Enfrentamento Das Doenças Negligenciadas No Estado De Pernambuco Sanar / 2019-2022* (Recife: Secretaria Estadual de Saúde), Vol. 48. (2019).

14. Facchini LA, Nunes BP, Felisberto E, da Silva JAM, da Silva Junior JB, Tomasi E. Assessment of a Brazilian public policy intervention to address schistosomiasis in Pernambuco State: the Sanar program, 2011-2014. *BMC Public Health* (2018) 18 (1):1200. doi: 10.1186/s12889-018-6102-5

15. Pernambuco. *Esquistossomose E Geo-Helmintíases: Relatório Das Condições De Saneamento Das Áreas/Localidades Hiperendêmicas Em Pernambuco* (Recife: Secretaria Estadual de Saúde), Vol. 134. (2013).

16. Xu J, Li SZ, Guo JG, Zhou XN, Djirmay AG. The who new guideline to control and eliminate human schistosomiasis: implications for the verification of transmission interruption and surveillance of schistosoma japonicum in China. *Infect Dis poverty* (2022) 11(1):79. doi: 10.1186/s40249-022-01003-w

17. WHO. *Who Guideline on Control and Elimination of Human Schistosomiasis* (Geneva: World Health Organization). (2022). p. 144.

18. Katz N, Chaves A, Pellegrino J. A simple device for quantitative stool thick-smear technique in schistosomiasis mansoni. *Rev Inst Med Trop Sao Paulo* (1972) 14 (6):397–400.

19. BRASIL. *Lei n° 11.445, De 5 De Janeiro De 2007* (Brasília: Presidência da República). (2007).

20. BRASIL and IBGE. *Censo Demográfico: 1950 Rio de Janeiro: IBGE, Departamento de População* (1950). Available at: https://biblioteca.ibge.gov.br/?view=detalhes&id=767.

21. Heller L. The human rights to water and sanitation, gender equality, and the state. *Lancet* (2023) 401(10378):728. doi: 10.1016/S0140-6736(23)00100-9

22. Barbosa FS, Pinto R, Souza OA. Control of schistosomiasis mansoni in a small north east Brazilian community. *Trans R Soc Trop Med Hygiene* (1971) 65(2):206–13. doi: 10.1016/0035-9203(71)90220-3

23. Ximenes R, Southgate B, Smith PG, Guimaraes Neto L. Socioeconomic determinants of schistosomiasis in an urban area in the northeast of Brazil. *Rev panamericana salud publica = Pan Am J Public Health* (2003) 14(6):409–21. doi: 10.1590/s1020-49892003001100006

24. Silva J, Ramos SB, Andrade Md. Análise multivariada da esquistossomose no Estado De Minas Gerais: análise de componentes principais. *ABCS Health Sci* (2018) 43 (2):84–90.

25. Barbosa FS, da Cruz OJ, Hollanda E, Siqueira SA, de Carvalho MA, Gomes ML, et al. [an alternative model for schistosomiasis control: the present status of the project in the state of Espirito Santo, Brazil]. *Cadernos saude publica* (1993) 9(1):85–9. doi: 10.1590/s0102-311x1993000100009

26. Enk MJ, Lima AC, Barros Hda S, Massara CL, Coelho PM, Schall VT. Factors related to transmission of and infection with schistosoma mansoni in a village in the South-Eastern region of Brazil. *Memorias do Instituto Oswaldo Cruz* (2010) 105 (4):570–7. doi: 10.1590/s0074-02762010000400037

27. Coura-Filho P, Farah MW, Rezende DF, Lamartine SS, Carvalho OS, Katz N. [Environmental and social determinants in schistosomiasis mansoni in Ravena, Minas Gerais, Brazil]. *Cadernos saude publica* (1995) 11(2):254–65. doi: 10.1590/s0102-311x1995000200009

28. Vasconcelos CH, Cardoso PC, Quirino WC, Massara CL, Amaral GL, Cordeiro R, et al. [Evaluation of schistosomiasis mansoni control measures in Sabara, Minas Gerais State, Brazil, 1980-2007]. *Cadernos saude publica* (2009) 25(5):997–1006. doi: 10.1590/s0102-311x2009000500006

29. Costa MF, Rocha RS, Magalhaes MH, Katz N. [a hierarchical model for analysis of socio-economic variables and water contact patterns associated with the hepatosplenic form of schistosomiasis]. *Cadernos saude publica* (1994) 10 Suppl 2:241–53. doi: 10.1590/S0102-311X1994000800002

30. Lima e Costa MF, Rocha RS, de Almeida Magalhaes MH, Katz N. A clinico-epidemiological survey of schistosomiasis mansoni in a hyperendemic area in minas gerais state (Comercinho, Brazil). I. Differences in the manifestations of schistosomiasis in the town centre and in the environs. *Trans R Soc Trop Med Hygiene* (1985) 79 (4):539–45. doi: 10.1016/0035-9203(85)90090-2

31. Sarvel AK, Oliveira AA, Silva AR, Lima AC, Katz N. Evaluation of a 25-year-program for the control of schistosomiasis mansoni in an endemic area in Brazil. *PloS Negl Trop Dis* (2011) 5(3):e990. doi: 10.1371/journal.pntd.0000990

32. Katz N. *Inquérito Nacional De Prevalência Da Esquistossomose Mansoni E Geo-Helmintoses*. Belo Horizonte: CPqRR (2018).

33. Poague K, Mingoti SA, Heller L. Water, sanitation and schistosomiasis mansoni: A study based on the Brazilian national prevalence survey (2011-2015). *Ciencia saude coletiva* (2023) 28(2):363–72. doi: 10.1590/1413-81232023282.09692022

34. Barbosa LM, Silva LK, Reis EA, Azevedo TM, Costa JM, Blank WA, et al. Characteristics of the human host have little influence on which local schistosoma mansoni populations are acquired. *PloS Negl Trop Dis* (2013) 7(12):e2572. doi: 10.1371/journal.pntd.0002572

35. Lima e Costa MF, Rocha RS, Leite ML, Carneiro RG, Colley D, Gazzinelli G, et al. A multivariate analysis of socio-demographic factors, water contact patterns and schistosoma mansoni infection in an endemic area in Brazil. *Rev Inst Med Trop Sao Paulo* (1991) 33(1):58–63. doi: 10.1590/s0036-46651991000100011

36. Massara CL, Peixoto SV, Barros Hda S, Enk MJ, Carvalho Odos S, Schall V. Factors associated with schistosomiasis mansoni in a population from the municipality of jaboticatubas, state of Minas Gerais, Brazil. *Memorias do Instituto Oswaldo Cruz* (2004) 99(5 Suppl 1):127–34. doi: 10.1590/s0074-02762004000900023

37. Santos MCS, Oliveira GL, Mingoti SA, Heller L. Effect of environmental factors in reducing the prevalence of schistosomiasis in schoolchildren: an analysis of three extensive national prevalence surveys in Brazil (1950-2018). *PloS Negl Trop Dis* (2023) 17(7):e0010804. doi: 10.1371/journal.pntd.0010804

38. Esrey SA, Potash JB, Roberts L, Shiff C. Effects of improved water supply and sanitation on ascariasis, diarrhoea, dracunculiasis, hookworm infection, schistosomiasis, and trachoma. *Bull World Health Organ* (1991) 69(5):609–21.

39. Grimes JE, Croll D, Harrison WE, Utzinger J, Freeman MC, Templeton MR. The relationship between water, sanitation and schistosomiasis: A systematic review and meta-analysis. *PloS Negl Trop Dis* (2014) 8(12):e3296. doi: 10.1371/journal.pntd.0003296

40. King CH, Bertsch D. Historical perspective: snail control to prevent schistosomiasis. *PloS Negl Trop Dis* (2015) 9(4):e0003657. doi: 10.1371/journal.pntd.0003657

41. McCullough FS, Gayral P, Duncan J, Christie JD. Molluscicides in schistosomiasis control. *Bull World Health Organ* (1980) 58(5):681–9.

42. Sokolow SH, Wood CL, Jones IJ, Swartz SJ, Lopez M, Hsieh MH, et al. Global assessment of schistosomiasis control over the past century shows targeting the snail intermediate host works best. *PloS Negl Trop Dis* (2016) 10(7):e0004794. doi: 10.1371/journal.pntd.0004794

43. Dai JR, Wang W, Liang YS, Li HJ, Guan XH, Zhu YC. A novel molluscicidal formulation of niclosamide. *Parasitol Res* (2008) 103(2):405–12. doi: 10.1007/s00436-008-0988-2

44. Coelho P, Caldeira RL. Critical analysis of molluscicide application in schistosomiasis control programs in Brazil. *Infect Dis poverty* (2016) 5(1):57. doi: 10.1186/s40249-016-0153-6

45. Li Y, Li PK, Roberts MJ, Arend RC, Samant RS, Buchsbaum DJ. Multi-targeted therapy of cancer by niclosamide: A new application for an old drug. *Cancer Lett* (2014) 349(1):8–14. doi: 10.1016/j.canlet.2014.04.003

46. Xu M, Lee EM, Wen Z, Cheng Y, Huang WK, Qian X, et al. Identification of small-molecule inhibitors of zika virus infection and induced neural cell death *via* a drug repurposing screen. *Nat Med* (2016) 22(10):1101–7. doi: 10.1038/nm.4184

47. al-Madani AA. Schistosomiasis control in Saudi Arabia with special reference to the period 1983-1988. *Public Health* (1990) 104(4):261–6. doi: 10.1016/s0033-3506(05)80475-5

48. Incani RN. The Venezuelan experience in the control of schistosomiasis mansoni. *Memorias do Instituto Oswaldo Cruz* (1987) 82 Suppl 4:89–93. doi: 10.1590/s0074-02761987000800014

49. Laamrani H, Khallaayoune K, Boelee E, Laghroubi MM, Madsen H, Gryseels B. Evaluation of environmental methods to control snails in an irrigation system in central Morocco. *Trop Med Int Health TM IH* (2000) 5(8):545–52. doi: 10.1046/j.1365-3156.2000.00606.x

50. Tanaka H, Tsuji M. From discovery to eradication of schistosomiasis in Japan: 1847-1996. *Int J Parasitol* (1997) 27(12):1465–80. doi: 10.1016/s0020-7519(97)00183-5

51. Sokolow SH, Jones IJ, Jocque M, La D, Cords O, Knight A, et al. Nearly 400 million people are at higher risk of schistosomiasis because dams block the migration of snail-eating river prawns. *Philos Trans R Soc London Ser B Biol Sci* (2017) 372(1722):1–12. doi: 10.1098/rstb.2016.0127

52. Steinmann P, Keiser J, Bos R, Tanner M, Utzinger J. Schistosomiasis and water resources development: systematic review, meta-analysis, and estimates of people at risk. *Lancet Infect Dis* (2006) 6(7):411–25. doi: 10.1016/S1473-3099(06)70521-7

53. BRASIL. *Vigilância E Controle De Moluscos De Importância Epidemiológica: Diretrizes Técnicas: Programa De Vigilância E Controle Da Esquistossomose (Pce). 2. ed.* Brasília: Editora do Ministério da Saúde (2008). p. 178.

54. Mesquita SG, Caldeira RL, Favre TC, Massara CL, Beck LCNH, Simões TC, et al. Assessment of the accuracy of 11 different diagnostic tests for the detection of. *Front Microbiol* (2022) 13:1048457. doi: 10.3389/fmicb.2022.1048457

55. Paraense W. Estado atual da sistemática dos planorbídeos Brasileiros. *Arq Mus Nac* (1975) 55:105–28.

56. Caldeira RL, Teodoro TM, Jannotti-Passos LK, Lira-Moreira PM, Goveia CO, Carvalho OD. Characterization of South American snails of the genus biomphalaria (Basommatophora: planorbidae) and schistosoma mansoni (Platyhelminthes: trematoda) in molluscs by Pcr-Rflp. *BioMed Res Int* (2016) 2016:1045391. doi: 10.1155/2016/1045391

57. Folmer O, Black M, Hoeh W, Lutz R, Vrijenhoek R. DNA primers for amplification of mitochondrial cytochrome C oxidase subunit I from diverse metazoan invertebrates. *Mol Mar Biol Biotechnol* (1994) 3(5):294–9.

58. Carvalho OS, Coelho PMZ, Lenzi HL. Técnicas utilizadas no estudo dos moluscos do gênero biomphalaria E na manutenção do ciclo de schistosoma mansoni. *Schistosoma Mansoni E Esquistossomose: Uma Visão Multidisciplinar. Editora Fiocruz* (2008). p:1124. doi: 10.7476/9788575413708

59. Alves Pinto H, de Melo AL. Larvas de trematódeos em moluscos do Brasil: panorama E perspectivas após um século de estudos. *Rev Patologia Trop / J Trop Pathol* (2014) 42(4):369–86. doi: 10.5216/rpt.v42i4.27922

60. Caldeira RL, Jannotti-Passos LK, Dos Santos Carvalho O. Use of molecular methods for the rapid mass detection of schistosoma mansoni (Platyhelminthes: trematoda) in Biomphalaria spp. *(Gastropoda: Planorbidae). J Trop Med* (2017) 2017:8628971. doi: 10.1155/2017/8628971

61. Fernandes JN, Dos Santos LMB, Chouin-Carneiro T, Pavan MG, Garcia GA, David MR, et al. Rapid, noninvasive detection of zika virus in aedes aEgypti mosquitoes by near-infrared spectroscopy. *Sci Adv* (2018) 4(5):eaat0496. doi: 10.1126/sciadv.aat0496

62. Valladares V, Pasquini C, Thiengo SC, Mello-Silva CC. Feasibility of near-infrared spectroscopy for species identification and parasitological diagnosis of freshwater snails of the genus biomphalaria (Planorbidae). *PloS One* (2021) 16(11):e0259832. doi: 10.1371/journal.pone.0259832

63. Carmo EH, Barreto ML. [Schistosomiasis mansoni in Bahia, Brazil: historical trends and control measures]. *Cadernos saude publica* (1994) 10(4):425–39. doi: 10.1590/s0102-311x1994000400002

64. Kloetzel K, Schuster NH. Repeated mass treatment of schistosomiasis mansoni: experience in hyperendemic areas of Brazil. I. Parasitological effects and morbidity. *Trans R Soc Trop Med Hygiene* (1987) 81(3):365–70. doi: 10.1016/0035-9203(87)90137-4

65. Barbosa FS, Costa DP. A long-term schistosomiasis control project with molluscicide in a rural area of Brazil. *Ann Trop Med Parasitol* (1981) 75(1):41–52. doi: 10.1080/00034983.1981.11687407

66. Katz N. Schistosomiasis control in Brazil. *Memorias do Instituto Oswaldo Cruz* (1998) 93 Suppl 1:33–5. doi: 10.1590/s0074-02761998000700005

67. Pieri OS, Goncalves JF, Sarquis O. Repeated focal molluscicide for snail control in a sugar-cane area of northeast Brazil. *Memorias do Instituto Oswaldo Cruz* (1995) 90(4):535–6. doi: 10.1590/s0074-02761995000400022

68. Vliet SM, Dasgupta S, Volz DC. Niclosamide induces epiboly delay during early zebrafish embryogenesis. *Toxicological Sci* (2018) 166(2):306–17. doi: 10.1093/toxsci/kfy214

69. Zhu B, He W, Yang F, Chen L. High-throughput transcriptome sequencing reveals the developmental toxicity mechanisms of niclosamide in zebrafish embryo. *Chemosphere* (2020) 244:125468. doi: 10.1016/j.chemosphere.2019.125468

70. Oliveira-Filho EC, Paumgartten FJ. Toxicity of euphorbia milii latex and niclosamide to snails and nontarget aquatic species. *Ecotoxicology Environ Saf* (2000) 46(3):342–50. doi: 10.1006/eesa.2000.1924

71. de Souza Gomes EC, Leal-Neto OB, Albuquerque J, Pereira da Silva H, Barbosa CS. Schistosomiasis transmission and environmental change: A spatio-temporal analysis in Porto de Galinhas, Pernambuco–Brazil. *Int J Health geographics* (2012) 11:51. doi: 10.1186/1476-072X-11-51

72. Palasio RGS, Bortoleto AN, Rosa-Xavier IG, Andrighetti MTM, Tuan R, Chiaravalloti-Neto F. Schistosomiasis in the middle paranapanema river region, state of Sao Paulo, Brazil: does it matter today for public health? *Rev da Sociedade Bras Medicina Trop* (2019) 52:e20180447. doi: 10.1590/0037-8682-0447-2018

73. Hillyer GV, Tsang VC, Vivas-Gonzalez BE, Noh J, Ahn LH, Vorndam V. Age-specific decrease in seroprevalence of schistosomiasis in Puerto Rico. *Am J Trop Med hygiene* (1999) 60(2):313–8. doi: 10.4269/ajtmh.1999.60.313

74. Coura-Filho P. [an alternative model for schistosomiasis control with active participation by the population through the unified health system (Sus) in Taquaracu de Minas (Minas gerais, Brazil) from 1985 to 1995]. *Cadernos saude publica* (1998) 14 Suppl 2:111–22. doi: 10.1590/S0102-311X1998000600010

75. Evan Secor W. Water-based interventions for schistosomiasis control. *Pathog Global Health* (2014) 108(5):246–54. doi: 10.1179/2047773214Y.0000000149

frontiers | Frontiers in Immunology

TYPE Original Research
PUBLISHED 23 February 2024
DOI 10.3389/fimmu.2023.1269336

OPEN ACCESS

EDITED BY
Thiago Almeida Pereira,
Stanford University, United States

REVIEWED BY
Sheila Donnelly,
University of Technology Sydney, Australia
Muhammad Ehsan,
Islamia University of Bahawalpur, Pakistan

*CORRESPONDENCE
Luciana C. C. Leite
luciana.leite@butantan.gov.br
Leonardo Paiva Farias
leonardo.farias@fiocruz.br
R. Alan Wilson
alan.wilson@york.ac.uk

†PRESENT ADDRESSES
Leonardo Paiva Farias,
Laboratório de Inflamação e Biomarcadores, Instituto Gonçalo Moniz, Fundação Oswaldo Cruz, Salvador, Brazil
Almiro Pires da Silva Neto,
Laboratório de Engenharia Genética e Enzimática, UNESP, Araraquara, Brazil

RECEIVED 29 July 2023
ACCEPTED 22 September 2023
PUBLISHED 23 February 2024

CITATION
Vance GM, Khouri MI, Neto APS, James S, Leite LCC, Farias LP and Wilson RA (2024) Antigenic epitope targets of rhesus macaques self-curing from *Schistosoma mansoni* infection.
Front. Immunol. 14:1269336.
doi: 10.3389/fimmu.2023.1269336

Antigenic epitope targets of rhesus macaques self-curing from *Schistosoma mansoni* infection

Gillian M. Vance[1], Mariana I. Khouri[2], Almiro Pires da Silva Neto[2†], Sally James[1], Luciana C. C. Leite[3*], Leonardo Paiva Farias[3*†] and R. Alan Wilson[1,4*]

[1]Department of Biology, University of York, York, United Kingdom, [2]Laboratório de Inflamação e Biomarcadores, Instituto Gonçalo Moniz, Fundação Oswaldo Cruz, Salvador, BA, Brazil, [3]Laboratório de Desenvolvimento de Vacinas, Instituto Butantan, São Paulo, SP, Brazil, [4]Biomedical Research Institute, University of York, York, United Kingdom

The self-cure of rhesus macaques from a schistosome infection and their subsequent strong immunity to a cercarial challenge should provide novel insights into the way these parasites can be eliminated by immunological attack. High-density arrays comprising overlapping 15-mer peptides from target proteins printed on glass slides can be used to screen sera from host species to determine antibody reactivity at the single epitope level. Careful selection of proteins, based on compositional studies, is crucial to encompass only those exposed on or secreted from the intra-mammalian stages and is intended to focus the analysis solely on targets mediating protection. We report the results of this approach using two pools of sera from hi- and lo-responder macaques undergoing self-cure, to screen arrays comprising tegument, esophageal gland, and gastrodermis proteins. We show that, overall, the target epitopes are the same in both groups, but the intensity of response is twice as strong in the high responders. In addition, apart from Sm25, tegument proteins elicit much weaker responses than those originating in the alimentary tract, as was apparent in IFNγR KO mice. We also highlight the most reactive epitopes in key proteins. Armed with this knowledge, we intend to use multi-epitope constructs in vaccination experiments, which seek to emulate the self-cure process in experimental animals and potentially in humans.

KEYWORDS

epitope mapping, tegument proteins, alimentary tract proteins, antigenic targets, esophageal glands, peptide array

1 Introduction

Despite the introduction of Praziquantel 45 years ago as a safe and effective drug (1) and, more recently, its use in mass chemotherapy, schistosomiasis stubbornly remains a public health problem in many countries where the disease is endemic. In 2019, the World Health Organization estimated in that at least 236.6 million people required preventive treatment for schistosomiasis (https://www.who.int/news-room/fact-sheets/detail/schistosomiasis), and given the increasing sensitivity of diagnostic techniques, that figure could be significantly higher (2, 3). Inevitably, this has led to calls for the development of vaccines as additional components in the toolbox of control measures (4). However, progress towards an effective schistosome vaccine has been slow, not least because of the difficulty in demonstrating specific acquired immunity following infection. The animal and human trials with single recombinant antigens have at best yielded only partial protection of uncertain duration (5, 6).

Nevertheless, work with animal models does indicate that substantial levels of protection can be induced. The radiation-attenuated (RA) cercarial vaccine delivered to both rodents and non-human primates is the most intensively researched (7, 8). Multiple exposures are required to achieve high levels of protection, the underlying immunological mechanisms are complex, and in the baboon, host immunity declines in parallel with antibody titer in the months after the last vaccination (8). The RA vaccine, with its shelf-life of hours, is best viewed as an experimental model to dissect the mechanism of protection, rather than a practical proposition. A second model, the rhesus macaque, was favored in early studies of protective immunity (43 papers cited on PubMed in the 1960s) before being replaced by cheaper rodent models. The principal attraction was the animal's ability to clear an established infection in a self-cure process, after which it was resistant to a cercarial challenge (9, 10). Given the slow progress with recombinant antigens, the model has been revisited in short-term (18–22 weeks) experiments with both *S. mansoni* (11) and *S. japonicum* (12) in the hope that it would provide pointers to the immune mechanisms, which can eliminate both established and challenge populations. Most recently, this work has been extended to a single large cohort of rhesus macaques given a primary infection followed by a cercarial challenge at 42 weeks, with protection determined at 60 weeks (13). In summary, the self-cure process begins approximately 10 weeks post-exposure but proceeds at different rates in individual animals. The animals that self-cured the most rapidly were the ones that showed the greatest degree of protection, some with virtually sterile immunity; no challenge worms achieved egg excretion, even in the slowest responders. Although the above models demonstrate acquired protection against a schistosome infection, it is no simple task to identify the antigens mediating that process in a macroscopic pathogen with a genome comprising ~12,000 protein coding genes, expressed in multiple organ systems. For this reason, array technologies have been developed for screening of sera from protected animals to assess their immune reactivity. Arrays comprising fractionated glycans have been used to identify the reactive epitopes in sera from rhesus macaques self-curing from *S. japonicum* (14) and baboons after multiple exposures to the RA *S. mansoni* vaccine (15). It remains unclear if these glycan antigens are involved in the protective response or provide a smokescreen to divert attention away from protective epitopes (16).

The rhesus macaque serum taken at weeks 12 and 20 has also been used to screen a large-scale array comprising *in vitro* translated proteins of *S. mansoni* (45) and *S. japonicum* (172) printed onto glass slides (17). Eight proteins were detected by the 22-week rhesus serum pool, but the only plausible candidate was an extracellular superoxide dismutase of unknown localization. The reactivity of target proteins can now be evaluated at the level of individual epitopes by printing of overlapping 15mer peptides onto glass slides for screening with immune sera. The technique was first applied to three such arrays encompassing 33 esophageal proteins from *S. japonicum* screened with serum from self-curing macaques, infected rabbits, and mice (18). While some reactivities were common to the three hosts (e.g., MEGs 4.1, 4.2, 11, 12, and an aspartyl protease), those to MEG-8.1 and 8.2 were largely confined to the macaques. Expanding on this epitope mapping approach, we have screened four peptide arrays comprising 55 secreted or exposed proteins from the alimentary tract and tegument of *S. mansoni with* sera from C57Bl/6 and IFNγR KO mice after multiple exposures to the RA vaccine. A list of priority peptides from 44 of the proteins was obtained for further investigation in multiepitope vaccine constructs and as targets of monoclonal antibodies (19). We now describe the reactivity of two pools of serum from rhesus macaques self-curing from *S. mansoni* (11) against the same four peptide arrays. We show that titer, not target, appears to determine the rate of self-cure, and we highlight the principal reactive epitopes of alimentary tract and tegument proteins for inclusion in a multi-epitope construct for vaccine experiments.

2 Methods

2.1 Source of self-curing sera and ethics statement

The high- and low-responder pools of rhesus sera used in the array screen came from the schistosomiasis serum archive at the University of York, acquired in the previously published study of self-cure undertaken at the Biomedical Primate Research Centre (BPRC), Rijswijk, The Netherlands (11). The experimental protocol was approved by the Institutional Animal Care and Use Committee at BPRC and the Biology Department Ethics Committee, University of York. The animals were exposed to 1,000 *S. mansoni* cercariae via the shaved abdominal skin for 30 min and the serum obtained by intravenous sampling at perfusion (week 18). The hi-responder pool combined serum from rhesus macaque R1 (12) and R6 (31) and the lo-responder pool from R2 (708) and R5 (249); numbers in parentheses are worms recovered. We also made computational comparisons with two of our previously published array studies: 1. IFNγR KO mice, which were capable of conferring ~50% passive protection on naive recipient mice (19) and 2. rhesus macaques self-curing from *S. japonicum* infection (18).

2.2 Array design and screening

The four previously described array designs (19) consisting of overlapping 15mer peptides, with a one, two, or three amino acid offset, were printed by PEPperPRINT (Heidelberg, Germany; https://www.pepperprint.com). The array slides were screened exactly as previously described (18, 19). These are the same arrays that were first reacted with mouse primary serum samples, with binding detected by Cy3-labeled goat anti-mouse IgG (19). A total of 55 alimentary tract and tegument proteins, exposed at or secreted from the intra-mammalian stages, were investigated, primarily selected by the presence of a signal peptide (which was excised from the sequence printed). Rhesus primary antibodies were applied at a 1:200 dilution for alimentary tract proteins and 1:100 for the tegument. Their binding was detected using Cy5-labeled goat anti-human IgG (H+L), pre-adsorbed using bovine, chicken, horse, mouse, pig, rabbit, and rat immunosorbents to remove cross-reactive antibodies (Abcam #97172), at 1:300 dilution. The two-color detection allowed the direct comparison of previously identified murine responses with the rhesus macaque reactivities. Detection specificity was confirmed by a pre-stain of each array with Cy5-labeled secondary antibody and a preliminary scan. Blocking, secondary antibody, and control antibody solutions were each incubated at room temperature for 30 min; primary antibody solutions were incubated overnight at 4°C. Arrays were scanned at 5 μm resolution using an Agilent Array scanner with High-Resolution SureScan Technology (Agilent Technologies LDA UK Limited, Stockport, Cheshire; model G2565CA). The instrument has a dynamic range > four orders of magnitude; by optimizing antibody dilutions, the arrays were never saturated, while weaker reactivities were still captured. A screengrab of the Agilent image was taken for orientation and editing purposes.

2.3 Data analysis

The Agilent.tif file output for each array was analyzed using the PepSlide® Analyzer (PSA) software as previously described (18). Heatmaps were then made from the cell scores for each array to facilitate visual interpretations. As the same aliquot of Cy5-Goat anti-human detection reagent was used throughout, the mean PSA scores for each position on the array allow comparisons of the intensity of reactive regions between individual samples. PSA scores were color-coded on a linear scale using the Conditional Formatting function in Excel to highlight reactive regions and facilitate comparisons between samples. An aggregate score for each reactive region was determined by summing adjacent peptide means above a predetermined threshold, down the array. In turn, these aggregates were combined to give a reactivity score for each of the 55 proteins under investigation. Additionally, we generated a reactivity-normalized score by dividing this last score by the total number of peptides for each protein. The sequence identity between the epitopes from *S. mansoni* and *S. japonicum* was calculated using the biostrings R package (https://bioconductor.org/packages/Biostrings). The two corresponding epitopes were aligned using the "pairwise Alignment" function with the global alignment option.

3 Results

3.1 Overview: proteins from the alimentary tract are generally more reactive than those from the tegument

The full data set obtained from screening the four arrays using high- and low-responder pools is provided in Supplementary Table S1 and presented in Figure 1 as a series of color-coded heatmaps to indicate the intensity of IgG binding against each 15mer peptide. The highest tegument array cell score was 44,974 units (Sm25) and for the alimentary tract, 55,163 units (ferritin heavy chain) (Supplementary Table S1). The number of neighboring reactive 15mer peptides ranged up to 20–23 (Sm25, calumenin), but was mostly smaller, in many cases likely representing a single epitope (Supplementary Table S1). Inspection of the heatmaps (Figure 1) reveals that, with one exception, the intensity of reactivity of the proteins printed on Array 1 (gastrodermal carrier proteins and esophageal secreted MEGs) and Array 2 (largely gastrodermal enzymes) showed the strongest reactivity. The striking exception is the short tegumental protein, Sm25 on Array 3, which shows the strongest overall visual signal. It is also apparent that the pool of hi-responder serum is more reactive against all the arrays, than the lo-responder pool, reacting weakly or not at all with the same targets. Only in MEG-8.2 does there appears to be a reactivity unique to the lo-responders.

3.2 Esophageal MEG and gastrodermal targets

The complexity of data presented in the heatmaps can be further reduced by summing the reactive regions within each protein (Supplementary Table S2) and plotting them in a bar chart (Figure 2). Viewed together, the heatmap (Figure 1) and bar chart (Figure 2) permit the proteins in each tissue of origin (Figure 1) to be graded by their overall reactivity. MEG-8.2 and MEG-4.2 were the most reactive esophageal secreted proteins followed by MEG-4.1 N and C termini and MEG-12. The MEG-8.1, MEG-9, VAL-7, and MEG-15 proteins reacted in descending order, while MEG-8.3 and MEG-22 were the weakest of all. However, four of these proteins reacted primarily at a single region: MEG-8.3 centrally, MEG-12 and MEG-22 at the extreme N-terminus, and VAL-7 at the C-terminus (Figure 1; Supplementary Table S2).

Among the gastrodermal secreted proteases, asparaginyl endopeptidase was the most reactive followed by cathepsins B1 and S (Figure 2B). Cathepsins B2 and L, plus beta xylosidase and DNAse, were moderately reactive over multiple regions of sequence. In contrast, Cathepsin D plus the N- and C-terminus of lysosomal-associated membrane protein, LAMP-1, were only weakly reactive. Among the lipid-transporting proteins secreted from the gastrodermis, only saposin-5 was moderately reactive, the others weakly so (Figure 2A), and the cholesterol-transporting Niemann-Pick 2 (NPC2) was barely detected (Figure 2B). In light of the single-cell sequencing results reported by Wendt et al. (2020), the strong reactivity of calcium binding calumenin and iron binding ferritin heavy chain may possibly originate in non-gastrodermal tissues.

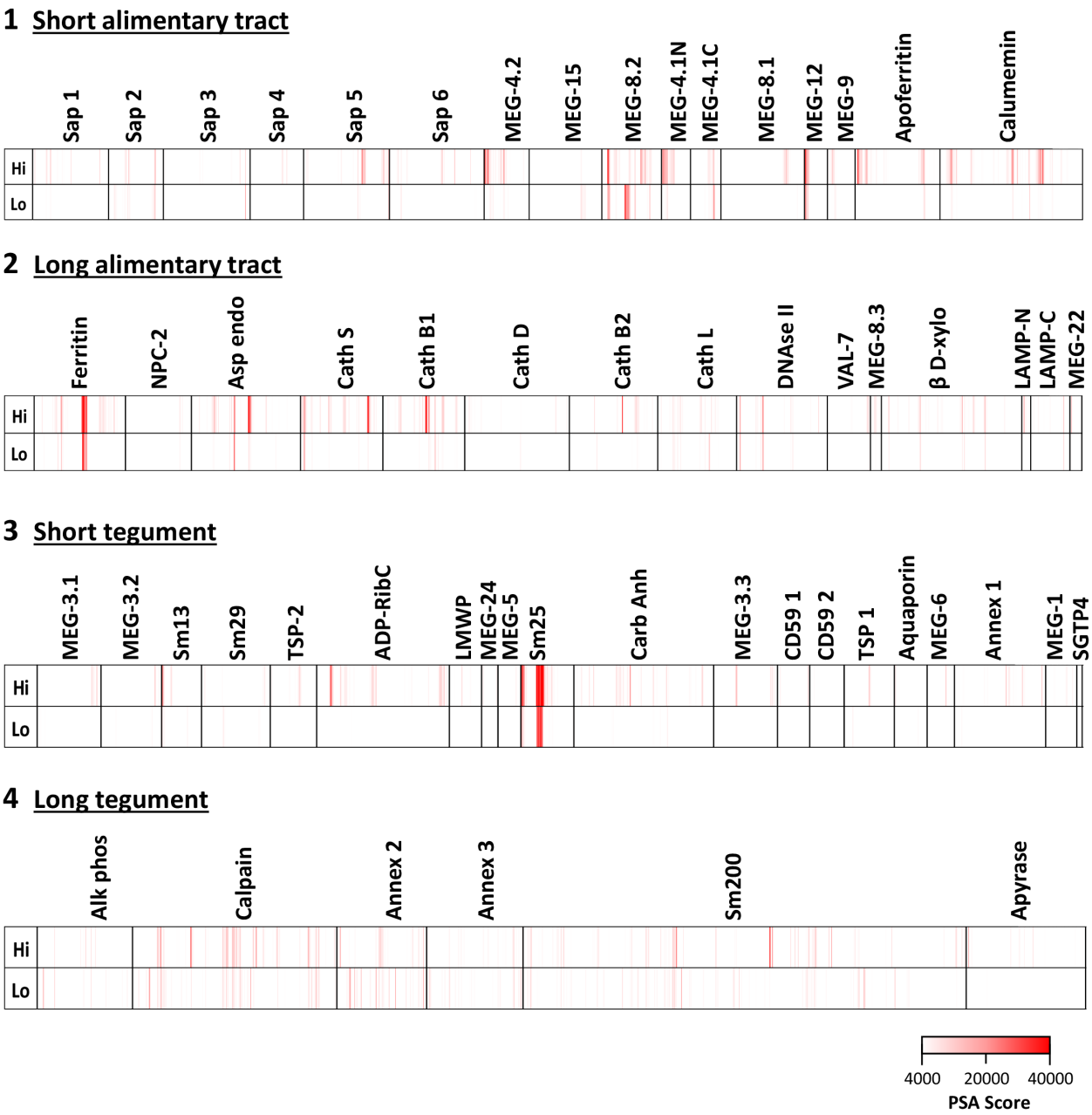

FIGURE 1
Heatmaps showing the reactivities of hi- and lo-responder rhesus macaque serum pools against the four peptide arrays: 1) short alimentary tract, 2) long alimentary tract, 3) short tegument surface, and 4) long tegument surface. The intense reactivity of tegument Sm25 is very evident.

3.3 Few tegument proteins show marked reactivity

Sm25 of unknown function was by far the most reactive tegument protein, more so in the hi- than lo-responder pool (Figure 2C). Among potential membranocalyx constituents, only Sm200 showed moderate reactivity (Figure 2D), but equally so in hi- and lo- responder pools. The vaccine candidate Sm-p80 calpain was similarly reactive with both pools (Figure 2D). The GPI-anchored tegument enzymes, ADP-ribosyl cyclase (Arc) and Carbonic anhydrase, on the outer leaflet of the plasma membrane, showed moderate reactivity with the hi-responder pool (Figure 2C). Finally, the three tegument annexins came next in rank order, two of them detected more strongly by the low responder pool. In contrast, GPI-anchored alkaline phosphatase and membrane-spanning apyrase (ATP-diphosphohydrolase), with a large extracellular domain, showed weak reactivity (Figures 2C, D). The N-terminus of Sm13 was weakly reactive with the hi-responder pool (Figure 1; Supplementary Table S2).

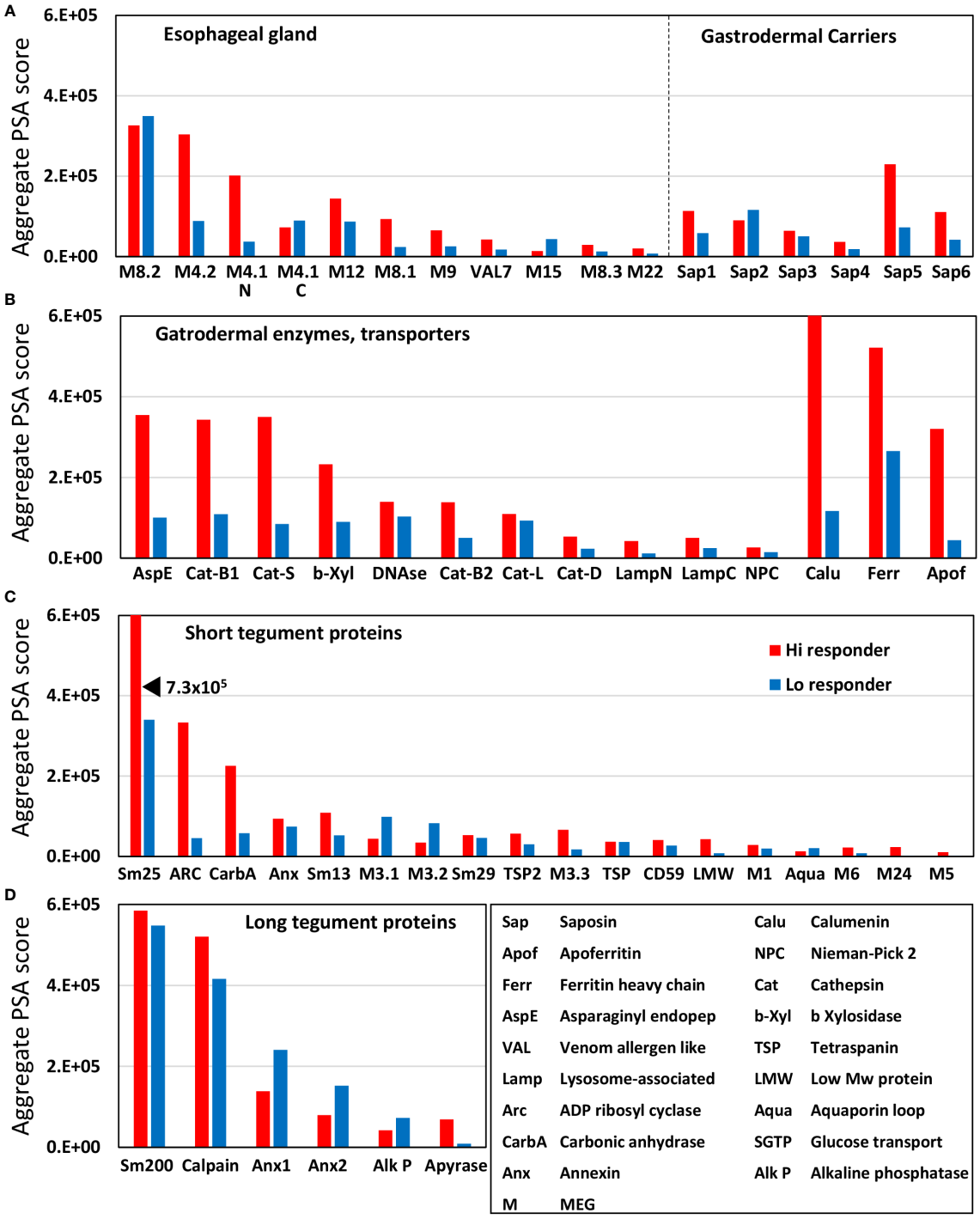

FIGURE 2
Bar chart summarizing the reactivity of all proteins on the four arrays, based on the data in Supplementary Table S2. The y-axis is the cumulative Agilent peptide score above zero for each protein, ignoring protein length. The proteins in each array have been rearranged along the x-axis according to functional group by reactivity. Three transporters with high reactivity on Array 2 were segregated on the basis of SchistoCyte predictions of their tissue localization. Note that the tegument arrays were hybridized with double the concentration of serum used for the alimentary tract arrays (1:100 versus 1:200).

3.4 Normalizing by number of peptides printed allows ranking of protein reactivity

The proteins printed on the four arrays differ in size from 8 to 200 kDa, and the amino acid offsets of the 15mer peptides vary between one and three, to accommodate the larger ones. This divergence was normalized to create a reactivity index by dividing the mean score (Supplementary Table S3) by the total number of peptides printed for each protein. The esophageal MEGs plus VAL-7 are the smallest targets ($\bar{x}$ 100 amino acids (AA). The 17

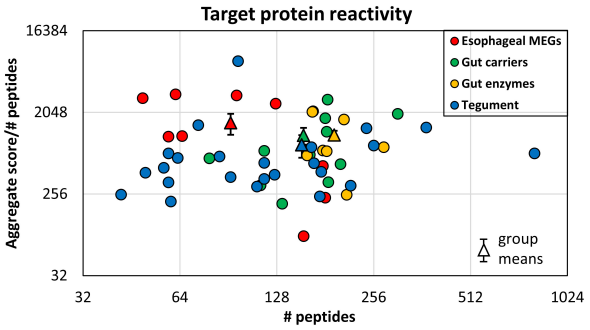

FIGURE 3
The mean reactivity of array proteins based on the data in Supplementary Table S3, normalized for number of peptides printed. This compensates for one, two, or three amino acid offsets. The proteins are color coded by function as esophageal MEGs, gastrodermal carriers, enzymes, and tegument. The differences in group reactivity were tested for significance using a t-test. Note the log x- and y-axis scales.

tegument proteins range between 44 and 1,630 AAs ($\bar{x}$ 262, skewed by Sm200; median = 129). The gastrodermal carriers plus LAMP are somewhat larger ($\bar{x}$ 166 AA), while, overall, the secreted hydrolases are the bulkiest targets ($\bar{x}$ 414 AA). The indexes, sorted by tissue of origin and displayed as a scatter plot (Figure 3), segregate into four distinct but overlapping groups. The esophageal MEGs cluster at the top left ($\bar{x}$ 1569 +/− S.E. 344). The gastrodermal carriers ($\bar{x}$ 1143+/− S.E. 255) and enzymes ($\bar{x}$ 1153 +/− S.E. 250) form a superimposed cluster in the center. Finally, the tegument proteins ($\bar{x}$ 898 +/− S.E. 286) spread across the whole plot with the lowest score. It is notable that no group mean is statistically significantly different from any other (all p-values > 0.05, NS). However, there are two outliers, Sm25 highly reactive for the tegument and MEG-15 under-reactive for the esophageal gland. If these are removed before analysis, then the mean tegument score ($\bar{x}$ 621 +/− S.E. 74) is significantly lower than the MEGs ($\bar{x}$ 1717 +/− S.E. 331,***), carriers ($\bar{x}$ as above,**) and enzymes ($\bar{x}$ as above,**) of alimentary tract origin (Supplementary Figure S1).

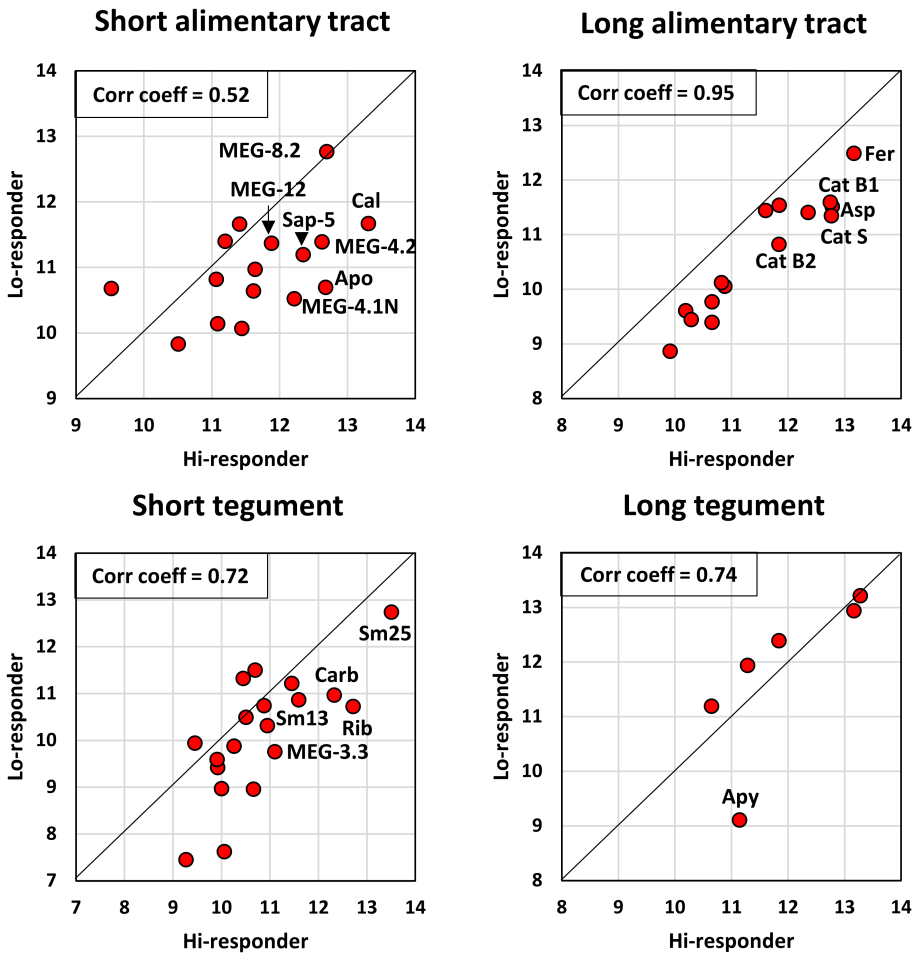

FIGURE 4
The reactivity of hi- and lo-responder pools compared for each array, based on the data in Supplementary Table S2. The linear relationship between the two variables was determined using Pearson's correlation coefficient, r. The offset from the diagonal midline provides a visual indication of the extent to which each protein reacts more with the hi-responder pool.

3.5 Hi-responders react more strongly with array peptides than lo-responders

It is clear from visual inspection of the bar charts (Figure 2) and the grand total aggregate scores for each array (Supplementary Table S3) that the hi-responder pool generally reacts more strongly with the 55 proteins printed on the arrays than the lo-responder pool. This is an important consideration when selecting target epitopes or proteins and can be visualized using an LN transform scatter plot of the aggregate scores for all proteins on the four arrays (Figure 4; Supplementary Table S3). The hi and lo scores for individual proteins on the long alimentary tract array 2 are strongly correlated (r = 0.95), but all hi-responder values are displaced from the median line by a factor of 2.4 times. The second highest correlation is between the six long tegument proteins (r = 0.74), but five of these lie along the median line,

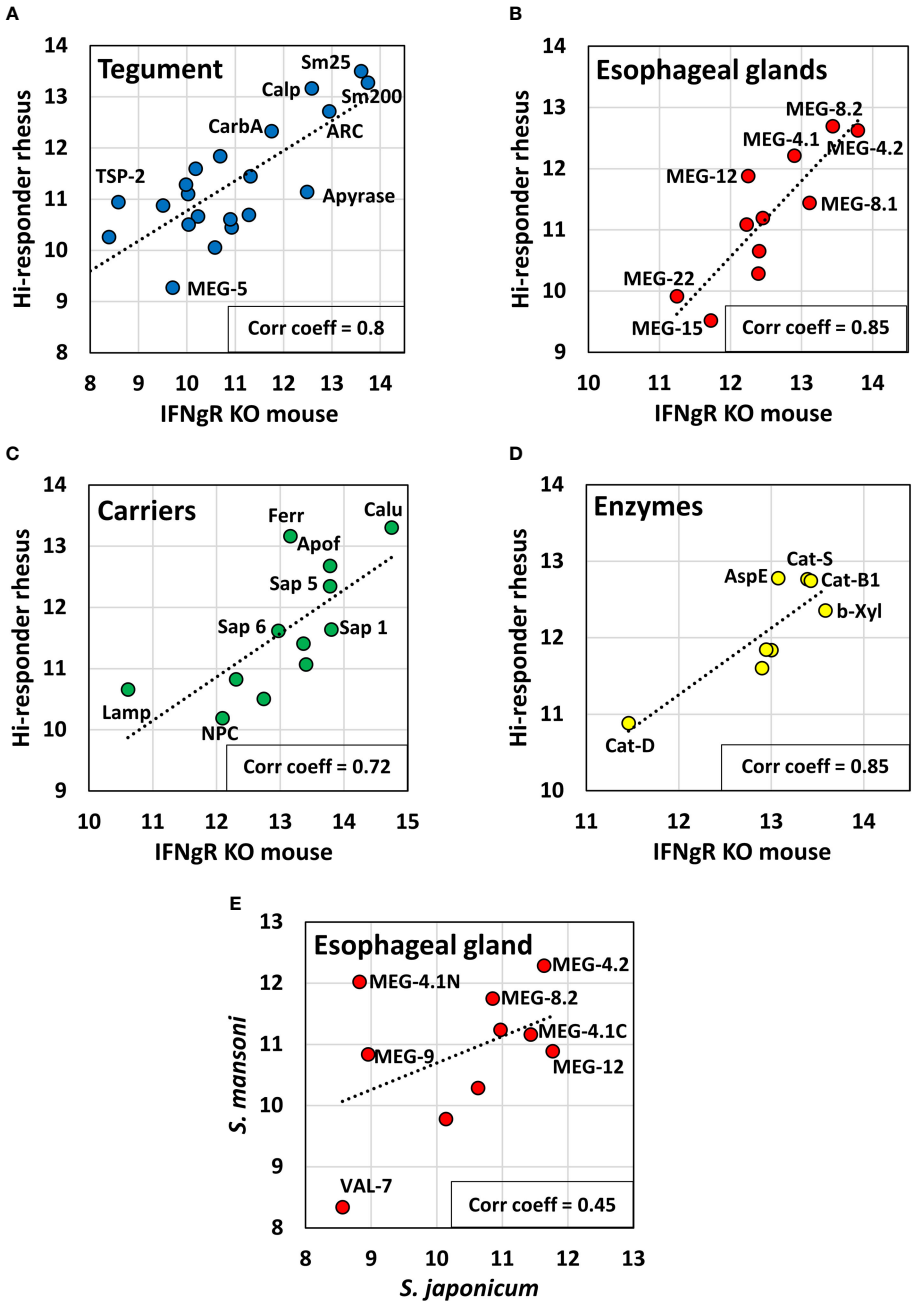

FIGURE 5
Scatter plots comparing the reactivity of hi-responder rhesus macaque sera with previously published data from IFNγR KO mice (19, Farias et al., 2021), screened on the same arrays, based on data in Supplementary Table S3, Sheet 3. The proteins were segregated by tissue of origin and function into: **(A)** tegument; **(B)** esophageal glands; **(C)** carriers; **(D)** enzymes. A strong relationship between the two data sets was revealed using Pearson's correlation coefficient, r. **(E)** shows the relationship between esophageal gland proteins from hi-responder macaques and previously published data from rhesus macaques recovering from *S. japonicum* (18, Li et al., 2020), presented in Supplementary Table S4. The correlation r, between the two data sets was weaker.

suggesting that responses to them are not a dominant component of self-cure. Only apyrase is an outlier, skewed towards the hi-responder pool, but the weakest of the six. The reactivity of short tegument proteins is moderately correlated (r = 0.72), twice as reactive with the hi-responder pool. Based on intensity and differential reactivity, Sm25, carbonic anhydrase, Sm13, and ADP-ribosyl cyclase are the most highly reactive tegument targets. The short alimentary tract proteins (MEGs, saposins) have the lowest correlation coefficient (r = 0.52), but almost all are more reactive with the hi-responder pool, by a factor of 2.21 times. However, the most reactive MEG-8.2 sits on the midline, while MEG-15 is an outlier, more reactive with the low-responder pool but at weak intensity (Figure 4).

3.6 There is a similarity in targets detected among IFNγR KO mice vaccinated with irradiated cercariae and rhesus macaques self-curing from *S. mansoni* and *S. japonicum*

Using all positive cell values, we compared the reactivity of the hi-responder macaques, which had eliminated most of their adult worms at 18 weeks, with already published data on the reactivity of the IFNγR KO mice (Figure 5). There was a good degree of concordance across the four arrays, with Pearson correlation coefficients between the two data sets of tegument (0.8), esophageal gland (0.85), carriers (0.72), and gut enzymes (0.85) (Figures 5A–D). It is apparent that the proteins highly reactive in the macaques self-curing from *S. mansoni* are similar to those eliciting a strong response in IFNγR KO mice. Assuming that the commonalities in macaque and mouse hosts represent potential protein targets of antibody-mediated protection, then for the tegument, Sm25, calpain, Sm200, ADP-ribosyl cyclase, and carbonic anhydrase are the most important. For the esophageal glands, the targets are the MEGs 4.1, 4.2, 8.1, 8.2, and 12. For the gastrodermal carriers, calumenin, ferritin heavy chain, apoferritin, and three saposins, and for the enzymes, cathepsins S and B1, asparaginyl endopeptidase, and beta xylosidase are the most shared. These data sets also indicate that proteins like MEGs 5, 15 and 22, Lamp, NPC-2, and cathepsin D show overall poor reactivity (Figure 5). Fortuitously, the hi-responder pool (Cy5) was reacted with short and long alimentary tract arrays previously used with the IFNγR KO mouse serum (Cy3), so a direct visual comparison can be made (Supplementary Figure S2). Although adjustment of the Cy3/Cy5 color balance needs care, visual inspection reveals that many identical runs of peptides are recognized by both sera. Good examples are the N-terminus of MEG-12 on the Array 1 and the C-terminus of VAL-7 on Array 2, both with "yellow" cells. However, other regions have discrete reactivity or greater intensity with one of the two sera. The N-terminus of MEG-4.1 on Array 1 is a good example (columns 41 and 42), where the reactive cells in descending order are three with mouse, four shared, and eight with rhesus macaque. On Array 2 (columns 21 and 22), there is a central region of cathepsin S with reactive cells: two mouse, one shared, five rhesus macaque, and two mouse. The previously mentioned poor reactivity of MEG-15 on Array 1 (columns 33–38) and cathepsin D on Array 2 (columns 27–34) is also very evident.

We were also able to compare the reactivity of the hi-responder macaques with an esophageal gland data subset, previously published (18) for macaques self-curing from *S. japonicum* (Figure 5E). The concordance between the two macaque groups responding to different schistosome species was lower, with a correlation coefficient of 0.45. MEG-12 was clearly more reactive in animals exposed to *S. japonicum*. The discrepancies are illustrated in a heatmap (Supplementary Figure S3) and in Supplementary Table S4. However, we highlight three regions within MEG-8.1, 8.2, and 8.3 proteins that had high sequence identity (>80%) between S. mansoni and S. japonicum and were strongly recognized by both macaque sera (labeled as regions 3, 4, and 5 in Supplementary Figure S3). Additionally, regions 1 and 2 with moderate sequence identity (40%–50%), in MEG-4.1 and 4.2, were strongly recognized by both macaque sera (Supplementary Figure S3). Our analysis suggests that these regions may exhibit a similar degree of spatial exposure in the native proteins of the two schistosome species. Although the N-terminus of MEG-12 (region 6) showed low sequence identity (~26%) in the two schistosomes, it was also strongly recognized by both macaque sera, again

TABLE 1 Principal reactive epitopes.

Tegument	P#	Epitope
Sm13	1	EPEPEPEPVPVSRNS
Sm25	3	PDGFPEYEFLNETSI
Sm25	2	QEAFHRNSDPDGFPE
Sm25	1	SNSIITDEDYDHYNS
ADP Ribosyl cyclase	1	NISCSEIWNSFESIL
Esophageal gland	**P#**	**Epitope**
MEG-4.1	1	SPLDDRFNDVNTINK
MEG-4.1	2	INKKQFTEEEFSRLI
MEG-4.2	1	DIEPRIQKEYYYNLH
MEG-4.2	2	RIQKEYYYNLHENNS
MEG-8.1	1	FFDLFSEQEFHPINH
MEG-8.2	3	SMFGSSDSSSGTNNK
MEG-8.2	1	VSKPTATVKPQPVNK
MEG-12	1	SGENYEQQLQQPKAY
VAL-7	1	PYDPIYPEDPYYLPG
Gastrodermis	**P#**	**Epitope**
Asparaginyl	4	TESSYGTFCDDPTIT
endopeptidase	1	YDDIAYNLMNPFPGK
Cathepsin B1.2	2	SKENHTGCEPYPFPK
Cathepsin B1.2	3	KCEHHTKGKYPPCGS

The amino acids in red indicate the reactivity center of the epitope.

suggesting that these N-termini must be exposed and accessible to B-cell antigen receptors.

3.7 Specific epitope targets of rhesus macaque serum in array proteins

The most reactive regions in the proteins printed on the four arrays are presented as putative epitopes, together with their aggregate scores, in Table 1 and Supplementary Table S5. This is equivalent to treating each replicate pair of cells on the array as a mini-ELISA, and then adding the adjacent cells to provide the score. In general, these scores are higher for the hi- than the lo-responder pool. On Array 1, short alimentary tract, peptide (P) 3 of MEG-8.2 stands out as more reactive with the lo-responder pool, but the rest are either equivalent or mostly much less reactive with the lo-responder serum. The most reactive peptides with scores >90,000 are P2 of saposin 5, P1 and P2 of MEG-4.2, P1 of MEG-8.2, P1 at the N-terminus of MEG-4.1, and P1 on MEG-12. On Array 2, long alimentary tract, all peptides with scores >75,000 are most reactive with the hi-responder serum, the most notable being P2 and P3 of the ferritin heavy chain, P4 of asparaginyl endopeptidase, P1 and P4 of cathepsin S, and P2 of cathepsin B1.2. Among the short tegument proteins (Array 3), only three stand out, the remainder having aggregate scores of<40,000. These are the very strongly reacting P1, P2, and P3 of Sm25; P1 of ADP-ribosyl cyclase; and the N-terminal P1 of Sm13. The long tegument proteins on Array 4 were weakly reactive, with only calpain and Sm200 surface protein having scores >30,000. It is notable that while P2–P5 of calpain reacted with the hi-responder pool, P2, P4, and P5 also reacted with the lo-responder pool. The same is true of P5 and P6 of Sm200, with lo responder scores very similar to hi responders. This appears to argue that host IgG responses against these long tegument proteins are not associated with protection in this model.

4 Discussion

We first consider the choice of proteins for printing on the four arrays. The axiom for selection was that proteins involved in protective immunity must be exposed on or secreted from external surfaces of the intra-mammalian parasite to be accessible to immune effector mechanisms. Internal proteins may be highly immunogenic but that is of no value if, in the live parasite, they are inaccessible to immune effectors. The proteins analyzed in this study were selected based on our extensive proteomic and transcriptomic analyses (listed in Farias et al., 2021 (19)). These studies were underpinned by bioinformatic analysis of transcripts, largely by the late Dr. Ricardo DeMarco. Localization of gene expression was performed by whole mount *in situ* hybridization (WISH) (20) and of protein by immunocytochemistry and high-resolution confocal microscopy, using monospecific antibodies (for the tegument, see (21)).

The arrays were designed and experiments executed before publication of the results of single-cell sequencing from disaggregated adult worms (22) and the creation of SchistoCyte atlas, a database searchable for the pattern of expression of schistosome gene transcripts by tissue (23). The database has already been interrogated using the tegument proteins on Arrays 3 and 4 (21); all were found in one or more of the eight tegument clusters, apart from LMWP (potentially parenchymal), which has been removed from the molecular model of the tegument apical surface. The alimentary tract proteins have now similarly been searched against SchistoCyte (Supplementary Table S6). Eight of the nine esophageal gland MEG proteins and VAL-7 are confirmed as exclusively expressed in the esophageal gland cluster. The exception is MEG-12, which was present diffusely at very low levels throughout. However, *in situ* hybridization has revealed that MEG-12 is expressed in the small anterior esophageal gland (24), which is not mentioned by Wendt et al. (22), so this tissue may not have been captured by their study. All six saposins, asparaginyl endopeptidase, and several of the cathepsins are located exclusively in the gastrodermis (gut cluster). Other enzymes, plus NPC-2 and LAMP (lysosomal-associated membrane protein) are present not only in the gastrodermis but also in other tissues. A recent comparative proteomic profile of microdissected male esophageal gland (ESO) versus extreme body posterior (BE) revealed that some proteins previously thought exclusive to the gastrodermal compartment do function in other worm tissues (25). Apoferritin may fall into this category since SchistoCyte atlas locates it not only in the gastrodermis but also in the internal parenchyma cluster/tissue. The Ferritin h chain is located in the tegument clusters, barely detected in the gut, and lacks a signal sequence (but then so does calpain from the tegument surface). SchistoCyte places calumenin in muscle cells, which lie beneath the tegument; indeed, it may derive from the sarcoplasmic reticulum of those cells. Thus, it is possible that the high reactivity scores of ferritin h chain and calumenin occur, since, due to their internal location, they had not been subject to selection pressure from the immune system in the live worm. Our stated axiom thus excludes them as vaccine candidates.

A clear message from the comparison of hi- versus lo-responder pools is that the dominant factor in the self-cure process is antibody titer, not a failure of lo responders to identify specific targets. The experimental animals were outbred, so diversity of MHC haplotypes might be expected to cause variation in antigen presentation. Using pools of two animals would have smoothed out some variation, but the single unique epitope detected by lo-responder animals in MEG-8.2 was the exception. This argues for a universality of protein epitopes mediating protection. The arrayed proteins were approximately twice as reactive with the hi-responder pool, the exceptions being five of the long tegument proteins (Sm200, calpain, two annexins and alkaline phosphatase). Does this mean that they are not involved in protection in the self-cure model? Another important conclusion is that, except for Sm25, tegument proteins were significantly less reactive than alimentary tract proteins (despite being screened with a higher antibody concentration). This could simply be a function of the degree of immunostimulation. Very probably, the release of alimentary tract proteins into the bloodstream is much greater than the release of tegument membranocalyx, so the

former are more likely to stimulate antibody production. Worms *in vivo* do not bind leukocytes (26), and we have argued that exposed tegument proteins must have been under selection pressure for "immunological silencing" (27).

The tegument exception, Sm25 (annotated as Smp_346910 on WormBase Parasite) deserves more detailed scrutiny. It was characterized before the genomic era as a tegument glycoprotein (28) and localized by immunocytochemistry (29) but does not appear to have been tested for protective potential. Direct evidence for its surface accessibility comes from proteomic analysis of culture supernatants from trypsinized live worms, where it was identified among a select group of host and worm proteins. The host proteins included immunoglobulins, complement factors, and CD44, clearly in the most external location. The other worm proteins were calpain, Sm200, three annexins, and two endophilins. Our best guess is that this group of proteins is involved in membranocalyx secretion deep at the base of tegument pits (21). They are accessible to trypsin (Mr ~ 20kDa) in the live worm. Would Sm25 be accessible to IgG (Mr ~ 150,000 kDa)? The protective potential of calpain (5) argues that it would.

Esophageal gland products were also preferentially detected by the hi-responder pool, namely, MEGs 4.1, 4.2, 8.1, 8.2, and 12. They are released into the anterior and posterior compartments of the esophageal lumen where initial processing of ingested blood takes place (20). Their precise roles in the uncoating of erythrocytes and disabling of leukocytes has not been established. However, co-detection of parasite protein and host IgG has been reported for MEGs 4.1, 4.2, 8.2, 9, 11, and VAL-7 in the esophageal lumen of *S. japonicum* worms from rhesus macaques (12). Additionally in the context of MEG-12 secreted from the anterior gland (24), there is strong morphological evidence in *S. japonicum* for blocking (constipation) of the secretory process. There is also much IgG deposition on the luminal surface, leading to a build-up of giant vesicles in the esophageal lining tissues (12). If this could be ascribed to antibody directed against the strongly reactive N-terminus of MEG-12, it would be an ideal vaccine candidate. A group of gastrodermal proteases are also more strongly recognized by the hi-responder pool. Antibody blocking of their activity by immune complex formation or neutralization is an attractive way to starve the worms of nutrients. Indeed, cathepsin B1 has been put forward as a vaccine candidate (30). A potential downside is the strong acidic environment in the gut lumen; the effect of a low pH on antibody activity does not appear to have been tested. Among the proteases, asparaginyl endopeptidase may be an attractive target, since it activates the other cathepsins in the hemoglobin hydrolysis cascade (31). Its neutralization could thus block the cascade.

The similarities in reactivity between the hi responder and IFNγR KO mouse sera reinforce the identities of the proteins mediating protection in the two models. For the tegument, Sm25 stands out, with Sm13, ADP ribosyl cyclase, and carbonic anhydrase as weaker but positive targets. Among esophageal gland products, the MEG-4 and 8 families are the most reactive, while MEG-12 is seen more strongly by the hi-responder pool. For the carriers, calumenin and ferritin are strongly detected by both sera but appear to be excluded by SchistoCyte. Apoferritin may be worth consideration, and saposin 5 is strongly detected by both sera. The problem with saposins as vaccine targets is that their multiplicity suggests a considerable overlap in uptake capabilities. We surmise a need to target all of them to achieve a biological effect, and they have for the moment been set aside. Asparaginyl endopeptidase and cathepsins B1 and S are prominent in both sera. The much lower correlation in the reactivities of rhesus macaques undergoing self-cure of *S. mansoni* and *S. japonicum* infections is striking. This could reflect the evolutionary distance, variously estimated as between 10 and 70 million years, between "basal" *S. japonicum* and *S. mansoni*, very much a parasite of *Homo sapiens* emerging in the last 0.3–0.4 million years (32). MEG-12, the N-terminus of MEG-4.1, and MEG-8.3 are the proteins with the stronger reaction in *S. japonicum*.

The foregoing appraisals are based on aggregate scores for the entire printed protein. A particular advantage of the peptide array approach is that it facilitates analysis at the level of a single antigenic epitope. The superimposed images of reactions to the two alimentary tract arrays highlight not only the existence of reactivities unique to macaque or mouse but also regions of overlap that may represent common epitopes, or even universal epitopes. As observed here and in unpublished work from other host species, the two N-terminal regions of Sm25 appear to be in this last category. Detailed analysis can also highlight "hot spots" within an otherwise poorly reactive subject. A region adjacent to the C-terminus of VAL-7 comes into this category in the IFNγR KO mouse.

How can we use the information generated in this study? It seems unlikely, but not impossible, that a single "magic bullet" antigen administered as a vaccine could replicate features of self-cure. Given the reported characteristics of the process (11–13), we have argued that sustained immunological pressure against multiple targets is needed over an extended period to eliminate established adults or challenge larvae in a self-cured macaque. This cannot be the whole explanation because self-cure proceeds at widely different rates in individual macaques ($t^{1/2}$ 2.8–8.7 weeks; 13). This is equally true of the elimination of a challenge of self-cured animals where fast-responder animals showed virtually complete immunity, whereas in slow-responders, blood feeding, judged by circulating antigen (CAA) levels, started before the infection was controlled but not completely eliminated. Proteomic and metabolomic analyses of rhesus plasma over this prolonged time course should provide pointers to the missing dimensions in the self-cure process, additional to the identity of target antigens.

In a proof of principle experiment, we have shown the feasibility of joining several short epitopes in a single construct that will elicit multiple antibody specificities in experimental animals (18). This is the approach we now propose to take with the principal reactive regions of tegument and alimentary tract proteins that we have identified. We will combine them in a single synthetic construct to assess their protective capacity in animal models and fine tune the composition of the construct to optimize its vaccine potential.

Data availability statement

The original contributions presented in the study are included in the article/Supplementary Material, further inquiries can be directed to the corresponding authors.

Ethics statement

The animal study was approved by Institutional Animal Care and Use Committee at Biomedical Primate Research Center, Rijswijk, The Netherlands, and by the Biology Department Ethics Committee, University of York, UK. The study was conducted in accordance with the local legislation and institutional requirements.

Author contributions

RW: Conceptualization, Data curation, Formal Analysis, Project administration, Supervision, Writing – original draft. GV: Formal Analysis, Investigation, Methodology, Writing – original draft. MK: Data curation, Methodology, Visualization, Investigation, Writing – original draft. AN: Methodology, Software, Visualization, Writing – review & editing. SJ: Investigation, Methodology, Resources, Writing – review & editing. LL: Conceptualization, Funding acquisition, Resources, Writing – review & editing. LF: Conceptualization, Data curation, Formal Analysis, Funding acquisition, Investigation, Methodology, Project administration, Resources, Writing – original draft.

Funding

The author(s) declare financial support was received for the research, authorship, and/or publication of this article. This work was supported by grants from Fundação de Amparo à Pesquisa do Estado de São Paulo to LF and LL (2012/23124-4) and to LL (2017/24832-6), Fundação Butantan, and by fellowships from CAPES to MK, and from Conselho Nacional de Desenvolvimento Científico e Tecnológico (CNPq) to LL and AN. This study was also financed in part by the Coordenação de Aperfeiçoamento de Pessoal de Nível Superior, Brasil (CAPES) - Finance code 001.

Conflict of interest

The authors declare that a patent related to this work has been deposited at INPI ((Instituto Nacional de Propriedade Intelectual): BR 10 2024 002799.

The authors declare that the research was conducted in the absence of any commercial or financial relationships that could be construed as a potential conflict of interest.

Publisher's note

Supplementary material

The Supplementary Material for this article can be found online at: https://www.frontiersin.org/articles/10.3389/fimmu.2023.1269336/full#supplementary-material

References

1. Gonnert R, Andrews P. Praziquantel, a new board-spectrum antischistosomal agent. *Z Parasitenkd.* (1977) 52(2):129–50. doi: 10.1007/BF00389899

2. Lindholz CG, Favero V, Verissimo CM, Candido RRF, de Souza RP, Dos Santos RR, et al. Study of diagnostic accuracy of Helmintex, Kato-Katz, and POC-CCA methods for diagnosing intestinal schistosomiasis in Candeal, a low intensity transmission area in northeastern Brazil. *PloS Negl Trop Dis* (2018) 12(3):e0006274. doi: 10.1371/journal.pntd.0006274

3. Klohe K, Koudou BG, Fenwick A, Fleming F, Garba A, Gouvras A, et al. A systematic literature review of schistosomiasis in urban and peri-urban settings. *PloS Negl Trop Dis* (2021) 15(2):e0008995. doi: 10.1371/journal.pntd.0008995

4. Hotez PJ, Bottazzi ME, Bethony J, Diemert DD. Advancing the development of a human schistosomiasis vaccine. *Trends Parasitol* (2019) 35(2):104–8. doi: 10.1016/j.pt.2018.10.005

5. Siddiqui AJ, Molehin AJ, Zhang W, Ganapathy PK, Kim E, Rojo JU, et al. Sm-p80-based vaccine trial in baboons: efficacy when mimicking natural conditions of chronic disease, praziquantel therapy, immunization, and Schistosoma mansoni re-encounter. *Ann N Y Acad Sci* (2018) 1425(1):19–37. doi: 10.1111/nyas.13866

6. Riveau G, Schacht AM, Dompnier JP, Deplanque D, Seck M, Waucquier N, et al. Safety and efficacy of the rSh28GST urinary schistosomiasis vaccine: A phase 3 randomized, controlled trial in Senegalese children. *PloS Negl Trop Dis* (2018) 12 (12):e0006968. doi: 10.1371/journal.pntd.0006968

7. Coulson PS. The radiation-attenuated vaccine against schistosomes in animal models: paradigm for a human vaccine? *Adv Parasitol* (1997) 39:271–336. doi: 10.1016/S0065-308X(08)60048-2

8. Kariuki TM, Farah IO, Yole DS, Mwenda JM, Van Dam GJ, Deelder AM, et al. Parameters of the attenuated schistosome vaccine evaluated in the olive baboon. *Infect Immun* (2004) 72(9):5526–9. doi: 10.1128/IAI.72.9.5526-5529.2004

9. McMullen DB, Ritchie LS, Oliver-Gonzalez J, Knight WB. Schistosoma mansoni in Macaca mulatta. Long-term studies on the course of primary and challenge infections. *Am J Trop Med Hyg* (1967) 16(5):620–7. doi: 10.4269/ajtmh.1967.16.620

10. Smithers SR. Acquired resistance to Schistosoma mansoni in the rhesus monkey (Macaca mulatta). *Ann Soc Belges Med Trop Parasitol Mycol* (1967) 47(1):87–95.

11. Wilson RA, Langermans JA, van Dam GJ, Vervenne RA, Hall SL, Borges WC, et al. Elimination of schistosoma mansoni adult worms by rhesus macaques: basis for a therapeutic vaccine? *PloS Negl Trop Dis* (2008) 2(9):e290. doi: 10.1371/journal.pntd.0000290

12. Li XH, Xu YX, Vance G, Wang Y, Lv LB, van Dam GJ, et al. Evidence that rhesus macaques self-cure from a schistosoma japonicum infection by disrupting worm esophageal function: A new route to an effective vaccine? *PloS Negl Trop Dis* (2015) 9(7):e0003925. doi: 10.1371/journal.pntd.0003925

13. Amaral MS, Santos DW, Pereira ASA, Tahira AC, Malvezzi JVM, Miyasato PA, et al. Rhesus macaques self-curing from a schistosome infection can display complete immunity to challenge. *Nat Commun* (2021) 12(1):6181. doi: 10.1038/s41467-021-26497-0

14. Yang YY, Li XH, Brzezicka K, Reichardt NC, Wilson RA, van Diepen A, et al. Specific anti-glycan antibodies are sustained during and after parasite clearance in Schistosoma japonicum-infected rhesus macaques. *PloS Negl Trop Dis* (2017) 11(2): e0005339. doi: 10.1371/journal.pntd.0005339

15. Yang YYM, Wilson RA, Thomas SRL, Kariuki TM, van Diepen A, Hokke CH. Micro array-assisted analysis of anti-schistosome glycan antibodies elicited by protective vaccination with irradiated cercariae. *J Infect Dis* (2019) 219(10):1671–80. doi: 10.1093/infdis/jiy714

16. Eberl M, Langermans JA, Frost PA, Vervenne RA, van Dam GJ, Deelder AM, et al. Cellular and humoral immune responses and protection against schistosomes induced by a radiation-attenuated vaccine in chimpanzees. *Infect Immun* (2001) 69 (9):5352–62. doi: 10.1128/IAI.69.9.5352-5362.2001

17. Pearson MS, Becker L, Driguez P, Young ND, Gaze S, Mendes T, et al. Of monkeys and men: immunomic profiling of sera from humans and non-human primates resistant to schistosomiasis reveals novel potential vaccine candidates. *Front Immunol* (2015) 6:213. doi: 10.3389/fimmu.2015.00213

18. Li XH, Vance GM, Cartwright J, Cao JP, Wilson RA, Castro-Borges W. Mapping the epitopes of Schistosoma japonicum esophageal gland proteins for incorporation into vaccine constructs. *PloS One* (2020) 15(2):e0229542. doi: 10.1371/journal.pone.0229542

19. Farias LP, Vance GM, Coulson PS, Vitoriano-Souza J, Neto A, Wangwiwatsin A, et al. Epitope mapping of exposed tegument and alimentary tract proteins identifies putative antigenic targets of the attenuated schistosome vaccine. *Front Immunol* (2020) 11:624613. doi: 10.3389/fimmu.2020.624613

20. Li XH, de Castro-Borges W, Parker-Manuel S, Vance GM, Demarco R, Neves LX, et al. The schistosome oesophageal gland: initiator of blood processing. *PloS Negl Trop Dis* (2013) 7(7):e2337. doi: 10.1371/journal.pntd.0002337

21. Wilson RA, Jones MK. Fifty years of the schistosome tegument: discoveries, controversies, and outstanding questions. *Int J Parasitol* (2021) 51(13-14):1213–32. doi: 10.1016/j.ijpara.2021.11.002

22. Wendt G, Zhao L, Chen R, Liu C, O'Donoghue AJ, Caffrey CR, et al. A single-cell RNA-seq atlas of Schistosoma mansoni identifies a key regulator of blood feeding. *Science* (2020) 369(6511):1644–9. doi: 10.1126/science.abb7709

23. Wendt GR, Reese ML, Collins JJ 3rd. SchistoCyte atlas: A single-cell transcriptome resource for adult schistosomes. *Trends Parasitol* (2021) 37(7):585–7. doi: 10.1016/j.pt.2021.04.010

24. Wilson RA, Li XH, MacDonald S, Neves LX, Vitoriano-Souza J, Leite LC, et al. The schistosome esophagus is a 'Hotspot' for microexon and lysosomal hydrolase gene expression: implications for blood processing. *PloS Negl Trop Dis* (2015) 9(12):e0004272.

25. Neves LX, Wilson RA, Brownridge P, Harman VM, Holman SW, Beynon RJ, et al. Quantitative proteomics of enriched esophageal and gut tissues from the human blood fluke schistosoma mansoni pinpoints secreted proteins for vaccine development. *J Proteome Res* (2020) 19(1):314–26. doi: 10.1021/acs.jproteome.9b00531

26. Keating JH, Wilson RA, Skelly PJ. No overt cellular inflammation around intravascular schistosomes in vivo. *J Parasitol* (2006) 92(6):1365–9. doi: 10.1645/GE-864R.1

27. Philippsen GS, Wilson RA, DeMarco R. Accelerated evolution of schistosome genes coding for proteins located at the host-parasite interface. *Genome Biol Evol* (2015) 7(2):431–43. doi: 10.1093/gbe/evu287

28. Ali PO, Jeffs SA, Meadows HM, Hollyer T, Owen CA, Abath FG, et al. Structure of Sm25, an antigenic integral membrane glycoprotein of adult Schistosoma mansoni. *Mol Biochem Parasitol* (1991) 45(2):215–22. doi: 10.1016/0166-6851(91)90088-N

29. Abath FG, Hirst EM, Hagan P, Simpson AJ. Ultrastructural localization of Sm15 and Sm25, two major tegumental adult worm antigens of Schistosoma mansoni. *Parasite* (1999) 6(3):243–7. doi: 10.1051/parasite/1999063243

30. El Ridi R, Tallima H, Dalton JP, Donnelly S. Induction of protective immune responses against schistosomiasis using functionally active cysteine peptidases. *Front Genet* (2014) 5:119.

31. Caffrey CR, McKerrow JH, Salter JP, Sajid M. Blood 'n' guts: an update on schistosome digestive peptidases. *Trends Parasitol* (2004) 20(5):241–8. doi: 10.1016/j.pt.2004.03.004

32. Lawton SP, Hirai H, Ironside JE, Johnston DA, Rollinson D. Genomes and geography: genomic insights into the evolution and phylogeography of the genus Schistosoma. *Parasit Vectors.* (2011) 4:131. doi: 10.1186/1756-3305-4-131

frontiers | Frontiers in Public Health

TYPE Original Research
PUBLISHED 28 May 2024
DOI 10.3389/fpubh.2024.1295081

OPEN ACCESS

EDITED BY
Roberta Lima Caldeira,
Oswaldo Cruz Foundation (Fiocruz), Brazil

REVIEWED BY
Iuliana Raluca Gheorghe,
Carol Davila University of Medicine and Pharmacy, Romania
Selorme Adukpo,
University of Ghana, Ghana

*CORRESPONDENCE
Yuanchun Mao
✉ myc449@hotmail.com
Wei Li
✉ liwei@jipd.com

RECEIVED 15 September 2023
ACCEPTED 10 May 2024
PUBLISHED 28 May 2024

CITATION
Wang Y, Li C, Zhang J, Mao Y and Li W (2024) Protection motivation theory in predicting intentional behaviors regards schistosomiasis: a WeChat-based qualitative study. *Front. Public Health* 12:1295081. doi: 10.3389/fpubh.2024.1295081

Protection motivation theory in predicting intentional behaviors regards schistosomiasis: a WeChat-based qualitative study

Yi Wang, Chengyuan Li, Jianfeng Zhang, Yuanchun Mao* and Wei Li*

National Health Commission Key Laboratory of Parasitic Disease Control and Prevention, Jiangsu Provincial Key Laboratory on Parasite and Vector Control Technology, Jiangsu Provincial Medical Key LaboratoryJiangsu Institute of Parasitic Diseases, Wuxi, China

Background: Modifications of behavior can help reduce the risk of transmission by disrupting the parasite life cycle. Behavior intension is a necessary intermediate step in behavior change. This study aimed to explore protection motivation theory (PMT) in predicting likelihood of engagement in protective behavior against infection with Schistosoma.

Methods: In China, a questionnaire for data collection was sent to users who followed the WeChat public account from June 2 to 6, 2023. Factors affecting intentional behavior of participants were analyzed using stepwise regression analysis and structural equation modeling.

Results: A total of 2,243 valid questionnaires were collected, with a mean age of 30 ± 8.4 years. Approximately 1,395 (62.2%) participants reported that they had been exposed to wild waters in daily work and life. About 51.0 and 50.7% of respondents reported never having been exposed to wild water in the last 3 and 6 months, respectively. Results indicated that prior knowledge of schistosomiasis was associated with the 7 PMT subconstructs, which then influenced future preventative behaviors.

Conclusion: Behavior intentionis a complicated and indispensable part of behavior change that is influenced by professional knowledge, socio-economic status, and personal characteristics. The effective dissemination of knowledge regards schistosomiasis should be strengthened to emphasize the effectiveness of protective measures against infection and severe disease.

KEYWORDS

behavior modification, schistosomiasis, education, protection motivation theory, behavior change

Introduction

Schistosomiasis, caused by *Schistosoma japonicum (S. japonicum)*, was highly prevalent in China before the initiation of the national schistosomiasis control program in the mid-1950s (1). The symptoms of schistosomiasis include abdominal pain, diarrhea, bloody stools, fever, enlarged spleen or liver, liver fibrosis, portal hypertension, and fluid accumulation in the peritoneal cavity (2). Remarkable progress in schistosomiasis control

has been achieved in China since the launch of the national program. Only 30,000 prevalent schistosomiasis patients were estimated across the country, with only five new infections detected in 2019 (3). However, a total of 53,254 existing habitats for the vector were identified, with three clusters in the Sichuan Basin, Dongting Lake, and Poyang Lake. These snail habitats are spread across 12 provinces covering an area of 3.58 billion m^2, where *Oncomelania hupensis* (*O. hupensis*) was identified through a nationwide survey in 2016 (4). Schistosomiasis can be acquired after exposure to freshwater cercariae released from *O. hupensis* (5). Consequently, these widespread intermediate hosts remain an important source of infection, particularly as the World Health Organization (WHO) aims to eliminate the disease in all endemic countries by 2030 (6). Thus, schistosomiasis remains a serious public health issue in China.

Various control measures have been developed and utilized over.

the past few decades, including snail control, personal hygiene attention, drug administration, improved sanitation, access to safe water, and health education (7). In February 2022, the WHO launched a new guideline for action against human schistosomiasis. This guideline suggests that strategies should include preventive chemotherapy, focal snail control, case management, health education, and behavior change (BC) interventions (8). Changing people's behavior can disrupt the life cycle of parasites and reduce the risk of transmission. Health education is a common strategy for BC, particularly focusing on individual-level improvements in knowledge of schistosomiasis. A previous study involved an assessment of 32 BC schistosomiasis interventions for shcistosomiasis (9), reporting a significant reduction in risky practices and a large increase in preventive measures after implementing such interventions. Although BC was not the primary objective, it played an important and ongoing role in schistosomiasis control (10). Another study suggested that knowledge activates a belief system, affecting emotions, and subsequently leading to an intention to perform a specific behavior (11). Therefore, behavior intention is a necessary intermediate step in BC initiatives.

The protection motivation theory (PMT) is a classical framework aimed at explaining and predicting behavior intention through threat and coping appraisal. Threat appraisal involves an individual's belief about the negative consequences of health threat (perceived severity), their vulnerability to these consequences (perceived vulnerability), and the benefits of the performance of the maladaptive behavior (intrinsic and extrinsic rewards). Coping appraisal is determined by beliefs about the effectiveness of preventative behavior (response efficacy), confidence in one's ability to perform the behavior (self-efficacy), and barriers to performing the behavior (response costs). Motivation, an important determinant of protective behavior, is often correlated with intention (12). Therefore, cognitive predictors such as severity, vulnerability, response efficacy, and self-efficacy are associated with intentions, serving as mediators of BC. PMT has shown moderate success in predicting health-related intentions and behaviors across contexts, including COVID-19 vaccination (13), diabetes mellitus type 2 (14), cervical cancer (15), schistosomiasis (16), and others. According to the most recent WHO program guidelines, effective BC is crucial for achieving the 2030 NTD roadmap goals (17). Our study aimed to explore PMT's role in predicting intention to engage in protective behaviors against schistosomiasis.

Materials and methods

Study design

This activity was conducted using a free online survey tool, the Jiangsu Institute of Parasite Disease's official WeChat account. Health information on parasitic diseases was available to followers on the account by JIPD since 2016. A questionnaire for data collection was sent via the official WeChat account from June 2 to 6, 2023 (Figure 1).

Questionnaire development

The questionnaire was entitled "Questionnaire on knowledge of schistosomiasis" and comprised 31 questions including demographics, schistosomiasis knowledge, awareness of schistosomiasis and exposure to wild water, previous protective behaviors and future behavior, and the schistosomiasis PMT scale (Supplementary file 1). The questionnaire was developed based on the constructs of the PMT model (Rogers, 1983) and related schistosomiasis topics such as schistosomiasis spread, schistosomiasis pathology, and prevention of schistosomiasis. Seven single-choice questions were used to assess participant knowledge of schistosomiasis. Participants earned one point for each correct response. Participants were asked for their awareness of schistosomiasis and exposure frequency to wild water through 5 questions, using 4 choices coded as follows:(0 = never, 1 = occasionally,2 = of tenor monthly, 3 = always or weekly). To measure past protective behaviors and future protective behaviors, four questions were asked using a 4-levelresponse scale: (0 = never, 1 = occasionally, 2 = often, 3 = always) and a 5-levelresponse scale (1 = very unlikely to 5 = very likely). The PMT scale consisted of 15 items assessing the7 PMT subconstructs using a 5-point Likert scale (1 = completely agree to 5 = completely disagree).

Statistical analysis

Data including demographics and scores were collected when the questionnaires were submitted. The factors affecting participant behavior intention were analyzed using stepwise regression analysis. Structural equation modeling (SEM) was performed to analyze the relationships of the questionnaire variables. SEM was assessed using 4 indices: goodness-of-fit index (GFI) >0.9, comparative-fit-index (CFI) >0.9, root mean square error of approximation (RMSEA) <0.05, and $\chi^2/df < 3$ [17]. Ap value <0.05 was considered statistically significant. Statistical analysis was completed using IBM SPSS, version 25.0 (Chicago, United States). An online statistics tool named SPSSAU (https://spssau.com/index.html) was used for structural equation modeling (SEM) and mediation analysis.

Results

Participant characteristics

A total of 2,243 valid questionnaires were collected from the network.1302 (58%) were male and 941 (42%) were female, with a mean age of 30 ± 8.4 years. Participants in the survey had a high

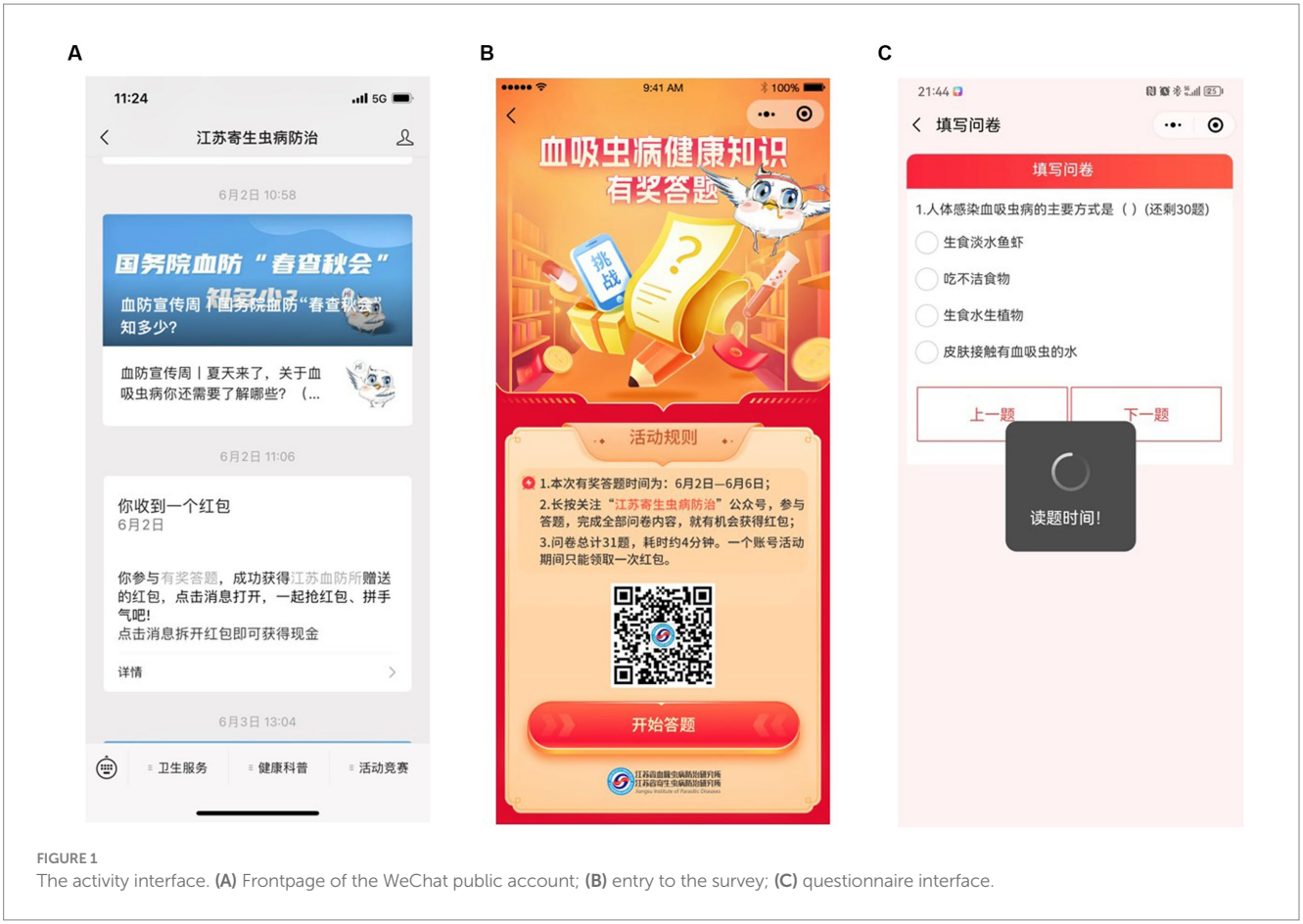

FIGURE 1
The activity interface. **(A)** Frontpage of the WeChat public account; **(B)** entry to the survey; **(C)** questionnaire interface.

TABLE 1 Participants characteristics.

		Total *n* (%)			Total *n* (%)
Gender			Career		
	Male	1,302 (58.0)		Farmer	290 (12.9)
	Female	941 (42.0)		Migrant workers	487 (21.7)
Education				Civil servant	769 (34.3)
	Primary school	112 (5.0)		Enterprise personnel	557 (24.8)
	High school	510 (22.7)		Student	141 (6.3)
	Bachelor's degree	1,321 (58.9)			
	Master's degree or above	300 (13.4)			

educational level, and more than half received an education beyond school level. Migrant workers, civil servants, and enterprise personnel comprised the main population at 80.8%. 35%participants said that they had suffered from schistosomiasis.Approximately1395 (62.2%) of participants reported that they had been exposed to recreational or wild waters through daily work and life (Table 1).

Descriptive statistics of the questionnaire

The reliability of PMT scale was 0.738 (Cronbach's α) and construct validity was 0.926 (KMO). The reliability of two subconstructs named threat and coping appraisal of PMT scale were 0.828, 0.739 (Cronbach's α) and construct validity were 0.901, 0.718 (KMO). The mean score for schistosomiasis knowledge was 3.0 ± 1.7 (the total score possible was 8 points). Only 20.7% of participants reported that they were always aware of schistosomiasis before exposure to recreational water and 34.8% said they had never been aware of it before exposure.51.0 and 50.7%respondents reported that they had never been exposed to wild water in the last 3 and 6 months, respectively. Approximately 38.1 and 42.0%ofparticipants reported that they were likely to avoid contact with wild water in the next3 and 12 months, respectively. The descriptive statistics from the questionnaire are presented in Figure 2.

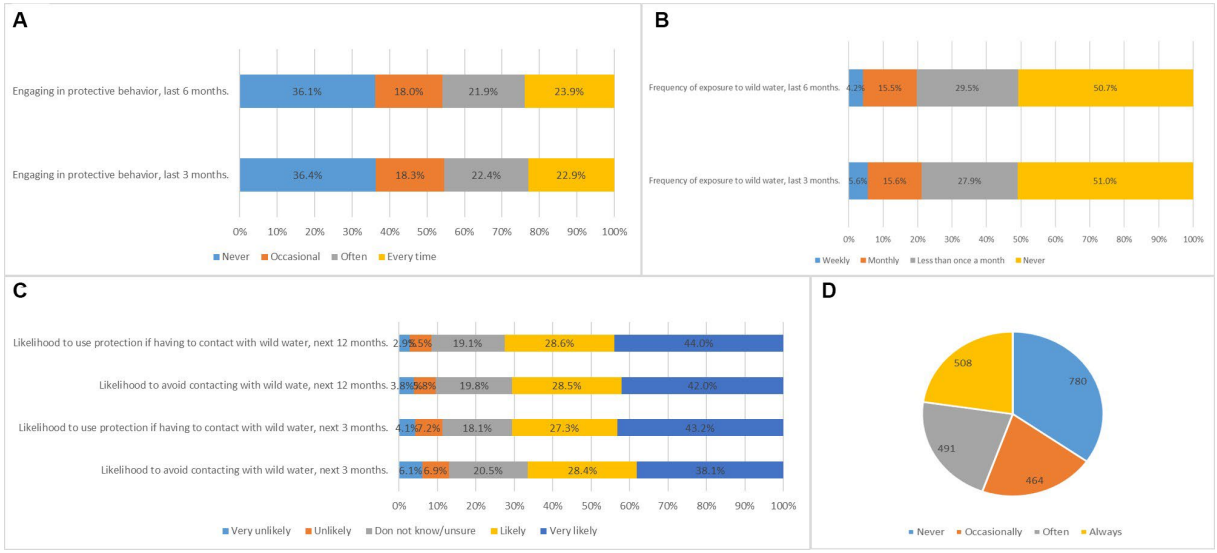

FIGURE 2
(A) Characteristics of engaging in protective behavior, last 3 and 6 months. **(B)** Frequency of exposure to wild water, last 3 and 6 months. **(C)** Characteristics of future protective behaviors. **(D)** Awareness of schistosomiasis before exposure to wild water.

TABLE 2 Results of the stepwise regression analysis.

Factors	B	*S.E*	T	*P*
Constant	14.757	0.245	60.336	0.000
Prior exposure	0.427	0.037	11.711	0.000
Prior protective behavior	−0.568	0.043	−13.340	0.001
Gender	−2.994	1.316	−2.276	0.012
schistosomiasis knowledge	0.109	0.049	2.219	0.027

*B, unstandardized regression coefficient; SE, standard error; $p < 0.05$.

Association between questionnaire variables and behavior intention

The stepwise regression analysis was used to analyze participant behavior intention. The main factors were gender, schistosomiasis knowledge, prior exposure, and prior protective behavior (Table 2). The hypothesized model analysis of this study showed a relatively good fit (χ^2/df = 3.0, GFI = 0.86, RMSEA =0.07, CFI =0.87). Results indicated that schistosomiasis knowledge was associated with the 7 PMT subconstructs, which then significantly influenced future protective behaviors (behavior intention). All parameters of SEM are illustrated in Figure 3.

Discussion

People can become infected with schistosomiasis by contact with freshwater harboring cercariae released from intermediate host snails. Therefore, schistosome infection is closely related to human behavior (18). Behavior change can improve schistosomiasis control by modifying risky practices (19). PMT is a theory that analyzes the cognitive process of behavior intention from the perspective of motivation. Behavior intentionis a decision made through a comprehensive assessment of both the threat of risk factors and the ability to coping with these and has been predicted widely using PMT. A pilot study of WeChat-based using PMT was conducted to predict behavior intentions against schistosomiasis.

Interventions combining information provision was an important part of BC. Despite adequate knowledge and positive attitudes, this did not translate to effective behavior changes, mainly due to the socio-cultural factors and participant environment. It is crucial to understand the social, cultural, and behavioral determinants that can bridge the knowledge-practice gap (20). According to our study, participant behavior intention was strongly associated with female gender, schistosomiasis knowledge, prior exposure, and prior protective behavior. Women were more likely than men to take protective measures. People who had been exposed to wild or recreational waters in the past were less likely to take protective measures in the future. One reason for this phenomenon may be survivorship bias (21). Even if these participants were exposed to wild waters, they were not infected with schistosomiasis. Therefore, they would not choose to take protective measures in the future. People who had taken protective measures in the past and achieved a high score on schistosomiasis knowledge were more likely to do so in the future. These finding showed that behavioral determinants should not only focus on knowledge transmission but also on early and acquired living habits.

As a result of the gaps observed between knowledge, attitude, and practices, more effective methods and considerable effort should be invested to better analyze the reasons for what motivates behavior change (22). The PMT framework for systematic behavior involved three phases: (1) assessing the risks; (2) benefiting from take protective measures; (3) making a decision. The result of the structural equation modeling analysis indicated that schistosomiasis knowledge was associated with all PMT subconstructs. Five of the seven subconstructs (severity, vulnerability, intrinsic reward, extrinsic reward, and response cost) were significantly associated with intention to engage in protective behavior. These results accentuated the necessity of schistosomiasis knowledge for subsequent behavior intention.

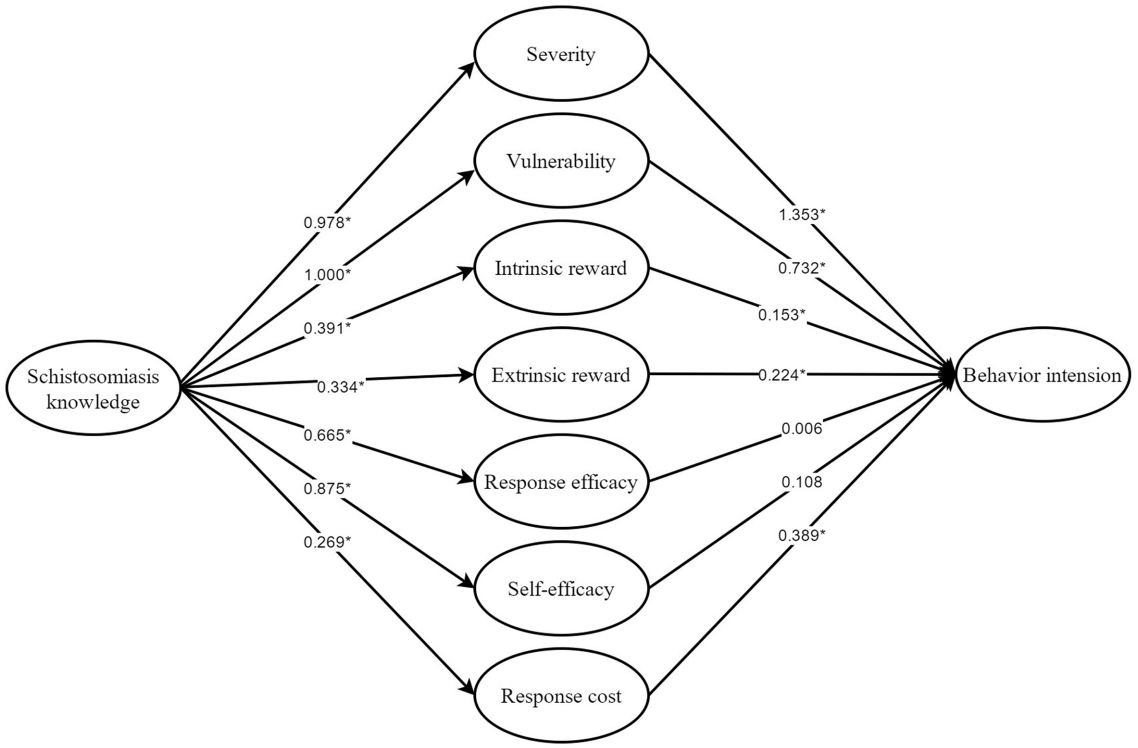

FIGURE 3
Structural equation modeling of schistosomiasis knowledge, schistosomiasis PMT constructs and behavior intention. *$p < 0.05$.

Focusing more on the emerging model, results indicated that schistosomiasis knowledge was significantly associated with four subconstructs including severity, vulnerability, self-efficacy, and response efficacy. Meanwhile, weaker associations were observed with intrinsic reward, extrinsic reward, and response cost. Severity and vulnerability were recognized as important clinical features of the disease. Response efficacy referred to the understanding of disease prevention and information concerning control. In most of these studies, the knowledge, attitudes, and practices (KAP) questionnaire on schistosomiasis control also included cause of infection, symptoms, prevention, and risky behaviors (23–25). Furthermore, not all the four substructures were closely associated with knowledge, which was associated with behavior intention. For example, self-efficacy represented confidence in one's ability to take protective behaviors. Moreover, three dimensions including intrinsic reward, extrinsic reward, and response cost were a comprehensive embodiment of personal cognition, social status, and culture. The three dimensions were weakly correlated with knowledge and strongly associated with behavior intention. So, for behavior intention, severity and vulnerability were the most important factors, which in turn were associated with knowledge of disease. However, another study suggested that severity, intrinsic reward and self-efficacy should be targeted (26, 27). It is possible that because this study focused on participants whose mean age was 30 years old, while the previous study focused on students whose mean age was 13 years old.

By and large, in combining BC approaches for schistosomiasis intervention programs, the content of behavior intention should be carefully considered. First, the characteristics of the target population should include age, gender, and early living habits. These appear to be important considerations for health education campaigns as part of disease control interventions. Second, the effective dissemination of information regarding schistosomiasis should be strengthened to consolidate knowledge on disease severity, vulnerability, and emphasis on the effectiveness of protective measures. Third, there is a high correlation between response costs and behavior intention, and this accentuates the need to develop economic and convenient protection to foster behavior intention.

Our study has some limitations. First, all participants may have had a higher socioeconomic background than the general public and thus are not representative of the entire population. To be able to generalize the results, participants who do not have access to smartphones should be included in the future. Second, response bias might be present because participant self-reporting of responses to questions about their capacity for healthy behaviors and skills might have been biased toward their responses and what the study investigators thought of these. Third, one individual may possess multiple phone lines connected to the WeChat platform, enabling them to provide duplicate responses in order to intentionally skew the data when contacted without their knowledge.

Conclusion

Behavior intentionis a complicated and indispensable component of behavior change that is influenced by professional knowledge, socio-economic status and personal characteristics. PMT highlighted that behavior intention and knowledge were inextricably linked in numerous ways and can mitigate against schistosomiasis infection.

Data availability statement

The original contributions presented in the study are included in the article/Supplementary material, further inquiries can be directed to the corresponding authors.

Ethics statement

The studies involving humans were approved by the Ethics Committee of the Parasitic Disease Control and Prevention in Jiang. The studies were conducted in accordance with the local legislation and institutional requirements. The participants provided their written informed consent to participate in this study.

Author contributions

YW: Project administration, Investigation, Writing – original draft. CL: Writing – review & editing, Investigation, Data curation. JZ: Writing – review & editing, Project administration. YM: Formal analysis, Writing – review & editing, Supervision. WL: Writing – review & editing, Project administration.

Funding

The author(s) declare financial support was received for the research, authorship, and/or publication of this article. This study was supported by the Jiangsu Province Capability Improvement Project through Science, Technology, and Education (No. ZDXYS202207).

Acknowledgments

We thank all participants who made this research possible.

Conflict of interest

The authors declare that the research was conducted in the absence of any commercial or financial relationships that could be construed as a potential conflict of interest.

Publisher's note

Supplementary material

The Supplementary material for this article can be found online at: https://www.frontiersin.org/articles/10.3389/fpubh.2024.1295081/full#supplementary-material

References

1. Wang W, Bergquist R, King CH, Yang K. Elimination of schistosomiasis in China: current status and future prospects. *PLoS Negl Trop Dis*. (2021) 15:e0009578. doi: 10.1371/journal.pntd.0009578

2. Zhu H, Liu JB, Xiao Y, Tu ZW, Shan XW, Li B, et al. Efforts to eliminate schistosomiasis in Hubei province, China: 2005–2018. *Acta Trop*. (2022) 231:106417. doi: 10.1016/j.actatropica.2022

3. Zhang LJ, Xu ZM, Dang H, Li YL, Lü S, Xu J, et al. Endemic status of schistosomiasis in People's republic of China in 2019. *Zhongguo Xue Xi Chong Bing Fang Zhi Za Zhi*. (2020) 32:551–8. doi: 10.16250/j.32.1374.2020263

4. Lv C, Li YL, Deng WP, Bao ZP, Xu J, Lv S, et al. The current distribution of Oncomelania hupensis snails in the People's Republic of China based on a Nationwide survey. *Trop Med Infect Dis*. (2023) 8:120. doi: 10.3390/tropicalmed8020120

5. Riaz S, Ahmed H, Kiani SA, Afzal MS, Simsek S, Celik F, et al. Knowledge, attitudes and practices related to neglected tropical diseases (schistosomiasis and fascioliasis) of public health importance: a cross-sectional study. *Front Vet Sci*. (2023) 10:1088981. doi: 10.3389/fvets.2023.1088981

6. WHO. *Ending the neglect to attain the Sustainable Development Goals: A road map for neglected tropical diseases 2021–2030*. https://www.who.int/publications/i/item/9789240010352 (Accessed August 3, 2023).

7. Gordon CA, Williams GM, Gray DJ, Clements ACA, Zhou XN, Li Y, et al. Schistosomiasis in the People's Republic of China - down but not out. *Parasitology*. (2022) 149:218–33. doi: 10.1017/S0031182021001724

8. Xu J, Li SZ, Guo JG, Zhou XN, Djirmay AG. The WHO new guideline to control and eliminate human schistosomiasis: implications for the verification of transmission interruption and surveillance of Schistosoma japonicum in China. *Infect Dis Poverty*. (2022) 11:79. doi: 10.1186/s40249-022-01003-w

9. Torres-Vitolas CA, Trienekens SCM, Zaadnoordijk W, Gouvras AN. Behaviour change interventions for the control and elimination of schistosomiasis: a systematic review of evidence from low-and middle-income countries. *PLoS Negl Trop Dis*. (2023) 17:e0011315. doi: 10.1371/journal.pntd.0011315

10. Trippler L, Hattendorf J, Ali SM, Ame SM, Juma S, Kabole F, et al. Novel tools and strategies for breaking schistosomiasis transmission: study protocol for an intervention study. *BMC Infect Dis*. (2021) 21:1024. doi: 10.1186/s12879-021-06620-8

11. Sule MN, Mosha J, Soboka TE, Kinung'hi SM, Sfynia C, Rafiq K, et al. A novel theatre-based behaviour change approach for influencing community uptake of schistosomiasis control measures. *Parasit Vectors*. (2022) 15:301. doi: 10.1186/s13071-022-05421-5

12. Hansen MF, Srensen PK, Srensen AE, Krogfelt KA. Can protection motivation theory predict protective behavior against ticks? *BMC Public Health*. (2023) 23:1214. doi: 10.1186/s12889-023-16125-5

13. Ansari-Moghaddam A, Seraji M, Sharafi Z, Mohammadi M, Okati-Aliabad H. The protection motivation theory for predict intention of COVID-19 vaccination in Iran: a structural equation modeling approach. *BMC Public Health*. (2021) 21:eng. doi: 10.1186/s12889-021-11134-8

14. Yao X, Zhang L, Du J, Gao L. Effect of information-motivation-behavioral model based on protection motivation theory on the psychological resilience and quality of life of patients with type 2 DM. *Psychiatry Q*. (2021) 92:49–62. doi: 10.1007/s11126-020-09783-w

15. Bai Y, Liu Q, Chen X, Gao Y, Gong H, Tan X, et al. Protection motivation theory in predicting intention to receive cervical cancer screening in rural Chinese women. *Psycho-Oncology*. (2018) 27:442–9. doi: 10.1002/pon.4510

16. Xiao H, Peng M, Yan H, Gao M, Li J, Yu B, et al. An instrument based on protection motivation theory to predict Chinese adolescents' intention to engage in protective behaviors against schistosomiasis. *Glob Health Res Policy*. (2016) 1:15. doi: 10.1186/s41256-016-0015-6

17. Lo NC, Bezerra FSM, Colley DG, Fleming FM, Homeida M, Kabatereine N, et al. Review of 2022 WHO guidelines on the control and elimination of schistosomiasis. *Lancet Infect Dis*. (2022) 22:e327–35. doi: 10.1016/S1473-3099(22)00221-3

18. Hamdan Alshammari M, Alboliteeh M. Structural equation modeling of the association between professional and cultural competencies of nurses in Saudi Arabia. *Nurse Educ Pract*. (2022) 63:103382. doi: 10.1016/j.nepr.2022.103382

19. Guan Z, Dai SM, Zhou J, Ren XB, Qin ZQ, Li YL, et al. Assessment of knowledge, attitude and practices and the analysis of risk factors regarding schistosomiasis among fishermen and boatmen in the Dongting Lake Basin, the People's Republic of China. *Parasit Vectors*. (2020) 13:273. doi: 10.1186/s13071-020-04157-4

20. Feng J, Wang X, Zhang X, Hu H, Xue J, Cao C, et al. Effect of health education on schistosomiasis control knowledge, attitude, and practice after schistosomiasis blocking: results of a longitudinal observational study in the field. *Trop Med Infect Dis*. (2023) 8:267. doi: 10.3390/tropicalmed8050267

21. Takeuchi R, Njenga SM, Ichinose Y, Kaneko S, Estrada CA, Kobayashi J. Is there a gap between health education content and practice toward schistosomiasis prevention among schoolchildren along the shores of Lake Victoria in Kenya? *PLoS Negl Trop Dis*. (2019) 13:e0007572. doi: 10.1371/journal.pntd.0007572

22. Pasqualetti F, Barberis A, Zanotti S, Montemurro N, De Salvo GL, Soffietti R, et al. The impact of survivorship Bias in glioblastoma research. *Crit Rev Oncol Hematol*. (2023) 188:eng. doi: 10.1016/j.critrevonc.2023.104065

23. Xue Q, Deng Y, Liu Y, Wang Y, Hu W, Huang Y, et al. A retrospective analysis of schistosomiasis related literature from 2011-2020: focusing on the next decade. *Acta Trop*. (2023) 238:106750. doi: 10.1016/j.actatropica.2022.106750

24. Assefa A, Erko B, Gundersen SG, Medhin G, Berhe N. Low awareness and common misconceptions about schistosomiasis in endemic lowland areas in Western Ethiopia: a mixed-methods study. *BMC Public Health*. (2021) 21:1064. doi: 10.1186/s12889-021-11106-y

25. Mwanga JR, Lwambo NJ. Pre-and post-intervention perceptions and water contact behaviour related to schistosomiasis in North-Western Tanzania. *Acta Trop*. (2013 Nov) 128:391–8. Epub 2012/10/13. doi: 10.1016/j.actatropica.2012.09.017

26. Shi L, Zhang JF, Li W, Yang K. Development of new Technologies for Risk Identification of schistosomiasis transmission in China. *Pathogens*. (2022) 11:224. doi: 10.3390/pathogens11020224

27. Xiao H, Li S, Chen X, Yu B, Gao M, Yan H, et al. Protection motivation theory in predicting intention to engage in protective behaviors against schistosomiasis among middle school students in rural China. *PLoS Negl Trop Dis*. (2014) 8:e3246. doi: 10.1371/journal.pntd.0003246

Frontiers in Immunology

Explores novel approaches and diagnoses to treat immune disorders.

The official journal of the International Union of Immunological Societies (IUIS) and the most cited in its field, leading the way for research across basic, translational and clinical immunology.

Discover the latest Research Topics

See more →

Frontiers

Avenue du Tribunal-Fédéral 34
1005 Lausanne, Switzerland
frontiersin.org

Contact us

+41 (0)21 510 17 00
frontiersin.org/about/contact